Natural Drivers of Antimicrobial Resistance

An exploration of the causative natural drivers of antimicrobial resistance, using a combination of metagenomic, evolutionary, and bioinformatic approaches. With a focus on the phytochemicals quercetin and berberine.

'Thesis submitted in accordance with the requirements from the Liverpool School of Tropical Medicine for the degree of Doctor of Philosophy by *William Hayden Hutton*'

September 2022

Abstract

Antibiotic resistance is a serious ongoing threat to both the medical and agricultural sectors, with far-reaching and diverse consequences. Historically, antibiotic resistance has been thought to be driven by the anthropogenic use of antibiotics in clinical and agricultural settings. However, there is a growing body of evidence that clearly demonstrates that antimicrobial resistance developed naturally, millions of years ago. Understanding these natural drivers of antibiotic resistance is key to managing the ongoing antimicrobial resistance problem.

One potential natural driver of antibiotic resistance are phytochemicals which are chemicals produced by plants for environmental interaction. Phytochemicals are being explored for their potential role as antibiotic replacements in the clinic, and in agriculture. We propose that the use of phytochemicals as antimicrobial replacements in multiple industries will have an equal, or worse impact on the problem of antibiotic resistance, due to their potential to select for cross-resistance to other antimicrobials such as antibiotics. Phytochemicals could drive antibiotic resistance in one of three ways: (1) The selection of genes which confer cross resistance to antibiotics. (2) The selection of plasmids carrying both phytochemical and antibiotic resistance genes and (3) the selection of bacteria which are known antimicrobial resistance reservoirs.

In this study, two antimicrobial phytochemicals, quercetin and berberine were explored for their role as natural drivers of antibiotic resistance.

This study was split into three different experimental methodologies. The first experimental methodology developed a novel phytochemical screening assay, which was then successfully used to screen an oral metagenomic library, and the Swab and Send bacterial isolate library. Screening the metagenomic library uncovered three isolates with tolerance to either

quercetin or berberine. These isolates contained inserts with multiple antibiotic resistance genes, including a glycosyltransferase and transpeptidase. Screening the Swab and Send library uncovered 20 isolates from 11 bacterial species containing antibiotic resistance genes with a phytochemical tolerant phenotype.

The second experimental methodology evolved *P. aeruginosa* NCTC 7244 and NCTC 9433 in sub-inhibitory concentrations of the phytochemicals for 30 days. This experiment was conducted see how environmental bacteria responded to phytochemical selective pressure. Eleven of the 12 isolates developed a 2-fold phytochemical tolerance after 30 days. The isolates contained multiple genetic mutations including mutations in a glycosyltransferase and transpeptidase gene.

The final experimental methodology explored the impact of phytochemical addition to chicken feed on the microbiome of chickens through two *in vitro* model experiments, and an *in vivo* chicken study. The studies also compared the viability of the two *in vitro* models as replacement for *in vivo* chicken experiments. Addition of both phytochemicals impacted microbiome development in all models compared to the control. Specifically increasing the levels of *Escherichia-shigella* and *Turicibacter* genera and decreasing levels of *Lactobacillus pontis* which may indicate an increase in disease incidence due to phytochemical supplementation.

This study shows that berberine and quercetin can act as a selective pressure for the maintenance and mutation of genes which confer antimicrobial resistance, and the selection of antimicrobial resistant isolates in isolate libraries and the chicken gastrointestinal system. Therefore, serious consideration should be given to the risks of using phytochemicals as antimicrobial replacements in both agricultural and clinical sectors.

Acknowledgements

Table of Contents

List of Figures

Figure 3-5 Bacterial insert contained on plasmid V5H10. The insert was 13,368 base pairs in length and contained a Di-tripeptide/cation symporter, Exinuclease subunit A, 4 hypothetical proteins, nitroreductase family protein, a 3'-5' oligoribonuclease bacillus type, two tRNA-CTT

and a penicillin binding protein. It maps to nucleotides 342032 − 355604 of Prevotella histolitica strain F0411 chromosome 2. All transposon mutagenesis insert sites are given as ΔTn, followed by the indication of the well from which they were located.

List of Tables

List of Equations

List of Abbreviations

ACT   –   Artemisinin combination therapy

AMR   –   Antimicrobial resistance

ARGs   –   Antimicrobial resistance genes

APGs   –   Antimicrobial growth promoters

BHI   –   Brain heart infusion

BP   –   Base pair

CDC   –   Centre for disease control

Ddl   –   d-alanine-d-alanine ligase

DMSO   –   Dimethyl-Sulfoxide

DNA   –   Deoxyribose nucleic acid

DPCo   –   Double principle component analysis

EUCAST   –   European committee on antimicrobial susceptibility testing

FAO   –   Food and agriculture organisation

GIS   –   Gastrointestinal system

HICs   –   High income countries

HGT   –   Horizontal gene transfer

HMR   –   Heavy metal resistance

IPM   –   Imipenem

LB   –   Lysogeny

LSTM   –   Liverpool School of Tropical Medicine

LTEE   –   Long-term evolution experiment

MDR   –   Multidrug resistant

MIC   –   Minimum inhibitory concentration

MGE   –   Mobile genetic element

MHA   –   Muller Hinton Agar

MHB   –   Muller Hinton Broth

MRSA   –   Methicillin-resistance *Staphylococcus aureus*

MSC   –   Minimum selective concentration

OTUs   –   Operational taxonomic unit

PAO1   –   *P. aeruginosa* O1

PBS   –   Phosphate buffered saline

PCoA   –   Principle component analysis

PCR   –   Polymerase chain reaction

PRI   –   Piperacillin

SOC   –   Sugar optimal broth with catabolite repression

TAE   –   Tris acetate-ethylenediaminetetraacetic acid

TSS   –   Transformation and storage solution

QS   –   Quorum Sensing

VRE   –   Vancomycin-resistant *Enterococcus*

WHO   –   World Health Organisation

WOAH   –   World Organisation for Animal Health

1 Introduction

1.1 The structure of the introduction

Antimicrobial resistance (AMR) is a global problem with far reaching consequences. The work presented in this thesis seeks to better understand one of the potential environmental drivers of AMR, phytochemicals, and how they contribute to AMR and the effects their increased use will have in the future, in both a clinical and an agricultural context.

This introduction will give a comprehensive overview of the current state of AMR, and the importance of natural drivers of AMR with a focus on the two key phytochemicals: quercetin and berberine. It will also outline the current gaps in our understanding between the relatedness of phytochemicals and AMR. It will then review several key studies on the interaction between phytochemicals and AMR bacteria. The introduction will also review the use of antimicrobials within the agricultural sector.

Subsequently, the introduction will review the key methodologies and techniques used within this thesis, namely the cultivation of *Escherichia coli* and *Pseudomonas aeruginosa,* the development of functional metagenomic screening procedures, bacterial evolution studies, and microbiome analysis using 16S rRNA gene sequencing.

This introduction will end with a summation of the aims and objectives of this thesis, and how the new knowledge generated contributes to the wider scientific understanding of the AMR problem.

1.2 Antimicrobial resistance: an overview

1.2.1 Antimicrobial resistance: the historical context

Antibiotics are natural, or synthetic compounds that can either kill, or inhibit the growth of bacteria, known as bactericidal and bacteriostatic activity, respectively. In most cases antibiotics do not damage the human or animal host. This is because they target specific

bacterial targets, which do not exist within the host. These include the bacterial cell wall, ribosome, or the essential bacterial metabolism and the enzymes which constitute the metabolic pathways (Hooper, 2001; Pankey & Sabath, 2004). Antimicrobials are compounds which kill microbes and are not necessarily antibiotics. This introduction will focus on antibiotics as drugs, but phytochemicals, and resistance as antimicrobial compounds and antimicrobial resistance, respectively.

Antibiotics contributed to the rapid extension of the human lifespan through their reduction of human mortality due to infectious diseases (Nicolaou & Rigol, 2018). They form an essential part of the modern healthcare system, not only for use in treating bacterial infections but also due to their use as prophylaxis during and after surgery, chemotherapy, transplantation, and childbirth (Crader & Varacallo, 2021; de Tejada, 2014; Gao et al., 2020).

Antibiotics, as we know them, were first discovered by Alexander Fleming in 1928 with his findings published in 1929. This antibiotic was penicillin from the fungus *Penicillium notatum* (Flemming, 1929). However, prior to this major discovery there was already limited use of antimicrobial therapy by humans. The first was the use of pyocyanase in 1899 produced by *Pseudomonas aeruginosa*, however its toxicity precluded further use (Hays et al., 1945). Pyocyanase was incorrectly assumed to be an enzyme, but is now thought to have been a combination of pyocyanin, a phenazine and a quinolone, which would have been toxic to both the respiratory tract and stomach (Hutchings et al., 2019). The second use of antimicrobials prior to the introduction of penicillin was the use of Salvarsan against the causative agent of syphilis (Ehrlich & Hata, 1910). Salvarsan, also known as arsphenamine, was an organoarsnic compound used as the first effective treatment for syphilis and African Trypanosomiasis (Vernon, 2019), though it was incredibly toxic and 'burnt veins'.

After the discovery of penicillin, the world entered what is now known as 'The Golden Age' of antibiotic discovery, with the first sulfadrug identified in 1932 and the discovery of five

new classes of antibiotics in the 1940s (Lewis, 2013). There are several antibiotic classes with different bacterial targets (Figure 1-1). These antibiotics have been isolated from both fungal and prokaryotic sources, with some being extensively chemically modified derivatives (e.g., amoxicillin and minocycline) and finally some being completely chemically synthesised (e.g. fluroquinolones and oxazolidinones) (Demain, 2009).
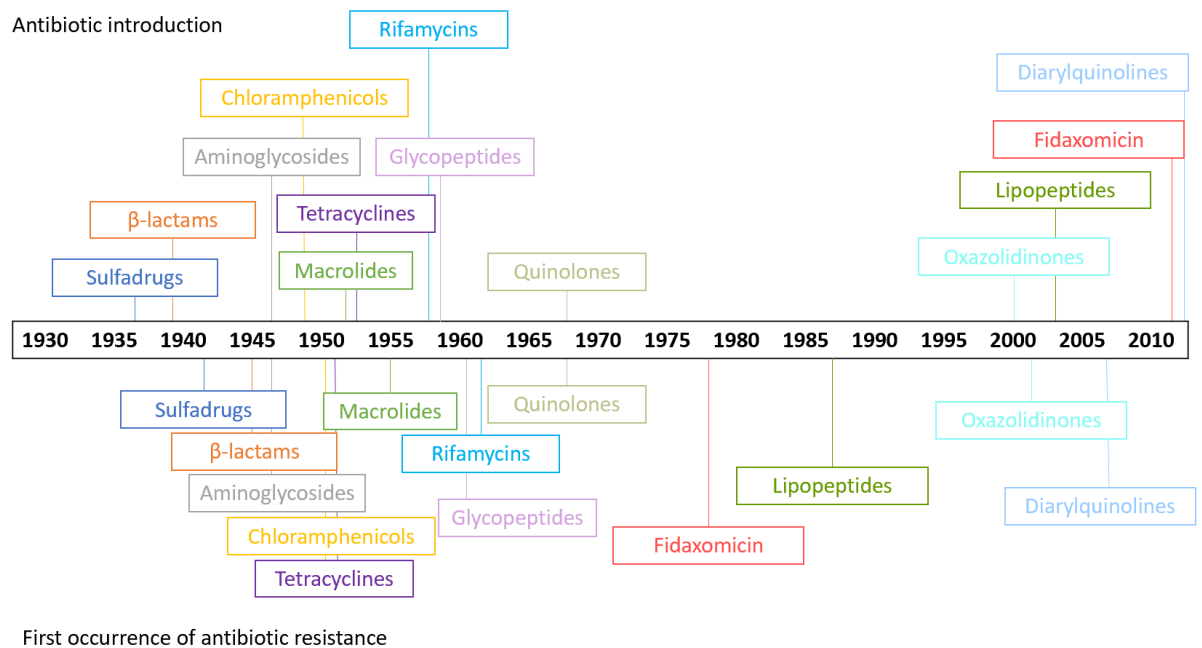
Figure 1-1 Antibiotic classes by year of introduction (top) and year of the first occurrence of antibiotic resistance to that class (bottom), adapted from data in Lewis et al., 2013.

Shortly following Flemming's discovery of penicillin, he observed that some bacteria, namely *Escherichia coli* and *Klebsiella pneumoniae* were able to coexist with the mould, despite the production of inhibitory molecules by the *Penicillium* fungi on a petri plate (Abraham & Chain, 1988). Following this discovery, the appearance of resistance to antibiotics has been followed, or even preceded by, their use in the clinic (Lewis, 2013) (Figure 1-1).

1.2.2 Antimicrobial resistance: the modern problem

AMR is the inherent or acquired capability of bacteria to survive exposure to a compound to which they were previously sensitive. Antibiotic resistance is a specific type of AMR where bacteria gain resistance to antibiotics. Microbial populations are inherently geared towards

the development of resistance due to their ability to respond to environmental challenges quickly and effectively. Microbial populations have distinct advantages in this arena such as high population generation turnover, highly mutable genomes, and horizontal gene transfer which all allow for rapid evolution of a bacterial population in stress conditions.

The problem of AMR is global, made worse by the widespread use, and misuse of antibiotics in both clinical and agricultural settings (Aslam et al., 2018; Ventola, 2015). Misuse includes inappropriate prescription (overprescribing, underprescribing, and incorrect prescribing practices), non-prescription purchasing of antibiotics, the use of fake or sub-standard antibiotics, and extensive overuse in agriculture as treatment, prophylaxis, and growth promotors. Additionally, international travel exacerbates the global problem of AMR, particularly when looking at healthcare related travel, with people infected pathologically, and colonised commensally, or mutually with AMR bacteria travelling between high, low, and middle income countries via air travel (Bokhary et al., 2021). This list of drivers is not exhaustive, with meat production, wastewater, biocide use, and agricultural waste amongst other factors also contribute to the AMR crisis (Singer et al., 2016).

The antibiotics currently in use are becoming less clinically effective, due to rising levels of AMR (Zaman et al., 2017). This has economic, healthcare, and social impacts. With the annual deaths due to AMR projected to reach 10 million globally to a cost of between 2-3.5% of global GDP (O'Neill, 2014). This rise was clearly shown in 2019, with deaths attributable to AMR estimated to be around 4.95 million (Murray et al., 2022). Importantly Murray et al, highlighted that there are significant issues in data gathering and analysis in low- and middle-income countries, and the reported deaths in 2019 suggest that the O'Neill report may have underestimate the potential burden of AMR globally.

This problem is compounded by a significant reduction in the development of new antibiotics, and a movement away from antibiotic development by the pharmaceutical

industry (Czaplewski et al., 2016; Plackett, 2020), with companies like Novartis and GSK actively announcing the end of their antibiotic development pipelines (Bulik, 2021; Carroll, 2018; Dall, 2018; LeMieux, 2018). Only 5 companies that developed antibiotics still work within the antibiotic space (Science, 2023).

1.2.3   Antimicrobial resistance: the role of the agricultural sector

One key driver of antibiotic resistance is the agricultural sector, where the AMR problem can broadly be categorised into three areas, (1) the use and misuse of antibiotics and other toxic molecules, (2) the prevalence of antimicrobial resistance genes (ARGs), and (3) the prevalence of antimicrobial resistant bacteria (Durso & Cook, 2014).

The use of antibiotics in agriculture is not new. Their use occurred simultaneously with their use in humans and continued throughout the 20th century. The first use was of Prontosil, the first effective drug against Gram-positive infections which was marketed for use in animals from 1938 onwards. Further, gramicidin was used to treat mastitis in cows from 1940, and in Britain and Denmark penicillinases were tested for use against mastitis due to the wartime importance of milk production in 1943 (Kirchhelle, 2018). This use surged throughout the 20th century due to the lack of an international standardisation of antibiotic use.

More antibiotics are used in the agricultural sector as both antibiotic growth promotors (APGs) and as therapeutics, than in humans (Dritz et al., 2002). Spending on antibiotics in the agricultural sector is high, and usage is projected to increase by two thirds by 2030. This increase will occur mainly in developing countries, due to rising demand for low cost meat (Laxminarayan et al., 2015). Further the use of antibiotics in agriculture has a clear impact on human health, as methicillin-resistant *S. aureus* (MRSA) and multi-drug-resistant (MDR) urinary tract infections originated in swine and poultry, respectively (Larsen et al., 2015; Nordstrom et al., 2013). It is thus clear that there is a need to produce new products and

farming policies which keep AMR low and produce high, instead of using antibiotics as was commonplace in the past.

AGPs are sub-therapeutic doses of antibiotics, usually added to feed, which are given to livestock to promote growth and reduce disease incidence. The first use of AGPs was in the mid-1940s when poultry and swine were fed dried mycelia of *Streptomyces aureofaciens* containing chlortetracycline residues, which improved their growth (Castanon, 2007; Dibner & Richards, 2005).

However, there is contention about the ethical use of AGPs due to fears they might exacerbate the problem of AMR in humans. Many European countries have banned the use of antibiotic growth promotors, as have many major food suppliers (Singer et al., 2016), and the world health organisation (WHO), Food and Agriculture Organisation (FAO), and World Organisation for Animal Health (WOAH) have all petitioned for the complete global ban of AGPs (Dibner & Richards, 2005).

Clear evidence links the use of antibiotics in agriculture to the rise of AMR, as in the case of vancomycin-resistant *Enterococcus* (VRE) spread due to the use of avoparcin in poultry (Aarestrup, 1995). These resistant bacteria have moved from the agricultural industries to become an ongoing global problem, direct cases of which are described below.

The removal of AGPs, however, has led to an increased incidence of disease in animals or higher economic costs (Casewell et al., 2003; Cogliani et al., 2011; Dritz et al., 2002; MacDonald & Wang, 2011). The agricultural industry in high income countries (HICs) such as Sweden and Denmark can combat this effect with higher use of antibiotic prophylaxis and veterinary prescriptions (Kirchhelle, 2018). This suggests that there is still a high reliance on antibiotics, despite the ban. Removal of AGPs led to producers receiving higher fees on contracts, suggesting they bear a higher cost to output ratio in broiler production after the

removal of APGs (MacDonald & Wang, 2011). There is also higher mortality and morbidity in both post-weaning pigs and broilers due to *E. coli and Lawsonia intracellularis* infections as a result of AGP removal, which led to the increased use of antibiotics as therapeutic treatments (Casewell et al., 2003). Alongside this, both the agricultural and pharmaceutical communities in America have lobbied for the preservation of the AGP market there, with success (Kirchhelle, 2018), highlighting the complicated nature of the relationship of AGPs, interest groups, and animal health.

1.2.4   Antimicrobial resistance: potential Solutions

A comprehensive strategy is required to manage the AMR crisis (O'Neill, 2014). This strategy will require a focus not only on development of new antibiotics and more effective treatment regimens; but also reinventing the antibiotic pipeline through 'push and pull incentives' such as antibiotic development bonuses and public partnerships (Morel et al., 2020; Singer et al., 2019a, 2019b). Further efforts are being made to develop of antimicrobial treatment profiles which reduce the development of AMR in the clinic (Lee et al., 2013).

Integral to this project, it is essential that the wider biological environment which underpins the development of AMR is properly understood. To determine the 'natural' predisposition of bacteria to develop resistance to antibiotics (Kirchhelle & Roberts, 2022).

1.2.5   Antimicrobial resistance: types of antibiotic resistance

Antibiotic resistance, as previously defined, can either be intrinsic, or acquired through mutation in chromosomal genes, or acquisition of resistance genes through horizontal gene transfer (HGT) from other bacteria (Reygaert, 2018).

1.2.5.1   *Intrinsic antimicrobial resistance*

Intrinsic antibiotic resistance is the inherent ability of bacteria to resist the activity of antibiotics of a particular class or agent through its innate structural or functional characteristics. This inherent resistance may be due to inaccessibility of the drug into the

bacterial cell, removal of the drug from the cell by chromosomally encoded exporters, production of antibiotic inactivating or degrading enzymes, or the absence of a particular drug target (Reygaert, 2018). A key intrinsic mechanism of resistance is the outer membrane peptidoglycan layer of Gram-negative bacteria, which conveys resistance to antibiotics such as vancomycin that are unable to penetrate the outer membrane (Miller, 2016). An example of a bacterium containing intrinsic resistance mechanisms is *Acinetobacter baumannii,* which not only has a highly impermeable membrane, but also chromosomally encoded β-lactamases (Peleg et al., 2008)

1.2.5.2   *Acquired resistance*

Acquired resistance, conversely, is the evolutionary process by which bacteria develop resistance to antibiotics, through several pathways (Van Hoek et al., 2011). These can include mutations in target genes, gene promotors, and repressors. Additionally, bacteria can acquire resistance through HGT, where ARGs are located on mobile genetic elements (MGEs) such as plasmids, transposons, and bacteriophages.

1.2.5.2.1   Chromosomal mutation mediated resistance

Chromosomally located AMR is the mutation of areas of the bacterial chromosome in such a way that it confers resistance to an antimicrobial compound. This involves mutation of the genes which encode for the targeted proteins, alongside modification of gene promotors and repressors, or of genes encoding for cellular structures, which affects access to the target site of the antibiotic (Doss, 1994).

Examples of chromosomally mediated AMR include: point mutations in the *gyrA* and *gyrB* genes of *Salmonella enterica* alongside many other bacteria, which confers resistance to fluoroquinolones (Acheampong et al., 2019) and mutations in the *ampC* promotor region causing cephalosporin resistance in *E. coli* (Paltansing et al., 2015). Further mutations include

the *uhpA, uhpB, uhpC, uhpT, and glpT* genes resulting in fosfomycin resistance in *E. coli* clinical isolates (Cattoir et al. 2020).

Horizontal gene transfer mediated resistance

Acquisition of DNA and thereby resistance through HGT is one of the major drivers of bacterial evolution, and the persistence of antibiotic resistance within the bacterial community. HGT often involves MGEs which carry resistance determinants from one bacterium to another, these MGEs include, insertion sequences, plasmids, transposons, and bacteriophages.

Plasmids are molecules of DNA which are able to replicate within the cell independently from the chromosome (Esser et al., 1986). Plasmids can carry resistance determinants on them, examples include plasmids with genes that encode for bla_{TEM-1}, a β-lactamase (Datta & Kontomichalou, 1965; Morin et al., 1987), or the quinolone resistance gene *qnrC* (Wang et al., 2009).

The acquisition of MGEs can occur through transformation, transduction, or conjugation (Peleg et al., 2008).

1.2.5.2.2.1 Transformation

Transformation is the ability of a bacterium, to take up foreign naked DNA from the environment followed by its subsequent integration into the bacterial chromosome by homologous recombination (Johnston et al., 2014). Transformation can also be used by bacteria to uptake other mobile genetic elements such as plasmids. Transformation has been shown to readily allow for the movement of DNA containing ARGs between bacterial species.

Transformation occurs when naturally transformable bacteria enter a transient physiological state called competence in which they are able to take up exogenous DNA and integrate it

into their chromosome, often through the expression of a multi-component DNA uptake system (Cattoir et al, 2020).

An example of this is *Acinetobacter baumannii* A118's ability to acquire DNA from *K. pneumoniae, Providencia rettgeri* and *Staphylococcus aureus* in an *in vitro* setting. In this experiment, the *A. baumannii* A118 cells were mixed with the naked DNA *in vitro*. The *K. pneumoniae* DNA carried multiple β-lactamases such as bla_{TEM-1}, and conferred resistance when acquired by *A. baumannii* (Traglia et al., 2019).

1.2.5.2.2.2 Transduction

Transduction is the movement of DNA from one bacterium to another, mediated by bacteriophages (Chiang et al., 2019). Bacteriophages are viruses that specifically target bacteria. When bacteriophages propagate they may encapsulate host DNA to form transducing particles that are then passed to the host of the new cell, where it can then undergo chromosomal recombination or replication into a plasmid (Chiang et al., 2019). Transduction allows for movement of AMR related genes between bacterial species. An example of this was the movement of the bla_{CMY-2} and *tet*(A) genes on the P24 phage, which transduced these genes from *Salmonella heidelberg* to *Salmonella typhimurium* (Colavecchio et al., 2017). There are two types of transduction, generalised and specialised. In the former, the bacteriophages will take any portio of the host genome, whereas in specialised transduction, the bacteriophages take only specific portions of the host DNA as part of the lysogenic cycle (Admin (2022) Transduction in bacteria: Definition, types, steps and advantages, BYJUS. BYJU'S. Available at: https://byjus.com/neet/transduction-in-bacteria/ (Accessed: February 27, 2023).)

1.2.5.2.2.3 Conjugation

Finally, conjugation is the transfer of genetic material between two bacteria with direct cell to cell contact (Koraimann & Wagner, 2014). Conjugation requires specific conjugation

machinery to work properly, known as the type 4 secretion system (Bhatty et al., 2013; Bidlack & Silverman, 2004). This machinery is usually part of the bacterial genome, however, it is possible for plasmids to contain genes that encode for this specific conjugation machinery, which allow them to spread (Smillie et al., 2010).

Plasmid conjugation is heavily involved in the spread of resistance. Examples include the transfer of bla_{TEM-1} (which confers resistance to penicillin and early cephalosporins) and bla_{CTX-M} (an extended spectrum β-lactamase, which confers resistance to third generation cephalosporins) between *E. coli* on plasmids (Li et al., 2019), or the presence of *flo*R (which confers resistance to florfenicol) on plasmids in *K. pneumoniae* species (Khezri et al., 2021), both of which are now globally spread.

1.2.6   Antimicrobial resistance: the mechanisms of antimicrobial resistance

There are four main mechanisms by which bacteria can develop resistance to antibiotics (Hemaiswarya et al., 2008) (Figure 1-2). These are (1) antibiotic target modification, (2) antibiotic modification and enzymatic degradation, (3) reduction of antibiotic concentration within the cell through either increasing active efflux levels, or (4) decreased membrane permeability preventing antibiotic permeation into the cell.

Phytochemicals, compounds produce by plants for environmental interaction and the main focus of this thesis, can work synergistically with antibiotics, by inhibiting these resistance mechanisms to restore bacterial sensitivity to antibiotics (Khare et al., 2021). Quercetin, reserpine, piperine and silybin have all been shown to inhibit efflux pump expression, which can restore antibiotic sensitivity (Miklasińska-Majdanik et al., 2018; Ohene-Agyei et al., 2014). Epigallocatechin gallate can inhibit the activity of β-lactamases, restoring β-lactam sensitivity (Zhao et al., 2002). Baicalin is able to modify the bacterial cell membrane, altering its permeability which allows the movement of antibiotics through the membrane (Liu et al., 2010; Ozma et al., 2021). Some phytochemicals such as quercetin (Vipin et al., 2020) and

Baicalin (Liu et al., 2010) have been shown to act synergistically with antibiotics in more than one way, as displayed in Figure 1-2.
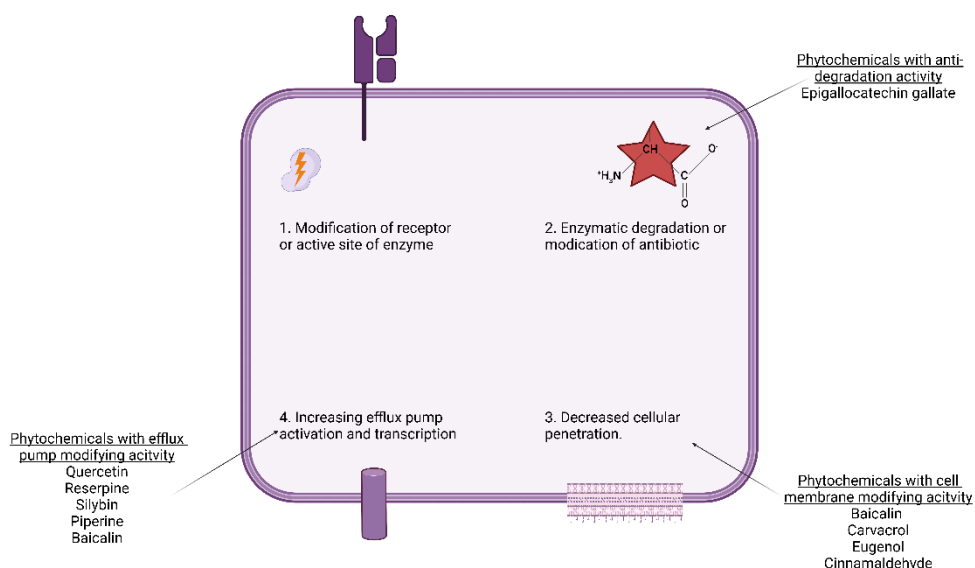
Figure 1-2 Methods of antibiotic resistance that are used by bacteria, which can be targeted by synergistic phytochemicals to restore antibiotic susceptibility. Example phytochemicals which can counter these synergistic effects are also given. Adapted from (Hemaiswarya et al., 2008).

1.3 Environmental drivers of antimicrobial resistance

1.3.1 Antimicrobial resistance predates anthropogenic use of antimicrobials

The time before the discovery of penicillin and antibiotics as we know them is usually referred to by the moniker 'the pre-antibiotic era', wound infections were usually treated with antiseptics, or not at all, and as such bacterial infections were much more commonly associated with high morbidity and mortality (Erdem et al., 2011; Walsh & Wright, 2005).

Despite this notion of a 'pre-antibiotic era,' there is a growing body of evidence which suggests that AMR is not simply a result of the widespread anthropogenic use of antimicrobials, and that AMR predates the development and use of antibiotics. D'Costa et al 2009 analysed bacterial DNA taken from soil samples 50 cm below 30,000-year-old ice-cores. Within this study AMR genes were discovered including genes that conferred resistance to tetracycline (via *tet*(M)), vancomycin (via *van*X), and β-lactams (*bla)*. The β-lactam ARGs were

between 53-84% identical to known clinical ARGs and clustered with characterised β-lactams. They located the *van*X gene, and in doing so located the *van*HAX operon surrounding the gene. The *van*HAX operon confers resistance to vancomycin by terminating D-alanine-D-lactate in place of D-alanine-D-alanine. They then attempted to synthesis four open reading frames containing *van*HAX operons of which two allowed for isolation of soluble protein. From this they managed to isolate a functional *van*HAX operon which was comparable, in both protein structure, and steady state kinetic parameters, to the clinically relevant *van*HAX operons seen in the clinic today (D'Costa et al., 2011). The only clear alterations between the modern clinically relevant *van*HAX operon were the concentration of Mg2+, ATP-γ phosphate coordination, and structural changes in the omega loop, which had 13 amino acid residues (223-246) missing, including H241 responsible for the proteins lactate sensitivity.

Further functional studies have also found ARGs in other pristine environments (environments thought to have never been exposed to humans), which demonstrates clear evidence of a need to develop AMR in the absence of widespread use of antibiotics. This need could be competition in an environmental niche, or a stressed environment. These include 800-1050 year old teeth with dental cavities (Warinner et al., 2014), which contained 337 putative ARGs including, but not limited to, efflux pumps, metallo-β-lactams and aminoglycoside phosphotransferases. A Tn*5042* mercury resistance transposon was located in 15-30,000 year old Siberian permafrost (Mindlin et al., 2005), and whole genome sequencing of *Paenibacillus* sp. LC231 from a 4-7,000,000 year old cave system (Pawlowski et al., 2016) found genes that conferred resistance to Linezolid (*cfr*), Streptogramin A (*vat*(L)) and Rifampicin (*rpo*B)

Alongside this, phylogenetic analysis suggests that ARGs, specifically class D oxacillin (OXA) β-lactamases (which confer resistance to β-lactam antibiotics, such as penicillin), were

mobilised onto plasmids on two independent occasions, between 320 and 574 million years ago. The first jump occurred prior to the divergence of the *S. aureus/B. subtilis group* from *Streptococcus* group (Barlow & Hall, 2002) and the second prior to divergence of the *Bacillus subtilis* from *Staphylococcus* (Barlow & Hall, 2002). They also determined that the OXA β-lactamase genes predate the emergence of cyanobacteria around 2 billion years ago. These studies highlight just how ancient these bacterial survival mechanisms are, and how horizontal gene transfer has been used to disseminate these resistance genes over time.

This new knowledge that environmental factors can cause AMR means that there is now a clear need to understand how the development of this resistance occurred in the absence of mass production and widespread global use of antibiotics and how resistance has persisted in environments absent of antibiotics. The evidence would suggest that specific compounds that naturally occur in the environment could select for genes which confer a selective advantage to the bacteria who are able to survive repeated exposure to them in the environment. It is possible that these genes also confer resistance to antibiotics, a phenomenon termed co-selection. These selective compounds include but are not limited to, heavy metals, naturally occurring antibiotics, biocides, and disinfectants and the focus of this study, phytochemicals.

Biocides, such as alcoholic hand gel, surface disinfectants and the like, are also associated with strains of antimicrobial resistant bacteria. Whilst they are not a focus of this study, nor this introduction, its worth highlighting that they are a parallel to phytochemicals with regards to there use everyday human products, and pose a risk to the antimicrobial resistance reservoir in the environment that is similar to that of phytochemicals (Chen et al., 2021).

1.3.2 The role of heavy metals in the development and maintenance of antibiotic resistance in the environment

Heavy metals are naturally occurring elements which have a high atomic weight and a density of at least five times greater than that of water, although the exact dimensions of the category are not well defined (Seiler & Berendonk, 2012; Smith, 2009; Tchounwou et al., 2012). They are mostly toxic, although the severity and type of toxicity can depend on the nature of exposure, and they are classified as human carcinogens in many cases. Heavy metals have been used for their antimicrobial activities, long before the establishment of germ theory or our understanding of antibiotics altogether (Alexander, 2009; Dollwet, 1985). Silver, for example has been used for at least 6000 years to combat malaise we now know to be microbial in origin (Alexander, 2009).

Multiple studies indicate a correlation between ARGs within bacteria and the presence of heavy metal pollution within the environment (de Vicente et al., 1990; Di Cesare et al., 2016; Knapp et al., 2011, 2017; Ohore et al., 2019). In Lake Taihu, China for example, there is a significant correlation by principal component analysis ($p < 0.05$) between tetracycline and sulphonamide resistance genes, and the presence of heavy metals including: iron, magnesium, copper, and zinc. This study measured at differing depths of the lake, and demonstrated that at lower depths there was a decrease in metal pollution, which was correlated with a decrease in heavy metal resistance (HMR) genes and ARGs (Ohore et al., 2019).

Heavy metals have been shown to co-select for ARGs. This occurs in three main ways (Nguyen et al., 2019). The first is that HMR and AMR can be expressed by the same gene, known as co-resistance. Key to this are efflux pumps, which can extrude both antibiotics, and heavy metals (Blanco et al., 2016). The *tet(L)* transporter from *B. subtilis* confers resistance to both

tetracycline and sodium (Cheng et al., 1996). Another example is the Ges transport system which can extrude chloramphenicol, fluoroquinolones and gold (Conroy et al., 2010).

The second method is co-regulation of the HMR and AMR genes. This is exemplified by the *czrR-czrS* two component regulator in *P. aeruginosa,* which controls resistance to cobalt. This system also affects expression of the *opr*D gene, which encodes for an imipenem resistance porin (Perron et al., 2004). .

The third method is co-localisation of HMR and AMR genes on the same MGE such as a plasmid or transposon (Mazhar et al., 2021). For example a *mer* operon which conferred resistance to mercury was contained on a putative transposon Tn*mer*1, the transposon was present on a streptomycin resistance plasmid pPPM1000 in *Enterococcus faecium* (Davis et al., 2005).

Alongside the previously mentioned methods of cross-resistance and co-localisation/regulation of resistance between HMR and AMR genes, subinhibitory concentrations of heavy metals can promote conjugative transfer of ARGs between bacteria (Zhang et al., 2018). In *E. coli*, subinhibitory concentrations of heavy metals causes production of reactive oxygen species, which, in turn, leads to oxidative stress and an SOS response. The SOS response leads to increased cell membrane permeability and upregulation of conjugation related genes that led to increased uptake of conjugative elements containing both HMR and AMR genes including *tet(L)*, *merE* and *oprD* (Y. Zhang et al., 2018). The induction of an SOS response in *E. coli* is specific to *E. coli* and other heavy metals will cause different cellular responses in different bacterial species, for example we theorise that the strength of the bacterial SOS response will differ between heavy metals. Together these studies demonstrate a clear instance of non-antibiotic, antimicrobial environmental contaminants selecting for AMR genes.

1.4 The role of plant phytochemicals in the development and maintenance of antimicrobial resistance in the environment

Secondary plant metabolites, also known as phytochemicals, are a range of chemicals produced by plants that are not essential for growth or reproduction of the plant. Instead, these chemicals are essential for interaction between the plant and their environment. These chemicals can potentially inhibit bacterial growth. We hypothesise that these chemicals, would have, long ago, selected for mechanisms of detoxification that are identical to, or predecessors of, mechanisms currently used by bacteria to resist antibiotics (e.g., cross-resistance).

There are over 40,000 known phytochemicals, and they cover a diverse area of chemical space. These include: phenolic compounds such as tannins, lignins, and quinolones, Acetyl-CoA based compounds such as lipids and polyketides, and pyruvic acid based compounds such as terpenes (Mendoza & Silva, 2018). Phytochemicals, particularly from different classes have extremely diverse chemical structures, and functions (Mendoza & Silva, 2018). Phytochemicals are ubiquitous in both the environment and within human settings, such as healthcare, the home, and in food products (Chandra et al., 2017; Woodrow et al., 2005). Examples of the use of phytochemicals by humans include citral (from citrus plants) in perfumes and cleaning products, to give the citrus smell, or tannins such as tannic acid in red wine. Tanbark, containing tannins was also historically used in the process of leather tanning (Chandra et al., 2017). Asprin, the painkiller is a derivative of the salicylic acid found in a variety of plants including the *Salix* genus (Chandra et al., 2017)

1.4.1 Phytochemicals: the story of artemisinin

One of the most important and well-known plant phytochemicals within the healthcare sphere is Artemisinin. Artemisinin is a drug used to treat malaria, and is a plant derived sesquiterpene lactone, discovered by the Nobel prize winner Professor Tu Youyou in 1972

(Su & Miller, 2015) and is now widely used as the most effective treatment for *Plasmodium falciparum* caused malaria cases globally (Takala-Harrison et al., 2015). Importantly, resistance to artemisinin is a growing concern globally, but specifically within the greater Mekong region. The WHO has issued strict guidelines highlighting the importance of using artemisinin alongside other antimalarials in a drug cocktail known as artemisinin combination therapy (ACT) to help control the spread of artemisias resistance (Ashley et al., 2014; Imwong et al., 2017; Müller et al., 2019; Ouji et al., 2018; Talundzic et al., 2015).

Artemisinin resistance can be overcome by using whole plant extract from *Artemisia annua* and use of the whole plant extract significantly slows the acquisition of resistance by *P. falciparum* to artemisinin, up to 3 times slower (Elfawal et al., 2015). This presents a potential parallel to the use of phytochemicals as antimicrobial compounds, highlighting that single compounds may have a higher chance of leading to an increase in resistance and that compound mixtures may slow down the development of resistance.

Alongside their evaluation as potential new antibiotic compounds, specific phytochemicals are being evaluated for their potential as new medicines in other fields, including, but not limited to, cancer (Choudhari et al., 2019) and liver disease (Chung et al., 2019). Some examples of this include: Paclitaxel, which is derived from the western yew tree (*Taxus brevifolia*) and used to treat leukaemia (Wani et al., 1971), tiotropium, derived from belladonna/deadly nightshade (*Atropa belladonna*), which is used to treat asthma and chronic obstructive pulmonary disease (Mundy & Kirkpatrick, 2004), and curcumin from turmeric (*Curcuma longa*) which is being evaluated as a treatment for breast cancer (NCT03072992, 2017).

1.4.2 Phytochemicals: key studies on the interaction between phytochemicals and bacteria

The next section of this introduction will outline several key studies that feed into the hypothesis of the thesis that phytochemicals have played an important role in the co-selection of antibiotic resistance genes.

1.4.2.1 Key study one: linalool resistance in isolates grown on supermarket basil led to increased antimicrobial tolerance in a clinical outbreak of Salmonella enterica

Kalily et al (2016), linked a clinical isolate of *Salmonella enterica* serovar Senftenberg which caused a *Salmonella* outbreak, back to contaminated supermarket basil (*Ocimum basilicum L.)* (Kalily et al., 2016, 2017). Basil produces many phytochemicals, including linalool, eugenol and estragenol. The *Salmonella* outbreak was determined to be an MDR strain that was also linalool resistant (Kalily et al., 2016). After the discovery of this isolate, Kalily et al (2016), wanted to determine the mechanisms by which co-resistance was selected. To do so they conducted serial transfers of *Salmonella* strains in Linalool supplimented Lysogeny (LB)-broth up to a concentration of 0.96 M linalool from a starting volume of 240 mM (the exact number of passaging attempts this took was not stated). This passaging led to an eight-fold increase in linalool resistance (Kalily et al., 2017). Subinhibitory concentrations of linalool led to the formation of small membrane pores in *S. enterica*. The linalool-resistant strains had reduced numbers of membrane pores in the presence of linalool. Further, the linalool resistance strains showed significant differences in fatty acid composition, particularly in the relative concentration of palmitoleic acid, cyclopropaneoctanoic acid 2-hexyl and methyldihydrosterculate. Alongside this linalool resistant strains overexpressed the efflux pump encoding genes *acr*AB, *mic*F, *mar*RAB, *sox*S, *rov* and *ram*A (Kalily et al., 2017).

Of key importance to this study, the linalool resistant strains demonstrated significantly increased tolerance to the antibiotics; trimethoprim (32-fold)/-sulfamethoxazole (8-fold),

chloramphenicol (2-fold), tetracycline (2-fold) and piperacillin (4-fold), and lower tolerance to amikacin, however the exact mechanisms of these changes were not researched (Kalily et al., 2017). These antibiotics all have various modes of action highlighting the development of resistance to linalool influences multiple bacterial resistance systems. This study highlights the potential cross-resistant impact of phytochemicals within the natural environment (plants) and how this may impact the level of antimicrobial resistant bacteria within the community and in the clinic. Further this study highlights the importance of adhering to best practice of using clean water, rather than grey or fresh water to irrigate food crops, as the phytochemicals produced by the crops may select for the MDR human pathogens in the water (Paulo et al., 2013).

1.4.2.2 *Key study two: the presence of d-cycloserine resistance genes in an oral metagenomic library where none of the sampled participants had undergone d-cycloserine treatment suggested a dietary driver of resistance*

The second study was conducted using an oral metagenomic library which was constructed from DNA isolated from the saliva of human volunteers in both Bangladesh and the United Kingdom. In this metagenomic library two *d-alanine-d-alanine ligase* (*ddl*) genes were found in the first position of an integron. An integron is a genetic element that contains site-specific recombination system that allows the system to integrate, express and exchange DNA elements known as gene cassettes. The first position of an integron is the first DNA element on the integron from the start codon. Genes in the first position of an integron are highly transcribed as they are next to the integron promoter, suggesting a selective pressure keeping these genes in the first position. The Ddl protein is essential for bacterial survival and is the target of D-cycloserine, a second line antibiotic reserved for the treatment of MDR-*Mycobacterium tuberculosis.* It is reserved for this use due to its neurotoxic side effects. None of the volunteers in this study reported *M. tuberculosis* or a recent infection. The study hypothesised that phytochemicals ingested in food might be the selective pressure due to

the structural similarities between the phytochemicals, notably: quercetin and apigenin, and D-cycloserine. This theory was tested using molecular docking (Figure 1-3) which indicated both D-cycloserine and the two phytochemicals bound in the D-alanine binding pocket of the Ddl protein (Rahman, 2017). This study highlighted how phytochemicals in food have the potential to select for genes conferring AMR in the absence of antibiotics in the oral cavity and informed the selection of quercetin as a key phytochemical worthy of evaluation.
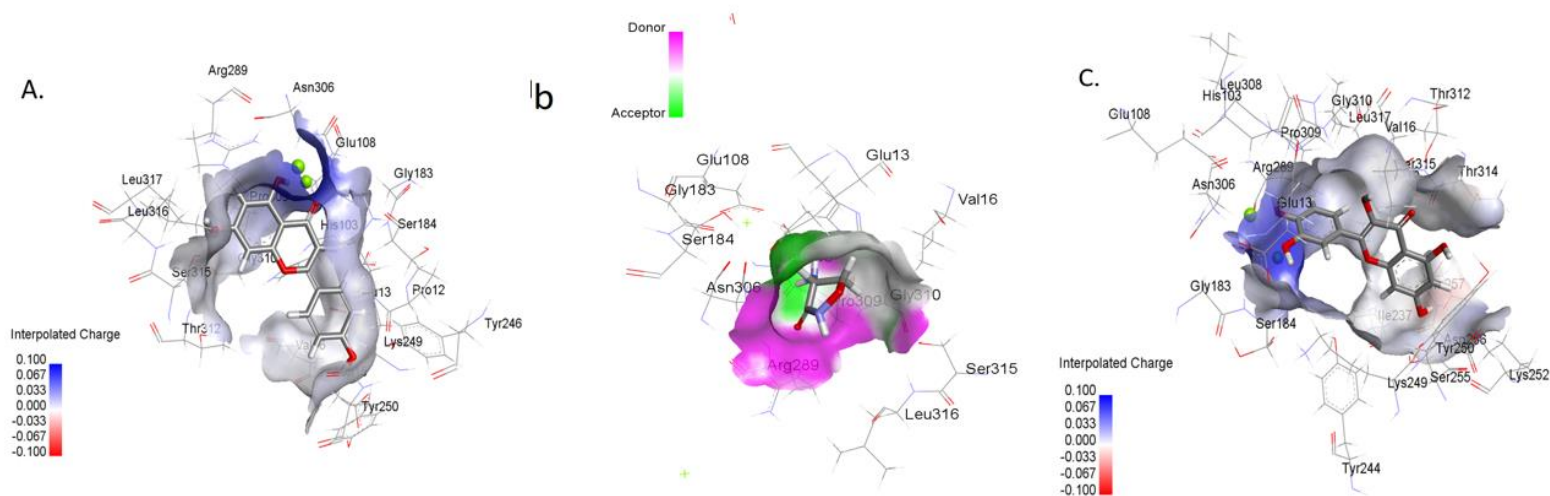
Figure 1-3 Molecular docking showing the interaction between the D-alanine binding site of D-alanine-D-alanine ligase and (A) apigenin (B) D-cycloserine and (C) quercetin. In each image the binding site is shown with the respective chemical docked, the various amino-acid residues around the binding site are given, and the colour change indicates the interpretated change in structure after docking of the relative molecule *(Figure adapted from (Rahman n.d.)).*

1.4.3 Phytochemicals: synergy between secondary plant metabolites and antibiotics

Some phytochemicals have been shown to act synergistically with other phytochemicals and antibiotics. When used in combination with antibiotics, treatment with phytochemicals restored sensitivity of drug resistant and multidrug resistant bacteria to those antibiotics (Langeveld et al., 2014) examples including cinnamon and amikacin against *A. baumannii* (Guerra et al., 2012) and coriander and chloramphenicol against *A. baumannii* (Moon et al., 2011). Another example of this is caffeic acid (which is found in all plants due to its role in lignin biosynthesis), which lowered the minimum inhibitory concentration (MIC) of erythromycin, ciprofloxacin and vancomycin against *Staphylococcus aureus* (Kępa et al., 2018).

Plant phytochemicals can counter bacterial resistance mechanisms and restore susceptibility to antibiotics. Examples of these include but are not limited to: (1) Carnosic acid from Rosemary (*Rosmarinus officinalis*) which restores susceptibility to tetracycline in MRSA by inhibition of the TETK and MSRA efflux pumps (Oluwatuyi et al., 2004), (2) Baicalin from a Chinese medical plant from the Skullcap family (*Scutellaria amoena),* which inhibits the activity of B-lactams, restoring susceptibility to methicillin in MRSA (Liu et al., 2010) and (3) Totatrol from the New Zealand Yew tree (*Podocarpus totara*) which restores susceptibility to methicillin in MRSA by inhibiting PBP 2a production (Pao et al., 1998) (Figure 1-2).

1.4.4 Phytochemicals: the development of resistance to secondary plant metabolites

Whilst many phytochemicals demonstrate antimicrobial qualities, there are very few studies which describe the genomic mechanisms by which bacteria develop or express resistance to phytochemicals. It has been suggested that it is difficult for bacteria to evolve resistance to phytochemicals (Khameneh et al., 2021). This is because plant chemicals often have multiple

bactericidal/bacteriostatic modes of action. As such, the combination of mutations required to overcome phytochemical inhibition would often be lethal to the bacteria, or so costly that in the absence of phytochemical inhibition they would be immediately lost (Jian-Ling et al., 2010), or the resistant strains out competed.

Becerril et. al (2012), reported that evolving *P. aeruginosa* in the presence of essential oils led to alterations in cell morphology. Resistant colonies were less mucoid and had a different pigmentation, which indicated alterations in lipopolysaccharide content/composition and changes in pigment production. However, changes in the lipopolysaccharide altered strains did not lead to changes in the strains MIC values against any of the essential oils (Becerril et al., 2012). However evolving *Serratia marcescens* in the presence of oregano oil increased the MIC of minocycline and chloramphenicol 1-fold, and the MIC of tetracycline 4-fold. The study also showed that in *Proteus mirabilis* passaged with whole plant oregano *(Origanum vulgare)* essential oil 50 times, the MIC of ampicillin was lowered from 64 to 8 μg/ml. This study did not investigate any underlying genomic changes responsible for the phenotypic changes.

Use of transposon mutagenesis in *E. coli* indicated that increased sensitivity to thymol was due to mutations in the *Ion, menA, yagF* and *cadB* genes, which are involved in regulation of menaquinone biosynthesis, membrane protein expression, and efflux pump expression, highlighting the diverse antimicrobial mechanisms of thymol (Shapira & Mimran, 2007).

Expression of the *tet*(A) gene encoding an efflux protein led to increased bacterial resistance to berberine in *E. coli* (Li et al., 2018)*.* Another study highlighted a total of 42 proteins that were differentially regulated in *E. coli* after long term exposure to berberine, with particular attention given to the *ompW* encoding a membrane protein which was upregulated within 8 hours of berberine exposure in every case (Budeyri Gokgoz et al., 2017). This suggests

OmpW plays a key role in cell proliferation under the selective conditions imposed by berberine.

1.4.5 Phytochemicals: the potential role of phytochemicals as a replacement for antibiotic growth promoters

The agricultural industry is always looking for something innovative, to meet rising demands and more recently global supply chain problems. The war in Ukraine has caused drastic reductions in the global supply of animal feed, and the agricultural industry will need every tool at its disposal to continue its current production levels (Welsh, 2022). As AGPs are banned, one solution globally is the use of phytochemicals as a potential replacement for AGPs due to their antimicrobial properties (Lillehoj et al., 2018).

Some examples of recent studies into phytochemical use as AGPs include: a commercially available mixture of carvacrol, cinnamaldehyde and capsicum, which actively improved dietary fat digestibility and weight gain in broiler chickens and improvement in energy utilisation for growth (Bravo et al., 2014). The addition of whole plant senna tora *(Cassia tora)* extract to feed led to increased growth parameters in broiler chickens including higher bodyweight at culling, and a higher feed conversion ratio (Sahu et al., 2017). Finally, magnolia *(Magnolia officinalis)* bark extract supplemented feed led to increase body weight and feed conversion in broilers alongside protection against *Clostridium perfringens* challenge when compared to a control group fed with just feed (Oh et al., 2018). Taken together it is clear that phytochemicals may offer an attractive and cheap alternative to traditional AGPs.

Whilst phytochemicals offer an attractive alternative to AGPs, little is known about how their use would contribute to the development and proliferation of ARGs in agricultural settings. The hypothesis underlying this thesis is that the mechanisms of resistance bacteria employ to survive exposure to phytochemicals may also confer cross resistance to antibiotics. If true, the use of phytochemicals as AGPs might be little different from the use antibiotics, which
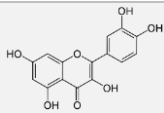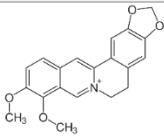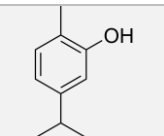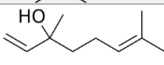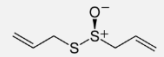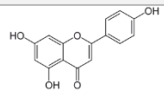
has been banned due to safety concerns around promoting and selecting for resistance. It is essential, therefore, as part of this project to understand how the use of phytochemicals alters not only bacteria at the individual gene and cellular scale, but also at the microbiome and resistome scales of animals of agricultural importance.
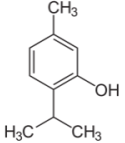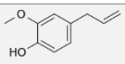
1.5   An overview of phytochemicals used in this study

Some phytochemicals have antimicrobial properties, with various modes of action. Furthermore, phytochemical pressure can select for AMR in various bacterial species. In this thesis, I will attempt to elucidate how two phytochemicals, quercetin and berberine, can function as natural drivers of AMR, and the role they may play as AGPs.

After initial literature-based evaluation of a range of phytochemicals (Table 1-1), two specific plant metabolites were selected for use during this PhD due to potent antimicrobial ability against the bacteria we aimed to study, cost, and ease of use. These two phytochemicals; quercetin and berberine, will be further explored in this section.

Table 1-1 An overview of the chemical structure and classification, plant origin, theoretical and proven antimicrobial activity and current further research on several phytochemicals initially selected for use for this thesis.

Secondary Plant Metabolite	Chemical Structure	IUPAC Name	Plant Origin	Antimicrobial Activity and Mechanism	Current exploration of uses
Quercetin		2-(3,4-dihydroxyphenyl)-3,5,7-trihydroxy-4*H*-chromen-4-one	*Morus alba, Maringa oleifera & Brassica species* (Anand David et al., 2016)	Pneumolysin inhibition (Lv et al., 2019). DNA Gyrase Inhibition (Plaper et al., 2003). Naphthoate Synthase (Das et al., 2019).	Cancer (Vafadar et al., 2020). Alzheimer's (Zhang et al., 2020). Depression (Macedo et al., 2017).
Berberine		5,6-Dihydro-9,10-dimethoxybenzo[*g*]-1,3-benzodioxolo[5,6-a] quinolizinium	*Berberis vulgaris* (Imenshahidi & Hosseinzadeh, 2016)	Surface protein inhibition (S.-H. Kim et al., 2004; S.-W. Kim et al., 2002)	Cancer (Ortiz et al., 2014). Diarrheal diseases and Neurodegeneration (Takase et al., 1993)
Carvacrol		2-Methyl-5-(propan-2-yl) phenol	*Origanum vulgare, Thymus vulgaris, Nigella Sativa* (Bayir et al., 2019)	Unknown but potent against resistant *E. coli* (Magi et al., 2015)	Cancer and growth promotion in poultry (Bayir et al., 2019; Lillehoj et al., 2018).
Linalool		3,7-Dimethyl-1,6-octadien-3-ol	*Lauraceae Lamiaceae,* and *Tuaceae* families	Disruption of cell morphology (Kalily et al., 2016, 2017; X. Liu et al., 2020).	Aquaculture (Bandeira Junior et al., 2018).
Allicin		*S*-Prop-2-en-1-yl prop-2-ene-1-sulfinothioate	Garlic	Unknown (Ankri & Mirelman, 1999)	Antimicrobial activity and food preservation (Ankri & Mirelman, 1999; Gutiérrez-Del-Río et al., 2018).
Apigenin		5,7-Dihydroxy-2-(4-hydroxyphenyl)-4*H*-1-benzopyran-4-one	Parsley, celery, and chamomile tea.	Inhibition of nucleic acid processing enzymes and D-alanine: D-alanine ligase inhibition (M. Wang et al., 2019).	Insomnia, Alzheimer's, Knee osteoarthritis and depression (Salehi et al., 2019)

Secondary Plant Metabolite	Chemical Structure	IUPAC Name	Plant Origin	Antimicrobial Activity and Mechanism	Current exploration of uses
Thymol		5-Methyl-2-(propan-2-yl) phenol	Thymus vulgaris	Membrane disruption (J. Xu et al., 2008)	Cholesterol and inflammation control (Agarwal et al., 2020).
Eugenol		2-Methoxy-4-(prop-2-en-1-yl) phenol	Clove, Cinnamon, Pepper, Turmeric, Thyme (Khalil et al., 2017)	Deregulation of *ydiC* (Mak et al., 2019)	Anti-inflammation and antioxidant (Barboza et al., 2018)

1.5.1   Quercetin

Quercetin (2-(3,4-dihydroxyphenyl)-3,5,7-trihydroxy-4H-chromen-4-one) (Figure 1-4), is a flavonoid widely found in many plants in nature, this includes red onion (*Allium cepa*) and broccoli *(Brassica oleracea var. italica),* amongst many others (Anand et al., 2016). It is an incredibly abundant compound in the human diet and the average consumption of quercetin through the diet can vary widely depending on location and diet, from 4 to 314 mg/day (Chun et al., 2007; Johnson et al., 2011; Nishimuro et al., 2015; Sampson et al., 2002; Somerset & Johannot, 2008; Sun et al., 2015; Zamora-Ros et al., 2010). Further, quercetin can be used as dietary supplement and is generally classified as safe (Andres et al., 2018). It can be active alone or as part of a soluble salt such as quercetin-chalcone, or hesperdin, methyl-chalcone, it is unknown if this daily intake is antimicrobial at this point, though its many health benefits are known.
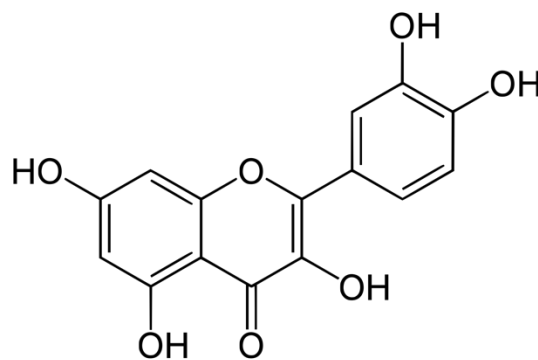
Figure 1-4 The chemical structure of quercetin (2-(2,4-dihydroxyphenyl-3,5,7-trihydroxy-4H-chromen-4-one).

Quercetin is being explored as a potential therapeutic for a range of conditions including, but not limited to: multiple different types of cancer (Albrecht et al., 2020; Ezzati et al., 2020; Greco et al., 2020; Jeong et al., 2009; Vafadar et al., 2020), polycystic ovarian syndrome (Neisy et al., 2019), high blood pressure (Ferenczyova et al., 2020; Marunaka et al., 2017; Patel et al., 2018), Alzheimer's (Elumalai & Lakshmi, 2016; Zhang et al., 2020), Parkinson's (Tamtaji et al., 2020), depression (Macedo et al., 2017), and allergies (Jafarinia et al., 2020).

Furthermore, quercetin is also being evaluated for its activity against human pathogens. Quercetin possesses antiviral properties against a range of RNA viruses including Ebola (Qiu et al., 2016), Zika (Wong et al., 2017), and porcine epidemic diarrhoea virus (Choi et al., 2009), however the mode of action is unknown.

1.5.1.1   The antimicrobial proprieties of quercetin

Quercetin demonstrates antimicrobial activity against a range of Gram-positive and Gram-negative bacteria (Wang et al., 2018). This antimicrobial activity is due to cell membrane damage which led to an increase of extracellular alkaline phosphatase, β-galactosidase, and soluble protein concentrations.

Quercetin also demonstrates activity against multi-drug resistant bacteria via the inhibition of bla_{NDM} and adeB expression in *P. aeruginosa* and *A. baumannii* (Pal & Tripathi, 2019). In addition, quercetin works synergistically with tetracycline in the treatment of multi-drug resistant *E. coli* (Qu et al., 2019). Further quercetin acts as an antibiofilm compound against a number of bacteria (Vipin et al., 2019; Zeng et al., 2019). In *P. aeruginosa,* quercetin treatment reduced the level of the quorum sensing associated virulence factors pyocyanin, siderophore and elastase. Quercetin resistant strains showed increased production of these virulence factors, suggesting that modification of the quorum sensing system can contribute to quercetin resistance (Ouyang et al., 2016).

Quercetin demonstrates at least four antimicrobial modes of action: (1) inhibition of bla_{NDM} and (2) adeB expression, (3) anti-biofilm, (4) and anti-quorum sensing, that function across multiple bacterial species. In addition, quercetin also demonstrates species specific inhibitory mechanisms. Quercetin acts as a pneumolysin inhibitor against *Streptococcus pneumoniae* infection (Lv et al., 2019). Further, quercetin has been shown in inhibit naphthoate synthase of multidrug resistant *Enterococcus faecalis*, which is an essential enzyme for menaquinone

synthesis, by directly binding with naphthoate synthase and inhibiting any catalytic activity (Das et al., 2019).

1.5.2 Berberine

Berberine (Figure 1-5) is a benzylisoquinoline alkaloid found in a number of plants including *Berberis* species (Freile et al., 2003) such as Barberry (*Berberis vulgaris*), and Tree Turmeric (*Berberis aristata*), alongside other plants including the Oregon grape (*Mahonia aquifolium)* (Cernáková & Kostálová, 2002) and Japanese goldthread (*Coptis japonica*). Berberine has been used for thousands of years in traditional medicine as a treatment for diarrhoea, intestinal parasites and ocular trachoma (Birdsall, 1997) with the earliest therapeutic use of berberine dating back to 650 BC (Neag et al., 2018).

Berberine is not usually consumed commonly in the normal human diet, however, it is a very common as an over the counter supplemental health treatment, and is generally classified as safe, and can now be produced by chemical synthesis (Battu et al., 2010). However, berberine has low oral bioavailability, which calls into question its ability to function as an oral therapeutic (Chen et al., 2011; Liu et al., 2016). However, this is less important if the site of action of the phytochemical is in the gastrointestinal system.
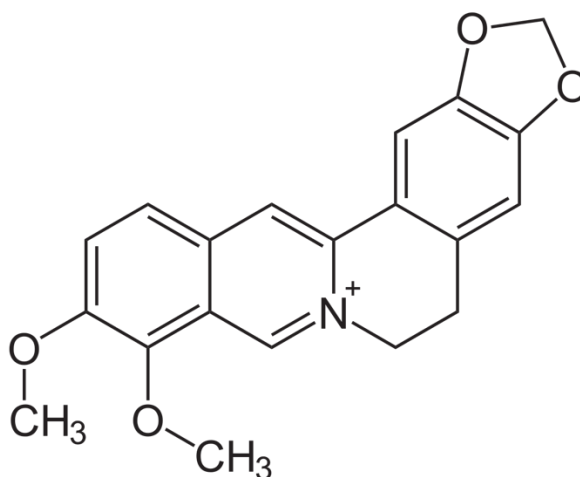
Figure 1-5 The structure of berberine (5,6-dihydro-9,10-dimethoxybenzo[g]-1,3-benzodioxolo[5,6-a] quinolizinium).

Berberine is being explored as a potential therapeutic for a range of conditions including: cancer (Ortiz et al., 2014) , Alzheimer's (Ahmed et al., 2015), inflammation (Zou et al., 2017), diabetes (Dong et al., 2012), cardiovascular diseases (Chang et al., 2012) and diarrhoea (Chen

et al., 2015; Rabbani et al., 1987). In many cases berberine has been used as a traditional agent to treat these illnesses, but it has little clinical analysis to confirm its affects.

1.5.2.1 The antimicrobial properties of berberine

Berberine antimicrobial qualities have been well studied as it is highly active against both gram positive and Gram-negative species (Bandyopadhyay et al., 2013). Berberine is also active against bacteria within a mixed species biofilm (Xie et al., 2012). The exact antimicrobial mode of action of berberine is a subject of some debate, but may involve a combination of surface protein inhibition, (Kim et al., 2004), and disruption of cell membrane integrity (Zhang et al., 2020).

In mice challenged with *Salmonella typhimurium,* intravenous treatment with 40 mg/kg of berberine increased survival rate of mice, but did not appear to show an effect on the level of bacterial infection of the mice (Chu et al., 2014). An additional study in *S. aureus* indicated that berberine may also play a role in the inhibition of bacterial-cell adhesion and intercellular invasion (Yu et al., 2005).

Further studies in *S. aureus* have indicated that berberine inhibits amyloid fibrils formation by binding with the phenyl ring of the phenol-soluble modulins which make up the fibrils, preventing hydrophobic interactions. This inhibition prevents proper formation of biofilms in MRSA (Chu et al., 2016) infections, although other studies have highlighted that sub-inhibitory concentrations of berberine (Tan et al., 2019) led to increased biofilm production.

1.6 An overview of the important experimental procedures and materials used in this thesis

To elucidate the mechanisms by which quercetin and berberine function as natural drivers of AMR, three lines of experimental investigation were undertaken. In this introduction, an overview of essential bacterial species and strains, and experimental procedure are given.

Chapter 3 and 4 explored the development of a metagenomic screening assay for an oral metagenomic library constructed using *E. coli* and later a bacterial isolate library resulting from the citizen science project Swab and Send (Roberts, 2020). The importance of *E. coli* as a model bacterium, and functional metagenomic screening as a procedure for gene discovery are discussed.

1.6.1 Escherichia coli

1.6.1.1 Introduction to E. coli

E. coli is an anaerobic, rod-shaped, Gram-negative pathogen from the family *Enterobacteriaceae,* first described by Theodore Escherich in 1885 (Escherich, 1998). The bacterium is found in the lower intestinal tract of animals, including humans. It is commonly discharged into the environment through faecal matter and wastewater effluent. However, it has been shown to survive for long periods of time and reproduce in the environment (Jang et al., 2017).

E. coli is usually commensal, however it is an opportunistic pathogen and can cause disease in the host (Proença et al., 2017). Common diseases caused by pathogenic *E. coli* include urinary tract infections, diarrhoea, and meningitis. Extended-spectrum β-lactamase producing *E. coli* are considered a serious threat by the United States Centre for Disease Control and Prevention (CDC), and a critical priority pathogen by the WHO.

In optimal growth conditions (37°C) *E. coli* can divide in as little as twenty minutes. Its genome is well characterised, and modified versions of the bacteria which are engineered for microbiological applications, such as transformation, are easily accessible, making it good model organism for use within a laboratory setting.

1.6.1.2   E. coli as a model organism

1.6.1.2.1   *E. coli* EPI300

EPI300[TM] Chemically Competent *E. coli* containing a pCC1BAC plasmid was previously used to construct the metagenomic library used in this study (Reynolds et al., 2016). This is due to the strain and plasmids combination, which contains the plasmid at a single copy number. This is important as an increased number of inserts would lead to a higher copy number of the genes on the inserts and therefore a higher expression of the encoded proteins which may cause toxicity issues. Alongside this the plasmid can be induced to high copy number if needed for the purposes of plasmid extraction.

1.6.1.2.2   *E. coli* DH5α

DH5α is an *E. coli* strain designed to possess increased transformation efficiency. This is defined by three mutations *rec*A1, *end*A1 and *lac*ZM15, the former two increase transformation efficacy and plasmid recombination and the latter allows for blue/white screening (Taylor et al., 1993) of the isolates.

These two strains of *E. coli* were selected because of the wealth of working knowledge available as part of the LSTM group where I underwent this PhD.

1.6.2   Functional metagenomic screening

Metagenomic screening is an technique which can be used to evaluate a library of all DNA isolated directly from an environment, discarding the need for isolation or cultivation, allowing for greater evaluation of diversity (due to the difficulties of diverse environmental culturing) (K. Chen & Pachter, 2005; Riesenfeld et al., 2004). It is possible for metagenomic

libraries to include DNA from other environmental microbes, such as viruses, fungi, or human DNA in the case of an oral library.

There are three methods of metagenomic screening: 1) sequencing based; 2) Polymerase Chain Reaction (PCR) based, and 3) function based. Sequencing based screening can be used to look for the presence of known genes in a metagenome, or for genes associated with known MGEs (P. Liu et al., 2019). Sequencing based screen has the advantage of requiring no laboratory work after the creation and sequencing of the library. PCR based screening can also be used to screen for known genes using primers, which has the advantage over sequencing based screening of not requiring full metagenomic sequencing, and is conductible on the raw metagenomic DNA (Johny & Bhat, 2017).

This study uses a functional screening approach, where the metagenomic DNA from a sample is ligated and cloned into a suitable vector, and the vector is transformed into a suitable host, the suitability of both the host and vector is based on several factors such as the bacterial host, the size of insert and the desired vector copy number. The constructed library is then introduced into the surrogate host and grown on or in appropriate media for phenotypic selection or functional analysis.

Functional metagenomic screening can be used to identify novel genes with functions of interest. Depending on the study design this type of screening can search for multiple functions. Functional screening can detect enzymes with particular activity, such as glycosyltransferases (Rabausch et al., 2013), by screening using selective substances such as enzyme substrates or chemical compounds.

The functional glycotransferase screening used quercetin as a broth additive. Sets of 96 pre preincubated cultures of *B. cereus/ B. subtilis* were pooled and the pooled samples were tested for the glycosyltransferase product by thin layer chromatography. Once a quercetin

modifying pool was found, the pool was continually halved until the flavonoid modifying isolate was located (Rabausch et al., 2013).

Functional screening can also be used to screen for genes which allow for growth under selective conditions, such as the presence of antibiotics or nutrient deficient conditions. One example of this was the discovery of a novel tetracycline resistance gene *tet*AB(60) using a functional metagenomic screen of the oral metagenomic library I will use in my study (Reynolds et al., 2016).

Finally functional screening can also search for genes encoding antimicrobial substances, by growing the library on an bacterial lawn and selecting colonies which produce a zone of inhibition (Chung et al., 2008; de Castro et al., 2014). This has elucidated several key antimicrobial compounds including polyketides and plantaricins (Gomes et al., 2013; Pal & Srivastava, 2014).

The benefit of the use of metagenomic functional screening is the ability to find novel gene families and functions from bacteria that are not yet culturable, and from sequences that are not already known. However, there are limitations with the expression of genes in heterologous hosts, as they may express genes from different origins differently or not at all (Iqbal et al., 2014). This can be due to several factors, such as promotor recognition differing between species, differing codon usage or transcription factors, to name a few (Iqbal et al., 2014). There may also be toxicity issues surrounding the expression of certain proteins in heterologous hosts, particularly at high copy numbers.

1.6.3 Functional screening of the Swab and Send bacterial isolate library

Following the development of the functional metagenomic screening assay, the protocol was also used in the screening assay to assess a bacterial isolate library known as the Swab and Send library (Roberts, 2020). To determine if inhibitory conditions of phytochemicals could

select for resistant bacteria, and if those resistant bacteria contained common AMR genes or genotypes.

The Swab and Send library is comprised of over 21,000 isolates from 2,200 swabs, taken from a wide variety of places around the globe (Roberts, 2020). The library is currently being used to search for new antibiotics, by plating the library onto lawns of pathogens, and looking for the appearance of zones of inhibition around the Swab and Send isolates.

1.6.4   Pseudomonas aeruginosa

Chapter 5 involved the evolution of *P. aeruginosa* in sub-inhibitory concentrations of both phytochemicals. The importance of *P. aeruginosa* and the role of bacterial evolution experiments in elucidating the mechanisms of resistance evolution is discussed.

P. aeruginosa, first recognised in the study 'The Blue Green Colouration of Bandages' by Carle Gessard in 1882 (Gessard, 1984) from the growth of organisms from cutaneous wounds, is a gram negative rod shaped bacterium of the family *Pseudomonadaceae* and is ubiquitous in the environment. It has a single flagellum, and produces several pigments, the most well-known of which is pyocyanin (Jayaseelan et al., 2014). Further environmental isolates of *P. aeruginosa* are often the same as clinical isolates with regards to infectivity, irrespective of their evolution and isolation environments, although this data is somewhat contentious (Fenner et al., 2006).

P. aeruginosa causes opportunistic infections in humans. These include burn wound infections (Morrison & Wenzel, 1984) causing soft tissue damage, and infection of immunocompromised patients (Sadikot et al., 2005) including those with morbidities such as cystic fibrosis (Bhagirath et al., 2016). *P. aeruginosa* colonizes ventilators, causing ventilator associated pneumonia and associated lung injury (Tsay et al., 2016). *P. aeruginosa* also causes community acquired pneumonia, although again this generally targets immunocompromised patients (Hatchette et al., 2000). Importantly *P. aeruginosa* infection is known for having distinctly higher mortality than other hospital acquired pneumonia (Osmon et al., 2004).

P. aeruginosa is categorised as a member of the ESKAPE pathogens by the CDC and is considered a priority pathogen by the WHO. This is because *P. aeruginosa* having generally very low antibiotic susceptibility due to a combination of resistance mechanisms including low outer membrane permeability, expression of efflux pumps, and the production of antibiotic degrading and inactivating enzymes (Pang et al., 2019). Alongside this they have a

highly mutable genome, via both horizontal gene transfer and mutational changes (Breidenstein et al., 2011; Pang et al., 2019). Further *P. aeruginosa* also produces a biofilm (Drenkard, 2003) which prevents antibiotic access to the bacterial cells. Finally, when exposed to a stressful condition a number of *P. aeruginosa* cells in a population can transform into environmentally tolerant persister cells, which can result in prolonged/recurrent infections in cystic fibrosis patients (Mulcahy et al., 2010).

Taken together these factors make *P. aeruginosa* an ideal organism for examining evolution in sub-inhibitory concentrations of plant metabolites, with the aim to reveal the role they play in the development of resistance to clinically relevant antibiotics in non-clinical environments.

1.6.5 Bacterial evolution and the development of resistance.

This study used an evolutionary approach to determine how the presence of sub-inhibitory concentrations of secondary plant metabolites would affect the susceptibility of bacteria after thirty days of continuous growth. The experiment was based on the procedure used for the *E. coli* long-term evolution experiment (LTEE) (Consuegra et al., 2021).

Evolutionary experiments have been previously conducted to determine if *E. coli* and *Pseudomonas fluorescens* could evolve resistance to the antimicrobial peptide pexiganan. Lineages of *E. coli* and *P. fluorescens* were grown over 600 generations in sub-inhibitory concentrations of pexiganan. All lineages displayed an increase in resistance to pexiganan, relative to the control isolates grown in the same media without pexiganan (Perron et al., 2006). The resistance remained stable after a further four passages and did not alter growth rate or maximal population density *in vivo*, although the exact genetic changes in the bacteria which conferred the resistance seen in this experiment were unknown.

P. aeruginosa sub-cultured in sub-MIC concentrations of ciprofloxacin over 940 generations had an increase in resistance to ciprofloxacin at 100 times the original MIC due to mutations

in the *gyrA* and *gyrB* genes (Jørgensen et al., 2013). Another study highlighted that *E. coli* and *S. enterica* can evolve resistance to tetracycline, ciprofloxacin and streptomycin resistance in sequential passaging up to 700 generations at sub-MIC conditions from 8-128 µg/ml (Gullberg et al., 2011).

Controls in evolution experiments are essential. Bacterial populations will evolve to adapt and grow in whatever conditions they encounter. As such, growth in laboratory conditions can have drastic effects on bacterial genomes and phenotypes (Hoang et al., 2016). Parallel control experiments are essential to determine which genetic changes are a result of growth in laboratory conditions, and which are a result of growth in treatment conditions.

An additional limitation to single population evolutionary experiments is selection for mechanisms of resistance unlikely to occur in nature. An example of this are pleiotropic mutations (Kawecki et al., 2012), mutations which affect multiple genes. Pleiotropic mutations can be positive and adverse. Evolution in natural environments will usually involve weak selective pressure in multiple areas, and thus pleiotropic mutations with multiple, or severe adverse effects are unlikely. Thus laboratory evolution studies may often overstate the importance of evolutionary trade-offs as the mutations in questions would rarely, if ever, appear and be sustained naturally in 'the wild' (Hillenmeyer et al., 2008). Finally, single isolate evolution experiments also miss out on multi-species interaction (Harrison & Brockhurst, 2012), which can be important in the development of bacterial tolerance, through the exchange of MGEs.

1.6.6   16S microbiome analysis

Chapters 6, 7 and 8 explored the role of quercetin and berberine as potential growth promoters in agriculture, specifically exploring their effects on the microbiome of chickens *in vitro* through batch culture and a caecal model fermenter system, and *in vivo*. This was conducted using 16S microbiome analysis.

16S microbiome analysis is a method of analysis which allows for detection of taxonomic changes within the microbiome down to a species level using bioinformatics techniques (Callahan, Sankaran, et al., 2016; Paulson et al., 2013). High throughout sequencing of PCR-amplified 16S sequences allows for analysis of complex bacterial communities that are largely unculturable. Whilst this method allows for establishment of species changes, it does not allow for exploration of the wider genomic changes within the microbial environment.

16S ribosomal RNA is a subunit of the 30S ribosomal subunit of the prokaryotic ribosome. It is slow to evolve and is essential for the survival of all prokaryotic species (Wimberly et al., 2000). However, the 16S ribosomal subunit contains 9 hypervariable regions which are different for distinct species of bacteria. The degree of nucleotide conservation varies, with highly conserved regions correlating to phyla class and order levels, and poorly conserved regions to family and species level. Full 16S sequencing can be conducted to establish isolate identity, as is used in our metagenomic and bacterial isolate library studies. However, the Illumina MiSeq platform can be used to sequence the hypervariable regions which allows for bacterial identification from population samples (Johnson et al., 2019).

The studies detailed in this thesis use 16S microbiome analysis to explore the speciation changes in multiple model chicken systems, following addition of phytochemicals. Whilst this experimental approach does not give an immediate indication of the antimicrobial genes the phytochemicals select for, it does, however, indicate the species these phytochemicals select for, which could potentially elucidate a rough overview of their antimicrobial mechanisms, and their impact on chicken growth (Valenzuela-Grijalva et al., 2017). Certain bacterial species can also harbour antibiotic resistance genes, acting as reservoirs for AMR within agricultural animal communities such as *E. coli* (Oladeinde et al., 2021)

1.7 Study aims and research value

The main aims of these studies were to investigate the interplay, and potential cross resistance between bacteria, antibiotic resistance genes, and phytochemicals in different environments, at the genomic, cellular, and population levels.

The specific aims are:

I. To develop a functional metagenomic screening methodology that can be used to screen both metagenomic libraries and bacterial isolate libraries for genes which confer, or bacteria who possess, phytochemical tolerance.

II. To evolve environmental isolates of bacteria in sub-inhibitory concentrations of the plant phytochemicals to determine the effects of phytochemical selective pressure on a genomic level.

III. To explore the effects phytochemicals supplementation in broiler chickens at a population level both *in vivo* and using two *in vitro* models.

1.7.1 Research Focus

This research will focus on the interplay between the environmental drivers of antibiotic resistance and the areas, both clinical and agricultural, that they effect.

1.7.2 The value of this research

This research will provide initial information into the baseline level of antibiotic resistance upon which the agricultural and clinical use of antibiotic is placed. It will also give insight into the basic biology by which bacteria can evolve resistance to plant metabolites and cross resistance to antibiotics. These data will be used to inform future decisions on the application of phytochemicals as new therapeutics, or growth promoters in meat and dairy production systems.

2   Materials and methods

2.1   Introduction

The materials and methods common across multiple chapters are detailed here. Specific methodologies used in only one chapter are outlined in the materials and methods section of that chapter.

2.2   Sources of chemicals, reagents, antibiotics, molecular biology kits and bacterial strains

Chemicals, solvents, culture media and antibiotics were all purchased from Sigma Aldrich Ltd (Dorset, UK) unless otherwise specified. Plasmid preparation kits were purchased from Qiagen (UK), and New England Biolabs (UK) as specified. Restriction enzymes were purchased from New England Biolabs (UK). *E. coli* competent cells were purchased from New England Biolabs (UK). Bacterial isolates were purchased from The National Collection of Type Cultures (UK) or provided by the Roberts Lab (LSTM). All primers were purchased from Integrated DNA technologies (UK). The ZymoBIOMICs DNA Miniprep Kits were provided by the Wigley Lab (University of Liverpool).

2.3   Plasmids, bacteria, and sequences

A comprehensive list of all plasmids and bacterial strains used in this thesis are given in Table 2-1.

Table 2-1 Strains and Plasmids used in this study. The strain, genotype, resistance marker in the case of plasmids, and the source of the strains and plasmids are given.

Strain/Plasmid	Genotype/Description	Resistance Marker	Reference/Source
Bacterial Strains			
E. coli **EPI300**	F⁻ mcrA Δ(mrr-hsdRMS-mcrBC) Φ80dlacZΔM15 ΔlacX74 recA1 endA1 araD139 Δ (ara, leu)7697 galU galK λ⁻ rpsL (Str^R) nupG trfA dhfr		Lucigen, Cambridge
E. coli **NEB5α**	fhuA2 Δ(argF-lacZ) U169 phoA glnV44 Φ80 Δ(lacZ)M15 gyrA96 recA1 relA1 endA1 thi-1 hsdR17		New England Biolabs, UK
***Pseudomonas aeruginosa* NCTC 7244**	Environmental strain isolated from a freshwater well in 1946 (Tobie, 1946)		National Collection of Type Cultures, UK
***Pseudomonas aeruginosa* NCTC 9433**	Environmental strain isolated from a tobacco plant in 1925 (Hoff & Drake, 1960)		National Collection of Type Cultures, UK
Plasmids			
pCC1BAC	Cloning Vector	Chloramphenicol	Lucigen, Cambridge

2.4 Standard optical density reading

Unless otherwise specified all optical density readings were taken at 600 nm using a CO8000 Biowave® Density Meter (VWR, UK) and a 1 ml cuvette.

2.5 Long term storage of bacterial isolates

Isolates were grown overnight in 10 ml Muller Hinton Broth (MHB) or Lysogeny (LB) broth depending upon the isolate, at 37°C and 200 rpm in 50 ml screw top falcon tubes. After 18-24 hours of growth 500 µl of the overnights were pipetted into a 2 ml screwcap tube using a 0.1-1 ml pipette. An additional 500 µl of sterile 40-80% glycerol/(MHB/LB) (v/v) was added to the 2 ml screwcap tube by pipetting, to a final concentration of 20-40% glycerol/broth. The contents of the 2 ml tube were mixed by inversion 5-10 times. Stocks were labelled with isolate name, date, and my name; these cultures were subsequently preserved at -80°C in a freezer.

2.6 Preparation of antibiotics and phytochemicals

All solid antibiotics and phytochemicals (berberine and quercetin) were weighed out in bijou tubes (VWR, UK) and then diluted using dH_2O, ethanol or dimethyl sulfoxide (DMSO) as stated in Table 2-2. The diluted compounds were then filter sterilised using 0.2 µM syringe filters (VWR, UK) in a category 2 hood and then diluted in growth media as stated in Table 2-2. All liquid secondary plant metabolites were diluted directly into growth media in a biological safety cabinet.

Table 2-2 Standard stock solutions of phytochemicals and antibiotics used in these experiments, containing information on standard stock concentration and solubility liquid, and working concentrations in media.

Compound	Standard Stock Solution	Working solution in media (LB/MHB)
Phytochemical		
Quercetin	10 mg/ml (DMSO)	2 mg/ml (MIC analysis using Clariostar) 1024 µg/ml (MIC analysis using EUCAST broth dilution) 320 µg/ml (Screening procedure concentration) 32 µg/ml (*Pseudomonas aeruginosa* sub-inhibitory growth conditions)
Berberine	10 mg/ml (DMSO)	2 mg/ml (MIC analysis using Clariostar) 1024 µg/ml (MIC analysis using EUCAST broth dilution) 320 µg/ml (Screening procedure concentration) 32 µg/ml (*Pseudomonas aeruginosa* sub-inhibitory growth conditions)
Antibiotic		
Novobiocin	10 mg/ml (dH_2O)	1024 µg/ml (MIC analysis using EUCAST broth dilution)
D-cycloserine	10 mg/ml (dH_2O)	1024 µg/ml (MIC analysis using EUCAST broth dilution)
Chloramphenicol	10 mg/ml (EtOH)	12.5 µg/ml
Tetracycline	10 mg/ml (dH_2O)	4 µg/ml

2.7 Standard DNA/colony PCR protocol

All polymerase chain reaction (PCR)s were conducted with MyTaq^{TM} Red Mix (Bioline, UK), a complete 2x reaction mixture containing a Taq DNA polymerase, red loading dye, 2.5 mM Mg^{++} and dNTPs.

A typical PCR of total volume 50 µl contained; 20 µM forward and reserve primers, 25 µl MyTaq^{TM} Red Mix (Bioline), 50-100 ng of DNA template or one bacterial colony from an overnight culture and dH$_2$O to a total volume of 50 µl.

The typical thermocycler parameters for PCR were: 95°C for 1 minute, then 35 cycles of 95°C for 15 seconds (denaturing), followed by an adjustable annealing temperature (50°C for 16S PCR), and then 72°C for 45 seconds (extension). Then hold at 4°C. The samples were then run on a 1% agarose gel. The annealing temperature was calculated using the melting temperatures (Tm)s of the oligos provided by the supplier. An overview of the primers used across this thesis are detailed in Table 2-3.

Table 2-3 Primers used in this study. Primer name, sequence from the 5' end, description and use, and origin are detailed within the table.

Primer Name	Sequence (5'-3')	Description/Use	Reference/Origin
8F	AGAGTTTGATCCTGGCTCAG	Ribosomal 16S Sequencing	(Edwards et al., 1989)
27F	AGAGTTTGATCMTGGCTC AG	Ribosomal 16S Sequencing	(J Lane, 1991)
1492R	CGGTTACCTTGTTAGACTT	Ribosomal 16S Sequencing	(Sneath, 1994)
518R	GTATTACCGCGGCTGCTGG	Ribosomal 16S Sequencing	(Muyzer et al., 1993)
U1492R	GGTTACCTTGTTACGACTT	Ribosomal 16S Sequencing	Universal
ITS1	TCCGTAGGTGAACCTGCGG	Fungal Primer	(White et al., 1990)
ITS2	GCATCGATGAAGAACGCAGC	Fungal Primer	(White et al., 1990)
T7	TAATACGACTCACTATAGGG	T7 Promoter Forward Primer	(Eberwine et al., 1992)
RP	CTCGTATGTTGTGTGGAATTGTGAGC	pCC1BAC/pEPIFOS Reverse Sequencing Primer	(CamBio, 2011)
FP	GGATGTGCTGCAAGGCGATTAAGTTGC	pCC1BAC/pEPIFOS Forward Sequencing Primer	(CamBio, 2011)
RP2	TACGCCAAGCTATTTAGGTGAGA	pCC1BAC/pEPIFOS Reverse Sequencing Primer 2	(CamBio, 2011)
SeqE	CGACACACTCCAATCTTTCC	Transposon Mutagen sequencing primer (east)	(*Thermo Scientific Template Generation System II Kit Technical Manual*, 2021)
SeqW	GGTGGCTGGAGTTAGACATG	Transposon Mutagen sequencing primer (west)	(*Thermo Scientific Template Generation System II Kit Technical Manual*, 2021)

2.8   Agarose gel preparation protocol

Agarose gels were cast using 50x Tris Acetate-Ethylenediaminetetraacetic Acid (TAE) Buffer

(VWR, UK) which was diluted to 1x TAE in dH$_2$O. Agarose gels were stained using 1:10,000

diluted GelRed® Nucleic Acid Gel Stain (Biotium, UK). PCR projects using MyTaq™ Red Mix

were directly loaded. All other products were loaded with 6x purple DNA loading dye (New

England Biolabs, UK). For example, a 6 µl sample would be a mix of 5 µl of PCR product and

1 µl of DNA loading dye, which would then be loaded into the agarose gel. The amount of PCR product loaded depended on the purpose of the electrophoresis (5 µl for visualisation of PCR result and 50 µl for DNA extraction).

2.9   PCR purification protocols

2.9.1   QIAquick PCR purification Kit protocol

Buffers for the QIAquick protocol were brought with the purification kit (Qiagen, UK). To start 5 volumes of PB buffer were added to 1 volume of the PCR Sample, and mixed (for example 250 µl of PB buffer would be added to 50 µl of PCR product). A QIAquick spin column was placed in the provided 2 ml collection tube. The sample was then bound to the QIAquick column by adding the sample to the column by pipetting and then centrifuging the column for 30-60 seconds at 16,000 *x g*. The flowthrough was discarded, and the column placed back in the same collection tube. Next, 750 µl of PB wash buffer was added to the tube and the tube was then centrifuged for 30-60 seconds at 16,000 *x g*. The flowthrough was discarded, and the column was placed back in the same tube and centrifuged for 1 minute at 16,000 *x g* to remove residual wash buffer. The column was then placed in a clean 1.5 ml microcentrifuge tube. The sample was eluted using 50 µl of DNase and RNase free water, allowed to stand for 1 minute and eluted by centrifugation for 1 minute at 16, 000 *x g*.

2.9.2   Monarch® PCR/DNA clean-up kit protocol

Buffers used in this protocol were purchased with the Monarch® PCR/DNA clean-up kit (New England Biolabs, UK). The PCR/DNA sample was first diluted 1:2 with DNA clean-up Binding Buffer (for example 100 µl of the sample was diluted with 200 µl of binding buffer). A Monarch® PCR/DNA Cleanup Kit column was then placed into the provided collection tube and the sample was loaded into the column by pipetting, and then the column was spun for 1 minute at 16,000 *x g*. The column was then re-inserted into the provided collection tube. Then 200 µl of DNA wash buffer was added to the column and the column was spun for 1

minute at 16,000 *x g*, this step was repeated twice. Then the column was transferred to a new clean 1.5 ml microcentrifuge tube, 20 µl of DNase and RNase free water was added to the column, and the sample eluted by centrifugation of the column for 1 minute at 16, 000 *x g*.

2.10 DNA sequencing and Analysis

Plasmid and chromosomal DNA was sequenced using the commercial service from GENEWIZ (GENEWIZ, Inc, UK). The different bioinformatics tools used as part of this analysis are detailed in Table 2-4.

Table 2-4 Software and tools used for nucleotide sequence analysis.

Program/Software	Uses/Purpose	Reference/Source
Nucleotide BLAST (megablast, discontinuous blast, blast and blastn)	To identify a query sequence or find nucleotide sequences with similar or identical identity to my query sequence.	(Altschul et al., 1990)
Translated BLAST	To find proteins with similar or identical translated nucleotide identity to the query sequence	(Altschul et al., 1990)
BioEDIT Sequence Editor	To align sequences.	(Hall, 1999)

2.11 Gel extraction protocols

2.11.1 Qiagen gel extraction kit protocol

All centrifugation steps were conducted at 17,900 *x g* in a benchtop centrifuge. Ethanol was added to buffer PE as directed.

The DNA fragment from the agarose gel was excised and placed in a clean microcentrifuge tube. The sample was then subsequently weighed, using an empty microcentrifuge tube as a zero. Then 3 volumes of buffer QG was added to 1 volume of the excised gel fragment. The tube was then incubated at 50°C until the gel fragment had fully dissolved. Then 1 gel volume of isopropanol was added to the dissolved sample and mixed. The sample was then

transferred via pipetting to the provided QIAquick spin column in a 2 ml collection tube. The sample was centrifuged for 1 minute and the flowthrough was discarded. Next 500 µl of buffer QG was added to the column and the column was then centrifuged for 1 minute, and the flowthrough was discarded. The sample was washed by adding 750 µl of buffer PE to the column and the column was then centrifuged for 1 minute, the flowthrough was discarded. The sample was centrifuged for 1 minute and the flowthrough discarded to remove residual was buffer. The column was placed in a clean 1.5 ml microcentrifuge tube. The sample was eluted by adding 30 µl of dH_2O, allowed to stand for 1 minute and then centrifuged for 1 minute.

2.11.2 Monarch® DNA gel extraction kit protocol

All centrifugation steps were conducted at 16,000 $x\,g$ to ensure all traces of buffer are eluted at every step. The DNA fragment was excised from the gel using a clean cutting tool and excessive agarose was trimmed. The remaining sample was transferred to a 1.5 ml microcentrifuge tube and weighed, using an empty 1.5 ml microcentrifuge tube as a zero. Following weighing of the sample 4 x the volume of the gel of Monarch Gel dissolving buffer was added to the tube with the gel slice (for example 400 µl of buffer was added to 100 µg of gel slice). The sample was then incubated on a heat block at 55°C and inverted periodically by hand until the sample was completely dissolved. The sample was added to a Monarch ® DNA gel extraction kit column in a fresh 2 ml collection tube and spun for 1 minute and the flowthrough was discarded. Next 200 µl of DNA wash buffer was added to the column, and the column was spun for 1 minute. This wash step was then repeated. The column was transferred to a clean 1.5 ml microcentrifuge tube and 30 µl of H_2O or DNA elution buffer was added to the column. The sample was incubated for 1 minute, and then spun for 1 minute, and the eluted DNA was stored at -20°C until use.

2.12 Plasmid extraction protocols

2.12.1 Qiagen miniprep kit protocol

All buffers used in this protocol were purchased with the extraction kit (Qiagen, UK). First, 1-5 ml of overnight culture was transferred to a 10 ml falcon tube and subsequently pelleted using a benchtop centrifuge at 3220 x g for 10 minutes, the remaining supernatant was discarded. The pellet was resuspended in 250 µl of P1 buffer and transferred to a microcentrifuge tube. Subsequently, 250 µl of P2 buffer was added to the resuspended colonies and mixed by hand via inversion. Next, 350 µl of N3 buffer was added to the resuspended colonies and the mixture was mixed immediately via inversion. The sample was centrifuged for 10 minutes at 17,900 x g in a benchtop centrifuge to pellet the bacterial waste. Next, without disturbing the waste pellet, 800 µl of supernatant was added to a QIAprep® 2.0 spin column, which was placed in a 2 ml waste collection tube. This column was centrifuged at 17,900 x g for 60 seconds. The flowthrough was then discarded and 750 µl of PE buffer was added to the column. The column was centrifuged at 17,900 x g for 60 seconds and the flowthrough discarded, residual buffer was removed via another 60 second centrifugation at 17,900 x g. The column was then placed in a clean 1.5 ml microcentrifuge tube and 30 µl of dH_2O was added to the column. The column was allowed to stand for 1 minute, and the sample eluted by centrifugation for 60 seconds at 17,900 x g.

2.12.2 Monarch plasmid miniprep kit protocol

Buffers used in this protocol were purchased with the Monarch® plasmid miniprep kit (New England Biolabs, UK). First, 1-5 ml of overnight culture was transferred to a 10 ml falcon tube and subsequently pelleted using a benchtop centrifuge at 3220 x g for 10 minutes, the remaining supernatant was discarded. The pellet was resuspended in 200 µl of B1 buffer and transferred to a microcentrifuge tube. Next 200 µl of B2 buffer was added to the resuspended pellet and the solution mixed by hand via inversion. Subsequently 400 µl of B3 buffer was

added and mixed immediately via inversion until the liquid turned yellow. The solution was centrifuged for 5 minutes at 17,900 x g to pellet the lysate. The supernatant was transferred to a Monarch® Spin column without disturbing the pellet. The column was placed in a 2 ml collection tube and centrifuged at 17,900 x g for 60 seconds. The flowthrough was discarded and 200 μl of wash buffer 1 was added to the column. The column was centrifuged for 60 seconds at 17,900 x g and the flowthrough discarded. Next, 400 μl of wash buffer 2 was added to the column. The column was centrifuged for 60 seconds at 17,900 x g and the flowthrough discarded. The column was placed in a clean 1.5 ml microcentrifuge tube and the plasmid was eluted in 30 μl of dH$_2$O via centrifugation for 60 seconds at 17,900 x g.

2.13 Determining the minimum inhibitory concentration of a compound against bacteria

2.13.1 European committee on antimicrobial susceptibility testing (EUCAST) broth dilution methodology

To assess the minimum inhibitory concentration, 100 μl of 2x the maximum concentration of the inhibitory concentration to be assessed, diluted in MHB, was added to the first three wells of row A (A1-3) in a sterile round bottom 96 well Corning® 3367 plate (Sigma-Aldrich, UK). For example, if the highest inhibitory concentration to be assessed was 512 μg/ml then 100 μl of 1024 μg/ml was added to the first wells in row A. A single column gap was left between each compound if assessing the MIC of multiple compounds (such that columns 4 and 8 were left empty). Subsequently 50 μl of MHB was added to each well below the first (B-H (1-3)). A series of doubling dilutions were conducted along each column, where 50 μl was removed from row A, added to row B via a multi-channel pipette, the pipette tips were discarded between each dilution. The final 50 μl was discarded at row G so that row H did not contain any drug and functioned as a positive control of MHB (Schön, et al, 2020).

A 10 ml overnight culture of bacteria was grown the day before at 37°C, 200 rpm from a single colony from a fresh plate of the -80°C stock. This 10 ml overnight was diluted to an OD of between 0.8 to 1 in MHB. Subsequently 10 µl of this dilution was added to 10 ml of MHB and mixed to give the final dilution concentration. Next 50 µl of this final dilution was added to each well of the plate with inhibitory compound, excluding the blank wells. Finally, 100 µl of sterile MHB was added to all rows in column 12 as a negative control.

Next, 1 µl of the final culture dilution was diluted in 999 µl of sterile PBS in a 1.5 ml Eppendorf. From this PBS dilution, 100 µl was spread, using a sterile single-use spreader, onto a sterile LB plate (supplemented with antibiotics as appropriate) for determination of colony forming units (CFUs). Both the 96 well plate and agar plates were incubated at 37°C for between 16-20 hours, and then read by eye. MIC was established by determining the final well in which the bacteria grew, and then the lowest concentration after was considered the MIC. For example, if bacteria grew in every well of 32 µg/ml the MIC was 64 µg/ml.

2.13.2 Antimicrobial susceptibility testing EUCAST disk diffusion method

Disk diffusion followed the protocol laid out in the EUCAST disk diffusion handbook (Eucast, 2022; Schön, et al, 2020).

Muller-Hinton agar (MHA) was prepared according to the manufacturer's instructions, and autoclaved. The medium for disk diffusion must have a depth level of 4.0 mm ± 0.5mm, which equates to 71 ml in a 150 mm circular petri-dish. These plates were created by adding freshly autoclaved agar to the 150 mm petri-dishes using a Stripette™. The plates were dried for 30 minutes at room temperature in a laminar flow hood, and then stored overnight at 4°C.

Cultures of the colonies to be assessed were prepared on MHA supplemented with appropriate antibiotic 24 hours before and grown at 37°C. Using a sterile loop, single colonies were taken from these overnight plates and suspended in 10 ml of saline, until the media

visually equated to the turbidity of a 0.5 McFarland turbidity standard. This suspension was always used to inoculate the plate within 15 minutes of preparation.

The previously prepared agar plates with standard depth were removed from the fridge and warmed to room temperature in a sterile category 2 hood. A sterile swab was dipped into the diluted bacteria and the plates inoculated with the swab by streaking across the entire plate in three directions (horizontally, vertically, and diagonally) leaving no gaps between streaks.

The pre-brought antimicrobial discs (Thermo Fisher Scientific, UK) were allowed to reach room temperature and then placed firmly onto the agar plates within 15 minutes of inoculation using forceps. With a maximum number of 12 discs on a 150mm plate.

Plates were incubated within 15 minutes of disc application at 37°C for 18 hours, with a maximum of five plates stacked on top of each other. After 24 hours a confluent lawn was expected, if individual colonies could be distinguished, the experiment was repeated. Zones of growth inhibition were measured on a light producing background from the back of the plate using a ruler.

2.14 Preparation of competent cells

Competent cells were prepared by the one step protocol from (Chung et al., 1989). A 5ml culture of *E. coli* DH5-alpha was prepared in LB broth and grown overnight at 37°C. Then, 500 µl of this culture was added to 50 ml of LB broth and grown at 37°C, 200 rpm until the OD$_{600}$ reached 0.5. The cells were centrifuged for 10 minutes at 1910 x g and 4°C, and the supernatant was discarded. The cells were then resuspended in 5 ml of Transformation and Storage Solution (TSS) buffer. TSS buffer was made with 85% LB medium, 10% (w/v) PEG MW 8000, 5% (v/v) DMSO and 50 mM magnesium chloride which was filter sterilised. The stored cells were divided into 100 µl stocks in 1.5ml Eppendorf tubes and stored at -80°C.

2.15 Transformation of DH5α

DH5α competent cells (New England Bioscience, UK) were thawed on ice until all ice in the tubes disappeared. The cells were mixed gently and 50 µl of cells were pipetted into individual 1.5 ml microcentrifuge tubes on ice. Next, 1-5 µl of plasmid DNA, at a DNA concentration of 0.2 pg-20 ng/µl (of a total volume 1 pg – 100 ng) was added to the cells and mixed by gently flicking the tube. The cells were then left on ice for 30 minutes. The cells were heat shocked at 42°C for 30 seconds, using a heat block, and immediately placed on ice for 5 minutes. After heat shock, 950 µl of room temperature sugar optimal broth with catabolite repression (SOC) media (New England Bioscience, UK) was added, and tubes were incubated at 37°C for 60 minutes with rotation. The cells were plated out onto pre-warmed 37°C agar containing 12.5 µg/ml of chloramphenicol and incubated at 37°C overnight.

2.16 DNA insolation protocols

2.16.1 ZymoBIOMICs DNA miniprep kit

All tubes and solutions used were purchased alongside the ZymoBIOMICs DNA miniprep kit (Zymo Research, UK). First, 200 mg of caecal sample was added to a ZR BashingBead™ Lysis Tube alongside 750 µl of ZymoBIOMICs™ Lysis solution. The sample was secured in a bead beater with a 2ml tube holder assembly attachment, and beaten according to specifications in ZymoBIOMICs™ DNA Miniprep Kit Protocol (Zymo Research, 2022). The sample tube was centrifuged for 1 minute at 10,000 *x g*. Next, 400 µl of the supernatant was transferred to a Zymo-Spin™ III-F Filter in a 2 ml collection tube and centrifuged at 8,000 *x g* for 1 minute. Next, 1200 µl of ZymoBIOMICs™ DNA binding buffer was added to the filtrate in the collection tube from the Zymo-Spin™ III-F Filter. Then, 800 µl of the sample plus binding buffer mixture was transferred to a Zymo-Spin IICR Column and centrifuged for 1 minute at 10,000 *x g*, the flowthrough discarded, and the step repeated with the remaining 800 µl of the sample. The ZymoSpin™ IICR column was washed with 400 µl of ZymoBIOMICs™ DNA wash buffer 1 and

centrifuged at 10,000 *x g* for 1 minute and the flowthrough was discarded. The ZymoSpin™ IICR column was washed with 700 μl of ZymoBIOMICs™ DNA wash buffer 2 and centrifuged at 10,000 *x g* for 1 minute and the flowthrough was discarded. The ZymoSpin™ IICR column was washed with 200 μl of ZymoBIOMICs™ DNA wash buffer 2 and centrifuged at 10,000 *x g* for 1 minute and flowthrough discarded. The ZymoSpin™ IICR column was transferred to a new 1.5 ml microcentrifuge tube and 50 μl of ZymoBIOMICs™ DNase/RNase Free Water was added directly to the column matrix, the column was incubated for 1 minute and ten centrifuged at 10,000 *x g* for 1 minute to elute the DNA. Then a Zymo-Spin™ III-HRC Filter was placed in a new collection tube and 600 μl of ZymoBIOMICs™ HRC prep solution was added. The filter was centrifuged at 8,000 *x g* for 3 minutes. The eluted DNA was transferred to the now prepared ZymoBIOMICs™ III-HRC filter, which was placed in a clean 1.5 ml microcentrifuge tube. This was centrifuged at exactly 16,000 *x g* for 3 minutes. The samples were stored at -20°C for downstream applications.

2.16.2 Qiagen bacterial genomic DNA extraction Kit

All buffers were prepared according to manufacturer's protocol. Firstly, -80°C long term storage cultures of bacteria were plated out onto LB agar plates supplemented with appropriate antibiotics and grown overnight at 37°C. A single colony from these cultures was taken and used to streak out a lawn on a fresh LB plate containing appropriate antibiotic supplementation and these lawns were grown overnight at 37°C. The cultures from these lawn plates were gathered using a sterile loop and resuspended in a 3.5 ml aliquot of B1 buffer after the addition of 7 μl of RNase solution to the buffer aliquot. The resuspended sample was vortexed at the maximum available speed of the benchtop vortex.

Next, 100 μl of proteinase K and 80 μl of lysozyme stock solution was added to the samples and the samples were incubated at 37°C for 30 minutes. Then 1.2 ml of buffer B2 was added to the samples and the mixture was vortexed and incubated at 50°C for 30 minutes.

While the sample was incubating a Qiagen Genomic Tip (100/g) was equilibrated with 4 ml of buffer QBT and tip to was allowed to empty by gravity. The bacterial sample was vortexed for 10 seconds after incubation at maximum speed and pipetted into the column. The bacteria were allowed to enter the resin by gravitational flow. Positive pressure was applied to the column, but the rate of flow was not allowed to exceed 10-20 drops per minute. The column was washed twice with 7.5 ml of buffer QC. The column was not allowed to run dry. The genomic DNA was eluted into a fresh tube using 5 ml of buffer QF. The DNA was precipitated by adding 3.5 ml of room temperature isopropanol to the eluted DNA. The DNA was mixed and centrifuged immediately at 7500 $x\ g$ for 15 minutes at 4°C. The centrifuged DNA pellet was washed with 2 ml of 70% ethanol at 4°C. The sample was vortexed briefly and centrifuged for 10 minutes at 4°C. The supernatant was removed without disturbing the pellet and the pellet was resuspend in 100 ml of H_2O and allowed to dissolve at 55°C for 2 hours. The DNA was stored at 4°C.

2.16.3 Fire monkey DNA extraction protocol

All tubes and solutions used were purchased alongside the Fire monkey DNA extraction kit (Revolugen, UK). First, 14 ml of 100% ethanol was added to the wash solution concentrate and mixed by gentle agitation. Bacterial cells were pelleted at 1,180 $x\ g$ and all supernatant was removed, and the pellet was washed in 1x phosphate buffered saline (PBS) solution. For Gram-negative bacteria, the pellet was incubated for 10 minutes in 100 µl of freshly prepared 3 mg/ml lysozyme solution (1.2% triton X-100 in H_2O) at 37°C. Then 10 µl of 20 mg/ml RNase A solution diluted in H_2O was added and the sample was mixed by vortexing. Next, 300 µl of Lysis solution DNA was added, followed by 20 µl of 20 mg/ml proteinase K and the solution was again vortexed. The sample was incubated at 56°C for 20 minutes. Two 1.5 ml sterile Eppendorf tubes were prewarmed to 80°C, and two further tubes were warmed containing 250 µl elution buffer each. During this, 350 µl of solution BS was added to the sample and the sample was vortexed briefly. This was followed by the addition of 400 µl of 75%

isopropanol. After the addition of isopropanol, the sample was vortexed briefly. A wide bore tip was then used to transfer 60 µl of the sample to the spin column.

At each following step involving the spin column the flowthrough was discarded. The sample was centrifuged at 4722 *x g* for 1 minute. A wide bore tip was then used to add the remainder of the sample to the column which was centrifuged again at 4722 x g for one minute. Then 500 µl of wash solution was added to the spin column and the column was centrifuged at 4722 x g for one minute. Then 500 µl of 90% ethanol was added to the spin column and the column was centrifuged at 14,462 *x g* for 3 minutes. The column was centrifuged again at 14,462 *x g*. The DNA was extracted by adding 100 µl EB to the spin column and incubating the column at 80°C for 1 minute. The DNA was eluted by centrifuging the column at 1,180 *x g* for 2 minutes, for fraction A. After the elution of fraction, A, 80 µl of fresh EB was added and the column transferred to a fresh pre warmed Eppendorf and incubated at 80°C for 1 minute. The sample was eluted at 1,180 *x g* for fraction B.

2.17 DNA sequencing protocols

2.17.1 MinION nanopore protocol

The DNA was prepared using the Oxford Nanopore technologies Native DNA barcoding protocol.

2.17.1.1 DNA Preparation

Firstly 1 µg of genomic DNA was placed into an Eppendorf DNA LoBind® tube and the volume was adjusted to 49 µl with nuclease free water. The tube was mixed by gently flicking and spinning down briefly in a microcentrifuge. In a separate thin-walled PCR tube, 48 µl of DNA, 3.5 µl of NEBNext Formalin-Fixed, Paraffin-Embedded DNA repair buffer, 2 µl NEBNext FFPE DNA Repair MIX, 3.5 µl Ultra II End-prep reaction buffer and 3 µl ultra II end prep enzyme mix was mixed. The solution was mixed by pipetting, or gently flicking the tube. The tube was incubated at 20°C for 5 minutes followed by 65°C for 5 minutes. The AMPure XP beads where

resuspended by vortexing. The clean DNA sample was transferred to a clean 1.5ml Eppendorf

DNA Lobind® Tube and 60 μl of AMPure beads were added to the tube and the tube was

mixed by flicking. The DNA was incubated on a rotator for 5 minutes at room temperature.

The sample was spun down and pelleted on a magnet. We then prepared 500 μl of fresh 70%

ethanol. The tube was kept on the magnet and the pellet was washed with 200 μl fresh 70%

ethanol. The ethanol was removed with a pipette and discarded. This was step was repeated.

The tube was spun down and placed back on the magnet, and a pipette was used to remove

any residual ethanol. The pellet was allowed dry for 30 seconds but to not the point of

cracking. The pellet was removed from the magnet and the DNA was resuspended in 25 μl of

DNA free water and allowed to incubate for 2 minutes at room temperature. The beads were

then pelleted on the magnet until the solution became clear and colourless. The 25 μl of

elution was removed by pipetting and retained in a clean LoBind® Eppendorf tube and

quantified using a Qubit Fluorometer.

2.17.1.2 Native Barcoding

The native barcodes were thawed with one barcode thawed per sample. The barcodes were

individually mixed by pipetting and placed on ice. Then 500 μg of prepared DNA was

aliquoted into 22.5 μl of nuclease free water in a clean LoBind® Eppendorf tube. Next 2.5 μl

of the barcode, followed by 25 μl of blunt/TA ligase mix was added to the DNA and the tube

was mixed by gently flicking between each addition. The reaction was incubated for 10

minutes at room temperature. The AMPure beads were resuspended by vortexing and 50 μl

of beads were added to each reaction tube. The reaction was incubated for 5 minutes at

room temperature with rotation. Then 70% ethanol in nuclease free water was prepared.

The sample was spun down and pelleted on a magnet. The supernatant was removed by

pipetting and the sample washed twice with 200 μl ethanol. The pellet was spun down and

placed back on the magnet, and allowed to dry for 30 minutes, without allowing the pellet

to crack. The pellet was then removed from the magnet and resuspended in 26 μl nuclease

free water. The beads were pelleted on the magnet until the elute was clear and colourless. The elution was removed by pipetting and retained in a 1.5 ml LoBind Eppendorf Tube. In preparation for the next step, equimolar amounts of the samples were pooled together and diluted to a total of 700 ng of pooled DNA in 65 µl nuclease free water.

2.17.1.3 Adapter Ligation and Clean up

Firstly, the elution buffer and ligation buffer were thawed at room temperature and mixed via vortexing, spun down and placed on ice. Then the T4 ligase and Adapter Mix II were spun down and placed on ice. To enrich for DNA fragments of all sizes, one tube of short fragment buffer was thawed, vortexed, spun down and placed on ice. The pooled DNA was mixed with 5 µl of adapter mix II, 20 µl NEBNext quick ligation reaction buffer (5x) and 10 µl quick T4 DNA ligase. The sample was mixed between each addition by flicking, and then spun down. The tube was incubated for 10 minutes at room temperature. Then the AMPure beads were resuspended by vortexing and 50 µl of the resuspended beads were added to the reaction and the reaction was mixed by pipetting. The reaction was then incubated at room temperature for 5 minutes on a rotator. The reaction was placed on a magnetic rack to pellet the beads and the supernatant was removed by pipetting. The beads were washed with 250 µl short fragment buffer, the beads were flicked to resuspend and subsequently the tube was returned to the magnetic rack to pellet. The supernatant was removed by pipetting. The wash step was repeated. The tube was spun down and placed back on the magnet and a pipette was used to remove any residual supernatant. The tube was allowed to dry for 30 seconds without allowing the pellet to crack. The pellet was removed from the magnetic holder and resuspended in 15 µl of elution buffer. The sample was then incubated for 10 minutes at room temperature and re-pelleted on the magnet until the solution is clear and colourless. The 15 µl elution was removed by pipetting and retained in a new 1.5 ml LoBind® Eppendorf tube.

2.17.1.4 Priming and loading the flow cell.

Firstly, the sequencing buffer, loading beads, flush tether and one tube of the flush buffer were thawed at room temperature. The tubes were placed on ice as soon as thawing was complete. Next, the sequencing buffer, flush buffer, and flush tether were all individually mixed by vortexing, subsequently spun down and returned to ice. The MinION lid was opened, and the flow cell was slid under the clip. The priming port cover was slid clockwise to open the priming port.

Following the opening, the next step was to check for an air bubble under the cover of the priming port and draw a small volume of water, to remove any bubbles. The water was drawn by setting a P1000 pipette to 200 µl and then inserting a tip into the priming port. The volume of the pipette was increased to 230 µl and a small amount of liquid was allowed to be drawn through the tip. Next 30 µl of thawed and mixed flush tether were added directly to the tube of thawed and mixed flush buffer and mixed by vortexing. Following this 800 µl of the priming mix was loaded into the flow cell via the priming port, avoiding the addition of air bubbles. Next, there was a 5-minute waiting period, to allow the priming mix to integrate fully.

The loading beads were mixed and resuspended immediately for use by pipetting. A new tube was prepared containing 37.5 µl of sequencing buffer, 25.5 µl of loading beads and 12 µl of the DNA library. The port cover was gently lifted and 200 µl of the priming mix was loaded into the flow cell via the priming port. The prepared library was mixed gently by pipetting and 75 µl of the sample was added to the sample port in a dropwise fashion. Next both the sample and priming port were gently closed, and the port cover was replaced followed by the lid. The MinION was run according to manufacturer's protocols.

2.18 Ethical approval

Ethical approval for the *in-vivo* poultry work in chapter 9 was obtained through the project licence P999B8C93 and personal licence of Dr Sian Pottenger (IE89D0D59), approved by the University of Liverpool Ethics Committee.

3 Development of a functional screening methodology for screening of both metagenomic and bacterial isolate libraries for resistance to phytochemicals

3.1 Introduction

In this chapter, we hypothesise that phytochemicals function as a selective pressure for the maintenance of the antimicrobial resistance gene reservoir in the oral cavity, enriching for genes that confer tolerance to phytochemicals, and that a subset of those genes may also confer cross-resistance to antibiotics. This chapter used two phytochemicals, quercetin and berberine, to develop a functional metagenomic screen. The developed functional metagenomic screening assay was used to examine a an oral metagenomic library for metagenomic inserts which contained gene conferring phytochemical tolerance, which would be subsequently evaluated for their antimicrobial resistance properties. These inserts underwent sequencing and bioinformatics analysis.

Functional screening is a powerful and well-known screening procedure used to isolate bacteria that possess desirable characteristics (Lam et al., 2015). Functional screening often acts synergistically with PCR-based screening approaches; where the genetic material of interest is searched for directly (Noureen et al., 2020). Functional metagenomic screening is a powerful procedure, however it is not without caveats. One of the key considerations is that the usual host for a metagenomic library, *E. coli,* may express cloned genes differently, or not at all, as compared to how they would be expressed in their original bacterial host (De Lorenzo et al., 2005). One possible way of addressing this would have been to use multiple different bacterial libraries with the same starting genomic DNA.

The theory assessed in this chapter was based on a study by Rahman et al (2020), which used an oral metagenome from Bangladeshi samples. In the study by Rahman et al (2020), a *ddl6*

and a *ddl7* gene had been identified, which theoretically conferred resistance to d-cycloserine. Notably, none of the donors to the library had previously had d-cycloserine treatment, which suggested there was another selective pressure for these genes (Rahman et al., 2020). This selective pressure in the oral cavity was theorised to be food, specifically the plant phytochemicals the food contained. Using molecular docking the flavonoid quercetin bound in the same binding pocket of the *ddl6* and *ddl7* (Rahman et al., 2020) as d-cycloserine, which led to the theory that the presence of this phytochemical acted as a selective pressure for the maintenance of these d-cycloserine resistance genes in the oral cavity.

The oral metagenomic library used in this study was created using saliva from the human oral cavity taken from people in the United Kingdom (Reynolds et al., 2016). The samples underwent whole DNA extraction and then the DNA was cleaved using the HindIII restriction enzyme. This cut DNA was then inserted into a plasmid vector, known as the metagenomic insert, and the vector ligated into *E. coli* in 96 well plates to form the library (Reynolds et al., 2016). One trade-off for oral metagenomic libraries is that they have previously been shown to contain high proportions of human DNA which is co-isolated during the DNA extraction from saliva or cheek swabs (Reynolds et al., 2016). This library was chosen because of its availability and link to a potential known phytochemical-antimicrobial resistance overlap.

3.2   Materials and methods

3.2.1   Selection of the plant metabolites and metagenomic library

The plant metabolites selected for this thesis have been discussed in Chapter 1.4. The metagenomic library selected was a previously constructed human oral metagenomic library (Reynolds et al., 2016). The metagenomic library was constructed of 96 well plates, where each well of the 96 well plates contained a single *E. coli* EPI300 isolate containing a unique metagenomic insert. The library contained human DNA on over 40% of inserts, and inserts containing bacterial DNA had been previously located with *tet*AB(60) genes present upon the insert (Reynolds et al., 2016). The library was at least 200,000 isolates, and the average insert size was unknown.

3.2.2   Induction of pCC1BAC to a high copy number in *E. coli* EPI300

To induce a high plasmid, copy number (~50 per cell), 1 ml of LB supplemented with 12.5 µg/ml of chloramphenicol was dispensed into sterile 1.5 ml Eppendorf tubes. Each tube was inoculated with a single isolated clone from an overnight agar plate. The 1.5 ml tubes were incubated at 37°C overnight without agitation. Following overnight incubation, the 1 ml of inoculated LB broth was added to 9 ml of LB supplemented with 12.5 µg/ml chloramphenicol in sterile 50 ml falcon tubes. Then 10 µl of 1000x EpiCentre CopyControl induction solution (Cambridge Bioscience) was added to the tubes, this compound induces high copy number through the origin of replication. These tubes were incubated at 37°C at 200 rpm for 5 hours. Following this incubation, the plasmid was extracted using the protocol in Chapter 2.12.

3.2.3   Development of the functional screening methodology

3.2.3.1   Protocol 1: Agar based screening of the metagenomic library

To screen the metagenomic library 90 ml LB agar plates were prepared containing doubling dilutions from 32 to 512 µg/ml of quercetin, berberine and reserpine, diluted from 30 mg/ml DMSO stock solutions plus 12.5 µg/ml of chloramphenicol (to select for the plasmid

containing the metagenomic DNA). These phytochemical concentrations were chosen because the current literature indicated that quercetin and berberine tolerance for *E. coli* fell within this range (Cushnie & Lamb, 2005; S. Wang et al., 2018). One 90 ml plate containing 5 µg/ml of tetracycline plus 12.5 µg/ml of chloramphenicol was also prepared. A single plate from the oral metagenomic library was replicated onto these plates using the procedure described below (Chapter 3.2.3.2). Growth was evaluated by eye after 24 hours.

3.2.3.2 Protocol 2: Broth dilution screening of the metagenomic library with endpoint reading

3.2.3.2.1 Broth dilution screening

The second screening procedure was conducted by adding 100 µl of MHB plus 2.5 times the MIC of the inhibitory compound to be assessed to each well of a sterile flat bottomed 96 well plate. Then using a sterile 96 pin replicator, the thawed 96 well metagenomic library plate was replicated into one of the fresh 96 well plates containing MHB plus inhibitory compound, a separate plate of just MHB plus the phytochemical was used as a blank. Plates were read at OD_{600} at 0 and 18 hours. The readings were fed into Equation 1(which was designed to account for noticeable precipitation of quercetin during the functional screen).

$$\left(\begin{array}{c} (OD600 \; of \; Inidividual \; Well \; at \; Time = 18) - \\ (OD600 \; of \; Individual \; well \; at \; Time = 0) - \left(\dfrac{\sum OD \; of \; all \; wells \; at \; Time = 18}{96} \right) \end{array} \right)$$

$$= Corrected \; Individual \; Well \; OD600$$

Equation 1 Equation for analysis of individual wells from a 96 well plate that considers both growth and plate precipitation average.

3.2.3.2.2 Secondary screening: MIC analysis of positive primary hits

Putative resistant isolates were grown overnight on LB agar supplemented with 12.5 µg/ml chloramphenicol. A single colony was used to inoculate 10 ml of MHB supplemented with 12.5 µg/ml of chloramphenicol which was incubated at 37°C, 200 rpm overnight. The culture was then diluted to OD_{600} 0.8-1 with MHB, and diluted 1:1000 to match the concentration of

bacteria used to determine the MIC. Then 50 µl of this cell suspension was added to 50 µl of 2x MIC dilution of the respective secondary plant metabolite in MHB to a final 1x MIC dilution. This was incubated overnight at 37°C. Growth in wells after overnight incubation indicated resistance.

3.2.3.2.3 Tertiary screening: confirmation of plasmid mediated resistance

The plasmids from the positive hits after secondary screening were extracted and re-transformed into DH5α. The protocols for the extraction and subsequent retransformation of the plasmids into DH5α is given in Chapter 2.15.

After transformation, a single colony was taken from each plate and used to inoculate 10 ml MHB supplemented with 12.5 µg/ml chloramphenicol, which was grown overnight at 37°C, 200 rpm. These transformed cells were evaluated for resistance to the secondary plant metabolites following the MIC protocol as previously described (Chapter 2.13.1).

3.2.3.2.4 Quaternary Screening: end sequencing of pCC1BAC plasmids from the metagenomic library

The inserts within pCC1BAC are flanked by pCC1/EpiFos Forward Sequence primer binding site, T7 Sequence and pCC1/EpiFos Reverse Sequence 1 and 2. These primers were used to end sequence the insert. If the sequences obtained through this process were of bacterial origin, they were subsequently analysed using BLAST and mapped to the relative bacterial genomes showing high identity and coverage.

3.2.3.3 Protocol 2: Transposon mutagenesis

Transposon mutagenesis was conducted using the Template Generation Kit II (Thermo Fisher Scientific, UK). One to 14 µl of target plasmid DNA for mutagenesis was mixed with 4 µl of 5x Reaction Buffer for MuA transposase, 1 µl of entranceposon (Cam®03 or Kan®-3 or Tet®-3), 1 µl of MUA transposase and then equalised to 20 µl using dH_2O. The reagents were mixed without vortexing and then incubated for 1 hour at 30°C. Then heated to 75°C for 1 minute

to deactivate the protease, they were then transformed using the transformation protocol (Chapter 2.15).

3.2.3.4 Protocol 3: Broth dilution screening of the metagenomic library with continuous reading

The third screening procedure was conducted by adding 100 µl of MHB supplemented with 1 mg/ml of the inhibitory compound to be assessed to each well of a sterile flat bottomed 96 well plate. Then using a sterile 96 well replicator, the thawed metagenomic library plate was replicated into one of the fresh 96 well plates containing MHB plus inhibitory compound. Plates were read for 24 hours at OD_{600} with a reading every 10 minutes at 37°C with shaking on the CLARIOstar plate reader to determine the growth dynamics over time in each well.

3.2.3.5 Snapgene inserts of positive hits

Full positive hit insert sequences can be found in appendix I.

3.3   Results

3.3.1   Determination of the MIC of EPI300 *E. coli* containing an empty pCC1BAC plasmid against a range of phytochemicals

Five plant metabolites were screened for their antimicrobial activity against EPI300 *E. coli* containing empty (no insert) pCC1BAC (Table 3-1). Quercetin and berberine had an MIC of 128 μg/ml, reserpine and apigenin had an MIC of 256 μg/ml and allicin did not demonstrate any inhibitory activity.

Table 3-1 MICs of Phytochemicals against EPI300 E. coli containing an empty pCC1BAC plasmid.

Phytochemical	Minimum Inhibitory Concentration (μg/ml)
Quercetin	128
Berberine	128
Reserpine	256
Allicin	No inhibition
Apigenin	256

3.3.2   Protocol 1: metagenomic library screening using agar plates supplemented with plant secondary metabolites

All 96 clones from the single (1) stamped library plate grew on all agar plates, except for the tetracycline plate, where no isolate grew. It was determined from this that the phytochemicals were inactive in agar, as a result, protocol 2 was developed.

3.3.3   Protocol 2: discovery of precipitation of quercetin during the broth dilution screening protocol

After development of the first stage screening procedure, it was noted that most wells contained a degree of quercetin precipitation after growth at 37°C for 18 hours (Figure 3-1). The wells containing berberine had no precipitation. As the two phytochemicals were the only difference between the experiments it was assumed quercetin was the precipitating factor.
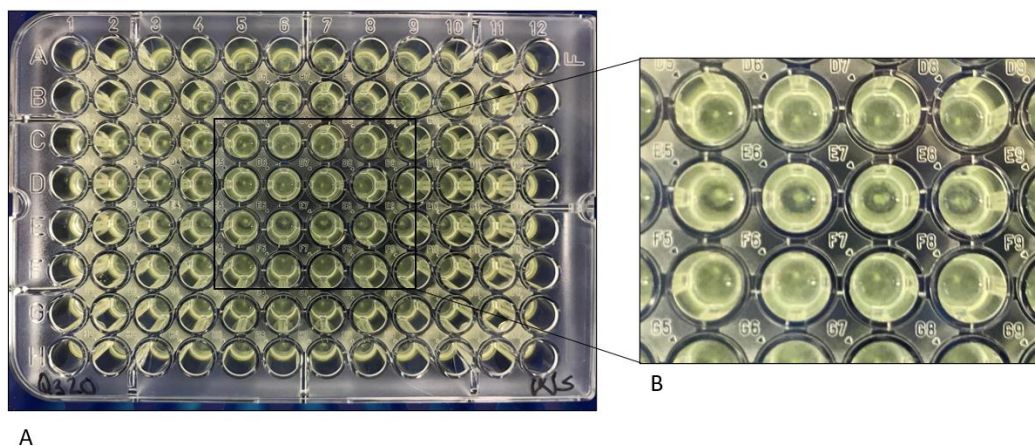
Figure 3-1 Discovery of quercetin precipitation from individual wells. (A) Whole plate view of plate screening W5. (B) Close up view of wells E5 to G9. In the centre of each well there is a clear deposit of quercetin in all wells.

3.3.4 Protocol 2: controlling for the precipitation of quercetin during the broth dilution screening protocol

To attempt to determine the conditions which caused the precipitation of quercetin, a plate was set up containing MHB plus the phytochemical at the concentration used for screening with and without bacteria and then left incubating for 18 hours at 37°C. There was no visible precipitation of any phytochemical in this experiment despite continued precipitation in the screening plates (Figure 3-2).
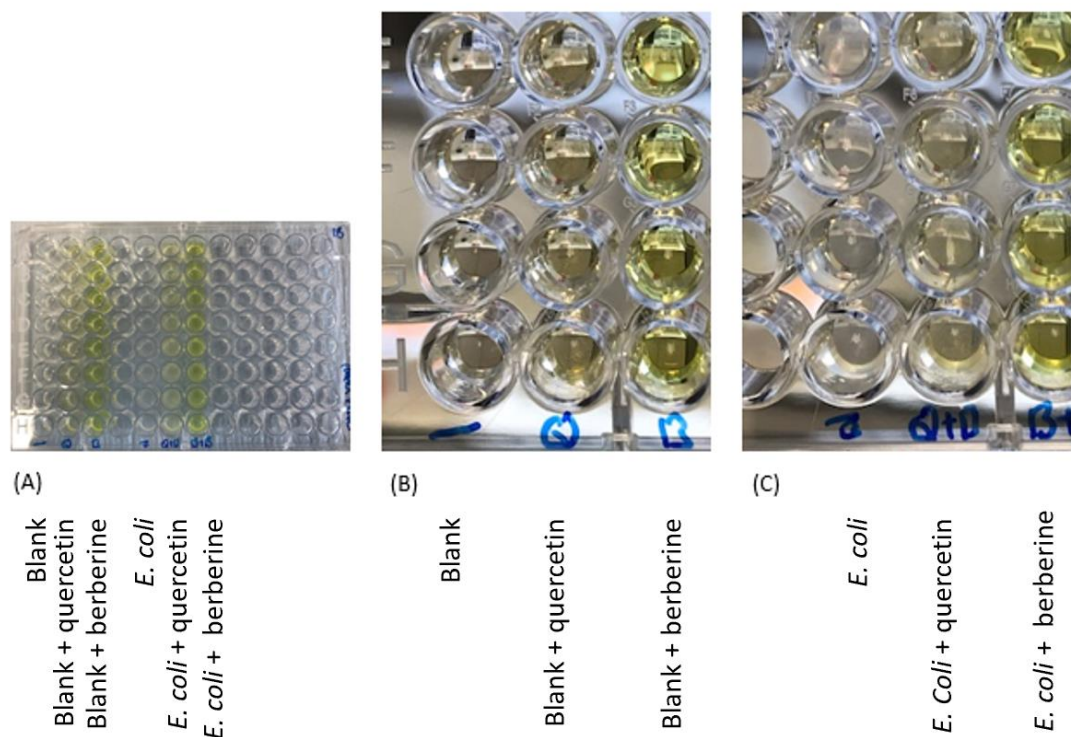
Figure 3-2 Testing to determine the reason for the precipitation of quercetin in the screening assay (A) Whole plate (B) Phytochemicals (C) Phytochemicals + EPI300 E. coli. In quercetin wells (marked Q and Q+B (for quercetin and bacteria) there is no precipitation.

3.3.5 Protocol 2: development of an equation-based method for controlling the impact of quercetin precipitation on the broth dilution screening protocol

To account for noticeable precipitation of quercetin during the functional screen, a theoretical equation which would control for this precipitation was designed. To control for the occurrence of precipitation in these experiments, an equation was designed which would be applied to the OD_{600} data from the screening procedure. The equation accounts for both growth, and precipitation, with a high cut off point to reduce the chance of false positives (Equation 1).Any OD_{600} value over 0.5 for an individual well after the application of this equation was considered a positive hit and taken forward to second stage screening.

3.3.6 Protocol 2: results from the first stage screening of the broth dilution screening protocol

The number of isolates screened, and those that presented resistance to one of the phytochemicals (known as a positive hit) are presented in. The number of positive isolates showing resistance to 320 μg/ml of quercetin was 37, or around 1 in 244, which is about 1 in every 2.5 96-well library plates. The number of positive isolates showing resistance to 320 μg/ml of berberine was 31, around 1 in 291, which is about 1 in every 3 library plates (Table 3-2).

Table 3-2 Overall number of isolates screened during the end point primary screening protocol, and the number of positive isolates showing resistance to 320 μg/ml of berberine, or quercetin Followed by the number of isolates remaining after every step of the screening protocol.

	Number of quercetin resistant isolates	Number of Berberine resistant Isolates	Total number of isolates screened
Primary Screen	37	31	9024
Secondary Screen	27	21	-
Tertiary Screen	20	19	-
Quaternary Screen	8	4	-

3.3.7 Protocol 2: development and outcome of a second stage screening procedure for protocol 2 using MIC analysis.

With concerns over the risks of false positives due to the precipitation of quercetin potentially obscuring the true OD_{600}, a second stage screen was developed. Any isolates that displayed resistance to one of the phytochemicals (positive hits) from the first stage screening underwent standard broth dilution MIC testing protocol (Chapter 2.13.1), to confirm that the isolate was indeed phytochemical resistant. Ten of 37 isolates (27%) of positive isolates showing resistance to 320 μg/ml of quercetin were lost at this stage and 10

of 31 isolates (33%) of positive isolates showing resistance to 320 µg/ml of berberine were lost at this stage (Table 3-2).

3.3.8 Protocol 2: development and outcome of a third stage screening procedure for protocol 2 using transformation and subsequent MIC analysis.

After determination that positive hits from the primary screening protocol displayed resistance to the respective phytochemical via MIC analysis, a third stage screening protocol was conducted. The third stage screening protocol was used to determine if the genes which encoded for proteins that led to resistance to the phytochemical were carried upon metagenomic insert on the plasmid. The pCC1BAC plasmids containing the inserts were extracted, and subsequently transformed into NEB5α (New England Bioscience, UK) (Chapter 2.15). The newly transformed bacteria underwent standard broth dilution MIC testing protocol (Chapter 2.13.13.3.8) to confirm that the resistance was plasmid mediated. After undergoing third stage screening 7 of 27 (26%) of positive isolates showing resistance to 320 µg/ml of quercetin were lost at this stage and 2 of 21 isolates (9%) of positive isolates showing resistance to 320 µg/ml of berberine were lost at this stage , when compared to positive hits from the second stage screening protocol (Table 3-2).

3.3.9 Protocol 2: quaternary screening: characterisation of plasmids from the metagenomic library isolates that displayed resistance to either phytochemical

Isolates that displayed resistance to either quercetin or berberine after third stage screening underwent end sequencing using the pCC1BAC/EPIFOS forward and reverse sequence primers. This was to determine which, if any, of the sequence inserts contained bacterial DNA. Eight of 20 (40%) of positive isolates showing resistance to 320 µg/ml of quercetin contained inserts of bacterial origin. Four of 19 (22.5%) of positive isolates showing resistance to 320 µg/ml of berberine contained inserts of bacterial origin. (Table 3-2). The isolates

showing resistance to either berberine or quercetin that contained a plasmid insert with a

bacterial origin are listed in Table 3-3.

*Table 3-3 Characterised strains from the protocol one screening procedure of the metagenomic library including the strain designation, the nature of the phytochemical tolerance element, the closest homologous species, ascension number and mapped insert location. * Indicates a sample for which only the forward or reverse end primer sequence is available. $^\varphi$ Indicates a sample for which both the forward and reverse sequence were available but mapped to separate locations on the genome.*

Strain Name	Selective compound	Closest Homologous Species	Ascension Number	Mapped location of insert (predicted)	Predicted size of Insert (bp)
V5H10	Quercetin	*Prevotella histolitica F0441*	CP72386.1	Chromosome 2 342032 – 355402	13,370
R1H3	Quercetin	*Prevotella jejuni F0106*	CP072365.1	Chromosome 1291767 - 1418766	126,999
J4H1	Quercetin	*Veillonella sp. S12025-13*	AP022322.1	Complete Genome 187391-197318	9,927
S11E1	Quercetin	*Veillonella parvula NCTC 11810*	LT906445.1	Chromosome 1 15522272 -? *	Unknown
T0E6	Quercetin	*Prevotella nigrescens FDAARGOS_1486*	CP082842.1	Chromosome 42373 – 68339	25,966
V2F12	Quercetin	*Prevotella sp. Oral taxon 475 strain F0059*	CP072334.1	Chromosome 1467400-1504169	36,769
Y2H1	Quercetin	*Veillonella nakazawae T1-7*	AP022321.1	Complete genome DNA 2033619 - 2056950	23,331
J4H3	Quercetin	*Prevotella dentalis DSM 3688*	CP003368.1	Chromosome 1 404352 -? *	Unknown
I10H5	Berberine	*Prevotella histolitica F0441*	CP72367.1	Chromosome 1 1517016 – 1525131	8,115
X2H5	Berberine	*Prevotella histolitica F0441*	CP72367.1	Chromosome 1 428334-466222	37,888
D0D12	Berberine	*Aggregatibacter sp. 2125159857*	CP072548.1	32470 =/=$^\varphi$ 42806	Unknown
G0B8	Berberine	*Prevotella histolitica F0411*	CP72367.1	Chromosome 1 1959020-1982471	23,451

3.3.10 Protocol 2: transposon mutagenesis of the first two positive hits from protocol 2 (I10H5 and V5H10)

After determination that the inserts which conferred resistance to the plant metabolites were of bacterial origin, transposon mutagenesis was conducted on the first two positive hits to come out of the functional screening pipeline. Transposon mutagenesis was conducted to determine which genes on the insert conferred the phytochemical tolerant phenotype. These two isolates were I10H5, a berberine resistant isolate, and V5H10 a quercetin resistant isolate.

The extracted plasmids first underwent transposon mutagenesis as explained in the materials and methods section, before being transformed into NEB5α. The grown transformants were then picked onto new plates and grown again for 24 hours before being stored in 96 well plates in glycerol.

Following transposon mutagenesis, the NEB5α isolates containing mutated pCC1BAC plasmids were replicated into inhibitory concentrations of the respective phytochemicals to which they were resistant. Figure 3-3 displays the growth of these isolates after 18 hours at 37°C. Six inserts with tolerance to 320 µg/ml of either berberine or quercetin which had undergone transposon mutagenesis lost their phytochemical tolerant phenotype, because of the mutagenesis. After propagation of the isolates containing these mutated inserts onto agar, only 4 and 2 isolates grew, respectively.

I10H5 (Plate 3)	1	2	3	4	5	6	7	8	9	10	11	12
A	0.177	0.242	0.2	0.183	0.227	0.063	0.254	0.187	0.322	0.237	0.12	0.145
B	0.016	0.22	0.124	0.219	0.002	0.127	0.179	0.181	0.112	0.205	0.092	0.18
C	0.264	0.111	0.219	0.203	0.188	0.144	0.108	0.151	0.248	0.149	0.103	0.181
D	0.251	0.211	0.127	0.211	0.206	0.144	0.132	0.155	0.116	0.152	0.229	0.199
E	0.257	0.11	0.228	0.164	0.191	0.037	0.247	0.169	0.127	0.2	0.121	0.14
F	0.271	0.254	0.174	0.212	0.187	0.257	0.142	0.009	0.141	0.159	0.104	0.274
G	0.214	0.182	0.196	0.227	0.307	0.25	0.218	0.26	0.432	0.352	0.417	0.111
H	0	0	0.002	0	0.002	0.001	0.004	0.001	0	0	0.001	0.005

V5H10 (Plate 3)	1	2	3	4	5	6	7	8	9	10	11	12
A	0.263	0.366	0.278	0.279	0.344	0.271	0.353	0.265	0.203	0.283	0.283	0.382
B	0.298	0.301	0.371	0.235	0.252	0.023	0.193	0.206	0.103	0.194	0.22	0.308
C	0.291	0.324	0.226	0.286	0.297	0.24	0.257	0.237	0.001	0.213	0.193	0.279
D	0.294	0.199	0.206	0.242	0.285	0.281	0.25	0.315	0.334	0.224	0.171	0.275
E	0.285	0.268	0.291	-0.001	0.268	0.241	0.247	0.087	0.025	0.282	0.241	0.403
F	0.27	0.24	0.304	0.31	0.266	0.295	0.267	0.287	0.287	0.374	0.381	0.218
G	0.305	0.292	0.226	0.326	0.263	0.262	0.268	0.226	0.338	0.344	0.296	0.319
H	0.197	0.281	0.386	0.35	0.227	0.06	0.23	0.198	0.229	0.319	0.286	0.432

Figure 3-3 Growth of NEB5α isolates containing mutated pCC1BAC plasmids containing either a I10H5 and V5H10 insert after replication into MHB supplemented with either 256 µg/ml of berberine or quercetin. Isolates marked in green and yellow did not grow after replication suggesting the mutagenesis had interrupted the resistance determinant. Row H on the I10H5 plate had no isolates and as such is marked in red. Isolates marked green were able to be propagated onto agar, isolates in yellow were not.

3.3.11 Protocol 2: whole Genome Sequence Analysis of V5H10 and I10H5

The whole genome sequence of EPI300 containing the pCC1BAC with either the I10H5 or V5H10 inserts were constructed using short read analysis at microbesNG™. Both plasmid inserts were contained on single contigs with no breaks, flanked by regions of the pCC1BAC plasmid. The plasmids were locatable by using the pCC1BAC primer sequences.

I10H5 was a 10,100 bp long insert that mapped to *P. histolitica* F0411 chromosome 1 (1517016 – 1523418 - 1526229) (CP72368.1) (Figure 3-4). This was the length and mapping

expected from the previous end sequencing experiments (Table 3-3). The insert contained 7

predicted protein encoding genes according to both Prokka and blastx analysis (Table 3-4).

Table 3-4 Translated protein names of gene encoding sequences present on the I10H5 plasmid. Given are the names of the translated proteins, length of the genes (in base pairs) and the method of gene identification using either Prokka or blastx analysis.

Translated protein name	Length of gene (bp)	Method of gene identification	
		Prokka	blastx
SGNH/GDSL hydrolase family protein	750		x
MBOAT family protein	1479		x
DUF4251 domain-containing protein	564		x
Hypothetical protein	456		x
Xanthine permease	1344	x	
Xanthine phosphoribosyltransferase	573	x	
TonB-dependent receptor	1866	x	
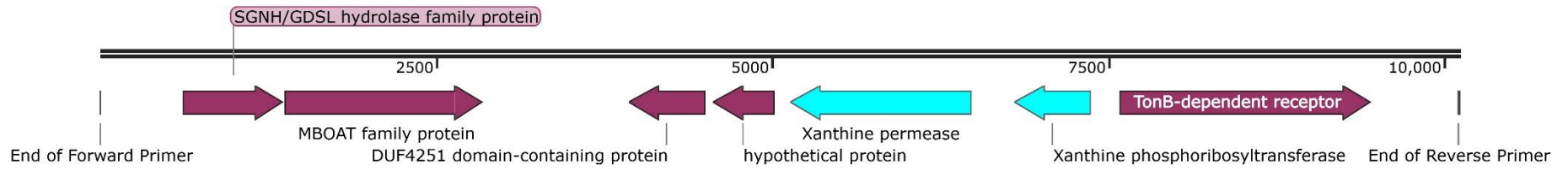
Figure 3-4 Bacterial insert contained on plasmid I10H5. The insert was 10,110 base pairs in length and contained an SGNH/GDSL Hydrolase, MBOAT, DUF4251 DCP, Hypothetical Protein, Xanthine/Purine Permease, Xanthine phosphoribosyltransferase and TonB dependant receptor gene sequences. It maps to nucleotides 1517016 – 1523418 Prevotella histolitica strain F0411 chromosome 1. The two members of the purine degradation pathway are highlighted in blue, all other open reading frames are in purple

V5H10 was a 13,572 bp long insert that mapped to *P. histolitica* F0411 chromosome 2 (342032 – 355604) (CP072368) (Figure 3-5). This was the length and mapping expected from the previous end sequencing experiments (Table 3-3). The insert contained 9 protein encoding genes according to both Prokka and blastx analysis (Table 3-5), and 2 tRNA encoding sequences.

Table 3-5 Translated protein names of gene encoding sequences present on the V5H10 plasmid. Given are the names of the translated proteins, length of the genes (in base pairs) and the method of gene identification using either Prokka or Blastx analysis.

Translated protein name	Length (bp)	Method of gene identification	
		Prokka	Blastx
Di-tripeptide/cation symporter	1512	x	
Exinuclease subunit A	2859	x	
Hypothetical protein 1	357		x
Hypothetical protein 2	672		x
Nitroreductase family protein	510	x	
3'-5' oligoribonuclease A	1038	x	
Hypothetical protein 3	912		x
Hypothetical protein 4	207		x
Peptidoglycan D, D-transpeptidase MrdA	1143	x	

The insertion sites of the transposon mutagenesis are shown in Figure 3-5 and elaborated upon in Table 3-6. When using the seqE and seqW primers to determine the location of these insertions on the plasmid, it was discovered that the sequences obtained from all the transposon primers, were identical to sequences from the V5H10 insert.

It was determined that due to a laboratory mistake, the transposon mutagenesis experiment had only been conducted on the V5H10 insert, and not the I10H5 insert. To reconfirm the

phenotype of the metagenomic isolates after this mistake, the MIC of both isolates to each

phytochemical were repeated.

Table 3-6 Location and function of the transposons inserted into V5H10 through the transposon mutagenesis procedure. The name of the transposon, its insertion site, and the location of the gene interruption (if existing) is given.

Transposon Name	Insertion Site (bp)	Gene interruption
ΔTnA6	12,963	No, it does not interrupt an open reading frame
ΔTnB1	11,018	Yes: Interrupts gene encoding hypothetical protein 4 at position 74 from the 5' end.
ΔTnE6	3059	Yes: Interrupts Exinuclease ABC subunit A at position 849 from the 3' end.
ΔTnF8	10,783	Yes: interrupts the second tRNA encoding sequence at position 10 from the 5' end
ΔTnE8	12,970	No, it does not interrupt an open reading frame
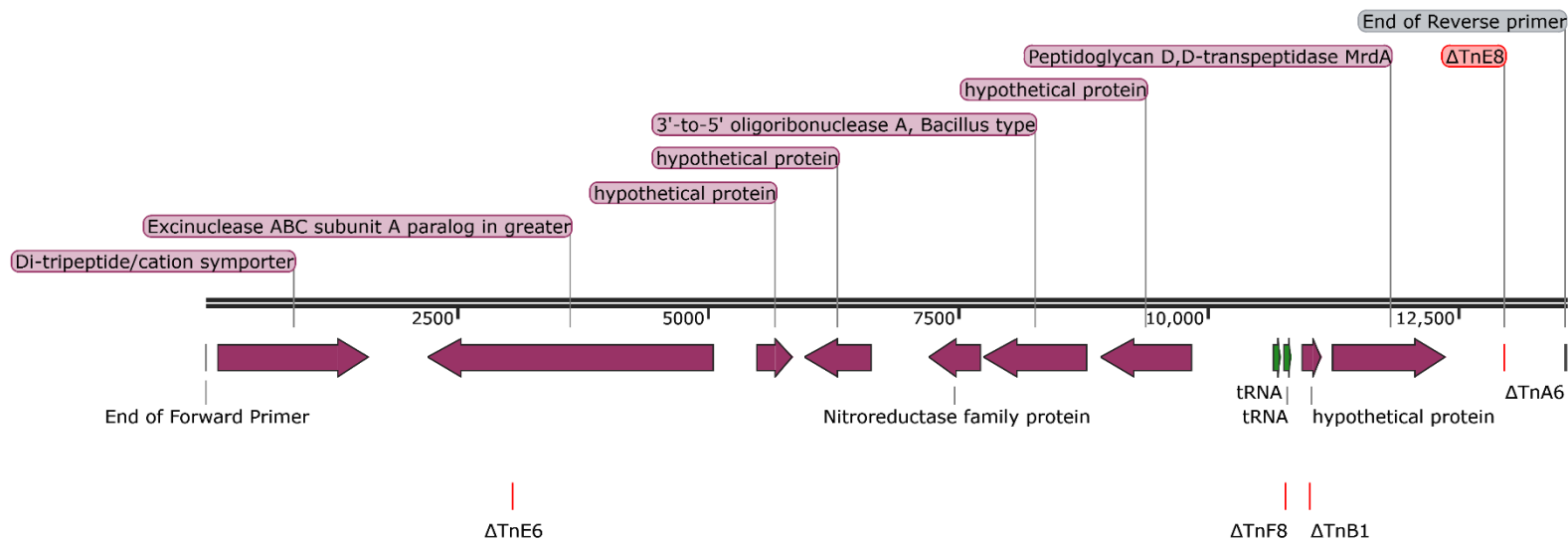
Figure 3-5 Bacterial insert contained on plasmid V5H10. The insert was 13,368 base pairs in length and contained a Di-tripeptide/cation symporter, Exinuclease subunit A, 4 hypothetical proteins, nitroreductase family protein, a 3'-5' oligoribonuclease bacillus type, two tRNA-CTT and a penicillin binding protein. It maps to nucleotides 342032 – 355604 of Prevotella histolitica strain F0411 chromosome 2. All transposon mutagenesis insert sites are given as ΔTn, followed by the indication of the well from which they were located.

3.3.12 Protocol 2: change in expected minimum inhibitory concentrations of pCC1BAC with and without metagenomic inserts to the phytochemicals quercetin and berberine as demonstrated using the MIC protocol

EPI300 *E. coli* containing an empty pCC1BAC vector, pV5H10, and pI10H5 underwent a second MIC analysis, to reconfirm phytochemical tolerance phenotype after the transposon mutagenesis experiment. All isolates had the same level of resistance to both plant metabolites (Table 3-7).

Table 3-7 MICs of the I10H5 and V5H10 isolates from the metagenomic screening procedure, alongside the library construct. The first two repeats showed every isolate having a resistance at 256 and the third showing every isolate had a resistance of 128 μg/ml.

Strain	Quercetin MIC (μg/ml)	Berberine MIC (μg/ml)
EPI300 *E. coli* containing an empty pCC1BAC	256-128*	256-128*
V5H10	256-128*	256-128*
I10H5	256-128*	256-128*

3.3.13 Protocol 2: change in expected minimum inhibitory concentrations of pCC1BAC with and without metagenomic inserts to the phytochemicals quercetin and berberine as demonstrated using the MIC protocol with continuous monitoring

MICs were then conducted using the same protocol, but with 24-hour growth curve analysis on the CLARIOstar® microplate reader. All isolates grew at 256 μg/ml of quercetin and 64 μg/ml berberine. This mirrored the result of the previous endpoint MIC experiments.

Further MIC analysis using continuous reading was conducted for all isolates. These experiments demonstrated that all isolates were inhibited at 512 μg/ml quercetin and had reduced growth at 256 μg/ml. The presence of either insert did not alter the level of resistance to quercetin (Figure 3-7).

The EPI300 isolate containing the I10H5 insert was able to grow, albeit at a reduced level in 128 µg/ml of berberine. However, 256 µg/ml of berberine was inhibitory to all isolates (Figure 3-6).
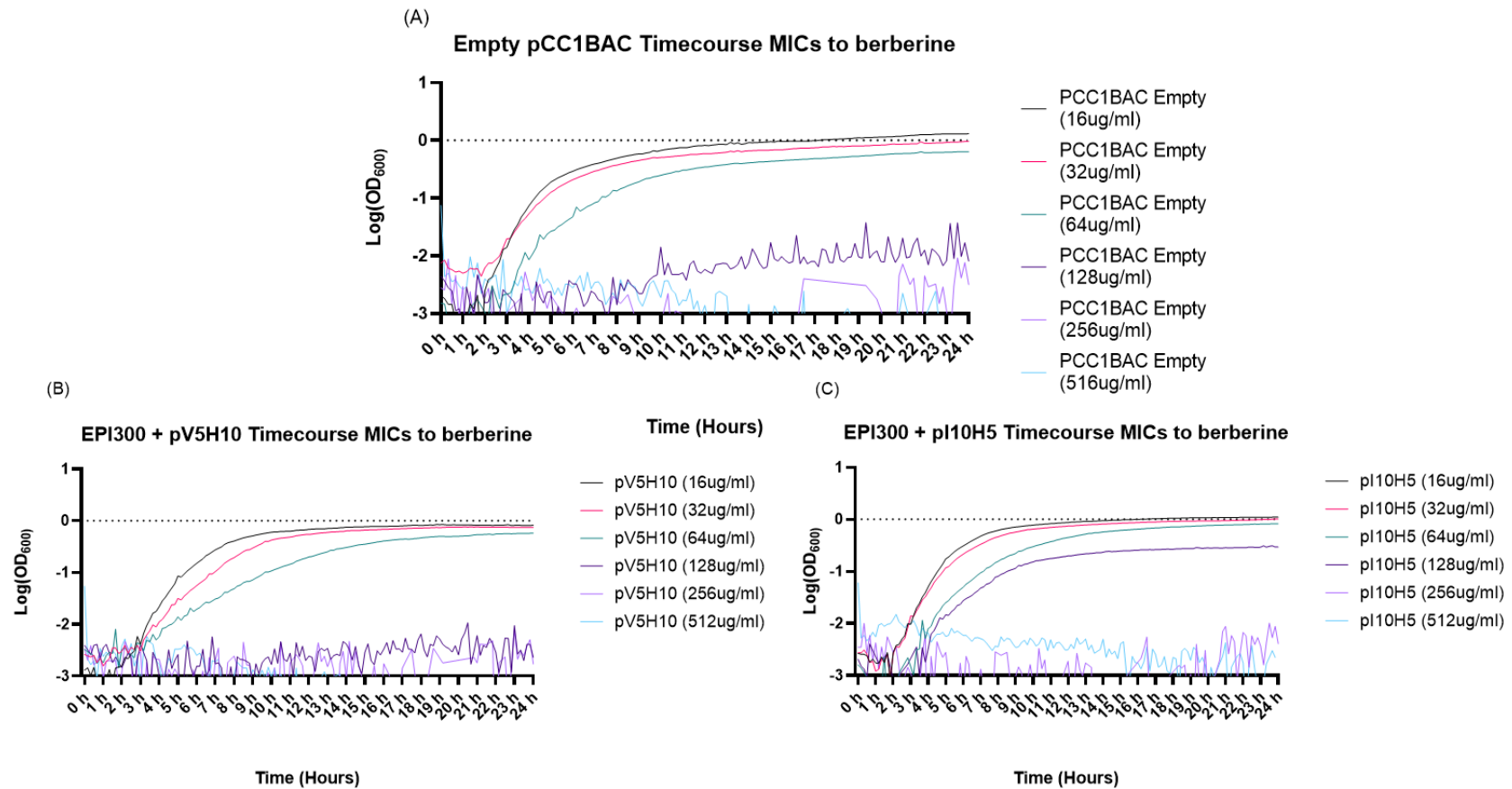
Figure 3-6 Growth curves of EPI300 isolates containing pCC1BAC plasmids with resistance inserts (V5H10 (B) or I10H5 (C)), or no insert (A), over 24 hours at 37C, 200 rpm (collation of 3 biological repeats and 9 technical repeats) in the presence of berberine from 16 – 512 μg/ml. All isolates were inhibited by 128 μg/ml of berberine except for the EPI300 isolate containing pI10H5 which grew at in 128 μg/ml of berberine at a reduced rate (C, purple line).

(A)

Empty pCC1BAC Timecourse MICs to quercetin

- pCC1BAC (16ug/ml)
- pCC1BAC (32ug/ml)
- pCC1BAC (64ug/ml)
- pCC1BAC (128ug/ml)
- pCC1BAC (256ug/ml)
- pCC1BAC (512ug/ml)

(B)

EPI300 + pV5H10 Timecourse MICs to quercetin

- pV5H10 (16ug/ml)
- pV5H10 (32ug/ml)
- pV5H10 (64ug/ml)
- pV5H10 (128ug/ml)
- pV5H10 (256ug/ml)
- pV5H10 (512ug/ml)

(C)

EPI300 + pI10H5 Timecourse MICs to quercetin

- pI10H5 (16ug/ml)
- pI10H5 (32ug/ml)
- pI10H5 (64ug/ml)
- pI10H5 (128ug/ml)
- pI10H5 (256ug/ml)
- pI10H5 (512ug/ml)

Figure 3-7 Growth curves of EPI300 isolates containing pCC1BAC plasmids with resistance inserts (V5H10 (B) or I10H5 (C)), or no insert (A), over 24 hours at 37C, 200rpm (collation of 3 biological repeats and 9 technical repeats) in the presence of quercetin from 16 – 512 µg/ml. All isolates were inhibited by 256 µg/ml of quercetin.

3.3.14 Protocol 2: quercetin precipitates out of the media at a level which interfered with the analysis of bacterial growth using optical density readings

As a result of quercetin precipitating causing readings at OD_{600} that could be equated to bacterial growth, an experiment was designed to evaluate the precipitation of berberine and quercetin in different bacterial growth media. It was noticed that quercetin precipitated in both media but berberine did not. As MHB was the media used for the screening and MIC protocols, it was decided to move forward evaluating only berberine (Figure 3-8).
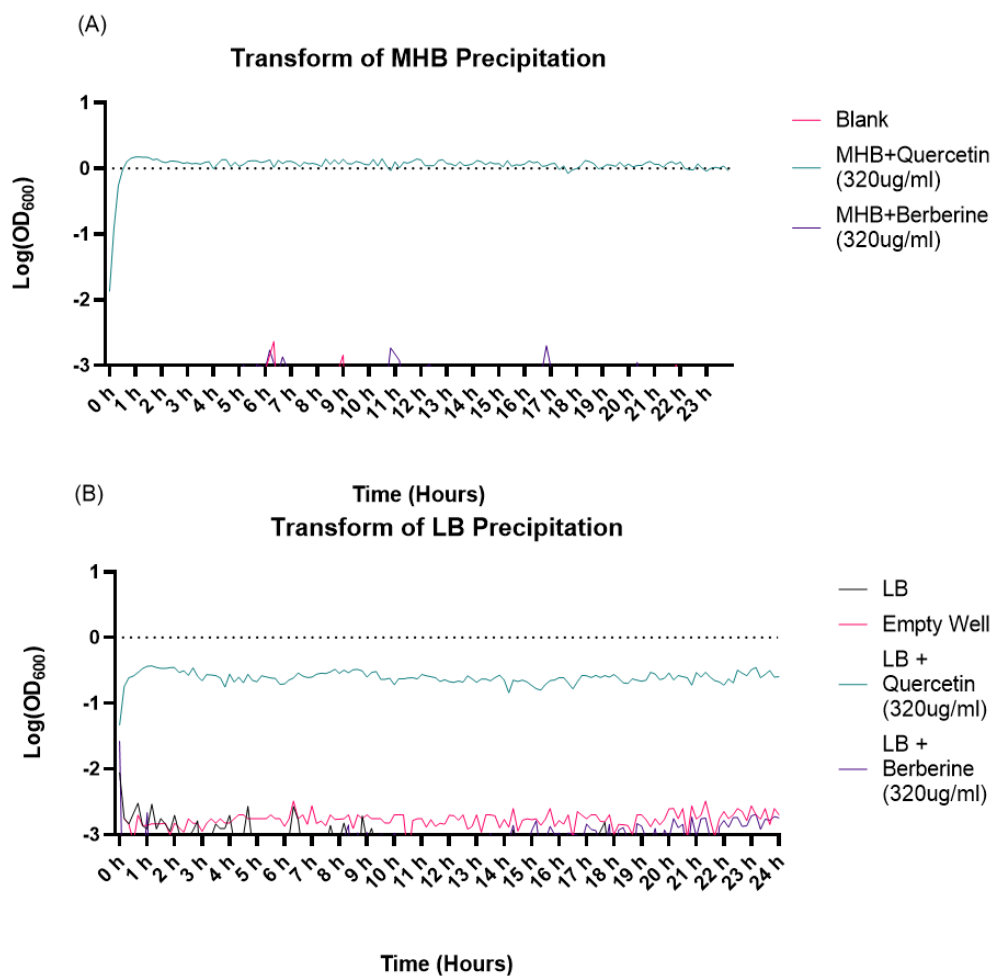
Figure 3-8 Time course assays of the precipitation of plant metabolites quercetin and berberine in Muller-Hinton broth (A) and lysogeny broth (B) over 24 hours at 37°C, 200 rpm shaking. q*uercetin precipitated in both media (blue line) at around 1.5 OD_{600} in lysogeny broth (A) and 0.4 in Muller-Hinton broth (B). The empty well, LB, and LB + berberine lines are all at 0.0 and are covered by the x axis.*

3.3.15 Protocol 2: analysis of isolates that passed through quaternary screening using continuous monitoring in 320 µg/ml of berberine

Isolates that passed through quaternary screening stage screening were subsequently assessed at 320 µg/ml of berberine with continuous reading on the Clariostar plate reader. All isolates grew at this concentration except for EPI300 *E. coli* without the pCC1BAC plasmid (Figure 3-9).

Growth of Lead Isolates and EPI300 *E. coli* with and without empty pCC1BAC over 24 hours in the presence of 320 ug/ml of berberine in MHB
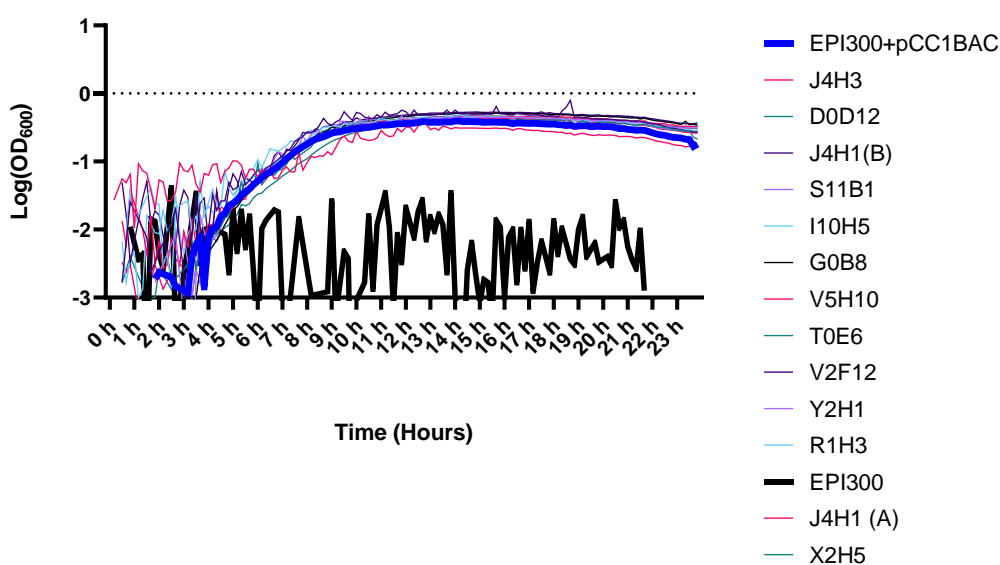
Figure 3-9 Growth of al isolates that passed through quaternary stage screening *and EPI300 E. coli with and without pCC1BAC over 24 hours in the presence of 320 µg/ml of berberine in MHB. All isolates except for EPI300 (the bold black line) grew in this concentration of berberine. This included EPI300 containing the empty pCC1BAC plasmid (the bold blue line).*

3.3.16 Protocol 3: serial dilution analysis of EPI300 *E. coli* containing an empty pCC1BAC vector or pI10H5 or pV5H10 using continuous monitoring

The isolates that had already undergone whole genome analysis (I10H5 and V5H10) underwent another round of MIC analysis on the CLARIOstar plate reader alongside EPI300 *E. coli* containing an empty pCC1BAC plasmid using a serial dilution from 2 mg/ml to 62.5 µg/ml of berberine. All isolates showed reduced growth at 0.5 mg/ml and no growth at 1

mg/ml (Figure 3-10). The minimum selective concentration (MSC) is therefore between 0.25 and 0.5 mg/ml.

(A)

(B)

(C)
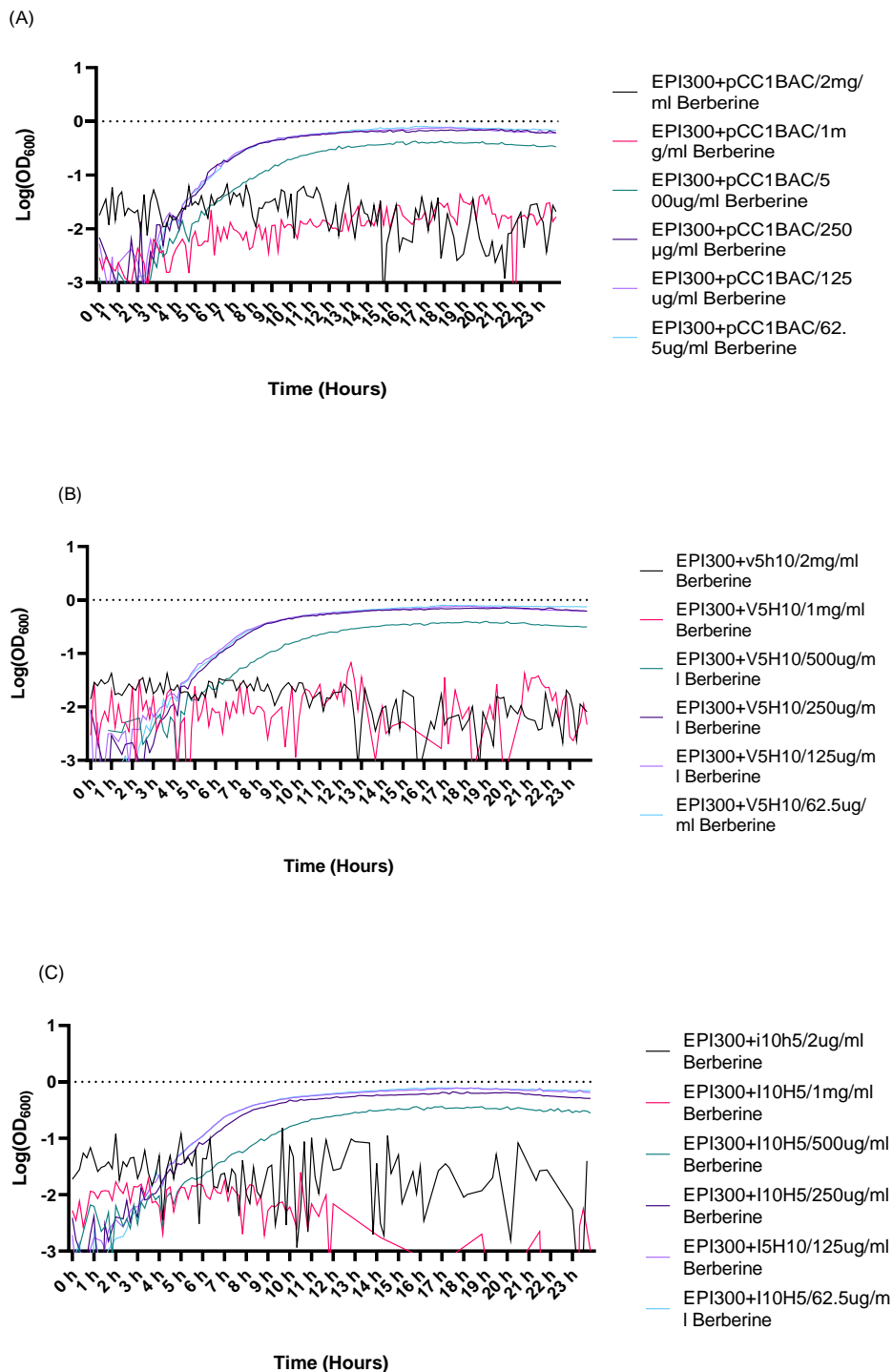
Figure 3-10 Time course analysis of the growth of EPI300 E. coli plus empty pCC1BAC (A), or pV5H10 (B), or pI10H5 (C) against a doubling dilution of beberine in MHB from 2 mg/ml to 62.5 µg/ml. All isolates had reduced growth at 500 µg/ml of berberine and growth was completely inhibited at 1 mg/ml and 2 mg/ml of the pytochemical.

3.3.17 Protocol 2: reassessment of isolates that passed through quaternary screening of protocol 2 using 1 mg/ml of berberine and continuous monitoring.

No isolates that passed through quaternary stage screening grew in 1 mg/ml of berberine, including *E. coli* EPI300 with or without pCC1BAC. As such they were deemed to be false positives.

3.3.18 Protocol 3: screening of the metagenomic library using protocol 3

Under this new protocol (Chapter 3.2.3.4) 2688 isolates were screened resulting in 1 positive hit (Figure 3-11).

Berberine (1mg/ml) Plate H4
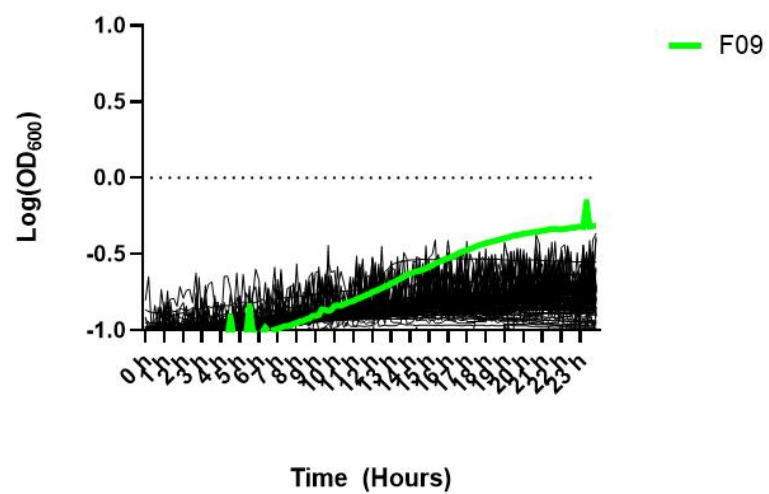
(A)

(B)

Figure 3-11 Positive hit H4F9. (A) Graphical representation of all growth curves from the H4 plate when selected with 1mg/ml of berberine over 24 hours, well F9 growth highlighted in green. Growth in well F9 was above plate background. (B) Picture of plate H4 after 24 hours growth in 1 mg/ml of berberine with well F9 highlighted in red. The well is cloudier than the rest of the wells, indicating growth.

3.3.19 Protocol 3: minimum inhibitory concentration analysis of the positive hit H4F9 from protocol 3 screening of the metagenomic library.

H4F9 underwent two rounds of MIC analysis, the first was a serial dilution from 2 mg/ml of berberine. In two of the biological repeats, a single technical repeat would grow in 1 mg/ml of berberine. No isolates of *E. coli* EPI300 plus an empty pCC1BAC vector grew during these experiments (Table 3-8).

Table 3-8 Minimum inhibitory concentrations and minimum selective concentrations of H4F9 compared to EPI300 E. coli containing an empty pCC1BAC plasmid. MIC conditions set as a serial dilution starting from 2 mg/ml, colony counts included.

	H4F9			EPI300 + Empty pCC1BAC		
	MSC (mg/ml)	MIC (mg/ml)	Colony Count	MSC (mg/ml)	MIC (mg/ml)	Colony Count
Biological Repeat 1	-	1-2	66	0.25 - 0.5	1	74
Biological Repeat 2	-	1-2	70	0.25 - 0.5	1	70
Biological Repeat 3	-	1	90	0.24 - 0.5	1	90

The second round was a series of simple dilutions from 1 mg/ml down to 0.5mg/ml. H4F9 grew at 1-0.9 mg/ml and EPI300 *E. coli* containing an empty pCC1BAC vector grew at 0.8-0.9 mg/ml of berberine (Table 3-9).

Table 3-9 Minimum inhibitory concentrations of H4F9 compared to EPI300 E. coli containing an empty pCC1BAC plasmid. MIC conditions set as a series of simple dilutions, from 1 mg/ml to 0.5 mg/ml (decreasing by 0.1 mg/ml in each dilution), colony counts included.

	H4F9		EPI300 + Empty pCC1BAC	
	MIC (mg/ml)	Colony Count	MIC (mg/ml)	Colony Count
Biological Repeat 1	0.9	39	0.8	61
Biological Repeat 2	1	72	0.8	54
Biological Repeat 3	1	58	0.9	51

3.3.20 Protocol 3: whole genome sequence analysis of H4F9

The H4F9 insert was 25,866 base pairs in length and mapped to the genome of *Veillonella nakazawae T1-7* (AP022321.1) between bases 1179146 and 1195608 (Figure 3-12). The insert contained 25 predicted protein encoding genes as determined by Prokka and blastx analysis (Table 3-10).

*Table 3-10 Translated protein names of open reading frames present on the H4F9 plasmid. Given are the names of the translated proteins, length of the genes (in base pairs) and the method of gene identification using either Prokka or blastx analysis. * Open reading frames discussed in the discussion section*

Translated protein code	Name	Length (bp)	Prokka	blastx
MDP*	Membrane dipeptidase	585		x
gmhA1	Phosphoheptose isomerase 1	570	x	
hldE	Bifunctional protein	1479	x	
hldD	ADP-L-glycero-D-manno-heptose-6-epimerase	966	x	
gmhB	D-glycero-beta-D-manno-heptose-1,7-bisphosphate 7-phosphatase	495	x	
gtf9*	Glycosyltransferase family 9 protein	1020		x
rfaQ	Lipopolysaccharide core heptosyltransferase	1041	x	
polC	DNA polymerase III PolC-type	984	x	
apeA	Putative M18 family aminopeptidase 1	1392	x	
hp*	Hypothetical protein	378		x
abcSBP_1*	ABC transporter substrate binding protein 1	978		x
abcSBP_2*	ABC transporter substrate binding protein 2	978		x
abcTP*	ABC transporter permease	873		x
yxdL	ABC transporter ATP-binding protein YxdL	798	x	
rpsO	30S ribosomal protein S15	267	x	
pnp	Polyribonucleotide nucleotidyltransferase	2070	x	
dut	Deoxyuridine 5'-triphosphate nucleotidohydrolase	450	x	
act	Methanol dehydrogenase activator	534	x	
deob	Phosphomannomutase	1173	x	
afa	AAA family ATPase	2205	x	
rpsT	30S ribosomal protein S20	261	x	
polA	DNA polymerase I	2262	x	
coaE	Dephospho-COA kinase	615	x	
slt	Soluble lytic murein transglycosylase	555	x	
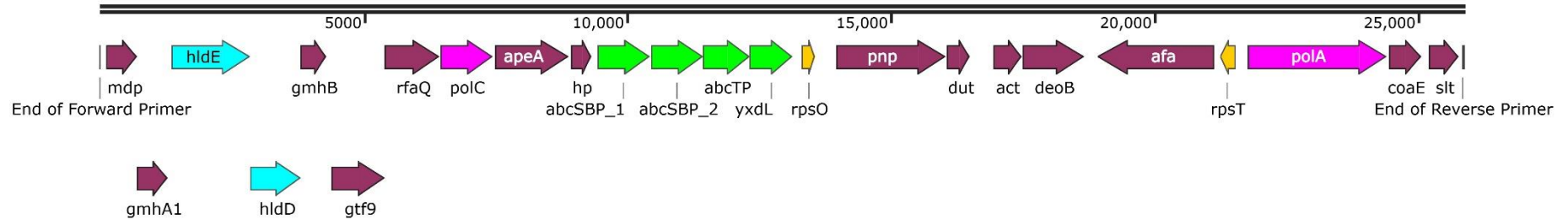
Figure 3-12 Bacterial insert contained on plasmid H4F9. The insert was 25,866 base pairs in length and contained 25 protein encoding genes. These are: a membrane dipeptidase, Phosphoheptose isomerase 1, a bifunctional protein (hld family: highlighted in blue), ADP-L-glycero-D-manno-heptose-6-epimerase (hld family: highlighted in blue, D-glcero-beta-D-manno-heptose-1,7-biphosphate 7-phosphatase, glycosyltransferase family-9-protein, lipopolysaccharide core heptosyltransferase, DNA polymerase III PolC-type (pol family: highlighted in pink), a putative M18 family amino peptidase 1, a hypothetical protein, ABC transporter substrate binding proteins 1 & 2 ABC transporter family: highlighted in green,, ABC transporter permease (ABC transporter family: highlighted in green), ABC transporter ATP-binding protein yxdL ABC transporter family: highlighted in green), 30S ribosomal protein S15 (rps family: highlighted in yellow), Polyribonucleotide nucleotidyltransferase, methanol dehydrogenase activator, Phosphomannomutase, AAA family ATPase, 30S ribosomal protein s20 (rps family: highlighted in yellow), a DNA polymerase I (pol family: highlighted in pink), Dephospho-COA kinase, and soluble lytic murein transglycosylase. The bacterial insert maps to nucleotides 1179146-1195608 of the Veillonella nakazawae T1-7 DNA complete genome.

3.4   Discussion

3.4.1   Development of protocol 2: screening of the oral metagenomic library using broth dilution and endpoint analysis

In this chapter, a screening procedure to detect resistance to the phytochemicals quercetin and berberine was developed.

The initial attempt to screen the metagenomic library using phytochemicals dissolved in agar was unsuccessful. Agar based screening has been previously used in metagenomic screening to identify proteases (Neveu et al., 2011), esterase's (Gao et al., 2016), lipases (Kouker & Jaeger, 1987), cellulases (Wang et al., 2012) and antimicrobial resistance genes (Reynolds et al., 2016) and it is the most high throughput and simple way of conducting functional screening (Ngara & Zhang, 2018).

It is possible that the phytochemicals selected may have been active in another agar, or that other phytochemicals may have retained activity when dissolved in agar. Examples include extractions of *Hydnora africana* (also known as the Jackal food plant) which was successfully used to inhibit the growth of *E. coli, Salmonella typhimurium, Enterococcus faecalis, and Pseudomonas aeruginosa,* amongst others (Wintola & Afolayan, 2015), and extractions of the leaves of *Aegle marmelos* (Indian bael) against *Enterobacter aerogenes, Klebsiella pneumoniae, Bacillus cereus, Staphylococcus epidermidis, and Staphylococcus aureus* (Mujeeb et al., 2014) in agar. However, the two specific phytochemicals chosen for this study did not show inhibitory activity in agar, necessitating an alternative screening methodology.

The second protocol developed used a liquid-broth based functional screen. Liquid-broth based functional screens have also been used to select for genes encoding for proteins with a variety of functions such as esterase's from an oil reservoir metagenome (Lewin et al., 2016). A liquid-broth based screen was previously used to screen this metagenomic library for resistance to the antiseptics triclosan and CTAB (Reynolds et al., 2016).

To account for noticeable precipitation of quercetin during the functional screen, a theoretical equation which would control for this precipitation was designed. Quercetin precipitation from the media presented a unique problem. Quercetin precipitation is a problem that occurs in multiple industries. Due to acid-hydrolysis during the winemaking process, quercetin precipitates out of the wine, forming a waste product at the bottom, and is dependent upon the specific species of grape used in the winemaking process. The solutions in this case include, oxygenation, wood aging and enzymatic treatment of the wines to prevent precipitation (Gambuti et al., 2020; Valls-Fonayet et al., 2022). Pessoa et al (2018), used quercetin without noted precipitation using tryptic soy agar and tryptic soy broth, however, the maximum concentration used by Pessoa et al (2018), was 125 μg/ml of quercetin (Pessoa et al., 2018).

Quercetins lack of bioavailability presents one of the key problems into its development as a pharmaceutical and contributes to its insolubility in multiple media. Attempts have been made to increase the bioavailability including, nanosuspension (Karadag et al., 2014), co-crystallisation with caffeine, methanol, isonicotinamide, and theobromine dihydrate (Smith et al., 2011), and solid dispersion (Kakran et al., 2011). However these are all time and chemically intensive protocols (Cai et al., 2013) which were outside the remit of this particular study. Further the aim of the study was to explore how environmental quercetin was associated with antimicrobial activity in the environment and these experiments, if conducted, would not have been representative of quercetin in the environment. Quercetin was selected because of the connection it held with previous oral microbiome studies, however in retrospect a further analysis of the ability of phytochemicals to dissolve would have been an essential step for this study.

It is here that I suspect many of the problems encountered during the construction of this screening protocol could be traced back to. These problems include the quercetin

precipitation, and the change in *E. coli EPI300* resistance throughout the course of the experiment. This was unlikely to have occurred due to mutation, as it was represented in every *E. coli* isolate in the library and the controls in later experiments. The replication of bacterial cultures from the original library into the screening plates did not allow room for any controls. This was done to increase the experimental throughput. It is possible that half of the metagenomic library plates been replicated onto the screening plates, and half of the plate left as controls. These controls could have included: blank wells, MHB, MHB plus the phytochemical, MHB plus *E. coli* EPI300 with and without the plasmid, and MHB plus the phytochemical plus *E. coli* EPI300 with and without the plasmid. These controls continually repeated with each metagenomic plate would have certainly given a clearer understanding of how the screen was functioning and indicated early into the development process that there was an issue with the initial MICs to the phytochemicals. However, at that point in development there was little reason to suspect a problem and throughput was prioritised.

Alongside the equation designed to try and account for precipitation, two further stages of the screening procedure were developed to try and avoid false positives. These stages were based upon standard MIC determination protocol as described in Chapter 2.13.1. These stages were designed to ensure the positive hits were in fact more resistant to the phytochemical than the library host containing the empty pCC1BAC, and that the resistant determinant was indeed located on the plasmid insert.

To finalise which inserts would be taken forward for analysis, end sequencing was conducted to determine which gene inserts were bacterial in origin, it was at this stage that we had the largest loss of positive hits, due to the inserts mostly containing DNA of human origin. Eight of 20 (40%) of positive isolates showing resistance to 320 µg/ml of quercetin contained inserts of bacterial origin. Four of 19 (22.5%) of positive isolates showing resistance to 320 µg/ml of berberine contained inserts of bacterial origin (Table 3-2). Thus 60% of all isolates

resistant to quercetin and 77.5% of all isolates resistant to berberine contained inserts of human DNA. This was slightly above the amount that was expected to be lost because of human DNA contamination of the library which was estimated at 40.625% (Reynolds, 2017).

3.4.2 Outcomes of protocol 2: the potential role that genes present on the metagenomic inserts V5H10 and I10H5 may play in antibiotic and phytochemical tolerance

End sequencing determined that two genera were highly represented in the positive hits. These were *Prevotella* species including *histolitica, dentalis, jejuni,* and *nigrescens (*8 of 12) and *Veillonella* species (3 of 12) including *paruva,* and *nakazawae*. The oral microbiome contains over 101 genera (Nasidze et al., 2009), though it is unknown exactly how many bacterial genera are present in this library.

Two inserts V5H10 and I10H5 were taken forward for further analysis. These isolates were the first to come out of the screening pipeline and were taken to the next step while the screening process was still ongoing. Further analysis of the other positive isolates from the library did not reach this stage, as the change in MIC of the library construct was noticed before they reached this point. The change in MIC necessitated a re-evaluation of the screening pipeline.

Both inserts (V5H10 and I10H5) show homology to the genome of *Prevotella histolitica*. *P. histolitica* is a human gut commensal (Shahi et al., 2019) and a facultative oral pathogen that affects both humans and other mammals including horses, causing dental cavities and infections (Shahi et al., 2019). *P. histolitica* can also be a cystic fibrosis colonising pathogen (Sherrard et al., 2013). Within *Prevotella* sp*.* antibiotic resistance is common, with many isolates producing β-lactamases, and tetracycline resistance genes, specifically *tet*(Q) (Sherrard et al., 2013, 2014; Veloo et al., 2019). The V5H10 insert contained the peptidoglycan D, D transpeptidase MdrA which is a known β-lactamase.

The V5H10 insert was a 13,572 bp long insert that mapped to *P. histolitica* F0411 chromosome 2. *Prevotella* species, including *P. histolitica* are well known for having 2 chromosomes, the second smaller chromosome being highly variable between species (Naito et al., 2016). The insert contains genes encoding for: 1) A truncated di-tripeptide/cation symporter 2) Exinuclease subunit A (uvrA), 3) four hypothetical proteins, 4) nitroreductase family protein, 5) A 3'-5' oligoribonuclease A, 6) two tRNA-lyase-CTT, and 7) a peptidoglycan D, D-transpeptidase MdrA.

Exinuclease subunit A is part of the larger UvrA protein complex, UvrA is a nucleotide excision repair protein which binds around the sight of DNA lesions, unwinds and repairs the DNA (Jaciuk et al., 2011; Truglio et al., 2006). UvrA is associated with the acquisition of antimicrobial resistance genes in *Acinetobacter baumannii* (Jaciuk et al., 2011; Norton et al., 2013).

The peptidoglycan D, D-transpeptidase MdrA was of particular interest. This is due to the appearance of genetic modifications to the gene encoding for a similar protein (the L, D-transpeptidase) when *P. aeruginosa* were evolved under the selective pressure of berberine for thirty days, as described in detail in Chapter 5. The appearance of transpeptidases in two separate experiments involving phytochemical selective pressure, via different methodologies, suggests that they may a play a key role in phytochemical tolerance.

Glycopeptides are a class of antibiotics often used as last resort antibiotics, and resistance mechanisms such as D-alanine ligases (Rahman et al., 2020), have been associated with both d-cycloserine resistance in the oral microbiome which may have been due to the selective pressure of quercetin. When run through a blastx for protein alignment the gene was determined to encode for a penicillin-binding protein. This, led to a theory of the synergistic role between quercetin and penicillin resistance. Quercetin has previously demonstrated

synergistic activity with multiple antibiotics including other β-lactams such as amoxicillin (Siriwong et al., 2016; Vipin et al., 2020). Quercetin has also demonstrated anti-β-lactamase activity in other synergistic studies (Siriwong et al., 2016). The β-lactamases are common across *Prevotella* species (Sherrard et al., 2013, 2014).

tRNA-derived fragments are a novel class of non-coding RNA sequences which are not well defined. They can be both simply degraded tRNA, and can function as sRNA (Martinez, 2018).The V5H10 insert contained two tRNA-CTT fragments. Alternative studies have linked these to cancer progression, cell cycle, chromatin and epigenetic modifications (Xie et al., 2020; Zhu et al., 2021).

All the transposon mutagenesis inserts, which led to an apparent loss of resistance to a plant metabolite, which could be correctly sequenced, mapped to different regions of the V5H10 insert. This included inside the uvrA subunit, one of the tRNA-CTT's, one of the hypothetical proteins, and two within the non-coding region between the pCC1BAC insert and the penicillin binding protein (Figure 3-5).

BPROM analysis (SoftBerry, 2020) indicated the existence of two potential promotors upstream of the four open reading frames (tRNA, Hypothetical Protein and MdrA). The ΔTnF8 and ΔTnB1 inserts inserted between these two predicted promotor regions and the MdrA protein, which impacted transcription. The final two transposons ΔTnA6 and ΔTnE6 inserted downstream of the MdrA gene between the MdrA gene and the end of the insert / start of the primer, and as such was assumed not to affect transcription of the genes.

3.4.2.2   Outcomes of protocol 2: I10H5

I10H5 was a 10,100 bp long insert that mapped to *P. histolitica* F0411 chromosome 1 (1517016 – 1523418 - 1526229) and contained genes encoding for: 1) an SGNH/GDSL hydrolase, 2) an MBOAT family protein, 3) a hypothetical protein, 4) a Xanthine/Purine

permease, 5) a xanthine phosphoribosyltransferase, 6) a DUF 4251 domain containing protein and 7) a TonB-dependant receptor protein.

Hydrolases are a category of enzymes that cleave a covalent bond using water, the GDSL family is little studied (Akoh et al., 2004) but is characterised by carrying four conserved residues of serine, glycine, asparagine and histidine within the active side (Mølgaard et al., 2000). GDSL's are associated with peptidoglycan O- / De-O-acetylation, which can be involved in AMR and immune response (Sychantha et al., 2018).

 The MBOAT family of proteins are membrane bound O-acyl transferases which transfer acyl groups from a coenzyme to another protein and act as drug targets for multiple human diseases (Chang et al., 2011; Ma et al., 2018).

Xanthine permeases transport key metabolites across the cell membrane (Karena et al., 2015) and xanthine phosphoribosyltransferase are involved in the same purine metabolism pathway (Krenitsky et al., 1970). The metabolism of nucleotides is a pathway oft used by bacteria in response to antibiotic induced stress (Lopatkin & Yang, 2021).

Finally, TonB-dependant receptors mediate substrate-specific transport across the outer membrane of bacteria (Fujita et al., 2019) and can be hijacked to force uptake of antimicrobial chemicals in *P. aeruginosa* (Luscher et al., 2018). Further, de-activation of TonB receptors led to a slower acquisition of mutations which conferred resistance to antibiotics, when *Aeromonas hydrophilia* was grown in the presence of oxytetracycline, compared to wildtype strains (Li et al., 2021). The removal of 4 TonB-dependant receptor-encoding genes from *Aeromonas hydrophilia* altered the level of spontaneous evolution to oxytetracycline compared to 2 wildtype isolates. This alteration could be either an increase, or decrease in spontaneous evolution levels, depending upon the TonB encoding genes removed.

At the time, the working theory was that all these membrane transporters worked in tandem to increase the efflux of berberine to which I10H5 was thought to be resistant to at the time.

3.4.3 Development of protocol 3: screening of the oral metagenomic library using broth dilution and continuous analysis

At this point it was noted that EPI300 *E. coli* containing an empty pCC1BAC plasmid and the pV5H10 and pI10H5 plasmids began behaving differently compared to previous MIC analysis, and new MICs were conducted on these isolates using the CLARIOstar microplate reader. These new MICs indicated that there was no discernible difference between the MICs of any isolate, and that the MIC of the *E. coli* EPI300 control was 2-fold higher than expected across 3 biological repeats.

This was thought to be a result of phytochemical precipitation out of the media during the screening protocol, and multiple experiments were set up to analyse this, which found quercetin precipitated in all media at concentrations which would be required for an inhibitory screen. At this point it was decided to proceed with only berberine.

All isolates that had been indicated to be previously resistant to either quercetin or berberine were put on a new plate, which was then screened using the new protocol over 24 hours in what was assumed to be an inhibitory concentration of berberine. All isolates grew. This was unexpected and the two most analysed isolates and the *E. coli* EPI300 with an empty pCC1BAC vector underwent another round of MIC analysis with 24-hour observation. At this point the MICs appeared to change again. Now, 1 mg/ml of berberine appeared to completely kill or inhibit the growth of all isolates and was used to then screen the isolates from the library that passes through quaternary stage screening. None of the isolates that passes through quaternary stage screening, or control isolates grew in this concentration.

Quercetins environmental concentrations vary by plant, to as high as 45 mg/100 g in onions, to as low as 0.9 mg/100 g in leeks, in processed foods such as red wine and black tea, the

concentration is quite low, at 2.5 mg and 3.16 mg per 100 ml respectively (Dabeek & Marra, 2019). *Berberis vulgaris* root contained approximately 0.6 mg of berberine per 1 mg of crude berberis extract (Abd El-Wahab et al., 2013). It is possible berberine concentration changes during the cooking process, as is the case with allicin from garlic (*Allium sativum*) when crushed (Lawson & Hunsaker, 2018).

Mice fed 20 mg tablets of quercetin or quercetin derivatives had a circulating quercetin level of 11.7 ± 1.5 μM in the blood (Morand et al., 2000), and the absorption of quercetin in rat models appears to be controlled by the sugar moieties they are attached too (Arts et al., 2004). Further studies indicated that the circulating levels of quercetin may not present the full picture, as over 50% of quercetin supplementation in a rat model bound to the intestinal lining without permeating (Carbonaro & Grant, 2005). This suggests that it is possible, with consumption of food containing quercetin that the compound may concentrate within the intestinal system at high concentrations. The phytochemicals may also concentrate in the faecal matter, or urine after deposition, providing another environment where selective concentrations may be achieved.

Further, wastewater from the production of rose essential oil, contained quercetin as part of the phytochemical waste in concentrations of up to 7.6 ± 0.3 mg/ml (Georgieva et al., 2021). This suggests this concentration is very reachable in wastewater resulting from industrial applications of plants, such as essential oil production.

The protocol 3 screening procedure followed a similar structure to the initial screening procedure, however, this time the plates were continually monitored, with an OD_{600} reading every 10 minutes for 24 hours, at a concentration of 1 mg/ml of berberine on the CLARIOstar microplate reader.

This screening procedure gave rise to a new positive hit isolate H4F9; this hit appeared promising for two reasons. Firstly, the isolate was in the middle of the plate rather than in

any of the outer wells, which can be a known issue with OD_{600} reading of 96 well plates. This is because the edge and corners are more prone to evaporation, changing the growth of bacteria within those wells compared to those in the middle (Mansoury et al., 2021) and the concentrations of any supplements.

Secondly, the *E. coli* isolate containing the H4F9 insert had a variable MIC alongside an *E. coli* isolate containing an empty pCC1BAC plasmid. This MIC was not consistent across repeats, with the MIC for the H4F9 insert containing *E. coli* falling between 2 mg/ml and 0.9 mg/ml and the MIC for the empty *E. coli* isolate falling between 0.9 mg/ml and 0.8 mg/ml of berberine. This suggests there was a slight overlap between the tolerance levels of the two isolates, but that there is a clear difference in the upper and lower ranges of the tolerance levels. Together this suggests that berberine tolerance may be fluid, and that the insert is likely to be carrying genes which encode for proteins that confer berberine tolerance.

A future step in this research pathway would be to conduct a screen of many bacteria, and strains to locate a sensitive strain to the phytochemicals, which could then be used to construct a metagenomic library where the difference between the control, and inserts conferring tolerance, was much larger. The majority of metagenomic libraries are constructed using *E. coli* (Knietsch et al., 2003) and the data from chapters 6, 7, and 8 suggest that *E. coli* may be intrinsically tolerant to these phytochemicals.

3.4.4 Outcomes of protocol 3: the potential role of genes present on the metagenomic inserts H4F9 for both antibiotic and phytochemical tolerance

The H4F9 insert was 25,866 base pairs in length and mapped to the genome of *Veillonella nakazawae T1-7,* the insert contained 25 protein encoding genes, we discuss here only those considered to be related to AMR or phytochemical tolerance.

The glycosyltransferase family 9 protein encoding gene present on the H4F9 insert is part of the larger glycosyltransferase family protein complex. Glycosyltransferases mediate AMR

through multiple mechanisms in *E. faecalis* (Dale et al., 2015). They form an integral part of the multiprotein peptidoglycan layer creation machinery, alongside transpeptidases, as part of the wider penicillin binding protein complex. Glycosyltransferases, alongside transpeptidases are attractive targets for the development of new antimicrobials (Sauvage & Terrak, 2016), as perturbation of the multiprotein complex of which penicillin binding protein is part appears to have multiple bactericidal consequences.

Glycosyltransferases from *Bacillus cereus* have been shown to modify flavonoids through the glycosylation pathway (Hyung Ko et al., 2006). The UDP-glycosyltransferase from *B. cereus* was able to use apigenin, genistein, kaempferol and quercetin as substrates, glycosylating preferentially the C-3 or C-7 hydroxyl group to produce a newly glycosylated phytochemical and UDP-degraded sugar moieties. Glycosylation is used as a process to stabilise, detoxify, or solubilise substrates in all kingdoms (Tian et al., 2016)

Finally, modification of genes encoding for proteins involved in glycosylation have been selected for by quercetin in our *P. aeruginosa* evolution study (Chapter 5). Further *Lactobacillus pontis* (a bacteria whose biological niche is defined by its high glycosylation activity) abundance was decreased *in vivo* after in feed phytochemical supplementation in chickens (Chapter 8). The connection between these different experimental results is explored further in the later chapters, and in the final discussion.

Taken together these studies suggest a strong linkage between glycosylation, AMR, and flavonoid tolerance.

The M18 family aminopeptidase is part of the larger M aminopeptidase family. In *P. falciparum* modifications to the M aminopeptidases can be involved as part of the artemisinin resistance complex (Bunditvorapoom et al., 2018; Teuscher et al., 2007).

ABC transporters are well known multi-drug resistance mechanisms across bacterial species (Saier & Paulsen, 2001), that act by removing the drug from the cell via an efflux pump (Choi, 2005). Further ABC transporters have been previously selected for by another phytochemical similar in structure to berberine, reserpine (Garvey & Piddock, 2008). Taken together with the data from this study it is possible that ABC transporters play a role in phytochemical tolerance, which would be a direct cross-resistance role if true, assuming the ABC transporter in question also effluxes antibiotics.

It is possible that there are potentially many bacterial proteins, or combinations of proteins which can confer resistance to phytochemicals. Combinations of genes together conferring antibiotic resistance is a common strategy employed by bacteria to deal with stressful conditions (Nikaido, 2009). In the case of H4F9, in combination with the evidence from the other chapters, it is likely that the phytochemical is being used as a substrate as part of the glycosylation pathways, which may be detoxifying or solubilising the phytochemical. Further, it is possible that the transpeptidases are also able to use the phytochemical as a substrate, which may be having further detoxification effects. Finally, the appearance of ABC transporters suggests the toxic phytochemical may be a target of the efflux systems. The multiple detoxification mechanisms would potentially explain the variable levels of berberine tolerance by the strain containing this isolate, as when all mechanisms work together in tandem, it may offer a higher level of tolerance than any single mechanism alone.

The next step in this research would be to further explore the open reading frames on the H4F9 insert, either by conducting the transposon mutagenesis step, or forward genetics, where the individual genes are cloned into a stable vector with control expression (Tarantino & Eisener-Dorman, 2012). These two approaches together would elucidate which of the genes on the H4F9 insert have an impact on berberine tolerance, and how expression of these genes modifies the tolerant phenotype.

3.5 Conclusion

This chapter had two main objectives, the first (1) was to develop a functional metagenomic screening procedure using the plant metabolites quercetin and berberine, that was able to discover key genes responsible for phytochemical tolerance from an oral metagenomic library. The second (2) was to determine if these genes were known antimicrobial resistance determinants or had antimicrobial resistance properties. Both individual objectives were achieved, albeit with caveats, due to the complex nature of the screening procedure and the unpredictable nature of the flavonoids.

Previous work has successfully used broth dilution to functionally screen metagenomic libraries. The precipitation of quercetin from the media, and the high concentration of berberine required for bactericidal or bacteriostatic activity suggests these two compounds may not have been the ideal phytochemicals for this type of screen, at least for this library construct.

In a similar vein it is possible that other libraries, metagenomic or otherwise, may present more ideal candidates for screening using a liquid broth dilution method, and it is this strand which I followed in Chapter 4 of this thesis.

Despite the often-contradictory nature of the positive hits that came out of the screening procedure, all three contained genes known to be involved in antimicrobial resistance, specifically efflux pumps. Further to this the screening procedure outcomes, both protocol 2 and 3, were metagenomic inserts from either *Prevotella* or *Veillonella* species (with 1 exception out of 14). This suggests that there is a potential link between AMR and phytochemical tolerance and these two bacterial genera. Be that co-location of genes on the inserts, or that efflux pumps may be able to remove both phytochemicals and antimicrobials from the bacterial cell.

Finally, genes present on the bacterial inserts that came out of the library, in particular the D, D-transpeptidase and glycosyltransferase, are similar in function to genes that contained mutations in *P. aeruginosa* after 30 days of evolution in subinhibitory concentrations of phytochemicals as we will see in the later chapters. The reduction in *L. pontis* abundance after quercetin supplementation in *in vivo* phytochemical feed studies in chickens was also noted. The appearance of these gene families in three independent research strands within this thesis suggests that there is a complex connection between transpeptidases, glycosyltransferases and phytochemical tolerance, which is explored further in the overall discussion.

4 Functional screening of the Swab and Send bacterial isolate library

4.1 Introduction

Following the design and implementation of the functional metagenomic screening protocol in chapter 3, the decision was taken to screen an available bacterial isolate library with berberine. This screen was conducted using a modified version of the protocol in chapter 3 using the high concentration of berberine (1 mg/ml) that was determined to have inhibitory activity against *Escherichia coli*.

The library screened was the Swab and Send library, available at the Liverpool School of Tropical Medicine (LSTM) (Roberts, 2020). Swab and Send is a citizen science project set up by Dr Adam Roberts in 2015, whereby people can pledge a small amount of money to the project and receive swabs, which they can then use to swab anything they find interesting. The bacteria and fungi from these swabs are then cultured by the group at LSTM. The cultured microorganisms are then tested for antimicrobial activity against a range of indicator strains including *Micrococcus luteus, Staphylococcus aureus, Escherichia coli,* and *Candida albicans or Candida auris,* to search for novel antibiotics (Roberts, 2020). This library was chosen due to the diverse nature of the bacteria within, and the knowledge that many of the bacteria possessed antimicrobial resistance (AMR) genes, such as a *Klebsiella grimontii* isolate that was shown to contain the bla_{OXY6-4} and fos_A resistance genes (Hubbard et al., 2020). The central idea behind the work presented in this chapter is that if antibiotic resistance genes confer increased tolerance to berberine then they should be common in those isolates that grow in high concentrations of berberine.

As such the aim of this chapter was threefold. First, to determine if the screening methodology developed in chapter 3 could be applied to isolate, rather than metagenomic

libraries. Secondly, to determine what bacterial species, could best survive in inhibitory concentrations of the berberine. Finally, to determine if there was any correlation between tolerance of inhibitory concentrations of berberine, and antibiotic resistance gene profile. We hypothesised that the presence of antibiotic resistance genes would be associated with phytochemical resistant bacteria, and that

4.2   Materials and methods

4.2.1   Modification of the functional screen for the Swab and Send library

A bacterial library was assembled with bacterial isolates grown from swabs from various places and things, primarily in the UK but also including samples from around the world. Some of these sample locations included but were not limited to pets, keyboards, humans, food, and bathhouses. These bacterial isolates were collected as part of the Swab and Send project. The individual bacterial isolates are stored in individual wells in multiple 96 well plates in brain heart infusion (BHI) broth with glycerol at -80°C. At the time of writing the Swab and Send library includes over 20,000 isolates.

These isolates were screened using the broth dilution methodology developed in chapter 3. One hundred µl of Muller-Hinton Broth (MHB) plus 1 mg/ml of berberine was added to each well of two sterile flat bottomed 96 well plates. Then using a sterile 96 pin replicator, the thawed Swab and Send library plate was replicated into one of the prepared plates. Plates were then read by eye after 24 hours growth at 37°C.

4.2.2   PCR and 16S Sequencing

16S PCR and sequencing was conducted following the protocol described in chapter 2.7 and chapter 2.10 respectively.

4.2.3   Whole genome sequencing

Whole genome sequencing was contracted to the company MicrobesNG. Protocols for this can be found at https://microbesng.com/microbesng-faq/, and sample submission was conducted according to these guidelines.

4.2.4 Bioinformatics analysis

Bioinformatics analysis of these genomes to determine antimicrobial resistance gene presence and isolate relatedness was conducted using the programmes described in Table 4-1.

Table 4-1 Bioinformatics tools used to analyse positive hits from the Swab and Send isolates.

Programme	Use	Reference
ABRicate	Mass screening of contigs for antimicrobial resistance genes.	(Seemann, 2022)
Resfinder	Database used during ABRicate analysis	(Zankari et al., 2012)
OrthoANI	To calculate Orthologous average nucleotide identity analysis (similarity values between genomes) and subsequently visualise this analysis (heatmaps)).	(Lee et al., 2016)
Clustal Omega	Calculate multiple sequence alignment (MSA) between genes of similar activity.	(Sievers et al., 2011)
Jalview	Visualisation of MSAs and calculation of minimum spanning trees of relatedness between genes.	(Waterhouse et al., 2009)
Snapgene	Visualisation of bacterial contigs from MicrobesNG.	(GSL Biotech, 2020)

4.3   Results

4.3.1   Determination of positive hits from the Swab and Send library

Twenty plates from the Swab and Send library housed at LSTM underwent screening according to the modified phytochemical based functional screening protocol. Seven out of the 20 plates had positive hits (Figure 4-1). Five of the 7 plates containing positive hits were labelled as SAS (Swab and Send) followed by the number of the plate, for example SAS183. A positive hit was a well in which the replicated colony grew in the presence of inhibitory concentrations of berberine or quercetin. Two of the 7 plates containing positive hits were labelled DRI and SOIL respectively, these two plates were labelled differently from the normal Swab and Send protocol as the isolates they contained were taken from agar letters used for public engagement purposes. The positive hits were distributed unequally across the plates, with some plates having more positive hits than others. The random distribution of positive hits suggests there was no apparent bias in the execution of the protocol we undertook. SAS214, SAS209 and SAS183 all had 1 single hit. SAS205 and the DRI plate had 3 hits each. The SOIL plate had 4 hits, and SAS216 had 8 hits.

(A) SAS 214

(B) SAS 216

(C) Soil Letters
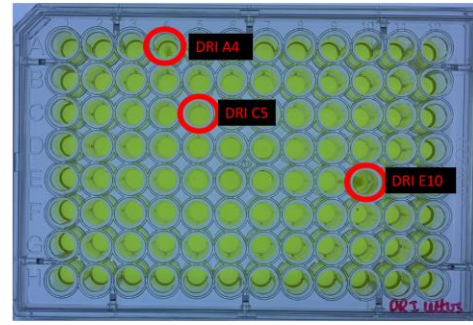
(D) DRI Letter
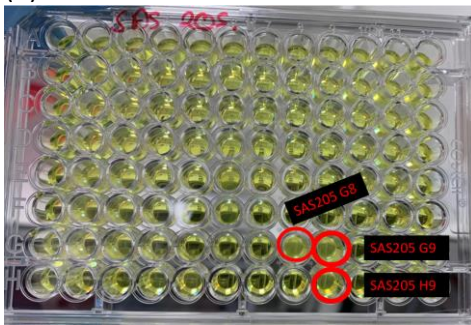
(E) SAS 205

(F) SAS 209
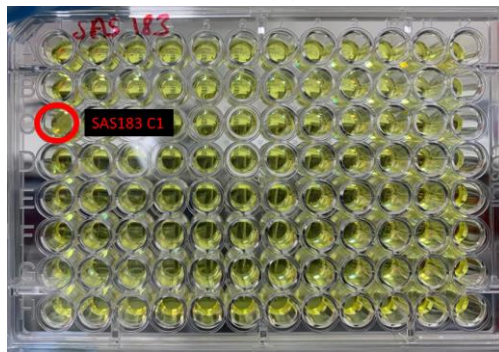
(G) SAS 183

Figure 4-1 Screening plates with positive hits from the Swab and Send library screen. Positive hits from the 7 plates are outlined in red circles. Samples are mapped to their respective wells on the plates (labelled in red). (A) SAS214 (B) SAS215 (C) Soil Letters plate (D) DRI Letters plate (E) SAS205 (F) SAS209 (G) SAS183.

4.3.2 There were many antibiotic resistant phenotypes across the positive hit isolates from the Swab and Send library which encoded for resistance to multiple antibiotics

After positive isolates were identified they were then subsequently plated out onto antibiotic free Muller-Hinton agar. At this point the isolate from plate SAS214, and a single isolate from plate SAS216, C5, did not grow. However, two different colonies grew from wells SAS216E7 and DRIC5, leaving a remaining total of 21 positive hits. Due to the nature of the library construction it is likely that a well could contain two or more isolates, as if a colony is not well isolated in the library construction it is picked anyway (Roberts, 2020).

Eight isolates from 3 plates were members of the *Enterobacter* genus, with 7 isolates being *Enterobacter ludwigii*. Seven isolates from 3 plates were members of the *Bacillus* genus, 3 isolates were *Bacillus pumilus,* 2 isolates were *Bacillus subtilis,* and the final 2 were *Bacillus altitudinis*. Finally, there were 2 *Serratia fonticola,* 1 *Leclercia adecarboxylata,* 1 *Staphylococcus warneri*, 1 *Staphylococcus cohnii,* and 1 *Escherichia coli* isolate spread across 3 plates (Table 4-2).

After whole genome sequencing, the genome sequences were analysed using ABRicate and Resfinder, to determine if there were any antimicrobial resistance genes present in the genomes. All *E. ludwigii* isolates from plates SAS205, SAS209 and 2 isolates from plate SAS216 contained the fos_{A2}, bla_{ACT-12}, oqx_{A9} and oqx_{B9} genes. The *E. ludwigii* isolates from SAS216 contained a bla_{ACT-22} gene instead of bla_{ACT-12}. The *E. hormaechei* isolate from DRIC5 contained all the same AMR genes as *E. ludwigii* except for bla_{ACT-17} in the place of $bla_{ACT-12}/bla_{ACT-17}$ gene.

The *S. fonticola* isolates from SAS216 both contained the bla_{FONA-1} gene. Whilst the *E. coli* from SAS216 contained a bla_{EC-13} gene. The *L. adecarboxylata* from plate SAS216 contained both an *mcr-9.1* and fos_{A8} gene.

The *Bacillus* isolates from plates SAS216, and SOIL contained the *cat*$_{86}$ and *bla*$_{BPU-1}$ genes, except for the isolate designated SOILG5, which contained the *rph*C, *aadK, mphK* and *vm1R* genes. The *B. subtilis* isolate from DRIA4 contained the same AMR genes as SOILG5, with the addition of the *sat*$_{A\_Bs}$ and *tet*(L) genes. The *S. cohnii* isolate contained the *fusF* and *erm*(C) genes. Finally, the *S. warneri* isolate contained no known AMR genes, according to Resfinder (Table 4-2). The name and function of these AMR genes is detailed in Table 4-3.

Table 4-2 Antimicrobial genes by isolate from the Swab and Send library. Three gene groups were present frequently and so specified as (Gene Group 1) containing fos_{A2}, bla_{ACT-12}, oqx_{A9} and oqx_{B9}, (Gene Group 2) containing cat86 and bla_{BPU-1} and (Gene group 3) containing fos_{A2}, bla_{ACT-22}, oqx_{A9} and oqx_{B9}. There were 21 positive isolates from 6 plates. Multiple isolates from the same plate came from the same sample location: (φ) A winogradsky column for isolates on SAS205, (*) A horse bridle for isolates on SAS216, (¥) A sewage sample for two isolates on SAS216, (ψ) A single soil sample for isolates on the SOIL plate, and (ω) a combined sample of handprints and soil for isolates on the DRI plate.

Sample Name	Sample Location	Species	AMR Genes
205G8	Winogradsky Column φ	*Enterobacter ludwigii*	**(Gene Group 1)** fos_{A2} (NG_050406.1) bla_{ACT-12} (NG_048559.1) oqx_{A9} (NG_0.050427.1) oqx_{B9} (NG_050458.1)
205G9	Winogradsky Column φ	*Enterobacter ludwigii*	**(Gene Group 1)**
205H9	Winogradsky Column φ	*Enterobacter ludwigii*	**(Gene Group 1)**
209E4	Toppersfield Brook, Riverbed	*Enterobacter ludwigii*	**(Gene Group 1)**
216H8	Horse Bridle *	*Enterobacter ludwigii*	**(Gene Group 3)** fos_{A2} (NG_050406.1) bla_{ACT-22} (NG_048559.1) oqx_{A9} (NG_0.050427.1) oqx_{B9} (NG_050458.1)
216A6	Sewage¥	*Serratia fonticola*	bla_{FONA-1} (NG_049092.1)
216E5	Sewage¥	*Serratia fonticola*	bla_{FONA-1} (NG_049092.1)
216E7-2	Horse Bridle *	*Enterobacter ludwigii*	**(Gene Group 3)**
216E7-1	Horse Bridle *	*Escherichia coli*	bla_{EC-13} (NG_049079.1)
216F7	Horse Bridle *	*Enterobacter ludwigii*	**(Gene Group 3)**
216F10	Horse Brush *	*Leclercia adecarboxylata*	*mcr-9.1* (NG_064792.1) fos_{A8} (NG_066545.1)
216B2	Shoe Cabinet	*Bacillus pumilus*	**(Gene Group 2)** *cat86* (NG_047563) bla_{BPU-1} (NG_050941.1)
183C1	Garden Hole	*Staphylococcus warneri*	N/A
SoilG5	Soil (Oxford) ψ	*Bacillus subtilis*	*rphC* (NG_063825.1) *aadK* (NG_047379.1) *mphK* (NG_065846.1) *vm1R* (NG_063831.1)
SoilG9	Soil (Oxford) ψ	*Bacillus altitudinis*	**(Gene Group 2)**
SoilG8	Soil (Oxford) ψ	*Bacillus pumilus*	**(Gene Group 2)**
SoilH5	Soil (Oxford) ψ	*Bacillus pumilus*	**(Gene Group 2)**
DRIE10	Soil (Oxford) & Hands ω	*Bacillus altitudinis*	**(Gene Group 2)**
DRIC5-1	Soil (Oxford) & Hands ω	*Staphylococcus cohnii*	*fusF* (NG_047903.1) *erm*(C) (NG_047806.123S)
DRIA4	Soil (Oxford) & Hands ω	*Bacillus subtilis*	*rphC* (NG_063825.1) *aadK* (NG_047379.1) *mphK* (NG_065846.1) *vm1R* (NG_063831.1) sat_{A_Bs} (NG_064662.1) *tet*(L) (NG_0.48202.1)
DRIC5-2	Soil (Oxford) & Hands ω	*Enterobacter hormaechei*	*fosA* (NG_050405.1) bla_{ACT-17} (NG_04803.1) oqx_{A9} (NG_0.050427.1) oqx_{B9} (NG_050458.1)

Table 4-3 Name and function of antimicrobial resistance genes found in the genomes of isolates tolerant to berberine from the swab and send library located using a combination of both ABRicate and Resfinder. Given is the antimicrobial resistance gene moniker, full name and function, and the antimicrobial(s) to which the gene confers resistance.

Antimicrobial Resistance Gene	Name/Function	Antimicrobial
Fosfomycin Resistance Genes		
fos$_A$	Fosfomycin resistance glutathione transferase	Fosfomycin
fos$_{A2}$	Fosfomycin resistance glutathione transferase	Fosfomycin
fos$_{A8}$	Fosfomycin resistance glutathione transferase	Fosfomycin
Beta-lactamase Genes		
bla$_{ACT-12}$	Cephalosporin-hydrolysing class C beta-lactamase	Cephalosporins
bla$_{ACT-17}$	Cephalosporin-hydrolysing class C beta-lactamase	Cephalosporins
bla$_{ACT-22}$	Cephalosporin-hydrolysing class C beta-lactamase	Cephalosporins
bla$_{EC-13}$	Cephalosporin-hydrolysing class C beta-lactamase	Cephalosporins
bla$_{FONA-1}$	class D beta-lactamase	Beta-lactams
bla$_{BPU-1}$	class D beta-lactamase	Beta-lactams
Quinolone Resistance Genes		
oqx$_{A9}$	multidrug efflux RND transporter periplasmic adaptor subunit	Quinolone
oqx$_{B9}$	multidrug efflux RND transporter permease subunit	Quinolone
Colistin Resistance Gene		
mcr-9	phosphoethanolamine--lipid A transferase	Colistin
Chloramphenicol Resistance Gene		
*cat*86	chloramphenicol O-acetyltransferase	Chloramphenicol
Rifamycin Resistance Gene		
rphC	rifamycin-inactivating phosphotransferase	Rifamycin
Streptomycin Resistance Gene		
aadK	aminoglycoside 6-adenylyltransferase	Streptomycin
Macrolide Resistance Gene		
mphK	macrolide 2'-phosphotransferase	Macrolide
erm(C)	rRNA (adenine (2058)-N (6))-methyltransferase	Macrolide
Linosamide & Streptogramin & Tiamulin Resistance Gene		
*vm*1R	ABC-F type ribosomal protection protein	Linosamide& Streptogramin & Tiamulin
Streptothricin Resistance Gene		
*sat*A_Bs	streptothricin N-acetyltransferase	Streptothricin
Tetracycline Resistance Gene		
tet(L)	tetracycline efflux MFS transporter	Tetracycline
Fusidic Acid Resistance Gene		
fusF	Fusidic acid resistance EF-G-binding protein	Fusidic Acid

4.3.3 Analysis of *bla* and *fos* antimicrobial resistance genes found in positive hits from the Swab and Send screening procedure determined that none of the genes were identical

Antimicrobial resistance genes discovered in the positive hits, which conferred resistance to the same antimicrobial underwent nucleotide similarity analysis using Clustal Omega. The sequence alignment, and phylogenetic relatedness trees were visualised using Jalview. This analysis was conducted to determine if the resistance genes were consistent in relatedness to their location in specific bacterial species, and to determine if there were any consistencies or outliers which may relate to phytochemical tolerance profile. Nucleotide alignment was a direct result of our DNA sequencing experiments, any protein alignments would have been theoretical based on these sequences.

None of the fosfomycin resistance genes were identical, however all genes were exactly 426 base pairs (bp) in length. Differences in the genes between the species did not encode for a mutation in the active site of the encoded protein and were consistent with the sequences expected for the designated gene (Figure 4-2). The *fos*$_A$ and *fos*$_{A2}$ genes were more closely related than *fos*$_{A8}$.

None of the *bla* genes were homologous. All *bla*$_{ACT}$ sequences were equal in length, but not equal in length to any other members of the *bla* gene family present in this study. Differences in the genes between the species encoded for differences in the active site of the encoded protein and were consistent with the sequences expected for the designated genes. The *bla*$_{ACT}$ genes were more related to *bla*$_{EC-13}$ and *bla*$_{FONA-1}$ genes than the *bla*$_{BPU-1}$ gene (Figure 4-3).

(1)

(2)

Figure 4-2 Sequence alignments of fos resistance genes. (1) Multiple sequence alignment image, 100% with alignment between sequences is given in dark blue, and alignment of only two sequences given in light blue. (2) Phylogenetic tree constructed using with nearest neighbour of the three fos resistance genes (fos$_A$, fos$_{A2}$ and fos$_{A8}$) present within samples from the Swab and Send library. The fos$_A$ and fos$_{A2}$ genes are more closely related than to fosA8.

(1)

(2)

Figure 4-3 Sequence alignments of bla resistance genes. (1) Multiple sequence alignment with 100% identity between sequences given in dark blue and alignment of >2 sequences given in light blue. (2) Phylogenetic tree constructed using nearest neighbour of the six Bla resistance genes (bla_{ACT-12}, bla_{ACT-17}, bla_{ACT-22}, bla_{FONA-1}, bla_{BPU-1}, and bla_{EC-13}) present within samples from the Swab and Send library. The three bla_{ACT-22} and bla_{ACT-12} are closely related, bla_{ACT-17} is equally related to both bla_{EC-13} and the other two bla_{ACT} genes. The bla_{FONA-1} and bla_{BPU} genes are very distant relations of the bla_{ACT-12} and bla_{ACT-22} genes. The bla_{FONA-1} is 691bp and bla_{BPU-1} genes are 776 base pairs, whilst all other bla genes present are 1040 base pairs.

4.3.4 Analysis of different isolates of the same bacterial species using average nucleotide identity analysis identified three groups of homologous clonal isolates from the same plate and swab location

Whole genome sequencing of isolates showed that several isolates of the same species from the same plate, and across plates contained the same resistance genes. This suggested that these isolates could be clonal. To determine if the screening methodology was indeed selecting for clonal isolates from the same plate, relatedness analysis was conducted using OrthoANI.

Analysis of isolates from the *Bacillus* genus, despite isolates of the same species containing the same AMR genes, and being from the same plate, none of the isolates were 100% homologous. This means that none of the *Bacillus* colonies were clonal. (Figure 4-4).
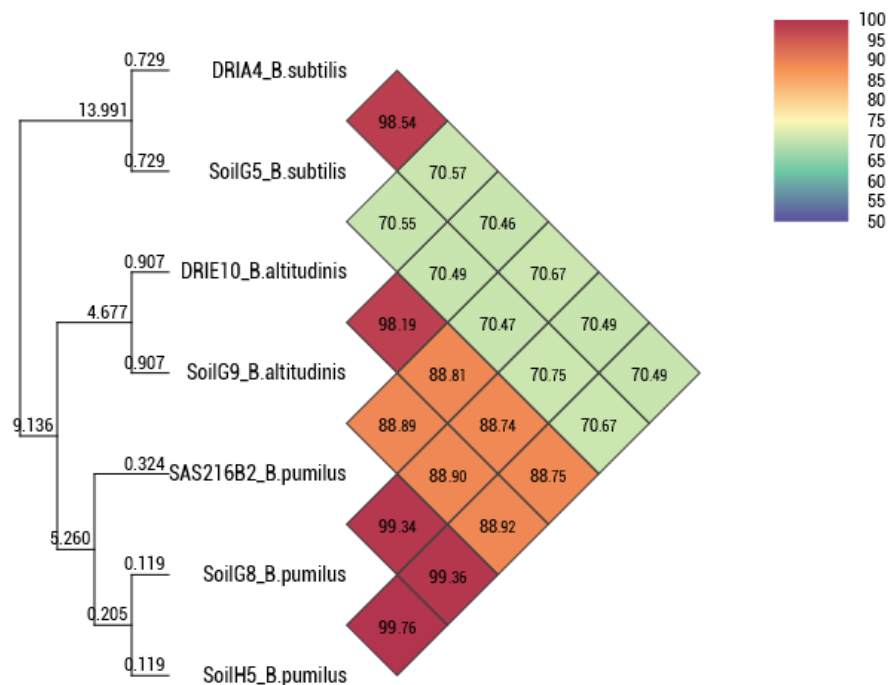
Figure 4-4 Heatmap showing relatedness between positive hits from the Bacillus genus of the Swab and Send library. Three B. pumilus, two B. altitudinis and two B. subtilis strains were selected for across three different plates by 1 mg/ml of berberine. The B. subtilis and altitudinis isolates came from different plates and were not 100% homologous suggesting they were not clonal. None of the B. pumilus strains were 100% homologous suggesting they were also not clonal, despite coming from the same plate.

When looking at the isolates from the *Enterobacter* genus, two groups of isolates were assumed to be clonal (Figure 4-5). The 3 hits from SAS216 are all 100% homologous to each other and came from the same swab (a horse bridle), which suggests that these 3 isolates are clonal. This clonal isolate was designated SAS216 *E. ludwigii* clonal isolate 1. The 3 hits from SAS205 are also all 100% homologous to each other and came from the same swab (a Winogradsky Column), which suggests that these 3 isolates are clonal. This clonal isolate was designated SAS205 *E. ludwigii* clonal isolate 1.

The *E. ludwigii* isolate from SAS209 was distinct from either *E. ludwigii* clonal isolates from the SAS216 and SAS205 plates and had only 99% homology, which was expected as it came from a completely different swab (a riverbed). Thus three *E. ludwigii* isolates and one *E. hormaechei* (Figure 4-5) remained.
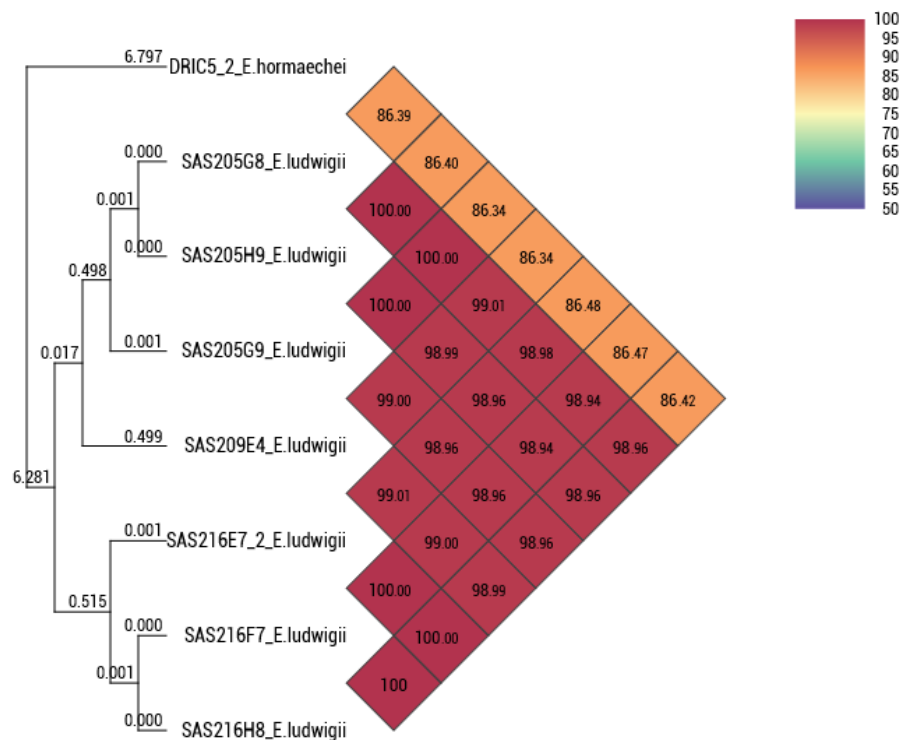
Figure 4-5 Heatmap showing relatedness between positive hits from the Enterobacter genus of the Swab and Send library. Seven Enterobacter ludwigii and one Enterobacter hormaechei isolates were selected across three different plates. The Enterobacter hormaechei isolate was less than 87% homologous to any other isolate, demonstrating it was clearly a distinct species. All E. ludwigii isolates from plate SAS205 were 100% homologous to each other and came from the same location (a Winogradsky column) suggesting they were clonal (SAS205 E. ludwigii clonal isolate 1). The E. ludwigii isolate from plate SAS209 was not 100% homologous to any other isolate.

Finally, the three isolates from plate SAS216 were 100% homologous to each other and came from the same location (a horse bridle) and therefore clonal (SAS205 E. ludwigii clonal isolate 1).

The two *S. fonticola* isolates from plate SAS216, were 100% identical to each other and came from the same swab (sewage) and were thus considered clonal (Figure 4-6). This clonal isolate was designated SAS216 *S. fonticola* clonal isolate 1. All remaining isolates were separate species.
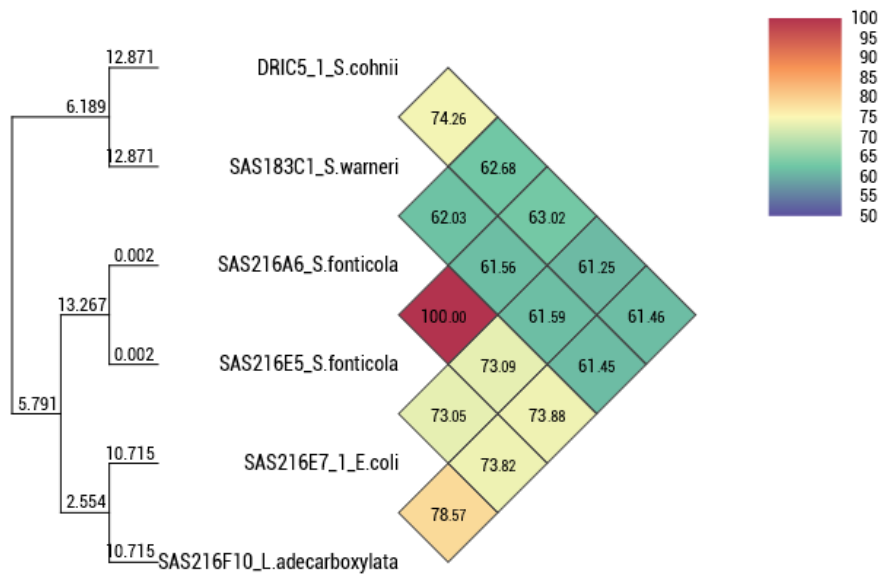
Figure 4-6 Heatmap showing the relatedness between the Staphylococcus, Serratia, Escherichia and Leclercia genera positive hit isolates from the Swab and Send library. In this case, only the two Serratia fonticola isolates were 100% identical from plate SAS216 and came from the same swab (sewage) suggesting they are clonal (SAS216 S. fonticola clonal isolate 1).

4.3.5 The species distribution of bacterial isolates after OrthoANI relatedness analysis demonstrated that inhibitory concentrations of berberine for multiple bacterial species across different genera and was highly selective for members of the *Bacillus* and *Enterobacter* genera

Following the OrthoANI relatedness analysis, it became clear that three clusters of isolates were clonal, and that the screening procedure was able to select for the same clonal isolate, multiple times, on the same plate but in distinct positions on that plate. These were: SAS216 *E. ludwigii* clonal group 1, which came from a horse bridle, SAS205 *E. ludwigii* clonal group 2, which came from a Winogradsky column, and SAS216 *S. fonticola* clonal group 3, which came from a sewage sample swab. After the reduction of these isolates into the clonal groups, 16 non-homologous isolates remained, and the species distribution of these isolates is displayed here (Figure 4-7).
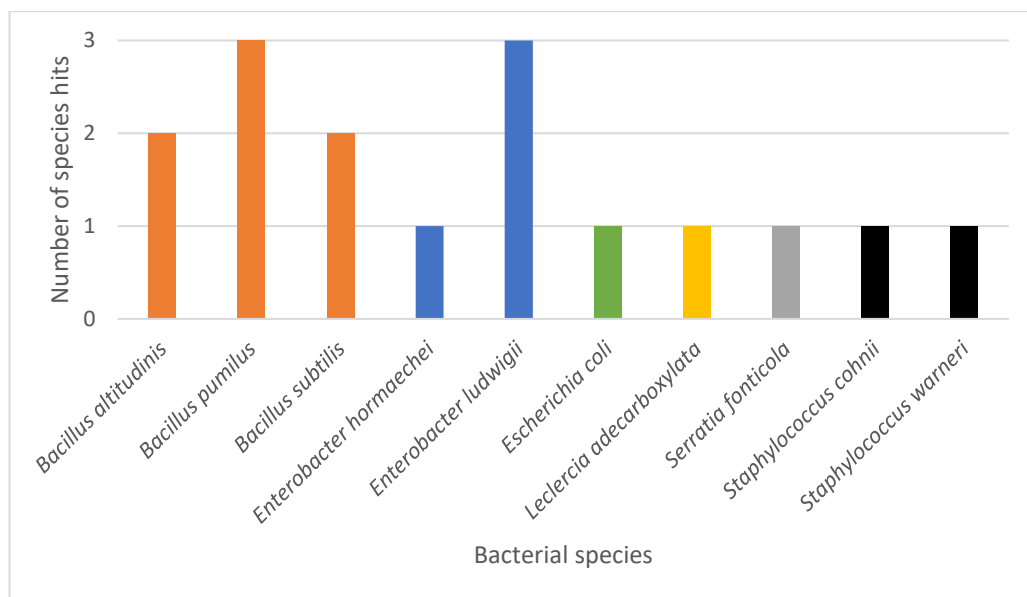
Figure 4-7 Species distribution of positive hits from the Swab and Send library using the metagenomic screening methodology. The most common species were Bacillus pumilus (orange) and Enterobacter ludwigii (blue) at three hits each, Bacillus altitudinis (orange) and Bacillus subtilis (orange) both appeared twice, and then Enterobacter hormaechei (blue), Leclercia adecarboxylata (yellow), Serratia fonticola (grey), Staphylococcus cohnii (black) and Staphylococcus warneri (black) all appeared once.

4.3.6 Three of the AMR genes present in the genomes of isolates from the Swab and Send library that had a berberine tolerant phenotype were located alongside transposable elements

The location of the AMR genes within the genomes of the respective bacteria was determined using Resfinder and visualised using Snapgene. Most of the resistant genes were located within the chromosomes of the respective bacteria; however, 3 resistance genes were associated with putative IS family transposase elements.

The streptothricin n-acetyltransferase *sat*$_{A9}$ and tetracycline efflux MFS transporter *tet*(L) found within the DRIA4 *Bacillus pumilus* isolate were co-located with an IS*1595* family transposase IS*CAC2*. The genes were downstream and upstream of the transposase respectively (Figure 4-8).
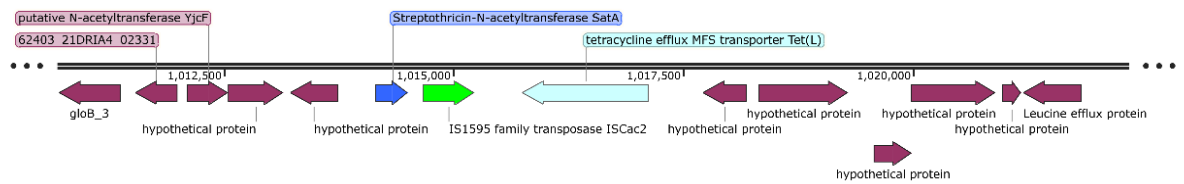
Figure 4-8 Location of the streptothricin (blue) and tetracycline (light blue) resistance genes from DRIA4 B. pumilus. The two genes were found located together and associated with the ISCac2 transposase (green).

The third gene that was collocated with a transposase was the *mcr-9.1* gene within the *L. carboxylata* isolate SAS216F10. This isolate contained two *mcr-9.1* genes, one was chromosomally located whilst the other was co-located with three different IS family elements, two downstream (IS*1R* and IS*1D*) and one upstream (IS*26*) of the gene (Figure 4-9). Also present next to IS*1R* was a tyrosine recombinase gene *xerD*, suggesting the whole region is mobile, as recombinases catalyse site-specific recombination sites, this one is specific for the *xerD* combination site.
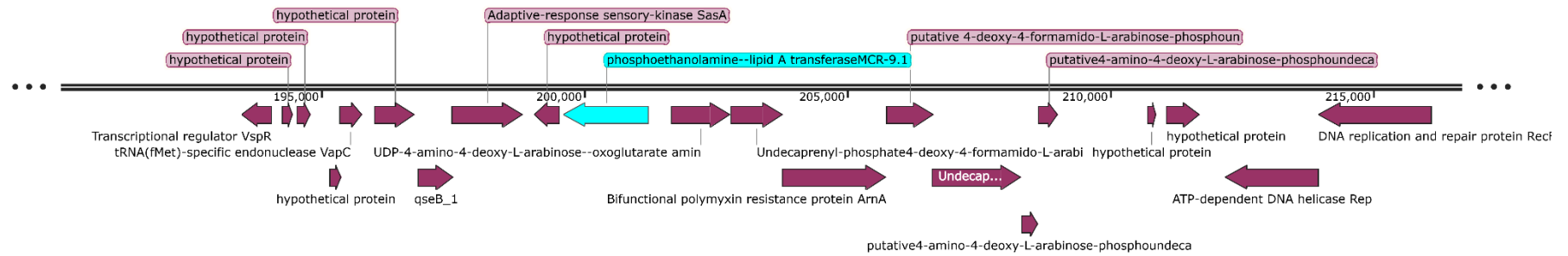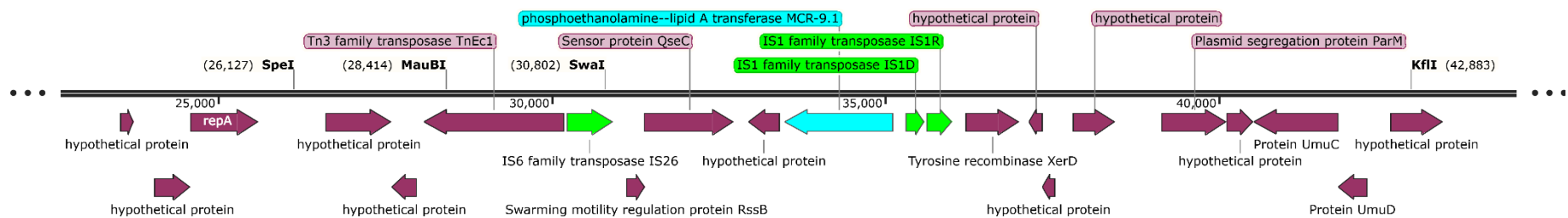
Figure 4-9 Location of the two mcr-9.1 genes (light blue) in SAS216F10 L. adecarboxylata. (1) Location of the mcr-9.1 present in the chromosomal DNA. (2) Location of the mcr-9.1 present in a possible mobile genetic element and associated with IS1R, IS1D downstream and IS26 upstream of the mcr-9.1 gene, the gene also located with a tyrosine recombinase xerD. The mcr-9.1 genes are highlighted in blue, the IS transposases in green, and all other protein encoding genes in purple.

4.4 Discussion

In this chapter, the functional metagenomic screening methodology previously developed in chapter 3, was used to screen an inhouse bacterial isolate library at LSTM using 1 mg/ml of berberine.

In total, 20 plates from the library were screened (containing an estimated 1920 bacteria). Twenty-one isolates grew in inhibitory concentrations of berberine, from 7 of the 20 plates. These isolates underwent 16S sequencing, to determine their bacterial species, followed by whole genome short-read sequencing.

All but one of the 21 isolates contained AMR resistance genes, this suggests clearly that berberine selects for isolates containing AMR resistance genes. Whilst the exact number of isolates containing AMR genes in the Swab and Send library is unknown, it is highly unlikely to be as high as 95%. The library is made up of bacterial and fungal isolates from environmental sources, and environmental bacteria can contain anywhere from 1.75% to 95% AMR gene carriage depending on the location and bacteria evaluated (Ibrahim et al., 2012; Lin et al., 2017). As such we hypothesise that berberine selects for bacteria carrying AMR genes. Determining the exact mechanisms for this is a key avenue for future research.

When the genomes of the isolates were elucidated, it became clear that several of the isolates were of the same species, from the same plates and from the same swab sample, and they contained the exact same resistance genes as determined by Resfinder. To determine if these isolates were clonal copies of each other OrthoANI analysis was conducted and the heatmaps visualised (Figure 4-4).

From this analysis it became clear that all three *E. ludwigii* isolates from plate SAS205 (SAS205 *E. ludwigii* clonal isolate 1) were clonal copies of each other, as were the *S. fonticola* isolates from plate SAS216 (SAS216 *S. fonticola* clonal isolate 1), and finally the *E. ludwigii* isolates from plate SAS216 (SAS216 *E. ludwigii* clonal isolate 1). It is important to note the *E.*

ludwigii clonal groups from SAS205 and SAS216 shared only 98.96% identity, and thus remained as two distinct clonal groups. This was expected as they came from two completely different swabs, a horse bridle, and a Winogradsky column.

According to the OrthoANI analysis none of the isolates from different plates were 100% identical, nor were any of the *Bacillus* isolates, despite multiple coming from the same plate. This gave us a strong degree of confidence that this screening procedure worked effectively at selecting berberine tolerant bacteria, as it was able to select clonal colonies that were present in different wells on the same plate, alongside isolates with similar AMR genotypes across different plates.

After integration of clonal colonies into their respective clonal groups, the distribution of bacterial species was given (Table 4-2). A number of these species have been previously explored in the literature regarding their tolerance to, and interaction with berberine.

The most common bacterial genus in our samples was *Bacillus*, and included *B. subtilis, B. pumilus* and *B. altitudinis*. Berberine as a constituent of the Mexican Prickly Polly (*Argemone Mexicana L*) extract has been previously shown to inhibit the growth of *B. cereus* (More et al., 2017) *and B. subtilis* (Cernáková & Kostálová, 2002). Interestingly at low concentrations of berberine (20 µg/ml) *B. subtilis* growth is increased, though high concentrations (100 µg/ml) inhibited growth (Kong et al., 2012). This 'high' concentration was ten times lower than the concentration used in our screening methodology. The use of a berberine/carvacrol combination led to a 4500-fold increase in efflux pump expression in *B. subtilis* (Atas et al., 2022). This combination of growth promotion at low concentrations and high efflux pump expression by *Bacillus* species in the presence of berberine may partially explain why 43.75% of positive hits were from the *Bacillus* genus.

The second most abundant genus in our samples was *Enterobacter,* of which two species were present: *E. hormaechei* and *E. ludwigii.* The *Enterobacter* genus constituted 25% of

positive hits from the library even after controlling for clonal colonies. Growth of the *Enterobacter* genus has previously been shown to be modified under the selective pressure of berberine in the gut microbiota, both positively (Wang et al., 2017) and negatively (Yao et al., 2020). Notably, all the *Enterobacter* in our samples contained genes encoding for an oqx_{AB9} efflux pump, the relevance of which is discussed further below.

Two *Staphylococcus* spp. were present: *S. warneri* and *S. cohnii. S. cohnii* is also a skin commensal, and is known for its high levels of AMR and potential role as an AMR gene reservoir (Lienen et al., 2021). These two members of the *Staphylococcus* genus are poorly studied, however, berberine has been previously shown to be antimicrobial against *S. aureus* and restored beta-lactam activity against MRSA (Yu et al., 2005). The inhibition of *S. cohnii* by berberine may occur through damage of the cell surface via lipid fluctuation (Zhang et al., 2020), or inhibition of amyloid fibril formation (Lienen et al., 2021). Alongside this, berberine has been previously shown to inhibit surface adhesion and biofilm formation of *Staphylococcus epidermis* (Wang et al., 2009)*.

The *S. warneri* isolate, contained no known AMR genes, suggesting very clearly berberine tolerance is not related to known AMR genes in this case. *S. warneri* from plate SAS183 was an environmental isolate, derived from a "garden hole" in the United Kingdom. *S. warneri* is a skin commensal and a rare causative pathogen of bacterial UTIs (Kanuparthy et al., 2020). *S. warneri* has high tolerance to berberine compared to other member of the *Staphylococcus* genus, suggesting it may be intrinsically resistant (Wojtyczka et al., 2014). Intrinsic resistance may have occurred due to one of the theoretical mechanisms discussed later in this thesis, such as via a glycosyltransferase, however it may also have been a mechanism of berberine resistance that is currently unknown.

Finally single isolates of *E. coli, L. adecarboxylata* and *S. fonticola* were also present within the positive hits. *E. coli* has been shown to respond to berberine exposure through the

upregulation of *omp*W (Budeyri Gokgoz et al., 2017). Berberine has multiple targets within *E. coli* (Karaosmanoglu et al., 2014) including the *fts*Z cell division protein (Domadia et al., 2008). It would be interesting to see if these berberine targets had genetic alterations in the isolate from the Swab and Send library, when compared to a berberine susceptible *E. coli* isolate.

No studies were found that related *L. adecarboxylata* and berberine together, though its previous characterisation as a *Escherichia* species (Tamura et al., 1986) would suggest that berberine inhibition likely functions along the same pathways. The lack of consistent efflux pump-based AMR genotypes across the two isolates would suggest that berberine tolerance in *Escherichia/Leclercia* occurs despite the lack of efflux pumps.

It would be interesting to determine how the distribution of genera/species isolated in this study, compare against the distribution of genera/species in the entire Swab and Send library. It is possible that a small number of species are tolerant to berberine, as seems apparent from the results presented here. However, it is also possible that we have an incomplete and biased understanding of the potential widespread nature of berberine tolerance within the Swab and Send collection.

No single gene, or antibiotic resistance phenotype was consistently present across all isolates. This would suggest that berberine tolerance is not directly attributable to one resistance genotype.

Beta-lactam resistance was common across all the *Enterobacter* and *Serratia* isolates, and several of the *Bacillus* isolates. The beta-lactam resistance genotype was absent in the *B. subtilis, L. adecarboxylata* and *Staphylococcus* isolates. Further analysis of the *bla* genes (Figure 4-2) highlighted that the bla_{ACT} genes were of similar length and sequence, with bla_{ACT-17} being more distantly related than bla_{ACT-12} and $blaA_{ACT-22}$ were with each other. This was expected as the former was isolated from *E. hormaechei* whist the latter two from *E. ludwigii*.

The bla_{EC}, bla_{BPU} and bla_{FONA-1} genes were all increasingly distant from the bla_{ACT} genes, with bla_{EC} being the most closely related. This is unsurprising as the bla_{ACT} and bla_{EC} genes offered protection from cephalosporins, whilst the others offered protection against first generation beta-lactams.

Importantly bla_{ACT} genes are intrinsic to *Enterobacter sp.* (Piotrowska et al., 2019)*.* Unlike in *Enterobacter* the other *bla* genes are not considered intrinsic resistance mechanisms. The bla_{FONA} genes are beta-lactams produced exclusively by *S. fonticola* (Blaak et al., 2014), and bla_{EC-13} is a beta-lactam first isolated from *E. coli* but not intrinsic to all MDR *E. coli* isolates (Iramiot et al., 2020). Finally, bla_{BPU} is a beta-lactam found exclusively but not intrinsically in the *Bacillus* genus (Toth et al., 2016).

 Taken together, this evidence suggests that it is unlikely that the presence of beta-lactams is the sole reason for bacterial tolerance to berberine. However, the frequency that isolates with non-intrinsic mechanisms of beta-lactam resistance were selected for (68.75% of all isolates) warrants further functional analysis, of the role of these genes in berberine tolerance.

The next most common antibiotic resistance phenotype was fosfomycin resistance. The fos_A genes (Figure 4-3), were found within all *Enterobacter* isolates and in the *L. adecarboxylata* isolate*.* The genes were all equal length, with several nucleotides changes across all three of the *fos* genes present. fos_{A8} was more distantly related than the other two fos_A genes. This makes sense as it was found in the *L. adecarboxylata* rather than the *Enterobacter* isolates. As with the *bla* genes, fos_A homologues are present in the majority of *Enterobacter* isolates (65.22-100%) (Ito et al., 2017), and as such their presence within the isolates selected for by berberine is not unexpected. It is unlikely that the *fos* genes are the only determining factor of berberine tolerance as they appeared in only three of the species isolated.

All other resistance genes were limited to one genera of bacteria, respectively. Of these genes, the majority were intrinsic.

Leclercia adecarboxylata carrying both *mcr*-4 (Sun et al., 2019) and *mcr*-9 (Garza-González et al., 2021) have been previously described in the literature. Though this study is the first known instance of a *L. adecarboxylata* isolate containing an *mcr-9* gene on a transposable element. However, the *L. adecarboxylata* described in this study did not contain an *mcr-4* gene.

In *Bacillus* spp. *rph*C genes are widespread (Spanogiannopoulos et al., 2014) as are *cat*86 genes, although the latter are not intrinsic (Harwood et al., 1983). The *aadk* genes are chromosomally located in *B. subtilis* (Honda et al., 2020) and *mph*K genes are found in 95.43% of *B. subtilis* isolates (McArthur et al., 2013) whilst *vm*1R genes are found in 91.43% of *B. subtilis* isolates (McArthur et al., 2013). Both *fus*F and *sat*A are chromosomally located in other *S. cohnii* isolates (McArthur et al., 2013).

Tetracycline resistance genes and *oqx*$_{AB}$ efflux pumps have been previous associated with berberine tolerance. The *oqx*$_{AB}$ genes are intrinsic to members of the *Enterobacter* genus although *oqx*$_B$ alone is generally found in only 2-6% of isolates (Li et al., 2019). The *oqx* genes are strong MDR efflux pumps, and these are highly associated with berberine tolerance (Li et al., 2021; Tegos et al., 2002). The *tet*(L) resistance gene was noted in one *B. subtilis* isolate from our plates. The *tet*(A) resistance gene has been previously highlighted in *E. coli* as a potential contributor to increased bacterial resistance to berberine (Li et al., 2018). The *tet*(A) and *tet*(L) gene both encode for bacterial efflux pumps which are specific for tetracycline (Roberts, 2005).

Of specific interest, however, is the occurrence of colistin, tetracycline and streptothricin resistance genes co-located with IS transposons. Other natural drivers of antibiotic resistance include heavy metals. Bacterial heavy metal resistance genes often co-locate on plasmids

which contain AMR genes (Gullberg et al., 2014; Silver & Misra, 1988). The selection of isolates by inhibitory concentrations of berberine containing mobile genetic element associated AMR genes in this study is concerning. Other studies have highlighted berberines ability to upregulate transposases in *S. aureus* at sub-inhibitory conditions (Wang et al., 2008).

Three isolates located in this study had AMR genes associated with IS transposable elements. Further the literature consensus is that berberine can upregulate MGE carriage in bacteria. Putting these data together, we hypothesise that berberine selective pressure may upregulate mobile genetic element carriage in bacteria. These mobile genetic elements may contain genes that confer AMR. This is a potential secondary mechanism of cross-resistance between phytochemicals and antibiotics.

Taken together this data suggests that resistance to berberine is not related to the occurrence of a single antibiotic resistance gene. It is possible that some of these genes play a role in berberine resistance, either individually or together, and further studies need to be conducted to investigate the individual and combinatorial effects in these genes compared to isogenic strains without them.

The next experimental steps for these isolates would include: the cloning of these specific resistance genes into berberine susceptible isolates for functional testing, further exploration of the genomic environment in which they are set, and I-TASSAR analysis of the binding of berberine into the pockets of the resistance genes.

4.5   Conclusion

This chapter successfully demonstrated the ability of the functional screening methodology developed in the previous chapter, to select for bacterial isolates with phenotypic tolerance to the plant metabolite berberine. The screen was able to select for clonal isolates on the same plate, and the same bacterial species between plates, alongside a diverse number of isolates across different plates and sample origins.

The screen selected for 21 isolates, of which 20 contained ARGs. It is incredibly unlikely that the Swab and Send library has an over 95% representation of ARGs within the isolates in the library. As such we hypothesise that berberine selects for bacterial isolates containing ARGs.

The resistance profiles of the isolates to antimicrobials were diverse, and there was no common AMR gene or genotype across all isolates, though some genes were common to many isolates, such as the *bla* family genes. Together these data suggest that resistance to berberine is not a direct result of one antimicrobial resistance gene. However, isolates containing efflux pumps (oqx_{AB} *and tet*(L)) were selected for. These efflux pumps, or similar in the case of *tet*(L) have previously been associated with berberine tolerance in the literature. Further, the screen also selected for berberine tolerant isolates that had AMR genes co-located with mobile genetic elements. This suggests a possibility that berberine may function as a natural driver of AMR through mobile genetic element selection, in a similar fashion to heavy metals.

 Finally, this study demonstrated the first instance of *L. adecarboxylata* containing an *mcr-9.1* colistin resistant element associated with a transposon in the current literature.

Further work on these isolates, including studies to assess individual and combinatorial effects in these genes compared to isogenic strains without them, and *in silico* protein docking of berberine with the proteins encoded for by these genes would be ideal for a

clearer understanding of the association of AMR genes, and berberine tolerance, within these strains.

5 Evolution of *Pseudomonas aeruginosa* in sub-inhibitory concentrations of berberine and quercetin

5.1 Introduction

5.1.1 The design of evolution experiments

In this chapter, we wanted to explore how bacteria evolved under the selective pressure of the phytochemicals berberine and quercetin. This experiment was designed and based around the *Escherichia coli* long-term evolution experiment (LTEE) (Consuegra et al., 2021). The LTEE is an ongoing experiment started by Professor Lenski which has been monitoring the growth of 12 initially identical populations of *E. coli* since 1988.

Evolution experiments allow us to study how a bacterial population evolves over a specific timeframe, under a specific set of conditions. Previous studies have used similar experimental methodologies to determine if *E. coli* and *Pseudomonas fluorescens* could evolve resistance to pexiganan (an antimicrobial peptide). Over 600 generations all isolates of *P. fluorescens* and *E. coli* isolates saw a significant increase in resistance relative to ancestral cells (Perron et al., 2006).

We theorised that by growing bacteria for 30 days in sub-inhibitory concentrations of our phytochemicals, we may see the occurrence of phytochemical resistance. We could then study the genomes of these evolved isolates to further our mechanistic understanding of any adaptive mutations, and if any of these phytochemical tolerance adaptations were related to AMR in the literature.

In this study we had three experimental groups, 32 µg/ml of quercetin, 32 µg/ml of berberine, and a control with no phytochemical addition. We attempted to account for the occurrence of changes due to adaptation of the strains to laboratory media and small amounts of glycerol by having three repeats of each experimental group, for each strain.

5.1.2 Bacterial adaptation to evolution in laboratory media

As much as possible, bacteria adapt to any non-lethal environment they live in, or challenge that they are presented with, especially when that challenge is prolonged (Santos-Lopez et al., 2019; Wiser et al., 2013). In our experiment, we wanted to explore specifically the adaptive mutations of *Pseudomonas aeruginosa* to selective pressure of the phytochemicals quercetin and berberine. The microbes we picked, NCTC 7244 and NCTC 9433, were environmental isolates and were not adapted for growth in laboratory media.

Bacteria adapt to growth in laboratory conditions, which are usually nutrient rich and at an optimal temperature for growth. In PAO1 *P. aeruginosa* for example, this has led to a change in the production of pyocyanin and exopolysaccharides (Chandler et al., 2019). It is also important to note here that genetic mutations are not always adaptive, and simply occur as part of the natural evolutionary process (Putnins & Androulakis, 2021). Therefore, there is a background of mutational activity in *P. aeruginosa,* and as such some mutations in our experiments may occur randomly, rather than due to selection.

5.1.3 Post-evolution assessment of the isolates

Strains underwent minimum inhibitory concentration (MIC) analysis the phytochemicals quercetin and berberine and to a range of antibiotics. They also underwent biofilm and pyocyanin production analysis (the relevance of which is discussed in the following section). We then conducted whole genome sequencing, followed by bioinformatics analysis on all control isolates, and any treatment isolates that displayed a change in phytochemical resistance phenotype as determined by the previous MIC analysis. This allowed us to capture many of the genetic changes occurring across all the isolates, which were likely to be a result of media adaptation, rather than treatment adaptation, and remove them from further analysis.

A general overview of the role, and importance of *P. aeruginosa* is given in chapter 1, and an overview of many of the major methodologies used in this study design are given in chapter 2.

5.1.4 The importance of pyocyanin and biofilm production in *P. aeruginosa* with relation of phytochemical and antibiotic resistance

Alongside assessing the isolates for a change in the phytochemical tolerance and antibiotic resistance phenotype, we also assessed them for changes in their biofilm and pyocyanin production phenotypes. We assessed production of biofilms and pyocyanin because both are important *P. aeruginosa* responses to stress conditions (Muller & Merrett, 2014; Pang et al., 2019). Production of both is also altered by the presence of phytochemicals (Memariani et al., 2019; Zhou et al., 2012) through the quorum sensing pathway. Finally, biofilms in particular are associated with antibiotic resistance phenotype, and horizontal gene transfer (Abe et al., 2020).

Thus, we hypothesised that adaptations to survival in sub-inhibitory concentrations of quercetin and berberine would be associated with an increase in production of pyocyanin and/or biofilms. This chapter introduction will now give a short overview of both pyocyanin, and biofilms.

5.1.4.1 The role of pyocyanin in P. aeruginosa

Pathogenic *P. aeruginosa* produces several virulence factors associated with disease severity (Alonso et al., 2020). These include the type III secretion systems (exoT, exoS, exoY and exoU) which together control expression of exotoxins (toxins secreted into the environment by bacteria which cause damage to the host), quorum sensing (QS) system proteins (lasR/I and rhlR/I), which allow for communication between bacterial cells, elastases (lasA and lasB) that disrupt the junctions between host epithelial cells allowing penetration of the bacteria, and

alginate production genes (*alg* genes), which produce alginate, the most abundant extracellular matrix polysaccharide in *P. aeruginosa* biofilms (Blanco-Cabra et al., 2020).

Finally, they produce pyocyanin, which is involved in oxidative stress, altering the mitochondrial electron transport systems of the host. Pyocyanin is a compound produced by *P. aeruginosa* during infection and is recovered in large quantities from infected patients (Wilson et al., 1988). Pyocyanin production is a complex system mediated by quorum sensing and accumulation of low molecular weight signal molecules (Ouyang et al., 2016). Pyocyanin has multiple negative effects on human cells including: inhibition of cell respiration, ciliary function, epidermal cell growth, and prostacyclin release (Kamath et al., 1995; Lau et al., 2004).

5.1.4.2 The role of biofilms in P. aeruginosa

Biofilms are a major mechanism by which cells can protect themselves from harmful chemicals and predation. Previous phytochemicals have been linked to a reduction in the formation of biofilms usually through inhibition of the quorum sensing system, these include ellagic acid (Sarabhai et al., 2013), clove oil (Husain et al., 2013), eugenol (Zhou et al., 2012) and naringenin (Vandeputte et al., 2011). Berberine specifically has been shown to inhibit biofilm formation in *Staphylococcus aureus* infection (Chu et al., 2016). Another study highlighted that sub-inhibitory concentrations of berberine led to increased biofilm production (Tan et al., 2019).

After evolution in sub-inhibitory concentrations of berberine, we theorised that there may be a change in biofilm production of the *P. aeruginosa* due to berberine's inhibitory activity against it, and thus adaptive mutations may be pro-biofilm. As such, an assay was used to examine the extent to which this occurred.

P. aeruginosa can produce biofilms, which enhance its ability to cause infection by physically protecting bacteria from host defences and chemotherapy used to treat bacterial infections. Biofilms are structures of bacterial cells encased in an extracellular matrix that can adhere to abiotic or biological surfaces (Flemming & Wingender, 2010; Rasamiravaka et al., 2015). They are also associated with surface adhesion. Biofilms are especially prevalent in implanted and indwelling devices in patients, compounding an already complex treatment profile. Biofilms are also understood to be polymicrobial in nature, presenting another complication in the clinic (Mulcahy et al., 2014); although this does not seem to be the case in regards to burn wound infections (Fazli et al., 2009), which make up the majority of cutaneous *P. aeruginosa* infections.

5.2 Materials and methods

5.2.1 Selection of *P. aeruginosa* isolates

Two *Pseudomonas* isolates NCTC 9433 and 7244 were selected for this study. These isolates were environmental isolates collected at a time when antibiotic use was in its infancy within clinical and agricultural settings in the 1950s, as previously discussed in Chapter 1. They both displayed no antimicrobial resistance phenotypes and were isolated from natural environments. This made them ideal candidates for evolutionary experiments focused upon exploring the natural background of antimicrobial resistance in the environment.

5.2.2 Evolving resistance to secondary plant metabolites

To evolve resistance to secondary plant metabolites in *P. aeruginosa* the experiment followed a 5-day weekly rhythm.

An initial broth of *P. aeruginosa* was created on Monday and a small aliquot was transferred to fresh media every 24 hr until Friday at which point a sub-culture was frozen and the cycle was repeated on Monday using 100 µg/ml of the frozen sub-culture from the previous Friday. This protocol was repeated 6 times for a total of 30 days. Three independent replicates were maintained in parallel.

This methodology was based upon the long term *Escherichia coli* evolution experiment (Lenski, 2017). The three experimental conditions were: (1) 32 µg/ml of berberine, or (2) 32 µg/ml of quercetin, or (3) without any sub-inhibitory plant metabolite.

Daily Propagation: Approximately 24 hours after the previous daily transfer 0.1ml was taken from the previous days 10 ml culture and added to 9.9 ml of fresh lysogeny broth (LB) containing sub-inhibitory concentrations of the respective phytochemicals. There were three replicates of each culture and phytochemical for a combination of 12 flasks per day. The new

flasks were then incubated at room temperature (18-21°C) with rotation. The previous days flasks were saved in the refrigerator.

Weekly Storage: Every Friday, 0.5ml of the previous day's cultures were taken and added to 0.5ml of 40% glycerol/LB (v/v) to a 2ml tube, label with the sample combination and week and stored at -80°C. Three replicates of each of the combinations and repeats were made so that there was one working solution and two backups, for a total of 36 tubes per week. After freezing on a Friday, the leftover cultures were autoclaved and disposed.

Weekly Restart: The experiment was then restarted the following Monday, by adding 100 µl of the frozen aliquot from the previous Friday to 10 ml of fresh MHB until a full 30 days of subculture was conducted. All treatment groups were propagated from the frozen cultures from the previous Friday, this kept the concentration, and potential evolution to glycerol consistent across all experimental groups.

5.2.3 Pyocyanin production assay

P. aeruginosa cultures were grown overnight at 37°C on MHA plates, and a single colony was taken a grown overnight in 10 ml of MHB at 37°C, 200 rpm. To extract the supernatant containing pyocyanin 1.5 ml of culture was transferred to Eppendorf tubes and centrifuged at 13000 x *g* for 2 minutes. Then 100 µl of supernatant was transferred to a single well of a 96 well plate and read at 695 nm compared to an MHB broth blank on a CLARIOstar plate reader.

5.2.4 Biofilm production assay

M9 Media was produced [(50% (v/v) M9 minimal salts), 100ul calcium chloride $MgCl_2$ (1M), 2mL magnesium Sulphate (1M) / 0.4% d-glucose, 4 mM magnesium sulphate and 0.05 mM calcium chloride] and subsequently adjusted to 1 L with sterile dH20 and filter sterilised into a sterile 1L Duran bottle.

Cultures of *P. aeruginosa* were grown from -80°C stocks on MHA plates grown overnight at 37°C. A single colony from each plate was taken and used to inoculate 10 ml of MHB. Overnight cultures were subsequently diluted to an OD of 0.01 in previously prepared M9 media. From this new dilution 150 µl was pipetted into four round bottom wells in a 96 well plate. Four wells of 150 µl of M9 media without bacteria were used as controls. The plate was then incubated for 48 hours at 37°C.

The planktonic cells were then disposed of by pipetting the contents of the wells out into the petri dish which contained an appropriate decontaminant. The now empty wells were then washed three times by pipetting 200 µl of sterile dH_2O into each well, and then removing it, each wash was disposed of into the waste petri dish. After the third wash the plate was dried within a class II cabinet for 45 minutes.

Following the drying step, 180 µl of 5% crystal violet was added to each well using a pipette and the plate was subsequently incubated at room temperature for 20 minutes. The excess crystal violet was discarded into a petri dish using a pipette and the plate was then washed three times again with sterile H_2O, following the previous procedure. The remaining stained crystal violet was solubilised by the addition of 200 µl of 30% acetic acid to each well using a pipette. The plate was then covered and incubated at room temperature for 20 minutes. After incubation each well was mixed by pipetting and 125 µl of liquid from each well was transferred to the corresponding well of a flat-bottomed microtiter plate.

The absorbance of each well was measured using the CLARIOstar plate reader at 600nm. A standard curve was constructed using a twofold serial dilution of 5% crystal violet in 30% acetic acid, and a background correction was conducted using just acetic acid.

5.2.5   Statistical Analysis

Statistical analysis was conducted in three separate experiments: (1) to compare levels of imipenem resistance between treatment and ancestral isolates, (2) to compare levels of

pyocyanin production between treatment and ancestral isolates, and (3) to compare levels of biofilm production between treatment and ancestral isolates.

Two tailed t-tests for independent means were conducted using https://www.socscistatistics.com/tests/studentttest/default2.aspx (Social Science Statistics, 2022). Two tailed t-tests were selected as it was unknown if resistance level, or production would increase or decrease as a consequence of evolution in sub-inhibitory concentrations of phytochemicals. Significance value was set at $p > 0.05$. Full calculations are given in appendix II.

5.2.6   Bioinformatics analysis

Bioinformatics analysis was conducted to determine genetic differences using evolved isolates using the programmes and websites described below (Table 5-1).

Table 5-1 Programmes used for bioinformatics analysis of P. aeruginosa isolates.

Programme / Website	Use	Reference
Bowtie	Read alignment of short and long read sequences for analysis using Breseq.	(Langmead & Salzberg, 2012)
Breseq	Detection of single nucleotide polymorphisms using long and short read sequencing.	(Deatherage & Barrick, 2014)
R	Required dependency for bioinformatics analysis.	(Team, 2020)
Porechop	Trims adapters from short read and long reads.	(*GitHub - Rrwick/Porechop: Adapter Trimmer for Oxford Nanopore Reads*, n.d.)
Filtlong	Filters reads depending on quality.	(*GitHub - Rrwick/Filtlong: Quality Filtering Tool for Long Reads*, n.d.)
Unicycler	Resolves bacterial genomes from long and short reads into a hybrid assembly.	(Wick et al., 2017)
www.kazusa.or.jp	Website which displays codon frequency per 1000 codons for bacterial species.	(Nakamura et al., 2000)

5.2.7   Triage methodology for evaluating Breseq outputs

Breseq is a bioinformatics pipeline used to determine the genetic differences between two isolates. Breseqs output gives a list of genetic differences for any given isolate, when compared to any other isolate. In this study, evolved isolates were compared to the ancestral strains NCTC 7244 or NCTC 9433. The lists of these mutations were combined, so that mutations occurring in any evolved isolate of a particular strain, could be compared to the mutations of any other evolved isolate of that strain.

After mutation analysis was conducted on whole genome sequences using Breseq, the mutations were triaged to determine which were likely to have occurred only in isolates grown under the selective pressure of phytochemicals, and which were likely to have occurred as a consequence of either evolution in laboratory conditions (media), or poor coverage in the hybrid assembly step of the bioinformatics analysis.

Triage step 1: Any mutations that occurred in more than one isolate, in different growth conditions or in the isolates grown in the absence of plant phytochemical was removed from the analysis, as it was these mutations were not specific to isolates grown in sub-inhibitory concentrations of phytochemicals and instead likely to be a result of growth in laboratory conditions. We kept however mutations that occurred in multiple isolates, but only a single treatment group.

Triage step 2: Any mutations that occurred in a single isolate but occurred within a gene or genetic region that was repeatedly mutated in other isolates, including the isolates grown in the absence of phytochemical, was removed. These regions / genes, with multiple mutations, were dubbed 'highly mutable locations' and mutations within were thought to be associated with either (1) poor/incorrect coverage in the hybrid assembly leading to incorrect mutation prediction by Breseq (this was considered to be a potential outcome if all experimentally evolved lineages from a particular ancestor had exactly the same mutations), (2) growth in

laboratory conditions, or (3) a result of these genes being naturally highly mutable and thus non-adaptive mutations.

5.3   Results

5.3.1   Minimum inhibitory concentrations of the phytochemicals; quercetin, berberine and the antimicrobials; d-cycloserine and against *P. aeruginosa* NCTC 7244 and 9433

Two environmental isolates of *P. aeruginosa* (NCTC 7244 and NCTC 9433) were selected for the following evolution experiments, both NCTC 7244 and NCTC 9433 displayed equal sensitivity to both quercetin and berberine at 128 µg/ml (Table 5-2).

Table 5-2 MIC of P. aeruginosa isolates NCTC 7244 and NCTC 9433 to the plant metabolites quercetin and berberine.

Phytochemical	NCTC 9433	NCTC 7244
Quercetin (µg/ml)	64-128	128
Berberine (µg/ml)	128	128

5.3.2   Sample flocculation of NCTC 7244 and 9433 in the presence of quercetin

It was subsequently noticed that both NCTC 9433 and NCTC 7244 flocculated in the presence of quercetin but not in the presence of berberine (Figure 5-1). This was repeatable and occurred in every instance throughout the evolution experiment and was equal across both isolates.
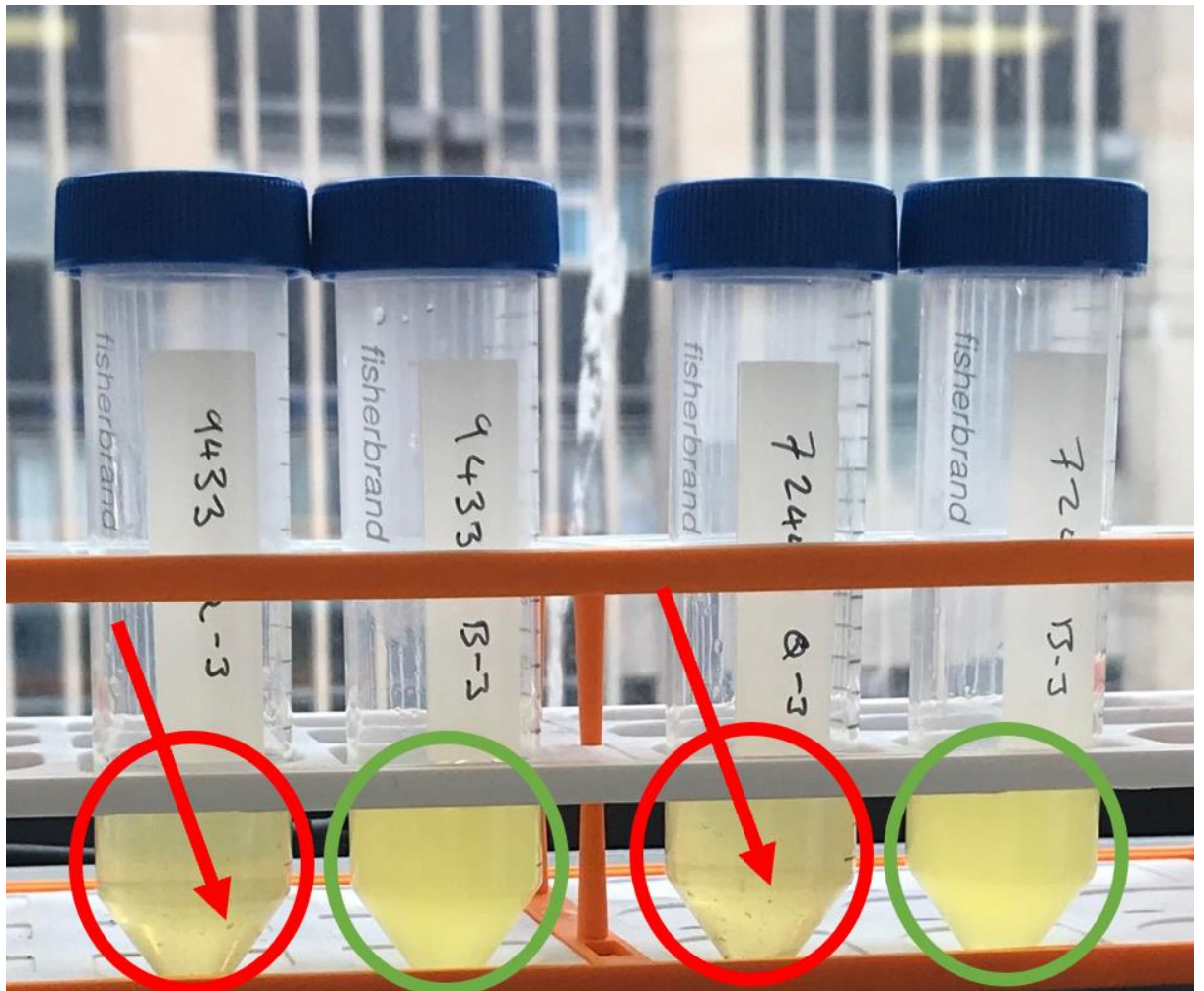
Figure 5-1 Flocculation occurred for both isolates in the presence of quercetin. One sample from each evolution experiment is given here demonstrating that flocculation occurred for both NCTC 7244 and NCTC 9433 in the presence of quercetin but not berberine. Isolates grown in the presence of quercetin are displayed using red circles, with red arrows pointing out an individual flock from each sample, the media is mostly clear in these samples further reinforcing that most planktonic bacteria are within the flocks. Isolates grown in the presence of berberine are displayed using green circles, there are no flocks, and the media is cloudy, suggesting the planktonic bacteria within are well dispersed.

5.3.3 Changes in the minimum inhibitory concentrations of quercetin and berberine of *P. aeruginosa* isolates after 30 days evolution in sub-inhibitory concentrations

The isolates were passaged for thirty days in one of three treatment groups, either 32 µg/ml of berberine or quercetin, or without any sub-inhibitory plant metabolite (labelled control),

following the protocol detailed above. The isolates then underwent MIC analysis against the plant metabolites.

Two of the three NCTC 7244 isolates grown in the presence of berberine had a 2-fold increase in berberine resistance in two replicates, and one had a 2-fold increase in two of the three MIC repeats. All NCTC 7244 isolates grown in the presence of quercetin had a 2-fold increase in two of the three MIC repeats. All NCTC 9433 isolates grown in the presence of berberine had a 2-fold increase in resistance. NCTC 9433 Quercetin 1 had a 2-fold increase in two of the three MIC repeats and NCTC 9433 Quercetin 2 had a 2-fold increase in resistance.

No control isolates displayed altered levels of susceptibility to the plant metabolites (Table 5-3). 9433 Quercetin 3 had no increase in resistance to quercetin.

Table 5-3 MIC of P. aeruginosa isolates to quercetin or berberine after 30-day evolution in either berberine or quercetin, control group also given.

Isolate Name	Quercetin (µg/ml)	Berberine (µg/ml)
P. aeruginosa **NCTC 7244**		
7244 Berberine 1	-	256
7244 Berberine 2	-	256
7244 Berberine 3	-	128-256
7244 Quercetin 1	128-256	-
7244 Quercetin 2	128-256	-
7244 Quercetin 3	128-256	-
7244 Control 1	128	128
7244 Control 2	128	128
7244 Control 3	128	128
P. aeruginosa **NCTC 9433**		
9433 Berberine 1	-	256
9433 Berberine 2	-	256
9433 Berberine 3	-	256
9433 Quercetin 1	128-256	-
9433 Quercetin 2	256	-
9433 Quercetin 3	128	-
9433 Control 1	128	128
9433 Control 2	128	128
9433 Control 3	128	128

5.3.4 Changes in minimum inhibitory concentrations of clinically relevant antibiotics for the *P. aeruginosa* isolates after evolution for thirty days in sub-inhibitory conditions of phytochemicals

Following MIC analysis of evolved isolates to the plant metabolites, changes to the resistance profiles to antimicrobials of clinical importance was measured using disc diffusion methodology, following the thresholds given in the EUCAST guidelines.

All changes in imipenem resistance between the evolved isolates and their respective ancestors underwent a two-tailed t-test statistical analysis, the full statistical results can be found in Appendix II.

When the data was visualised their appeared to be a change in the level of resistance to imipenem (IPM) from susceptible to resistant, across all NCTC 9433 isolates irrespective of condition, with the exception of NCTC 9433 Control 1, and NCTC 9433 Berberine 3 (Figure 5-2, Figure 5-3, and Figure 5-4). However, none of these changes were significant (Appendix II).

The difference in imipenem resistance was greatest between NCTC 9433 (Mean = 19.00, Standard deviation = 6.0) and NCTC 9433 Berberine 2 (Mean = 16.00, Standard deviation = 8.00) however this was not statistically significant ($p = 0.121004$).

None of the isolates appeared to develop resistance to any of the other antibiotics analysed after visualisation of the data. Thus, no other statistical analysis was conducted on this data.
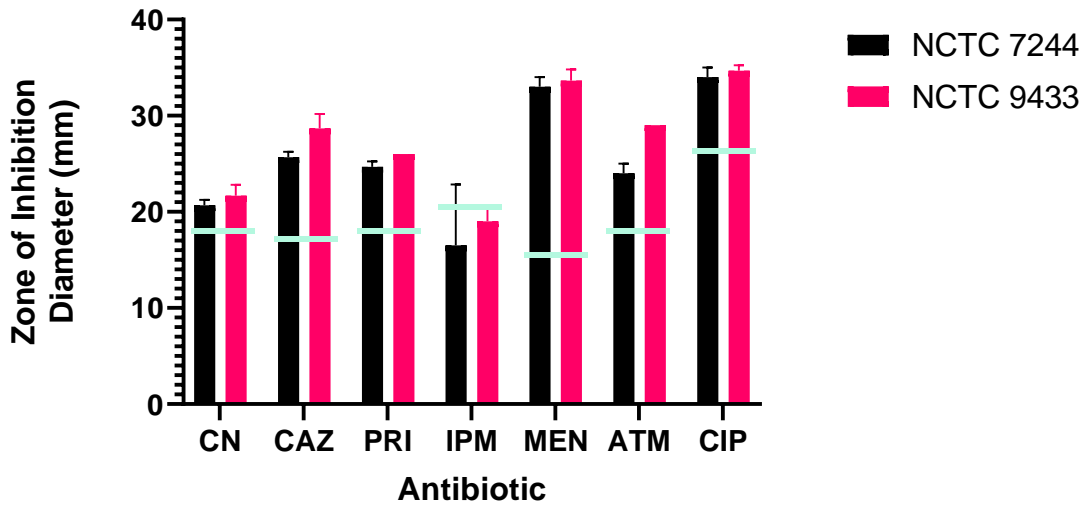
Figure 5-2 Antibiotic susceptibility of ancestral NCTC 7244 and NCTC 9433 to a range of clinically relevant antibiotics according to the disk diffusion method. Antibiotics evaluated were gentamycin (CN), ceftazidime (CAZ), piperacillin (PRI), imipenem (IPM), meropenem (MEN), aztreonam (ATM), and ciprofloxacin (CIP). Threshold denotation, as provided by EUCAST guidelines is given with a light blue bar. The ancestral isolates NCTC 7244 or NCTC 9433 were not resistant to any antibiotic.
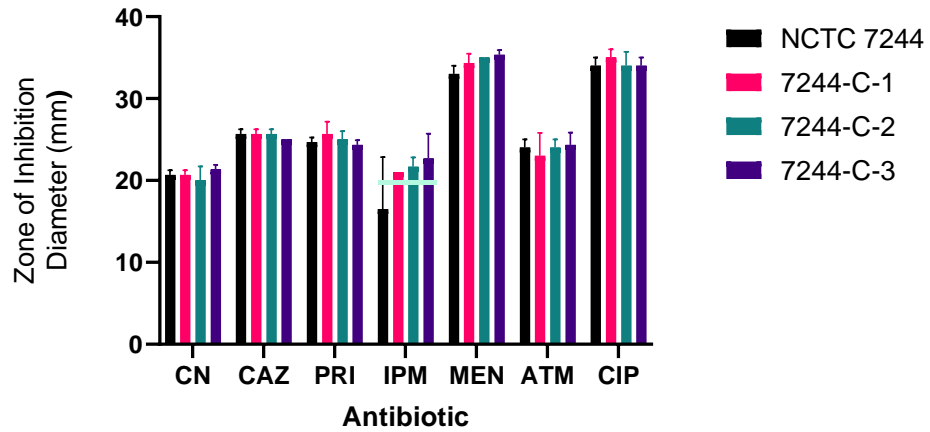
(1)
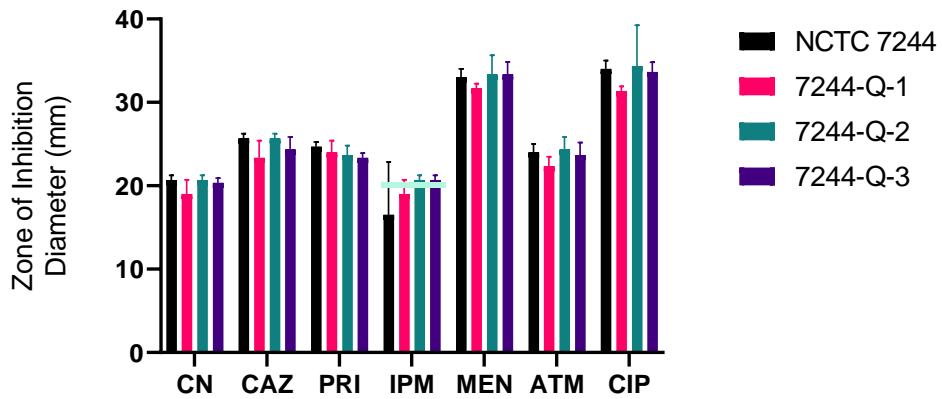
(2)
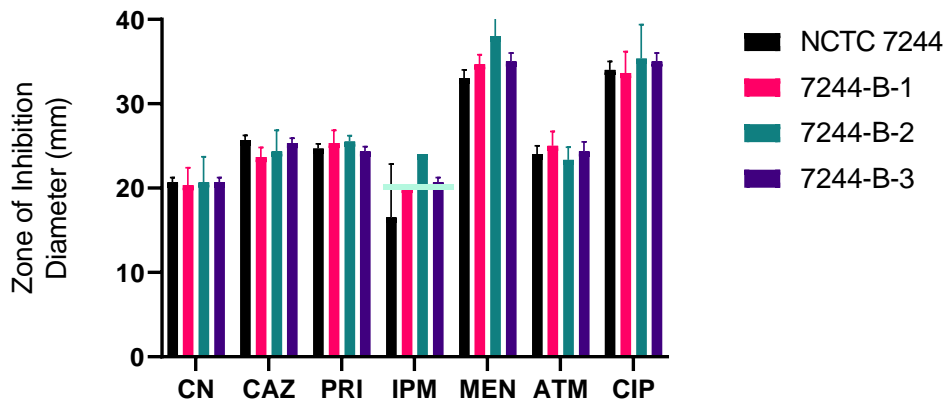
(3)

Figure 5-3 Antibiotic susceptibility of isolates of NCTC 7244 (control (1), quercetin (2) and berberine (3)), to a range of clinically relevant antibiotics according to the desk diffusion method. There was no clear change in any of the antibiotic susceptibility profiles. There was an increase in IPM exclusion zones in all cases, however, these changes were not statistically significant (Appendix II).
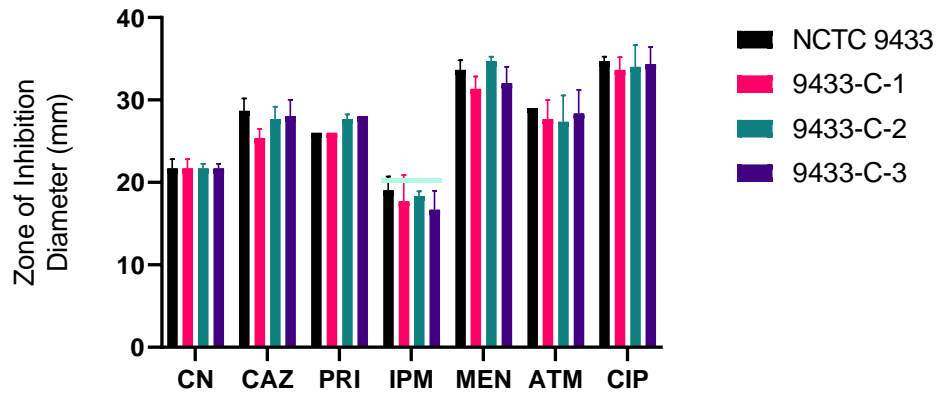
(1)
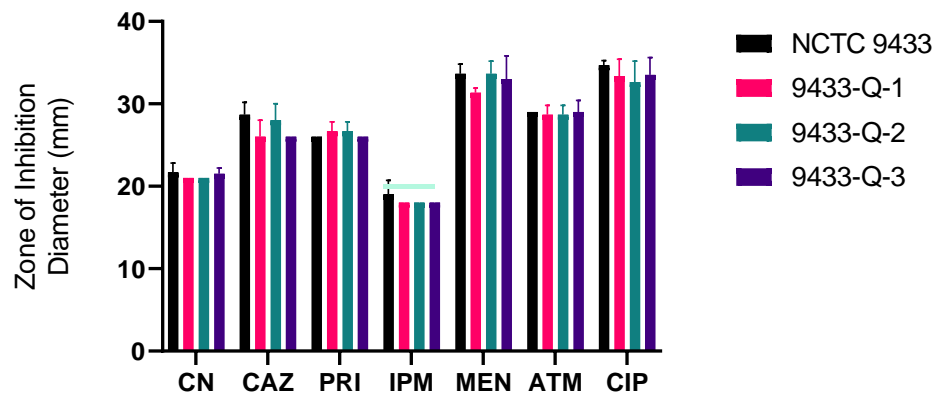
(2)
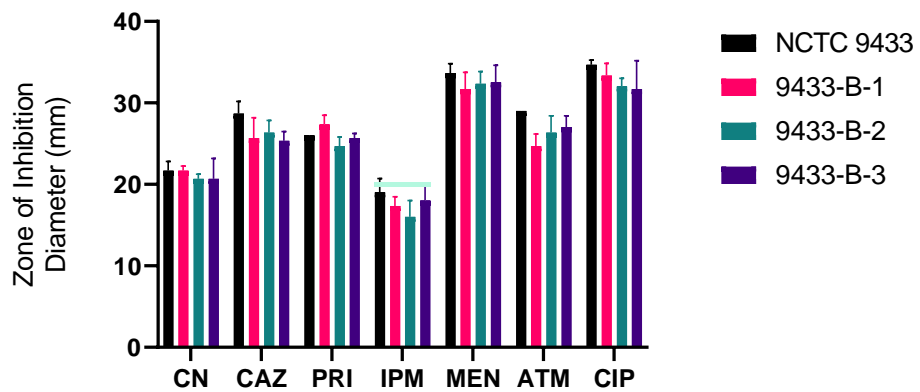
(3)

Figure 5-4 Antibiotic susceptibility of isolates of NCTC 9433 (control (1), quercetin (2) and berberine (3)), to a range of clinically relevant antibiotics according to the desk diffusion method. There was a slight change in the level of resistance to IPM from susceptible to resistant, across all 9433 isolates irrespective of condition, apart from NCTC 9433 Control 1, and NCTC 9433 Berberine 3 however none of these changes were statistically significant (Appendix II).

5.3.5 Appearance of D-zones in MIC analysis of evolved isolates

It was noted during the disc diffusion analysis that alongside the lack of changes that a D-zone appeared with all isolates in piperacillin (PRI), when placed next to the imipenem (IPM), such that the exclusion zone around the PRI was smaller on the side adjacent to the IPM disc (Figure 5-5). This was noted in 20 out of 20 isolates, including all ancestral strains and evolved isolates. PRI zones of inhibition were measured from at the widest points, avoiding the D-zone, for MIC analysis.
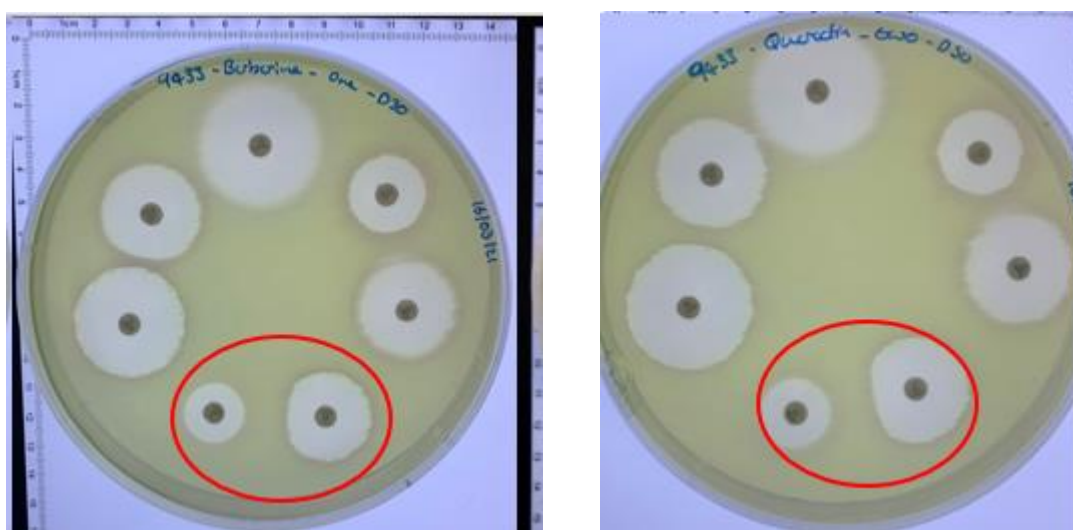
Figure 5-5 D-zone appearance in 9433 isolates between IPM and PRI. D-zones in the PRI exclusion zone appeared when place next to IPM. D-zone areas highlighted in red. 9433 Berberine 1 (left) and 9433 Quercetin 2 (right) are given as representatives of the isolates.

5.3.6 Changes in the production of pyocyanin by NCTC 7244 and NCTC 9433 isolates after evolution for thirty days in sub-inhibitory conditions of phytochemicals

After exploration of changes in MIC, the evolved isolates were subsequently evaluated against the ancestral isolate and a control *P. aeruginosa* NCTC 13437 (a clinical isolate), for production of pyocyanin, one of the major virulence factors of *P. aeruginosa*. This was conducted to determine if evolution in the presence of sub-inhibitory concentrations of the phytochemical altered the pyocyanin production phenotype of the isolates, compared to the ancestral strains (Figure 5-6). As pyocyanin production has previously been shown to be inhibited by phytochemicals.

All changes in pyocyanin production between the evolved isolates and their respective ancestors underwent a two-tailed t-test statistical analysis, the full statistical results can be found in appendix II.

NCTC 9433 berberine 2, NCTC 9433 berberine 3, and NCTC 9344 control 3 had a statistically significant increase in pyocyanin production. Pyocyanin production of NCTC 9433 (M = -0.01, SD = 0.00) was significantly different to NCTC 9433 berberine 2 (M = 0.00, SD = 0.00) (p = 0.00472), and pyocyanin production of NCTC 9433 (M = -0.01, SD = 0.00) was significantly different to NCTC 9433 berberine 3 (M = 0.00, SD = 0.00) (p = 0.035189). Pyocyanin production of NCTC 9433 (M = -0.01, SD = 0.00) was significantly different to NCTC 9433 control 3 (M = 0.00, SD = 0.00) (p = 0.027255).

No other isolates had significantly different pyocyanin production compared to their respective ancestral strain (appendix II).
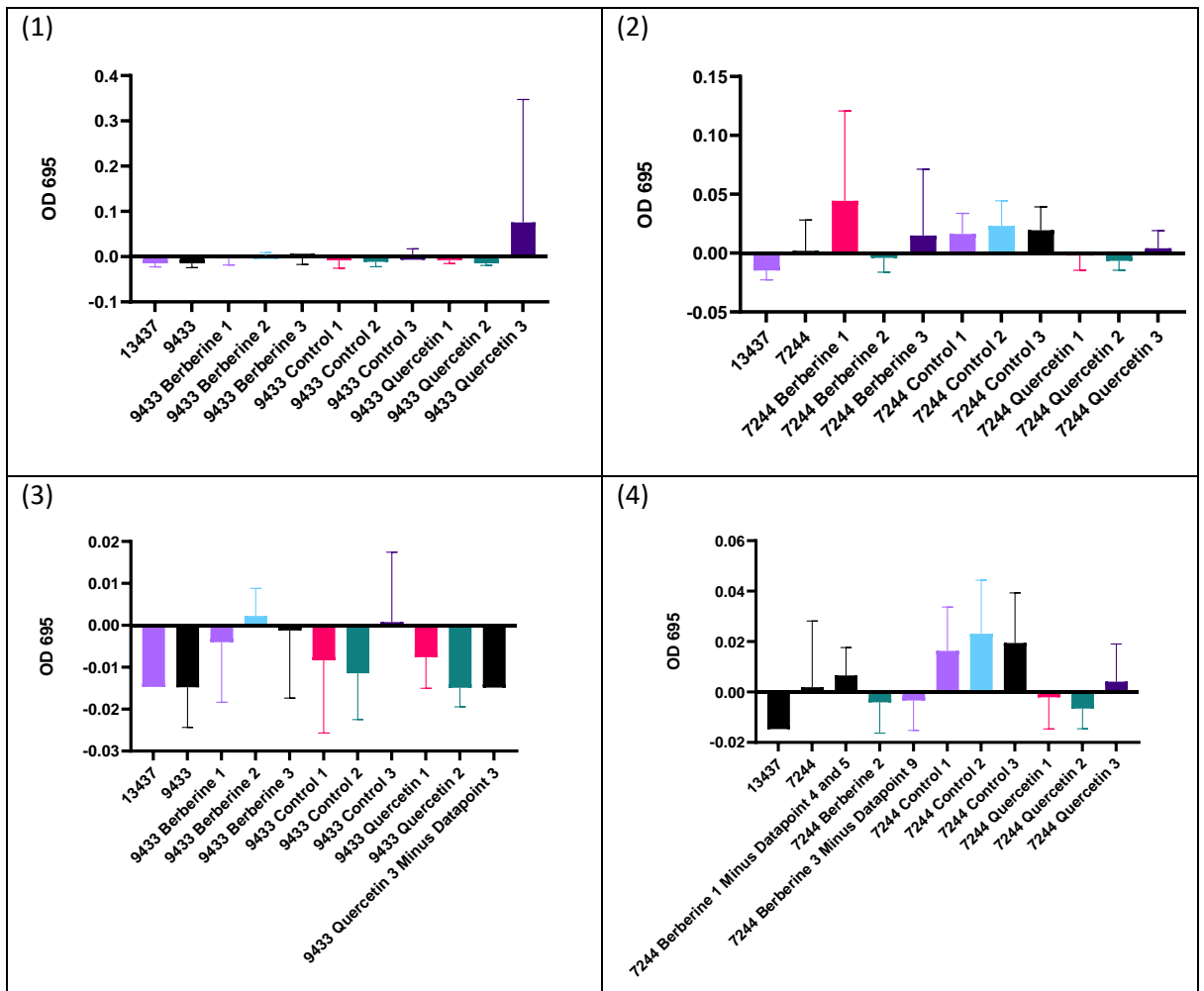
Figure 5-6 Changes in pyocyanin production after evolution in subinhibitory concentrations of either berberine or quercetin for thirty days for P. aeruginosa *NCTC 7244 (1) and NCTC 9433 (2). Both isolates were poor pyocyanin producers, NCTC 9433 quercetin 3 appeared to have dramatically increased pyocyanin production (1), but this was determined to be a single outlier datapoint, and removal indicated that all isolates produced a similar level of pyocyanin (3). NCTC 7244 Berberine 1 and 3 appeared to have increased pyocyanin production, but these were again found to be two outlier datapoints, and they were subsequently removed (4), the 7244 isolates evolved without plant metabolite pressure had increased pyocyanin production (2 & 4). NCTC 13437 was measured and included in all graphs, to give a consistent* P. aeruginosa *to measure by as a sense check.*

5.3.7 Changes in the biofilm production of NCTC 7244 and NCTC 9433 isolates after evolution for thirty days in sub-inhibitory conditions of phytochemicals

After evaluating the evolved isolates for increased pyocyanin production, they were also evaluated for biofilm production. Biofilms are a major mechanism by which cells can protect themselves from harmful chemicals and predation. In this study, it was hypothesised that chronic exposure to a harmful phytochemical could select for biofilm formation. As such, this assay aimed to examine the extent to which this

occurred. This assay specifically evaluated static biofilm production, and not flocculation which was observed when cells were passaged in the presence of sub-inhibitory concentrations of quercetin.

Biofilm production has been shown to be altered by the presence of phytochemicals and is associated with AMR phenotype in *P. aeruginosa*. As such we sought to examine if growth in sub-inhibitory concentrations of quercetin and berberine altered the biofilm producing phenotype of our isolates and if that was related to any of the genetic mutations we saw (Figure 5-7).

All changes in biofilm production between the evolved isolates and their respective ancestors underwent a two-tailed t-test statistical analysis, the full statistical results can be found in appendix II.

Only NCTC 9433 quercetin 2 had a statistically significant difference in biofilm production when compared to the ancestral isolate. Biofilm production of ancestral NCTC 9433 (M = 0.05, SD = 0.01) and NCTC 9433 quercetin 2 (M = 0.03, SD = 0.00) was significantly different (p = 0.040077). This was a decrease in biofilm production.

No other isolates had significantly increased or decreased pyocyanin production compared to their respective ancestor (appendix II).
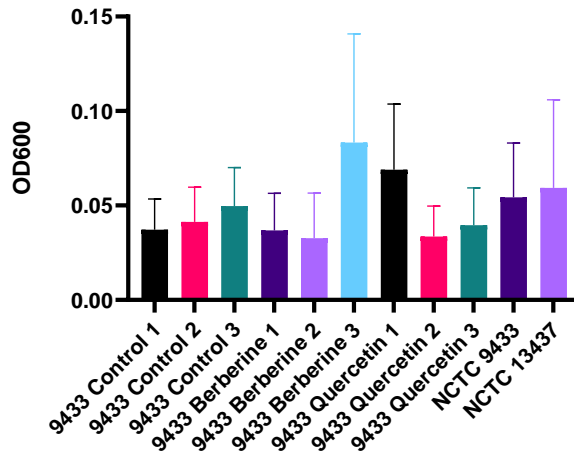
(1)
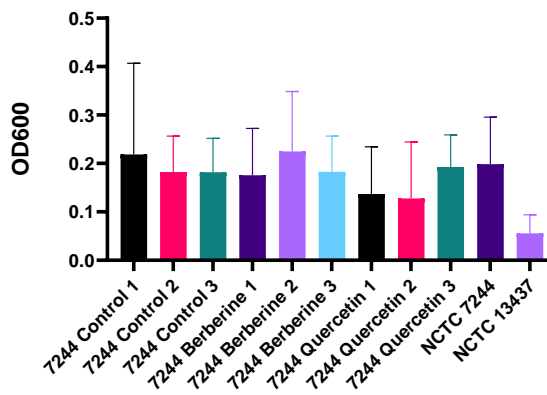
(2)
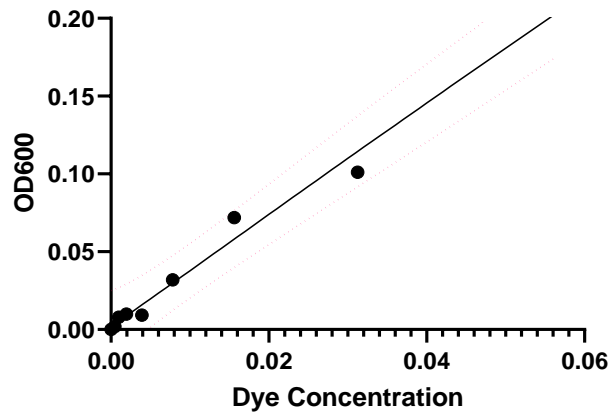
(3)

Figure 5-7 Changes in the biofilm production of P. aeruginosa NCTC 9433 and NCTC 7244 after evolution in subinhibitory concentration of either berberine or quercetin for thirty days. NCTC 9433 isolates (1) and NCTC 7244 isolates (2), and the standard curve that was created and used for this experiment (3) are shown.

5.3.8 Genomic changes in evolved isolates of NCTC 7244 and NCTC 9433 isolates after evolution for thirty days in sub-inhibitory conditions of phytochemicals, compared to ancestral strains.

After evolution for thirty days in the presence, or absence of the plant metabolites berberine or quercetin, the evolved lineages that displayed a phenotypic change in phytochemical resistance, and all the control lineages underwent whole genome sequencing. The resultant short read data was compared to the hybrid assemblies of the ancestral strains to examine the data for any mutations that fit the criteria outlined in the methods section, in the genomes of the evolved isolates.

Mutation prediction for each of the evolved isolates from the ancestral isolates was determined using Breseq. The number of mutations varied between isolates, with a maximum of 110 for NCTC 9433 berberine 3, to a minimum of 34 for NCTC 7244 quercetin 2 and NCTC 7244 berberine 2, generally all NCTC 9433 isolates had more mutations than all NCTC 7244 Isolates (Table 5-4 and Table 5-5). This list of mutations was triaged, following the methodology laid out in chapter 5.2.7.

The first triaging step removed mutations which occurred in multiple isolates, despite differences in phytochemical supplementation during evolution. After this step, 26 mutations remained, examples of mutations removed from analysis at this stage are given in (Table 5-6).

The second triaging step removed mutations which, despite occurring in only a single isolate, occurred within a gene, or genetic location, with many mutations, which were given the alias 'highly mutable locations'. After removal of mutations that occurred within these highly mutable locations, 7 mutations remained (Table 5-7). These seven mutations are detailed in this chapter, and examples of triaged mutations from this step are given in (Table 5-4 and

Table 5-5). Further three mutations were located across multiple NCTC 9433 isolates grown

in sub-inhibitory concentrations of berberine (Table 5-12).

An overview of all genes present across all isolates are displayed in Figure 5-8 and Figure 5-9.
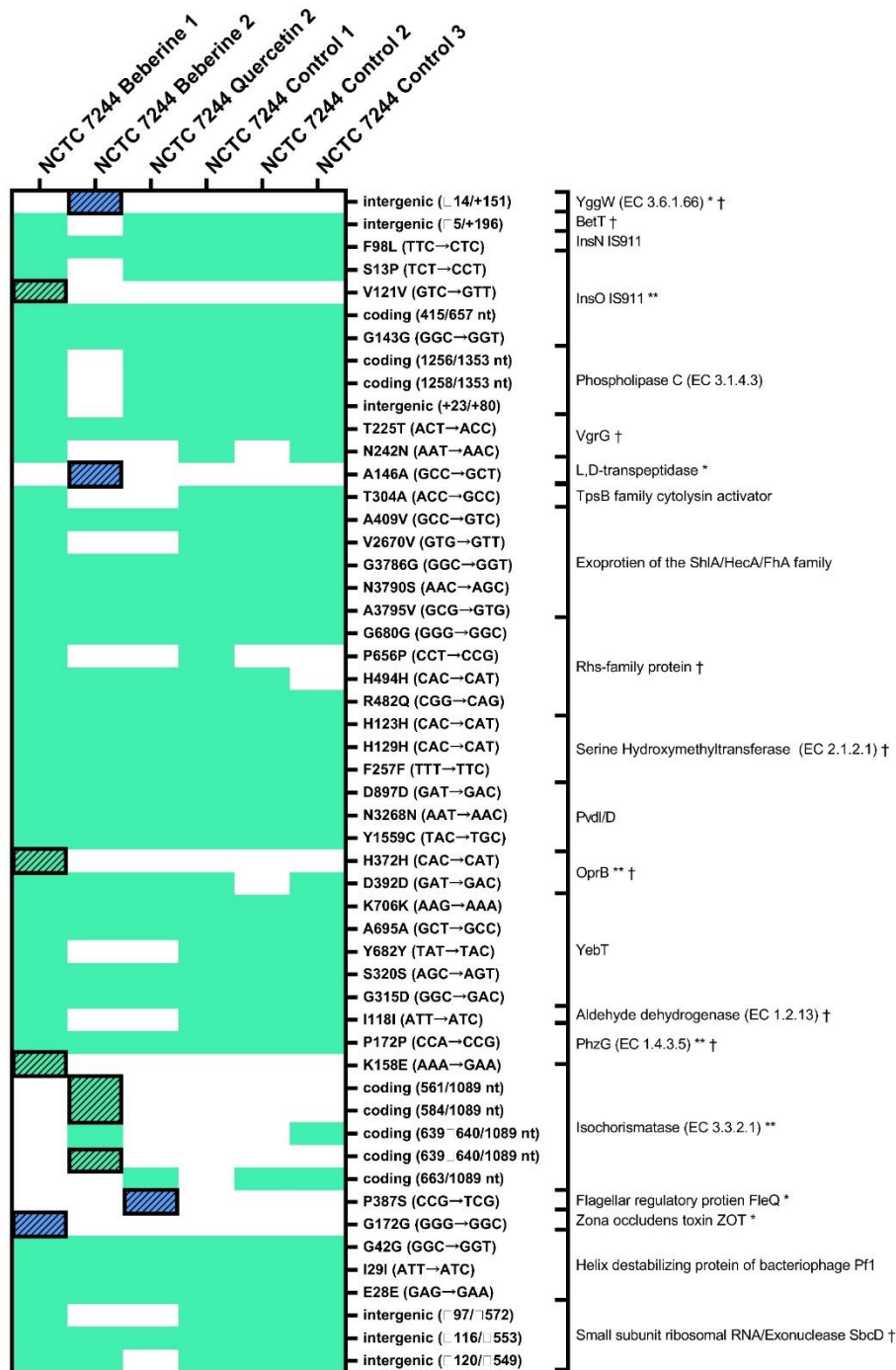
Figure 5-8 Categorical 2-variable heatmap of predicted mutations of NCTC 7244 isolates grown in the presence of phytochemicals with a two-fold increase in phytochemical resistance, and isolates grown in the absence of phytochemical.

Isolates are designated on the X-axis and predicted mutations, and associated genes on the Y-axis. Green & blue denotes the presence of a mutation, and white the absence. (*) Denotes a predicted mutation that occurred only once across all isolates, and where no other mutation occurred in the gene across other isolates. These are also highlighted with a blue shaded box. These mutations are: YggW, L, D-transpeptidase, FleQ and ZOT. (**) Denotes a gene containing a predicted mutation that occurred in only a single isolate, but where multiple mutations occurred in that gene across all isolates: Examples include InsO and Isochrismatase. (†) Denotes a gene where mutations were present in both NCTC 9433 and NCTC 7244 isolates. These are: yggW, betT, vgrG, Rhs-family protein, Serine Hydroxymethyltransferase, OprB, Aldehyde dehydrogenase and SbcD. No mutations were identical across isolates, only genes containing them.
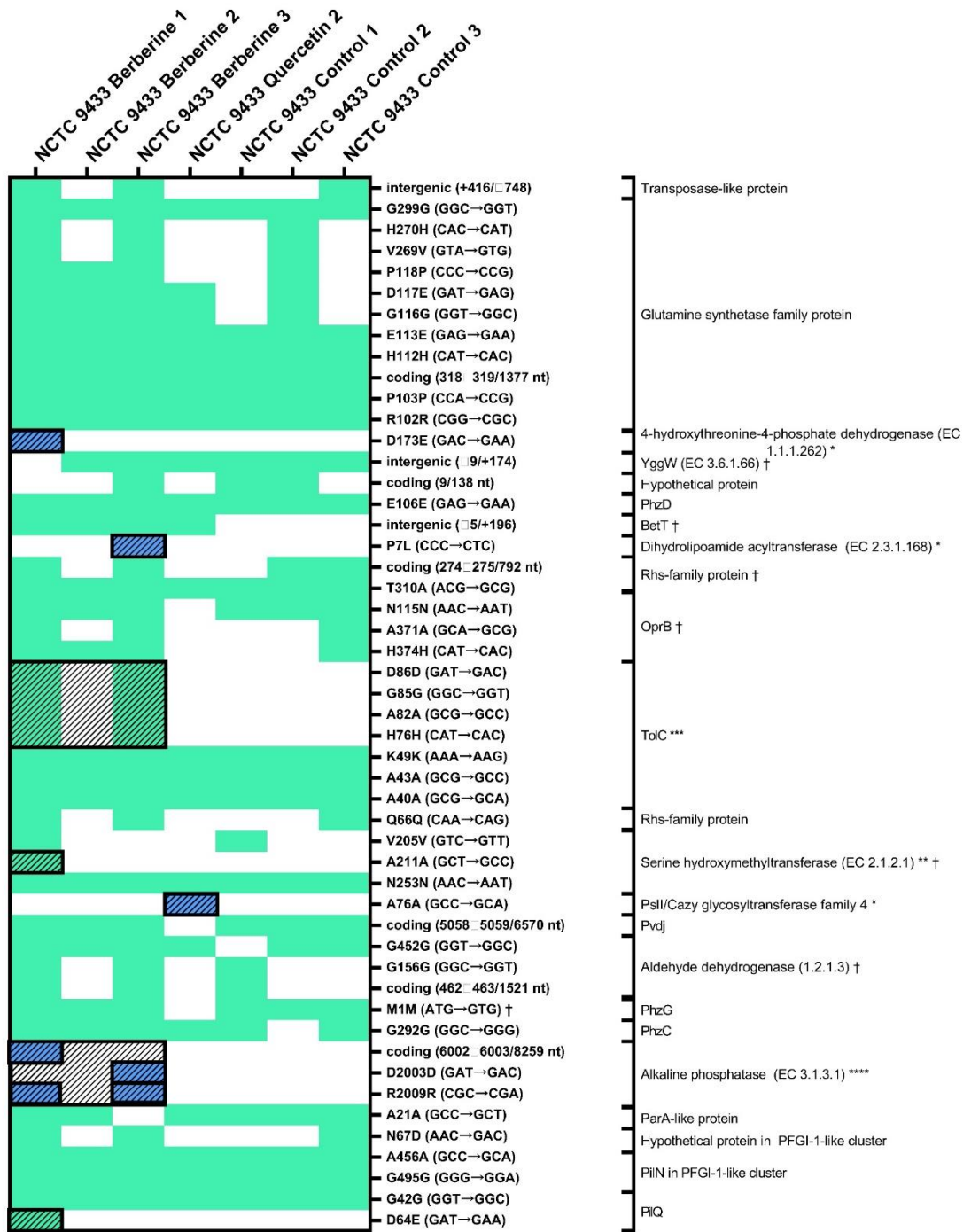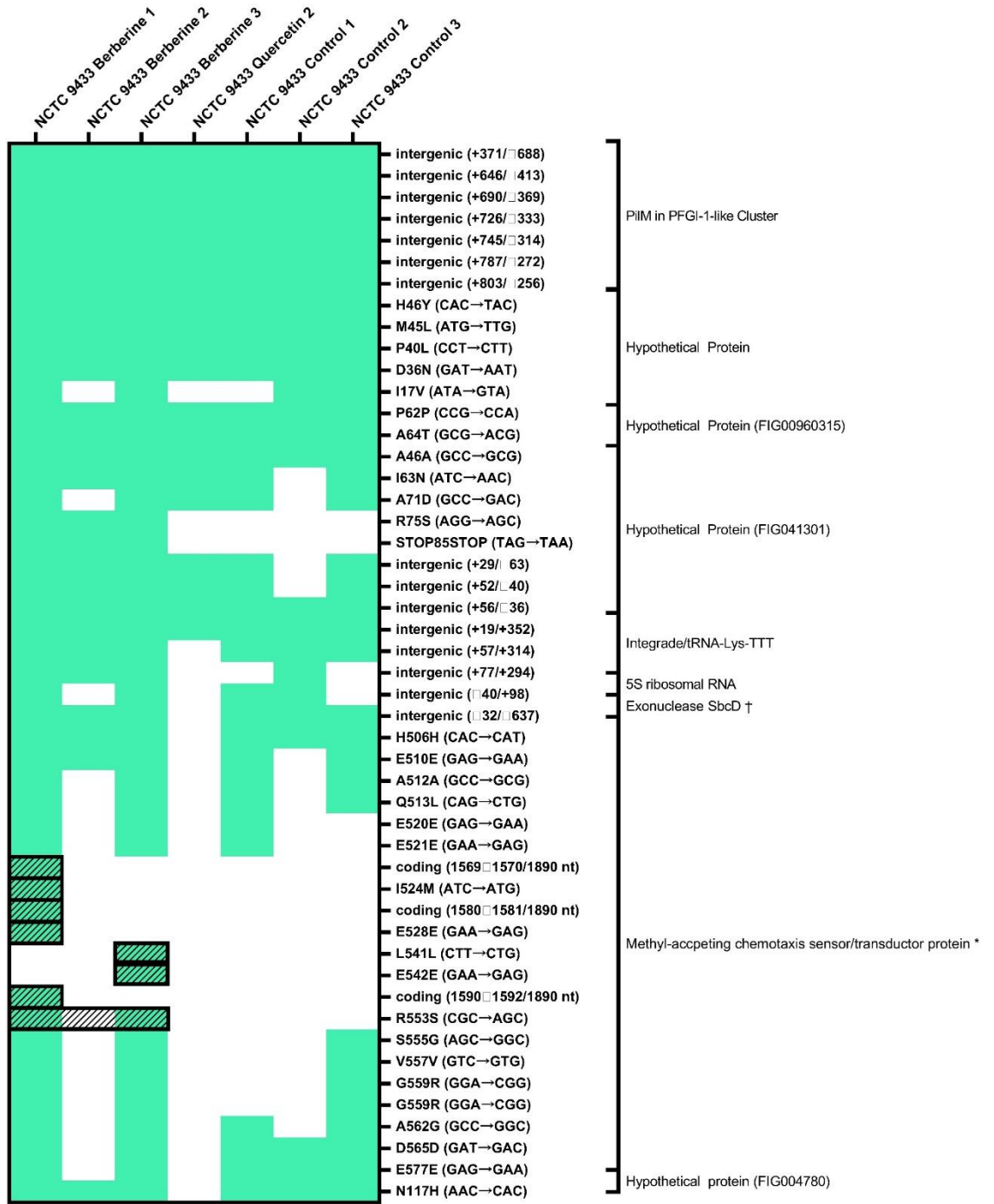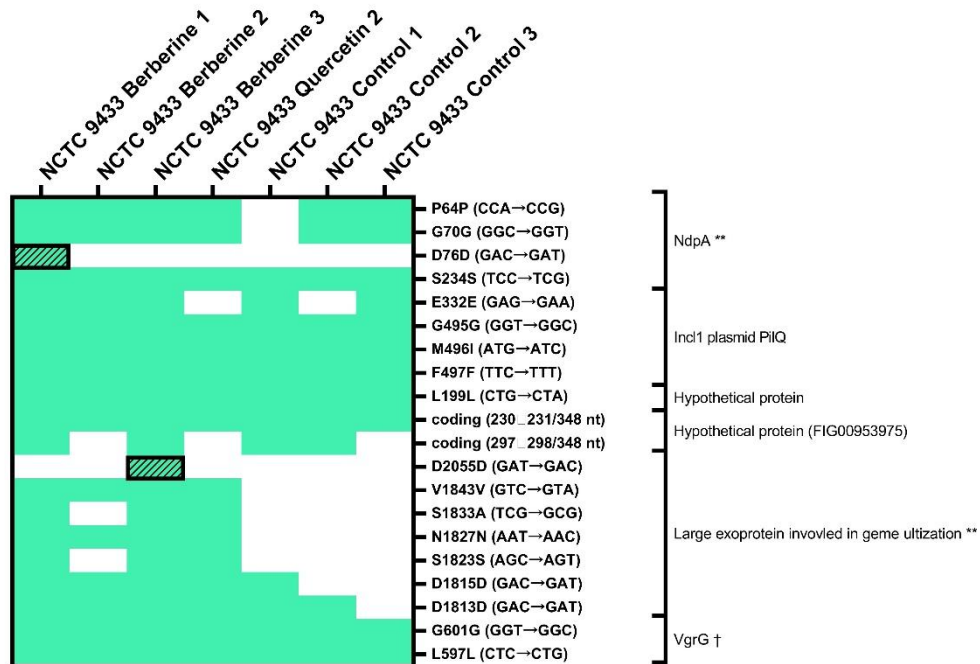
Figure 5-9 Categorical 2-variable heatmap of predicted mutations of NCTC 9433 isolates grown in the presence of phytochemicals with a two-fold increase in phytochemical resistance, and isolates grown in the absence of phytochemical.

Isolates are designated on the X-axis and predicted mutations, and associated genes on the Y-axis. Green & blue denotes the presence of a mutation, and white the absence. (*) Denotes a predicted mutation that occurred only once across all isolates, and where no other mutation occurred in the gene across other isolates. These are also highlighted with a blue shaded box. These mutations are: 4-H-4-P dehydrogenase, Dihydrolipoamide acyltransferase, Cazy. (**) Denotes a gene containing a predicted mutation that occurred in only a single isolate, but where multiple mutations occurred in that gene across all isolates. (***) Denotes a gene containing a set of predicted mutations unique to a growth condition, but that had other mutations across growth conditions. The clearest example of this were the predicted mutations in the tolC gene, which had 4 mutations unique to the berberine treatment groups, but a further 3 predicted mutations across all treatment groups. (****) Denotes a gene containing a set of different mutations that are unique to a growth condition, specifically mutations in the alkaline phosphatase gene grown in the presence of berberine. (†) Denotes a gene where mutations were present in both NCTC 9433 and NCTC 7244 isolates. These are: YggW, BetT, VgrG, Rhs-family protein, Serine Hydroxymethyltransferase, OprB, Aldehyde dehydrogenase and SbcD. No mutations were identical across isolates, only genes containing them.

Table 5-4 Overview of the triage methodology for each lineage of NCTC 7244 isolates evaluated. Isolate name, the total number of mutations overall, after triage step 1, and after triage step 2 displayed. Also displayed are the details of predicted mutations for each lineage after the final triage step.

Isolate	Total number of mutations	Triage Step 1. Number of mutations present in only this isolate	Triage Step 2. Number of mutations present in only this isolate; not contained in a highly mutable location	Mutations present in this isolate after passing through the triage step.
NCTC 7244 Berberine 1	44	4	1	Zona occludens toxin (ZOT) C→G G172G (GGC→GGG)
NCTC 7244 Berberine 2	34	5	2	L, D-transpeptidase C→T A146A (GCC→GCT)
				Oxygen-Independent coproporphyrinogen-III oxidase-like protein YggW/ RdgB (EC 3.6.1.66) +G Intergenic (-14/+151)
NCTC 7244 Quercetin 2	34	1	1	Flagellar regulatory protein FleQ C→T P387S (CCG→TCG)
NCTC 7244 Control 1	40	0	N/A	N/A
NCTC 7244 Control 2	38	0	N/A	N/A
NCTC 7244 Control 3	40	0	N/A	N/A

Table 5-5 Overview of the triage methodology for each lineage of NCTC 9433 isolates evaluated. Isolate name, the total number of mutations overall, after triage step 1, and after triage step 2 displayed. Also displayed are the details of predicted mutations for each lineage after the final triage step.

Isolate	Total number of mutations	Triage Step 1. Number of mutations present in only this isolate	Triage Step 2. Number of mutations present in only this isolate; not contained in a highly mutable location	Mutations present in this isolate after passing through the triage step.
NCTC 9433 Berberine 1	111	10	1	4-hydroxythreonine-4-phosphate dehydrogenase (EC 1.1.1.262) C→A D173E (GAC→GAA)
NCTC 9433 Berberine 2	69	0	N/A	N/A
NCTC 9433 Berberine 3	106	5	1	Dihydrolipoamide acyltransferase component of branched-chain alpha-keto acid dehydrogenase complex (EC 2.3.1.168) C→T P7L (CCC→CTC)
NCTC 9433 Quercetin 2	59	1	1	Pellicle/biofilm biosynthesis protein PsIi, CAZy glycosyltransferase family 4 C→A A76A (GCC→GCA)
NCTC 9433 Control 1	70	0	N/A	N/A
NCTC 9433 Control 2	65	0	N/A	N/A
NCTC 9433 Control 3	74	0	N/A	N/A

Table 5-6 Examples of mutations removed from our analysis by step 1 of our triage methodology. Location of the mutations, the mutations (base pair change, codon change and predicted amino acid change given) and the predicted gene name and function given from RAST analysis. Also displayed are the isolates that the predicted mutation is present in, and the number of mutations within this area.

Location of Mutation	Mutation	Gene Name/Function	Isolates present in	Number of Mutations within that Highly Mutable location
2,728,223	C→T A409V (GCC→GTC)	Putative large exoprotein involved in heme utilization or adhesion of ShlA/HecA/FhaA family	7244 Berberine 1 7244 Berberine 2 7244 Quercetin 2 7244 Control 1 7244 Control 2 7244 Control 3	1: This mutation occurred in all NCTC 7244 Isolates.
314,956	C→T G299G (GGC→GGT)	Glutamine synthetase family protein	9433 Berberine 1 9433 Berberine 2 9433 Berberine 3 9433 Quercetin 2 9433 Control 1 9433 Control 2 9433 Control 3	11: This mutation occurred in all NCTC 9433 isolates, and there was a total of 11 mutations in this gene across all NCTC 9433 isolates.

Table 5-7 Examples of mutations removed from our analysis by step 2 of our triage methodology. Location of the mutations, the mutations (base pair change, codon change and predicted amino acid change given) and the predicted gene name and function given from RAST analysis. Also displayed are the isolates that the predicted mutation is present in, and the number of mutations within this area

Location of Mutation	Mutation	Gene Name/Function	Isolates present in	Number of Mutations within that Highly Mutable location
3,455,085	A→G K158E (AAA→GAA)	Pyridoxamine 5'-phosphate oxidase PhzG (EC 1.4.3.5)	7244 Berberine 1	2: This mutation occurred in only a single isolate, however another mutation in this gene was present in all NCTC 7244 Isolates.
5,151,201	C→T D76D (GAC→GAT)	Nucleoid-associated protein NdpA	9433 Berberine 1	3: This mutation was present only a single isolate, however 3 mutations were present in this gene in all other NCTC 9433 isolates.
2724321, 2724324, 2724333, 2724351	T→C D86D (GAT→GAC) C→T G85G (GGC→GGT) G→C A82A (GCG→GCC) T→C H76H (CAT→CAC)	Type I secretion outer membrane protein TolC family	9433 Berberine 1 & 3	7: These 4 mutations were present in multiple NCTC 9433 isolates grown I n the berberine conditions, however 3 other mutations in this gene were present in all NCTC 9433 isolates.

5.3.9 Further analysis of the predicted mutations dataset across the *P. aeruginosa* isolates.

5.3.9.1 Synonymous mutations

Further analysis was conducted on the seven predicted mutations that passed successfully through the triage methodology. Of the 7 mutations remaining after triage, 3 were synonymous mutations (Table 5-8). A synonymous mutation is a mutation in the nucleic acid sequence, which does not confer a change in the amino-acid sequence of the protein it encodes. For these mutations, the codon frequency of the pre-, and post-mutation codons is given. Codons usage bias within a genome correlates with the charged amino-acyl tRNA copy numbers (Andersson & Kurland, 1990; Ikemura, 1981). Alongside this, essential and highly expressed genes usually contain a higher frequency of optimal codons (Gouy & Gautier, 1982). By this it can be inferred that a synonymous mutation, from a frequently used codon, to an infrequently used codon, is associated with a movement from an amino acyl tRNA with high copy numbers, to low copy numbers, thereby potentially limiting the level of transcription of this gene.

Codon frequency was determined from www.kazusa.or.jp (Nakamura et al., 2000), which used *P. aeruginosa strain O1* (PAO1), though, it is possible NCTC 7244 or 9433 have slightly different codon frequencies than PAO1. In our case, all mutations led to the selection of a codon with a lower frequency (Table 5-8).

Table 5-8 Synonymous mutations, and codon frequency from our triaged mutations.

Gene Name & Function	Location of Mutation	Mutation	Codon frequency per 1000 (PAO1)	Strain and Phytochemical
Pellicle/biofilm biosynthesis protein PslI, CAZy glycosyltransferase family 4	3,052,141	C→A A76A (GCC→ GCA)	GCC: 67.7 GCA: 4.8	NCTC 9433 Quercetin
Zona occludens toxin (ZOT)	4,794,585	C→G G172G (GGC→ GGG)	GGC: 61.9 GGG 9.9	NCTC 7244 Berberine
L, D-transpeptidase	2,279,005	C→T A146A (GCC→ GCT)	GCC: 67.7 GCT/U: 4.8	NCTC 7244 Berberine

5.3.9.2   Non-synonymous mutations

The 3 mutations were non-synonymous. A non-synonymous mutation is one which does confer a change to the amino-acid sequence of the protein it encodes. An overview of the relation of each of these mutations to functional sites on their respective encoded proteins is given in Table 5-9 and Table 5-10.

Table 5-9 Non-synonymous mutations that remained after triaging from NCTC 9433 Isolates, the codon frequency of the mutations, and the relationship of the mutation to the functional sites of the protein.

Gene Name & Function	Location of Mutation	Mutation	Codon frequency per 1000 (PAO1)	Strain and Phytochemical	Relation to functional sites on the protein
4-hydroxythreonine-4-phosphate dehydrogenase (EC 1.1.1.262)	634,601	C→A D173E (GAC→ GAA)	GAC: 42.6 GAA: 23.4	NCTC 9433 Berberine	The homodimer structure has multiple binding sites, to the substrate between the amino acids (AAs) 136-137 and 273-292 AAs, and to the metal at 166 AA, 211 AA and 266 AA. The mutation is predicted to cause an amino acid change in the alpha helix ring of the substrate binding site, this predicted change is unlikely to directly interact with the substrate or with metal binding, but may possibly change the binding site structure, or alter the homodimer structure (Bateman et al., 2021).
Dihydrolipoamide acyltransferase component of branched-chain alpha-keto acid dehydrogenase complex (EC 2.3.1.168)	1,673,443	C→T P7L (CCC→ CTC)	CCC: 13.0 CTC: 27.8	NCTC 9433 Berberine	From our mutation we predict an amino acid change within the initial highly variable region of the protein which is normally attached to the transit peptide which moves the protein around the cell. This inferred change may affect attachment of the protein to the transit peptide, or interactions with other subunits of the pyruvate dehydrogenase complex but is unlikely to affect the function of the protein, or substrate binding (Bateman et al., 2021).

Table 5-10 Non synonymous mutations that remained after triaging from NCTC 9433 Isolates, the codon frequency of the mutations, and the relationship of the mutation to the functional sites of the protein.

Gene Name & Function	Location of Mutation	Mutation	Codon frequency per 1000 (PAO1)	Strain and Phytochemical	Relation to functional sites on the protein
Flagellar regulatory protein FleQ	4,370,672	C→T P387S (CCG→ TCG)	CCG: 33.3 T/UCG: 13.0	NCTC 7244 Quercetin	There are multiple binding sites including AA 142, 147, 334 and 363 within the 177-182, 186-189 and 330-341 regions. Various mutations from residues 29 to 334 completely inhibit biofilm formation and pel transcription. Our predicted amino acid change is on the outer edge of the protein, towards the N terminal residues. It is entirely possible that it would affect the proteins' function, due to the ability of various changes to residues at the edge of the protein to have been shown to do so previously (Bateman et al., 2021).

5.3.9.3   Intergenic mutations

One mutation occurred in the intergenic region between the YggW and RdgB encoding open reading frames. This mutation was unlikely to affect protein structure directly, but may impact transcription of the surrounding open reading frames (Table 5-11).

Table 5-11 Intergenic region mutations that remained after triaging from NCTC 9433 Isolates, the codon frequency of the mutations, and the relationship of the mutation to the functional sites of the protein.

Gene Name & Function	Location of Mutation	Mutation	Codon frequency per 1000 (PAO1)	Strain and Phytochemical	Relation to functional sites on the protein
Oxygen-Independent coproporphyrinogen-III oxidase-like protein YggW/ RdgB (EC 3.6.1.66)	410,893	+G Intergenic (-14/+151)	N/A	NCTC 7244 Berberine	This mutation is an insertion of a G after the reference position of 410,893, this mutation is 6 nucleotides upstream of the YggW gene encoding region and +151 nucleotides downstream of the RdgB+ protein. We predict that it is unlikely to affect the protein, but may affect transcription of the surrounding open reading frames.

5.3.9.4   The presence of varied mutations in the Alkaline phosphatase of NCTC 9433 isolates grown in the presence of berberine

Additionally, four other mutations in one other gene passed through our triage methodology, though these mutations did not meet the above categories.

Instead, the Alkaline phosphatase gene (EC 3.1.3.1) from NCTC 9433 had three predicted mutations, one of which occurred in two isolates undergoing

evolution in the same selective pressure of berberine. However, all these mutations were clustered within the NCTC 9433 isolates grown in sub-inhibitory

concentrations of berberine (Table 5-12).

Table 5-12 Group of predicted mutations in the Alkaline phosphatase gene (EC 3.1.3.1) that occurred only in the NCTC 9433 berberine evolved isolates, the codon frequency of the mutations, and the relationship of the mutation to the functional sites of the protein.

Gene Name & Function	Location of Mutation	Mutation	Codon frequency per 1000 (PAO1)	Strain and Phytochemical	Relation to functional sites on the protein
Alkaline phosphatase (EC 3.1.3.1)	4244312	2 bp→AT coding (6002 -6003 /8259 nt)	N/A	NCTC 9433 Berberine 1	A multiple base substitution at this region, this would suggest the original protein is not produced after this region. However this protein is predicted to be over 2000 AA long, far larger than the standard 450-500 AA for E.C.3.1.3.1 (Bateman et al., 2021).
Alkaline phosphatase (EC 3.1.3.1)	4244319	T→C D2003D (GAT→GAC)	GAT: 10.5 GAC: 42.6	NCTC 9433 Berberine 3	N/A
Alkaline phosphatase (EC 3.1.3.1)	4244337	C→A R2009R (CGC→CGA)	CGC: 49.4 CGA: 2.4	NCTC 9433 Berberine 1 & 3	N/A

5.3.9.5   Multiple genes contained predicted mutations in both the NCTC 7244 and 9433 isolates, across treatment conditions

Finally, predicted mutations in the YggW, BetT, VgrG, Rhs-family protein, Serine Hydroxymethyltransferase, OprB, Aldehyde dehydrogenase and SbcD genes were present in both NCTC 9433 and NCTC 7244 isolates (Figure 5-8 and Figure 5-9). No identical mutations were detected, however the YggW gene mutation occurred only in NCTC 7244 berberine 2 isolate (Table 5-4), but across all growth conditions in NCTC 9433 (Table 5-5) though as previously stated the YggW / RdgB mutation in NCTC 7244 berberine 2 was intergenic (Table 5-11).

5.4   Discussion

The main findings from this study can be broken down into the following:

(1) Eleven of twelve isolates had a 2-fold increases in their resistance profile to either quercetin, or berberine, respectively. (2) None of our isolates had a significant change in their antibiotic resistance phenotype after 30-day evolution in sub-inhibitory concentrations of berberine or quercetin. (3) When evaluated visually it was clear that all samples flocculated when cultured with sub-inhibitory concentrations of quercetin, but not berberine. (4) Piperacillin developed a D-zone in all isolates when placed next to imipenem (5) NCTC 9433 berberine 2, NCTC 9433 berberine 3, and NCTC 9344 control 3 had a statistically significant increase in pyocyanin production. (6) Only NCTC 9433 quercetin 2 had significantly different level biofilm production compared to the ancestral strain. NCTC 9433 quercetin 2 had decrease biofilm formation compared to the ancestral strain. This decrease was associated with a mutation in the *cazY* gene. (7) We hypothesise that ten mutations across our isolates occurred due to growth in selective concentrations of quercetin and berberine. Two of these mutations, the L, D, transpeptidase and the glycosyltransferase occurred in genes present on inserts in phytochemical tolerant isolates from chapter 3.

5.4.1   Eleven of twelve isolates had increased resistance to phytochemicals after evolution in subinhibitory concentrations of the respective phytochemical

Eleven of the 12 isolates had a 2-fold increase to the phytochemical they were passaged under selective pressure of. This increase was from 128 µg/ml to 256 µg/ml.

Previous studies have highlighted the ability of bacteria to develop an 8-fold increase resistance to other phytochemicals such as linalool (Kalily et al., 2016) as a result of environmental exposure. This increase was 4-fold higher than the resistance increase seen in this study. Our study clearly demonstrates that *P. aeruginosa* can develop resistance to our two plant metabolites, quercetin and berberine. A twofold increase in resistance is not

always considered clinically relevant, or enough to change a bacterial status from susceptible to resistance (Kowalska-Krochmal & Dudek-Wicher, 2021). However, this usually occurs for MIC in concentrations below 32 µg/ml (EUCAST, 2022), and the inhibitory concentration of phytochemicals against the ancestral strains in our experiments is much higher than this, at 128 µg/ml.

5.4.2   Sample flocculation occurred when *P. aeruginosa* was exposed to quercetin in sub-inhibitory concentrations

All our isolates demonstrated flocculation after exposure to quercetin in subinhibitory concentrations, but not to berberine, and they did not demonstrate this ability when grown in the absence of phytochemicals.

Flocculation is the ability of *Pseudomonas sp.* to form clumps of cells through cellular aggregation, and can also involve the cells changing structure shape, from rods to cocci. Flocculation, also known as auto-aggregation, is a strategy employed by many bacterial species to increase survival in hostile environments when there is no surface to colonise (Trunk et al., 2018), and can be thought of as a type of planktonic biofilm.

Flocculation is controlled by the polysaccharides glucose, glucuronic acid, mannose and xylose (Li et al., 2013). Flocculation is being explored for its use in controlling sewage treatment (Lee et al., 2017), heavy metal contamination of oil-field formation water (Pathak et al., 2014) and desulfurization (Li et al., 2011). This suggests that there is a possible industrial application of quercetin-based flocculation in the control of water contaminants (Fakhruddin & Quilty, 2007).

 In *Pseudomonas putida,* flocculation occurs as a result of magnesium depletion (Corkill, 1989). Metal depletion in the environment may be the cause of our flocculation in these experiments, as quercetin has been shown to effectively chelate calcium, magnesium and nickel (de Castilho et al., 2018).

We theorise that the flocculation seen in this study is a result of bacterial adaptation to quercetin stress conditions. Selection for flocculation by these strains likely occurred as a result of the evolution methodology which had continued growth in shaking laboratory media, thus reducing the ability of the cells to form biofilms.

5.4.3 There was a D-zone at the interface between piperacillin and imipenem, across all isolates

All isolates had a clear D-zone on the interface between piperacillin and imipenem, such that the zone of inhibition around piperacillin was reduced.

The D-zone suggests that when piperacillin is placed next to imipenem, the bacteria are potentially becoming more resistant to imipenem. *P. aeruginosa* isolates can develop resistance to both piperacillin and carbapenems, however these antibiotics have diverse modes of action and thus, bacterial develop different resistant mechanisms for both (Mokaddas & Sanyal, 1999).

Zones of inhibition are usually uniform, however they do not always have clear or regular borders (Microchem Laboratory, 2022). Disc diffusion methodology can be used to determine synergy or antagonistic activity between two different antibiotics, the latter which is seen with the flattening of the zone of resistance between the two antibiotics (Laishram et al., 2017), although the results are usually qualitive and open to interpretation.

This could suggest that piperacillin and imipenem are antagonistic antibiotics in the case of our two *P. aeruginosa* isolates which has been previously reported for 10 aminoglycoside-susceptible and 25 aminoglycoside-resistant clinical isolates (Betram & Young, 1984) and 25 imipenem resistant clinical strains of *P. aeruginosa* (Farzana & Shamsuzzaman, 2015). The literature in this field suggests that this is the probable cause of this D-zone appearance.

5.4.4 Three isolates had increased pyocyanin production

NCTC 9433 berberine 2, NCTC 9433 berberine 3, and NCTC 9344 control 3 had a statistically significant increase in pyocyanin production. (Figure 5-6).

High pyocyanin production is associated with septic shock, and death in bacteraemia patients infected with *P. aeruginosa* (Gupte et al., 2021) and is associated with low bacterial mobility. Previous studies have linked pyocyanin production to heavy metal resistance (Muller & Merrett, 2014). Alongside this, pyocyanin is highly associated with multidrug resistance (MDR). One study by Gajdács et al, suggested there is no correlation between virulence factors and resistance in the laboratory across a range of 302 clinical isolates of *P. aeruginosa* with a range of antimicrobial resistance profiles (Gajdács et al., 2021), with the notable exception of pyocyanin, which was correlated with MDR strains. Quercetin has been previously reported as a pyocyanin inhibitor (Ouyang et al., 2016).

The higher pyocyanin production in NCTC 9433 control isolates could be a result of cell adaptation to growth in high nutrient concentration laboratory conditions, although its use as virulence factor would suggest that pyocyanin production should decrease with adaptation to laboratory conditions, as is the case with PAO1 (Chandler et al., 2019). Pyocyanin production between *Pseudomonas sp.* isolates can vary between strain and media used (Amly et al., 2021; El-Fouly et al., 2015). Royal jelly supplementation in media increases pyocyanin production (Amly et al., 2021), and of 20 isolates of *P. aeruginosa,* containing both clinical and environmental isolates, the two highest producing strains were isolated from a rice-cultivating soil, and urinary tract infection, producing 9.3 and 5.9 µg/ml pyocyanin respectively on glucose supplemented nutrient medium (El-Fouly et al., 2015).

Taken together, these data suggest repetition of this experiment may be required in alternative media, to understand fully the pyocyanin producing phenotype of these isolates. However, these data suggest that pyocyanin production may be increased by passaging in

sub-inhibitory concentrations of berberine, and thus there may be a linkage between berberine tolerance and pyocyanin production.

5.4.5 NCTC 9433 quercetin 2 had a statistically significant decrease in biofilm formation compared to the ancestral isolate

Only NCTC 9433 quercetin 2 had a statistically significant difference in biofilm production when compared to the ancestral isolate. This difference was a decrease in biofilm production compared to the ancestral isolate. The *cazY* mutation was found in NCTC 9433 Quercetin 2, the only isolate with a statistically significant decrease in biofilm formation. We theorise that the *cazY* mutation was transcribed less, as a result of this mutation, this hypothesis is strengthened by the decrease in biofilm formation of this isolate.

Biofilm formation in *P. aeruginosa* is contentious with regards to its relationship to antimicrobial resistance, and phytochemical tolerance. One study by Abdulhaq et al, evaluated a total of 52 clinical isolates of *P. aeruginosa* of which 20 were MDR isolates, all MDR isolates in this study were biofilm producers, and 90% of isolates were positive for the *pslA* gene, which is the first gene of the *pslA* gene cluster, involved in exopolysaccharide biosynthesis. (Abdulhaq et al., 2020). Further Kamali et al, demonstrated that across 80 clinical isolates of *P. aeruginosa* having a MDR phenotype was associated with biofilm production in 17.91% of the samples (Kamali et al., 2020). However, in Gajdács et al, 2021, 302 isolates of *P. aeruginosa* were used to assess the relatedness of AMR phenotype and biofilm production. Gajdács et al., determined that there was no overall significant correlation between AMR phenotype and biofilm production across all 302 isolates (Gajdács et al., 2021).

Both quercetin (Mu et al., 2021; Vipin et al., 2019; Zeng et al., 2019) and berberine (Chu et al., 2016; Wang et al., 2009) have been shown to inhibit biofilm formation across many bacterial species including members of the *Pseudomonas* and *Staphylococcus* genera. As

such we would have expected to see mutations which led to increased biofilm formation in our evolved strains, though this was not seen as part of this study.

One potential reason for decreased biofilm production is that this experimental design was conducted in large volumes of constantly shaken media, which would encourage the growth of planktonic bacteria (Garrett et al., 2008). The passaging methodology avoided taking bacteria from the edges of the media, where biofilm may have formed on the tube surface. As such, our experimental design may have actively selected for bacteria which did not form a static biofilm. Instead, we posit that out experimental methodology selected for planktonic cells, with a flocculation phenotype, rather than a static biofilm.

5.4.6 The presence of sub-inhibitory concentrations of phytochemicals led to the appearance of seven unique mutations across six isolates and an additional group of mutations in one gene across all NCTC 9433 isolates grown in sub-inhibitory concentrations of berberine

After phytochemical resistance, antimicrobial resistance and pyocyanin and biofilm producing phenotypes were established, the isolates that displayed an increase in resistance to either phytochemical, or the control groups, subsequently underwent whole genome sequencing. These genomes were compared to the ancestral isolates, to determine the predicted mutations that occurred across the strains during the experimental evolution. Over both strains, and all assessed isolates, there were a total of 170 predicted mutations. These mutations went through the previously described triage, which resulted in the determination of 7 predicted mutations which are theorised to have occurred as a consequence of growth under the selective pressure of the plant phytochemicals in one of the isolates (Table 5-8, Table 5-9, Table 5-10, and Table 5-11). In addition, 3 further mutations in the same gene were theorised to have occurred because of NCTC 9433 growth under the selective pressure of berberine (Table 5-12).

5.4.6.1   The relevance of synonymous mutations

Of the seven changes that occurred in only a single isolate, three of the changes were predicted to be synonymous mutations. Synonymous mutations are changes in a single DNA residue in a codon, which does not alter the translated protein sequence. An example of a synonymous mutation would be CAU to CAC, both of which encode for Histidine. Synonymous mutations do not change the translated amino acid. However, they are able to change protein structure, as depending on the context, codon usage can regulate translated protein folding (Yu et al., 2015) and affect the ribosome during translation (Pechmann et al., 2014; Pechmann & Frydman, 2013). An example of this is that two firefly luciferases with the same amino-acid sequence, but different codons had different resistances to trypsin digestion and different levels of luciferase activity, indicating that the synthesised polypeptides must differ structurally (Yu et al., 2015).

Synonymous mutations can affect gene expression in a number of settings, including cancer (Gutman et al., 2021), bacterial growth (Horton et al., 2021) and immune disorders (Petry & Loos, 2005). Synonymous mutations cause changes in gene expression by altering mRNA stability, which subsequently affects translation rates, shaping expression levels of individual genes (Granneman et al., 2009). They also alter gene expression in a second way, certain codons are more highly represented in the cell than others and this is usually correlated with amino acyl tRNA levels, a shift in codon from a highly represented to poorly represented codon, can indicate a change from a more to less available tRNA, this can lower gene expression, and vice versa. For example, in PAO1 the frequency of the codons CAU and CAC is 6.3 and 15.4 per thousand, respectively. It is possible that a mutation of these codons, despite both encoding for histidine, would result in a change in the expression level of the protein for which they encode.

We posit in this study, that our synonymous mutations could be altering the gene expression, or protein structure of the proteins of the genes in question, in either a positive or negative fashion, and that this may be a consequence of growth in sub-inhibitory concentrations of phytochemicals. However, exploration of protein activity, and gene expression would be needed to confirm this.

Synonymous mutations as a method of gene expression alteration is common in *P. aeruginosa* (Grocock & Sharp, 2002; Gupta & Ghosh, 2001)*,* and is often seen in relation to flagella activity (Spangenberg et al., 1996) and adaptation to cystic fibrosis lung (Smith et al., 2006). The appearance of synonymous mutations within this experiment supports the idea that our evolution experiment accurately encapsulates the mechanisms of gene alteration by *P. aeruginosa* gene expression in response to stress conditions.

The three genes containing a predicted synonymous mutation as determined by our analysis where the L, D-transpeptidase gene, the zot protein encoding gene, and the biofilm related glycotransferase family four protein encoding gene. These mutations will now be discussed individually

5.4.6.2   L, D transpeptidase

The predicted L, D transpeptidase mutation occurred in a single isolate of NCTC 7244 grown in sub-inhibitory concentrations of berberine. The mutation was C→T (GCC→GCT), and the codon frequency of codons used decreased from GCC: 67.7 to GCT/U: 4.8 (per thousand codons).

L,D transpeptidases catalyse the cleavage and bonding of peptidoglycans, and are essential for building bacterial cell walls (Magnet et al., 2008). Inhibition of L, D transpeptidases within *Mycobacterium tuberculosis* is possible using carbapenems (Cordillot et al., 2013; Kim et al., 2013), and causes complete bacterial inhibition (Erdemli et al., 2012; Zandi & Townsend, 2021). Similar studies have been conducted in *Enterococcus faecium* (Triboulet et al., 2013).

Other environmental contaminants, such as copper (Peters et al., 2018), have also been shown to inhibit the function of the L,D-transpeptidase. In Caprari et al, a *P. aeruginosa* L, D transpeptidase was discovered and functionally classified using an *in-silico* approach. And this study suggested that this protein would confer resistances to beta-lactam antibiotics (Caprari et al., 2019), though the *in vivo* work required to prove this was not completed.

In chapter 3, the D, D-transpeptidase MdrA was discovered on a plasmid insert in an isolate that displayed berberine resistance, which had been identified by metagenomic screening. This gene falls within the same overall transpeptidase family as the L, D-transpeptidase in this chapter. The appearance of a predicted mutation after in sub-inhibitory growth in berberine, and a transpeptidase gene in our inhibition-based screening assay suggests that this family may play a key role in berberine resistance, and potentially cross-resistance to antibiotics.

Berberine acts as an inhibitor of the surface protein transpeptidase, sortase in *S. aureus* (Kim et al., 2004)*,* though the exact mode of action is unknown. Transpeptidases are members of the penicillin binding protein family, and are inhibited by beta-lactams by the formation of covalent bonds with the penicillin binding protein active site (Georgopapadakou et al., 1986), and resistance to beta-lactams can be conveyed by overproduction or mutation of transpeptidases, including the L, D-transpeptidase (Hugonnet et al., 2016). We theorise that if part of the antimicrobial mechanism of berberine is binding to transpeptidases, that mutation, or overproduction of these transpeptidases may result in sequestration of the berberine allowing the cell to overcome berberine selective pressure.

5.4.6.3   Zona occludens toxin

The predicted ZOT mutation occurred in one isolate of NCTC 7244 after growth in sub-inhibitory concentrations of berberine. The mutation was C→G (GGC→GGG), and the codon frequency of the codons used decreased from GGC: 61.9 to GGG 9.9 (per thousand codons).

The ZOT is a bacterial toxin which allows for increased membrane permeability, particularly within the human gastrointestinal system by multiple bacterial species, but is particularly common in the *Vibrio* genus (Marinaro et al., 2003; Mauritzen et al., 2020; Pérez-Reytor et al., 2020). In *P. aeruginosa,* it specifically allows for polarization and thus transportation across epithelial monolayers (Soong et al., 2008). The protein is not heavily associated with any antimicrobial or antimicrobial resistance pathway, and the mutation occurs within the highly variable region at the cleavage site (Bateman et al., 2021). We theorise that this mutation has occurred due to *P. aeruginosa* growth in laboratory conditions and is not directly tied with the selective pressure of the phytochemical because this gene is not associated with antibiotic, or phytochemical resistance in previous literature, is used for epithelial penetration, and because the predicted mutation suggests the use of a much rarer codon.

5.4.6.4   *Pellicle/biofilm biosynthesis protein PslI / CAZy Glycopeptidase family four protein*

The predicted *cazY* mutation occurred in a single isolate of NCTC 7244 after growth in sub-inhibitory concentrations of quercetin. The mutation was C→A (GCC→GCA), and the codon frequency of the codons used decreased from GCC: 67.7 to GCA: 4.8 (per thousand codons).

The CAZy glycosyltransferase family four protein specifically catalyses glycopeptides, as opposed to peptidoglycans, and the CAZy protein forms an important part of the biofilm pathway. The protein allows for the matrix to form within the biofilm (Fong & Yildiz, 2015). We have discussed previously how quercetin has an antibiofilm activity (Mu et al., 2021), and the altered expression of this particular gene results in restoration of that biofilm formation. However, altered biofilm expression was not seen for any isolate in this study, so further work to characterise the effect of this gene's expression on biofilm expression, with and without quercetin supplementation is warranted.

Once again, the codon shift for this predicted mutation, would suggest that the cell is producing less of this protein, due to the mutation in the gene. We theorised that the reduction in this biofilm associated gene would be a result of growth in an evolution experiment which did not select for biofilm producing Isolates. This was confirmed as NCTC 7244 quercetin 2, the isolate containing this mutation, had significantly lower levels of biofilm production when compared to the ancestral NCTC 7244 isolate. We further postulate that due to our methodology, we positively selected for planktonically growing cells, particularly those that flocculate.

5.4.7 Predicted non-synonymous mutations

The next three mutations were non-synonymous, and the predicted mutation within the gene is theorised to lead to an alteration within the amino acid sequence of the encoding protein.

5.4.7.1 4-hydroxythreonine-4-phosphate dehydrogenase (EC 1.1.1.262)

The predicted mutation C→A (GAC→GAA) in the 4-hydroxythreonine-4-phosphate dehydrogenase (*pdx*A) gene led to a D173E in the translated protein sequence. The codon frequency of the codons used in this predicted mutation decreased from GAC: 42.6 to GAA: 23.4. This predicted mutation was present in an NCTC 9433 isolate after growth in sub-inhibitory concentrations of berberine. This predicted D173E mutation in the translated protein sequences of PdxA would lie within the outer alpha helix ring of the substrate binding site.

PdxA catalyses an oxidoreductase reaction, and participates in the metabolism of vitamin B_6 (Cane et al., 1998) and the pyridoxal phosphate biosynthesis pathway in *E. coli* (Sivaraman et al., 2003). The levels of PdxA are increased in infectious models of *E. coli* that produce the Shiga toxin, suggesting it may function as a virulence factor (Koutsoumanis et al., 2020). Mutation in the gene encoding for the PdxA protein in *Campylobacter jejuni* resulted in an

almost complete loss of flagellum mediated motility and reduced growth (Asakura et al., 2013), this is particularly interesting, as this is the first of two mutations that affected the flagella of *P. aeruginosa* as a result of berberine selection.

With relation to AMR, PdxA is a target of meropenem, and is essential in glucose minimal conditions in *E. coli* (Pearcy et al., 2021). A mutation in this gene could well have anti-meropenem activity and contribute to a natural background of meropenem resistance. We suggest that the occurrence of mutations in multiple genes, with flagella associated function, in isolates grown in the presence of berberine alone, indicates that overcoming berberine selective pressure involves modification of flagella genes. Though it is possible that due to the shaking of the cultures during passaging, the requirement of these isolates to have a functioning flagellum was reduced, thus unintentionally creating a selective pressure for mutations that decrease flagella function.

5.4.7.2   Dihydrolipoamide acyltransferase (EC 2.3.1.168)

The predicted (CCC→CTC) mutation of the dihydrolipoamide acyltransferase gene led to a P7L mutation in the translated protein sequence. The codon frequency of the codons used in this predicted mutation increased from CCC: 13.0 to CTC: 27.8. This predicted mutation was present in a single NCTC 9433 isolate after growth in sub-inhibitory concentrations of berberine. This predicted P7L mutation in the translated protein sequence falls within the highly variable C-terminal region next to the carriage peptide cleavage site.

This dihydrolipoamide acyltransferase is an essential part of the much more extensive pyruvate dehydrogenase complex, in both pro-, and eukaryotic life (Millar et al., 1999). The protein does play an essential role in *Mycobacterium tuberculosis* pathogenicity (Shi & Ehrt, 2006). However, it is not a known antimicrobial drug target.

The location of the predicted mutation of the translated protein sequence within the highly variable cleavage site, suggests that the mutation may be a result of natural variation within

that region rather than growth in laboratory conditions, or sub-inhibitory concentrations of the berberine. The location of the mutation could have no effect on the active sites of the protein or could completely inhibit peptide cleavage. Though it is hard to develop a concrete theory on this, without supporting *in vivo* evidence.

5.4.7.3   Flagellar regulatory protein FleQ

FleQ is a transcriptional regulator that controls motility, adhesion and biofilm production in *P. aeruginosa* (Arora et al., 1997; Kao et al., 2016). The predicted (CCG→TCG) mutation of the *fleQ* gene, led to a predicted mutation P387S in the translated protein sequence. This predicted mutation occurred in a single NCTC 7244 isolate grown in sub-inhibitory concentrations of quercetin. The codon frequency of codons used for this mutation decreased from CCG: 33.3 to T/UCG: 13.0 (per thousand codons).

This predicted genetic mutation would lead to a predicted mutation P387S in the translated protein sequence. This mutation would be found on the outer edge of the N-terminal region away from the active site. However, multiple mutations (for example F26N, N185A and R334E) across the protein resulted in either complete loss of biofilm formation or 75% repression of pel transcription (Su et al., 2015). We posit that our predicted mutation may impact protein function, despite its location on the outer edge of the n-terminal region.

This is the second occurrence of a flagella modifying protein mutation in an isolate grown in sub-inhibitory concentrations of berberine. In *Pseudomonas putida* the FleQ protein is responsible for the control of the two component system TarR-TarS which controls resistance to multiple antibiotics including chloramphenicol, kanamycin, tetracycline and imipenem (Y. Xiao et al., 2021). The isolate, which contained this predicted mutation did not have a change of resistance to any of the antibiotics measured, including imipenem. Which suggests this mutation alone was not sufficient to make the isolate antibiotic resistant. However, the occurrence of a predicted mutation in these gene suggests there may be linkage between

the TarR-TarS system and phytochemical resistance.

5.4.8   Predicted intergenic mutations

The final mutation seen in only a single isolate was the intergenic +G mutation in the non-coding region between the *ygg*W and *rdg*B genes, which did not change the amino-acid sequence of the surrounding proteins.

5.4.8.1   *Oxygen-Independent coproporphyrinogen-III oxidase-like protein YggW/Nucleoside 5-trophosphatase RdgB (dHAPTP, dITP, XTP-specific) (EC 3.6.1.66)*

The final mutation that occurred in only a single isolate was a +G (-14/+151) in the intergenic region, between the *ygg*W and *rdg*B genes in NCTC 7244 after growth in sub-inhibitory concentrations of berberine. Intergenic evolution predominantly targets transcriptional processes to alter the expression of downstream genes in *P. aeruginosa* (Hossein Khademi et al., 2019). As such we theorise that this mutation in the intergenic region is altering the transcription of the surrounding *yggW* and *rdgB* genes.

The YggW protein is part of the larger heme biosynthesis pathway, and is upregulated as a result of heat/cold conditions in *S. aureus* (Karki et al., 2020)*.* The *yggW* gene was also mutated in a planktonic *Acinetobacter baumannii* after growth in subinhibitory conditions of chloramphenicol, although not in inhibitory conditions, or in competent biofilm producing isolates (Santos-Lopez et al., 2019). Suggesting that overcoming chloramphenicol inhibition may involve mutations in the *yggW* gene.

The level of *rdgB* gene expression was also decreased in an antibiotic administered sludge, affecting the anaerobic digestion of the bacteria within (Xu et al., 2019). Suggesting that *rdgB* gene expression is negatively correlated with survival in the presence of antibiotics.

This presence of this predicted intergenic mutation suggests there may be a potential overlap between chloramphenicol and berberine resistance mechanisms. As mutation in the *yggW*

gene led to chloramphenicol tolerance, and the intergenic mutation in this study may related to the berberine tolerant phenotype.

We therefore hypothesise that *yggW* may control both controls chloramphenicol resistance and berberine tolerance, and thus be a mechanism of cross resistance. This cross resistance between chloramphenicol and berberine may explain why the *EPI300 E. coli* isolates containing the pCC1BAC had such high berberine tolerance in chapter 3. As the pCC1BAC plasmid used to construct the metagenomic library was chloramphenicol resistant.

5.4.9 There were three predicted mutations in the Alkaline Phosphatase (EC 3.1.3.1) across two isolates of NCTC 9433 grown in the presence of berberine

Finally, there were three predicted mutations in the Alkaline Phosphatase (EC 3.1.3.1) gene of *P. aeruginosa* NCTC 9433, grown in the presence of sub-inhibitory concentrations of berberine (Table 5-12). These mutations occurred across two isolates and one of the mutations occurred in both isolates (R2009R). Two of these mutations synonymous, and one was a 2-base pair AT insertion (6002-6003/8259 nucleotide). The (GAT→GAC) mutation which resulted in a predicted D2003D change to the translated protein sequence had an increase in the relative frequency of the codons used from GAT: 10.5 to GAC: 42.6 per 1000 codons, whilst the (CGC→CGA) mutation which resulted in a predicted R2009R change to the translated protein sequence had a relative decrease from CGC: 49.4 to CGA: 2.4 per 1000 codons.

This alkaline phosphatase gene is extremely large, at 8259 base pairs. When putting this sequence into blast only 22 hits were returned, of which 15 from were *P. aeruginosa* at 100% query length, the other 7 hits had between 0-5% query coverage, suggesting they were false positives (Altschul et al., 1990). This suggests that this gene is only known to be present in *P. aeruginosa*. The best prediction of this protein was a calcium binding haemolysing protein

(Doyle, 2018), and it is much larger than the standard EC.3.1.3.1 protein submissions on Uniprot (Bateman et al., 2021).

Alkaline phosphatase takes a phosphate monoester + H_2O and results in an alcohol + a phosphate (Bateman et al., 2021), and is present in both pro and eukaryotic life and is essential in tackling pathogenic gut infections as part of the normal human immune system (Sharma et al., 2014). Alkaline phosphatase can be inhibited by both chloramphenicol (Faccioli et al., 2016) and imipenem (Chakraborty et al., 2012). Alongside this, berberine supplementation in rats inhibits the rise of alkaline phosphatase, supporting hepatoprotection (Janbaz & Gilani, 2000).

In summary there were three predicted mutations in total across two isolates of NCTC 9433 grown in the presence of sub-inhibitory concentrations of berberine. There was no significant change in imipenem resistance profile between the ancestral NCTC 9433 and the NCTC 9433 isolates grown in sub inhibitory concentrations of berberine. However, NCTC 9433 berberine 1 and 2 displayed closest p values to significance across all the isolates (p = 0.237796 and p = 0.121004 respectively). Alkaline phosphatase is inhibited by both imipenem and berberine. This thesis hypothesises that mutations in alkaline phosphatase of *P. aeruginosa* NCTC 9433 may cause cross resistance between berberine and imipenem and certainly warrants further investigation.

5.4.10 Study Limitations

We selected two environmental isolates NCTC 9433 and NCTC 7244 to evolve as part of this study, after careful evaluation of the pros and cons of environmental vs standard laboratory strains. We will now briefly discuss these pros and cons. We also discuss some of the limitations of this type of experimental work, which must be considered when evaluating the phenotypic and genotypic changes discussed above.

Standard laboratory strains of *P. aeruginosa* were considered but eventually discounted for this analysis, as bacterial growth in laboratory conditions and media leads to the loss or change of genes responsible for growth in environmental conditions, an aspect of laboratory based evolutionary experiments we sought to minimise. The most common laboratory strain of *P. aeruginosa* is PAO1. PAO1 has a loss of function in the oxidoreductase gene (*mexS*), which activates a stress response controlled by a positive regulator *mexT*. The selection for mutations with higher fitness in PAO1 often inadvertently leads to the selection of *mexT* negative isolates due to the loss of function of the *mexS* gene in the strain (S. Lee et al., 2021). Another study by Chandler et al, highlighted that pyocyanin production and exopolysaccharide (components of the biofilm) production were altered in PAO1 strains from 10 different laboratories and strain banks worldwide (Chandler et al., 2019) due to prolonged growth in laboratory conditions. The presence of these laboratory derived mutations led to the discounting of PAO1 and other laboratory strains for this set of experiments.

The central question of this thesis posits that environmental interaction, and natural drivers are responsible for the occurrence of phytochemical resistance and that this phytochemical resistance has the potential to lead to cross resistance against antibiotics. The use of laboratory adapted strains may have allowed for selection of phytochemical resistance quicker, as these strains would not be primed to phytochemical resistance, and as such the pressure to mutate would have been greater in these strains. However, we decided that using environmental strains would be more appropriate, due to the lack of antibiotic resistance they displayed, and the potential for them to be primed towards phytochemical resistance.

Another important consideration is that resistance to an antibiotic may require multiple mutations to achieve, with multiple mutations combining to yield high-level resistance (Igler et al., 2021). In *P. aeruginosa* multi-step mutations are common when developing resistance

during chronic cystic fibrosis lung infections (Oliver et al., 2000). An example of multi-step mutational process conferring resistance is the co-occurrence of the loss of the bla_{NDM-1} gene and acquiring of Y150S and N346H mutations in CMY-16 enzyme in *Klebsiella pneumoniae,* the combination of which led to aztreonam/avibactam resistance (Niu et al., 2020). In our environmental isolates some of these mutations may be pre-existing, where they would not be in laboratory strains, which may make resistance easier to acquire in our study. A caveat to this is that the concentration of phytochemicals used in our study are much higher than those found in the environment, and as such our selective pressure may be biased for single high-value mutations.

It was important to consider during our study that our strains would evolve as result of growth within the laboratory conditions with example factors such as nutrient rich media, highly motile environment and lack of competitors influencing the requirement for specific genes. Alongside growth in sub-inhibitory concentrations of phytochemicals, controls of the strains grown in flavonoid free MHB for 30 days were used to evaluate how these strains evolved in media, and how this impacted pyocyanin and biofilm production alongside flavonoid and antibiotic resistance, and to give us a greater understanding of the mutational landscape because of growth in laboratory media.

Understanding which mutations occurred because of growth in laboratory media was incredibly important for our study. All isolates that had a 2-fold increase in tolerance had at least 30 genetic mutations. All but those mentioned in this discussion were also present in the control isolates. An example of this is the predicted 314,959 G→A mutation in the gene encoding the glutamine synthetase family protein, which was present in every NCTC 9433 isolate, across the control and experimental groups (Table 5-6).

5.4.10.2 Potential pitfalls of the study design

We posit that the mutations discussed above are adaptive mutations to growth under selective pressure of the respective phytochemical. However, this study did not explore if there was a direct causal link between each mutation, and growth under inhibitory conditions of the plant metabolite. It is possible that these mutations are non-adaptive (Putnins & Androulakis, 2021). Non-adaptive mutations are primarily random mutations which occur regardless of whether they improve the fitness of the isolate. It is possible that a single mutation may have occurred in a single strain due to these random forces and passed through our triage.

One additional limitation to consider is that we did not work with the genomes of the isolates grown for thirty days in sub-inhibitory concentrations of the plant metabolites that only had a partial, or no change in the resistance profile to the phytochemical they were grown in the presence of. It would be valuable to sequence those isolates and compare the predicted mutations to the predicted mutations of the isolates evaluated here, to determine if more genes were associated with a single growth supplementation, notwithstanding the phytochemical resistance phenotype. This was not conducted initially as we were focused specifically on the isolates that had a change in phytochemical resistance phenotype, as we did not expect there to be an elevated level of mutation across the isolates.

5.4.11 Next steps

The next logical step in this experimental pathway would be to construct plasmids containing the mutated genes discovered in this study, however this would come with the caveat of the wildtype genes still being present within the genome. It may be possible further to use CRISPR-cas9 edit these mutations directly into the genome of the bacterial host (Ratner et al., 2016), though this would be both time consuming and expensive. This would allow us to see if this presence of this mutation directly resulted in a change of phenotype from susceptible to resistant. This would clarify if any of our mutations were a result of non-adaptive forces. Given unlimited time and money, this would be my first choice as a continuation of this thesis experiment.

An alternative option would be to use competition to determine how well our isolates containing these mutations survived when cultured with isolates without the mutations in stressed conditions. If our mutants out competed the wildtype, or ancestor it would be clear that the mutation was beneficial.

5.5   Conclusion

This chapter explored the effect of the selective pressure of berberine and quercetin on two isolates of *P. aeruginosa* to determine how the evolution of resistance to these phytochemicals affected the bacteria. Resistance was developed to both phytochemicals in both isolates successfully. This resistance was not associated with a statistically significant increase in resistance to any antibiotic tested, according to disc diffusion methodology.

The resistance that was developed to the plant metabolites was associated with seven different genetic mutations. Three of these mutations were synonymous, suggesting that the mutation influenced the transcription of the gene, but not the function of the translated protein. Three of the remaining mutations were non-synonymous, and one which was intergenic. Several isolates did not display any genomic changes because of phytochemical selective pressure, and it is possible that the change in phytochemical resistance in these cases may be a result of transcriptional changes not seen through whole genome sequence analysis. An additional three mutations were predicted in Alkaline Phosphatase of NCTC 9433 after growth in sub-inhibitory concentrations of berberine

Of the mutations, we note the re-occurrence of glycotransferases and transpeptidases, as seen in chapter 3, suggesting that these genes may play a key role in phytochemical resistance. We also saw the occurrence of two genes associated with chloramphenicol resistance, which may explain, in part, why the EPI300 *E. coli* containing the chloramphenicol resistant gene carrying pCC1BAC was tolerant of high concentrations of berberine.

We also see here that there is a clear overlap between phytochemical resistance, and AMR genes, despite the lack of AMR phenotype. We also see the occurrence of two genes associated with flagella and motility in *P. aeruginosa* due to berberine selection highlighting motility as a potential key target of berberine inhibition. Of particular interest are the mutations in the Alkaline Phosphatase gene that occurred in NCTC 9433 Berberine 1 and 3.

We suggest that mutations in this gene may provide a potential link between phytochemical and antibiotic resistance.

6 Analysis of chicken caecum microbiomes using a pilot study of the fermenter gut model after media supplementation with berberine or quercetin

6.1 Introduction

One of the potential new uses of phytochemicals are as growth promoters in the agricultural industry. This potential use is in part driven by the ban of antimicrobial growth promotors. The central concern of this approach is that if phytochemical growth promoters select for cross-resistance to antibiotics, then the use of phytochemical based growth promoters may exacerbate antimicrobial resistance (Figure 6-1).
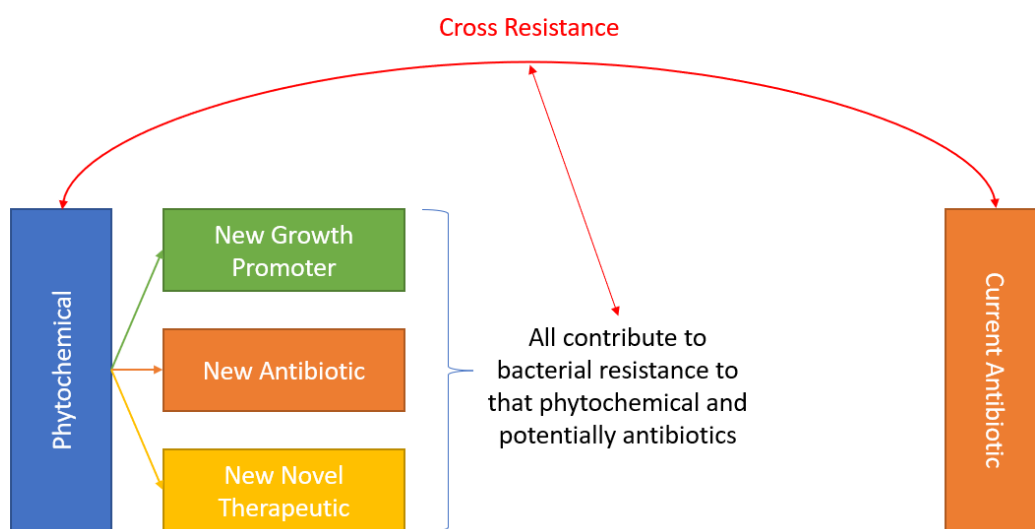
Figure 6-1 A graphical overview of the overlapping issues that may result in the use of phytochemicals as new therapeutics. Individual phytochemicals are being developed simultaneously as new growth promoters, antibiotics, and non-antibiotic-based therapeutics. These will all contribute to the selection of the emergence and spread of AMR to phytochemicals, further phytochemicals encourage cross resistance to current therapeutic antibiotic.

Despite this danger, several licenced phytochemical growth promoters are already on the market (Table 6-1), highlighting how quickly this field is moving in the absence of data on the AMR effects of these growth promoters.

Table 6-1 Examples of four commercially available phytochemical-based growth promotors and constituting phytochemical.

Product Name and Company	Compounds contained	Animal Growth Promoter	Reference
Turmafeed™ M/s Akay Flavours and Aromatics Pvt. Ltd., Kochi, India.	Curcumin, desmethoxycurcumin, and bisdemethoxycurcumin	Broiler Chickens	(Nm et al., 2018)
Biostrong® Actifor® Fresta ® Aromex® Decalon, Europe	Thyme and Star Anise	Poultry, Ruminants, Swine, Swine	(Delacon, 2020)
Novacid™ Zeus Biotech Private Limited	Organic acids, glucomannan and phytochemicals	Poultry	(Manafi et al., 2019)
Digestarom® Biomin	L-methol, D-carvone, carvacrol, thymol, methyl salicylate	Poultry, pigs, ruminants, and agriculture	(Murugesan et al., 2015)

6.1.1   Phytochemical based growth promoters in poultry

One of the key industries in which the use of phytochemical-based growth promotors is being explored is the poultry industry, and many studies have been conducted into their effectiveness in this industry (Lillehoj et al., 2018). According to the US department of agriculture, global chicken meat production is an estimated 100,509 tonnes as of April 2020, with the largest producers being the US, China and Brazil, with the largest consumers being the US, China and the EU (United States Department of Agriculture, 2022). This market is estimated to each US$347.27 billion by 2027 (Coherent Market Insights, 2020).

An overview of some phytochemicals assessed for use as antimicrobial growth promoters is given in appendix III. This assessment is broken down into three categories, growth promotive effect, physiological effect, and antimicrobial effect, across multiple different

measurements. Appendix III contains data pertaining to both chickens (in broiler and free-range conditions) and quails, which are a smaller component of the poultry market.

There is little chemical repetition in the literature, due to the diversity of chemicals available. However, this has led to a knowledge gap in the understanding of how the effects of these phytochemicals vary on a between agricultural species and breeds. This is exemplified by black cumin (*Nigella sativa L.)* (Abd El-Hack et al., 2018; Arif et al., 2018; Kumar et al., 2017) and thyme (*Thymus vulgaris)* (Dehghani et al., 2019; Hesabi Nameghi et al., 2019) which have differential effects in broiler chickens compared to quails.

Many of these compounds have positive effects on growth performance; including the plume poppy (*Macleaya cordata)* and magnolia tree (*Magnolia officinalis*) bark (P. Huang et al., 2018; Park, Oh, et al., 2020). Others demonstrated little to no growth promotive effect, including fever tea (*Lippia javanica)* (Matshogo et al., 2018) and quebracho (*Schinopsis sp*) essential oil (Díaz Carrasco et al., 2018).

The physiological effects varied widely between studies. These effects included alteration to peri-oxidation levels with sickle senna (*Senna tora)* extract supplementation (Sahu et al., 2017), changes in the villus-crypt ratio after supplementation with synthetic phytochemical blend (Galli et al., 2020), and increased Newcastle disease antibody titres after supplementation with extracts of tanners sumac (*Rhus coriaria)* and thyme *(T. vulgaris)* (Ahmadian et al., 2020).

The antimicrobial effects of these compounds also varied. A synthetic blend of thymol, curcumin and cinnamaldehyde decreased overall bacterial colonisation at day 22, but this was restored by day 45 (Galli et al., 2020). Sickle senna *(S. tora)* extract had high antimicrobial activity against *Escherichia coli, Staphylococcus aureus and Pseudomonas aeruginosa* (Sahu et al., 2017). A synthetic blend of thyme (*T. vulgaris)*, peppermint (*Metha x piperita)* and eucalyptus *(Eucalyptus* sp*.)* oil lowed ileum *E. coli* abundance and increased *Lactobacilli*

abundance in broiler chickens (Hesabi Nameghi et al., 2019). Finally, magnolia (*M. officinalis)* bark supplementation led to increased survival in chickens after *Clostridium perfringens* challenge compared to a control (Oh et al., 2018).

6.1.2   Development of the chicken fermenter model

Studies on the effects of antimicrobial compounds as growth promoters *in vivo* are usually conducted on live chickens from birth through to culling at day 45, following the full farmed chicken lifecycle (Galli et al., 2020; Zimmerman et al., 2020; Wang et al., 2018). These experiments allow for an immediate understanding of the actions of supplementation upon the chicken gut microbiome, and resistome. This work is essential to understand the effects of phytochemicals on growth performance and the wider chicken microbial community.

Alongside this, model systems can be used to mimic the chicken gastrointestinal system (GIS), for exploration of microbiome analysis without the ethical and environmental costs of live chicken experiments (Card et al., 2017). These models have effectively demonstrated the transfer of a multi-drug resistant plasmid from *Salmonella sp* to *E. coli* in a chicken intestinal system. In this study the model system is used to understand how phytochemical supplementation impacts the chicken GIS microbiome.

This chapter builds on previous analysis of quercetin and berberine as antimicrobial compounds. Previous chapters have explored how quercetin and berberine select for specific genes in *P. aeruginosa* serial cultures. This chapter will evaluate how these compounds function as modulators of the microbiome in chicken gut model system, alongside chapter 7 and chapter 8 which will explore *in vitro* batch culture and *in vivo* chicken gut microbiomes, respectively, using a bioinformatics approach.

6.2   Material and Methods

6.2.1   Chicken cecum content extraction and storage

6.2.1.1   Collection

Whole gastrointestinal systems (GIS) were collected from slaughterhouse chickens within two hours of slaughter and transported to Wageningen University and Research (WUR) Lelystad campus in the Netherlands at room temperature.

6.2.1.2   Extraction

Caecum were extracted from the whole GIS using scissors. The caecal content was extracted by washing the cecum in alcohol and then squeezing the content out into a fresh paper cup.

6.2.1.3   Pooling

The individual caecum contents were pooled into three separate pools with 17 samples (approx. 100 g) each.

6.2.1.4   Storage

First, 2.5 g of caecal pool was added to 22.5 ml of PBS/Glycerol (30%) and then 0.1 ml of cystine was added, as cystine greatly improves the growth of bacteroides, similar to the gut microbiome. The bottle was then flushed with nitrogen. A separate 0.5 g of caecal pool was stored in 2 ml PBS/Glycerol. Both samples were stored at -80°C. Finally, a separate 0.2 g of caecal content was stored at room temperature.

6.2.2   Applikon bioreactor system setup

6.2.2.1   Vimogut Media

Vimogut media was made by mixing 2.5 g of Beef/Meat extract, 5 g of yeast extract, 2.5 g of Glucose, 10 g of Tryptose, 0.6 g of L-cysteine hydrochloride, 5 g of NaCl, 4ml (0.025 weight/volume) Resazurin and H_2O to a total volume of 1 L. This was then autoclaved, and

sterile 0.05 g Haemin and 0.000984 g Vitamin K was added. NaOH and HCL were used as an acid and base respectively to adjust the pH to 4.

6.2.2.2 Vimogut System Setup

The model system was set up using an Applikon® Bioreactor and *my*-control package system, using the Applikon® bioprocess software from Applikon®. The computer system was set up according to manufacturing instructions. The system had a single fermentation vessel with an inflow, outflow, nitrogen sparging, ph detector, temperature sensor, and then an adjustable amount of inflows for the addition of further compounds, such as acids and bases and phytochemicals, the total vessel volume was 2 L, however max valume of liquid was 1 L.

A single fermentation vessel was used for maintenance of the chicken caecal microbiota. The pH was maintained throughout at between 6.5 and 6.7 to simulate the chicken caecal conditions. The temperature was maintained at 41°C. Anaerobic conditions were attempted to be maintained using nitrogen sparging, however this was not possible due to issues with the nitrogen sensor. The culture was stirred at 500 rpm for 5 seconds every 30 seconds.

Samples were taken every 24 hours, and media fed into the sample at a rate of 3.3 ml/h. Experiments were run for 8 to 9 days. Four experiments were performed, two controls and two with supplement of quercetin or berberine, respectively. Biofilm samples were taken from the biofilm around the edge of the fermenter.

Phytochemicals were added after T = 2 sampling (after 72 hours) of the experiment, as this was when chicken microbiomes usually stabilise, and when chicks are move from starter feed to full feed which would contain the phytochemical/antibiotic growth promoter in agricultural settings. Phytochemical supplementation conducted at a concentration of 320 µg/ml.

DNA was extracted following the Zymobiomics DNA extraction protocol (Chapter 2.16.1).

6.2.3   DNA sequencing

16S sequencing of the microbiome samples was conducted by Wageningen University and Research.

6.2.4   Bioinformatics analysis setup

Bioinformatics analysis was conducted on the sequenced data using R (Team, 2020). Session info for the R environment is given below (Figure 6-2). Major pre-processing of the 16S microbiome samples was done using the packages DADA (Callahan, McMurdie, et al., 2016), Phangorn (Schliep, 2011), DECIPER (Wright, 2016) and Phyloseq (McMurdie & Holmes, 2013). Major analysis was conducting using the packages Phyloseq (McMurdie & Holmes, 2013), ggPlot (Wickham, 2009) and ggNetwork (Tyner et al., 2017). Full code is given in Appendix IV.

```
> sessionInfo()
R version 4.1.2 (2021-11-01)
Platform: x86_64-pc-linux-gnu (64-bit)
Running under: Ubuntu 20.04.3 LTS

Matrix products: default
BLAS:   /usr/lib/x86_64-linux-gnu/blas/libblas.so.3.9.0
LAPACK: /usr/lib/x86_64-linux-gnu/lapack/liblapack.so.3.9.0

locale:
 [1] LC_CTYPE=en_GB.UTF-8       LC_NUMERIC=C              LC_TIME=en_GB.UTF-8       LC_COLLATE=en_GB.UTF-8    LC_MONETARY=en_GB.UTF-8    LC_MESSAGES=en_GB.UTF-8
 [7] LC_PAPER=en_GB.UTF-8       LC_NAME=C                LC_ADDRESS=C              LC_TELEPHONE=C            LC_MEASUREMENT=en_GB.UTF-8 LC_IDENTIFICATION=C

attached base packages:
[1] parallel  stats4    stats     graphics  grDevices utils     datasets  methods   base

other attached packages:
 [1] reshape2_1.4.4       randomForest_4.7-1   e1071_1.7-9          pls_2.8-0            miniUI_0.1.1.1       dplyr_1.0.8
 [7] phangorn_2.8.1       ggrepel_0.9.1        ape_5.6-1            ade4_1.7-18          DECIPHER_2.22.0      RSQLite_2.2.9
[13] Biostrings_2.62.0    GenomeInfoDb_1.30.1  XVector_0.34.0       IRanges_2.28.0       S4Vectors_0.32.3     BiocGenerics_0.40.0
[19] dada2_1.22.0         Rcpp_1.0.8           gridExtra_2.3        ggnetwork_0.5.10     igraph_1.2.11        phyloseqGraphTest_0.1.0
[25] networkD3_0.4        data.table_1.14.2    ggplot2_3.3.5        biomformat_1.22.0    phyloseq_1.38.0      BiocManager_1.30.16
[31] shinythemes_1.2.0    shiny_1.7.1          structSSI_1.1.1

loaded via a namespace (and not attached):
 [1] colorspace_2.0-2     rjson_0.2.21         hwriter_1.3.2        class_7.3-20         ellipsis_0.3.2
 [6] GenomicRanges_1.46.1 proxy_0.4-26         rstudioapi_0.13      farver_2.1.0         bit64_4.0.5
[11] fansi_1.0.2          codetools_0.2-18     splines_4.1.2        cachem_1.0.6         knitr_1.37
[16] jsonlite_1.7.3       Rsamtools_2.10.0     cluster_2.1.2        png_0.1-7            compiler_4.1.2
[21] Matrix_1.4-0         fastmap_1.1.0        cli_3.1.1            later_1.3.0          htmltools_0.5.2
[26] tools_4.1.2          gtable_0.3.0         glue_1.6.1           GenomeInfoDbData_1.2.7 ShortRead_1.52.0
[31] fastmatch_1.1-3      Biobase_2.54.0       vctrs_0.3.8          rhdf5filters_1.6.0   multtest_2.50.0
[36] nlme_3.1-155         iterators_1.0.14     xfun_0.29            stringr_1.4.0        mime_0.12
[41] lifecycle_1.0.1      zlibbioc_1.40.0      MASS_7.3-55          scales_1.1.1         promises_1.2.0.1
[46] MatrixGenerics_1.6.0 SummarizedExperiment_1.24.0 rhdf5_2.38.0 RColorBrewer_1.1-2   memoise_2.0.1
[51] latticeExtra_0.6-29  stringi_1.7.6        foreach_1.5.2        permute_0.9-7        BiocParallel_1.28.3
[56] rlang_1.0.1          pkgconfig_2.0.3      matrixStats_0.61.0   bitops_1.0-7         lattice_0.20-45
[61] purrr_0.3.4          Rhdf5lib_1.16.0      GenomicAlignments_1.30.0 htmlwidgets_1.5.4 labeling_0.4.2
[66] bit_4.0.4            tidyselect_1.1.1     plyr_1.8.6            magrittr_2.0.2       R6_2.5.1
[71] generics_0.1.2       DelayedArray_0.20.0  DBI_1.1.2            pillar_1.7.0         withr_2.4.3
[76] mgcv_1.8-38          survival_3.2-13      RCurl_1.98-1.6       tibble_3.1.6         crayon_1.4.2
[81] utf8_1.2.2           jpeg_0.1-9           grid_4.1.2           blob_1.2.2           vegan_2.5-7
[86] digest_0.6.29        xtable_1.8-4         httpuv_1.6.5         RcppParallel_5.1.5   munsell_0.5.0
[91] quadprog_1.5-8
```

Figure 6-2 Session info for the R environment used in the workflow for this thesis.

6.3   Results

6.3.1   Pre-processing of all samples

From the 16S sequences two random forward and reverse sequences were visualized (Figure 6-3). This allowed for determination of the optimal filtering (removal of sequences) and trimming (trimming of the sequence) conditions. Trimming of the forward sequences was conducted at 265 base pairs and 200 base pairs for the reverse sequence. The forward sequences were of better quality than the reverse sequences at greater than 200 base pairs. This step removed reads below a certain quality level and length, whilst also trimming all reads to a consistent length. The first 10 nucleotides are also trimmed from both the forward and reverse reads due the observation that these reads are often of inferior quality.
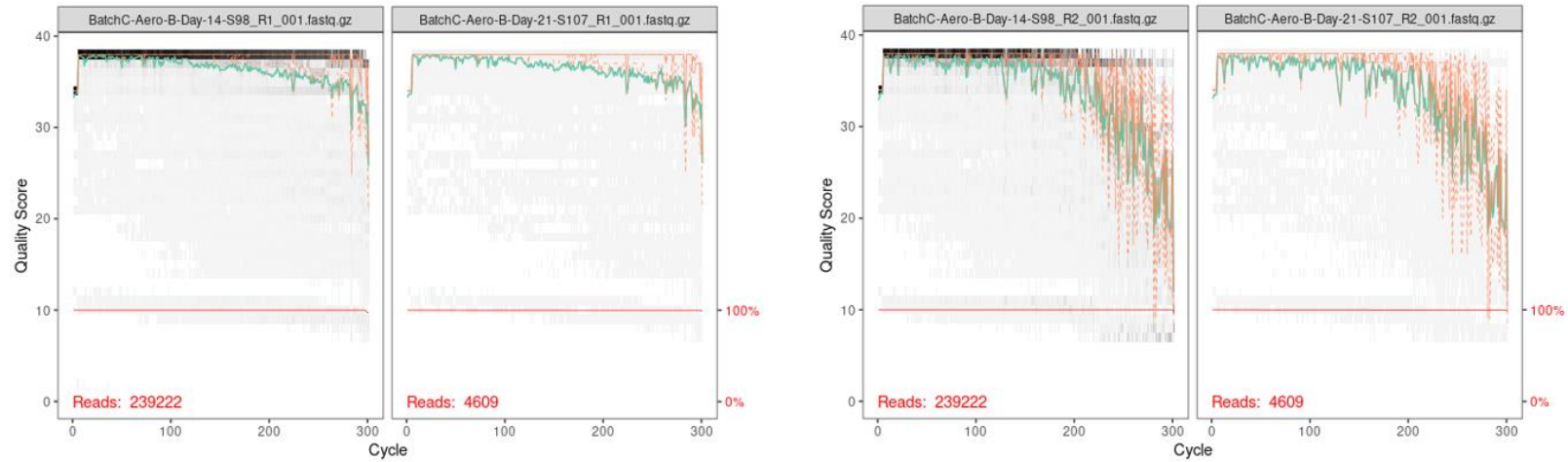
Figure 6-3 Quality of two random forward (left) and reverse (right) 16S sequences from the 16S sequencing step. After DNA extraction and prior to bioinformatics analysis, sequences must be filtered (removed) and trimmed (low quality base pairs removed). The read quality of the forward and reverse isolates was displayed on the y-axis, and base pairs (bp) on the x-axis. The forward reads remain high quality untill 270 bp, and the reverse reads remain high quality till 200 bp, where they lose quality sharply, comparitively to the forward reads. The decision was made to trim the forward reads at 265 bp and the reverse reads at 200 bp, whilst also removing the first 10 bp from all sequences. Forward sequences shorter than 265 bp and reverse seuqences shorter than 200bp were filtered.

The reads are then inferred into sequences using DADA2, and then de-replicated to remove redundancy. The error rates from the DADA2 step are visualised, with the red line indicating the optimal, or 'expected' error rates, to determine if they were well estimated (Figure 6-4). This step is conducted to ensure that the ribosomal sequence variants are conferred correctly and allows the DADA2 to distinguish between sequencing errors and true biological variance.
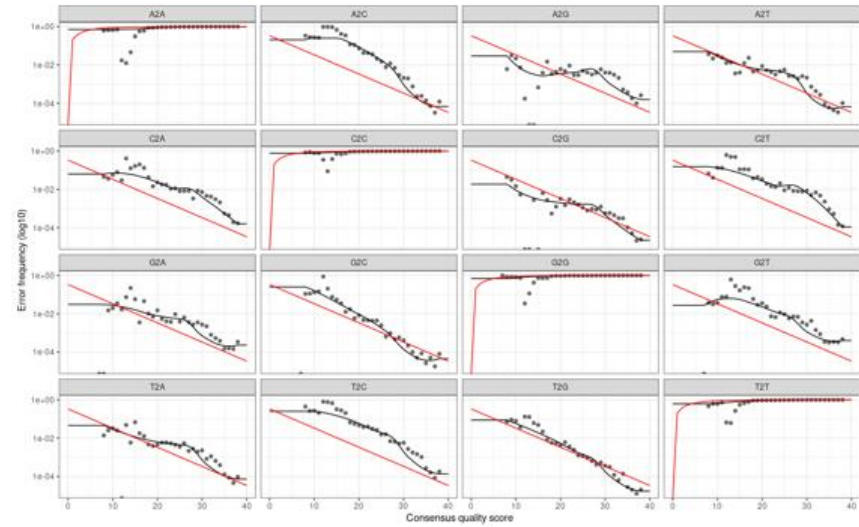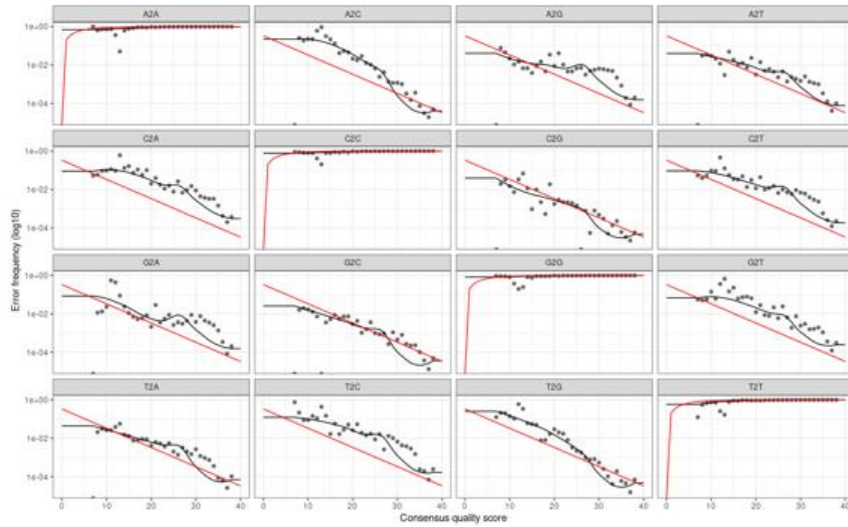
Figure 6-4 Error rates after dereplication of samples using DADA2, the error rates for each sample are plotted as black dots, the trend across also samples as a black line, with the optimal theoretical line plotted in red. The trends followed as expected for all errors. The y-axis is the error frequency, and the x-axis is the consensus quality score. DADA2 infers ribosomal sequence variants (RSVs) without using arbitrary thresholds, to attempt to resolve variants by as little as one nucleotide, using a parameterized model of substitution errors to distinguish between sequence errors, and true biological variation, using an unsupervised learning technique to make the sample inference and parameter estimation consistent.

6.3.2 Processing of samples from the fermenter system

Often when working with complex microbiome datasets, the data can be very time, and computationally intensive. One solution to this is to agglomerate the operational taxonomic units (OTUs) by genus or a fixed distance, especially if the data contains a large amount of species redundancy.

To determine the effect of agglomerating of specific species, or subspecies, two additional phylogenetic trees were constructed to determine the level of sequence variance seen by taxonomic agglomeration at the genus rank or a fixed distance of 0.4 (Figure 6-5). Neither agglomeration method demonstrated a clear simplification of the data and this the original phylogenetic tree by OTUs was kept.
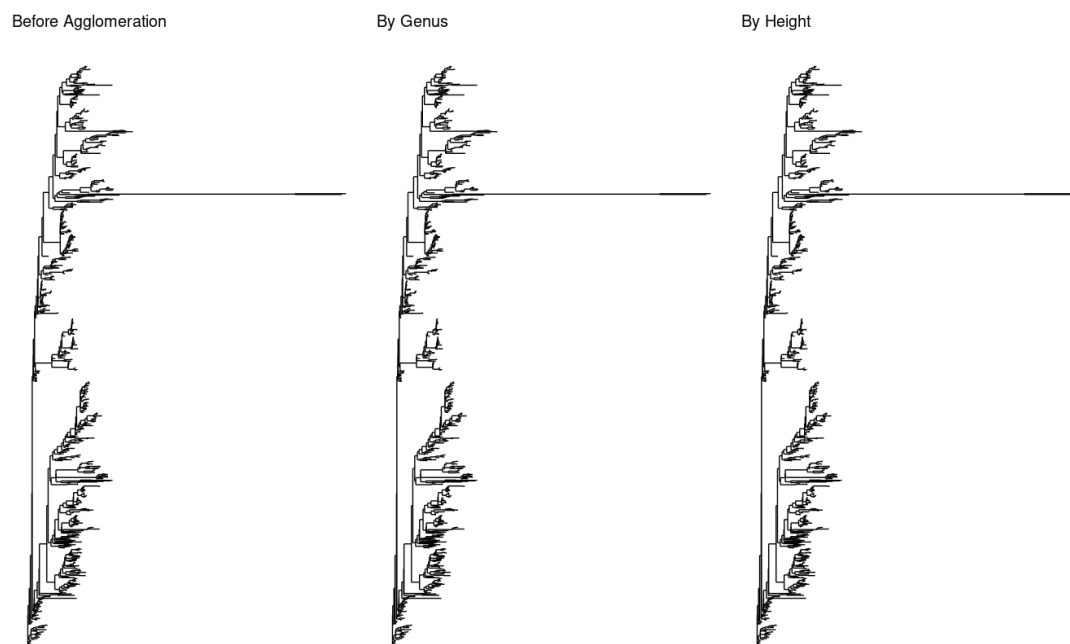
Figure 6-5 Phylogenetic trees were constructed with the sample data from the fermenter system. The phylogenetic trees shown are prior to any agglomeration (left), agglomeration by genus (middle), and agglomeration with a set height of 0.4 (right). Often with complex biological data it can become much simpler to analyse when the tips are agglomerated by genus or by height, however in this data case agglomeration did not significantly decrease data complexity.

After taxonomic tree analysis and prior to dataset analysis, the abundance of phyla across all samples was visualised (Figure 6-6). This allowed removal of phyla that were present in only

a small number of samples, as this study was designed to investigate the major changes between the treatment groups. This data highlighted a diverse range of bacterial phyla, with a number present in less than 5% of samples. From this data the phyla present in less than 5% of all samples were removed, and the distribution of samples redisplayed (Figure 6-7).
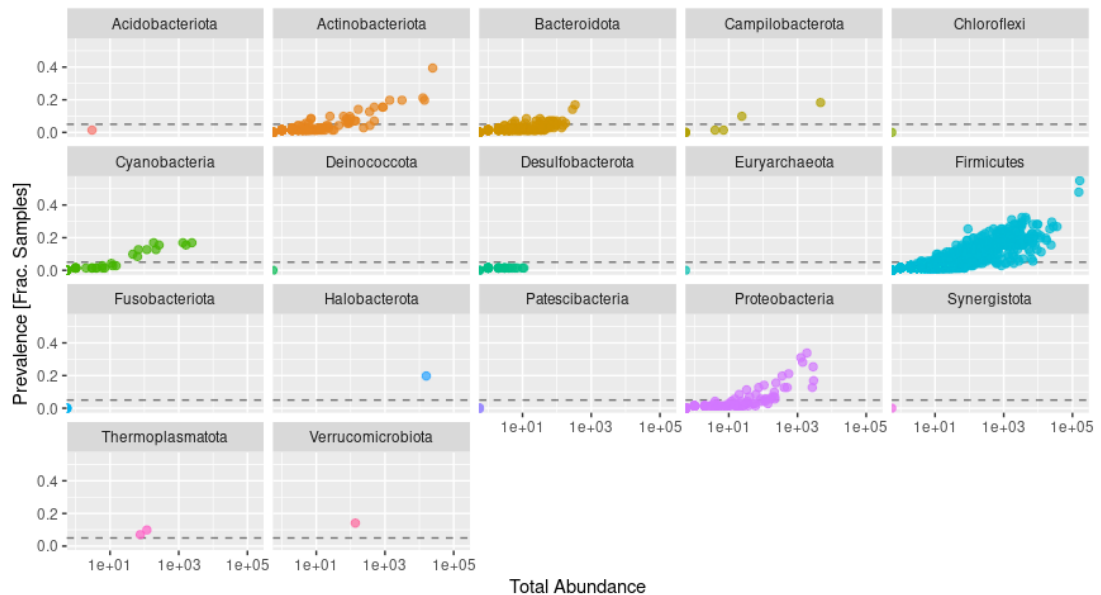
Figure 6-6 Phyla present across all samples from the fermenter system are plotted, each dot represents a particular taxon of bacteria from within the phyla. The y-axis is the prevalence of the species in as a fraction of samples from 0 (no samples) to 0.4 (40% of samples) and the x-axis is the log abundance of the species within that sample. The dashed black line indicates a prevalence of 0.05, or 5% of samples.

After removal of phyla present in less than 5% of samples it is immediately visible that the samples are dominated by the *Firmicutes* phyla, which are both the most abundant and most prevalent. There is a lower abundance of *Proteobacteria, Bacteroidota, Cyanobacteria and Actinobacteriota* which had an equally low prevalence, alongside a few single members of *Verrucomicrobiota, Thermoplasmatota, Halobacterota and Campilobacterota* phyla present in around 10-15% of the samples (Figure 6-7).
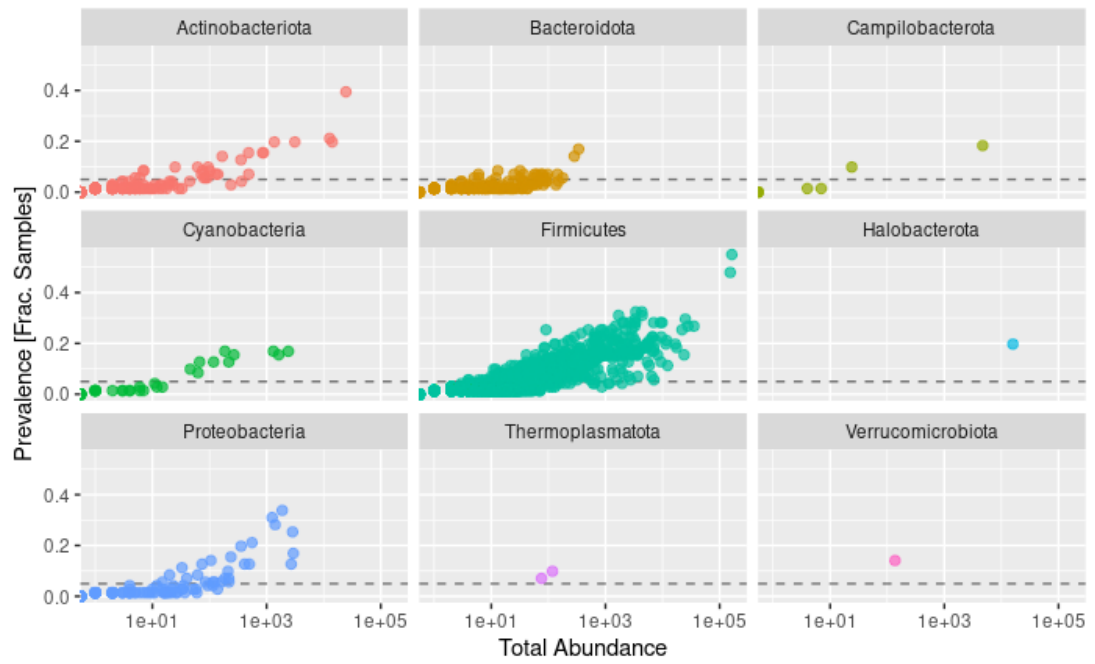
Figure 6-7 Plot of all Phyla present within the model system after removal of phyla with no species present in more than 5% of all samples. The y-axis is the prevalence of the species in as a fraction of samples from 0 (no samples) to 0.4 (40% of samples) and the x-axis is the log abundance of the species within that sample. The dashed black line indicates a prevalence of 0.05, or 5% of samples.

6.3.3 Detection of outlier samples from within the fermenter system samples using sample depth and ordination

After taxonomic abundance analysis, the data was then further processed to remove outliers. Sample sequencing depth by read counts as both normal, and log counts was plotted (Figure 6-8). Two samples contained approximately 0 reads, these were the berberine treatment group samples at timepoint 4 and 6.
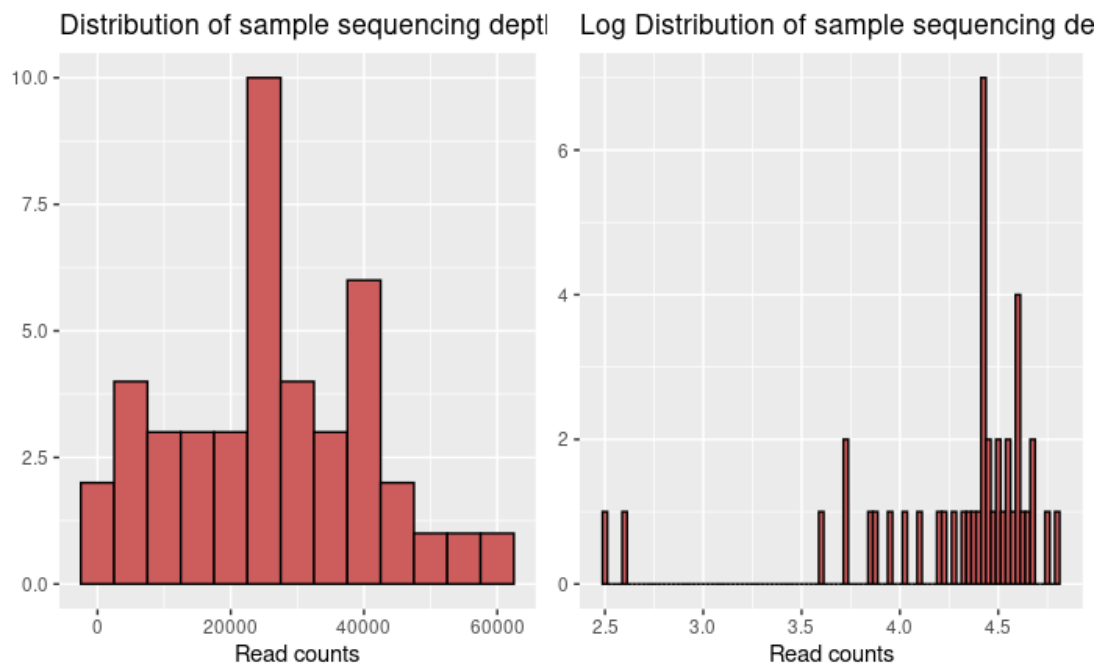
Figure 6-8 Histogram of read count distribution from samples from the fermenter system (left) and log adjusted (right). The number of samples is given on the y-axis and the read counts are plotted along the x-axis. The two samples with low read counts were the berberine condition at time point 4 and time point 6.

Different bioinformatics methodologies and analyses can often give different results, despite attempting to mine a specific dataset for the same answer (Nearing et al., 2021, 2022). As such multiple ordination and networking techniques were used to interrogate the dataset in this study. An outline of the different bioinformatics techniques used to interrogate the dataset are given at each point, and representative images of the analyses are shown and discussed.

Principle component analysis (PCoA) was conducted using Bray-Curtis dissimilarity, and Weighted-UniFrac on the entire dataset. The conclusions were identical so only the weighted UniFrac analysis is shown as it explained more of the ordination on two axes (85.1% vs. 65.3%). To determine if these samples affected the overall grouping of points on the graph (Figure 6-9). This did not appear to be the case using either ordination method; however, those samples were removed as the lack of sequencing depth may have affected later analysis.
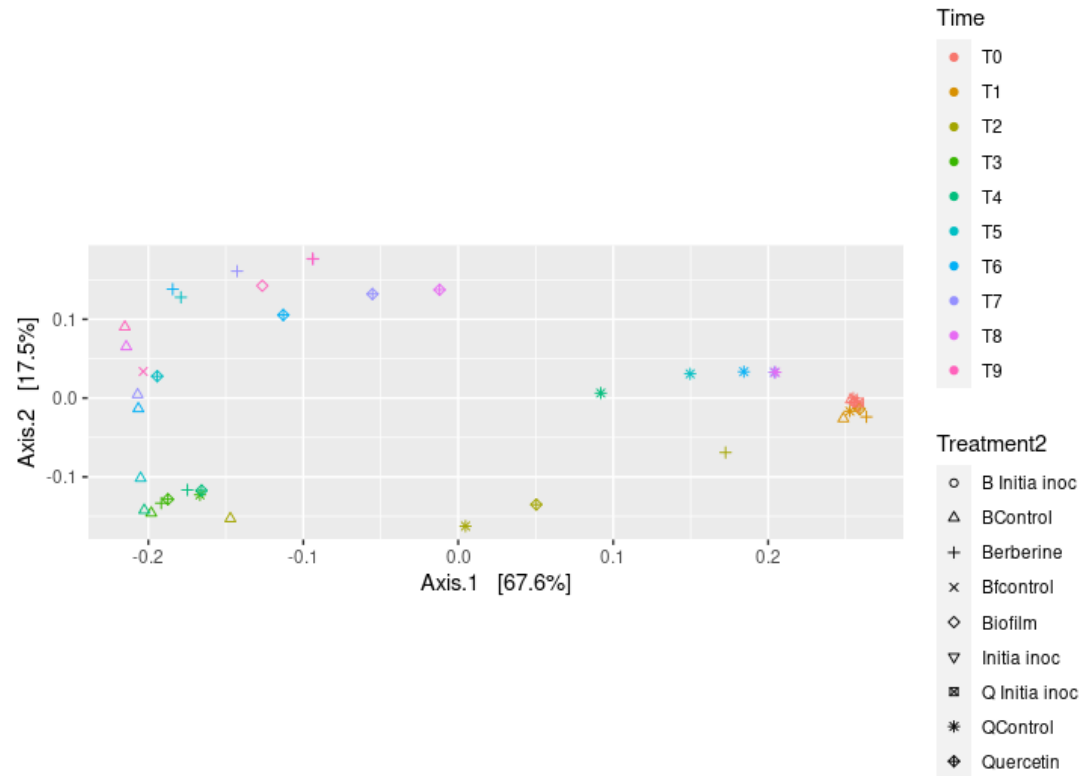
Figure 6-9 Ordination of samples from the fermenter system using MDS-weighted UniFrac analysis prior to the removal of low read counts to determine the ordination of outliers. Samples are ordinated according to axis.1 (x-axis) which accounts for 67.6% of the ordination, and axis.2 (y-axis) which accounts for 17.5% of the ordination. Samples are labelled by timepoint (colour) and treatment group (shape). The two low read count samples do not appear to be clear outliers, however the lack of read counts means they were removed from further analysis

.

6.3.4 Ordination analysis of fermenter system samples after removal of samples with low read count

Following removal of the low read samples as explained in 6.3.3, PCoA analysis using Bray-Curtis dissimilarity and DPCoA analysis were conducted. The conclusions of the two analyses were identical, thus only DPCoA was shown as it explained more of the ordination (92.2% vs. 69.7%). There is a clear grouping of samples at T = 0 and T = 1, on the right of the graph, and T = 2 and T = 3 on the bottom left. Then the ordination diversifies in the later samples. Treatments were added at T = 3, which would match well with the diversification of the samples. The x-axis accounts for 83.8% of the ordination and is most likely to represent the impact that time has on our ordination. The y-axis accounts for 8.4% of the ordination and represents the effect of treatment (Figure 6-10). A key point to mention here is that the quercetin control group, is clearly distinct from any other treatment group in the middle of the ordination, suggesting this control does not follow the same diversification of bacteria, as the other conditions.
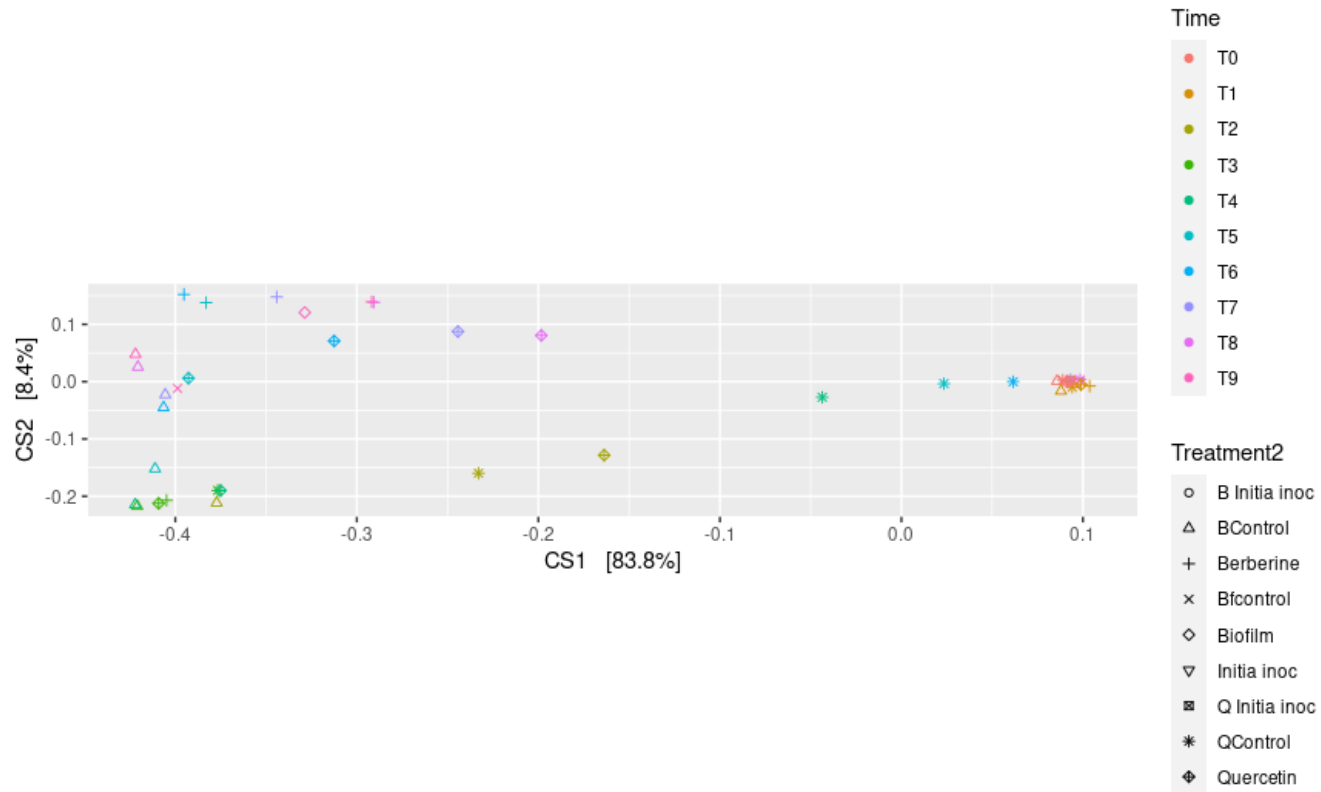
Figure 6-10 Ordination of samples from the fermenter system using DPCoA analysis after the removal of low read counts. Samples are ordinated according to CS1 (x-axis) which accounts for 83.8% of the ordination, and CS2 (y-axis) which accounts for 8.4% of the ordination. Samples are labelled by timepoint (colour) and treatment group (shape). The T=0-1 samples group on the right of the graph, with the T=2-3 on the bottom left and the T=4-9 spreading from the bottom left to top left and middle.

The analogous graph (Figure 6-11) used DPCoA on the samples, but instead plotted where the phyla would ordinate, rather than the samples themselves. Combined with the previous figure, this demonstrates that the diversity in *Firmicutes* changes along the x axis. The *Proteobacteria*, *Bacteroidota* and *Proteobacteria*, are confined to specific areas on the x axis, which correspond to the quercetin control, and the two treatment groups respectively (Figure 6-11). The y axis is responsible for diversity within the phyla.
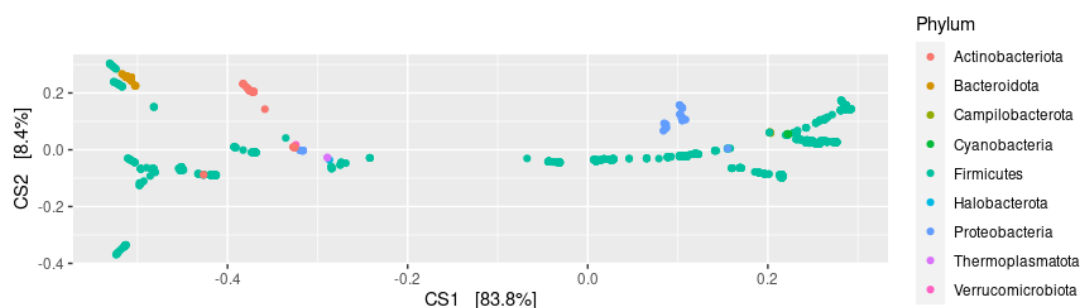
Figure 6-11 Ordination of samples from the fermenter system using DPCoA analysis after the removal of low read counts. Samples are ordinated according to x-axis which accounts for 83.8% of the ordination, and CS2 y-axis which accounts for 8.4% of the ordination and correspond to time and treatment, respectively. Datapoints are taxon from phyla organised by colour. The analogous graph to Figure 6-10.

6.3.5   Network analysis of the samples from the fermenter system.

Following ordination analysis, the next step was to conduct network analysis on the samples from the fermenter systems, to determine grouping between samples. The first was a simple network analysis using the Jaccard-Dissimilarity matrix (Figure 6-12Figure 6-12). This highlighted that the samples tended to group by age (represented as colour), with a loose level of interconnectedness by treatment type (represented by shape), which was stronger at later timepoints.
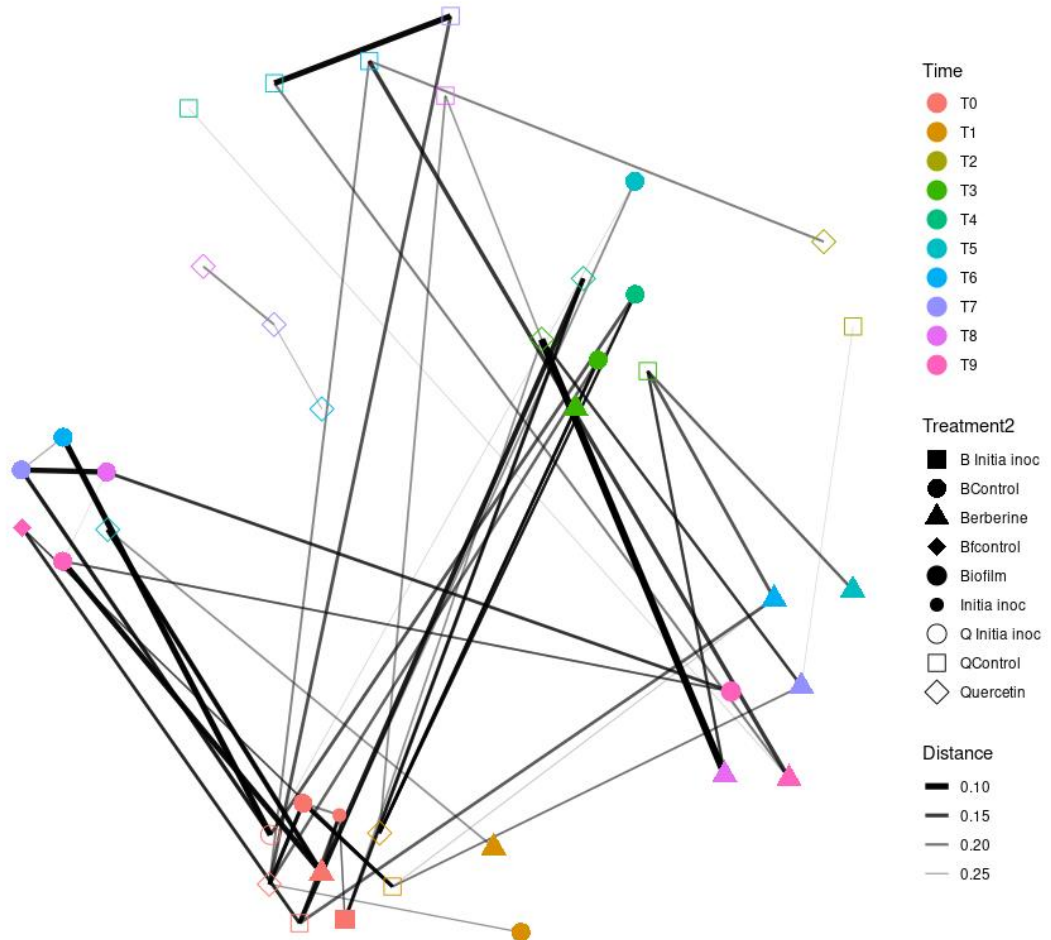
Figure 6-12 Network analysis of samples from the fermenter system created using thresholding with the Jaccard-Dissimilarity matrix. Samples are denoted by timepoint (colour) and treatment group (shape). The T = 0 and T = 1 samples grouped, as did several the T = 2 and T = 3 samples. There was a large amount of diversity in the later timepoints, although samples grouped together loosely by condition.

The next step was to evaluate the samples using networking methodologies including: Jaccard, K-nearest neighbour, bray, and bray enforced edges. All methodologies agreed in their conclusions, thus only the results from the Jaccard analyses are shown (Figure 6-13). The p value was < 0.5 for both treatment and time, and so the hypothesis that the samples came from the same treatment, or timepoint was rejected. Several members of each treatment group associated together more than expected by chance. The early timepoint samples, regardless of treatment condition (T = 0 through to T = 3) also grouped together

clearly. This backs up earlier analysis that addition of phytochemical on day 3 had a profound impact on sample diversity.
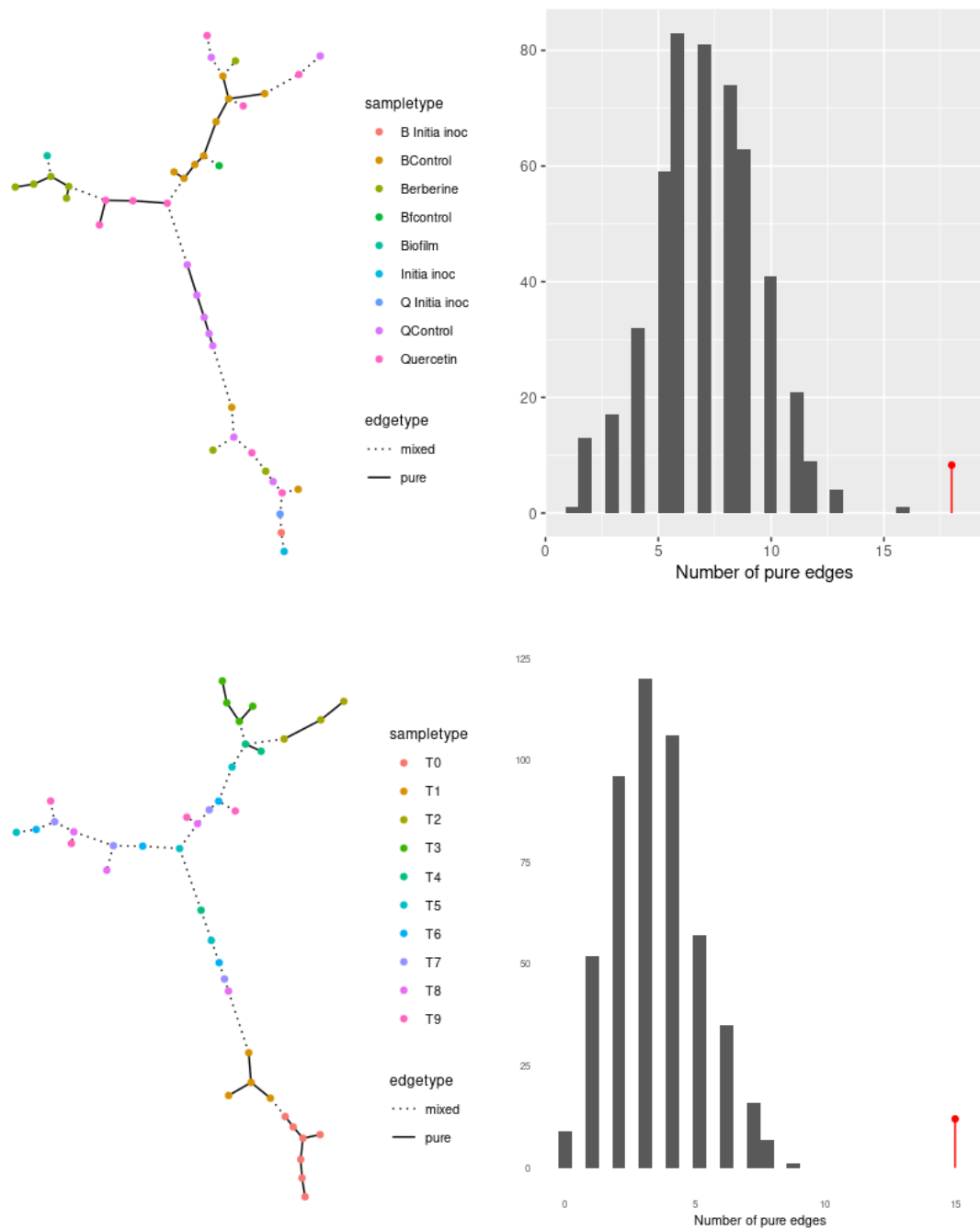
Figure 6-13 Network analyses of samples from the fermenter system using minimum spanning tree with Jaccard similarity by treatment group (top (p = 0.002)) and time (bottom (p=0.002)), networks (left), permutation of edges histograms (right). Samples are denoted by timepoint and treatment group (colour), in their respective graphs. Several members of the berberine, quercetin, and control groups mapped together. However there was clear diveristy between specific members of each group, which is likely to correlate to the later time points of the experiment. Samples mapped together at early treatment points, but poorly after T = 3.

6.3.6 Shannon diversity of samples from the fermenter system

After networking, linear modelling was used to predict and plot the Shannon diversity of all the samples by treatment and timepoint (Figure 6-14). This was conducted to explore the effect of phytochemical supplementation on overall sample diversity. Diversity is highest in the T = 0 and T = 1 samples and is a similar level of diversity as the initial inoculum. Sample diversity dropped markedly at T = 2 and T = 3, before recovering slowly through to T = 9. This recovery never matched the initial diversity. The diversity was lower in the berberine control and the quercetin treatment group. However, in all cases the predicted intervals crossed, suggesting more samples are needed to confirm these findings.
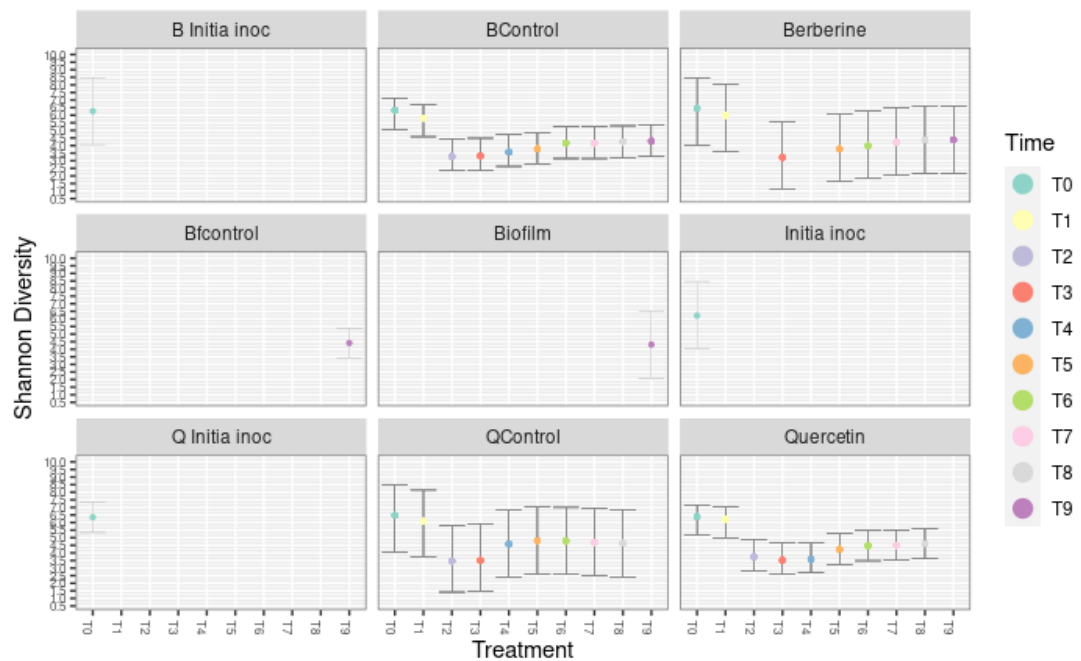
Figure 6-14 Shannon diversity of samples from the model system, faceted by sample treatment group and indicated by time in colour and on the x-axis, each point indicates the Shannon diversity at one timepoint for each treatment group. Shannon diversity is given on the y-axis. Diversity of the berberine initial inoculum is higher than that of the quercetin initial inoculum, the biofilm on the control is less diverse than the biofilm from the berberine samples. The berberine control is less diverse across all timepoints than the quercetin control or berberine and has a similar level of diversity to the quercetin. All samples have higher diversity at T = 0 and T = 1, which then drops at T = 2 and slowly increases marginally from T = 3 to T = 8/9. The prediction intervals for each sample obtained from the mix-effects modelling are overlaid.

6.3.7 Assessment of abundance of phyla in the fermenter system samples visualised using stacked bar charts

The final visualisation conducted on these samples was a stacked bar chat of phyla in each treatment condition. First the sample abundance was normalised to the average across all samples. This was conducted to normalise all sample numbers to a specific value (Figure 6-15Figure 6-15) to allow for analysis across the data despite the difference in raw read numbers from the different samples.
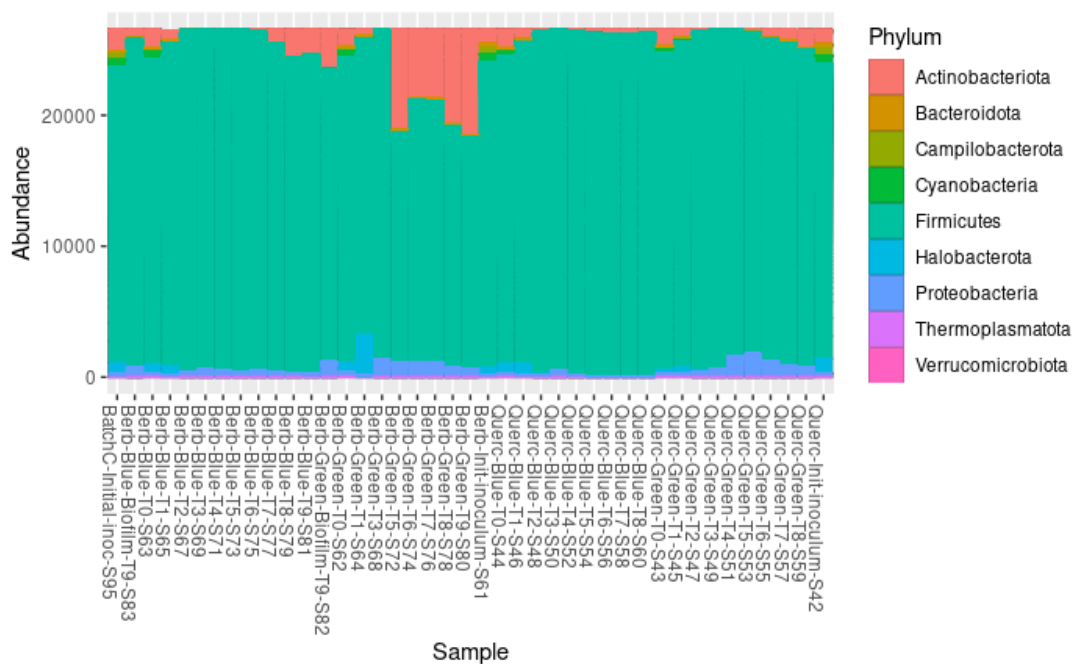
Figure 6-15 Stacked bar chart of all samples from the fermenter system, homogenised to relative abundance between the samples. The relative abundance is plotted on the y-axis and samples are plotted on the x-axis. Phyla are coloured according to the label (right). In the later time points in each condition are more heavily dominated by the Actinobacteriota phyla and the middle time points have an increase in the presence of Proteobacteria. Halobacterota dominates in the early time points of the berberine, and quercetin control samples. Cyanobacteria is seen intermittently throughout the earlier stages of each sample and the initial inoculum.

Within the berberine associated treatment samples (Figure 6-16), the samples were composed of *Firmicutes*. At T = 0 there were a small number of the *Actinobacteriota, Proteobacteria and Thermoplasmatota* phyla. At T = 1 The *Firmicutes* increasingly took over the sample, although in the berberine treatment group fermenter, there was an isolated increase in *Halobacterota*. From T = 2 to T = 4, the *Firmicutes* completely dominated the control sample and at from T = 3 in the treatment sample.

The removal of the T = 2 and T = 4 berberine treatment samples due to low reads makes the phyla level movement of the berberine samples harder to assess. Berberine supplementation was started at T = 3. After T = 4 there is divergence of the samples, leading to an increase in the number of *Actinobacteriota*, which decrease at T = 6 and T = 7, before increasing again at T = 8 and T = 9. The berberine control group saw a slight increase in *Actinobacteriota* at T = 7 onwards, but not as marked as the treatment group. Alongside this in the berberine treatment group there was an increase in the number of *Proteobacteria* and *Verrucomicrobiota* compared to the control.

Sample assessment was done on the raw abundance reads from a single sample, and as such we were unable to perform statistical analysis on this dataset. Thus, it is unknown if these changes are statistically significant. Future experiments would need to be conducted using 16S qPCR on multiple samples at each timepoint, for a true statistical analysis of the dataset.
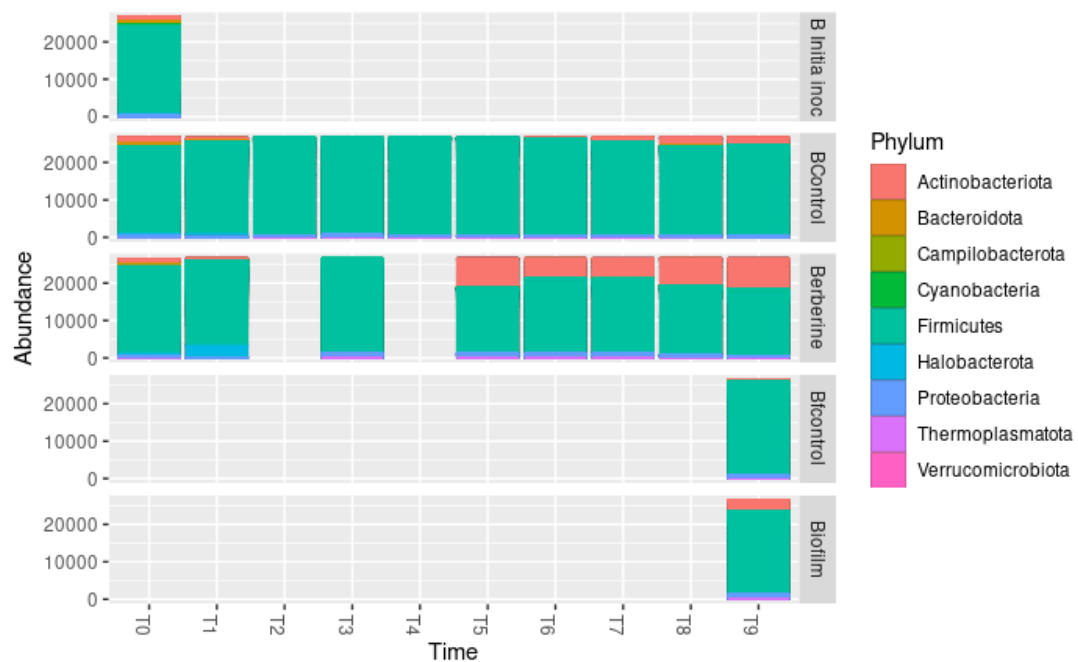
Figure 6-16 Stacked bar chart of the berberine associated samples from the fermenter system, homogenised to relative abundance between the samples. The relative abundance is plotted on the y-axis and samples are plotted on the x-axis. Phyla are coloured according to the label (right). The initial inoculum and T = 0 of samples were dominated by Firmicutes with low levels of Thermoplasmatota, Verrucomicrobiota and Actinobacteriota. Firmicutes dominate from T = 2 to T = 5, although there is a noticeable increase in Halobacterota in the berberine condition at T = 2. In the berberine condition at T = 5 there is an increase in the number of Actinobacteriota, which

In the quercetin associated samples (Figure 6-17) the difference was not as marked as in the berberine samples. The bacterial breakdown of the samples was equal at T = 0, as expected, and similarly distributed as those seen in the berberine associated samples. The *Firmicutes* dominated the samples by T = 2. For the quercetin control group, they continued to completely dominate the sample until T = 8. Whereas at T = 4 and T = 5, *Proteobacteria* started to appear in the quercetin treatment group, which decreased by T = 8, there was a minor increase in the number of *Actinobacteriota* in the quercetin treatment group at T = 6, T = 7, and T = 8.

Together these results indicate that the samples are diverse at T = 0, settle to a *Firmicute* dominated environment by T = 3. The quercetin treatment group diversified after the addition of phytochemical, which was more marked in the berberine treatment group.
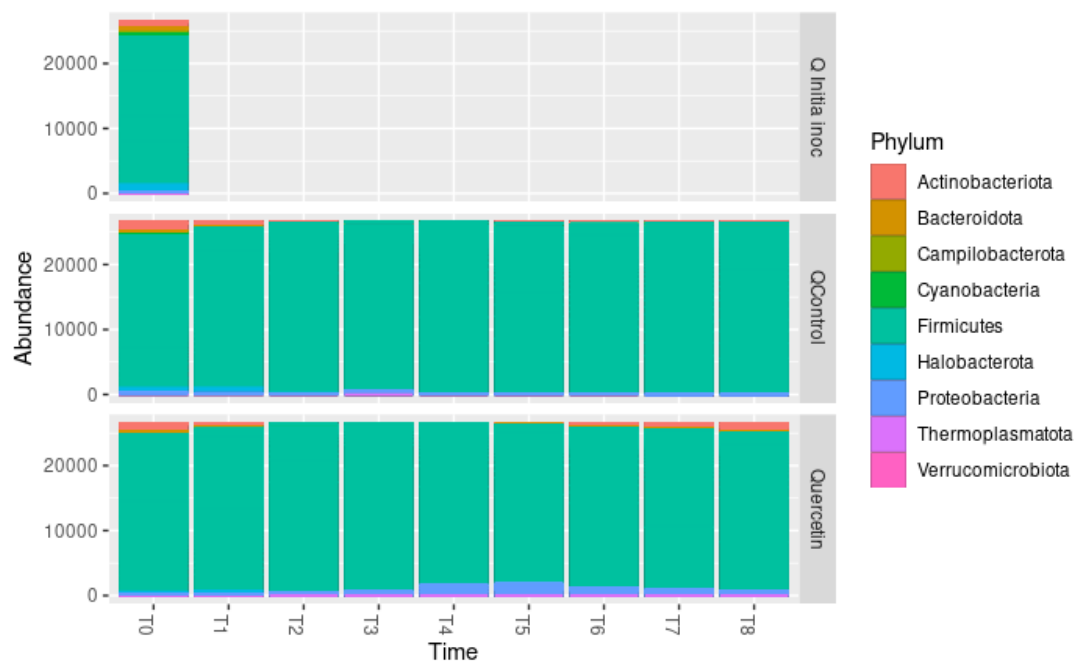
Figure 6-17 Stacked bar chart of the quercetin associated samples from the fermenter system, homogenised to relative abundance between the samples. The relative abundance is plotted on the y-axis and samples are plotted on the x-axis. Phyla are coloured according to the label (right). The initial inoculum and T = 0 were mostly Firmicutes with a small number of Actinobacteriota, Campilobacterota, and Cyanobacteria. The sample became completely dominated by Firmicutes for all samples at T = 2. At T = 3 a minor increase was seen in both conditions in Proteobacteria and Thermoplasmatota, this decreased again at T = 4 and T = 5 in the control. The levels of

Proteobacteria increased dramatically at T = 4 and T = 5 in the quercetin group. At T = 6 Actinobacteriota began to appear in the quercetin treatment group, the abundance of which increased through to T = 8.

6.3.8 Violin plot visualisation determined that the *Escherichia-shigella* genus was present only in the quercetin and control samples.

Violin plots were visualised for all phyla, by class faceted by order and order faceted by genus. Here the *Eubacteriales* order faceted by genus is shown (Figure 6-18). The most abundant genus was the *Aquamonas,* which was present in all samples. The *Consenzaea* genus was not present in the control samples, which the *Escherichia-Shigella* genus was present only in the control and quercetin samples.

Figure 6-18 Violin plot of the Enterobacterales order faceted by genus, with log abundance plotted on the y-axis (adjusted log abundance across all samples) and treatment group plotted along the x-axis. Each dot is a specific taxon within that genus, with the bimodal distribution for each sample plotted as a violin shape (black). The Aquamonas genus was most present in the control and quercetin conditions, as was the Escherichia-shigella, the Consenzaea genus was not present in the control but was present in the berberine and quercetin conditions.

6.4 Discussion

This chapter followed the analysis of a set of experiments conducted on chicken caecal content within a Vimogut fermenter system. This system was set up to model the chicken cecum. To determine, in a model environment, what the effect of phytochemical based growth promoters would have upon the chicken gut microbiome.

The key findings from this research can be broken down into the following statements: (1) *Firmicutes* were the dominant phyla across all treatments, with *Actinobacteriota* and *Proteobacteria* also present in large numbers in some samples (Figure 6-7). (2) Time was the most important factor across all ordination methodologies, and treatment was the second most important factor across all ordinations (Figure 6-9, Figure 6-10, and Figure 6-11). (3) The quercetin control samples were uniquely diverse compared to all other treatment groups (Figure 6-14). (4) The diversity of all samples, including the control was higher at the start of the experiments, and dropped sharply after 48 hours, followed by a gradual increase throughout the remainder of the experiment but never quite recovering to the initial diversity. (5) The addition of berberine led to a change in relative abundance of the phyla between *Firmicutes* and *Actinobacteriota* (Figure 6-16). (6) The addition of quercetin led initially to an increase in *Proteobacteria*, which was followed by a minor increase in the abundance of *Actinobacteriota* at the expense of *Firmicutes* (Figure 6-17).

6.4.1 Firmicutes were the dominant phyla across all samples

Firmicutes are a mostly Gram-positive bacterial phylum, and one of the two dominate phyla found in the gut of humans and chickens, along with *Bacteroidota* (Mariat et al., 2009; Rychlik, 2020), split, mainly, into the *Clostridia* and *Bacilli* classes, each with multiple orders, and over 200 genera. Although most of the members of the *Firmicutes* are Gram-positives, members of the *Negativicutes* class, which includes the *Veillonella* genus, are Gram-negatives (Vesth et al., 2013).

Firmicutes dominated sample abundance across all experimental conditions, this is expected, as *Firmicutes* tend to be the dominant phyla within chicken GIS systems naturally. However, *Firmicutes* normally compromise only 44-56% of a normal chicken caecal microbiome (Shang et al., 2018), with *Bacteroidota* representing the other 45%, and *Actinobacteriota* and *Proteobacteria* the other 2-3% (Rychlik, 2020). Between 10-90% of chicken gut microbiota can be *Bacteroidota*, with equally variable number of other phyla, such as *Verrucomicrobiota* (Rychlik, 2020), as found in this study. Other studies suggest that at a caeca level, *Bacteroidota* can often be the most dominant phyla (Xiao et al., 2017).

Whilst the fermenter system did well at maintaining the microbiome it was supplied, that inoculum was not perfectly representative of chicken caeca. This experiment attempted to control for this by using an inoculum from a pool of, on average, 5 chickens, all from the same farm, which were immediately frozen after collection at -80°C. This method of pooling and storage does not alter the microbe composition at a phylum level for human gut microbiomes (Fouhy et al., 2015; Ilett et al., 2019), suggesting it is likely that our samples were naturally dominated by *Firmicutes.*

It would be interesting to repeat these experiments with an initial inoculum that contained a higher percentage of *Bacteroidota*, to determine how the effects of phytochemical supplementation would affect varied chicken microbiomes.

6.4.2 Differences in order and genera diversity abundance was mostly between the control/treatment groups

The orders and genera of bacteria varied between treatments. Each case is considered here, and the relevance of these phyla distributions discussed, alongside how well they match up with known chicken caeca datasets.

Bacteroidota were less abundant than expected within the fermenter system and was comprised of the *Bacteroidales* order. When faceting that order by genus it became clear

that the major component genus *Bacteroides* was not highly abundant within the initial inoculum. The *Bacteroides* genus, however, was more abundant in all treatment groups and controls. This suggests that the model system works well at mimicking a chicken caecum, despite a *Firmicutes* dominated inoculum. *Bacteroides* are a non-spore forming, anaerobic, Gram-negative bacteria that are usually commensal in the gut, but can act as opportunistic pathogens in the event of environmental stress (Wexler, 2007). These bacteria are involved in carbohydrate fermentation and host energy requirements (Hooper et al., 2002). Clinically these bacteria have demonstrated resistance to multiple antibiotics including tetracycline (Shoemaker et al., 2001), clindamycin, imipenem and piperacillin/tazobactam (Sood et al., 2021).

The *Proteobacteria* were split into two orders, the *Enterobacterales* and the *Rhodospirales*. Within the *Enterobacterales* there were two genera of interest, the *Aquamonas* which comprised much of the order, and the *Escherichia-Shigella* genus, which was present only in the control and quercetin samples. *Proteobacteria* are a normal component of the chicken caeca (1-16%) (Rychlik, 2020). Despite being a normal member of a healthy gut microbiome in both chickens, humans, and other mammals (Carrasco et al., 2019; Moon et al., 2018), the *Proteobacteria* contains well known opportunistic pathogens, including *E. coli, Salmonella* sp, and *Shigella* sp.

The *Proteobacteria* phyla is associated with the expression of pro-inflammatory cytokine expression (Oakley & Kogut, 2016) and poor growth performance parameters when found in high numbers in adult chickens including bodyweight (Bae et al., 2017) and residual feed intake (Siegerstetter et al., 2017). These bacteria are important due to their potential to carry carbapenem resistance (Ghaith et al., 2019). The selection for *Proteobacteria*, particularly the *Escherichia-Shigella* genus by quercetin supplementation, is concerning, from both a growth performative and AMR perspective.

The *Actinobacteriota*, was comprised of two main orders, the *Bifidobacteriales* and the *Coriobacteriales*. The *Coriobacteriales* were dominated by two major genera, the *Gordonibacter* and CHCKC1002. *Actinobacteriota* are non-spore forming, non-motile, strictly anaerobic gram positives, with a high GC content (65%) and small genome size that usually comprise around 2-3% of the total GIS phyla (Rychlik, 2020). *Actinobacteriota* are normally present in the healthy gut microbiota of chickens (Shang et al., 2018), and when found in high quantities in the caecum it can be associated with positive growth parameters (Bae et al., 2017). They are more predominantly found in free-range chickens, due to their role as a common soil bacteria (Huang et al., 2018).

Finally, the most abundant phyla were the *Firmicutes*, and was also the most complex. The major orders were the *Clostridia* UCG-O14 group, *Clostridia vandin* BB60 group, *Clostridia*, *Lachnospirales*, *Lactobacillales*, *Oscillospirales* and *Eubacteriales* groups. Of the *Eubacteriales* group it was comprised of *Eubacterium* and *Anerofusitis* classes the latter of which was not present in high abundance in the control groups. Studies vary on association between *Firmicutes* and growth performance parameters, although they generally tend to be positive (Bae et al., 2017; Rubio et al., 2015). In particular the *Clostridium*, *Clostridia,* and *Clostridiales* genera are associated with both positive and negative growth outcomes based in different trials (Stanley et al., 2016).

6.4.3   Time was the main determinant of sample ordination and network grouping

The combined ordination plots highlight that time was the main determining factor when looking at sample diversity and varied from being worth 25% to greater than 80% of the variance between samples, depending on ordination method. When comparing the ordination by sample to the analogous ordination by phyla, the picture becomes clearer, with time being responsible for the movement from *Firmicutes*, to P*roteobacteria* and *Bacteroidota,* and the treatment being responsible for intra-phyla, diversity.

Microbiome phyla ratio naturally changes with time, in both humans and chickens (Mariat et al., 2009; Rychlik, 2020). The development of a 'mature' microbiota in broilers is thought to occur during days 15-22 (Ranjitkar et al., 2016). Though this is variable between studies (Awad et al., 2016).

One key thing to highlight is the initial inoculum in the fermenter system came from 42-day old, culled chickens, and represents the GIS microbiome at the end-stages of the chicken life cycle (in high throughput farming practices only, chickens can live for between 3 to 20 years naturally). In this experiment we attempted to replicate the early stage of chicken microbiome development, between 0 and 8 days (Kubasova et al., 2019; Varmuzova et al., 2016). We propose that the use of mature chicken caecal content biased the microbiomes in this experiment towards late-stage chicken microbiomes.

In natural settings, the gut microbiota of chicks is a combination of microbiota of the mother hen, contact with hens after birth, and environment after birth (Awad et al., 2016a; Varmuzova et al., 2016). This facet is hard to introduce into the fermenter system, which is designed to be sterile prior to inoculation and closed to environmental bacteria. Another aspect missed by this system would have been diet diversity between chickens raised on different farms, however in cohort experiments chickens are usually kept on a strict identical diet with the exception of the tested product.

6.4.4 The quercetin control group samples where uniquely diverse compared to the rest of the samples.

Further to the ordination analysis, it became clear that the quercetin control group was uniquely diverse. Further analysis highlighted that this diversity was not due to inter-phyla change, but instead intra-phyla change within the *Firmicutes* phyla. Diversity within the *Firmicutes* over time is common in the GIS of chickens (Awad et al., 2016). Microbiome studies are inherently largely variable, and highly variable controls, with unique diversity

compared to the other groups, are not outside the realm of possibility (Sinha et al., 2015). Microbiome variation can be seen between scientific facilities that have identical genotypes of mice (Friswell et al., 2010) or between spouses in the same house (Shaw et al., 2017).

As such, we suggest that the combination of these factors, elevated levels of microbiome variation inherently, and the natural diversification of *Firmicutes* in the GIS as chickens age means that this unique clustering of the control samples is normal. Additionally, it positively displays that the model system accurately models the development of the microbiome in the GIS of chickens. Multiple replications of the current system using the same and different inoculum, would be needed to confirm what a 'normal' control looks like in this fermenter system. This was outside the remit of this study, as it was the first time the model system was used.

6.4.5 Sample diversity decreased immediately following inoculation but increased after 72 hours

The Shannon diversity of the samples was highest in the initial inoculum and the preliminary stages of each experiment. The diversity then fell drastically at the second and third timepoint and slowly increased towards the end. This drop in diversity, is of twofold interest. The first point of interest is that it accurately models the expected stabilisation of the microbiome usually seen after 72 hours in new born chicks (Glendinning et al., 2019). During the early days of chicken life, they are exposed to a wide variety of microbes in the environment (Awad et al., 2016), with an increase in diversity at day 8. In Awad et al., 2016, diversity rose at day 8 above initial levels, and continued to rise until the end of the experiments at day 28. It would be interesting to see if the diversity of the samples within the fermenter system continued to change over the whole 45 days of the broiler chicken life cycle, however that was outside the scope of this experiment.

Phytochemicals were added before T = 3 and this is where we see an increase in the diversity of the two treatment groups. This highlights that the phytochemicals are perturbing the microbiome, causing an increase in bacterial diversity, which can have both positive and negative growth performative effects as discussed in the following section

6.4.6 The addition of phytochemicals shifted the phyla from *Firmicutes* to *Actinobacteriota* and *Proteobacteria*

The addition of the phytochemicals led to a clear alteration in the microbiome of the fermenter system, from being solely *Firmicutes*, to *Firmicutes* and *Actinobacteriota*, in the case of berberine, and *Firmicutes, Proteobacteria* and *Actinobacteriota* in the case of quercetin.

Berberine supplementation increased the number of *Actinobacteriota,* specifically the *Gordonibacter* which are associated with positive growth parameters in broilers (Bae et al., 2017). The *Gordonibacter*, which were the most common genera in the samples, metabolise dietary polyphenols into urolithin, and is generally thought to be a positive candidate for probiotic supplementation (Selma et al., 2014; Toney et al., 2020). The ability of *Gordonibacter* to metabolise tannins, a class of phytochemicals is previously noted (Sallam et al., 2021), and the ability to metabolise phytochemicals may go some way to explaining the abundance of this genus after berberine supplementation.

Berberine is thought to reduce the diversity of intestinal microbiomes in mice (Chen et al., 2020; Guo et al., 2016) was noted in the previous section. Further, *Actinobacteriota* were reduced in the human GIS after berberine supplementation over 13 weeks (Zhang et al., 2020), though this was mostly limited to *Bifidobacterium.* This reduction was also seen in rats (Xu et al., 2017). These studies also indicated a decrease in *Firmicutes.* The decrease in *Firmicutes* but increase in *Actinobacteriota* is an interesting result present in our data, and different from what would be expected after literature analysis. However, the deeper

exploration of the genera that compose this would suggest this is positive for chicken health, and growth parameters. No published data exists detailing the role of *Gordonibacter* in AMR, or the potential of *Gordonibacter* to function as a reservoir for AMR genes. This data would be useful for evaluating berberines potential as a growth promotive supplement in chickens and represents a potential new line of work stemming from this thesis.

Quercetin supplementation led to an increase in *Proteobacteria* at day 4 and 5, and then a subsequent increase in *Actinobacteriota* at day 7 and 8. Relative to the berberine treatment group the increase in *Actinobacteriota* is minor and limited to the *Gordinibacter* genus. On the other hand, the increase in *Proteobacteria* abundance was unique to the quercetin treatment group. This increase was limited totally to the *Aquamonas* genus. However, there was also an increase in *Escherichia-Shigella* genus. The *Escherichia-Shigella* genus contains two pathogens of interest in poultry health, *E. coli* and *Shigella sp. E. coli* can cause secondary infections in both birds and humans (Stromberg et al., 2017), and is a reservoir of AMR genes (Ibrahim et al., 2019), and is negatively associated with chicken growth performance (EL-Sawah et al., 2018). This highlights clearly that quercetin supplementation has potential negative consequences for both growth performance parameters, and the AMR crisis.

6.4.7   Limitations and corrective modifications for future experiments

There were several limitations with this study. Firstly, this set of experiments was conducted using an inoculum that was dominated by *Firmicutes*. Whilst this was a biologically possible representation of the chicken GIS microbiome (Rychlik, 2020), it is not common, as the chicken GIS is usually represented by four phyla, two major and two minor. Future experiments would be prudent to determine if the changes we see in this study are consistent across microbiomes with a different initial inoculum, particularly with a higher relative abundance of *Bacteroidota*.

A second major limitation is that the fermenter system does not allow for challenge of the microbiome with new bacteria due to its sterile nature, as would happen in agriculture. As such it is not a perfect model for chickens gut microbiomes. In future experiments it may be possible to feed new, varied inoculum into the fermenter systems throughout the study, to better model the environment that the GIS of broilers and free-range chickens would be exposed too.

Thirdly, we only took a single extraction once a day from each of the systems. *In vivo* chicken experiments would usually be conducted with multiple chickens in each group and our single bioreactor runs model only a single chicken. Future experiments would be prudent running multiple bioreactors simultaneously and taking multiple samples. The bioinformatics analysis was conducted on single samples from each time point, and as such detailed statistics were unable to be run on this data. Further statistical analysis on repeats of this experiment, and qPCR would be ideal for determining the statistical relevance of the phyla level movement seen in this study.

6.5 Conclusion

Berberine supplementation led to an increase in *Actinobacteriota*, particularly *Gordonibacter*. This genus is charactered by their ability to metabolise phytochemicals such as tannins. They also have a positive impact on broiler health and growth performance parameters. This suggests berberine supplementation may be a good replacement for antimicrobial growth promoters in terms of chicken health.

Quercetin supplementation on the other hand led to an increase in the relative abundance of *Proteobacteria* and *Actinobacteriota*, the former of which specifically included a rise in the *Escherichia-Shigella* genus. This genus contains species that are pathogenic, function as AMR reservoirs, and have negative effects on growth performance parameters. This suggests that quercetin supplementation is a poor replacement for antimicrobial growth promoters, both from a growth performative standpoint, and due to its ability to increase the relative abundance of 'AMR reservoir' bacteria.

Berberine and quercetin supplementation was explored further using batch culture in chapter 7 and an *in vivo* experiment in chapter 8. To determine how well this fermenter system models the chicken GIS, and how it compares to other microbiome culture methodologies. Comparisons between the model system, and those experiments are given in the relative chapters, and final discussion.

7 Analysis of batch culture microbiomes and comparison to the model system

7.1 Introduction

To further explore how phytochemical supplementation alters microbiome composition within the chicken gastrointestinal system (GIS), a batch culture experiment was designed and implemented. This experiment used the same initial inoculum as the fermenter model detailed in Chapter 6.

Batch culture is a process by which all nutrients are provided to a bioreactor (Bhatia et al., 2015; Godbey, 2022), in this case a 2 ml bijou, at the start of a given experiment. There are other types of culture-based experiments. These include fed batch, wherein nutrients are added at specific time points to extend the culture duration, and continuous batch culture wherein media and in some cases a growth promoting or limiting substance is given throughout an experiment to maintain a specific microbial density. The previous experiment in Chapter 6 was an example of a continuous batch culture experiment, which is both more expensive, and more complicated to maintain.

In this chapter a limited fed batch culture experiment was carried out. Additional media and phytochemicals were added at three specific timepoints, as replacement for sampling extract at day 7, day 14, and day 21. The samples were grown in anaerobic, aerobic, and microaerophilic conditions, to model the different aerobic conditions present in the chicken GIS.

Simple batch culture experiments are useful to asses quick, high level overviews of the effect of supplementation on a particular microbiome (Yousi et al., 2019). They are relatively much cheaper and simpler to run than continuous assessment. If the batch culture successfully models the fermenter system in chapter 6 and the *in vivo* studies in chapter 8, it would prove

an extremely cheap and high throughput method of assessing many phytochemical compounds. This would allow it to act as an efficient exploratory step, before compounds were assessed using the more time, cost, and labour-intensive *in vivo* studies.

This chapter will evaluate how phytochemicals function as modulators of the chicken GIS microbiome. Comparisons will be drawn to chapter 6 and chapter 8 which explore *in vitro* model fermenter systems and *in vivo* chicken gut microbiomes respectively, using a bioinformatics approach.

7.2 Materials and Methods

7.2.1 Caecal content extraction, DNA extraction, sequencing, and bioinformatics methods

Materials and methods for collection of the caecal material, DNA extraction, and sequencing were identical to those in Chapter 6. Bioinformatics analysis outline is given in chapter 6, and full bioinformatics code is given in appendix IV.

7.2.2 Batch culture setup

In a 5 ml Bijou 350 µg of caecal content (identical to the initial inoculum used in Chapter 6), 50 µl of 10 mg/ml quercetin or berberine diluted in DMSO (filter sterilised), and 1.6 ml of MHB were mixed. These samples were then stored in either anaerobic, aerobic, or microaerophilic conditions at 42°C. Then 200 ml of the sample was extracted at day 7, day 14, and day 21 which was replaced with 200 µl of fresh MHB supplemented with phytochemical. The final concentration of phytochemical was equal to that of the previous model system experiments 320 µg/ml.

7.3 Results

7.3.1 Processing of samples from the batch culture.

Overall sample processing prior to taxonomic analysis was conducted as part of the bioinformatics pipeline detailed in Chapter 6.

As detailed in Chapter 6, often when working with complex microbiome datasets, the data can be very time, and computationally intensive. One possible solution to this is to agglomerate the operational taxonomic units (OTUs) by genus or a fixed height, especially if the data contains a large amount of species redundancy.

Phylogenetic trees (Figure 7-1) were constructed to determine if the agglomeration of the dataset by genus, or by a set height (0.4), would impact the distribution of the samples. In our dataset the agglomeration by genus, and height, did not have a marked impact on the phylogenetic tree, and thus future analysis was conducted using the pre-agglomeration dataset.

Before Agglomeration By Genus By Height
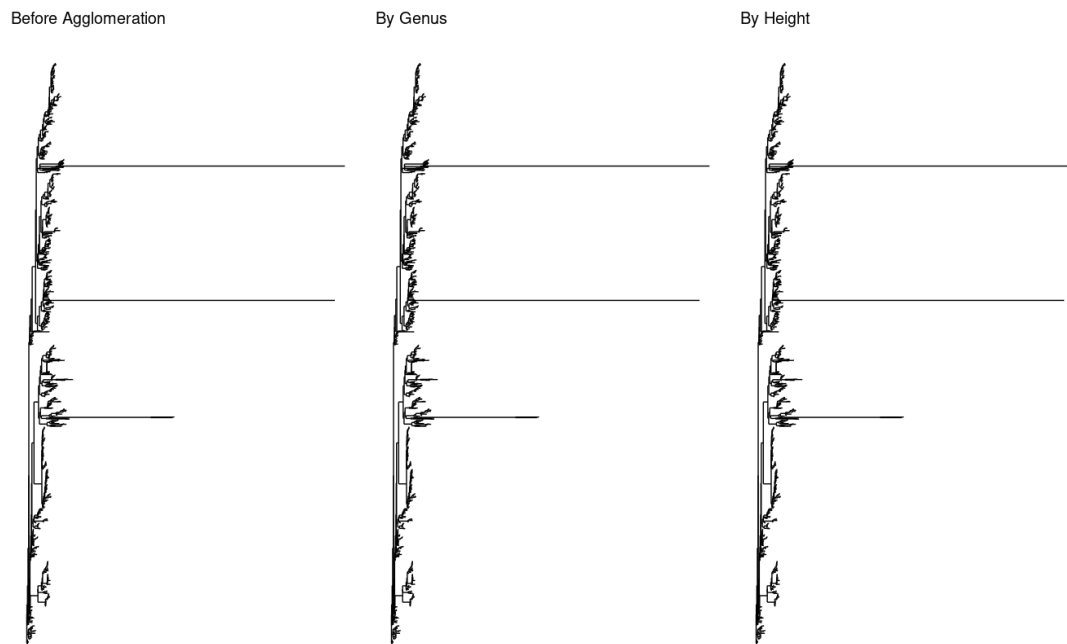
Figure 7-1 Phylogenetic trees were constructed with the sample data from the batch culture. The phylogenetic trees shown are prior to any agglomeration (left), agglomeration by genus (middle), and agglomeration with a set height of 0.4 (right). Often with complex biological data it can become much simpler to analyse when the tips are agglomerated by genus or by height, however in this data case agglomeration did not alter agglomeration.

Following agglomeration analysis, the phyla present within the dataset were then plotted (Figure 7-2), and all phyla present in less than 5% of samples regardless of abundance were removed (Figure 7-3). The most abundant phyla were the *Firmicutes*, with a small number of *Bacteroidota, Actinobacteriota, Cyanobacteria* and *Proteobacteria*. The removed phyla were present in less than 5% of samples at less than 5% abundance, these boundaries were selected because this experiment was concerned with the high-level changes between the different treatment conditions, and the presence of phyla in less than 5% of samples, or 5% of abundance was outside the remit of the analysis.
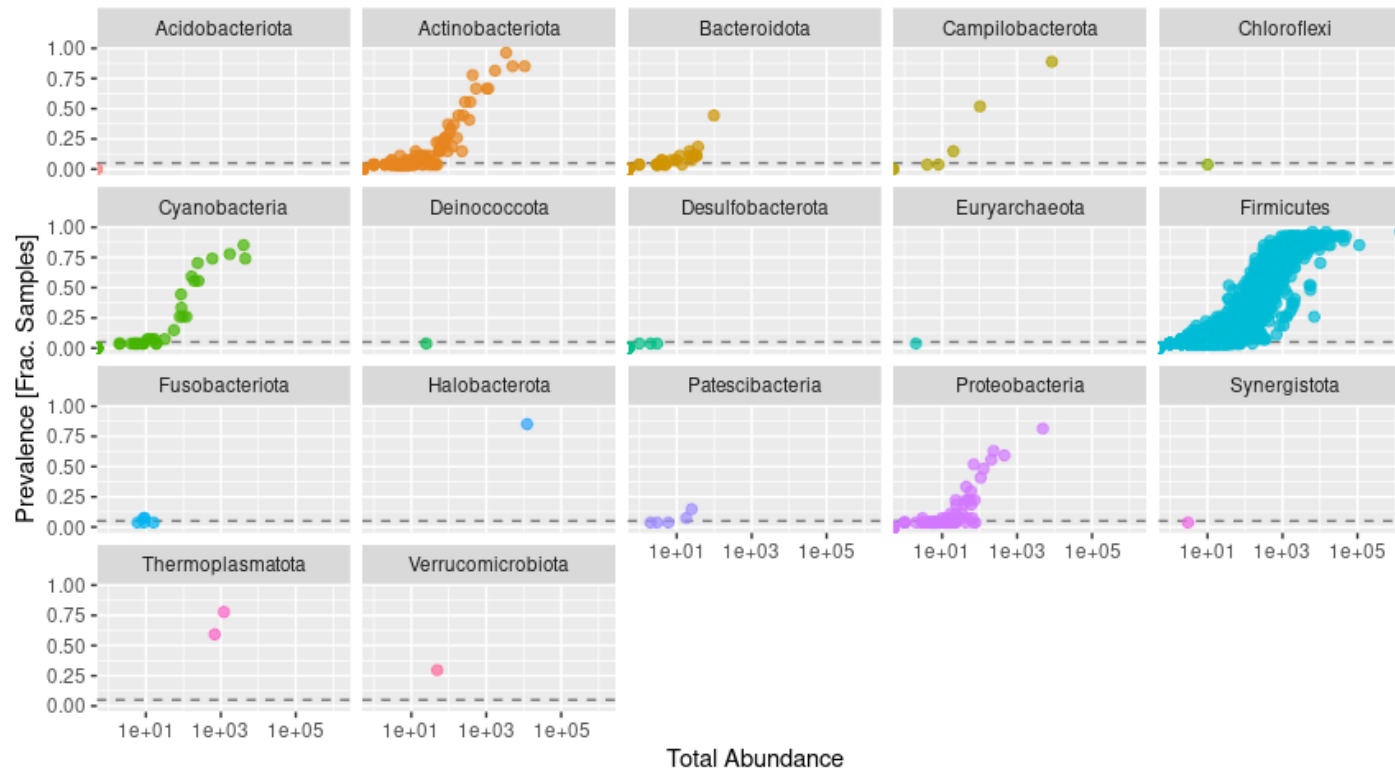
Figure 7-2 Phyla present across all samples from the batch culture are plotted, each dot represents a particular taxon of bacteria from within the phyla. The y axis is the prevalence of the species in as a fraction of samples from 0 (no samples) to 0.4 (40% of samples) and the x axis is the log abundance of the species within that sample. The dashed black line indicates a prevalence of 0.05, or 5% of samples.
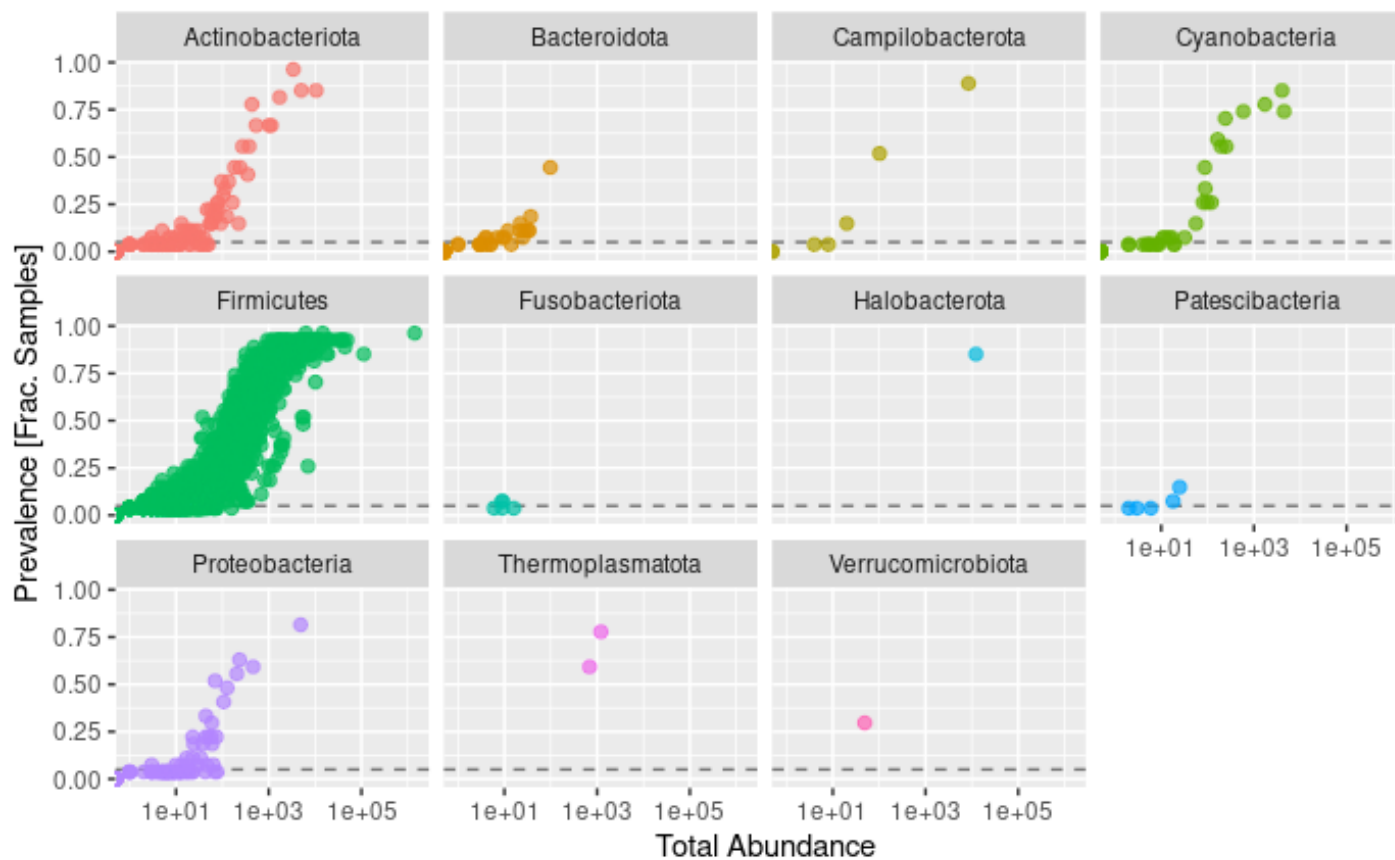
Figure 7-3 Plot of all Phyla present within the batch culture after removal of phyla with no species present in more than 5% of all samples. The y axis is the prevalence of the species in as a fraction of samples from 0 (no samples) to 0.4 (40% of samples) and the x axis is the log abundance of the species within that sample. The dashed black line indicates a prevalence of 0.05, or 5% of samples.

7.3.2 Detection of outlier samples from within the batch culture samples using sample depth and ordination

After taxonomic abundance analysis the next step was to determine which samples from the dataset were outliers. When plotting read counts present from all the batch culture samples, both as normal and log data there were six datapoints that had noticeably lower read counts than the rest of the dataset (Figure 7-4). These were: Berberine-Aerobic-D14, Berberine-Aerobic-D21, Quercetin-Aerobic-D7, Berbeine-Anerobic-D21, Quercetin-Anerobic-D7, and Quercetin-Anerobic-D21.

The removal of samples from the study due to noticeably lower read counts could have one of two potential causes. The first could be methodological errors, such as poor DNA extraction, amplicon library construction, or DNA sequencing. The second could be that the phytochemicals antimicrobial properties are causing complete bacterial inhibition in these samples. This latter possibility is consistent with the low read count samples all being from the phytochemical treatment groups. However, the fact that 3 out of 9 of each treatment group sample were lost, suggests it may not be a complete story.
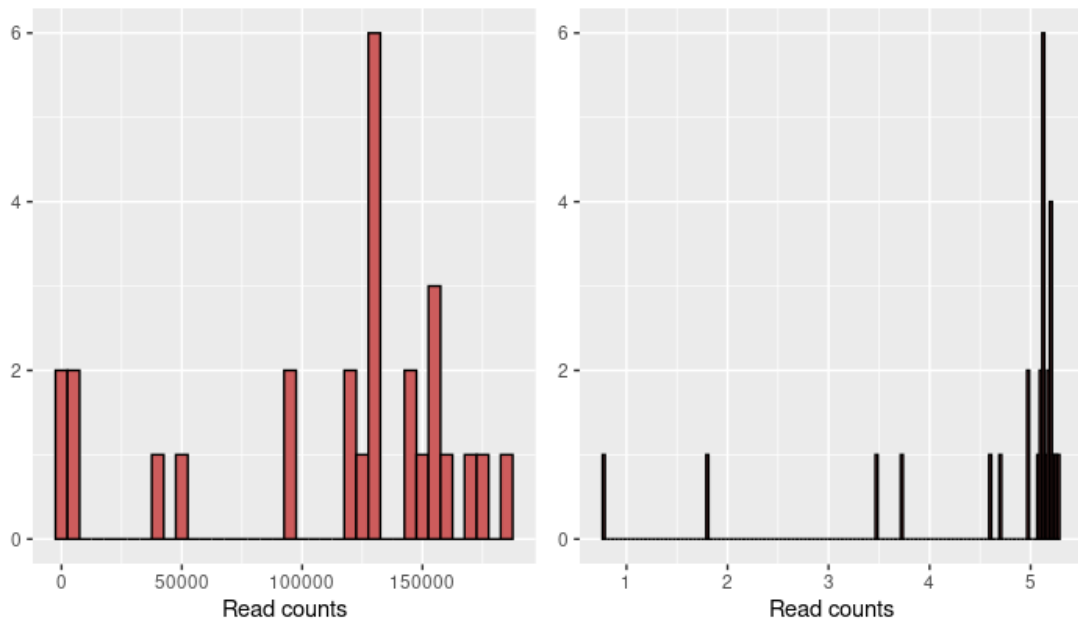
Figure 7-4 Histogram of read count distribution from samples from the batch culture (left) and log adjusted (right). The number of samples is given on the y-axis and the read counts are plotted along the x-axis. The samples removed at this stage were below 52000 reads and included, Berberine-Aerobic-D14, Berberine-Aerobic-D21, Quercetin-Aerobic-D7, Berbeine-Anerobic-D21, Quercetin-Anerobic-D7, and Quercetin-Anerobic-D21.

As previously discussed in Chapter 6 different bioinformatics methodologies and analyses can often give different results, despite attempting to mine a specific dataset for the same answer (Nearing et al., 2021, 2022). Multiple ordination and networking techniques were used to interrogate the dataset in this study. An outline of the different bioinformatics techniques used to interrogate the dataset are given at each point, and representative images of the analyses are shown and discussed.

PCoA using Bray-Curtis dissimilarity was conducted on the entire dataset (Figure 7-5). The lower read count samples cultured in the centre and the bottom right of the graph. Whilst the rest of the samples clustered on the left-hand side of the x axis, across the entire y axis. This suggests that these low read count samples did not well represent the ordination expected of the rest of the samples. These samples were removed from further analysis of the batch culture dataset.
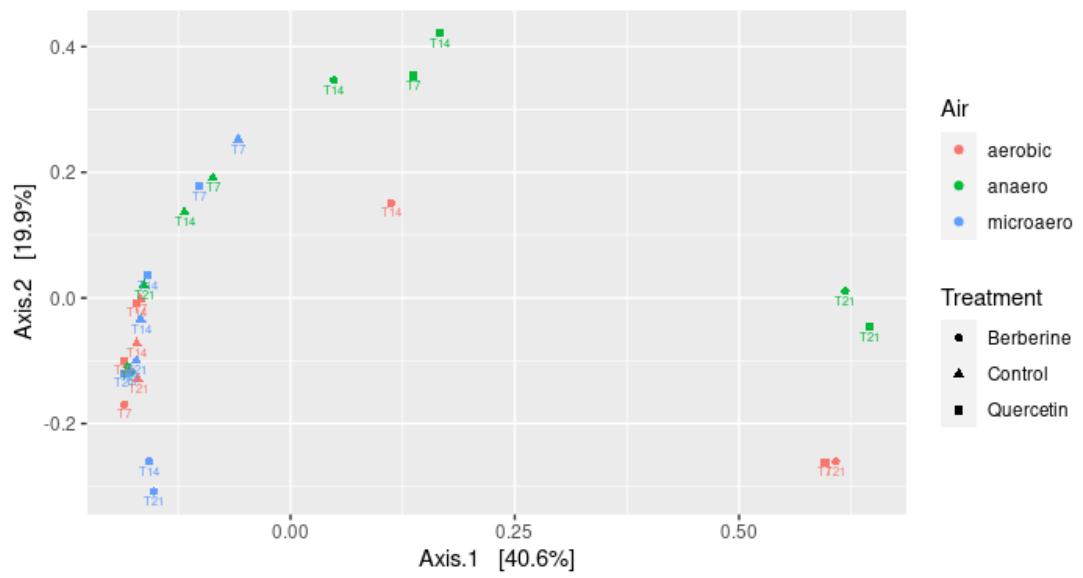
Figure 7-5 Ordination of samples from the batch culture using MDS-bray analysis prior to the removal of low read counts to determine the ordination of outliers. Samples are ordinated according to x axis which accounts for 40.6% of the ordination, and y axis which accounts for 19.9% of the ordination. Samples are labelled by aerobic conditions (colour), treatment group (shape) and timepoint according to text label.

7.3.3 Ordination analysis of batch culture samples after removal of samples with low read count

A PCoA ordination was then conducted using Weighted-UniFrac (Figure 7-6) on the remaining samples. In this ordination the x axis is now responsible for 46% of the ordination, and there are only two datapoints both treatment groups at day 14 on the right side of the axis. The y axis in this ordination accounted for 23.1% of the ordination, and represents time, with the T = 7 samples clustering at the top, the T = 14 samples towards the centre, and T = 21 samples at the bottom.
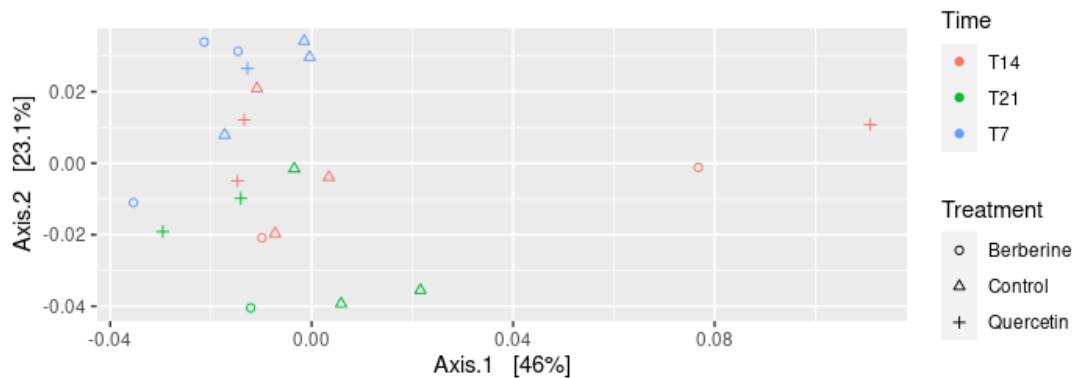
Figure 7-6 Ordination of samples from the batch culture PCoA-Weighted UniFrac analysis after the removal of low read counts to determine the ordination of outliers. Samples are ordinated according to axis.1 (x-axis) which accounts for 46% of the ordination, and axis.2 (y-axis) which accounts for 23.1% of the ordination. Samples are labelled by time conditions (colour) and treatment group (shape).

Next, the analogous graph to Figure 7-6 was constructed, plotting phyla rather than sample, on the ordination. Here the firmicute diversity is a result of both the x and y axis. The *Proteobacteria, Bacteroidota,* and *Actinobacteriota* clustered at the lower end of the y axis, which correlated with the later timepoints of the experiment (Figure 7-7).
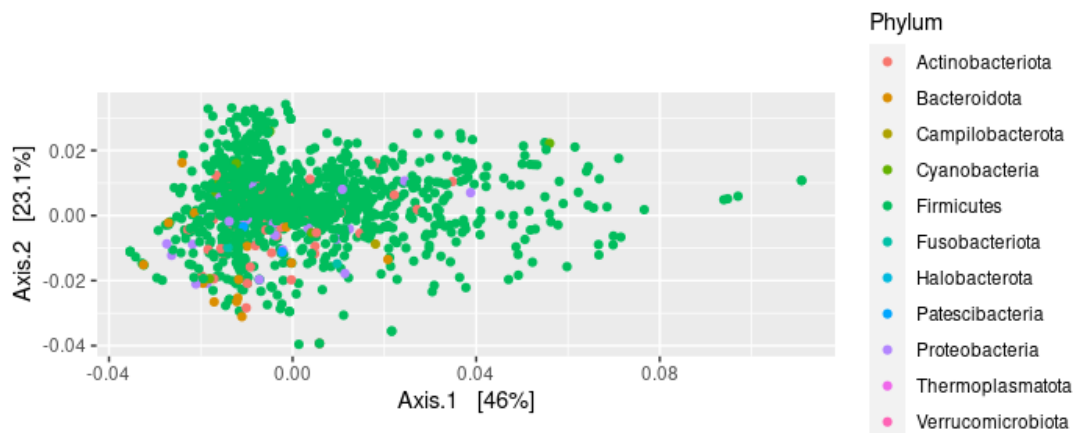
Figure 7-7 Ordination of samples from the fermenter system using PCoA-Weighted UniFrac analysis after the removal of low read counts. Samples are ordinated according to x axis which accounts for 46% of the ordination, and the y axis which accounts for 23.1% of the ordination. Datapoints are taxon from phyla organised by colour. Most of the diversity from non-firmicutes seems to be dominated by the bottom of the y axis and the right side of the x axis.

7.3.4 Network analysis of samples from the batch culture

After ordination analysis the next step was to conduct network analysis to assess sample relatedness and determine groupings. The first was a network using the Jaccard-Dissimilarity matrix. Samples were denoted by aerobic condition and treatment group (Figure 7-8). The microaerophilic and aerobic samples were mixed. Two members of the aerobic group at day 14, likely to the two samples that were outliers in the ordination analysis, did not associate with any other samples.
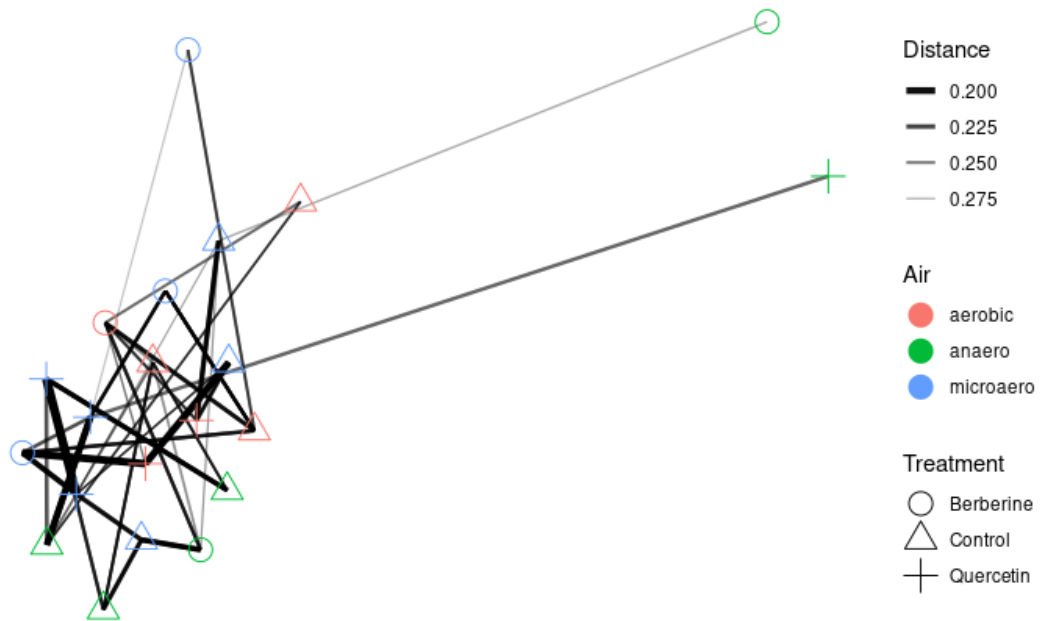
Figure 7-8 Network analysis of samples from the batch culture created using thresholding with the Jaccard-Dissimilarity matrix. Samples are denoted by air condition (colour) and treatment group (shape). Two day 14 samples, likely to be those that did not ordinate well with the other samples did not associate where expected. The samples grouped closer by air condition than by treatment point.

The next networking analysis was conducted using minimum spanning trees with Jaccard similarity to test for the relatedness by treatment, time, and air condition (Figure 7-9). Our null hypotheses for this analysis were that time, treatment, and aerobic condition did not affect sample relatedness.

All quercetin samples grouped together, as did all the control samples. However, the berberine samples did not group together, likely due to the loss of three berberine samples due to low read counts. The microaerophilic samples grouped together, as did several of the aerobic samples. However, the anaerobic samples did not group together. The minimum spanning tree analysis on sample distance according to time was not statistically significant.

From this analysis we can assume that both treatment group, and aerobic condition were significant determinants of sample relatedness (P < 0.05), however time was not a statistically significant factor in sample relatedness (P = 0.572).
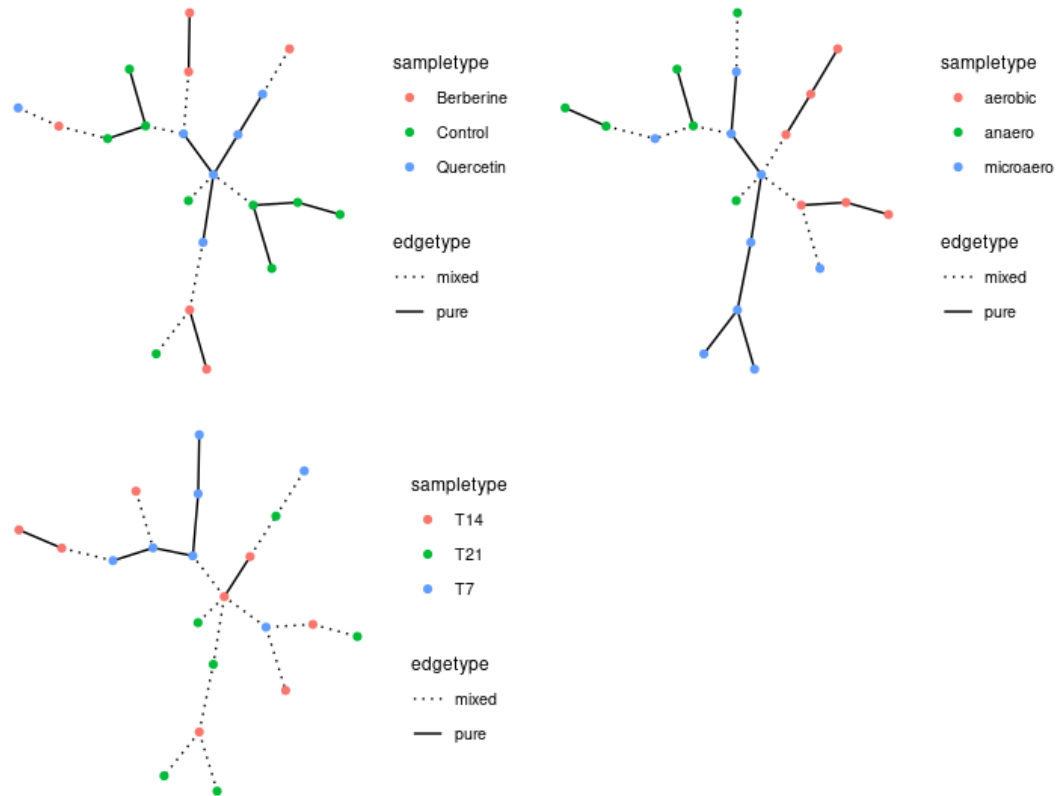
Figure 7-9 Network analysis of samples from the batch culture using minimum spanning tree with Jaccard similarity, by chemical addition (top left) (p = 0.018), air condition (top right, p = 0.008) and time (bottom left, p = 0.572). Where chemical addition, air condition and time point are given by colour in each of their respective graphs.

7.3.5   Shannon diversity of samples from the batch culture

After networking, linear modelling was used to plot the Shannon diversity of all the samples

(Figure 7-10). The berberine microaerophilic, control aerobic, and control microaerophilic

conditions have the lowest diversity overall. In all samples bar the control, anaerobic sample

diversity appeared to decrease by T = 21, although the severity of the change at T = 14 was

variable depending on the sample. However, in all cases, the predicted intervals crossed,

suggesting more samples are needed to confirm these findings. This consistent reduction in

diversity across all samples suggests that the inoculum did not survive well in the batch

culture experimental system.
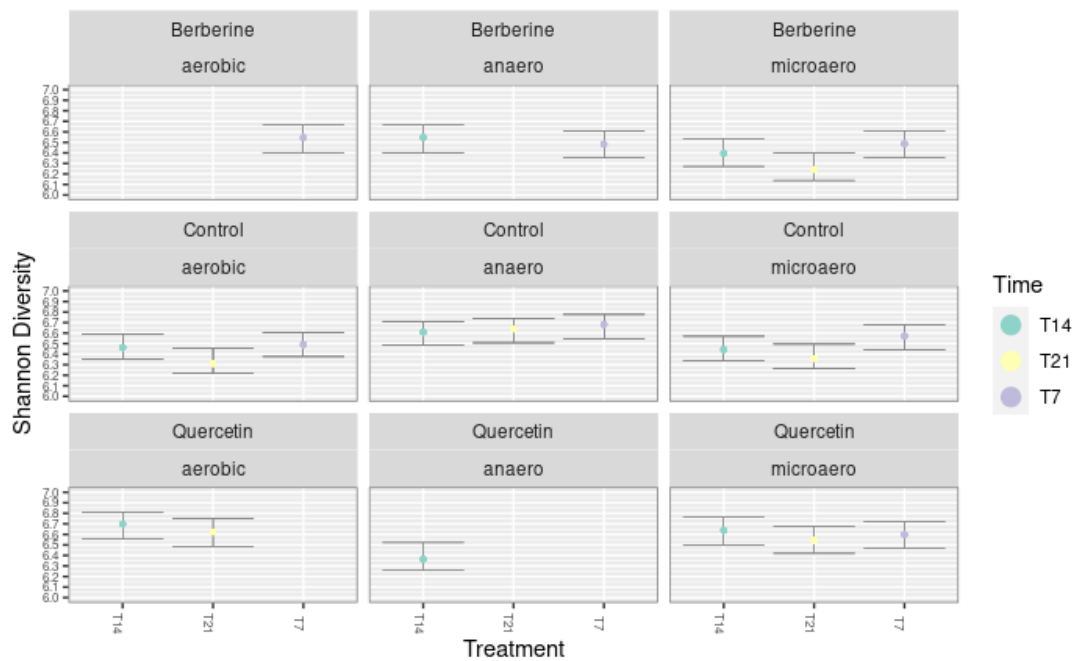
Figure 7-10 Shannon diversity of samples from the batch culture, faceted by sample treatment group and indicated by time in colour and on the x axis, each point indicates the Shannon diversity at one timepoint for each treatment group. Shannon diversity is given on the y axis. The prediction intervals for each sample obtained from the mix-effects modelling are overlaid. Diversity was similar across samples, with the control anaerobic and the quercetin aerobic conditions having slightly higher diversity and T = 21 samples having lower diversity.

7.3.6 Assessment of abundance of phyla in the batch culture samples visualised using stacked bar charts

The final set of visualisations was to look at the sample abundances by phyla by treatment group, faceted by air and timepoint. In all cases *Firmicutes* are the most dominant phyla, and the only one that has comparable abundances between the treatment groups.

Firstly, when evaluating the control groups, faceted by time and treatment it became clear that the aerobic control group was dominated by *Clostridiales* with a small number of *Lachnospirales* and *Oscillospirales*, and that the relative abundance of the *Clostridiales* increased over time. This pattern of dominance of *Clostridiales* was repeated in both the control anaerobic and microaerophilic conditions. However, both the anaerobic and microaerophilic control conditions had a higher ratio of *Lachnospirales* and *Oscillospirales* than the aerobic condition throughout each timepoint (Figure 7-11). This suggests that the

Clostridiales were particularly competent at survival in aerobic conditions in our batch culture experiment, without phytochemical supplementation.
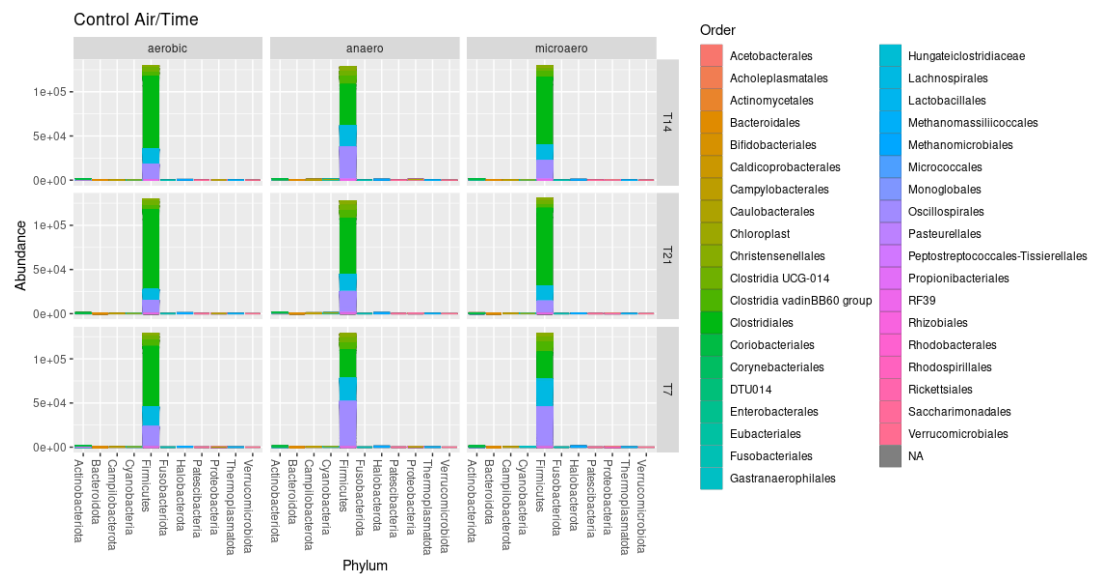
Figure 7-11 Stacked bar chart of control treatment group samples from the batch culture system, homogenised to relative abundance between the samples. The relative abundance is plotted on the y-axis and samples are plotted on the x axis. Phyla are coloured according to the label (right). Charts are faceted by timepoint and air condition. Firmicutes dominated sample abundance.

In the berberine group two of the day 21 and one of the day 7 samples were removed due to low read abundance. These samples may have had low read counts due to methodological errors, or the biocidal activity of berberine. This made it difficult to determine exactly how important time is in the ratios of the different orders within the *Firmicutes* phyla in these samples.

In the aerobic and microaerophilic conditions after berberine supplementation, the ratio of *Clostridiales* increased with time relative to all other orders and that they are the most abundant order, as they were in the control samples.

In the anaerobic sample at day 14, which was previously highlighted as an outlier sample in both the ordination and networking analyses, there was an increased ratio of *Lachnospirales* and *Oscillospirales* compared to *Clostridiales.* This ratio was increased at T = 14, relative to the berberine anaerobic sample at T = 7 (Figure 7-12).

This suggests that the addition of berberine was positive for the growth of *Lachnospirales and Oscillospirales* in anaerobic conditions, which most closely model the conditions of the chicken GIS.
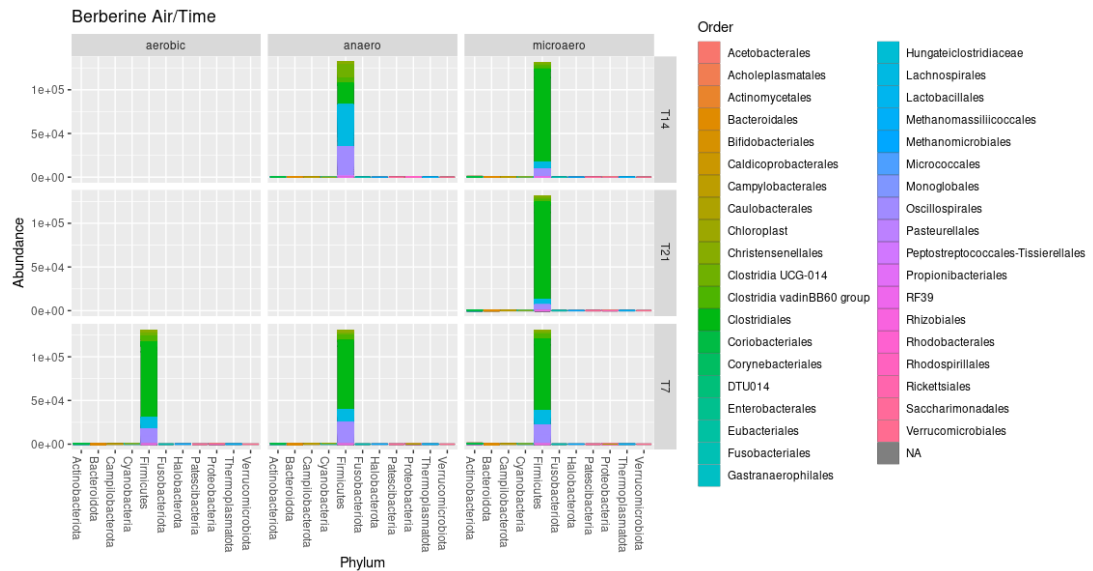
Figure 7-12 Stacked bar chart of Berberine treatment group samples from the batch culture system, homogenised to relative abundance between the samples. The relative abundance is plotted on the y-axis and samples are plotted on the x-axis. Phyla are coloured according to the label (right). Charts are faceted by timepoint and air condition. The diversity of Firmicutes appeared to be a single order in all samples apart from the anaerobic T14 sample.

Finally, in the case of quercetin, one sample from day 7 and one sample from day 21 were removed from the analysis due to low read count. These samples may have had low read counts due to methodological errors, or the biocidal activity of quercetin. This again makes the temporal aspect of this set of experiments hard to quantify.

The aerobic and microaerophilic conditions are similar those seen in the control and berberine groups with an increase in the relative abundance of the *Clostridiales* over time. The microbiome of the anaerobic group appears to mirror that of berberine at day 14 with a higher relative abundance of *Lachnospirales* and *Oscillospirales* than *Clostridiales*. This again matches with the earlier ordination conclusions (Figure 7-13).

This suggests that phytochemical supplementation is positive for the growth of the *Lachnospirales* and *Oscillospirales* orders, particularly in anaerobic conditions.
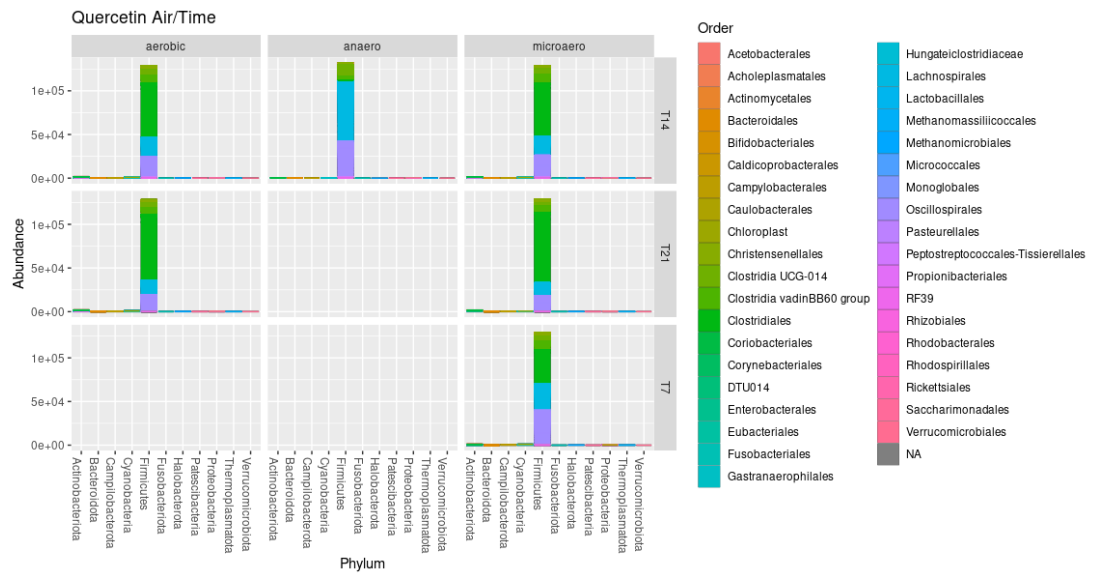
Figure 7-13 Stacked bar chart of quercetin treatment group samples from the batch culture system, homogenised to relative abundance between the samples. The relative abundance is plotted on the y axis and samples are plotted on the x axis. Phyla are coloured according to the label (right). Charts are faceted by timepoint and air condition.

7.3.7 Violin plot visualisation determined that the *Escherichia-shigella* genus was present only in the quercetin samples.

Violin plots were visualised for all phyla, by class faceted by order and order faceted by genus. Here the *Eubacteriales* order faceted by genus is shown (Figure 7-14). Within the Enterobacterales the Aquamonas was the most abundant genera present in both the berberine and quercetin treatment groups, and the *Escherichia-Shigella* was present in higher abundance in the quercetin group than the berberine group.
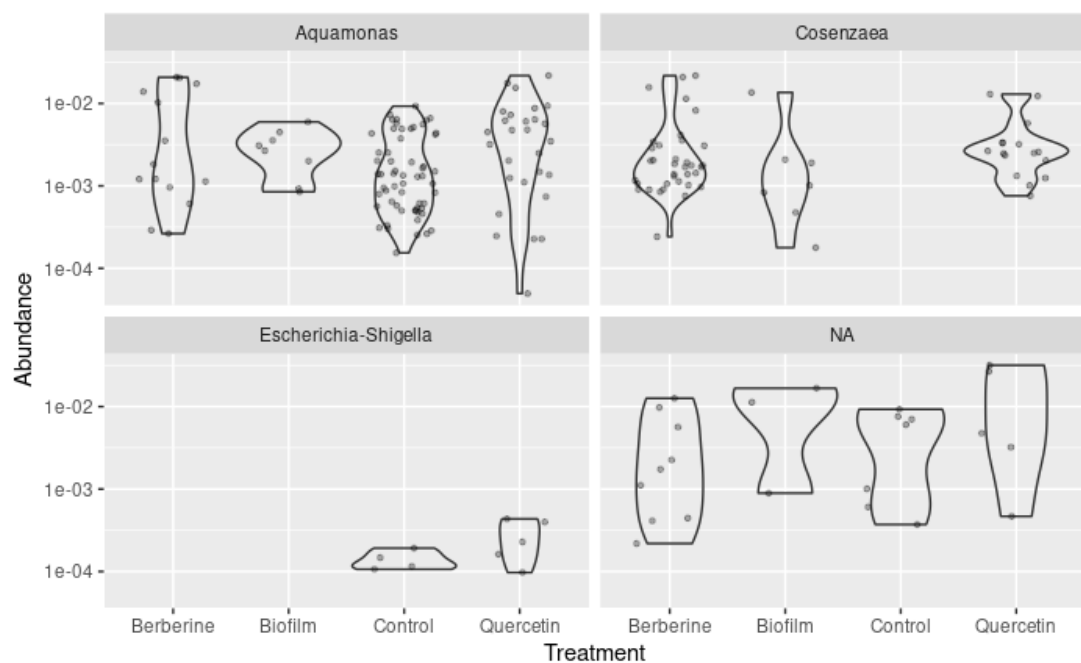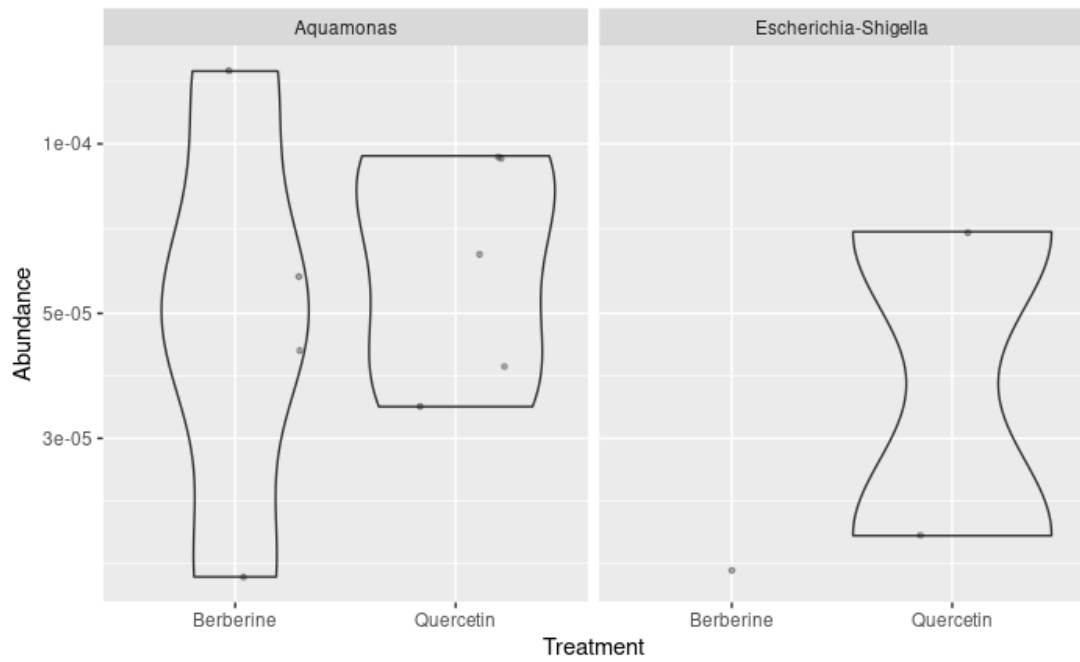
Figure 7-14 Violin plot of the Enterobacterales order faceted by genus, with log abundance plotted on the y-axis and treatment group plotted along the x-axis. Each dot is a specific taxon within that genus, with the bimodal distribution for each sample plotted as a violin shape (black). The Aquamonas genus was most present in the berberine and quercetin conditions, the Escherichia-shigella, was most present in quercetin.

7.4 Discussion

This chapter followed a set of batch culture experiments conducted on a chicken caecal inoculum over a period of 21 days and was used as a comparative experiment to the more intensive and complex fermenter experiment described in Chapter 6, and the *in vivo* studies in Chapter 8.

The key findings from this chapter can be broken down as the following: (1) The phytochemicals may have had complete biocidal effects in the batch culture system (Figure 7-4). (2) *Firmicutes* were the dominant phyla within the sample (Figure 7-3). (3) Aerobic condition, treatment group, and time all had an impact on both ordination analysis, and network analysis (Figure 7-6, Figure 7-7, and Figure 7-9). (4) Changes in Shannon diversity were limited (Figure 7-10). (5) The ratio of *Lachnospirales* and *Oscillospirales* decreased and the ratio of *Clostridiales* increased across all conditions as timepoints progressed (Figure 7-11, Figure 7-12, and Figure 7-13). However, in aerobic conditions after the addition of either quercetin or berberine, the ratio of *Lachnospirales* and *Oscillospirales* increased and the ratio of *Clostridiales* decreased. (6) The *Escherichia-Shigella* group was once again present in samples after the addition of quercetin, mirroring the Fermenter studies (Figure 7-14).

7.4.1 The phytochemicals may be completely biocidal

Three of the nine samples from each treatment group were removed from the analysis due to low read count. None of the samples from the control group were removed. There were two hypothesised reasons for the low read count of these samples. First, methodological errors in the content extraction, DNA extraction, or sequencing could have led to poor read count. The lack of multiple samples means we were unable to repeat these experiments to account for this.

Alternatively, it may be possible that the biocidal activities of quercetin (Das et al., 2019; Wang et al., 2018) and berberine (Freile et al., 2003) in the nutrient limited settings of the batch culture experiment led to a complete collapse of the microbiome. This hypothesis is further supported by the fact only samples from the treatment group had low sequence reads.

Multiple samples from the fermenter study in chapter 6 also were removed due to low reads from the berberine treatment groups. However, these samples were only single days, and the preceding and following day samples had high abundance. In that study, we theorise the low read count was due to methodological factors, as discussed above.

The potential collapse of the microbiome due to phytochemical addition in this study suggests that the batch culture is a poor model for the chicken GIS, when compared to the fermenter system where the microbiome was sustained. The potential biocidal activity of these compounds against chicken GIS microbiomes, may have industrial application.

7.4.2   Firmicutes were the most abundant phyla within the batch culture experiment

Within our samples *Firmicutes* were the most abundant phyla. As previously highlighted *Firmicutes* are one of the two major GIS phyla (Shang et al., 2018), and the initially inoculum was known to be *Firmicutes* dominated (chapter 6). The degree to which they dominated in the treatment group conditions was surprising, given that *Actinobacteriota* and *Proteobacteria* both increased in abundance after phytochemical supplementation in our fermenter system experiment (chapter 6). This increase in abundance of these alternative phyla were not seen in this experiment. This data highlights that the fermenter model system is better at modelling the chicken GIS than traditional batch culture methodologies. The fermenter system is better because it can maintain a multi-phyla microbiome, which allows the exploration of the effects of phytochemicals on multiple phyla, which is more representative of a normal chicken GIS.

It is important to note that our first timepoint was at day 7, in the fermenter system from Chapter 6 the quercetin control groups at this point were also almost entirely *Firmicutes* based. It's possible that conducting this experiment and taking daily samples for microbiome analysis may show that there is are diverse phyla present within the initial inoculum, which is followed by a stabilisation, or rapid contraction of the detectable species, of species present within the microbiome during the initial 7-day period. The inability to capture the initial stages of microbiome development was also an issue in the *in vivo* study.

7.4.3 Aerobic condition had the largest impact on sample ordination

Aerobic condition appeared to have the most notable effect on ordination analysis, accounting for between 40-60% of the ordination analysis on the data. It was expected that aerobic conditions would have a significant impact on the microbiome development given that the chicken gut is primarily composed of anaerobic bacteria (Shin et al., 2019). The faecal matter quickly changes from an anaerobic to an aerobic bacterial composition after deposition (Wong et al., 2016). The importance of the aerobic condition highlights that work on potential phytochemical growth should be limited to the bacteria present in a normal chicken GIS under GIS conditions, as comparative experiments on aerobic and microaerophilic conditions would likely mask the true impact of the phytochemicals.

7.4.4 Time was the second most important factor within the ordination analysis

Time accounted for between 15-30% of the ordination on normal data. Only three timepoints were taken, at day 7, day 14, and day 21. By contrast, the fermenter system was only run for 8 days. Time in the fermenter system model was responsible for anywhere between 25-80% of the ordination depending on ordination method. This decrease in the importance of time in the batch culture experiments is likely a result of the chicken GIS microbiome stabilising after 3 days, the early developmental stages of the microbiome being missed out in this experiment (Kubasova et al., 2019; Varmuzova et al., 2016). Although the development of

the mature microbiota from day 14 (the start of development) through day 21 (the end of development) was explorable through this experimental design (Ranjitkar et al., 2016).

7.4.5 The effects of treatment were not modelled by our ordination analysis

Treatment did not appear to influence the ordination analysis conducted. However, all our ordination analysis was conducted to visualise only the top two principal components. The DPCoA graph which accounted for the largest percentage of all ordination analysis, only accounted for 85.9% of the ordination. As such treatment probably falls as the third most important component in our ordination and the use of three dimensional PCoA plots may elucidate this data (Lever et al., 2017). Triple principal component analysis was conducted in Chapter 8, to effectively visualise the role of treatment in the *in vivo* work and would be the next step in this bioinformatics pipeline on these data.

7.4.6 Changes in Shannon diversity were small

Variation in the Shannon diversity between samples remained between 6.2 and 6.9, including predicted value ranges. Compared to the fermenter system model, the Shannon diversity ranged from 1.0 to 9.0, including predicted values. In the aerobic and microaerophilic conditions, diversity decreased from day 7 to day 21, and the quercetin anaerobic condition had the lowest diversity overall, whilst the control anaerobic condition had the highest. This highlights two things, firstly, that the initial inoculum contained a higher abundance of species that could survive in anaerobic conditions, as expected from caecal extract. Secondly it suggests that phytochemical supplementation lowers microbial diversity, which would make sense due to its intrinsic antimicrobial nature. This is likely harmful for chicken welfare as lower microbial diversity is negative for chicken growth (Yadav & Jha, 2019). This reduction in chicken growth suggests these phytochemicals would not function well as growth promoters in the agricultural industry.

This, like the decrease in Shannon diversity seen after phytochemical addition in the fermenter model, was unexpected. This is because chicken microbiomes tend to increase in diversity as they get older (Awad et al., 2016a; Xiao et al., 2021). This difference between *in vitro* and *in vivo* studies may be due to the inability to capture the effect of repeated exposure to bacteria from the environment and other chickens that would be present in *in vivo* studies.

The decrease in diversity may also be due to the limited nature of the batch culture systems. The bacteria likely reached exponential growth very quickly, and the species that could survive at later timepoints were likely adapted to growth in lower resource settings. This suggests that using the batch culture to assess the effects of phytochemicals on the microbiome of chickens, may have an unintended consequence of selecting for bacteria that thrive in nutrient limited settings.

7.4.7 Clostridiales was the most dominant order in all samples (With the notable exception of the aerobic cultures supplemented with either quercetin or berberine)

Almost all bacterial diversity and abundance within the batch culture experiment was confined to the *Firmicutes* phyla. *Clostridiales* was the dominant order, followed by *Lachnospirales* and *Oscillospirales*, these latter two orders decreased at the later timepoints in all conditions, where the sample became increasingly *Clostridiales* dominated. The exceptions to this rule were the quercetin and berberine sample in anaerobic conditions at day 14. Both samples ordinated together, but separately from the rest of the group, and this is due to a change in the relative abundance of the orders of the *Firmicutes* where *Clostridiales* decreased, to be replaced by increasing numbers of *Lachnospirales* and *Oscillospirales*. This suggests both quercetin and berberine, in anaerobic conditions, select for *Lachnospirales* and *Oscillospirales*. Both the *Lachnospiracae* and *Oscillospiraceae* were found in high abundance in the *in vivo* chicken studies, in the caeca samples (Chapter 8). This

suggests that the batch culture systems do have the ability to maintain a modifiable microbiome of *Firmicutes,* though it does not appear to allow for the survival of any other phyla and is certainly not representative of the complex chicken GIS microbiome.

7.4.7.1 Clostridiales

Clostridiales are an order within the *Clostridia* class. The *Clostridiales* are a diverse order of microbes and include important poultry pathogens such as *Clostridia perfringens. C. perfringens* is a normal member of soil and gut flora, and an opportunistic pathogen causing necrotic enteritis. *C. perfringens* infections is a growing problem in chicken flocks in countries that have eliminated the use of AGPs (Van Immerseel et al., 2004). Other members of the *Clostridiales* order are used as probiotics for chickens (Guo et al., 2020; Huang et al., 2019), with positive effects on the growth performance. This highlights the diversity of impacts this class can have on chicken growth performance. Importantly, the *Clostridia* class is considered incredibly important for gut immune response (Round & Mazmanian, 2009), and can cause both reduced and excessive inflammatory responses. The *Clostridiales* are not normally the most dominant order within caecal systems (Rychlik, 2020). This suggests that they may be being selected for by the nutrient limited setting of the batch culture system. This is backed up by previous studies that highlight the *Clostridiales* grow well in water stressed conditions (Zhang et al., 2019).

7.4.7.2 Oscillospirales

Oscillospirales an order of the *Firmicutes* from within the class of *Clostridia*. They are most well known for being obligate anaerobes. In the human gut microbiome, the presence of *Oscillospirales* is associated with positive outcomes for several health conditions. These include obesity related diseases, constipation, and weight loss (Konikoff & Gophna, 2016). In general, the *Oscillospirales* are considered good for GIS health. Further the *Oscillospirales* are being considered as a candidate for next generation probiotics (Yang et al., 2021). Although

some studies indicated that high abundance of *Oscillospirales* can promote constipation (Chen et al., 2020). Presence of the *Oscillospirales* in poultry is consistently associated with lower residual feed intake (Liu et al., 2021), highlighting its potential negative consequences on chicken growth. Though some members of the *Oscillospiraceae* have been associated with positive growth outcomes (Lundberg et al., 2021).

7.4.7.3   Lachnospirales

The *Lachnospirales* are members of the *Clostridia* class and they are associated with both positive and negative growth outcomes in chickens, depending upon the species (Liu et al., 2021). They are particularly abundant during early and late stage microbiome development in poultry (Richards et al., 2019) and are usually more common in the caecum than in the ileum (Glendinning et al., 2019). They are also present in the caeca samples from Chapter 8, alongside the *Oscillospirales.*

7.4.8   The *Escherichia-Shigella* genus abundance increased after addition of quercetin mirroring the results seen in the model fermenter system study

Finally, as seen in chapter 6. The *Escherichia-Shigella* genus was present in samples after supplementation with quercetin. The increase in *Escherichia-Shigella* abundance in quercetin supplemented samples suggests that quercetin is likely to be a poor growth promoting additive (EL-Sawah et al., 2018). Further, *E. coli* acts as an antibiotic resistance reservoir in agricultural settings (Wang et al., 2020). The presence of *E. coli* in samples after phytochemical supplementation is consistent across the three growth promoter studies and discussed in depth in the final discussion (chapter 9).

This result further reinforces the idea that some of the effects of phytochemical supplementation on the chicken microbiome can be discovered through batch culture experiments, though it is still a poor model.

7.4.9   Limitations and future work

Two key limitations are: (1) That 6 datapoints were removed of the total of 27 (22%), and (2) only that a single sample was taken from each batch culture at each timepoint. The removal of these samples limited the ability of the bioinformatics pipelines to drawn comparisons between treatment group, time, and anaerobic condition. Alongside these limiting factors two samples appeared to be outliers in terms of their microbiome composition. These samples were kept in because they represented the treatment groups at anaerobic conditions, which were important samples due to their relatedness to the fermenter system.

Future experiments using batch culture methodology would be best conducted with multiple biological replicates, this would increase the confidence in our findings, and mitigate the risks of potential sample loss due to low read count, which impacted this experiment. Direct comparison to chicken faecal, or caecal content at these time points would also be ideal, to determine how closely the control microbiome is represented in the batch culture.

7.5   Conclusion

The addition of the two phytochemicals changed the composition of the microbiome of the batch culture system, from *Clostridiales* dominant to a more balanced ratio of *Clostridiales*, *Oscillospirales,* and *Lachnospirales* which are beneficial for gut health. This was only true in the case of the anaerobic samples, which most closely resemble the GIS conditions.

The most noticeable difference between the results from Chapter 6 and this chapter is the lack of abundance of the other phyla after phytochemical addition. This suggests that the initial inoculum microbiome balance may have a much greater impact on the results from the batch culture, as there was no continued addition of media. Due to this, the phyla that dominated in the early stages were likely positioned better to dominate after the exponential growth phase was finished. Further, the lack of continuous feeding may have inadvertently selected for bacteria that grew well in nutrient poor conditions, such as the *Clostridiales*.

The results from this chapter indicate that the batch culture is a poor representation of the chicken GIS, and the addition of phytochemicals in this nutrient starved environment may lead to complete biocidal activity. The fermenter system model from chapter 6 models many of the important attributes of the chicken GIS that the batch system does not, such as movement, and continuous feeding. These factors, combined with the ability of the model system to maintain a multiple phyla microbiome, suggest it is a much better system. However, the batch culture may have some utility for high throughput exploration of phytochemical effects on the chicken microbiome by industry, before committing to the time and cost of an intensive model system and subsequent *in vivo* studies.

The batch culture experiments also picked up the increase in *Escherichia-Shigella* genus after quercetin addition. This was equivalent to the increase in the *Escherichia-Shigella* genus after quercetin supplementation in our model fermenter system study. We theorise that the selection for *E. coli* by quercetin in these models would have negative impacts for both

chicken welfare, and antimicrobial resistance persistence in agricultural systems, if quercetin

was used as a growth promoter.

8 *In vivo* analysis of the chicken caecal and ileal microbiome after in-feed supplementation of food with phytochemicals

8.1 Introduction

This chapter considers the effects of in-feed supplementation of quercetin and berberine on the caecal and ileal microbiota of chickens. This chapter is the final member of the triad of work (Chapters 6-8), exploring the potential effects of berberine and quercetin, as growth promoters in chickens.

Antibiotics are used in the agricultural sector as antibiotic growth promotors (APGs) and as therapeutics. More antibiotics are used in the agricultural sector than in the medical sector (Dritz et al., 2002). The spending on antibiotics by the agricultural sector is high, and usage is projected to increase by two thirds by 2030, due to rising demand for low cost meat (Laxminarayan et al., 2015).

Antibiotics in agriculture have a clear impact on human health. Examples of the antibiotic resistant bacterial infections which originated in the agricultural sector include methicillin-resistant *S. aureus* (MRSA) and multi-drug-resistant (MDR) urinary tract infections which originated in swine and poultry, respectively (Larsen et al., 2015; Nordstrom et al., 2013).

European countries and many food suppliers have banned the use of antibiotic growth promotors in their products (Singer et al., 2016). Further a number of international organisations including the World health organisation (WHO), Food and Agriculture Organisation (FAO), and World Organisation for Animal Health (WOAH) have suggested a complete ban of AGP use (Dibner & Richards, 2005).

The removal of AGPs, however, has in some cases led to an increased incidence of disease in animals or higher economic costs (Casewell et al., 2003; Cogliani et al., 2011; Dritz et al., 2002; MacDonald & Wang, 2011).

One solution to the removal of AGPs is the use of phytochemicals due to their antimicrobial properties (Lillehoj et al., 2018). Whilst phytochemicals offer an attractive alternative to AGPs, little is known about how their use would contribute to the development and proliferation of ARGs in agricultural settings. If phytochemicals can select for antimicrobial resistance, as explored in chapters 3-5, the use of phytochemicals as AGPs might be little different from the use antibiotics, worsening the AMR crisis.

In vivo microbiome studies have been previously used to assess the impact of a range of chemicals upon the caecal microbiome, including: plant essential oils (Chen et al., 2020), bacitracin, avilamycin, virginiamycin, and narasin (Plata et al., 2022), and heavy metals including calcium, phosphorous, and trace levels of others including iron (S. Acheampong, 2022).

The literature on the use of phytochemicals in feed showed diverse changes in the microbiome composition, depending upon the phytochemical used. Curcumin supplementation increased the relative abundance of *Faecalibacterium* and *Enterococcus* (Leyva-Diaz et al., 2021)*.* Whilst the *Lactobacilli* count was increased in chickens fed a diet supplemented with rosemary extract (Petričević et al., 2018). The varied nature of plant extracts and their constituting phytochemicals suggests that no two plant chemicals will have the same biological effect on the microbiome composition.

8.2 Materials and methods

8.2.1 Chicken rearing and the in-feed additive procedure feeding procedure

For the first two weeks of their lives, the chickens were fed 3 mm HPS poultry starters (802110) (Mazuri Zoo Foods, Witham). HPS poultry starters include barley, wheat, maize, soya bean oil, and additional vitamins (A, D3, and E), the feed also contains <1% of calcium, phosphorous, sodium and magnesium.

For the rest of their lives, they were fed Poultry Grower HPS (802104) (Mazuri Zoo Foods, Witham). This feed included wheat, wheat feed, maize, toasted soya, and the same additional vitamins and minerals as the poultry starter.

This was supplemented with either 320 µg/g of quercetin or berberine dried powder, which was mixed in with the feed before scattering, and subsequently eaten by the birds. The concentration of phytochemical was based upon the concentrations of phytochemicals provided in available phytochemical based growth promoter supplemented feed (Delacon, 2020).

8.2.2 Chicken caecal and ileal content extraction

At the time of extraction all chickens were 14 (3 chickens per group) or 21 (10 chickens per group) days of age, the birds were not sexed. Birds were killed via neck dislocation; subsequently the abdominal cavity was opened to expose the intestinal tract. The caecum and ileum are parts of the chicken gastrointestinal system (GIS). The blind ended caecum (caecal sacs attached to the intestine from which content moves circularly back into the intestine) and the ileum (the second to last part of the GIS in chickens, prior to the colon) were located and removed. Caecal and ileal contents were collected in separate clear sterile falcon tubes, and immediately snap frozen in liquid nitrogen. These were then stored at -80°C until further use (Dr Sian Pottenger (University of Liverpool) external communication (20/1/20)).

8.2.3 DNA extraction and preparation

DNA extraction was conducted using the ZymoBIOMICs® whole DNA extraction protocol (chapter 1.16).

8.2.4 16S sequencing and microbiome analysis

16S sequencing of the V4 region, amplicon library generation using the Illumina MiSeq™, and microbiome analysis were conducted under contract by the Centre for Genomic Research at the University of Liverpool (Liverpool, United Kingdom).

8.2.5 Data visualisation and analysis, and time constraints.

Data analysis was contracted out to the Centre for Genomic Research at the University of Liverpool (Liverpool, United Kingdom). Dataset analysis was provided with 7 weeks remaining before the final hand in date of the thesis. Therefore, analysis of the data was only conducted within this platform, and future work building on this PhD would be ideally placed to dive properly into this data.

The data analyses were visualised using Qiime2 version 2022.2. accessed using the following link view.qiime2.org.

8.2.6 Statistical analysis

Statistical analysis was conducted to determine if the abundance of *Escherichia-Shigella* was statistically different between the control and treatment groups.

Two tailed t-tests for independent means were conducted using https://www.socscistatistics.com/tests/studentttest/default2.aspx (Social Science Statistics, 2022). Two tailed t-tests were selected as it was unknown if resistance level, or production would increase or decrease because of evolution in sub-inhibitory concentrations of

phytochemicals. Significance value was set at p > 0.05. Full calculations are given in appendix V.

8.2.7 Ethics

Ethical approval for the *in-vivo* poultry work in chapter 9 was obtained through the project licence P999B8C93 and personal licence of Dr Sian Pottenger (IE89D0D59), approved by the University of Liverpool Ethics Committee (chapter 1.18).

8.3   Results

8.3.1   Samples were processed in two separate batches according to read quality

Sample were processed into two separate lanes (MiSeq sequencing runs) for the analysis, this was due to several reads being poorer quality, facilitating the need for separate analysis (MiSeq lane 1 and lane 2). The data shown in this chapter is taken from MiSeq lane 1, unless otherwise stated. The data shown are representative of both sample runs, unless otherwise stated.

8.3.2   Samples grouped strongly according to body part and loosely by treatment group within that body part according to taxonomic analysis.

Frequency of bacteria present across all samples was visualised using a heatmap, at varying levels of phylogenetic hierarchy. These heatmaps were analysed at the phyla, class, and order level. The most notable features of these heatmaps could be seen at the phyla level (Figure 8-1). The day 21 caecal samples all grouped together, with some outliers (samples 26, 28, 46, 73 and 75). The control samples grouped together within that (apart from samples 73 and 75), and then the two treatment sample groups grouped together, with little distinction. The caecal samples were characterised by a high relative frequency of the *Firmicutes* phyla and a lower relative frequency of the *Actinobacteriota* phyla. The ileal and caecal samples from day 14 all grouped together, treatment group notwithstanding. These were distinct from the day 21 samples as they were characterised by the absence of the *Actinobacteriota* phyla. A small number of samples contained members of the *Cyanobacteria, Bacteroidota* and *Spirochaeta* phyla, however, abundances of these phyla were limited and did not correlate with treatment group or body part (sample 33, 38 and 66).
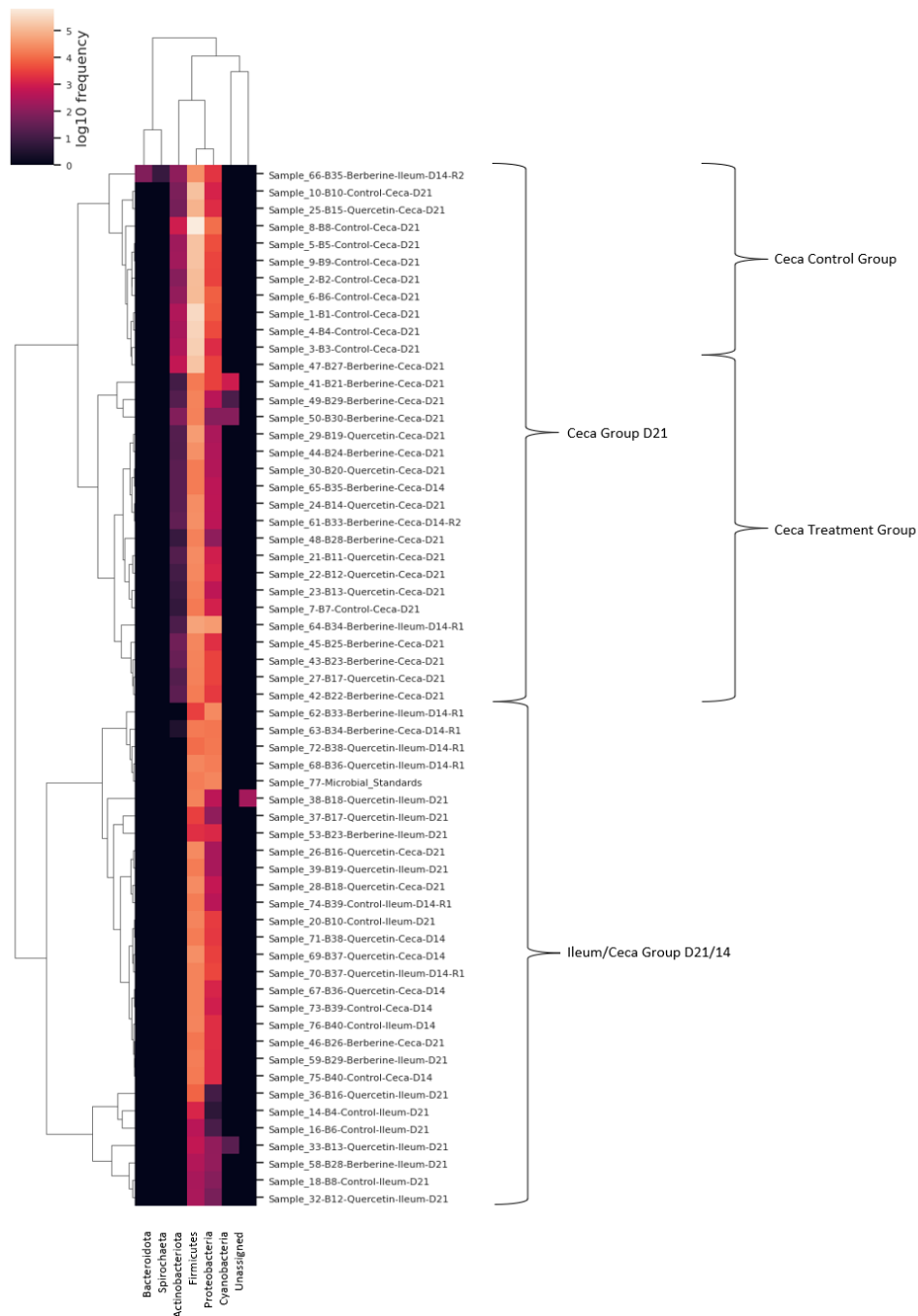
Figure 8-1 Bacterial abundance frequency heatmap of bacteria present in all samples classified at the phyla level. Bacterial phyla are displayed along the bottom x-axis with samples displayed on the right y-axis. Sample clustering is given using phylogenetic trees on the left y-axis, and relatedness of phyla displayed using phylogenetic trees on the top x-axis. Samples cluster into two main groups: (1) caecal samples from day 21 and (2) the ileum samples from day 14 and 21 and the caecal samples from day 14. The day 21 caecum group further splits into two groups, the caecum control samples, and the caecum treatment samples (from birds fed diets supplemented with either quercetin or berberine). The main difference between the two larger groups appears to be the presence of Actinobacteriota within the day 21 samples from the caeca. Within the subgroup of caecum day 21 there is a higher abundance of firmicutes in the control samples, and a lower abundance in the treatment samples.

8.3.3 Inter-organ differences in the microbiome are characterised by changes in the phyla

8.3.3.1 *Diversity analysis indicated that the caecal samples were significantly more diverse than the ileal samples, and that the two body parts were significantly different in terms of microbial diversity*

Samples underwent both α and β diversity analysis according to body site. α-diversity analysis determines the diversity of samples from each body part and compares them. Analysis was conducted using a range of α-diversity analytical techniques (evenness, faith_pd, Shannon, Simpson, and singles). We display here the Shannon diversity (Figure 8-2). The caecal samples were significantly more diverse than the ileal samples (p = 0.002) at a Shannon entropy index of 4.6-6.5 vs 1.8-2.2.
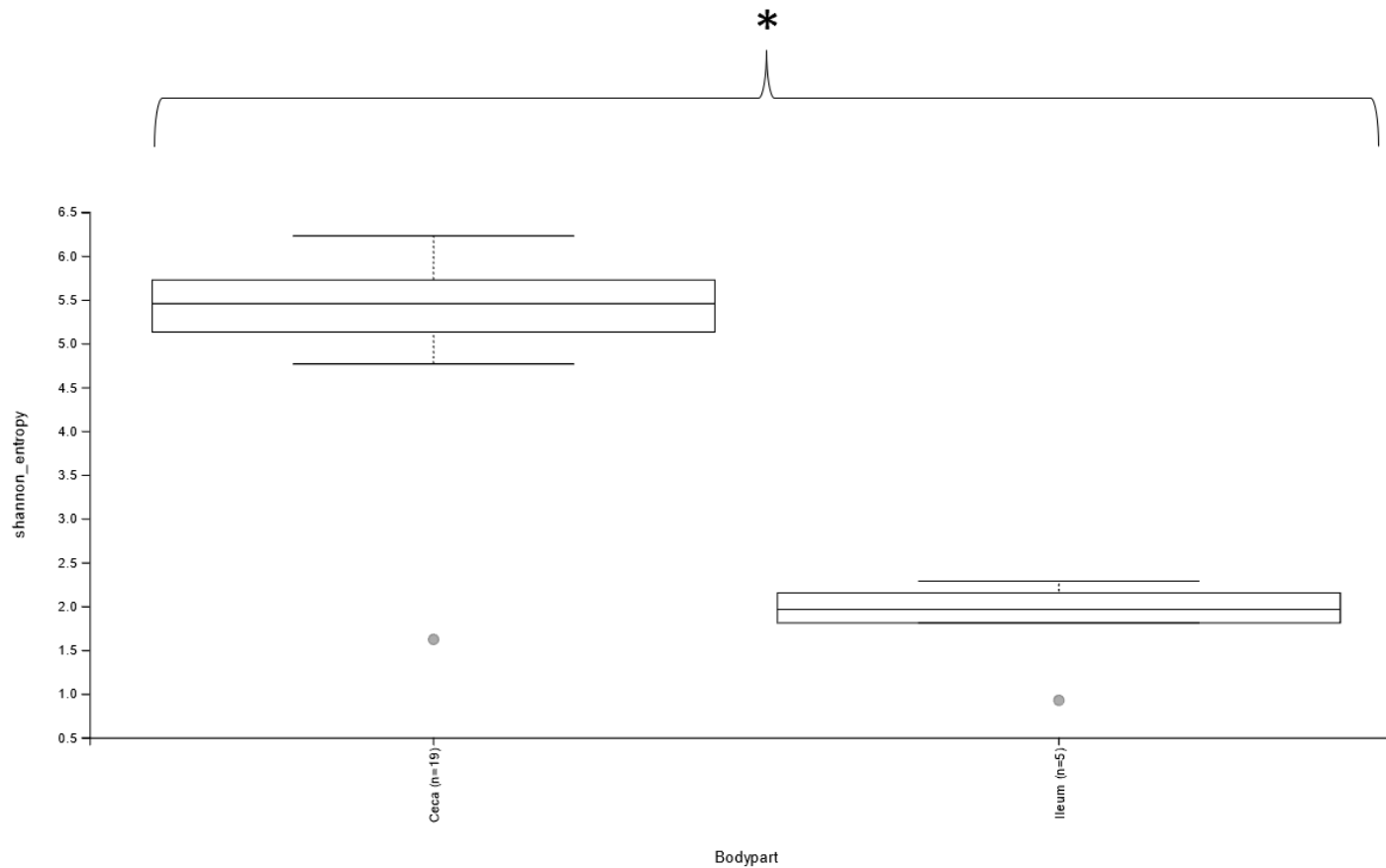
Figure 8-2 Shannon diversity plot displaying α-diversity between samples according to body part (caecum or ileum). Shannon entropy is given on the y-axis and body part is given on the x-axis. The caecum had a median Shannon entropy of 5.5, whilst the ileum had a median Shannon entropy of 2. There was a statistically significant difference between the diversity of the two body parts (Kruskal-Wallis, H=9.561, p-value = 0.002, q-value = 0.002 (rounded to 2 decimal places)). Statistical significance is indicated with braces and an asterisk.

β-diversity analysis compared the diversity of the two groups to each other and compared the distance of the samples within each group to a predetermined indicator of the samples. β-diversity analysis was conducted using a range of different statistical techniques (ANOISM, PERMANOVA and PERMDISP) for each metadata category within each of the diversity matrixes (Bray-Curtis, Jaccard, weighted UniFrac, and unweighted UniFrac). Displayed here is the outcome of the PERMANOVA statistical test on the weighted UniFrac diversity matrix (Figure 8-3). The diversity of the ileal and the caecal samples was significantly different according to PERMANOVA analysis on the weighted UniFrac diversity matrix (p = 0.001). This was also true of ANOISM statistical test (p = 0.001), but not the PERMDIST test (p = 0.402).
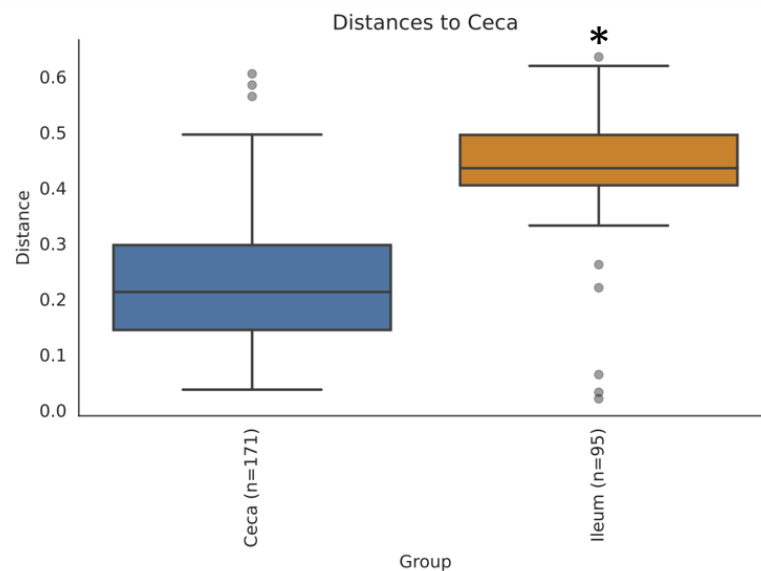
Figure 8-3 Distance plot displaying β-diversity between the body parts across all samples (caecum and ileum). Distance from samples to the average diversity of the body part is plotted along the y-axis, and body part plotted along the x-axis. Distances in the displayed graph were determined using weighted UniFrac PERMNOVA methodology. The ileum is significantly different in diversity from the caecum (PERMNOVA, p-value = 0.001, # of permutations = 999).

8.3.3.2   Differential abundance of bacteria in the caecum and ileum was characterizable by the alterations at the phyla level

Samples underwent differential abundance analysis using the ANCOM test at various phylogenetic levels. Shown here is the differential abundance analysis of samples categorised by body part at the class level (Figure 8-4). Four classes of bacteria were most differentially

abundant between the two body parts. Within the *Firmicutes* the *Clostridia* class was most differentially abundant, heavily weighted, and decreased in the ileum (W (weight of the difference, the higher the w the larger the difference in abundance between conditions) = 11, caecal abundance = 515,796, ileal abundance = 15,560). Similarly, the unclassified members of *Firmicutes* phyla were also decreased in the ileum (W = 9, caecal = 1203, ileum = 49). The *Coriobacteriia* from the *Actinobacteriota* followed a similar pattern (W = 8, caecal abundance = 901, ileum abundance = 31).

Conversely, the *Gammaproteobacteria* from the *Proteobacteria* phyla were more abundant in the ileum than in the cecum (W = 9, caecal abundance = 13,432, ileum abundance = 39907).
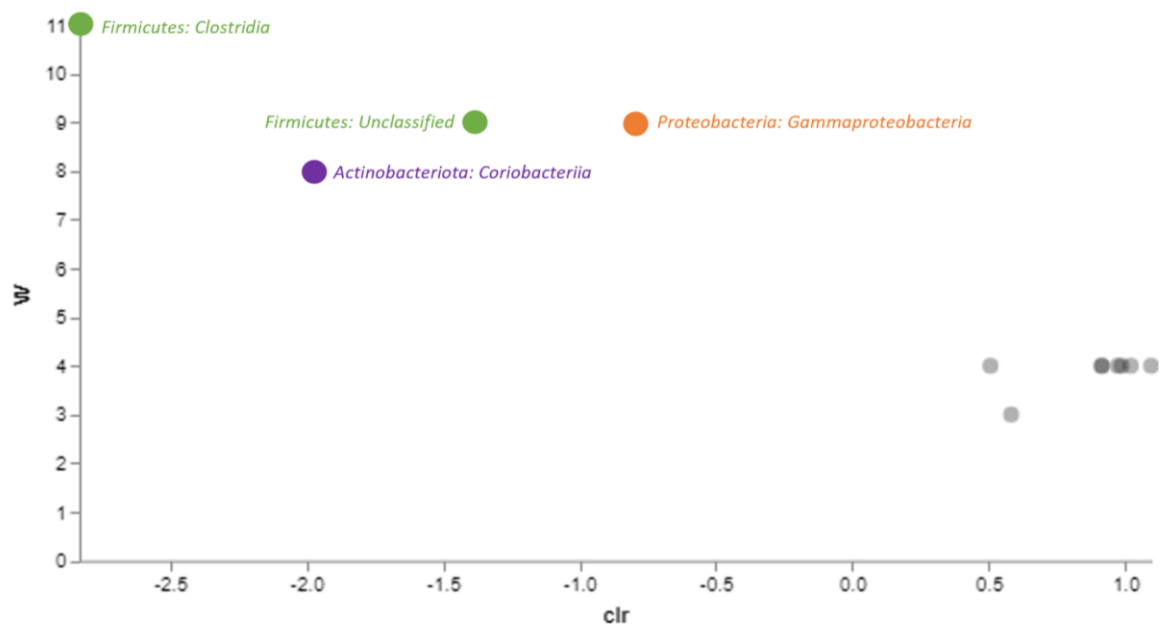
Figure 8-4 Differential abundance plot of bacteria present in samples according to body part at the class level. The y-axis displayed the weight (W) of the bacterial class (how important the bacterial class is in terms of determining the body part the sample comes from). The x-axis displays the differential abundance (clr) of species between body part. The four most important bacterial classes are Clostridia (W = 11, caecal abundance = 515,796, ileal abundance = 15,560), and Unclassified (W = 9, caecal abundance = 1302, ileal abundance = 49) members of the Firmicutes phyla (green), the Gammaproteobacteria (W = 9, caecal abundance = 13,432, ileal abundance = 39907) from the Proteobacteria phyla (orange) and the Coriobacteriia (W = 8, caecal abundance = 901, ileum abundance = 31) from the Actinobacteriota phyla (red). The grey dots are the remaining classes.

Further differential abundance analysis at the family level elucidated 4 species that were the most differentially abundant between the caecum and ileum (Table 8-1). Three were members of the *Firmicutes* phyla and one was a member of the *Actinobacteriota* phyla. However, one bacterium could only be determined at the group level. The 3 most important *Firmicutes* were the *Candidatus arthromitus* group, which was increased in abundance in the ileum, and the *Lachnospiracae* and *Oscillospiraceae* families which were increased in abundance in the caecum. The only member of an alternative phyla was an unculturable member of the *Eggerthellacae* family, which was increased in abundance in the caecum.

Table 8-1 Differential abundances of bacteria according to body part (caecum or ileum) at the lowest phylogenetic level possible for this analysis. Given are the bacterial classification (at the lowest known level), the weight (how important they are), the clr (centred log ratio), the number of the given bacteria in the caecum and ileum, and the fold change from caecum to ileum of the bacterial species.

Bacteria (At the lowest known level)	Weight	clr	# In Caecum	# In Ileum	Fold Change
Firmicutes, Clostridia					
Group: *Candidatus arthromitus*	207	3	176	810	4.6
Family: *Lachnospiracae*	203	-4.7	86802	2439	0.0281
Family: Oscillospiraceae	203	-4.65	21177	348	0.0164
Actinobacteriota					
Family Eggerthellacae	164	-1.25	689	31	0.04499

8.3.4 Differences in the microbiome according to phytochemical treatment were characterised by changes at the order level within the *Firmicutes* phyla

8.3.4.1 Alpha diversity according to Shannon was significantly different between the berberine and control treatment groups

Samples underwent both α and β diversity analysis according to treatment group. There was no significant difference between all the samples using a Kruskal-Wallis test (p = 0.075), though not significant (p < 0.05), the value is close and there is a visualisable difference between all the treatment groups. However, there was a significant difference in a pairwise Kruskal-Wallis test between the control and berberine samples (p = 0.023) at a Shannon entropy index of 1.9-5.25 vs 5.25-6.25 (Figure 8-5).
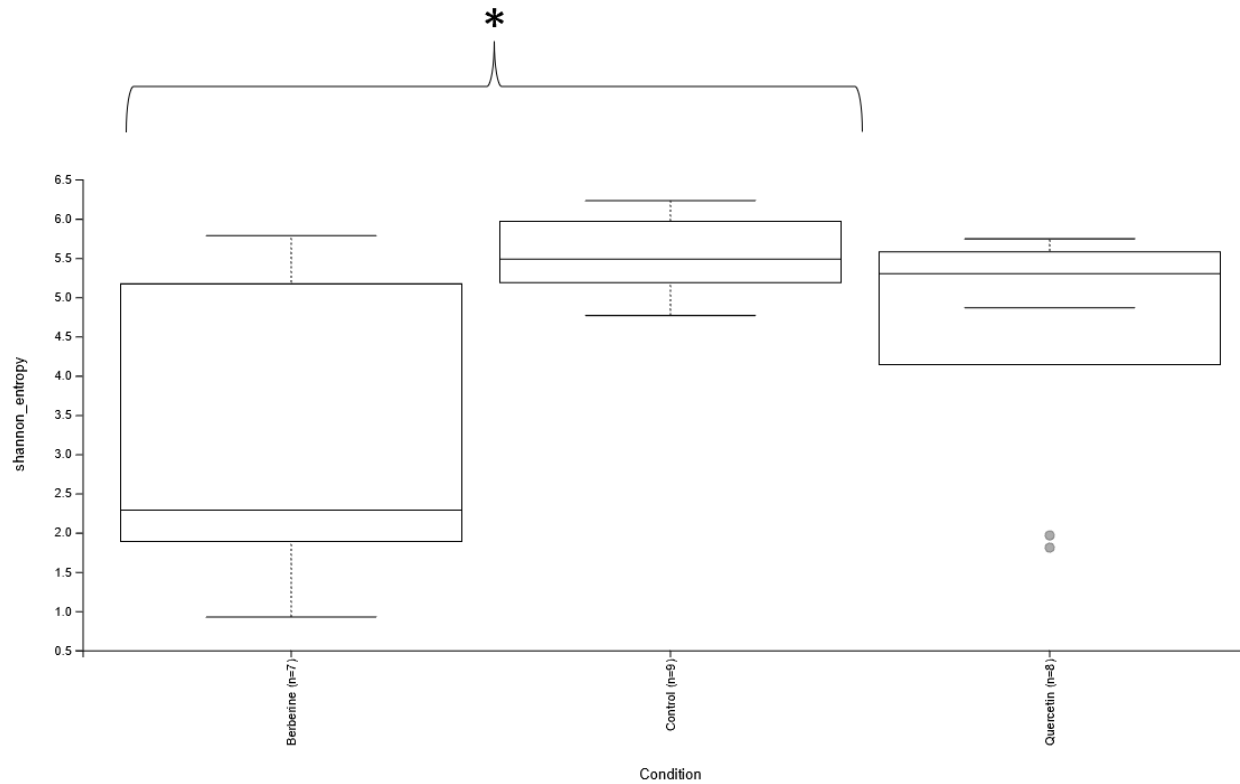
Figure 8-5 Shannon diversity plot displaying α-diversity between samples according to treatment group (berberine, quercetin or control (no phytochemical addition)). Shannon entropy is given on the y-axis and treatment group is given on the x-axis. There was a statistically significant difference between the diversity of the berberine and control groups (Kruskal-Wallis pairwise, H = 5.179, p-value = 0.023, q-value = 0.069 (rounded to 2 decimal places)). Statistical significance is indicated with braces and an asterisk. There was no statistically significant difference between quercetin and either the control or berberine groups (p-value = 0.298 and 0.248 respectively).

The diversity of treatment groups was not significantly different according to PERMDISP analysis on the weighted UniFrac diversity matrix (p = 0.083). However, the berberine and control groups were significantly different from each other using pairwise PERMDISP analysis (p = 0.01) (Figure 8-6). This was true for both the PERMNOV (p = 0.003) and ANOISM analysis (p = 0.002).
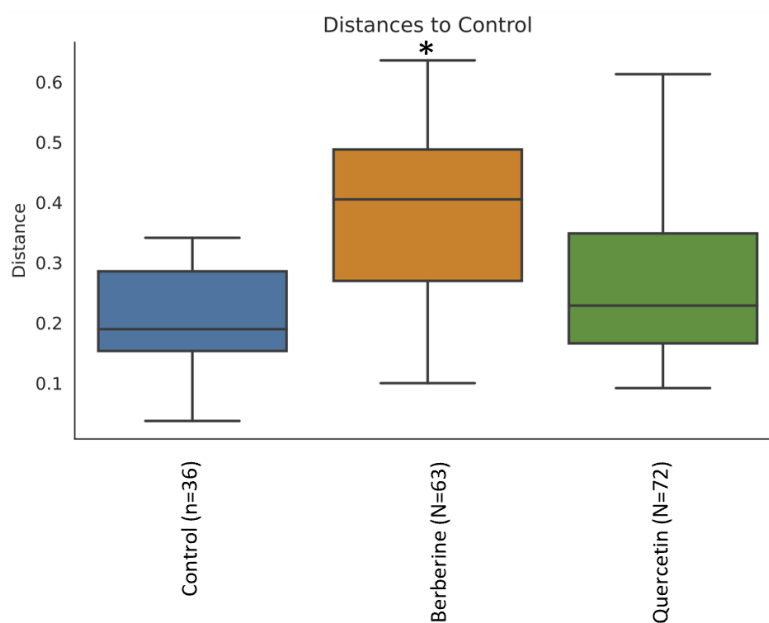
Figure 8-6 Distance plot displaying β-diversity between the treatment groups across all samples (berberine, quercetin and control). Distance from samples to the average diversity of the treatment group is plotted along the y-axis, and treatment group is plotted along the x-axis. Distances in the displayed graph were determined using weighted UniFrac PERMDISP methodology. The berberine treatment group is significantly different from the control (PERMDISP pairwise, F-value = 15.079, p-value = 0.010, q-value = 0.030, # of permutations = 999) indicated by an asterisk. Quercetin was not significantly different from either the control or berberine treatment groups.

8.3.4.2 Differences in abundance diversity across treatment groups were characterised by changes within the orders of the firmicutes phyla

Samples underwent differential abundance analysis using the ANCOM test at various phylogenetic levels. Differential abundance analysis of samples categorised by treatment group at the order level are shown here (Figure 8-7Figure 8-4). Four orders of bacteria were differentially abundant between samples based upon their treatment group, and all were

members of the *Firmicutes* phyla. The *Clostridiales (W = 19)* and *Peptostreptococcales-tissierallales (W = 22)* orders were both members of the *Clostridia* class and were more abundant in the control groups than the berberine group, and the quercetin group than the control group. One unclassified member of the *Firmicutes* phyla was more present in the berberine and the control groups than in the quercetin treatment group samples (W = 24). Finally, the abundance of the *Erysipelotrichales* order of the *Bacilli* class (W = 13) differed between treatment groups.
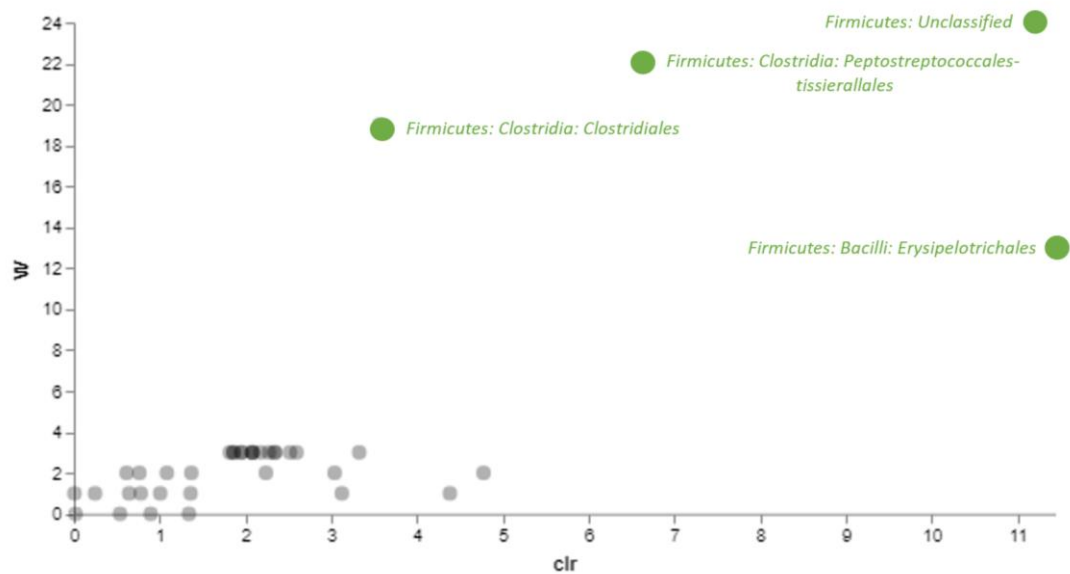
Figure 8-7 Differential abundance plot of bacteria present in samples according to treatment group at the order level. The y-axis displayed the weight (W) of the bacterial order (how important the bacterial order is in terms of determining treatment group the sample comes from). The x-axis displays the differential abundance (central log ratio (clr)) of species between treatment groups. All of the most important orders in this analysis were members of the Firmicutes phyla, two of the Clostridia class: the Clostridiales (W = 19, berberine sample abundance = 566, control sample abundance = 662, quercetin sample abundance 810), the Peptostreptococcales-tissierallales (W = 22, berberine sample abundance = 3114, control sample abundance = 5337, quercetin sample abundance = 7873) and one unclassified (W = 24, berberine sample abundance = 1302, control sample abundance = 1087, quercetin sample abundance = 58), and one member of the Bacilli class: the Erysipelotrichales (W = 13, abundances unknown). The remaining classes are indicated in grey.

8.3.4.3 Two species were considered the most important in explaining the difference between the microbiomes of the different treatment groups

The abundance of two bacterial species of the *Bacilli* class of *Firmicutes* phyla were differed between treatment groups (Table 8-2). The first was an unclassifiable species from the

Turicibacter genus, this species was almost absent in the control group, present at 1×10^3 in the berberine group and present at 2.3×10^3 in the quercetin group. The second was *Lactobacillus pontis* which was absent in the berberine group, present at 0.8×10^3 in the quercetin group and highly abundant in the control group at 6.7×10^3.

Table 8-2 Differential abundances of bacteria according to treatment at the genus and species level. Given are the bacterial names (at the lowest known level), the weight (how important they are), the clr, and the number of the given bacteria in the treatment groups. The two bacteria highlighted are both members of the bacilli class of the Firmicutes phyla, from the genus Turicibacter which was absent in the control group and present in the berberine and quercetin groups. Lactobacillus pontis was absent in the berberine samples, but present in the control samples and to a lesser extent the quercetin samples.

Bacteria (At the lowest known phylogenetic level)	Weight	clr	# In berberine	# In Control	# In Quercetin
Genus: Turicibacter	210	35.3	1207	87	2316
Species: Lactobacillus pontis	197	28.6	1	6667	799

8.3.5 Intra-phyla variability within the *Firmicutes* is responsible for treatment group variability, whilst phyla level changes are responsible for the inter-organ variability

Relative frequency of the different bacterial classes was plotted using a stacked bar chart (Figure 8-8). The samples were grouped by body part, timepoint and treatment group. The caecal samples were mostly compromised of the *Firmicutes* phyla, more specifically the *Clostridia* class alongside a small number of the *Bacilli* class and *Gammaproteobacteria* from the *Proteobacteria* phyla. One single sample taken from the berberine caecal group at day 21 was instead composed mostly of *Gammaproteobacteria* and *Bacilli* classes, but this outlier was unable to be removed from the analysis. The quercetin and control groups had what appeared to be a small increase in the *Bacilli* group, when compared to the berberine group, which by the previous ANCOM analysis is likely the *Erysipelotrichales,* specifically *Lactobacillus pontis* (Figure 8-7)*.* The ileum samples had increased abundance of the *Gammaproteobacteria* and *Bacilli* classes.
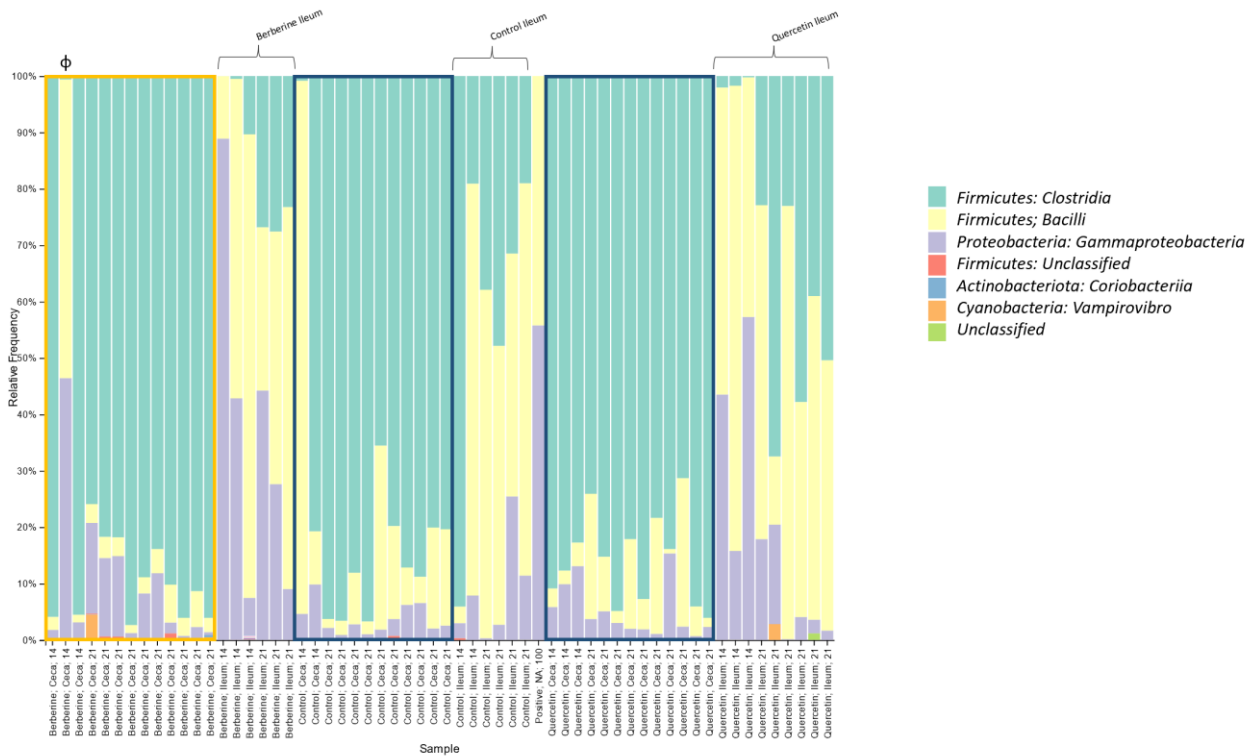
Figure 8-8 Stacked bar chart of relative species frequency across all samples at the class level. Relative frequency is on the y-axis with samples on the x-axis, divided by treatment group, body part, and time of microbiome extraction. Bacterial classes are represented on the graph in colour: Clostrdia in cyan, Bacilli in cream, Gammaproteobacteria in grey, Unclassified firmicutes in red, Coriobacteriia in blue, Vampirovibro in orange and unclassified bacteria in light green. All caecal samples are composed of the Clostridia phyla (outlined in either orange or blue boxes) and all ileal samples are comprised by the Bacilli and Gammaproteobacteria classes (indicated using braces at the top). Within the caeca samples there is a minor increase in the Bacilli class between the berberine samples (outlined in orange) and the control and quercetin samples (outlined in blue). Φ One single berberine caecum sample is highlighted due to its clear nature as an outlier from the caeca dataset, due to the dominance of Gammaproteobacteria and Bacilli, rather than the Clostridia.

8.3.6 Two thirds of the difference in the microbiome samples can be explained by inter-organ variability, and a further 14% by treatment

Finally, principal component analysis (PCoA) was conducted on the samples to determine how related the samples were to each other (Figure 8-9). PCoA was conducted using four different distance matrixes (Bray-Curtis, Jaccard, weighted UniFrac, and unweighted UniFrac). Weighted UniFrac explained the largest proportion of the distance matrix within both 2 and 3 axes (89.12%), and thus was used to display the conclusions from this analysis.

The PCoA (Figure 8-9) over three axes together explained 89.12% of the sample distribution. 65.52% of the distribution was explained by the axis 1, where samples grouped by body part.

There were two exceptions (1) the positive control and (2) the berberine sample that was previously discussed to be an outlier (Figure 8-8). Neither of these samples were removed from the data prior to further analysis. Axis 2 explained 12.26% of the distance matrix between samples. This axis was associated with the treatment groups, the control group grouped towards the north of the axis, and the berberine group to the south, with the quercetin group being interspersed within both. Axis 3 accounted for 9.34% of the distance matrix between samples, but it was not clear from the analysis or plot what may explain this, one potential reason for this axis representation could be the sex of the birds, which was not determined, the final 10.88% of the explanation was not plotted.
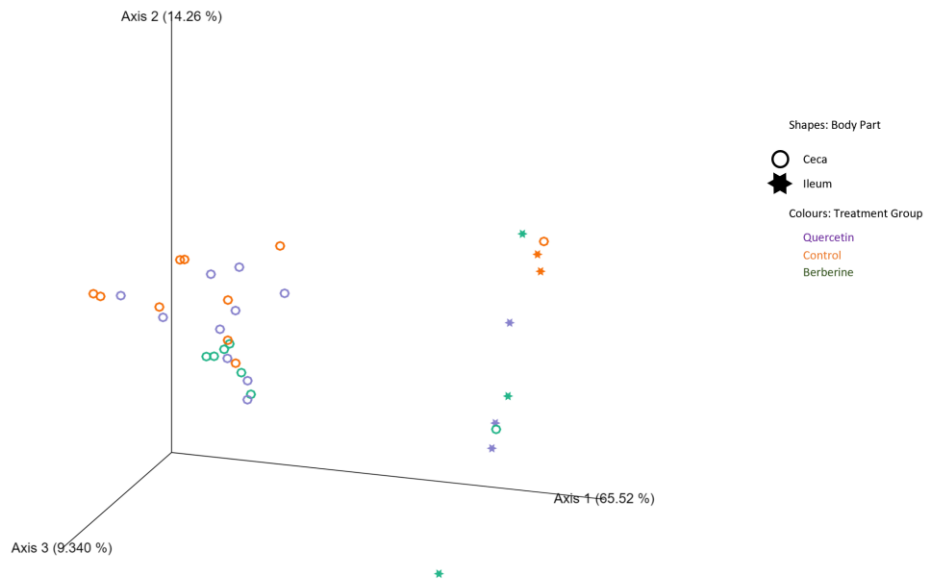
Figure 8-9 Principal component analysis on all samples. Principal component analysis was conducted using weighted UniFrac, with axes 1, 2 and 3 comprising 89.12% of the total distance between the samples. Samples are categorised by body: caecum (indicated by a circle) and ileum (indicated by a star). Samples are further categorised by treatment group according to colour, quercetin in purple, control in orange and berberine in green. Axis 1 is responsible for 65.52% of the distance between the samples, and there is a clear grouping of the samples along axis 1 by body part, with caecal samples on the left, and ileum samples on the right. This demonstrates that inter-organ variability is the most important for determining the microbiome of the samples. Secondary is axis 2 which is responsible for 14.26% of the variance. Samples group along axis 2 by treatment group with control samples to the top, quercetin samples in the middle, and berberine samples at the bottom. There is a clear mixing of quercetin between both the berberine and control samples in the caecal group, and to a lesser extent in the ileum samples. Axis 3 compromises 9.34% of the variance and represents an unknown quantity, the remaining 10.88% of the variance is not shown on the graph and was compromised of at least 2 more categories of unknown quantities.

8.3.7   Escherichia-Shigella abundance was altered in samples

The average *Escherichia-Shigella* abundance compared to all bacterial genera abundance increased in the microbiome of chickens supplemented with phytochemicals, relative to the respective time control in all cases except for the ileum samples supplemented with quercetin at day 21 (Figure 8-10). This was only significant in the case of the berberine cercal samples at day 21 (M = 0.17, SD = 0.13) compared to the control caecal samples at day 21 (M = 0.07, SD = 0.00) (p = 0.0427). Full statistical test analysis is given in appendix V.

	Berberine Ceca 14	Berberine Ceca 21	Berberine Ileum 14	Berberine ileum 21	Control Ceca 14	Control Ceca 21	Control Ileum 14	Control Ileum 21	Quercetin Ceca 14	Quercetin Ceca 21	Quercetin Ileum 14	Quercetin Ileum 21
Average	17%	7%	46%	27%	7%	3%	5%	10%	9%	4%	39%	7%
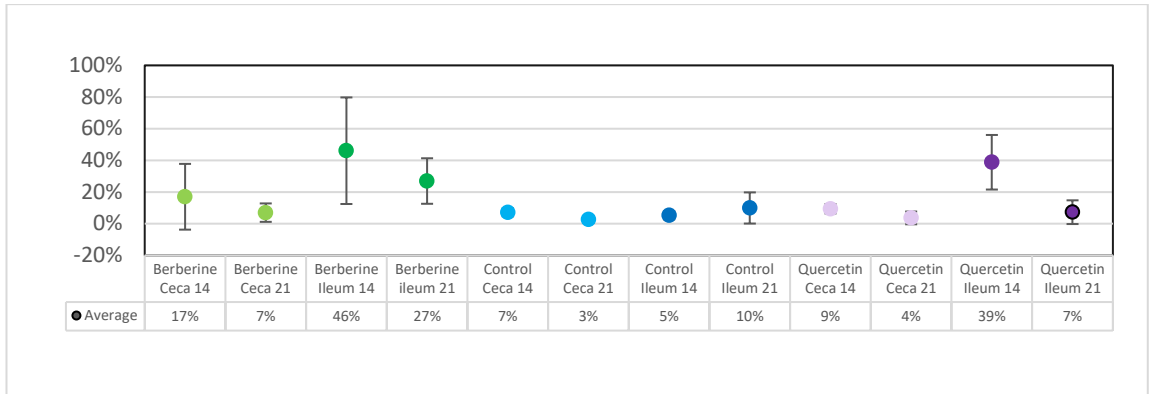
Figure 8-10 Average abundance of Escherichia-Shigella across all samples from the in vivo chicken experiment. Escherichia-Shigella abundance was increased in treatment samples, compared to the control sample at the corresponding timepoint regardless of location. The only exception was the quercetin ileal sample at day 21, which had 7% Escherichia-Shigella abundance, compared to the control ileal samples at day 21 which had 10% abundance. This was only significant in the case of berberine cercal samples at day 21 (M = 0.17, SD = 0.13) compared to the control caecal samples at day 21 (M = 0.07, SD = 0.00) (p = 0.0427).

8.4   Discussion

This chapter considers the effects of in-feed addition of the phytochemicals berberine and quercetin on the caecal and ileal microbiome of chickens. Microbiome collection was conducted after 14 and 21 days, and the samples then underwent DNA extraction. The following 16S sequencing and bioinformatics analysis was conducted by the Centre for Genomics Research at the University of Liverpool. Finally, data visualisation was then conducted using Qiime2.

8.4.1   The microbiomes of the caecal and ileal samples were different irrespective of treatment group

The microbiome of the caecum and ileum were significantly different in this study when evaluated using both α and β diversity analysis. Further, using PCoA, the body part of the sample accounted for over 65% of the sample ordination. Further, α-diversity analysis highlighted that the caecal samples were significantly more diverse than their ileal counterparts. This is not wholly unsurprising, as caecal and ileal microbiota are separate parts of the chicken GIS, and are known to be geographically and microbially distinct from one another in a normal chicken lifecycle after only three days (Lu et al., 2003). One study indicated that the ileum had a higher relative abundance of *Lactobacilli* (Bjerrum et al., 2006). Whereas another suggested that the caecum had higher relative abundance of the *Proteobacteria*

(Glendinning et al., 2019)*,* the higher abundance of *Proteobacteria* was contrary to the findings in this study.

It is generally accepted that the abundance of *Bacteroidota, Firmicutes, Actinobacteriota* and *Proteobacteria* can vary significantly in the chicken GIS (Aruwa et al., 2021)*,* which makes the direct comparison between the studies outlined in this thesis and others difficult to interpret

but does confirm that the microbiomes obtained in this work fall within the expected phyla described in the literature.

The diversity of the samples between the body parts was most clearly visible when looking at differences in phyla. The caecal samples were composed of the *Firmicutes* phyla, in particular members of the *Clostridia* class. The ileum samples were instead composed of the *Bacilli* class from the same phyla, alongside the *Gammaproteobacteria* from the *Proteobacteria* phyla. Despite its low overall abundance, one class of the *Actinobacteriota,* the abundance of *Coriobacteriia* was also markedly different between the two body parts. *Coriobacteriia* abundance within the chicken intestinal flora has been previously associated with amoxicillin treatment (Zhao et al., 2022). Though when looking at the relative frequency (Figure 8-8) we can see that this phylum represents less than 5%, and usually less than 1% of all bacteria within the samples.

Four families were differed significantly in their abundance between the caeca and ilea. Three were significantly increased in the caecum: *Lachnospiracae* and *Oscillospiraceae* from the *Clostridia* class of the *Firmicutes* and *Eggerthellacae* from the *Coriobacteriia* class of the *Actinobacteriota*.

The *Lachnospiracae* are common members of the caecal flora and are associated with both positive and negative growth outcomes, depending upon the species (Liu et al., 2021). They are particularly abundant during early and late stage microbiome development in poultry (Richards et al., 2019). Further, they are also usually more common in the caecum than in the ileum (Glendinning et al., 2019) as seen in this study. The *Oscillospiraceae* are usually associated with positive growth outcomes (Lundberg et al., 2021) and are a normal part of the caecal flora as well (Zenner et al., 2021). Finally, the *Eggerthellacae* have previously been shown to be upregulated in chicken models fed with sulphate trace minerals, alongside

supporting lower microbial diversity and unchanged growth performance (van Kuijk et al., 2021).

One genus, *Candidatus arthromitus* from the *Clostridiaceae* of the *Firmicutes* phyla was significantly more abundant in the ileum. *C. arthromitus* was initially found in the hindgut of terminates and other arthropods (Thompson et al., 2012). However, more recent microbiome studies have shown its existence in vertebrates, leading to the suggestion of a new provisional name of *Candidatus savagella*. *C. arthromitus* has been shown to be a commensal in vertebrates including mice and turkeys, by attaching itself to the epithelial tissue of the ileum. It has also been shown to increased Th17 cell maturation, and immunoglobulin A production and is significantly more abundant in high-performing turkey flocks than lower preforming flocks (Hedblom et al., 2018).

Taken together, these results suggest that the bacteria of both the ileum and caecum well represents the expected diversity in current literature. It also suggests that the chickens in this study are healthy, growing well and have a diverse microbiome appropriate for each body part.

8.4.2 Berberine supplementation significantly altered the diversity of the microbiome compared to the control irrespective of body part

The microbiome of chickens fed with additional berberine supplementation was significantly different from those of the control groups by both α and β diversity analysis. Further, PCoA analysis suggested that the difference between the in-feed treatment groups accounted for around 14% of sample difference. The α-diversity analysis suggested that the berberine treatment group samples were less diverse than those of the control group. There was no significant difference between the quercetin treatment group and either the control or berberine group in terms of diversity. The reduction diversity by berberine suggests that it is an active compound within the chicken microbiome with regards to its antimicrobial activity

and suggests it may be a strong candidate for further examination of its agricultural application.

The differences in microbiome between the two treatment groups were limited to changes within the *Firmicutes* phyla. Specifically, alterations to the relative abundance of the *Clostridia* and *Bacilli* classes. In the *Clostridia* class the *Peptostreptococcales-tissierallales* and the *Clostridiales* were highly differentially abundant, whilst in the *Bacilli* class the relative abundance of the *Erysipelotrichales* was altered.

Members of the *Peptostreptococcales-tissierallales* are markedly decreased in the human gut microbiota after treatment with tetracyclines (Nel Van Zyl et al., 2022). Their presence in the chicken GIS is usually associated with the early stage microbiota development (Videnska et al., 2014), though other studies demonstrated it was most frequent at day 28 (Jurburg et al., 2019), highlighting again that the development of the chicken microbiome is not consistent or easily comparable between studies. The *Peptostreptococcales-tissierallales* class produce butyric acid (Hang et al., 2012), which improves gut nutrient absorption. With regards to antibiotic resistance, the presence of *Peptostreptococcales-tissierallales* is also highly associated with the presence of the *tetA* gene in the metagenome of the chicken gut microbiome (Juricova et al., 2021), suggesting its potential role as a reservoir for tetracycline resistance. This suggests that berberine or quercetin supplementation may have a unique ability to reduce the abundance of bacteria that contain specific AMR reservoirs.

The *Erysipelotrichales* are one of the major classes of the *Firmicutes* found in normal chicken gut microbiota (Rychlik, 2020). In a single experiment the *Erysipelotrichales* class was significantly more abundant in day 28 in the chicken gut microbiome than day 14 (Ballou et al., 2016), suggesting they may be associated with middle and late stage chicken microbiome development. *Erysipelotrichales* are also associated with immune system modification in human models (Kaakoush, 2015). They are significantly more abundant after kidney

transplantation (Lee et al., 2014), and high abundance is associated with elevated tumour necrotic factor levels (Dinh et al., 2015). This increase in inflammatory markers would be associated with negative growth performance in chickens, due to the extra energy expenditure required.

Erysipelotrichales decrease in abundance after vancomycin treatment in the gut microbiome of hamsters (Peterfreund et al., 2012), and they were associated with a lower number of tetracycline resistance genes in the gut bacteria of dairy farm cows in Japan (Katada et al., 2021). *Erysipelotrichales* are also increased in the human gut microbiota after macrolide treatment (Korpela et al., 2016) and increased in abundance after gentamicin treatment in the rat gut (Zhao et al., 2013). This suggests that the taxonomic class has a varied antibiotic resistance profile, depending upon the species and genes present in any one experiment. The inability to determine in what treatment group this class was increased and decreased means it is difficult to draw conclusions, however, if it follows the same pattern as the *Peptostreptococcales-tissierallales,* then it is likely that phytochemical supplementation may also reduce the antimicrobial resistance (AMR) reservoir in this class.

8.4.3 The *Turicibacter genus* and *Lactobacillus pontis* differed between the treatment groups

One bacterial genus the *Turicibacter, and* one bacterial species *Lactobacillus pontis* differed in their abundance between treatment groups. The members of the *Turicibacter* genus were absent in the control groups, but highly increased in the berberine and quercetin groups. *Lactobacillus pontis* was almost absent in berberine, and limited in quercetin group, whilst being highly abundant in the control group. This suggests in-feed addition of berberine, and quercetin is negative for the growth of *L. pontis* but positive for the growth of the *Turicibacter genus.*

Turicibacter and *Lactobacillus pontis* were not part of the original search criteria of the model system or batch culture analysis, and re-analysis of that dataset would be prudent knowing that these species/genera are altered after phytochemical supplementation.

8.4.3.1 Turicibacter

Turicibacter members occupy the mucosal lining of the chicken GIS (Marmion et al., 2021) and they are common in the GIS of other avian species such as the herring gull (*Larus argentinus*) (Merkeviciene et al., 2017). The genus has two formally described members: *Turicibacter sanguinis* and *Turicibacter bilis* (Maki & Looft, 2022)*.* It is likely that the recent discovery of these two species, within the last year, meant that they were not included within the metadata used to classify the samples in this chapter. This would explain why the classification of these samples stops at the group level.

Turicibacter have been discovered within both the caecum and ileum of chickens, but are usually more abundant in the ileum (Siegerstetter et al., 2017). They are also associated with a lower residual feed measurement, which is favourable for feed conversion intake in broiler chicken models (Siegerstetter et al., 2017). The genus is also associated with conventional caged, rather than free range chickens (Wiersema et al., 2021). In pigs, *Turicibacter* growth is associated with *S. enterica* infection (Aljahdali et al., 2020), suggesting the group may thrive in sick and stressed animals. Both species of *Turicibacter* are resistant to colistin, but sensitive to vancomycin, penicillin, and kanamycin (Maki & Looft, 2022).

We were unable to determine in this study if the modification of the gut microbiome by quercetin and berberine to being positive for *Turicibacter* growth involved the antimicrobial properties of these compounds. However, positive conditions for *Turicibacter* growth may increase the colistin resistance reservoir in chickens after supplementation with phytochemicals if the intrinsic *Turicibacter* resistance to colistin can mobilise.

Lactobacillus pontis, as with all members of the *Lactobacillus* genus, is capable of converting sugars into lactic acid (Vogel et al., 1994). It is almost always present in the GIS of both chickens and guinea fowl (Bhogoju et al., 2018). It is generally associated with positive growth outcomes in poultry (Kalavathy et al., 2008) including increased feed conversion ratio and daily weight gain (Fesseha et al., 2021; Peng et al., 2016), and members of the group can prevent the growth of pathogenic chicken bacteria such as *E. coli, S. typhimurium* and *C. perfringens* (Murry et al., 2004).

Despite their positive role on growth performance, *Lactobacillus* strains can harbour many AMR genes, including genes encoding for resistance to kanamycin, tetracycline, streptomycin, enrofloxacin, erythromycin, lincosamides, gentamycin, chloramphenicol, and vancomycin (Dec et al., 2020). Over 79.5% of 88 *Lactobacillus* isolates taken from chicken gut samples were multidrug resistance (MDR) and the same study demonstrated a phenotypic resistance to ampicillin from these isolates, with no known ampicillin resistance genes present (Dec et al., 2017). All members of the genus are intrinsically resistant to aminoglycosides, ciprofloxacin and trimethoprim (Campedelli et al., 2019).

The literature is mixed on the role that *L. pontis* plays in the risk of chickens becoming infected with necrotic enteritis (NE). With some studies showing that *L. pontis* abundance is increased in NE infection (Stanley et al., 2012), and others showing that it is decreased (Q. Yang et al., 2021). The relative increase in abundance of *Lactobacillus* spp. after addition of *Macleaya cordata* extract, has been previously noted (Huang et al., 2018), suggesting that *L. pontis* may respond well to phytochemical based in-feed additives.

One of the ways *L. pontis* may be impacted by phytochemicals lies in its biological niche. *L. pontis* has a unique biological niche in that it contains many glycosyltransferases of which 2, GT2 and GT4, are widely distributed across all *L. pontis* strains. These two

glycosyltransferases are focused on carbohydrate metabolism (Liu et al., 2021). This observation represents the third chapter in this thesis, alongside chapter 3 and 5, where glycosyltransferases have been associated with berberine or quercetin selective pressure. In chapter 5 a synonymous A76A mutation in the GT4 protein was found in a P. *aeruginosa* isolate that was grown for 30 days in sub-inhibitory concentrations of quercetin. This was hypothesised to lead to a decrease in the protein transcription due to the relative rarity of the tRNA corresponding to the mutated codon.

The fact that species containing these glycotransferases were less abundant in this study, and the glycotransferases were potentially less transcribed in the study from Chapter 5, suggests that the presence of phytochemicals acts as a selective pressure which reduces the abundance of species containing glycosyltransferases, and that a reduction in the transcription of glycosyltransferases was positive for the growth of *P. aeruginosa* in the presence of quercetin. We hypothesise that the glycosyltransferation of phytochemicals may lead to a toxic bioproduct within the bacterial cell which is bactericidal. This conclusion is challenged by the positive selection of inserts containing glycosyltransferases in Chapter 3, suggesting a more complicated relationship of glycosyltransferase than first appears. This relationship is explored more in previously highlighted chapters and the final discussion.

8.4.4 The addition of berberine significantly increased the abundance of *Escherichia-coli* in the ceca

The abundance if the *Escherichia-shigella* group occurred in all samples after phytochemical supplementation. However, this was only significant in the berberine caecal samples at day 21. This result is consistent with the results from chapter 6, and chapter 7. Though in those chapters the increase in *Escherichia-shigella* abundance was limited to the quercetin group.

E. coli is one of the most important species of the chicken microbiota, as it's a reservoir of AMR genes as well as being potentially pathogenic (Oladeinde et al., 2021). The occurrence

of *E. coli* could potentially be negative for chicken growth due to its pathogenic role (Dho-Moulin & Fairbrother, 1999), and the previous literature which highlights that *E. coli* presence is usually associated with poor chicken growth (Diarra et al., 2007; Stromberg et al., 2017) . The consistency of this result across all members of the chicken triad is discussed in depth in the final discussion section.

8.4.5   Comparisons to the model system and batch culture studies

The *Firmicutes* were consistently the most abundant phyla in all three members of the phytochemical additive studies triad: the model system (Chapter 6), the batch culture (Chapter 7) and the *in vivo* work described here. Again it is noted here that while this is possible as *Firmicutes* can comprise over 95% of a healthy chicken microbiota, it may not be the most common. However, in the model system study, the addition of phytochemicals led to an increase in other phyla, a result that was not noted in the *in vivo* study. There was no bacterial addition after the initial inoculation in the batch culture or model system work, which means that all the phyla present were part of the initial inoculum. Whereas in the *in vivo* study the birds were constantly exposed to the environment, which would have allowed for greater microbial diversity, but the microbiomes may have also been limited, due to the additional stressors that come with an *in vivo* system (such as the immune system, or surrounding environment). It has been demonstrated that chickens often have a drastic change in phyla makeup as they age (Awad et al., 2016), or after antibiotic treatment (Kairmi et al., 2022), so this phyla level microbial shift is possible in *in vivo work*. The fact that this major microbial shift in samples from the treatment group was present in the model system study but not the *in vivo* study may indicate that the model system allows for determination of the microbiome changes that are overlooked in larger more complex *in vivo* studies.

Additionally, the model system work explored microbiome changes for only 8 days following initial inoculation and the 5 days following the additional of phytochemicals, whereas the *in*

vivo work looked specifically at days 14 and 21 and did not explore the immediate effects of phytochemical addition. This difference in scope makes the two studies more complex to compare. However, the data within these chapters is well positioned to support a more closely aligned model system / *in vivo* set of experiments, where faecal content could be examined daily, and the model system could be run for a full 21 to 45 days, alongside the previously mentioned additional transcriptomic and genomic analysis.

Finally, *Turicibacter* and *Lactobacillus pontis* were not part of the original search criteria of the model system analysis, and re-analysis of that dataset would be prudent knowing that these species/genera are altered after phytochemical supplementation.

8.4.6   Limitations and future work

The study had several limitations. Firstly, prior to the data analysis, 16 of the 78 samples failed to produce an amplicon library, or generated incredibly low yields after extraction, and were unable to be further analysed. These removed samples were mostly members of the ileal samples at day 21. The ileal samples from day 14 were frozen prior to DNA extraction, and this was considered to have damaged the integrity of the DNA, and as such day 21 ileal samples were not frozen prior to DNA extraction. Further, several of the remaining amplicon libraries were of low quality. This necessitated two separate MiSeq runs and data analysis pipelines to analyse the samples (known as run 1 and run 2), to account for the low-density clustering. However, the conclusions were identical between the two runs.

One further limitation to this study was the final culling of the chickens at day 21 instead of day 45. Farmed chickens are usually reared for 45 days prior to culling. It has been shown that caecal microbiota differ in makeup throughout the lifecycle of chickens up until culling (Richards et al., 2019). Thus, it remains to be seen how phytochemicals would affect the gut microbiota in both the early and late-stage life cycle of chickens (pre 14 and post 21 days). This experiment was conducted in collaboration with Professor Paul Wigley, and Dr Sain

Pottenger at the University of Liverpool. The initial experiment was planned for March 2020, however the covid-19 pandemic led to complete facilities closure and a backlog of experiments for the University of Liverpool group. When the facilities became available for this study in January of 2021, Professor Paul Wigley and Dr Sain Pottenger were both in their final 3 weeks at the University of Liverpool, and as such the experiment was only conductible for a maximum of 21 days.

8.5   Conclusion

This chapter aimed to determine how in-feed phytochemical addition affected the microbiome of chickens over 21 days. In the discussion it aimed to determine how these changes were associated with growth performance, disease, and AMR. Finally, it looked to explore how well the chicken model system seen in chapter 6, the batch culture experience in chapter 7, and modelled the results of an *in vivo* study.

The key findings from this study were that berberine had a significant impact on the caecal and ileal microbiomes of the chickens, when compared to the control group. Specifically, this difference was in the abundance of different members of the *Firmicutes* phyla, particularly *Lactobacillus pontis* and the *Turicibacter* group.

The caecal microbiomes were similar in both this study, and the model system present in chapter 6, although the species of import and phyla level movement, differed between the two experiments. Suggesting that the effect of berberine on the microbiome is complex, and the surrounding factors present in *in vivo* studies have an impact on the final outcomes.

This triad of work assessing the impact of phytochemical addition as replacements for antibiotic growth promoters in poultry highlights that the biological interactions between bacteria and phytochemicals are complex, often inconsistent, and may have wide ranging consequences in terms of both animal health and the maintenance of AMR reservoirs within agricultural systems.

9 Conclusions and future work

9.1 Foreword

The antimicrobial resistance crisis is an ongoing, worsening global problem with far reaching and diverse consequences (Aslam et al., 2018; Ventola, 2015). Antibiotics are becoming less effective in clinical settings (Zaman et al., 2017). This affects not only bacterial infections, but treatments for diseases such as cancer, or routine surgery, which require antibiotic prophylaxis to be successful (Crader & Varacallo, 2021). The reduction in antibiotic development is compounding the problem (Bulik, 2021; Dall, 2018). These factors together necessitate the need to change the paradigm, from a focus on a single 'silver bullet' antibiotic solution created by industry, to a more varied response. These responses include reinventing the antibiotic development pipeline (Singer et al., 2019b), the development of treatment programmes which reduce the development of resistance (Lee et al., 2013), and understanding how the environment drives antibiotic resistance (Kirchhelle & Roberts, 2022). It is within this final response that this thesis is situated.

Antimicrobial resistance is now accepted to predate the anthropogenic use of antibiotics (Barlow & Hall, 2002; D'Costa et al., 2011). There are several known environmental drivers of this resistance including, heavy metals (Ohore et al., 2019), biocides (Singer et al., 2016), and antibiotics in the environment (Kelly & Brooks, 2018). The work presented in this thesis sought to determine if secondary plant metabolites, also known as phytochemicals, functioned as an additional natural driver of antibiotic resistance.

This data is quickly becoming essential for the current crisis. Phytochemicals are ubiquitous in the environment, and in products for human use, such as cleaning wipes and perfumes (Chandra et al., 2017; Woodrow et al., 2005). Alongside this, they are being explored for their use in human medicine, both for their antimicrobial activity (Vipin et al., 2020), and their potential as treatments for myriad of other conditions (Abd El-Wahab et al., 2013). Finally,

they are being evaluated for their potential use as growth promoters in agriculture (Guaragni et al., 2020).

The central concept, and concern that this thesis seeks to explore is as follows: If phytochemicals function as a natural driver of antibiotic resistance and select for mechanisms of resistance which confer cross-resistance to antibiotics, then the use of phytochemicals in multiple competing industries could worsen the already critical antimicrobial resistance crisis.

The aims of the thesis were threefold, we will discuss the success of each of these aims in turn, and the wider impacts of the results of this thesis on the AMR landscape. The aims were as follows:

IV.   To develop a functional metagenomic screening methodology which can be used to screen both metagenomic libraries and bacterial isolate libraries for genes which confer, or bacteria who possess, phytochemical tolerance.

V.   To evolve environmental isolates of bacteria in sub-inhibitory concentrations of the plant phytochemicals to determine the effects of phytochemical selective pressure on a genomic level.

VI.   To explore the effects phytochemicals supplementation in broiler chickens at a population level both *in vivo* and using two *in vitro* models.

9.2   Outcomes of the novel screening assay

A screening assay, which could be used to screen both the oral metagenomic library (Reynolds et al., 2016) and The Swab and Send Library (Roberts, 2020), was successfully developed and deployed in Chapters 3 and 4.

In Chapter 3, three positive hits were taken forward for whole genome sequencing to allow determination of the genes contained upon the metagenomic inserts in the isolates. Two of

these positive hits were removed from later analysis due to loss of phytochemical tolerance. Despite their removal from later analysis both inserts contained genes encoding for proteins that are associated with antimicrobial resistance. These included a Exinuclease subunit A (Jaciuk et al., 2011; Norton et al., 2013), TonB-dependant receptors (Fujita et al., 2019; W. Li et al., 2021), and a D, D-transpeptidase.

The final positive hit H4F9 was clearly more tolerant to berberine at concentrations of between 1-2 mg/ml, this was higher than the MIC of the *E. coli* library host containing the empty pCC1BAC plasmid. The metagenomic insert in isolate H4F9 contained 25 putative protein encoding open reading frames. Proteins encoded for by these ORFs included an M18 aminopeptidase, and an ABC transporter, which have been associated with artemisinin and antibiotic resistance respectively (Choi, 2005; Garvey & Piddock, 2008; Saier & Paulsen, 2001). ABC transporters can efflux antibiotics out of the cell by sacrificing the ATP hydrolysis (C. H. Choi, 2005), and can form protein complexes with TolC receptors to further extrude antibiotics (Greene et al., 2018). Further the H4F9 insert contained a glycotransferase family 9 protein encoding gene, the importance of which is discussed later.

Further, 13 of the 14 isolates which came out of the various stages of the oral metagenomic library screening procedure contained inserts with DNA from either *Prevotella* or *Veillonella* genera. The oral microbiome contains over 101 genera (Nasidze et al., 2009). We hypothesise that the over-representation of these two genera suggest they are likely to be intrinsically tolerant to plant phytochemicals. *Veillonella* is one of the few seemingly Gram-negative members of the *Firmicutes* phyla (Vesth et al., 2013), and *Prevotella* is a Gram-negative member of the *Bacteroidota* phyla (Kau et al., 2021). It is hypothesised that the Gram-negative wall structure they both contain may play a part in the phytochemical tolerance that isolates containing their DNA display.

In Chapter 4, the novel screening procedure was used to screen the Swab and Send library (A. P. Roberts, 2020) with inhibitory concentrations of berberine. This experiment resulted in 21 positive hits that displayed tolerance to berberine, of which 20 hits contained known antibiotic resistance genes when the WGS was analysed. The percentage of isolates that contained antibiotic resistance genes in the library is unknown, however the library is constructed of environmental isolates. Prevalence of AMR genes in bacterial isolates in the environment can be as low as 1.75%, or as high as 95% (Ibrahim et al., 2012; Lin et al., 2017; Xu et al., 2018) depending upon the gene, bacteria, and location combination. Whilst it is possible that the library contains 95.24% (the rate of AMR genes in our positive hits) prevalence of AMR genes, it is highly unlikely, and thus it shows clearly that berberine selects for isolates containing AMR genes. Determining the mechanistic reasons for this selection is a clear avenue for future research.

There were 23 antibiotic resistance genes across all 20 isolates, some genes occurred in more than one isolate. However, no antibiotic resistance gene was consistent across all positive hits from the Swab and Send Library, though β-lactamases were present in the genomes of 68.75% of isolates, and fosfomycin resistance in all *Enterobacter* and *L. adecarboxylata* isolates. Efflux pump mediated resistance was apparent in many of the isolates. Finally, a number of the genes including *tet*(A) (Li et al., 2018)and *oqxAB* (Li et al., 2021; Tegos et al., 2002) have been previously associated with berberine resistance. This would suggest that a single antibiotic resistance gene is unlikely to responsible for berberine resistance, but that antibiotic resistance gene presence is clearly linked to berberine tolerance. This thesis hypothesises that these genes play a role in berberine resistance, either individually or together with other genes, and further studies should be conducted to elucidate the exact resistance, and selection mechanisms occurring here.

One additional potential mechanism of cross-resistance between phytochemicals and antibiotics would be through selection for the same mobile genetic elements containing these resistance mechanisms, as is seen with heavy metal resistance and antimicrobial resistance gene colocation (Yu et al., 2017; Zhang et al., 2017). This evaluation of these genomes was outside the remit of the study but would be an excellent starting point for a new project focused on co-selection and co-location of phytochemical and antimicrobial resistance genes.

9.3 *P. aeruginosa* evolution in sub-inhibitory concentrations of phytochemicals

The second aim of this thesis was to explore how sub-inhibitory concentrations of phytochemicals impacted the evolution of bacteria in the environment, specifically with regards to their antibiotic and phytochemical tolerance. The experiment was modelled after the long-term *E. coli* evolution experiment (Lenski, 2017). Two environmental isolates, NCTC 7244 isolated from well water in 1946, and NCTC 9433 isolated from a tobacco plant in 1960 were selected for this study due to their isolation prior to widespread antibiotic use. Both isolates were *Pseudomonas aeruginosa,* which was selected due to its environmental and clinical ubiquity, and its role in AMR (Awad et al., 2016b; Doyle, 2018).

Eleven of the 12 evolved isolates had a 2-fold increase in phytochemical resistance, this was not associated with an increase in resistance to any antibiotics. None of the controls evolved for 30 days in the absence of antibiotics had an increase in phytochemical tolerance or antibiotic resistance. After whole genome sequencing of both the controls and the isolates that had increased resistance to either compound, 6 genetic mutations were hypothesised to have occurred due to growth under the selective pressure of the phytochemical. Though five isolates with increased resistance had no detectable genetic mutations that could be assigned to the treatment alone.

Two genetic mutations of further import were: (1) An A146A mutation in the translated protein sequence of the L, D transpeptidase of NCTC 7244 after growth in sub-inhibitory concentrations of quercetin and (2) An A76A mutation in translated protein sequence of the CAZy glycosyltransferases. Both synonymous mutations were associated with a codon change to a codon with less abundance in *P. aeruginosa* which suggests they are transcribed less in the mutated isolates. Synonymous mutations can also interrupt transcription through the distortion of mRNA secondary structures (Wong et al., 2022). The occurrence of a glycosyltransferase and transpeptidase in this chapter is further discussed later.

The hypothesise after this work is that genetic mutations are not the only cause of phytochemical resistance. Though mutations did occur in AMR associated genes after growth in sub-inhibitory concentrations of the phytochemicals, there was no direct link between phytochemical tolerance and antimicrobial resistance phenotype.

Future steps in this research pathway include constructing plasmids containing the mutated genes discovered, or to use CRISPR-cas9 edit these mutations directly into the genome of the bacterial host (Ratner et al., 2016). Theoretical binding of quercetin and berberine too these proteins could be explored through *in silico* modelling (Moro et al., 2016), which would allow determination of the potential interaction between the phytochemicals and the proteins.

9.4 Comparisons and cooperation between the *in vitro* and *in vivo* chicken studies

The final aim of this thesis was to explore how phytochemicals affected the AMR crisis when used as replacements for antibiotic growth promoters. Phytochemicals make extremely attractive alternatives to antibiotic growth promoters, due to their diversity, safety, and myriad of health benefits (Rezaeiamiri et al., 2020).

The triad of studies in Chapters 6, 7, and 8 explored how phytochemical in-feed addition affected the chicken microbiome using two *in vitro* model systems and one *in vivo* study. The

objectives of this experimental triad were threefold: (1) To determine how effectively the *in vitro* systems modelled the *in vivo* study, (2) To determine how phytochemical addition altered the chicken gut microbiome, and chicken health, and finally (3) to explore how phytochemical supplementation affected AMR gene carriage in the chicken GIS.

Firmicutes were the dominant phyla across all the chicken experiments. This is not wholly unsurprising, as *Firmicutes* are one of two major phyla in the GIS (the other being *Bacteroidota*), and one of the four phyla usually present in the GIS system (the final two being *Actinobacteriota* and *Proteobacteria* (Rychlik, 2020). However, the relative proportions of the *Firmicutes* differed between the studies.

In the batch culture experiment in Chapter 6, the *Firmicutes* phyla accounted for greater than 99% of all bacteria present. This suggests it was extremely sensitive to the initial inoculum, which was *Firmicutes* dominated. The initial 7 days of microbiome development were not assessed, suggesting that this experiment may have missed the microbiome stabilisation that usually occurs in the chicken GIS during the early stages of the chicken life cycle (Kubasova et al., 2019; Varmuzova et al., 2016). Additionally, we hypothesise that the lack of additional media input into this experiment may have led to a selective pressure towards bacteria which survive well in low resource settings. This is reinforced by the dominant bacterial order throughout the batch culture experiments being *Clostridiales,* which are known for their ability to survive in stressed environments (R. Zhang et al., 2019). Addition of the phytochemicals caused an increase in the relative proportions of *Oscillospirales* and *Lachnospirales*. Finally, the batch culture was able to determine that *Escherichia-Shigella* genera abundance increased after phytochemical supplementation, a consistency across the chicken experiment triad.

The model system in Chapter 7 was a more advanced version of the batch culture experiment, allowing for continuous feeding and sampling. The model caeca were kept at

conditions properly mimicking the chicken gut, including movement, anaerobia, GIS content mimicking media, and constant replacement of nutrients. The *Proteobacteria* and *Bacteroidota* phyla both increased in abundance after photochemical addition, and the Shannon-diversity was much more varied between samples than in the batch culture experiments. This highlights that this system is much better positioned for mimicking the complex chicken GIS. Once again, the abundance of *Escherichia-Shigella* increased after the addition of quercetin in this system.

The *in vivo* experiment conducted in Chapter 8 allowed for comparison between the two model systems and the chicken GIS. Nine chickens were culled at day 14 and the remaining 30 at day 21. This allowed for two direct timepoint comparisons to the batch culture experiment but once again made the assessment of the early stage of microbiome development impossible (Kubasova et al., 2019; Varmuzova et al., 2016). The *in vivo* experiment allowed the determination of the two bacterial species most responsible for the microbiome differences between the treatment groups. These were *Turicibacter sp* and *Lactobacillus pontis*. This level of analysis which was much more specific than the order and phyla level examination that occurred in the batch culture and model system studies, respectively. Supplementation of chicken feed with either phytochemical led to an increase in the abundance of *Escherichia-Shigella*. From this we can be assured that the results of Chapter 6 and 7 are changes because of phytochemical addition rather than artifacts of model systems. This is further supported by the difference in location of these experiments, Chapter 6 and 7 were conducted using pooled caecal content from Dutch chickens, whilst Chapter 8 used Chickens from English eggs, grown, and reared in Liverpool. The consistency in outcomes, despite geographical distance suggests clearly that what we are seeing is true biological adaptation to the presence of the phytochemicals.

Previous work in chicken microbiome modelling has used static *in vitro* models which do not accurately represent the chicken GIS (De Maesschalck et al., 2015), similar to the batch culture in Chapter 6. We suggest here that both our *in vitro* models well matched our *in vivo* experiment, though to different degrees, and thus have distinct roles to play in future research in this area. The batch culture is ideally placed for quick, cheap, and efficient analysis of the thousands of phytochemicals being explored for their role as dietary supplements (Rezaeiamiri et al., 2020), as long as careful attention is paid to supplying a phyla balanced initial inoculum. The model fermenter system is then well placed to assess the compounds before *in vivo* experiments, and has a particularly effective niche in being able to explore the daily microbiome changes, without culling or assessment of chick faecal content, which is often poorly representative of the chicken GIS microbiome (Stanley et al., 2015). The model is also well placed to support existing models in other animals such as the SHIME human model (De Wiele et al., 2004), the TIM-2 porcine model (Long et al., 2020), and the recently developed avian ALIMEntary tRact mOdel-2 (Oost et al., 2021). Finally, the *in vivo* experiments continue to occupy the same space as the ultimate step between product development, and product deployment.

9.4.1   The role of phytochemicals in chicken health

Chapter 6, 7, and 8 also sought to explore the role of phytochemical supplementation on chicken GIS to determine how these compounds affected chicken health through modulation of the microbiome. The microbiome is a key indicator of chicken health and has clear linkage to growth performance (Huang et al., 2018). All experiments of the chicken triad of chapters (6-8) had an increase in *Escherichia-shigella* abundance after phytochemical addition which is discussed in depth in the concluding section.

Within the batch culture system, the addition of both phytochemicals in anaerobic conditions led to an increase in the relative abundance of the *Lachnospirales* and *Oscillospirales*. Both

bacterial orders are associated with positive and negative chicken growth performance depending upon the study in question (Liu et al., 2021; Lundberg et al., 2021). Both orders were equally increased in the *in vivo* studies, suggesting this is a true biological result. Though the impact on growth parameters was indiscernible within the model system.

The fermenter system had an increase in the relative abundance of *Proteobacteria* and *Actinobacteria* specifically *Gordonibacter* after the addition of berberine. We hypothesise that the increase in *Gordonibacter* is a direct result of its ability to metabolise phytochemicals (Sallam et al., 2021). *Gordonibacter* is positive for chicken growth (Selma et al., 2014; Toney et al., 2020). We thus conclude in this specific instance that berberine supplementation promotes chicken growth performance through the modification towards a *Gordonibacter* positive environment. No published data exists on the role of *Gordonibacter* in relation to antimicrobial resistance, or ARGs in the environment.

In the *in vivo* experiments in feed supplementation with berberine and quercetin is negative for the growth of *Lactobacillus pontis,* but positive for the growth of members of the *Turicibacter* genus. The *Turicibacter* has two recently discovered members (Maki & Looft, 2022), and are generally associated with poor growth performance in chickens (Siegerstetter et al., 2017) and *S. enterica* infections in pigs (Aljahdali et al., 2020). They are also intrinsically resistant to colistin (Maki & Looft, 2022). *L. pontis* on the other hand is considered positive for chicken growth (Fesseha et al., 2021; Murry et al., 2004; Peng et al., 2016). *Lactobacillus* are reservoirs for many antimicrobial resistance genes and over 79.5% of isolates contain them (Dec et al., 2017). Taken together we can hypothesise that the addition of phytochemicals modulates the microbiome in a way that is negative for chicken growth.

9.5 Phytochemicals as natural drivers of antibiotic resistance: Emerging narratives

After all experimental strands were completed, two narratives emerged from the collective results which drew the different studies together.

9.5.1 Glycosyltransferases and transpeptidases

The first of these two narratives involved glycosyltransferases and transpeptidases. The appearance of these genes occurred in three chapters. In Chapter 3, genes encoding for these proteins where present on the positive hits from the metagenomic library inserts. In Chapter 5, genes encoding for these proteins were mutated in *P. aeruginosa* evolved under selective pressure of the phytochemicals. Finally, in Chapter 8, the single most differentially abundant bacterial species between the treatment groups in the *in vivo* chicken study is characterised by the presence of these glycosyltransferases.

In the initial end point screening procedure, quercetin selected for the V5H10 insert, which amongst the other genes it contained, contained the MdrA D, D transpeptidase encoding gene. The second occurrence of a transpeptidase in our studies was the A146A mutation in the translated protein of the L, D transpeptidase gene (and the codon frequency of codons used decreased from GCC: 67.7 to GCT/U: 4.8) in *P. aeruginosa* after growth in sub-inhibitory concentrations of berberine. These proteins catalyse the cleavage and linkage of peptidoglycans, and are essential for the building of cell walls (Magnet et al., 2008), are well known β-lactamases (Georgopapadakou et al., 1986), and overproduction and mutation of transpeptidases can lead to β-lactam resistance (Hugonnet et al., 2016). Further berberine is a known inhibitor of the surface protein transpeptidase in *S. aureus* models (Kim et al., 2004).

The continuous screening assay using 1 mg/ml of berberine selected for the H4F9 insert, which was clearly berberine tolerant, and amongst the other genes present contained a gene encoding for the glycosyltransferase family 9 protein. The second occurrence of the

glycosyltransferases in our studies was the A76A mutation in the translated protein sequence of the *cazy* gene (the codon frequency of the codons used decreased from GCC: 67.7 to GCA: 4.8). The third occurrence of the glycosyltransferases in our study was during the *in vivo* chicken experiment where *L. pontis* abundance was decreased after the in-feed supplementation of either phytochemical, as it is characterised by the production of multiple glycosyltransferases (Vogel et al., 1994). Glycosyltransferases, alongside transpeptidases are involved in the peptidoglycan layer formation and the larger penicillin binding protein complex (Sauvage & Terrak, 2016). Glycosyltransferases have been previously shown to modify flavonoids, preferentially glycosylating the C-3 or C-7 hydroxyl group (Hyung Ko et al., 2006), and are able to stabilise, detoxify, or solubilise substrates in all kingdoms (Tian et al., 2016).

Initially after the metagenomic screening study, we theorised that the presence of the transpeptidase and glycosyltransferase conferred tolerance to the phytochemical through glycosylation. However, the evidence from both the *P. aeruginosa* and *in vivo* chicken work would suggest that the presence of these glycosyltransferases is negative for cell survival in phytochemical stress conditions.

We suggest here multiple hypothetical reasons for this conflicting information. In the first hypothesis: None of the glycosyltransferases or transpeptidases selected for or modified in our studies were identical. These protein families are extremely broad and have different substrate specificities (Breton et al., 2006) and are involved in various pathways (Jacobitz et al., 2017). As such the different enzymes may have different specificities for detoxification of the phytochemicals, and those selected for by the metagenomic screening assay were potentially able to use the phytochemicals as substrates, whilst those in the *P. aeruginosa* experiments were not. The reduction in the transcription of these proteins in *P. aeruginosa* may have paved the way for a concurrent increase in the expression of other genes, through

transcriptomic mechanisms (Lee & Young, 2013) or post translational modifications (Darling & Uversky, 2018) which fell outside of the scope of this genomic only study.

In the second hypothesis, we again return to the idea that these enzymes may not only have different substrate specificity, but also produce different biproducts. Glycosyltransferases are well known for their ability to detoxify substrates, or modifications that allow efflux (Tian et al., 2016). However they are also used as toxins in bacterial competition (Jank et al., 2015), and can induce cell apoptosis through toxification of substrates. We theorise that the modified enzymes in the *P. aeruginosa* study in this scenario toxify, rather than detoxify the phytochemicals, whilst the selected enzymes from Chapter 3, detoxify rather than toxify. It is possible, however, that the theoretical reduction in transcription of these two enzymes in *P. aeruginosa* is due to their lack of requirement as toxins in a non-competitive laboratory environment, however they only occurred in their respective isolates and not in any control isolates, and as such this is highly unlikely.

The third hypothesis to explore is based on the new knowledge that post-translational modification of efflux pumps by glycosyltransferases is essential for the correct functioning of these proteins, and the glycosyltransferase modifications can determine the substrate preferentially removed by the pumps (Abouelhadid et al., 2020). We hypothesise, again, that the glycosyltransferases selected for by the screening procedure, may alter the specificity of the efflux pumps in *E. coli* to preferentially remove the phytochemicals, whilst the glycosyltransferases in *P. aeruginosa* do not. This hypothesis is particularly interesting, as the modification of these efflux pumps is also key for multi-drug resistance and antibiotic efflux by bacteria. As such the selection for a particular efflux pump / glycosylation combination by phytochemical pressure, may have an impact on the resistance profile of the bacteria in question.

One final consideration in this discussion is that the metagenomic inserts contained in the oral genetic library on isolates with increased phytochemical tolerance were not originally *E. coli* DNA. As such the expression of those isolates is likely to be less efficient than those of wild-type *E. coli* glycosyltransferases or transpeptidases by EPI300 *E. coli*. As such it is possible that the presence of these genes titrated out the wildtype proteins, leading to an overall reduction in enzymatic activity of glycosyltransferases and transpeptidases within the EPI300 *E. coli* construct. If this is true, then there would be a consistent stream of glycosyltransferase activity reduction leading to increased phytochemical tolerance throughout the thesis. This potential reduction in glycosyltransferase activity was outside of the remit of that experiment and presents an avenue for future exploration of this work.

The narrative around glycosyltransferases. transpeptidases, antibiotic resistance, phytochemical tolerance, berberine, and quercetin is complex, and any number of the hypothesises presented here could be true and working in tandem. Further studies to elucidate the exact relationship between these factors are essential and could include expression of all these genes in laboratory strains, to site directed mutagenesis, or screening procedures for glycosyltransferase activity and subsequent phytochemical tolerance analysis.

9.5.2   *Escherichia-shigella* and *Escherichia coli*

The second narrative was the selection of *Escherichia-shigella* and *E. coli* by the phytochemicals in multiple experimental lines. In Chapter 4, the screening assay selected for *E. coli* and *L. adecarboxylata* isolates from the Swab and Send Library. In Chapter 6, and 7, the addition of quercetin in both *in vitro* chicken trails led to an increase in abundance of the *Escherichia-Shigella* group. Finally in Chapter 8, the addition of both quercetin and berberine led to an increase in the abundance of the *Escherichia-Shigella* group in both the caecal and ileal samples.

The *Escherichia-Shigella* genus contains two important bacterial pathogens which are negatively associated with chicken growth performance (EL-Sawah et al., 2018; Stromberg et al., 2017). Alongside the negative impacts on chicken growth performance, *E. coli* is a well-known reservoir of AMR genes within the agricultural environment (Ibrahim et al., 2019). *E. coli* responds to berberine exposure through the upregulation of *ompW* (Budeyri Gokgoz et al., 2017), and berberine has multiple targets within *E. coli* including the *ftsZ* cell division gene (Domadia et al., 2008; Karaosmanoglu et al., 2014). Finally, *E. coli* resistance to berberine has been previously associated with the expression of the *tet*(A) tetracycline resistance gene (Li et al., 2018).

We hypothesise from these results that *E. coli* can survive well in phytochemical stressed conditions and further that the selection for *E. coli* by these two phytochemicals is negative for the growth of poultry, and potentially increases the AMR gene carriage in agricultural systems, particularly the carriage of tetracycline resistance genes.

Finally, the difficulties in the development of the initial screening procedure in Chapter 4. may have been in part due to the intrinsic tolerance of *E. coli* to the phytochemicals. *E. coli* was used to construct the metagenomic library. Assuming our previous hypothesise that *E. coli* is well positioned to survive in phytochemical stressed conditions is correct, then an E. coli library would have been a poor choice for the screening assay. It would explain why the MIC of berberine and quercetin to EPI300 *E. coli* was so high, and why phytochemical tolerance was inconsistent between the positive hits and the library constructs. As such we suggest that future studies to explore the relationship between *E. coli* and phytochemical tolerance would be an immediate next step.

9.6   Priorities for future research

This thesis found a clear link between: (1) phytochemical tolerance and selection for antimicrobial resistance genes, (2) phytochemical tolerance, glycosyltransferases, and

transpeptidases, (3) phytochemical tolerance and chicken caecal health and (4) phytochemical supplementation, led to the increased abundance of *Escherichia-shigella* in the chicken caecal microbiome. Further studies, such as those suggested below, would be beneficial in adding further detail to the narratives begun within this thesis.

- The novel screening procedure could be used to screen other libraries, particularly those not constructed using *E. coli* to see if there are any consistencies in genes contained on the metagenomic inserts.

- Genes from the metagenomic inserts, and the mutated genes from the *P. aeruginosa* experimental streams could be cloned into *E. coli*, *P. aeruginosa* or other laboratory bacterial strains, to see if the presence of these genes, or mutations directly leads to increased phytochemical tolerance. Particularly important would be to conduct these experiments with the glycosyltransferases and transpeptidases identified.

- The chicken experimental triad could be repeated with more close alignment of the methodologies, running all models for 45 days, alongside chicken growth assessment, taking daily samples of chicken faecal content, running multiple models and batch cultures, and taking more than one sample from the model system per day. This would allow a more exact alignment of the different models.

- Further experiments would be prudent to explore the relationship between *E. coli* and phytochemical tolerance. Through a panel of minimum inhibitory concentration experiments against multiple strains of *E. coli* to see if phytochemical tolerance is strain or species specific.

References

Aarestrup, F. M. (1995). Occurrence of glycopeptide resistance among Enterococcus faecium isolates from conventional and ecological poultry farms. *Microbial Drug Resistance*, *1*(3), 255–257. https://doi.org/10.1089/mdr.1995.1.255

Abd El-Hack, M. E., Mahgoub, S. A., Hussein, M. M. A., & Saadeldin, I. M. (2018). Improving growth performance and health status of meat-type quail by supplementing the diet with black cumin cold-pressed oil as a natural alternative for antibiotics. *Environmental Science and Pollution Research International*, *25*(2), 1157–1167. https://doi.org/10.1007/s11356-017-0514-0

Abd El-Wahab, A. E., Ghareeb, D. A., Sarhan, E. E. M., Abu-Serie, M. M., & El Demellawy, M. A. (2013). In vitro biological assessment of berberis vulgaris and its active constituent, berberine: Antioxidants, anti-acetylcholinesterase, anti-diabetic and anticancer effects. *BMC Complementary and Alternative Medicine*, *13*(1), 1–12. https://doi.org/10.1186/1472-6882-13-218/TABLES/5

Abdulhaq, N., Nawaz, Z., Zahoor, M. A., & Siddique, A. B. (2020). Association of biofilm formation with multi drug resistance in clinical isolates of Pseudomonas aeruginosa. *EXCLI Journal*, *19*, 201. https://doi.org/10.17179/EXCLI2019-2049

Abe, K., Nomura, N., & Suzuki, S. (2020). Biofilms: hot spots of horizontal gene transfer ({HGT}) in aquatic environments, with a focus on a new {HGT} mechanism. *{FEMS} Microbiology Ecology*, *96*(5). https://doi.org/10.1093/femsec/fiaa031

Abouelhadid, S., Raynes, J., Bui, T., Cuccui, J., & Wren, B. W. (2020). Characterization of posttranslationally modified multidrug efflux pumps reveals an unexpected link between glycosylation and antimicrobial resistance. *MBio*, *11*(6), 1–19. https://doi.org/10.1128/MBIO.02604-20/SUPPL_FILE/MBIO.02604-20-SF005.JPG

Abraham, E. P., & Chain, E. (1988). An enzyme from bacteria able to destroy penicillin. 1940. *Reviews of Infectious Diseases*, *10*(4), 677–678. https://www.ncbi.nlm.nih.gov/pubmed/3055168

Acheampong, G., Owusu, M., Owusu-Ofori, A., Osei, I., Sarpong, N., Sylverken, A., Kung, H. J., Cho, S. T., Kuo, C. H., Park, S. E., Marks, F., Adu-Sarkodie, Y., & Owusu-Dabo, E. (2019). Chromosomal and plasmid-mediated fluoroquinolone resistance in human Salmonella enterica infection in Ghana. *BMC Infectious Diseases*, *19*(1), 1–10. https://doi.org/10.1186/S12879-019-4522-1/FIGURES/2

Acheampong, S. (2022). The Impact of Heavy Metals on the Chicken Gut Microbiota and their Health and Diseases. In *Broiler Industry [Working Title]*. IntechOpen. https://doi.org/10.5772/intechopen.105581

Agarwal, S., Tripathi, S., & Mishra, N. (2020). Pharmacological potential of thymol. In P. Mishra, R. R. Mishra, & C. O. Adetunji (Eds.), *Innovations in food technology: current perspectives and future goals* (pp. 489–500). Springer Singapore. https://doi.org/10.1007/978-981-15-6121-4_34

Ahmadian, A., Seidavi, A., & Phillips, C. J. C. (2020). Growth, Carcass Composition, Haematology and Immunity of Broilers Supplemented with Sumac Berries (Rhus coriaria L.) and Thyme (Thymus vulgaris). *Animals : An Open Access Journal from {MDPI}*, *10*(3). https://doi.org/10.3390/ani10030513

Ahmed, T., Gilani, A.-U.-H., Abdollahi, M., Daglia, M., Nabavi, S. F., & Nabavi, S. M. (2015). Berberine and neurodegeneration: A review of literature. *Pharmacological Reports*, *67*(5), 970–979. https://doi.org/10.1016/j.pharep.2015.03.002

Akoh, C. C., Lee, G. C., Liaw, Y. C., Huang, T. H., & Shaw, J. F. (2004). GDSL family of serine esterases/lipases. *Progress in Lipid Research*, *43*(6), 534–552. https://doi.org/10.1016/J.PLIPRES.2004.09.002

Albrecht, C., Cittadini, M. C., & Soria, E. A. (2020). Pharmacological Activity of Quercetin and 5 caffeoylquinic Acid Oral Intake in Male Balb/c Mice with Lung Adenocarcinoma. *Archives of Medical Research*, *51*(1), 8–12. https://doi.org/10.1016/j.arcmed.2019.11.006

Alexander, J. W. (2009). History of the medical use of silver. *Surgical Infections*, *10*(3), 289–292. https://doi.org/10.1089/sur.2008.9941

Aljahdali, N. H., Sanad, Y. M., Han, J., & Foley, S. L. (2020). Current knowledge and perspectives of potential impacts of Salmonella enterica on the profile of the gut microbiota. *BMC Microbiology 2020 20:1*, *20*(1), 1–15. https://doi.org/10.1186/S12866-020-02008-X

Alonso, B., Fernández-Barat, L., Domenico, E. G. Di, Marín, M., Cercenado, E., Merino, I., Pablos, M. de, Muñoz, P., & Guembe, M. (2020). Characterization of the virulence of Pseudomonas aeruginosa strains causing ventilator-associated pneumonia. *BMC Infectious Diseases 2020 20:1*, *20*(1), 1–8. https://doi.org/10.1186/S12879-020-05534-1

Altschul, S. F., Gish, W., Miller, W., Myers, E. W., & Lipman, D. J. (1990). Basic local alignment search tool. *Journal of Molecular Biology*, *215*(3), 403–410. https://doi.org/10.1016/S0022-2836(05)80360-2

Amly, D. A., Hajardhini, P., Jonarta, A. L., Yulianto, H. D. K., & Susilowati, H. (2021). Enhancement of pyocyanin production by subinhibitory concentration of royal jelly inPseudomonas aeruginosa. *F1000Research*, *10*, 14. https://doi.org/10.12688/F1000RESEARCH.27915.4

Anand David, A. V., Arulmoli, R., & Parasuraman, S. (2016). Overviews of biological importance of quercetin: A bioactive flavonoid. *Pharmacognosy Reviews*, *10*(20), 84–89. https://doi.org/10.4103/0973-7847.194044

Andersson, S. G. E., & Kurland, C. G. (1990). Codon preferences in free-living microorganisms. *Microbiological Reviews*, *54*(2), 198–210. https://doi.org/10.1128/MR.54.2.198-210.1990

Andres, S., Pevny, S., Ziegenhagen, R., Bakhiya, N., Schäfer, B., Hirsch-Ernst, K. I., & Lampen, A. (2018). Safety aspects of the use of quercetin as a dietary supplement. *Molecular Nutrition \& Food Research*, *62*(1). https://doi.org/10.1002/mnfr.201700447

Ankri, S., & Mirelman, D. (1999). Antimicrobial properties of allicin from garlic. *Microbes and Infection*, *1*(2), 125–129. https://doi.org/10.1016/s1286-4579(99)80003-3

Arif, M., Rehman, A., Abd El-Hack, M. E., Saeed, M., Khan, F., Akhtar, M., Swelum, A. A., Saadeldin, I. M., & Alowaimer, A. N. (2018). Growth, carcass traits, cecal microbial counts, and blood chemistry of meat-type quail fed diets supplemented with humic acid and black cumin seeds. *Asian-Australasian Journal of Animal Sciences*, *31*(12), 1930–1938. https://doi.org/10.5713/ajas.18.0148

Arora, S. K., Ritchings, B. W., Almira, E. C., Lory, S., & Ramphal, R. (1997). A transcriptional activator, FleQ, regulates mucin adhesion and flagellar gene expression in Pseudomonas aeruginosa in a cascade manner. *Journal of Bacteriology*, *179*(17), 5574–5581. https://doi.org/10.1128/JB.179.17.5574-5581.1997

Arts, I. C. W., Sesink, A. L. A., Faassen-Peters, M., & Hollman, P. C. H. (2004). The type of sugar moiety is a major determinant of the small intestinal uptake and subsequent biliary excretion of dietary quercetin glycosides. *British Journal of Nutrition*, *91*(6), 841–847. https://doi.org/10.1079/BJN20041123

Aruwa, C. E., Pillay, C., Nyaga, M. M., & Sabiu, S. (2021). Poultry gut health – microbiome functions, environmental impacts, microbiome engineering and advancements in characterization technologies. *Journal of Animal Science and Biotechnology*, *12*(1). https://doi.org/10.1186/S40104-021-00640-9

Asakura, H., Hashii, N., Uema, M., Kawasaki, N., Sugita-Konishi, Y., Igimi, S., & Yamamoto, S. (2013). Campylobacter jejuni pdxA Affects Flagellum-Mediated Motility to Alter Host Colonization. *PLoS ONE*, *8*(8). https://doi.org/10.1371/JOURNAL.PONE.0070418

Ashley, E. A., Dhorda, M., Fairhurst, R. M., Amaratunga, C., Lim, P., Suon, S., Sreng, S., Anderson, J. M., Mao, S., Sam, B., Sopha, C., Chuor, C. M., Nguon, C., Sovannaroth, S., Pukrittayakamee, S., Jittamala, P., Chotivanich, K., Chutasmit, K., Suchatsoonthorn, C., … to Artemisinin Collaboration (TRAC), T. R. (2014). Spread of artemisinin resistance in Plasmodium falciparum malaria. *The New England Journal of Medicine*, *371*(5), 411–423. https://doi.org/10.1056/{NEJMoa1314981}

Aslam, B., Wang, W., Arshad, M. I., Khurshid, M., Muzammil, S., Rasool, M. H., Nisar, M. A., Alvi, R. F., Aslam, M. A., Qamar, M. U., Salamat, M. K. F., & Baloch, Z. (2018). Antibiotic resistance: a rundown of a global crisis. *Infection and Drug Resistance*, *11*, 1645–1658. https://doi.org/10.2147/{IDR}.S173867

Atas, B., Aksoy, C. S., Avci, F. G., Sayar, N. A., Ulgen, K., Ozkirimli, E., & Akbulut, B. S. (2022). Carvacrol Enhances the Antimicrobial Potency of Berberine in Bacillus subtilis. *Current Microbiology*, *79*(5), 135. https://doi.org/10.1007/S00284-022-02823-7

Awad, W. A., Mann, E., Dzieciol, M., Hess, C., Schmitz-Esser, S., Wagner, M., & Hess, M. (2016a). Age-Related Differences in the Luminal and Mucosa-Associated Gut Microbiome of Broiler Chickens and Shifts Associated with Campylobacter jejuni Infection. *Frontiers in Cellular and Infection Microbiology*, *6*(NOV). https://doi.org/10.3389/FCIMB.2016.00154

Awad, W. A., Mann, E., Dzieciol, M., Hess, C., Schmitz-Esser, S., Wagner, M., & Hess, M. (2016b). Age-Related Differences in the Luminal and Mucosa-Associated Gut Microbiome of Broiler Chickens and Shifts Associated with Campylobacter jejuni Infection. *Frontiers in Cellular and Infection Microbiology*, *6*(NOV). https://doi.org/10.3389/FCIMB.2016.00154

Bae, Y., Koo, B., Lee, S., Mo, J., Oh, K., & Mo, I. P. (2017). Bacterial diversity and its relationship to growth performance of broilers. *Korean Journal of Veterinary Research*, *57*(3), 159–167. https://doi.org/10.14405/KJVR.2017.57.3.159

Ballou, A. L., Ali, R. A., Mendoza, M. A., Ellis, J. C., Hassan, H. M., Croom, W. J., & Koci, M. D. (2016). Development of the Chick Microbiome: How Early Exposure Influences Future Microbial Diversity. *Frontiers in Veterinary Science*, *3*(JAN), 20. https://doi.org/10.3389/FVETS.2016.00002

Bandeira Junior, G., Sutili, F. J., Gressler, L. T., Ely, V. L., Silveira, B. P., Tasca, C., Reghelin, M., Matter, L. B., Vargas, A. P. C., & Baldisserotto, B. (2018). Antibacterial potential of phytochemicals alone or in combination with antimicrobials against fish pathogenic bacteria. *Journal of Applied Microbiology*, *125*(3), 655–665. https://doi.org/10.1111/jam.13906

Bandyopadhyay, S., Patra, P. H., Mahanti, A., Mondal, D. K., Dandapat, P., Bandyopadhyay, S., Samanta, I., Lodh, C., Bera, A. K., Bhattacharyya, D., Sarkar, M., & Baruah, K. K. (2013). Potential antibacterial activity of berberine against multi drug resistant enterovirulent Escherichia coli isolated from yaks (Poephagus grunniens) with haemorrhagic diarrhoea. *Asian Pacific Journal of Tropical Medicine*, *6*(4), 315–319. https://doi.org/10.1016/S1995-7645(13)60063-2

Barboza, J. N., da Silva Maia Bezerra Filho, C., Silva, R. O., Medeiros, J. V. R., & de Sousa, D. P. (2018). An Overview on the Anti-inflammatory Potential and Antioxidant Profile of Eugenol. *Oxidative Medicine and Cellular Longevity*, *2018*, 3957262. https://doi.org/10.1155/2018/3957262

Barlow, M., & Hall, B. G. (2002). Phylogenetic analysis shows that the OXA β-lactamase genes have been on plasmids for millions of years. *Journal of Molecular Evolution*, *55*(3), 314–321. https://doi.org/10.1007/s00239-002-2328-y

Bateman, A., Martin, M. J., Orchard, S., Magrane, M., Agivetova, R., Ahmad, S., Alpi, E., Bowler-Barnett, E. H., Britto, R., Bursteinas, B., Bye-A-Jee, H., Coetzee, R., Cukura, A., da Silva, A., Denny, P., Dogan, T., Ebenezer, T. G., Fan, J., Castro, L. G., … Zhang, J. (2021). UniProt: the universal protein knowledgebase in 2021. *Nucleic Acids Research*, *49*(D1), D480–D489. https://doi.org/10.1093/NAR/GKAA1100

Battu, S. K., Repka, M. A., Maddineni, S., Chittiboyina, A. G., Avery, M. A., & Majumdar, S. (2010). Physicochemical characterization of berberine chloride: a perspective in the development of a solution dosage form for oral delivery. *{AAPS} {PharmSciTech}*, *11*(3), 1466–1475. https://doi.org/10.1208/s12249-010-9520-y

Bayir, A. G., Kiziltan, H. S., & Kocyigit, A. (2019). Plant family, carvacrol, and putative protection in gastric cancer. In *Dietary interventions in gastrointestinal diseases* (pp. 3–18). Elsevier. https://doi.org/10.1016/B978-0-12-814468-8.00001-6

Becerril, R., Nerín, C., & Gómez-Lus, R. (2012). Evaluation of bacterial resistance to essential oils and antibiotics after exposure to oregano and cinnamon essential oils. *Foodborne Pathogens and Disease*, *9*(8), 699–705. https://doi.org/10.1089/fpd.2011.1097

Betram, M. A., & Young, L. S. (1984). Imipenem antagonism of the in vitro activity of piperacillin against Pseudomonas aeruginosa. *Antimicrobial Agents and Chemotherapy*, *26*(2), 272–274. https://doi.org/10.1128/AAC.26.2.272

Bhagirath, A. Y., Li, Y., Somayajula, D., Dadashi, M., Badr, S., & Duan, K. (2016). Cystic fibrosis lung environment and Pseudomonas aeruginosa infection. *{BMC} Pulmonary Medicine*, *16*(1), 174. https://doi.org/10.1186/s12890-016-0339-5

Bhatia, S., Sharma, K., Dahiya, R., & Bera, T. (2015). Modern Applications of Plant Biotechnology in Pharmaceutical Sciences. *Modern Applications of Plant Biotechnology in Pharmaceutical Sciences*, 1–439. https://doi.org/10.1016/C2014-0-02123-5

Bhatty, M., Laverde Gomez, J. A., & Christie, P. J. (2013). The expanding bacterial type IV secretion lexicon. *Research in Microbiology*, *164*(6), 620–639. https://doi.org/10.1016/J.RESMIC.2013.03.012

Bhogoju, S., Nahashon, S., Wang, X., Darris, C., & Kilonzo-Nthenge, A. (2018). A comparative analysis of microbial profile of Guinea fowl and chicken using metagenomic approach. *PLoS ONE*, *13*(3). https://doi.org/10.1371/JOURNAL.PONE.0191029

Bidlack, J. E., & Silverman, P. M. (2004). An active type IV secretion system encoded by the F plasmid sensitizes Escherichia coli to bile salts. *Journal of Bacteriology*, *186*(16), 5202–5209. https://doi.org/10.1128/JB.186.16.5202-5209.2004/ASSET/9DAA3BFB-4527-4B3D-AB9C-60405F992FF2/ASSETS/GRAPHIC/ZJB0160439270007.JPEG

Birdsall, & T. C. (1997). Berberine : Therapeutic Potential of Alkaloid Found in Several Medicinal Plants. *Altern. Med. Rev.* https://ci.nii.ac.jp/naid/10016482634/

Bjerrum, L., Engberg, R. M., Leser, T. D., Jensen, B. B., Finster, K., & Pedersen, K. (2006). Microbial community composition of the ileum and cecum of broiler chickens as revealed by molecular and culture-based techniques. *Poultry Science*, *85*(7), 1151–1164. https://doi.org/10.1093/PS/85.7.1151

Blaak, H., van Hoek, A. H. A. M., Veenman, C., Docters van Leeuwen, A. E., Lynch, G., van Overbeek, W. M., & de Roda Husman, A. M. (2014). Extended spectrum ß-lactamase- and constitutively AmpC-producing Enterobacteriaceae on fresh produce and in the agricultural environment. *International Journal of Food Microbiology*, *168–169*, 8–16. https://doi.org/10.1016/J.IJFOODMICRO.2013.10.006

Blanco-Cabra, N., Paetzold, B., Ferrar, T., Mazzolini, R., Torrents, E., Serrano, L., & LLuch-Senar, M. (2020). Characterization of different alginate lyases for dissolving Pseudomonas aeruginosa biofilms. *Scientific Reports 2020 10:1*, *10*(1), 1–10. https://doi.org/10.1038/s41598-020-66293-2

Blanco, P., Hernando-Amado, S., Reales-Calderon, J. A., Corona, F., Lira, F., Alcalde-Rico, M., Bernardini, A., Sanchez, M. B., & Martinez, J. L. (2016). Bacterial Multidrug Efflux Pumps: Much More Than Antibiotic Resistance Determinants. *Microorganisms 2016, Vol. 4, Page 14*, *4*(1), 14. https://doi.org/10.3390/MICROORGANISMS4010014

Bokhary, H., Pangesti, K. N. A., Rashid, H., Abd El Ghany, M., & Hill-Cawthorne, G. A. (2021). Travel-Related Antimicrobial Resistance: A Systematic Review. *Tropical Medicine and Infectious Disease*, *6*(1). https://doi.org/10.3390/TROPICALMED6010011

Bravo, D., Pirgozliev, V., & Rose, S. P. (2014). A mixture of carvacrol, cinnamaldehyde, and capsicum oleoresin improves energy utilization and growth performance of broiler chickens fed maize-based diet. *Journal of Animal Science*, *92*(4), 1531–1536. https://doi.org/10.2527/jas.2013-6244

Breidenstein, E. B. M., de la Fuente-Núñez, C., & Hancock, R. E. W. (2011). Pseudomonas aeruginosa: all roads lead to resistance. *Trends in Microbiology*, *19*(8), 419–426. https://doi.org/10.1016/j.tim.2011.04.005

Breton, C., Šnajdrová, L., Jeanneau, C., Koča, J., & Imberty, A. (2006). Structures and mechanisms of glycosyltransferases. *Glycobiology*, *16*(2), 29R-37R. https://doi.org/10.1093/GLYCOB/CWJ016

Budeyri Gokgoz, N., Avci, F. G., Yoneten, K. K., Alaybeyoglu, B., Ozkirimli, E., Sayar, N. A., Kazan, D., & Sariyar Akbulut, B. (2017). Response of Escherichia coli to Prolonged Berberine Exposure. *Microbial Drug Resistance*, *23*(5), 531–544. https://doi.org/10.1089/mdr.2016.0063

Bulik, B. S. (2021). *GlaxoSmithKline to shut down antibiotics production, cut 300 jobs in wake*

of Novartis buyout. https://www.fiercepharma.com/pharma/gsk-set-to-close-u-k-antibiotics-business-after-novartis-sandoz-sale#:~:text=Pharma-,GlaxoSmithKline to shut down antibiotics production%2C cut 300,in wake of Novartis buyout&text=GlaxoSmithKline plans to shut down,prod

Bunditvorapoom, D., Kochakarn, T., Kotanan, N., Modchang, C., Kümpornsin, K., Loesbanluechai, D., Krasae, T., Cui, L., Chotivanich, K., White, N. J., Wilairat, P., Miotto, O., & Chookajorn, T. (2018). Fitness Loss under Amino Acid Starvation in Artemisinin-Resistant Plasmodium falciparum Isolates from Cambodia. *Scientific Reports*, *8*(1), 1–9. https://doi.org/10.1038/s41598-018-30593-5

Cai, X., Fang, Z., Dou, J., Yu, A., & Zhai, G. (2013). Bioavailability of quercetin: problems and promises. *Current Medicinal Chemistry*, *20*(20), 2572–2582. https://doi.org/10.2174/09298673113209990120

Callahan, B. J., McMurdie, P. J., Rosen, M. J., Han, A. W., Johnson, A. J. A., & Holmes, S. P. (2016). DADA2: High resolution sample inference from Illumina amplicon data. *Nature Methods*, *13*(7), 581. https://doi.org/10.1038/NMETH.3869

Callahan, B. J., Sankaran, K., Fukuyama, J. A., McMurdie, P. J., & Holmes, S. P. (2016). Bioconductor Workflow for Microbiome Data Analysis: from raw reads to community analyses. *F1000Research*, *5*, 1492. https://doi.org/10.12688/f1000research.8986.2

CamBio. (2011). *CopyControl ™ Fosmid Library Production Kit with pCC1FOS ™ Vector CopyControl ™ HTP Fosmid Library Production Kit with pCC2FOS ™ Vector*. 1–32.

Campedelli, I., Mathur, H., Salvetti, E., Clarke, S., Rea, M. C., Torriani, S., Ross, R. P., Hill, C., & O'Toole, P. W. (2019). Genus-wide assessment of antibiotic resistance in Lactobacillus spp. *Applied and Environmental Microbiology*, *85*(1). https://doi.org/10.1128/AEM.01738-18/SUPPL_FILE/AEM.01738-18-S0001.PDF

Cane, D. E., Hsiung, Y., Cornish, J. A., Robinson, J. K., & Spenser, I. D. (1998). Biosynthesis of vitamin B6: The oxidation of 4-(phosphohydroxy)-L-threonine by PdxA. *Journal of the American Chemical Society*, *120*(8), 1936–1937. https://doi.org/10.1021/JA9742085

Caprari, S., Brandi, V., Pasquadibisceglie, A., & Polticelli, F. (2019). Uncovering the structure and function of Pseudomonas aeruginosa periplasmic proteins by an in silico approach. *Https://Doi.Org/10.1080/07391102.2019.1683468*, *38*(15), 4508–4520. https://doi.org/10.1080/07391102.2019.1683468

Carbonaro, M., & Grant, G. (2005). Absorption of Quercetin and Rutin in Rat Small Intestine. *Annals of Nutrition and Metabolism*, *49*(3), 178–182. https://doi.org/10.1159/000086882

Card, R. M., Cawthraw, S. A., Nunez-Garcia, J., Ellis, R. J., Kay, G., Pallen, M. J., Woodward, M. J., & Anjum, M. F. (2017). An in Vitro chicken gut model demonstrates transfer of a multidrug resistance plasmid from Salmonella to commensal Escherichia coli. *MBio*, *8*(4). https://doi.org/10.1128/MBIO.00777-17/SUPPL_FILE/MBO003173381ST7.XLSX

Carrasco, J. M. D., Casanova, N. A., & Miyakawa, M. E. F. (2019). Microbiota, Gut Health and Chicken Productivity: What Is the Connection? *Microorganisms*, *7*(10). https://doi.org/10.3390/MICROORGANISMS7100374

Carroll, J. (2018). *Novartis joins the Big Pharma exodus out of antibiotics, dumping research, cutting 140 and out-licensing programs*. Endpoints News. https://endpts.com/novartis-joins-the-big-pharma-exodus-out-of-antibiotics-dumping-research-cutting-140-and-

out-licensing-programs/

Casewell, M., Friis, C., Marco, E., McMullin, P., & Phillips, I. (2003). The European ban on growth-promoting antibiotics and emerging consequences for human and animal health. *The Journal of Antimicrobial Chemotherapy*, *52*(2), 159–161. https://doi.org/10.1093/jac/dkg313

Castanon, J. I. R. (2007). History of the use of antibiotic as growth promoters in European poultry feeds. *Poultry Science*, *86*(11), 2466–2471. https://doi.org/10.3382/ps.2007-00249

Cattoir, V. et al. (2020) "Novel chromosomal mutations responsible for fosfomycin resistance in Escherichia coli," Frontiers in microbiology, 11, p. 575031. doi: 10.3389/fmicb.2020.575031.

Cernáková, M., & Kostálová, D. (2002). Antimicrobial activity of berberine--a constituent of Mahonia aquifolium. *Folia Microbiologica*, *47*(4), 375–378. https://doi.org/10.1007/bf02818693

Chakraborty, S., Ásgeirsson, B., Minda, R., Salaye, L., Frère, J. M., & Rao, B. J. (2012). Inhibition of a cold-active alkaline phosphatase by imipenem revealed by in silico modeling of metallo-β-lactamase active sites. *FEBS Letters*, *586*(20), 3710–3715. https://doi.org/10.1016/J.FEBSLET.2012.08.030

Chandler, C. E., Horspool, A. M., Hill, P. J., Wozniak, D. J., Schertzer, J. W., Rasko, D. A., & Ernsta, R. K. (2019). Genomic and phenotypic diversity among ten laboratory isolates of Pseudomonas aeruginosa PAO1. *Journal of Bacteriology*, *201*(5), 595–613. https://doi.org/10.1128/JB.00595-18/SUPPL_FILE/JB.00595-18-S0005.PDF

Chandra, H., Bishnoi, P., Yadav, A., Patni, B., Mishra, A. P., & Nautiyal, A. R. (2017). Antimicrobial Resistance and the Alternative Resources with Special Emphasis on Plant-Based Antimicrobials-A Review. *Plants*, *6*(2). https://doi.org/10.3390/plants6020016

Chen, B. et al. (2021) Biocide-tolerance and antibiotic-resistance in community environments and risk of direct transfers to humans: Unintended consequences of community-wide surface disinfecting during COVID-19?, Environmental pollution (Barking, Essex : 1987). U.S. National Library of Medicine. Available at: https://www.ncbi.nlm.nih.gov/pmc/articles/PMC8019131/ (Accessed: March 7, 2023).

Chang, C. C. Y., Sun, J., & Chang, T.-Y. (2011). Membrane-bound O-acyltransferases (MBOATs). *Frontiers in Biology 2011 6:3*, *6*(3), 177–182. https://doi.org/10.1007/S11515-011-1149-Z

Chang, X., Yan, H., Xu, Q., Xia, M., Bian, H., Zhu, T., & Gao, X. (2012). The effects of berberine on hyperhomocysteinemia and hyperlipidemia in rats fed with a long-term high-fat diet. *Lipids in Health and Disease*, *11*, 86. https://doi.org/10.1186/1476-{511X}-11-86

Chen, C., Tao, C., Liu, Z., Lu, M., Pan, Q., Zheng, L., Li, Q., Song, Z., & Fichna, J. (2015). A Randomized Clinical Trial of Berberine Hydrochloride in Patients with Diarrhea-Predominant Irritable Bowel Syndrome. *Phytotherapy Research*, *29*(11), 1822–1827. https://doi.org/10.1002/ptr.5475

Chen, H., Zhang, F., Zhang, J., Zhang, X., Guo, Y., & Yao, Q. (2020). A Holistic View of Berberine Inhibiting Intestinal Carcinogenesis in Conventional Mice Based on Microbiome-Metabolomics Analysis. *Frontiers in Immunology*, *11*. https://doi.org/10.3389/FIMMU.2020.588079

Chen, K., & Pachter, L. (2005). Bioinformatics for whole-genome shotgun sequencing of microbial communities. *{PLoS} Computational Biology*, *1*(2), 106–112. https://doi.org/10.1371/journal.pcbi.0010024

Chen, W., Miao, Y.-Q., Fan, D.-J., Yang, S.-S., Lin, X., Meng, L.-K., & Tang, X. (2011). Bioavailability study of berberine and the enhancing effects of {TPGS} on intestinal absorption in rats. *{AAPS} {PharmSciTech}*, *12*(2), 705–711. https://doi.org/10.1208/s12249-011-9632-z

Chen, Y. ran, Zheng, H. min, Zhang, G. xia, Chen, F. lan, Chen, L. dan, & Yang, Z. cong. (2020). High Oscillospira abundance indicates constipation and low BMI in the Guangdong Gut Microbiome Project. *Scientific Reports 2020 10:1*, *10*(1), 1–8. https://doi.org/10.1038/s41598-020-66369-z

Chen, Y., Wang, J., Yu, L., Xu, T., & Zhu, N. (2020). Microbiota and metabolome responses in the cecum and serum of broiler chickens fed with plant essential oils or virginiamycin. *Scientific Reports*, *10*(1). https://doi.org/10.1038/S41598-020-60135-X

Cheng, J., Hicks, D. B., & Krulwich, T. A. (1996). The purified Bacillus subtilis tetracycline efflux protein TetA(L) reconstitutes both tetracycline-cobalt/H+ and Na+(K+)/H+ exchange. *Proceedings of the National Academy of Sciences of the United States of America*, *93*(25), 14446–14451. https://doi.org/10.1073/PNAS.93.25.14446

Chiang, Y. N., Penadés, J. R., & Chen, J. (2019). Genetic transduction by phages and chromosomal islands: The new and noncanonical. *PLoS Pathogens*, *15*(8). https://doi.org/10.1371/JOURNAL.PPAT.1007878

Choi, C. H. (2005). ABC transporters as multidrug resistance mechanisms and the development of chemosensitizers for their reversal. *Cancer Cell International*, *5*, 30. https://doi.org/10.1186/1475-2867-5-30

Choi, H.-J., Kim, J.-H., Lee, C.-H., Ahn, Y.-J., Song, J.-H., Baek, S.-H., & Kwon, D.-H. (2009). Antiviral activity of quercetin 7-rhamnoside against porcine epidemic diarrhea virus. *Antiviral Research*, *81*(1), 77–81. https://doi.org/10.1016/j.antiviral.2008.10.002

Choudhari, A. S., Mandave, P. C., Deshpande, M., Ranjekar, P., & Prakash, O. (2019). Phytochemicals in cancer treatment: from preclinical studies to clinical practice. *Frontiers in Pharmacology*, *10*, 1614. https://doi.org/10.3389/fphar.2019.01614

Chu, M., Ding, R., Chu, Z., Zhang, M., Liu, X., Xie, S., Zhai, Y., & Wang, Y. (2014). Role of berberine in anti-bacterial as a high-affinity {LPS} antagonist binding to {TLR4}/{MD}-2 receptor. *{BMC} Complementary and Alternative Medicine*, *14*, 89. https://doi.org/10.1186/1472-6882-14-89

Chu, M., Zhang, M.-B., Liu, Y.-C., Kang, J.-R., Chu, Z.-Y., Yin, K.-L., Ding, L.-Y., Ding, R., Xiao, R.-X., Yin, Y.-N., Liu, X.-Y., & Wang, Y.-D. (2016). Role of Berberine in the Treatment of Methicillin-Resistant Staphylococcus aureus Infections. *Scientific Reports*, *6*, 24748. https://doi.org/10.1038/srep24748

Chun, O. K., Chung, S. J., & Song, W. O. (2007). Estimated dietary flavonoid intake and major food sources of U.S. adults. *The Journal of Nutrition*, *137*(5), 1244–1252. https://doi.org/10.1093/jn/137.5.1244

Chung, C. T., Niemela, S. L., & Miller, R. H. (1989). One-step preparation of competent Escherichia coli: transformation and storage of bacterial cells in the same solution. *Proceedings of the National Academy of Sciences of the United States of America*, *86*(7),

2172–2175. https://doi.org/10.1073/pnas.86.7.2172

Chung, E. J., Lim, H. K., Kim, J.-C., Choi, G. J., Park, E. J., Lee, M. H., Chung, Y. R., & Lee, S.-W. (2008). Forest soil metagenome gene cluster involved in antifungal activity expression in Escherichia coli. *Applied and Environmental Microbiology*, *74*(3), 723–730. https://doi.org/10.1128/{AEM}.01911-07

Chung, M.-Y., Song, J.-H., Lee, J., Shin, E. J., Park, J. H., Lee, S.-H., Hwang, J.-T., & Choi, H.-K. (2019). Tannic acid, a novel histone acetyltransferase inhibitor, prevents non-alcoholic fatty liver disease both in vivo and in vitro model. *Molecular Metabolism*, *19*, 34–48. https://doi.org/10.1016/j.molmet.2018.11.001

Cogliani, C., Goossens, H., & Greko, C. (2011). Restricting Antimicrobial Use in Food Animals: Lessons from Europe. *Microbe Magazine*, *6*(6), 274–279. https://doi.org/10.1128/microbe.6.274.1

Coherent Market Insights. (2020). *Global Poultry Market to Reach US$ 347,265.8 Mn by 2027*. https://www.businesswire.com/news/home/20191119005491/en/

Colavecchio, A., Cadieux, B., Lo, A., & Goodridge, L. D. (2017). Bacteriophages contribute to the spread of antibiotic resistance genes among foodborne pathogens of the Enterobacteriaceae family - A review. *Frontiers in Microbiology*, *8*(JUN), 1108. https://doi.org/10.3389/FMICB.2017.01108/BIBTEX

Conroy, O., Kim, E. H., McEvoy, M. M., & Rensing, C. (2010). Differing ability to transport nonmetal substrates by two RND-type metal exporters. *FEMS Microbiology Letters*, *308*(2), 115–122. https://doi.org/10.1111/J.1574-6968.2010.02006.X

Consuegra, J., Gaffé, J., Lenski, R. E., Hindré, T., Barrick, J. E., Tenaillon, O., & Schneider, D. (2021). Insertion-sequence-mediated mutations both promote and constrain evolvability during a long-term experiment with bacteria. *Nature Communications 2021 12:1*, *12*(1), 1–12. https://doi.org/10.1038/s41467-021-21210-7

Cordillot, M., Dubée, V., Triboulet, S., Dubost, L., Marie, A., Hugonnet, J. E., Arthur, M., & Mainardia, J. L. (2013). In vitro cross-linking of Mycobacterium tuberculosis peptidoglycan by L,D-transpeptidases and inactivation of these enzymes by carbapenems. *Antimicrobial Agents and Chemotherapy*, *57*(12), 5940–5945. https://doi.org/10.1128/AAC.01663-13

Corkill, M. (1989). *Characterisation of a occulating strain of pseudomonas putida* [Durham University]. http://etheses.dur.ac.uk/6419/

Crader, M. F., & Varacallo, M. (2021). Preoperative Antibiotic Prophylaxis. In *StatPearls*. {StatPearls} Publishing. https://www.ncbi.nlm.nih.gov/pubmed/28723061

Cushnie, T. P. T., & Lamb, A. J. (2005). Antimicrobial activity of flavonoids. *International Journal of Antimicrobial Agents*, *26*(5), 343–356. https://doi.org/10.1016/j.ijantimicag.2005.09.002

Czaplewski, L., Bax, R., Clokie, M., Dawson, M., Fairhead, H., Fischetti, V. A., Foster, S., Gilmore, B. F., Hancock, R. E. W., Harper, D., Henderson, I. R., Hilpert, K., Jones, B. V, Kadioglu, A., Knowles, D., Ólafsdóttir, S., Payne, D., Projan, S., Shaunak, S., … Rex, J. H. (2016). Alternatives to antibiotics-a pipeline portfolio review. *The Lancet Infectious Diseases*, *16*(2), 239–251. https://doi.org/10.1016/S1473-3099(15)00466-1

D'Costa, V. M., King, C. E., Kalan, L., Morar, M., Sung, W. W. L., Schwarz, C., Froese, D., Zazula, G., Calmels, F., Debruyne, R., Golding, G. B., Poinar, H. N., & Wright, G. D. (2011).

Antibiotic resistance is ancient. *Nature*, *477*(7365), 457–461. https://doi.org/10.1038/nature10388

Dabeek, W. M., & Marra, M. V. (2019). Dietary Quercetin and Kaempferol: Bioavailability and Potential Cardiovascular-Related Bioactivity in Humans. *Nutrients*, *11*(10). https://doi.org/10.3390/NU11102288

Dale, J. L., Cagnazzo, J., Phan, C. Q., Barnes, A. M. T., & Dunny, G. M. (2015). Multiple roles for Enterococcus faecalis glycosyltransferases in biofilm-associated antibiotic resistance, cell envelope integrity, and conjugative transfer. *Antimicrobial Agents and Chemotherapy*, *59*(7), 4094–4105. https://doi.org/10.1128/AAC.00344-15/SUPPL_FILE/ZAC007154135SO1.PDF

Dall, C. (2018). *Novartis drops antibiotic development program*. Center for Infectious Disease Research and Policy. http://www.cidrap.umn.edu/news-perspective/2018/07/novartis-drops-antibiotic-development-program

Darling, A. L., & Uversky, V. N. (2018). Intrinsic disorder and posttranslational modifications: The darker side of the biological dark matter. *Frontiers in Genetics*, *9*(MAY), 158. https://doi.org/10.3389/FGENE.2018.00158/BIBTEX

Das, S., Batra, S., Gupta, P. P., Kumar, M., Srivastava, V. K., Jyoti, A., Singh, N., & Kaushik, S. (2019). Identification and evaluation of quercetin as a potential inhibitor of naphthoate synthase from Enterococcus faecalis. *Journal of Molecular Recognition*, e2802. https://doi.org/10.1002/jmr.2802

Datta, N., & Kontomichalou, P. (1965). Penicillinase synthesis controlled by infectious R factors in Enterobacteriaceae. *Nature*, *208*(5007), 239–241. https://doi.org/10.1038/208239a0

Davis, I. J., Roberts, A. P., Ready, D., Richards, H., Wilson, M., & Mullany, P. (2005). Linkage of a novel mercury resistance operon with streptomycin resistance on a conjugative plasmid in Enterococcus faecium. *Plasmid*, *54*(1), 26–38. https://doi.org/10.1016/J.PLASMID.2004.10.004

de Castilho, T. S., Matias, T. B., Nicolini, K. P., & Nicolini, J. (2018). Study of interaction between metal ions and quercetin. *Food Science and Human Wellness*, *7*(3), 215–219. https://doi.org/10.1016/J.FSHW.2018.08.001

de Castro, A. P., Fernandes, G. da R., & Franco, O. L. (2014). Insights into novel antimicrobial compounds and antibiotic resistance genes from soil metagenomes. *Frontiers in Microbiology*, *5*, 489. https://doi.org/10.3389/fmicb.2014.00489

De Lorenzo, V., Watanabe, K., & Uchiyama, T. (2005). Problems with metagenomic screening. *Nature Biotechnology 2005 23:9*, *23*(9), 1045–1045. https://doi.org/10.1038/nbt0905-1045a

De Maesschalck, C., Eeckhaut, V., Maertens, L., De Lange, L., Marchal, L., Nezer, C., De Baere, S., Croubels, S., Daube, G., Dewulf, J., Haesebrouck, F., Ducatelle, R., Taminau, B., & Van Immerseel, F. (2015). Effects of Xylo-Oligosaccharides on Broiler Chicken Performance and Microbiota. *Applied and Environmental Microbiology*, *81*(17), 5880. https://doi.org/10.1128/AEM.01616-15

de Tejada, B. (2014). Antibiotic use and misuse during pregnancy and delivery: benefits and risks. *International Journal of Environmental Research and Public Health*, *11*(8), 7993–8009. https://doi.org/10.3390/ijerph110807993

de Vicente, A., Avilés, M., Codina, J. C., Borrego, J. J., & Romero, P. (1990). Resistance to antibiotics and heavy metals of Pseudomonas aeruginosa isolated from natural waters. *The Journal of Applied Bacteriology*, *68*(6), 625–632. https://www.ncbi.nlm.nih.gov/pubmed/2118131

De Wiele, T. Van, Boon, N., Possemiers, S., Jacobs, H., & Verstraete, W. (2004). Prebiotic effects of chicory inulin in the simulator of the human intestinal microbial ecosystem. *FEMS Microbiology Ecology*, *51*(1), 143–153. https://doi.org/10.1016/J.FEMSEC.2004.07.014

Deatherage, D. E., & Barrick, J. E. (2014). Identification of mutations in laboratory evolved microbes from next-generation sequencing data using breseq. *Methods in Molecular Biology (Clifton, N.J.)*, *1151*, 165. https://doi.org/10.1007/978-1-4939-0554-6_12

Dec, M., Stępień-Pyśniak, D., Nowaczek, A., Puchalski, A., & Urban-Chmiel, R. (2020). Phenotypic and genotypic antimicrobial resistance profiles of fecal lactobacilli from domesticated pigeons in Poland. *Anaerobe*, *65*. https://doi.org/10.1016/J.ANAEROBE.2020.102251

Dec, M., Urban-Chmiel, R., Stępień-Pyśniak, D., & Wernicki, A. (2017). Assessment of antibiotic susceptibility in Lactobacillus isolates from chickens. *Gut Pathogens*, *9*(1), 1–16. https://doi.org/10.1186/S13099-017-0203-Z/TABLES/6

Dehghani, N., Afsharmanesh, M., Salarmoini, M., & Ebrahimnejad, H. (2019). In vitro and in vivo evaluation of thyme (Thymus vulgaris) essential oil as an alternative for antibiotic in quail diet1. *Journal of Animal Science*, *97*(7), 2901–2913. https://doi.org/10.1093/jas/skz179

Delacon. (2020). *Phytogenic solutions for animal nutrition*. https://www.delacon.com/

Demain, A. L. (2009). Antibiotics: natural products essential to human health. *Medicinal Research Reviews*, *29*(6), 821–842. https://doi.org/10.1002/med.20154

Dho-Moulin, M., & Fairbrother, J. M. (1999). Avian pathogenic Escherichia coli ({APEC}). *Veterinary Research*, *30*(2–3), 299–316. https://www.ncbi.nlm.nih.gov/pubmed/10367360

Di Cesare, A., Eckert, E. M., D'Urso, S., Bertoni, R., Gillan, D. C., Wattiez, R., & Corno, G. (2016). Co-occurrence of integrase 1, antibiotic and heavy metal resistance genes in municipal wastewater treatment plants. *Water Research*, *94*, 208–214. https://doi.org/10.1016/j.watres.2016.02.049

Diarra, M. S., Silversides, F. G., Diarrassouba, F., Pritchard, J., Masson, L., Brousseau, R., Bonnet, C., Delaquis, P., Bach, S., Skura, B. J., & Topp, E. (2007). Impact of feed supplementation with antimicrobial agents on growth performance of broiler chickens, Clostridium perfringens and enterococcus counts, and antibiotic resistance phenotypes and distribution of antimicrobial resistance determinants in Escheric. *Applied and Environmental Microbiology*, *73*(20), 6566–6576. https://doi.org/10.1128/{AEM}.01086-07

Díaz Carrasco, J. M., Redondo, E. A., Pin Viso, N. D., Redondo, L. M., Farber, M. D., & Fernández Miyakawa, M. E. (2018). Tannins and bacitracin differentially modulate gut microbiota of broiler chickens. *{BioMed} Research International*, *2018*, 1879168. https://doi.org/10.1155/2018/1879168

Dibner, J. J., & Richards, J. D. (2005). Antibiotic growth promoters in agriculture: history and

mode of action. *Poultry Science*, *84*(4), 634–643. https://doi.org/10.1093/ps/84.4.634

Dinh, D. M., Volpe, G. E., Duffalo, C., Bhalchandra, S., Tai, A. K., Kane, A. V., Wanke, C. A., & Ward, H. D. (2015). Intestinal Microbiota, Microbial Translocation, and Systemic Inflammation in Chronic HIV Infection. *The Journal of Infectious Diseases*, *211*(1), 19. https://doi.org/10.1093/INFDIS/JIU409

Dollwet, H. H. (1985). Historic uses of copper compounds in medicine. *Trace Elem. Med.* https://ci.nii.ac.jp/naid/10030099966/

Domadia, P. N., Bhunia, A., Sivaraman, J., Swarup, S., & Dasgupta, D. (2008). Berberine targets assembly of Escherichia coli cell division protein FtsZ. *Biochemistry*, *47*(10), 3225–3234. https://doi.org/10.1021/BI7018546

Dong, H., Wang, N., Zhao, L., & Lu, F. (2012). Berberine in the treatment of type 2 diabetes mellitus: a systemic review and meta-analysis. *Evidence-Based Complementary and Alternative Medicine*, *2012*, 591654. https://doi.org/10.1155/2012/591654

Doss, S. A. (1994). Chromosomally-mediated antibiotic resistance and virulence. *Journal of Medical Microbiology*, *40*(5), 305–306. https://doi.org/10.1099/00222615-40-5-305/CITE/REFWORKS

Doyle, S. (2018, June 17). *Pseudomonas aeruginosa strain NCTC9433 genome assembly, chromosome: 1* . National Library of Medicine. https://www.ncbi.nlm.nih.gov/nucleotide/LS483497.1?report=genbank&log$=nuclalign&blast_rank=1&RID=8WEXNYVS016&from=4237845&to=4246103

Drenkard, E. (2003). Antimicrobial resistance of Pseudomonas aeruginosa biofilms. *Microbes and Infection*, *5*(13), 1213–1219. https://doi.org/10.1016/j.micinf.2003.08.009

Dritz, S. S., Tokach, M. D., Goodband, R. D., & Nelssen, J. L. (2002). Effects of administration of antimicrobials in feed on growth rate and feed efficiency of pigs in multisite production systems. *Journal of the American Veterinary Medical Association*, *220*(11), 1690–1695. https://www.ncbi.nlm.nih.gov/pubmed/12051512

Durso, L. M., & Cook, K. L. (2014). Impacts of antibiotic use in agriculture: what are the benefits and risks? *Current Opinion in Microbiology*, *19*, 37–44. https://doi.org/10.1016/j.mib.2014.05.019

Eberwine, J., Yeh, H., Miyashiro, K., Cao, Y., Nair, S., Finnell, R., Zettel, M., & Coleman, P. (1992). Analysis of gene expression in single live neurons. *Proceedings of the National Academy of Sciences of the United States of America*, *89*(7), 3010. https://doi.org/10.1073/PNAS.89.7.3010

Edwards, U., Rogall, T., Blöcker, H., Emde, M., & Böttger, E. C. (1989). Isolation and direct complete nucleotide determination of entire genes. Characterization of a gene coding for 16S ribosomal RNA. *Nucleic Acids Research*, *17*(19), 7843–7853. https://doi.org/10.1093/NAR/17.19.7843

Ehrlich, P., & Hata, S. (1910). *Die experimentelle Chemotherapie der Spirillosen*. Springer Berlin Heidelberg. https://doi.org/10.1007/978-3-642-64926-4

El-Fouly, M. Z., Sharaf, A. M., Shahin, A. A. M., El-Bialy, H. A., & Omara, A. M. A. (2015). Biosynthesis of pyocyanin pigment by Pseudomonas aeruginosa. *Journal of Radiation Research and Applied Sciences*, *8*(1), 36–48. https://doi.org/10.1016/J.JRRAS.2014.10.007

EL-Sawah, A. A., Dahshan, A. H. M., El-Nahass, E.-S., & El-Mawgoud, A. I. A. (2018). Pathogenicity of Escherichia coli O157 in commercial broiler chickens. *Beni-Suef University Journal of Basic and Applied Sciences*, *7*(4), 620–625. https://doi.org/10.1016/J.BJBAS.2018.07.005

Elfawal, M. A., Towler, M. J., Reich, N. G., Weathers, P. J., & Rich, S. M. (2015). Dried whole-plant Artemisia annua slows evolution of malaria drug resistance and overcomes resistance to artemisinin. *Proceedings of the National Academy of Sciences of the United States of America*, *112*(3), 821–826. https://doi.org/10.1073/pnas.1413127112

Elumalai, P., & Lakshmi, S. (2016). Role of quercetin benefits in neurodegeneration. *Advances in Neurobiology*, *12*, 229–245. https://doi.org/10.1007/978-3-319-28383-8_12

Erdem, H., Tetik, A., Arun, O., Besirbellioglu, B. A., Coskun, O., & Eyigun, C. P. (2011). War and infection in the pre-antibiotic era: the Third Ottoman Army in 1915. *Scandinavian Journal of Infectious Diseases*, *43*(9), 690–695. https://doi.org/10.3109/00365548.2011.577801

Erdemli, S. B., Gupta, R., Bishai, W. R., Lamichhane, G., Amzel, L. M., & Bianchet, M. A. (2012). Targeting the Cell Wall of Mycobacterium tuberculosis: Structure and Mechanism of L,D-Transpeptidase 2. *Structure*, *20*(12), 2103–2115. https://doi.org/10.1016/J.STR.2012.09.016

Escherich, T. (1998). The intestinal bacteria of the neonate and breast-fed infant. 1884. *Reviews of Infectious Diseases*, *10*(6), 1220–1225. https://doi.org/10.1093/clinids/10.6.1220

Esser, K., Kück, U., Lang-Hinrichs, C., Lemke, P., Osiewacz, H. D., Stahl, U., & Tudzynski, P. (1986). *Plasmids of Eukaryotes*. Springer Berlin Heidelberg. https://doi.org/10.1007/978-3-642-82585-9

EUCAST. (2022). *Clinical breakpoints and dosing of antibiotics*. https://www.eucast.org/clinical_breakpoints/

Ezzati, M., Yousefi, B., Velaei, K., & Safa, A. (2020). A review on anti-cancer properties of Quercetin in breast cancer. *Life Sciences*, 117463. https://doi.org/10.1016/j.lfs.2020.117463

Faccioli, C. K., Chedid, R. A., Mori, R. H., Amaral, A. C. do, Franceschini-Vicentini, I. B., & Vicentini, C. A. (2016). Acid and alkaline phosphatase localization in the digestive tract mucosa of the Hemisorubim platyrhynchos. *Acta Histochemica*, *118*(7), 722–728. https://doi.org/10.1016/j.acthis.2016.08.001

Fakhruddin, A. N. M., & Quilty, B. (2007). Measurement of the growth of a floc forming bacterium Pseudomonas putida CP1. *Biodegradation*, *18*(2), 189–197. https://doi.org/10.1007/S10532-006-9054-X

Farzana, A., & Shamsuzzaman, S. M. (2015). In vitro efficacy of synergistic antibiotic combinations in imipenem resistant Pseudomonas aeruginosa strains. *Bangladesh Journal of Medical Microbiology*, *9*(1), 3–8. https://doi.org/10.3329/BJMM.V9I1.31332

Fazli, M., Bjarnsholt, T., As, Kirketerp-Møller, K., Jørgensen, B., Andersen, A. S., Krogfelt, K. A., Givskov, M., & Tolker-Nielsen, T. (2009). Nonrandom distribution of Pseudomonas aeruginosa and Staphylococcus aureus in chronic wounds. *Journal of Clinical Microbiology*, *47*(12), 4084–4089. https://doi.org/10.1128/JCM.01395-09

Fenner, L., Richet, H., Raoult, D., Papazian, L., Martin, C., & La Scola, B. (2006). Are clinical

isolates of Pseudomonas aeruginosa more virulent than hospital environmental isolates in amebal co-culture test? *Critical Care Medicine*, *34*(3), 823–828. https://doi.org/10.1097/01.{CCM}.0000201878.51343.F1

Ferenczyova, K., Kalocayova, B., & Bartekova, M. (2020). Potential implications of quercetin and its derivatives in cardioprotection. *International Journal of Molecular Sciences*, *21*(5). https://doi.org/10.3390/ijms21051585

Fesseha, H., Demlie, T., Mathewos, M., & Eshetu, E. (2021). Effect of Lactobacillus Species Probiotics on Growth Performance of Dual-Purpose Chicken. *Veterinary Medicine : Research and Reports*, *12*, 75. https://doi.org/10.2147/VMRR.S300881

Flemming, A. (1929). On the Antibacterial Action of Cultures of a Penicillium, with Special Reference to Their Use in the Isolation of B. influenzae. *British Journal of Experimental Pathology*, *10*, 226–236.

Flemming, H., & Wingender, J. (2010). The biofilm matrix. *Nature Reviews. Microbiology*, *8*(9), 623–633. https://doi.org/10.1038/NRMICRO2415

Fong, J. N. C., & Yildiz, F. H. (2015). Biofilm Matrix Proteins. *Microbiology Spectrum*, *3*(2). https://doi.org/10.1128/MICROBIOLSPEC.MB-0004-2014

Fouhy, F., Deane, J., Rea, M. C., O'Sullivan, Ó., Ross, R. P., O'Callaghan, G., Plant, B. J., & Stanton, C. (2015). The Effects of Freezing on Faecal Microbiota as Determined Using MiSeq Sequencing and Culture-Based Investigations. *PLOS ONE*, *10*(3), e0119355. https://doi.org/10.1371/JOURNAL.PONE.0119355

Freile, M. L., Giannini, F., Pucci, G., Sturniolo, A., Rodero, L., Pucci, O., Balzareti, V., & Enriz, R. D. (2003). Antimicrobial activity of aqueous extracts and of berberine isolated from Berberis heterophylla. *Fitoterapia*, *74*(7–8), 702–705. https://doi.org/10.1016/S0367-{326X}(03)00156-4

Friswell, M. K., Gika, H., Stratford, I. J., Theodoridis, G., Telfer, B., Wilson, I. D., & McBain, A. J. (2010). Site and Strain-Specific Variation in Gut Microbiota Profiles and Metabolism in Experimental Mice. *PLOS ONE*, *5*(1), e8584. https://doi.org/10.1371/JOURNAL.PONE.0008584

Fujita, M., Mori, K., Hara, H., Hishiyama, S., Kamimura, N., & Masai, E. (2019). A TonB-dependent receptor constitutes the outer membrane transport system for a lignin-derived aromatic compound. *Communications Biology 2019 2:1*, *2*(1), 1–10. https://doi.org/10.1038/s42003-019-0676-z

Gajdács, M., Baráth, Z., Kárpáti, K., Szabó, D., Usai, D., Zanetti, S., & Donadu, M. G. (2021). No correlation between biofilm formation, virulence factors, and antibiotic resistance in pseudomonas aeruginosa: Results from a laboratory-based in vitro study. *Antibiotics*, *10*(9). https://doi.org/10.3390/ANTIBIOTICS10091134

Galli, G. M., Gerbet, R. R., Griss, L. G., Fortuoso, B. F., Petrolli, T. G., Boiago, M. M., Souza, C. F., Baldissera, M. D., Mesadri, J., Wagner, R., da Rosa, G., Mendes, R. E., Gris, A., & Da Silva, A. S. (2020). Combination of herbal components (curcumin, carvacrol, thymol, cinnamaldehyde) in broiler chicken feed: Impacts on response parameters, performance, fatty acid profiles, meat quality and control of coccidia and bacteria. *Microbial Pathogenesis*, *139*, 103916. https://doi.org/10.1016/j.micpath.2019.103916

Gambuti, A., Picariello, L., Rinaldi, A., Forino, M., Blaiotta, G., Moine, V., & Moio, L. (2020). New insights into the formation of precipitates of quercetin in Sangiovese wines.

Journal of Food Science and Technology 2020 57:7, *57*(7), 2602–2611. https://doi.org/10.1007/S13197-020-04296-7

Gao, W., Wu, K., Chen, L., Fan, H., Zhao, Z., Gao, B., Wang, H., & Wei, D. (2016). A novel esterase from a marine mud metagenomic library for biocatalytic synthesis of short-chain flavor esters. *Microbial Cell Factories*, *15*(1), 1–12. https://doi.org/10.1186/S12934-016-0435-5/FIGURES/5

Gao, Y., Shang, Q., Li, W., Guo, W., Stojadinovic, A., Mannion, C., Man, Y.-G., & Chen, T. (2020). Antibiotics for cancer treatment: A double-edged sword. *Journal of Cancer*, *11*(17), 5135–5149. https://doi.org/10.7150/jca.47470

Garrett, T. R., Bhakoo, M., & Zhang, Z. (2008). Bacterial adhesion and biofilms on surfaces. *Progress in Natural Science*, *18*(9), 1049–1056. https://doi.org/10.1016/J.PNSC.2008.04.001

Garvey, M. I., & Piddock, L. J. V. (2008). The efflux pump inhibitor reserpine selects multidrug-resistant Streptococcus pneumoniae strains that overexpress the {ABC} transporters {PatA} and {PatB}. *Antimicrobial Agents and Chemotherapy*, *52*(5), 1677–1685. https://doi.org/10.1128/{AAC}.01644-07

Garza-González, E., Bocanegra-Ibarias, P., Rodríguez-Noriega, E., González-Díaz, E., Silva-Sanchez, J., Garza-Ramos, U., Contreras-Coronado-Tovar, I. F., Santos-Hernández, J. E., Gutiérrez-Bañuelos, D., Mena-Ramirez, J. P., Ramírez-De-los-Santos, S., Camacho-Ortiz, A., & Morfín-Otero, R. (2021). Molecular investigation of an outbreak associated with total parenteral nutrition contaminated with NDM-producing Leclercia adecarboxylata. *BMC Infectious Diseases*, *21*(1), 1–8. https://doi.org/10.1186/S12879-021-05923-0/FIGURES/1

Georgieva, A., Ilieva, Y., Kokanova-Nedialkova, Z., Zaharieva, M. M., Nedialkov, P., Dobreva, A., Kroumov, A., Najdenski, H., & Mileva, M. (2021). Redox-modulating capacity and antineoplastic activity of wastewater obtained from the distillation of the essential oils of four bulgarian oil-bearing roses. *Antioxidants*, *10*(10). https://doi.org/10.3390/ANTIOX10101615/S1

Georgopapadakou, N. H., Dix, B. A., & Mauriz, Y. R. (1986). Possible physiological functions of penicillin-binding proteins in Staphylococcus aureus. *Antimicrobial Agents and Chemotherapy*, *29*(2), 333–336. https://doi.org/10.1128/AAC.29.2.333

Gessard, C. (1984). On the Blue and Green Coloration that Appears on Bandages. *Clinical Infectious Diseases*, *6*(Supplement_3), S775–S776. https://doi.org/10.1093/clinids/6.Supplement_3.S775

Ghaith, D. M., Mohamed, Z. K., Farahat, M. G., Aboulkasem Shahin, W., & Mohamed, H. O. (2019). Colonization of intestinal microbiota with carbapenemase-producing Enterobacteriaceae in paediatric intensive care units in Cairo, Egypt. *Arab Journal of Gastroenterology*, *20*(1), 19–22. https://doi.org/10.1016/J.AJG.2019.01.002

GitHub - rrwick/Filtlong: quality filtering tool for long reads. (n.d.). Retrieved August 10, 2021, from https://github.com/rrwick/Filtlong

GitHub - rrwick/Porechop: adapter trimmer for Oxford Nanopore reads. (n.d.). Retrieved August 10, 2021, from https://github.com/rrwick/Porechop

Glendinning, L., Watson, K. A., & Watson, M. (2019). Development of the duodenal, ileal, jejunal and caecal microbiota in chickens. *Animal Microbiome*, *1*(1).

https://doi.org/10.1186/S42523-019-0017-Z

Godbey, W. T. (2022). Cell growth. *Biotechnology and Its Applications*, 117–150. https://doi.org/10.1016/B978-0-12-817726-6.00005-8

Gomes, E. S., Schuch, V., & de Macedo Lemos, E. G. (2013). Biotechnology of polyketides: new breath of life for the novel antibiotic genetic pathways discovery through metagenomics. *Brazilian Journal of Microbiology : [Publication of the Brazilian Society for Microbiology]*, *44*(4), 1007–1034. https://doi.org/10.1590/s1517-83822013000400002

Gouy, M., & Gautier, C. (1982). Codon usage in bacteria: correlation with gene expressivity. *Nucleic Acids Research*, *10*(22), 7055–7074. https://doi.org/10.1093/NAR/10.22.7055

Granneman, S., Kudla, G., Petfalski, E., & Tollervey, D. (2009). Identification of protein binding sites on U3 {snoRNA} and pre-{rRNA} by {UV} cross-linking and high-throughput analysis of {cDNAs}. *Proceedings of the National Academy of Sciences of the United States of America*, *106*(24), 9613–9618. https://doi.org/10.1073/pnas.0901997106

Greco, S., Islam, M. S., Zannotti, A., Carpini, G. D., Giannubilo, S. R., Ciavattini, A., Petraglia, F., & Ciarmela, P. (2020). Quercetin and indole-3-carbinol inhibit extracellular matrix expression in human primary uterine leiomyoma cells. *Reproductive Biomedicine Online*. https://doi.org/10.1016/j.rbmo.2020.01.006

Greene, N. P., Kaplan, E., Crow, A., & Koronakis, V. (2018). Antibiotic resistance mediated by the MacB ABC transporter family: A structural and functional perspective. *Frontiers in Microbiology*, *9*(MAY), 950. https://doi.org/10.3389/FMICB.2018.00950/BIBTEX

Grocock, R. J., & Sharp, P. M. (2002). Synonymous codon usage in Pseudomonas aeruginosa PA01. *Gene*, *289*(1–2), 131–139. https://doi.org/10.1016/S0378-1119(02)00503-6

GSL Biotech. (2020). *SnapGene® software (www.snapgene.com)*. https://www.snapgene.com/

Guaragni, A., Boiago, M. M., Bottari, N. B., Morsch, V. M., Lopes, T. F., & da Silva, A. (2020). Feed supplementation with inulin on broiler performance and meat quality challenged with Clostridium perfringens: Infection and prebiotic impacts. *Microbial Pathogenesis*, *139*, 103889. https://doi.org/10.1016/j.micpath.2019.103889

Guerra, F. Q. S., Mendes, J. M., Sousa, J. P. de, Morais-Braga, M. F. B., Santos, B. H. C., Melo Coutinho, H. D., & Lima, E. de O. (2012). Increasing antibiotic activity against a multidrug-resistant Acinetobacter spp by essential oils of Citrus limon and Cinnamomum zeylanicum. *Natural Product Research*, *26*(23), 2235–2238. https://doi.org/10.1080/14786419.2011.647019

Gullberg, E., Albrecht, L. M., Karlsson, C., Sandegren, L., & Andersson, D. I. (2014). Selection of a multidrug resistance plasmid by sublethal levels of antibiotics and heavy metals. *MBio*, *5*(5), e01918-14. https://doi.org/10.1128/{mBio}.01918-14

Gullberg, E., Cao, S., Berg, O. G., Ilbäck, C., Sandegren, L., Hughes, D., & Andersson, D. I. (2011). Selection of resistant bacteria at very low antibiotic concentrations. *{PLoS} Pathogens*, *7*(7), e1002158. https://doi.org/10.1371/journal.ppat.1002158

Guo, P., Zhang, K., Ma, X., & He, P. (2020). Clostridium species as probiotics: Potentials and challenges. *Journal of Animal Science and Biotechnology*, *11*(1), 1–10. https://doi.org/10.1186/S40104-019-0402-1/FIGURES/2

Guo, Y., Zhang, Y. C., Huang, W. H., Selwyn, F. P., & Klaassen, C. D. (2016). Dose-response effect of berberine on bile acid profile and gut microbiota in mice. *BMC Complementary and Alternative Medicine*, *16*(1). https://doi.org/10.1186/S12906-016-1367-7

Gupta, S. K., & Ghosh, T. C. (2001). Gene expressivity is the main factor in dictating the codon usage variation among the genes in Pseudomonas aeruginosa. *Gene*, *273*(1), 63–70. https://doi.org/10.1016/S0378-1119(01)00576-5

Gupte, A., Jyot, J., Ravi, M., & Ramphal, R. (2021). High pyocyanin production and non-motility of Pseudomonas aeruginosa isolates are correlated with septic shock or death in bacteremic patients. *PloS One*, *16*(6). https://doi.org/10.1371/JOURNAL.PONE.0253259

Gutiérrez-Del-Río, I., Fernández, J., & Lombó, F. (2018). Plant nutraceuticals as antimicrobial agents in food preservation: terpenoids, polyphenols and thiols. *International Journal of Antimicrobial Agents*, *52*(3), 309–315. https://doi.org/10.1016/j.ijantimicag.2018.04.024

Gutman, T., Goren, G., Efroni, O., & Tuller, T. (2021). Estimating the predictive power of silent mutations on cancer classification and prognosis. *Npj Genomic Medicine 2021 6:1*, *6*(1), 1–15. https://doi.org/10.1038/s41525-021-00229-1

Hall T. (1999). BioEdit: Biological sequence alignment editor for Win95/98/NT/2K/XP. *Nucl Acids Symp Ser*, *41*, 95–98. https://www.scirp.org/(S(351jmbntvnsjt1aadkozje))/reference/referencespapers.aspx?referenceid=1306776

Hang, I., Rinttila, T., Zentek, J., Kettunen, A., Alaja, S., Apajalahti, J., Harmoinen, J., de Vos, W. M., & Spillmann, T. (2012). Effect of high contents of dietary animal-derived protein or carbohydrates on canine faecal microbiota. *BMC Veterinary Research*, *8*, 90. https://doi.org/10.1186/1746-6148-8-90

Harrison, E., & Brockhurst, M. A. (2012). Plasmid-mediated horizontal gene transfer is a coevolutionary process. *Trends in Microbiology*, *20*(6), 262–267. https://doi.org/10.1016/j.tim.2012.04.003

Harwood, C. R., Williams, D. M., & Lovett, P. S. (1983). Nucleotide sequence of a Bacillus pumilus gene specifying chloramphenicol acetyltransferase. *Gene*, *24*(2–3), 163–169. https://doi.org/10.1016/0378-1119(83)90076-8

Hatchette, T. F., Gupta, R., & Marrie, T. J. (2000). Pseudomonas aeruginosa community-acquired pneumonia in previously healthy adults: case report and review of the literature. *Clinical Infectious Diseases*, *31*(6), 1349–1356. https://doi.org/10.1086/317486

Hays, E. E., Wells, I. C., Katzman, P. A., & Cain, C. K. (1945). Antibiotic Substances produced by Pseu-domonas aeruginosa. *Biological \textellipsis*. https://www.cabdirect.org/cabdirect/abstract/19462700179

Hedblom, G. A., Reiland, H. A., Sylte, M. J., Johnson, T. J., & Baumler, D. J. (2018). Segmented filamentous bacteria - metabolism meets immunity. *Frontiers in Microbiology*, *9*(AUG), 1991. https://doi.org/10.3389/FMICB.2018.01991/XML/NLM

Hemaiswarya, S., Kruthiventi, A. K., & Doble, M. (2008). Synergism between natural products and antibiotics against infectious diseases. *Phytomedicine: International Journal of Phytotherapy and Phytopharmacology*, *15*(8), 639–652.

https://doi.org/10.1016/j.phymed.2008.06.008

Hesabi Nameghi, A., Edalatian, O., & Bakhshalinejad, R. (2019). Effects of a blend of thyme, peppermint and eucalyptus essential oils on growth performance, serum lipid and hepatic enzyme indices, immune response and ileal morphology and microflora in broilers. *Journal of Animal Physiology and Animal Nutrition*, *103*(5), 1388–1398. https://doi.org/10.1111/jpn.13122

Hillenmeyer, M. E., Fung, E., Wildenhain, J., Pierce, S. E., Hoon, S., Lee, W., Proctor, M., St.Onge, R. P., Tyers, M., Koller, D., Altman, R. B., Davis, R. W., Nislow, C., & Giaever, G. (2008). The chemical genomic portrait of yeast: Uncovering a phenotype for all genes. *Science*, *320*(5874), 362–365. https://doi.org/10.1126/SCIENCE.1150021/SUPPL_FILE/HILLENMEYER.SOM.PDF

Hoang, K. L., Morran, L. T., & Gerardo, N. M. (2016). Experimental evolution as an underutilized tool for studying beneficial animal-microbe interactions. *Frontiers in Microbiology*, *7*(SEP), 1444. https://doi.org/10.3389/FMICB.2016.01444/BIBTEX

Hoff, J. C., & Drake, C. H. (1960). Susceptibility of Pseudomonas polycolor to Pseudomonas aeruginosa bacteriophages. *Journal of Bacteriology*, *80*, 420–421. https://doi.org/10.1128/JB.80.3.420-421.1960/ASSET/36CC30A6-4D02-44C8-9C99-64D17A431098/ASSETS/JB.80.3.420-421.1960.FP.PNG

Honda, R., Tachi, C., Yasuda, K., Hirata, T., Noguchi, M., Hara-Yamamura, H., Yamamoto-Ikemoto, R., & Watanabe, T. (2020). Estimated discharge of antibiotic-resistant bacteria from combined sewer overflows of urban sewage system. *Npj Clean Water*, *3*(1), 15. https://doi.org/10.1038/s41545-020-0059-5

Hooper, D. C. (2001). Mechanisms of action of antimicrobials: focus on fluoroquinolones. *Clinical Infectious Diseases*, *32 Suppl 1*, S9–S15. https://doi.org/10.1086/319370

Hooper, L. V., Midwedt, T., & Gordon, J. I. (2002). How host-microbial interactions shape the nutrient environment of the mammalian intestine. *Annual Review of Nutrition*, *22*, 283–307. https://doi.org/10.1146/ANNUREV.NUTR.22.011602.092259

Horton, J. S., Flanagan, L. M., Jackson, R. W., Priest, N. K., & Taylor, T. B. (2021). A mutational hotspot that determines highly repeatable evolution can be built and broken by silent genetic changes. *Nature Communications*, *12*(1). https://doi.org/10.1038/S41467-021-26286-9

Hossein Khademi, S. M., Sazinas, P., & Jelsbak, L. (2019). Within-Host Adaptation Mediated by Intergenic Evolution in Pseudomonas aeruginosa. *Genome Biology and Evolution*, *11*(5), 1385. https://doi.org/10.1093/GBE/EVZ083

Huang, P., Zhang, Y., Xiao, K., Jiang, F., Wang, H., Tang, D., Liu, D., Liu, B., Liu, Y., He, X., Liu, H., Liu, X., Qing, Z., Liu, C., Huang, J., Ren, Y., Yun, L., Yin, L., Lin, Q., … Zeng, J. (2018). The chicken gut metagenome and the modulatory effects of plant-derived benzylisoquinoline alkaloids. *Microbiome*, *6*(1), 211. https://doi.org/10.1186/s40168-018-0590-5

Huang, T., Peng, X. Y., Gao, B., Wei, Q. L., Xiang, R., Yuan, M. G., & Xu, Z. H. (2019). The Effect of Clostridium butyricum on Gut Microbiota, Immune Response and Intestinal Barrier Function During the Development of Necrotic Enteritis in Chickens. *Frontiers in Microbiology*, *10*, 2309. https://doi.org/10.3389/FMICB.2019.02309/BIBTEX

Hubbard, A. T. M., Newire, E., Botelho, J., Reiné, J., Wright, E., Murphy, E. A., Hutton, W., &

Roberts, A. P. (2020). Isolation of an antimicrobial-resistant, biofilm-forming, Klebsiella grimontii isolate from a reusable water bottle. *MicrobiologyOpen*, e1023. https://doi.org/10.1002/mbo3.1023

Hugonnet, J. E., Mengin-Lecreulx, D., Monton, A., den Blaauwen, T., Carbonnelle, E., Veckerlé, C., Yves, V. B., van Nieuwenhze, M., Bouchier, C., Tu, K., Rice, L. B., & Arthur, M. (2016). Factors essential for L,D-transpeptidase-mediated peptidoglycan cross-linking and β-lactam resistance in Escherichia coli. *ELife*, *5*(OCTOBER2016). https://doi.org/10.7554/ELIFE.19469

Husain, F. M., Ahmad, I., Asif, M., & Tahseen, Q. (2013). Influence of clove oil on certain quorum-sensing-regulated functions and biofilm of Pseudomonas aeruginosa and Aeromonas hydrophila. *Journal of Biosciences 2013 38:5*, *38*(5), 835–844. https://doi.org/10.1007/S12038-013-9385-9

Hutchings, M., Truman, A., & Wilkinson, B. (2019). Antibiotics: past, present and future. *Current Opinion in Microbiology*, *51*, 72–80. https://doi.org/10.1016/J.MIB.2019.10.008

Hyung Ko, J., Gyu Kim, B., & Joong-Hoon, A. (2006). Glycosylation of flavonoids with a glycosyltransferase from Bacillus cereus. *{FEMS} Microbiology Letters*, *258*(2), 263–268. https://doi.org/10.1111/j.1574-6968.2006.00226.x

Ibrahim, M. E., Bilal, N. E., & Hamid, M. E. (2012). Increased multi-drug resistant Escherichia coli from hospitals in Khartoum state, Sudan. *African Health Sciences*, *12*(3), 368. https://doi.org/10.4314/AHS.V12I3.19

Ibrahim, R. A., Cryer, T. L., Lafi, S. Q., Basha, E. A., Good, L., & Tarazi, Y. H. (2019). Identification of Escherichia coli from broiler chickens in Jordan, their antimicrobial resistance, gene characterization and the associated risk factors. *BMC Veterinary Research*, *15*(1), 1–16. https://doi.org/10.1186/S12917-019-1901-1/TABLES/8

Igler, C., Rolff, J., & Regoes, R. (2021). Multi-step vs. single-step resistance evolution under different drugs, pharmacokinetics, and treatment regimens. *ELife*, *10*. https://doi.org/10.7554/ELIFE.64116

Ikemura, T. (1981). Correlation between the abundance of Escherichia coli transfer RNAs and the occurrence of the respective codons in its protein genes: A proposal for a synonymous codon choice that is optimal for the E. coli translational system. *Journal of Molecular Biology*, *151*(3), 389–409. https://doi.org/10.1016/0022-2836(81)90003-6

Ilett, E. E., Jørgensen, M., Noguera-Julian, M., Daugaard, G., Murray, D. D., Helleberg, M., Paredes, R., Lundgren, J., Sengeløv, H., & MacPherson, C. (2019). Gut microbiome comparability of fresh-frozen versus stabilized-frozen samples from hospitalized patients using 16S rRNA gene and shotgun metagenomic sequencing. *Scientific Reports 2019 9:1*, *9*(1), 1–11. https://doi.org/10.1038/s41598-019-49956-7

Imenshahidi, M., & Hosseinzadeh, H. (2016). Berberis vulgaris and berberine: an update review. *Phytotherapy Research*, *30*(11), 1745–1764. https://doi.org/10.1002/ptr.5693

Imwong, M., Suwannasin, K., Kunasol, C., Sutawong, K., Mayxay, M., Rekol, H., Smithuis, F. M., Hlaing, T. M., Tun, K. M., van der Pluijm, R. W., Tripura, R., Miotto, O., Menard, D., Dhorda, M., Day, N. P. J., White, N. J., & Dondorp, A. M. (2017). The spread of artemisinin-resistant Plasmodium falciparum in the Greater Mekong subregion: a molecular epidemiology observational study. *The Lancet Infectious Diseases*, *17*(5), 491–497. https://doi.org/10.1016/S1473-3099(17)30048-8

Iqbal, H. A., Craig, J. W., & Brady, S. F. (2014). Antibacterial enzymes from the functional screening of metagenomic libraries hosted in Ralstonia metallidurans. *FEMS Microbiology Letters*, *354*(1), 19–26. https://doi.org/10.1111/1574-6968.12431

Iramiot, J. S., Kajumbula, H., Bazira, J., De Villiers, E. P., & Asiimwe, B. B. (2020). Whole genome sequences of multi-drug resistant Escherichia coli isolated in a Pastoralist Community of Western Uganda: Phylogenomic changes, virulence and resistant genes. *PLOS ONE*, *15*(5), e0231852. https://doi.org/10.1371/JOURNAL.PONE.0231852

Ito, R., Mustapha, M. M., Tomich, A. D., Callaghan, J. D., McElheny, C. L., Mettus, R. T., Shanks, R. M. Q., Sluis-Cremer, N., & Doi, Y. (2017). Widespread fosfomycin resistance in Gram-negative bacteria attributable to the chromosomal fosA gene. *MBio*, *8*(4). https://doi.org/10.1128/MBIO.00749-17/ASSET/9090A787-FDFA-497D-A5CD-1EFAFAE17BE3/ASSETS/GRAPHIC/MBO0041734580002.JPEG

J Lane, D. (1991). 16S/23S rRNA sequencing,. In *Nucleic acid techniques in bacterial systematics* (pp. 115–147). https://www.scirp.org/(S(lz5mqp453edsnp55rrgjct55))/reference/ReferencesPapers.aspx?ReferenceID=1870033

Jaciuk, M., Nowak, E., Skowronek, K., Tañska, A., & Nowotny, M. (2011). Structure of UvrA nucleotide excision repair protein in complex with modified DNA. *Nature Structural & Molecular Biology 2011 18:2*, *18*(2), 191–197. https://doi.org/10.1038/nsmb.1973

Jacobitz, A. W., Kattke, M. D., Wereszczynski, J., & Clubb, R. T. (2017). Sortase Transpeptidases: Structural Biology and Catalytic Mechanism. *Advances in Protein Chemistry and Structural Biology*, *109*, 223–264. https://doi.org/10.1016/BS.APCSB.2017.04.008

Jafarinia, M., Sadat Hosseini, M., Kasiri, N., Fazel, N., Fathi, F., Ganjalikhani Hakemi, M., & Eskandari, N. (2020). Quercetin with the potential effect on allergic diseases. *Allergy, Asthma, and Clinical Immunology : Official Journal of the Canadian Society of Allergy and Clinical Immunology*, *16*, 36. https://doi.org/10.1186/s13223-020-00434-0

Janbaz, K. H., & Gilani, A. H. (2000). Studies on preventive and curative effects of berberine on chemical-induced hepatotoxicity in rodents. *Fitoterapia*, *71*(1), 25–33. https://doi.org/10.1016/S0367-326X(99)00098-2

Jang, J., Hur, H.-G., Sadowsky, M. J., Byappanahalli, M. N., Yan, T., & Ishii, S. (2017). Environmental Escherichia coli: ecology and public health implications-a review. *Journal of Applied Microbiology*, *123*(3), 570–581. https://doi.org/10.1111/jam.13468

Jank, T., Belyi, Y., & Aktories, K. (2015). Bacterial glycosyltransferase toxins. *Cellular Microbiology*, *17*(12), 1752–1765. https://doi.org/10.1111/CMI.12533

Jayaseelan, S., Ramaswamy, D., & Dharmaraj, S. (2014). Pyocyanin: production, applications, challenges and new insights. *World Journal of Microbiology \& Biotechnology*, *30*(4), 1159–1168. https://doi.org/10.1007/s11274-013-1552-5

Jeong, J.-H., An, J. Y., Kwon, Y. T., Rhee, J. G., & Lee, Y. J. (2009). Effects of low dose quercetin: cancer cell-specific inhibition of cell cycle progression. *Journal of Cellular Biochemistry*, *106*(1), 73–82. https://doi.org/10.1002/jcb.21977

Jian-Ling, J., Guo-Qiang, H., Zhen, M., & Gao, P.-J. (2010). Antibacterial Mechanisms of Berberine and Reasons for Little Resistance of Bacteria. *Chinese Herbal Medicines*, *3*(1), 27–35. http://timings.rs/storage/public/productrs/tips/7.pdf%5C_1553942082.pdf

Johnson, A. C., Yoshitani, J., Tanaka, H., & Suzuki, Y. (2011). Predicting national exposure to a point source chemical: Japan and endocrine disruption as an example. *Environmental Science \& Technology*, *45*(3), 1028–1033. https://doi.org/10.1021/es103358t

Johnson, J. S., Spakowicz, D. J., Hong, B. Y., Petersen, L. M., Demkowicz, P., Chen, L., Leopold, S. R., Hanson, B. M., Agresta, H. O., Gerstein, M., Sodergren, E., & Weinstock, G. M. (2019). Evaluation of 16S rRNA gene sequencing for species and strain-level microbiome analysis. *Nature Communications 2019 10:1*, *10*(1), 1–11. https://doi.org/10.1038/s41467-019-13036-1

Johnston, C., Martin, B., Fichant, G., Polard, P., & Claverys, J. P. (2014). Bacterial transformation: distribution, shared mechanisms and divergent control. *Nature Reviews Microbiology 2014 12:3*, *12*(3), 181–196. https://doi.org/10.1038/nrmicro3199

Johny, T. K., & Bhat, S. G. (2017). PCR in Metagenomics. *Methods in Molecular Biology (Clifton, N.J.)*, *1620*, 249–265. https://doi.org/10.1007/978-1-4939-7060-5_17

Jørgensen, K. M., Wassermann, T., Jensen, P. Ø., Hengzuang, W., Molin, S., Høiby, N., & Ciofu, O. (2013). Sublethal ciprofloxacin treatment leads to rapid development of high-level ciprofloxacin resistance during long-term experimental evolution of Pseudomonas aeruginosa. *Antimicrobial Agents and Chemotherapy*, *57*(9), 4215–4221. https://doi.org/10.1128/AAC.00493-13/SUPPL_FILE/ZAC999102092SO1.PDF

Jurburg, S. D., Brouwer, M. S. M., Ceccarelli, D., van der Goot, J., Jansman, A. J. M., & Bossers, A. (2019). Patterns of community assembly in the developing chicken microbiome reveal rapid primary succession. *MicrobiologyOpen*, *8*(9), e00821. https://doi.org/10.1002/MBO3.821

Juricova, H., Matiasovicova, J., Kubasova, T., Cejkova, D., & Rychlik, I. (2021). The distribution of antibiotic resistance genes in chicken gut microbiota commensals. *Scientific Reports 2021 11:1*, *11*(1), 1–10. https://doi.org/10.1038/s41598-021-82640-3

Kaakoush, N. O. (2015). Insights into the Role of Erysipelotrichaceae in the Human Host. *Frontiers in Cellular and Infection Microbiology*, *5*(NOV), 84. https://doi.org/10.3389/FCIMB.2015.00084

Kairmi, S. H., Taha-Abdelaziz, K., Yitbarek, A., Sargolzaei, M., Spahany, H., Astill, J., Shojadoost, B., Alizadeh, M., Kulkarni, R. R., Parkinson, J., & Sharif, S. (2022). Effects of therapeutic levels of dietary antibiotics on the cecal microbiome composition of broiler chickens. *Poultry Science*, *101*(6), 101864. https://doi.org/10.1016/J.PSJ.2022.101864

Kakran, M., Sahoo, N. G., & Li, L. (2011). Dissolution enhancement of quercetin through nanofabrication, complexation, and solid dispersion. *Colloids and Surfaces. B, Biointerfaces*, *88*(1), 121–130. https://doi.org/10.1016/J.COLSURFB.2011.06.020

Kalavathy, R., Abdullah, N., Jalaludin, S., Wong, C. M. V. L., & Ho, Y. W. (2008). Effect of Lactobacillus Cultures and Oxytetracycline on the Growth Performance and Serum Lipids of Chickens. *International Journal of Poultry Science*, *7*(4), 385–389.

Kalily, E., Hollander, A., Korin, B., Cymerman, I., & Yaron, S. (2016). Mechanisms of resistance to linalool in Salmonella Senftenberg and their role in survival on basil. *Environmental Microbiology*, *18*(11), 3673–3688. https://doi.org/10.1111/1462-2920.13268

Kalily, E., Hollander, A., Korin, B., Cymerman, I., & Yaron, S. (2017). Adaptation of Salmonella enterica Serovar Senftenberg to Linalool and Its Association with Antibiotic Resistance and Environmental Persistence. *Applied and Environmental Microbiology*, *83*(10).

https://doi.org/10.1128/{AEM}.03398-16

Kamali, E., Jamali, A., Ardebili, A., Ezadi, F., & Mohebbi, A. (2020). Evaluation of antimicrobial resistance, biofilm forming potential, and the presence of biofilm-related genes among clinical isolates of Pseudomonas aeruginosa. *BMC Research Notes*, *13*(1), 1–6. https://doi.org/10.1186/S13104-020-4890-Z/FIGURES/2

Kamath, J. M., Britigan, B. E., Cox, C. D., & Shasby, D. M. (1995). Pyocyanin from Pseudomonas aeruginosa inhibits prostacyclin release from endothelial cells. *Infection and Immunity*, *63*(12), 4921–4923. https://doi.org/10.1128/IAI.63.12.4921-4923.1995

Kanuparthy, A., Challa, T., Meegada, S., Siddamreddy, S., & Muppidi, V. (2020). Staphylococcus warneri: Skin Commensal and a Rare Cause of Urinary Tract Infection. *Cureus*, *12*(5). https://doi.org/10.7759/CUREUS.8337

Kao, W. T. K., Gagnon, P. M., Vogel, J. P., & Chole, R. A. (2016). FleQ, a Transcriptional Activator, is Required for Biofilm Formation in vitro but Does Not Alter Virulence in a Cholesteatomas Model. *Otology & Neurotology : Official Publication of the American Otological Society, American Neurotology Society [and] European Academy of Otology and Neurotology*, *37*(7), 977. https://doi.org/10.1097/MAO.0000000000001088

Karadag, A., Ozcelik, B., & Huang, Q. (2014). Quercetin nanosuspensions produced by high-pressure homogenization. *Journal of Agricultural and Food Chemistry*, *62*(8), 1852–1859. https://doi.org/10.1021/JF404065P

Karaosmanoglu, K., Sayar, N. A., Kurnaz, I. A., & Akbulut, B. S. (2014). Assessment of berberine as a multi-target antimicrobial: a multi-omics study for drug discovery and repositioning. *Omics : A Journal of Integrative Biology*, *18*(1), 42–53. https://doi.org/10.1089/OMI.2013.0100

Karena, E., Tatsaki, E., Lambrinidis, G., Mikros, E., & Frillingos, S. (2015). Analysis of conserved NCS2 motifs in the Escherichia coli xanthine permease XanQ. *Molecular Microbiology*, *98*(3), 502–517. https://doi.org/10.1111/MMI.13138/SUPPINFO

Karki, A. B., Neyaz, L., & Fakhr, M. K. (2020). Comparative Genomics of Plasmid-Bearing Staphylococcus aureus Strains Isolated From Various Retail Meats. *Frontiers in Microbiology*, *11*. https://doi.org/10.3389/FMICB.2020.574923/FULL

Katada, S., Fukuda, A., Nakajima, C., Suzuki, Y., Azuma, T., Takei, A., Takada, H., Okamoto, E., Kato, T., Tamura, Y., & Usui, M. (2021). Aerobic Composting and Anaerobic Digestion Decrease the Copy Numbers of Antibiotic-Resistant Genes and the Levels of Lactose-Degrading Enterobacteriaceae in Dairy Farms in Hokkaido, Japan. *Frontiers in Microbiology*, *12*, 2845. https://doi.org/10.3389/FMICB.2021.737420/BIBTEX

Kau, S., Mansfeld, M. D., Šoba, A., Zwick, T., & Staszyk, C. (2021). The facultative human oral pathogen Prevotella histicola in equine cheek tooth apical/ periapical infection: a case report. *BMC Veterinary Research*, *17*(1), 1–13. https://doi.org/10.1186/S12917-021-03048-9/FIGURES/9

Kawecki, T. J., Lenski, R. E., Ebert, D., Hollis, B., Olivieri, I., & Whitlock, M. C. (2012). Experimental evolution. In *Trends in Ecology and Evolution* (Vol. 27, Issue 10, pp. 547–560). Elsevier Current Trends. https://doi.org/10.1016/j.tree.2012.06.001

Kelly, K. R., & Brooks, B. W. (2018). *Global aquatic hazard assessment of ciprofloxacin: exceedances of antibiotic resistance development and ecotoxicological thresholds*. Elsevier. https://doi.org/10.1016/bs.pmbts.2018.07.004

Kępa, M., Miklasińska-Majdanik, M., Wojtyczka, R. D., Idzik, D., Korzeniowski, K., Smoleń-Dzirba, J., & Wąsik, T. J. (2018). Antimicrobial Potential of Caffeic Acid against Staphylococcus aureus Clinical Strains. *{BioMed} Research International*, *2018*, 7413504. https://doi.org/10.1155/2018/7413504

Khalil, A. A., Rahman, U. ur, Khan, M. R., Sahar, A., Mehmood, T., & Khan, M. (2017). Essential oil eugenol: sources, extraction techniques and nutraceutical perspectives. *{RSC} Adv.*, *7*(52), 32669–32681. https://doi.org/10.1039/{C7RA04803C}

Khameneh, B., Eskin, N. A. M., Iranshahy, M., & Fazly Bazzaz, B. S. (2021). Phytochemicals: A Promising Weapon in the Arsenal against Antibiotic-Resistant Bacteria. *Antibiotics*, *10*(9). https://doi.org/10.3390/ANTIBIOTICS10091044

Khare, T., Anand, U., Dey, A., Assaraf, Y. G., Chen, Z. S., Liu, Z., & Kumar, V. (2021). Exploring Phytochemicals for Combating Antibiotic Resistance in Microbial Pathogens. *Frontiers in Pharmacology*, *12*, 1726. https://doi.org/10.3389/FPHAR.2021.720726/XML/NLM

Khezri, A., Avershina, E., & Ahmad, R. (2021). Plasmid Identification and Plasmid-Mediated Antimicrobial Gene Detection in Norwegian Isolates. *Microorganisms*, *9*(1), 1–13. https://doi.org/10.3390/MICROORGANISMS9010052

Kim, H. S., Kim, J., Im, H. N., Yoon, J. Y., An, D. R., Yoon, H. J., Kim, J. Y., Min, H. K., Kim, S. J., Lee, J. Y., Han, B. W., & Suh, S. W. (2013). Structural basis for the inhibition of Mycobacterium tuberculosis L,D-transpeptidase by meropenem, a drug effective against extensively drug-resistant strains. *Acta Crystallographica. Section D, Biological Crystallography*, *69*(Pt 3), 420–431. https://doi.org/10.1107/S0907444912048998

Kim, S.-H., Shin, D.-S., Oh, M.-N., Chung, S.-C., Lee, J.-S., & Oh, K.-B. (2004). Inhibition of the bacterial surface protein anchoring transpeptidase sortase by isoquinoline alkaloids. *Bioscience, Biotechnology, and Biochemistry*, *68*(2), 421–424. https://doi.org/10.1271/bbb.68.421

Kim, S.-W., Chang, I.-M., & Oh, K.-B. (2002). Inhibition of the bacterial surface protein anchoring transpeptidase sortase by medicinal plants. *Bioscience, Biotechnology, and Biochemistry*, *66*(12), 2751–2754. https://doi.org/10.1271/bbb.66.2751

Kirchhelle, C. (2018). Pharming animals: a global history of antibiotics in food production (1935–2017). *Palgrave Communications 2018 4:1*, *4*(1), 1–13. https://doi.org/10.1057/s41599-018-0152-2

Kirchhelle, C., & Roberts, A. P. (2022). Embracing the monsters: moving from infection control to microbial management. *The Lancet Microbe*, *0*(0). https://doi.org/10.1016/S2666-5247(22)00225-7

Knapp, C. W., Callan, A. C., Aitken, B., Shearn, R., Koenders, A., & Hinwood, A. (2017). Relationship between antibiotic resistance genes and metals in residential soil samples from Western Australia. *Environmental Science and Pollution Research International*, *24*(3), 2484–2494. https://doi.org/10.1007/s11356-016-7997-y

Knapp, C. W., McCluskey, S. M., Singh, B. K., Campbell, C. D., Hudson, G., & Graham, D. W. (2011). Antibiotic resistance gene abundances correlate with metal and geochemical conditions in archived Scottish soils. *Plos One*, *6*(11), e27300. https://doi.org/10.1371/journal.pone.0027300

Knietsch, A., Waschkowitz, T., Bowien, S., Henne, A., & Daniel, R. (2003). Construction and Screening of Metagenomic Libraries Derived from Enrichment Cultures: Generation of

a Gene Bank for Genes Conferring Alcohol Oxidoreductase Activity on Escherichia coli. *Applied and Environmental Microbiology*, *69*(3), 1408. https://doi.org/10.1128/AEM.69.3.1408-1416.2003

Kong, W. J., Xing, X. Y., Xiao, X. H., Zhao, Y. L., Wei, J. H., Wang, J. B., Yang, R. C., & Yang, M. H. (2012). Effect of berberine on Escherichia coli, Bacillus subtilis, and their mixtures as determined by isothermal microcalorimetry. *Applied Microbiology and Biotechnology*, *96*(2), 503–510. https://doi.org/10.1007/S00253-012-4302-Y

Konikoff, T., & Gophna, U. (2016). Oscillospira: a Central, Enigmatic Component of the Human Gut Microbiota. *Trends in Microbiology*, *24*, 523–524. https://doi.org/10.1016/j.tim.2016.02.015

Koraimann, G., & Wagner, M. A. (2014). Social behavior and decision making in bacterial conjugation. *Frontiers in Cellular and Infection Microbiology*, *4*(APR), 54. https://doi.org/10.3389/FCIMB.2014.00054/BIBTEX

Korpela, K., Salonen, A., Virta, L. J., Kekkonen, R. A., Forslund, K., Bork, P., & De Vos, W. M. (2016). Intestinal microbiome is related to lifetime antibiotic use in Finnish pre-school children. *Nature Communications 2016 7:1*, *7*(1), 1–8. https://doi.org/10.1038/ncomms10410

Kouker, G., & Jaeger, K. E. (1987). Specific and sensitive plate assay for bacterial lipases. *Applied and Environmental Microbiology*, *53*(1), 211–213. https://doi.org/10.1128/AEM.53.1.211-213.1987

Koutsoumanis, K., Allende, A., Alvarez-Ordóñez, A., Bover-Cid, S., Chemaly, M., Davies, R., De Cesare, A., Herman, L., Hilbert, F., Lindqvist, R., Nauta, M., Peixe, L., Ru, G., Simmons, M., Skandamis, P., Suffredini, E., Jenkins, C., Monteiro Pires, S., Morabito, S., … Bolton, D. (2020). Pathogenicity assessment of Shiga toxin-producing Escherichia coli (STEC) and the public health risk posed by contamination of food with STEC. *EFSA Journal*, *18*(1), e05967. https://doi.org/10.2903/J.EFSA.2020.5967

Kowalska-Krochmal, B., & Dudek-Wicher, R. (2021). The Minimum Inhibitory Concentration of Antibiotics: Methods, Interpretation, Clinical Relevance. *Pathogens*, *10*(2), 1–21. https://doi.org/10.3390/PATHOGENS10020165

Krenitsky, T. A., Neil, S. M., & Miller, R. L. (1970). Guanine and Xanthine Phosphoribosyltransfer Activities of Lactobacillus casei and Escherichia coli: THEIR RELATIONSHIP TO HYPOXANTHINE AND ADENINE PHOSPHORIBOSYLTRANSFER ACTIVITIES. *Journal of Biological Chemistry*, *245*(10), 2605–2611. https://doi.org/10.1016/S0021-9258(18)63113-8

Kubasova, T., Kollarcikova, M., Crhanova, M., Karasova, D., Cejkova, D., Sebkova, A., Matiasovicova, J., Faldynova, M., Pokorna, A., Cizek, A., & Rychlik, I. (2019). Contact with adult hen affects development of caecal microbiota in newly hatched chicks. *PLoS ONE*, *14*(3). https://doi.org/10.1371/journal.pone.0212446

Kumar, P., Patra, A. K., Mandal, G. P., Samanta, I., & Pradhan, S. (2017). Effect of black cumin seeds on growth performance, nutrient utilization, immunity, gut health and nitrogen excretion in broiler chickens. *Journal of the Science of Food and Agriculture*, *97*(11), 3742–3751. https://doi.org/10.1002/jsfa.8237

Laishram, S., Pragasam, A., Bakthavatchalam, Y., & Veeraraghavan, B. (2017). An update on technical, interpretative and clinical relevance of antimicrobial synergy testing methodologies. *Indian Journal of Medical Microbiology*, *35*(4), 445–468.

https://doi.org/10.4103/IJMM.IJMM_17_189

Lam, K. N., Cheng, J., Engel, K., Neufeld, J. D., & Charles, T. C. (2015). Current and future resources for functional metagenomics. *Frontiers in Microbiology*, *6*(OCT), 1196. https://doi.org/10.3389/fmicb.2015.01196

Langeveld, W. T., Veldhuizen, E. J. A., & Burt, S. A. (2014). Synergy between essential oil components and antibiotics: a review. *Critical Reviews in Microbiology*, *40*(1), 76–94. https://doi.org/10.3109/{1040841X}.2013.763219

Langmead, B., & Salzberg, S. L. (2012). Fast gapped-read alignment with Bowtie 2. *Nature Methods 2012 9:4*, *9*(4), 357–359. https://doi.org/10.1038/nmeth.1923

Larsen, J., Petersen, A., S\orum, M., Stegger, M., van Alphen, L., Valentiner-Branth, P., Knudsen, L. K., Larsen, L. S., Feingold, B., Price, L. B., Andersen, P. S., Larsen, A. R., & Skov, R. L. (2015). Meticillin-resistant Staphylococcus aureus {CC398} is an increasing cause of disease in people with no livestock contact in Denmark, 1999 to 2011. *Euro Surveillance*, *20*(37). https://doi.org/10.2807/1560-7917.{ES}.2015.20.37.30021

Lau, G. W., Hassett, D. J., Ran, H., & Kong, F. (2004). The role of pyocyanin in Pseudomonas aeruginosa infection. *Trends in Molecular Medicine*, *10*(12), 599–606. https://doi.org/10.1016/J.MOLMED.2004.10.002

Lawson, L. D., & Hunsaker, S. M. (2018). Allicin Bioavailability and Bioequivalence from Garlic Supplements and Garlic Foods. *Nutrients*, *10*(7). https://doi.org/10.3390/NU10070812

Laxminarayan, R., Teillant, A., & Van Boeckel, T. (2015). *The Economic Costs of Withdrawing Antimicrobial Growth Promoters from the Livestock Sector*. https://doi.org/10.1787/5js64kst5wvl-en

Lee, C.-R., Cho, I. H., Jeong, B. C., & Lee, S. H. (2013). Strategies to minimize antibiotic resistance. *International Journal of Environmental Research and Public Health*, *10*(9), 4274–4305. https://doi.org/10.3390/ijerph10094274

Lee, H. D., Nara, O., Lee, E., & Suh, H. H. (2017). Flocculating Properties of Bioflocculant Biopol32 from Pseudomonas sp. GP32. *Journal of Life Science*, *27*(8), 930–936. https://doi.org/10.5352/JLS.2017.27.8.930

Lee, I., Kim, Y. O., Park, S. C., & Chun, J. (2016). OrthoANI: An improved algorithm and software for calculating average nucleotide identity. *International Journal of Systematic and Evolutionary Microbiology*, *66*(2), 1100–1103. https://doi.org/10.1099/IJSEM.0.000760

Lee, J. R., Muthukumar, T., Dadhania, D., Toussaint, N. C., Ling, L., Pamer, E., & Suthanthiran, M. (2014). Gut Microbial Community Structure and Complications Following Kidney Transplantation: A Pilot Study. *Transplantation*, *98*(7), 697. https://doi.org/10.1097/TP.0000000000000370

Lee, S., Gallagher, L., & Manoil, C. (2021). Reconstructing a Wild-Type Pseudomonas aeruginosa Reference Strain PAO1. *Journal of Bacteriology*, *203*(14). https://doi.org/10.1128/JB.00179-21

Lee, T. I., & Young, R. A. (2013). Transcriptional Regulation and its Misregulation in Disease. *Cell*, *152*(6), 1237. https://doi.org/10.1016/J.CELL.2013.02.014

LeMieux, J. (2018). *As Novartis Exits, Who Will Make New Antibiotics?* Genetic Engineering and Biotechnology News. https://www.genengnews.com/insights/as-novartis-exits-

who-will-make-new-antibiotics/

Lenski, R. E. (2017). Experimental evolution and the dynamics of adaptation and genome evolution in microbial populations. *The ISME Journal 2017 11:10*, *11*(10), 2181–2194. https://doi.org/10.1038/ismej.2017.69

Lever, J., Krzywinski, M., & Altman, N. (2017). Points of Significance: Principal component analysis. *Nature Methods*, *14*(7), 641–642. https://doi.org/10.1038/NMETH.4346

Lewin, A., Strand, T. A., Haugen, T., Klinkenberg, G., Kotlar, H. K., Valla, S., Drabløs, F., Wentzel, A., Lewin, A., Strand, T. A., Haugen, T., Klinkenberg, G., Kotlar, H. K., Valla, S., Drabløs, F., & Wentzel, A. (2016). Discovery and Characterization of a Thermostable Esterase from an Oil Reservoir Metagenome. *Advances in Enzyme Research*, *4*(2), 68–86. https://doi.org/10.4236/AER.2016.42008

Lewis, K. (2013). Platforms for antibiotic discovery. *Nature Reviews. Drug Discovery*, *12*(5), 371–387. https://doi.org/10.1038/nrd3975

Leyva-Diaz, A. A., Hernandez-Patlan, D., Solis-Cruz, B., Adhikari, B., Kwon, Y. M., Latorre, J. D., Hernandez-Velasco, X., Fuente-Martinez, B., Hargis, B. M., Lopez-Arellano, R., & Tellez-Isaias, G. (2021). Evaluation of curcumin and copper acetate against Salmonella Typhimurium infection, intestinal permeability, and cecal microbiota composition in broiler chickens. *Journal of Animal Science and Biotechnology*, *12*(1), 1–12. https://doi.org/10.1186/S40104-021-00545-7/FIGURES/5

Li, J., Zhang, H., Ning, J., Sajid, A., Cheng, G., Yuan, Z., & Hao, H. (2019). The nature and epidemiology of OqxAB, a multidrug efflux pump. *Antimicrobial Resistance and Infection Control*, *8*(1), 1–13. https://doi.org/10.1186/S13756-019-0489-3/FIGURES/2

Li, O., Lu, C., Liu, A., Zhu, L., Wang, P. M., Qian, C. D., Jiang, X. H., & Wu, X. C. (2013). Optimization and characterization of polysaccharide-based bioflocculant produced by Paenibacillus elgii B69 and its application in wastewater treatment. *Bioresource Technology*, *134*, 87–93. https://doi.org/10.1016/J.BIORTECH.2013.02.013

Li, Q., Chang, W., Zhang, H., Hu, D., & Wang, X. (2019). The role of plasmids in the multiple antibiotic resistance transfer in ESBLs-producing Escherichia coli isolated from wastewater treatment plants. *Frontiers in Microbiology*, *10*(APR), 633. https://doi.org/10.3389/FMICB.2019.00633/BIBTEX

Li, W., Zhao, Y., Yu, J., Lin, L., Ramanathan, S., Wang, G., Lin, X., & Pang, H. (2021). TonB-Dependent Receptors Affect the Spontaneous Oxytetracycline Resistance Evolution in Aeromonas hydrophila. *Journal of Proteome Research*, *20*(1), 154–163. https://doi.org/10.1021/acs.jproteome.9b00708

Li, Y., Cao, Z.-T., Wang, X.-Y., & Ge, X.-Z. (2018). Expression of the {TetA} gene encoding {TetA} efflux protein in E. coli contributes to its increased bacterial resistance toward berberine. *Journal of Asian Natural Products Research*, *20*(4), 374–384. https://doi.org/10.1080/10286020.2017.1384818

Li, Y., Li, W., Gao, H., Xing, J., & Liu, H. (2011). Integration of flocculation and adsorptive immobilization of Pseudomonas delafieldii R-8 for diesel oil biodesulfurization. *Journal of Chemical Technology & Biotechnology*, *86*(2), 246–250. https://doi.org/10.1002/JCTB.2510

Li, Y., Wen, H., & Ge, X. (2021). Hormesis Effect of Berberine against Klebsiella pneumoniae Is Mediated by Up-Regulation of the Efflux Pump KmrA. *Journal of Natural Products*,

84(11), 2885–2892. https://doi.org/10.1021/ACS.JNATPROD.1C00642

Lienen, T., Schnitt, A., Hammerl, J. A., Marino, S. F., Maurischat, S., & Tenhagen, B. A. (2021). Multidrug-resistant Staphylococcus cohnii and Staphylococcus urealyticus isolates from German dairy farms exhibit resistance to beta-lactam antibiotics and divergent penicillin-binding proteins. *Scientific Reports 2021 11:1*, *11*(1), 1–11. https://doi.org/10.1038/s41598-021-85461-6

Lillehoj, H., Liu, Y., Calsamiglia, S., Fernandez-Miyakawa, M. E., Chi, F., Cravens, R. L., Oh, S., & Gay, C. G. (2018). Phytochemicals as antibiotic alternatives to promote growth and enhance host health. *Veterinary Research*, *49*(1), 76. https://doi.org/10.1186/s13567-018-0562-6

Lin, J. L., Peng, Y., Ou, Q. T., Lin, D. X., Li, Y., Ye, X. H., Zhou, J. L., & Yao, Z. J. (2017). A molecular epidemiological study of methicillin-resistant Staphylococci environmental contamination in railway stations and coach stations in Guangzhou of China. *Letters in Applied Microbiology*, *64*(2), 131–137. https://doi.org/10.1111/LAM.12700

Liu, C.-S., Zheng, Y.-R., Zhang, Y.-F., & Long, X.-Y. (2016). Research progress on berberine with a special focus on its oral bioavailability. *Fitoterapia*, *109*, 274–282. https://doi.org/10.1016/j.fitote.2016.02.001

Liu, I., Durham, D., & Richards, M. (2010). Baicalin Synergy with β-Lactam Antibiotics Against Methicillin-resistant Staphylococcus aureus and Other β-Lactam-resistant Strains of S. aureus. *Journal of Pharmacy and Pharmacology*, *52*(3), 361–366. https://doi.org/10.1211/0022357001773922

Liu, J., Stewart, S. N., Robinson, K., Yang, Q., Lyu, W., Whitmore, M. A., & Zhang, G. (2021). Linkage between the intestinal microbiota and residual feed intake in broiler chickens. *Journal of Animal Science and Biotechnology*, *12*(1), 1–16. https://doi.org/10.1186/S40104-020-00542-2/FIGURES/10

Liu, P., Wang, W., Zhao, J., & Wei, D. (2019). Screening novel β-galactosidases from a sequence-based metagenome and characterization of an alkaline β-galactosidase for the enzymatic synthesis of galactooligosaccharides. *Protein Expression and Purification*, *155*, 104–111. https://doi.org/10.1016/J.PEP.2018.12.001

Liu, Q., Liu, C., Li, W., & Liu, W. (2021). *Comparative Genomic Analysis of Limosilactobacillus Pontis Reveals Genetic Characteristics of High GC Content and Potential Niches Adaptations*. https://doi.org/10.21203/rs.3.rs-969439/v1

Liu, X., Cai, J., Chen, H., Zhong, Q., Hou, Y., Chen, W., & Chen, W. (2020). Antibacterial activity and mechanism of linalool against Pseudomonas aeruginosa. *Microbial Pathogenesis*, *141*, 103980. https://doi.org/10.1016/j.micpath.2020.103980

Long, C., de Vries, S., & Venema, K. (2020). Polysaccharide source altered ecological network, functional profile, and short-chain fatty acid production in a porcine gut microbiota. *Beneficial Microbes*, *11*(6), 591–610. https://doi.org/10.3920/BM2020.0006

Lopatkin, A. J., & Yang, J. H. (2021). Digital Insights Into Nucleotide Metabolism and Antibiotic Treatment Failure. *Frontiers in Digital Health*, *0*, 12. https://doi.org/10.3389/FDGTH.2021.583468

Lu, J., Idris, U., Harmon, B., Hofacre, C., Maurer, J. J., & Lee, M. D. (2003). Diversity and succession of the intestinal bacterial community of the maturing broiler chicken. *Applied and Environmental Microbiology*, *69*(11), 6816–6824.

https://doi.org/10.1128/AEM.69.11.6816-6824.2003

Lundberg, R., Scharch, C., & Sandvang, D. (2021). The link between broiler flock heterogeneity and cecal microbiome composition. *Animal Microbiome*, *3*(1). https://doi.org/10.1186/S42523-021-00110-7

Luscher, A., Moynie, L., Auguste, P. Saint, Bumann, D., Mazza, L., Pletzer, D., Naismith, J. H., & Köhlera, T. (2018). TonB-Dependent Receptor Repertoire of Pseudomonas aeruginosa for Uptake of Siderophore-Drug Conjugates. *Antimicrobial Agents and Chemotherapy*, *62*(6). https://doi.org/10.1128/AAC.00097-18

Lv, Q., Zhang, P., Quan, P., Cui, M., Liu, T., Yin, Y., & Chi, G. (2019). Quercetin, a pneumolysin inhibitor, protects mice against Streptococcus pneumoniae infection. *Microbial Pathogenesis*, 103934. https://doi.org/10.1016/j.micpath.2019.103934

Ma, D., Wang, Z., Merrikh, C. N., Lang, K. S., Lu, P., Li, X., Merrikh, H., Rao, Z., & Xu, W. (2018). Crystal structure of a membrane-bound O-acyltransferase. *Nature*, *562*(7726), 286. https://doi.org/10.1038/S41586-018-0568-2

MacDonald, J. M., & Wang, S.-L. (2011). Foregoing Sub-therapeutic Antibiotics: the Impact on Broiler Grow-out Operations. *Applied Economic Perspectives and Policy*, *33*(1), 79–98. https://doi.org/10.1093/aepp/ppq030

Macedo, D., Filho, A. J. M. C., de Sousa, C. N., Quevedo, J., Barichello, T., Júnior, H. V. N., & de Lucena, D. (2017). Antidepressants, antimicrobials or both? Gut microbiota dysbiosis in depression and possible implications of the antimicrobial effects of antidepressant drugs for antidepressant effectiveness. *Journal of Affective Disorders*, *208*, 22–32. https://doi.org/10.1016/j.jad.2016.09.012

Magi, G., Marini, E., & Facinelli, B. (2015). Antimicrobial activity of essential oils and carvacrol, and synergy of carvacrol and erythromycin, against clinical, erythromycin-resistant Group A Streptococci. *Frontiers in Microbiology*, *6*, 165. https://doi.org/10.3389/fmicb.2015.00165

Magnet, S., Dubost, L., Marie, A., Arthur, M., & Gutmann, L. (2008). Identification of the l,d-Transpeptidases for Peptidoglycan Cross-Linking in Escherichia coli. *Journal of Bacteriology*, *190*(13), 4782. https://doi.org/10.1128/JB.00025-08

Mak, K.-K., Kamal, M., Ayuba, S., Sakirolla, R., Kang, Y.-B., Mohandas, K., Balijepalli, M., Ahmad, S., & Pichika, M. (2019). A comprehensive review on eugenol's antimicrobial properties and industry applications: A transformation from ethnomedicine to industry. *Pharmacognosy Reviews*, *13*(25), 1. https://doi.org/10.4103/phrev.phrev_46_18

Maki, J. J., & Looft, T. (2022). Turicibacter bilis sp. nov., a novel bacterium isolated from the chicken eggshell and swine ileum. *International Journal of Systematic and Evolutionary Microbiology*, *72*(1). https://doi.org/10.1099/IJSEM.0.005153

Manafi, M., Hedayati, M., Pirany, N., & Omede, A. A. (2019). Comparison of performance and feed digestibility of the non-antibiotic feed supplement (Novacid) and an antibiotic growth promoter in broiler chickens. *Poultry Science*, *98*(2), 904–911. https://doi.org/10.3382/ps/pey437

Mansoury, M., Hamed, M., Karmustaji, R., Al Hannan, F., & Safrany, S. T. (2021). The edge effect: A global problem. The trouble with culturing cells in 96-well plates. *Biochemistry and Biophysics Reports*, *26*. https://doi.org/10.1016/J.BBREP.2021.100987

Mariat, D., Firmesse, O., Levenez, F., Guimarães, V. D., Sokol, H., Doré, J., Corthier, G., & Furet,

J. P. (2009). The firmicutes/bacteroidetes ratio of the human microbiota changes with age. *BMC Microbiology*, *9*(1), 1–6. https://doi.org/10.1186/1471-2180-9-123/FIGURES/1

Marinaro, M., Fasano, A., & De Magistris, M. T. (2003). Zonula occludens toxin acts as an adjuvant through different mucosal routes and induces protective immune responses. *Infection and Immunity*, *71*(4), 1897–1902. https://doi.org/10.1128/IAI.71.4.1897-1902.2003/ASSET/614C20ED-E5DF-48D3-9803-511AB4FD0407/ASSETS/GRAPHIC/II0431174005.JPEG

Marmion, M., Ferone, M. T., Whyte, P., & Scannell, A. G. M. (2021). The changing microbiome of poultry meat; from farm to fridge. *Food Microbiology*, *99*, 103823. https://doi.org/10.1016/J.FM.2021.103823

Marunaka, Y., Marunaka, R., Sun, H., Yamamoto, T., Kanamura, N., Inui, T., & Taruno, A. (2017). Actions of quercetin, a polyphenol, on blood pressure. *Molecules (Basel, Switzerland)*, *22*(2). https://doi.org/10.3390/molecules22020209

Martinez, G. (2018) TRNA-derived small RNAS: New players in Genome Protection against retrotransposons, RNA biology. U.S. National Library of Medicine. Available at: https://www.ncbi.nlm.nih.gov/pmc/articles/PMC5798961/ (Accessed: March 6, 2023)

Matshogo, T. B., Mlambo, V., Marume, U., & Sebola, N. (2018). Growth performance, blood parameters, carcass characteristics and meat quality traits in Potchefstroom Koekoek chickens fed Lippia javanica leaf meal. *Tropical Animal Health and Production*, *50*(8), 1787–1795. https://doi.org/10.1007/s11250-018-1620-9

Mauritzen, J. J., Castillo, D., Tan, D., Svenningsen, S. Lo, & Middelboe, M. (2020). Beyond Cholera: Characterization of zot-Encoding Filamentous Phages in the Marine Fish Pathogen Vibrio anguillarum. *Viruses*, *12*(7). https://doi.org/10.3390/v12070730

Mazhar, S. H., Li, X., Rashid, A., Su, J., Xu, J., Brejnrod, A. D., Su, J.-Q., Wu, Y., Zhu, Y.-G., Zhou, S. G., Feng, R., & Rensing, C. (2021). Co-selection of antibiotic resistance genes, and mobile genetic elements in the presence of heavy metals in poultry farm environments. *The Science of the Total Environment*, *755*(Pt 2), 142702. https://doi.org/10.1016/j.scitotenv.2020.142702

McArthur, A. G., Waglechner, N., Nizam, F., Yan, A., Azad, M. A., Baylay, A. J., Bhullar, K., Canova, M. J., De Pascale, G., Ejim, L., Kalan, L., King, A. M., Koteva, K., Morar, M., Mulvey, M. R., O'Brien, J. S., Pawlowski, A. C., Piddock, L. J. V, Spanogiannopoulos, P., … Wright, G. D. (2013). The comprehensive antibiotic resistance database. *Antimicrobial Agents and Chemotherapy*, *57*(7), 3348–3357. https://doi.org/10.1128/{AAC}.00419-13

McMurdie, P. J., & Holmes, S. (2013). phyloseq: An R Package for Reproducible Interactive Analysis and Graphics of Microbiome Census Data. *PLOS ONE*, *8*(4), e61217. https://doi.org/10.1371/JOURNAL.PONE.0061217

Memariani, H., Memariani, M., & Ghasemian, A. (2019). An overview on anti-biofilm properties of quercetin against bacterial pathogens. *World Journal of Microbiology & Biotechnology*, *35*(9). https://doi.org/10.1007/S11274-019-2719-5

Mendoza, N., & Silva, E. M. E. (2018). Introduction to Phytochemicals: Secondary Metabolites from Plants with Active Principles for Pharmacological Importance. *Phytochemicals - Source of Antioxidants and Role in Disease Prevention*. https://doi.org/10.5772/INTECHOPEN.78226

Merkeviciene, L., Ruzauskaite, N., Klimiene, I., Siugzdiniene, R., Dailidaviciene, J., Virgailis, M., Mockeliunas, R., & Ruzauskas, M. (2017). Microbiome and Antimicrobial Resistance Genes in Microbiota of Cloacal Samples from European Herring Gulls (Larus Argentatus). *Journal of Veterinary Research*, *61*(1), 27. https://doi.org/10.1515/JVETRES-2017-0004

Microchem Laboratory. (2022). *Zone of Inhibition Test for Antimicrobial Activity*. https://microchemlab.com/test/zone-inhibition-test-antimicrobial-activity/

Miklasińska-Majdanik, M., Kępa, M., Wojtyczka, R. D., Idzik, D., & Wąsik, T. J. (2018). Phenolic Compounds Diminish Antibiotic Resistance of Staphylococcus Aureus Clinical Strains. *International Journal of Environmental Research and Public Health*, *15*(10). https://doi.org/10.3390/IJERPH15102321

Millar, A. H., Leaver, C. J., & Hill, S. A. (1999). Characterization of the dihydrolipoamide acetyltransferase of the mitochondrial pyruvate dehydrogenase complex from potato and comparisons with similar enzymes in diverse plant species. *European Journal of Biochemistry*, *264*(3), 973–981. https://doi.org/10.1046/J.1432-1327.1999.00707.X

Miller, S. I. (2016). Antibiotic resistance and regulation of the Gram-negative bacterial outer membrane barrier by host innate immune molecules. *MBio*, *7*(5). https://doi.org/10.1128/MBIO.01541-16

Mindlin, S., Minakhin, L., Petrova, M., Kholodii, G., Minakhina, S., Gorlenko, Z., & Nikiforov, V. (2005). Present-day mercury resistance transposons are common in bacteria preserved in permafrost grounds since the Upper Pleistocene. *Research in Microbiology*, *156*(10), 994–1004. https://doi.org/10.1016/j.resmic.2005.05.011

Mokaddas, E. M., & Sanyal, S. C. (1999). Resistance patterns of Pseudomonas aeruginosa to carbapenems and piperacillin/tazobactam. *Journal of Chemotherapy (Florence, Italy)*, *11*(2), 93–96. https://doi.org/10.1179/JOC.1999.11.2.93

Mølgaard, A., Kauppinen, S., & Larsen, S. (2000). Rhamnogalacturonan acetylesterase elucidates the structure and function of a new family of hydrolases. *Structure*, *8*(4), 373–383. https://doi.org/10.1016/S0969-2126(00)00118-0

Moon, C. D., Young, W., Maclean, P. H., Cookson, A. L., & Bermingham, E. N. (2018). Metagenomic insights into the roles of Proteobacteria in the gastrointestinal microbiomes of healthy dogs and cats. *MicrobiologyOpen*, *7*(5). https://doi.org/10.1002/MBO3.677

Moon, S.-E., Kim, H.-Y., & Cha, J.-D. (2011). Synergistic effect between clove oil and its major compounds and antibiotics against oral bacteria. *Archives of Oral Biology*, *56*(9), 907–916. https://doi.org/10.1016/j.archoralbio.2011.02.005

Morand, C., Manach, C., Crespy, V., & Remesy, C. (2000). Respective bioavailability of quercetin aglycone and its glycosides in a rat model. *BioFactors*, *12*(1–4), 169–174. https://doi.org/10.1002/BIOF.5520120127

More, N. V., Kharat, K. R., & Kharat, A. S. (2017). Berberine from Argemone mexicana L exhibits a broadspectrum antibacterial activity. *Acta Biochimica Polonica*, *64*(4), 653–660. https://doi.org/10.18388/ABP.2017_1621

Morel, C. M., Lindahl, O., Harbarth, S., de Kraker, M. E. A., Edwards, S., & Hollis, A. (2020). Industry incentives and antibiotic resistance: an introduction to the antibiotic susceptibility bonus. *The Journal of Antibiotics*. https://doi.org/10.1038/s41429-020-

0300-y

Morin, C. J., Patel, P. C., Levesque, R. C., & Letarte, R. (1987). Monoclonal antibodies to TEM-1 plasmid-mediated beta-lactamase. *Antimicrobial Agents and Chemotherapy*, *31*(11), 1761. https://doi.org/10.1128/AAC.31.11.1761

Moro, S., Sturlese, M., Ciancetta, A., & Floris, M. (2016). In Silico 3D Modeling of Binding Activities. *Methods in Molecular Biology (Clifton, N.J.)*, *1425*, 23–35. https://doi.org/10.1007/978-1-4939-3609-0_2

Morrison, A. J., & Wenzel, R. P. (1984). Epidemiology of Infections Due to Pseudomonas aeruginosa. *Clinical Infectious Diseases*, *6*(Supplement_3), S627–S642. https://doi.org/10.1093/clinids/6.Supplement_3.S627

Mu, Y., Zeng, H., & Chen, W. (2021). Quercetin Inhibits Biofilm Formation by Decreasing the Production of EPS and Altering the Composition of EPS in Staphylococcus epidermidis. *Frontiers in Microbiology*, *12*, 251. https://doi.org/10.3389/FMICB.2021.631058/BIBTEX

Mujeeb, F., Bajpai, P., & Pathak, N. (2014). Phytochemical evaluation, antimicrobial activity, and determination of bioactive components from leaves of aegle marmelos. *BioMed Research International*, *2014*. https://doi.org/10.1155/2014/497606

Mulcahy, L. R., Burns, J. L., Lory, S., & Lewis, K. (2010). Emergence of Pseudomonas aeruginosa strains producing high levels of persister cells in patients with cystic fibrosis. *Journal of Bacteriology*, *192*(23), 6191–6199. https://doi.org/10.1128/{JB}.01651-09

Mulcahy, L. R., Isabella, V. M., & Lewis, K. (2014). Pseudomonas aeruginosa biofilms in disease. *Microbial Ecology*, *68*(1), 1. https://doi.org/10.1007/S00248-013-0297-X

Muller, M., & Merrett, N. D. (2014). Pyocyanin production by Pseudomonas aeruginosa confers resistance to ionic silver. *Antimicrobial Agents and Chemotherapy*, *58*(9), 5492–5499. https://doi.org/10.1128/AAC.03069-14

Müller, O., Lu, G. Y., & von Seidlein, L. (2019). Geographic expansion of artemisinin resistance. *Journal of Travel Medicine*, *26*(4). https://doi.org/10.1093/jtm/taz030

Mundy, C., & Kirkpatrick, P. (2004). Tiotropium bromide. *Nature Reviews. Drug Discovery*, *3*(8), 643–644. https://doi.org/10.1038/NRD1472

Murray, C. J., Shunji Ikuta, K., Sharara, F., Swetschinski, L., Robles Aguilar, G., Gray, A., Han, C., Bisignano, C., Rao, P., Wool, E., Johnson, S. C., Browne, A. J., Give Chipeta, M., Fell, F., Hackett, S., Haines-Woodhouse, G., Kashef Hamadani, B. H., P Kumaran, E. A., McManigal, B., … Resistance Collaborators, A. (2022). Global burden of bacterial antimicrobial resistance in 2019: a systematic analysis. *The Lancet*, *0*(0). https://doi.org/10.1016/S0140-6736(21)02724-0

Murry, A. C., Hinton, A., & Morrison, H. (2004). Inhibition of Growth of Escherichia coli, Salmonella typhimurium, and Clostridia perfringens on Chicken Feed Media by Lactobacillus salivarius and Lactobacillus plantarum. *International Journal of Poultry Science*, *3*(9), 603–607.

Murugesan, G. R., Syed, B., Haldar, S., & Pender, C. (2015). Phytogenic feed additives as an alternative to antibiotic growth promoters in broiler chickens. *Frontiers in Veterinary Science*, *2*, 21. https://doi.org/10.3389/fvets.2015.00021

Muyzer, G., De Waal, E. C., & Uitterlinden, A. G. (1993). Profiling of complex microbial

populations by denaturing gradient gel electrophoresis analysis of polymerase chain reaction-amplified genes coding for 16S rRNA. *Applied and Environmental Microbiology*, *59*(3), 695–700. https://doi.org/10.1128/aem.59.3.695-700.1993

Naito, M., Ogura, Y., Itoh, T., Shoji, M., Okamoto, M., Hayashi, T., & Nakayama, K. (2016). Editor's choice: The complete genome sequencing of Prevotella intermedia strain OMA14 and a subsequent fine-scale, intra-species genomic comparison reveal an unusual amplification of conjugative and mobile transposons and identify a novel Prevotella-lineage-specific repeat. *DNA Research: An International Journal for Rapid Publication of Reports on Genes and Genomes*, *23*(1), 11. https://doi.org/10.1093/DNARES/DSV032

Nakamura, Y., Gojobori, T., & Ikemura, T. (2000). Codon usage tabulated from international DNA sequence databases: status for the year 2000. *Nucleic Acids Research*, *28*(1), 292. https://doi.org/10.1093/NAR/28.1.292

Nasidze, I., Li, J., Quinque, D., Tang, K., & Stoneking, M. (2009). Global diversity in the human salivary microbiome. *Genome Research*, *19*(4), 636–643. https://doi.org/10.1101/GR.084616.108

NCT03072992. (2017). "Curcumin" in Combination With Chemotherapy in Advanced Breast Cancer. *Https://Clinicaltrials.Gov/Show/NCT03072992*. https://clinicaltrials.gov/ct2/show/NCT03072992

Neag, M. A., Mocan, A., Echeverría, J., Pop, R. M., Bocsan, C. I., Crişan, G., & Buzoianu, A. D. (2018). Berberine: botanical occurrence, traditional uses, extraction methods, and relevance in cardiovascular, metabolic, hepatic, and renal disorders. *Frontiers in Pharmacology*, *9*, 557. https://doi.org/10.3389/fphar.2018.00557

Nearing, J. T., Comeau, A. M., & Langille, M. G. I. (2021). Identifying biases and their potential solutions in human microbiome studies. *Microbiome*, *9*(1), 113. https://doi.org/10.1186/s40168-021-01059-0

Nearing, J. T., Douglas, G. M., Hayes, M. G., MacDonald, J., Desai, D. K., Allward, N., Jones, C. M. A., Wright, R. J., Dhanani, A. S., Comeau, A. M., & Langille, M. G. I. (2022). Microbiome differential abundance methods produce different results across 38 datasets. *Nature Communications 2022 13:1*, *13*(1), 1–16. https://doi.org/10.1038/s41467-022-28034-z

Neisy, A., Zal, F., Seghatoleslam, A., & Alaee, S. (2019). Amelioration by quercetin of insulin resistance and uterine {GLUT4} and {ERα} gene expression in rats with polycystic ovary syndrome ({PCOS}). *Reproduction, Fertility, and Development*, *31*(2), 315–323. https://doi.org/10.1071/{RD18222}

Nel Van Zyl, K., Matukane, S. R., Hamman, B. L., Whitelaw, A. C., & Newton-Foot, M. (2022). Effect of antibiotics on the human microbiome: a systematic review. *International Journal of Antimicrobial Agents*, *59*(2), 106502. https://doi.org/10.1016/J.IJANTIMICAG.2021.106502

Neveu, J., Regeard, C., & Dubow, M. S. (2011). Isolation and characterization of two serine proteases from metagenomic libraries of the Gobi and Death Valley deserts. *Applied Microbiology and Biotechnology*, *91*(3), 635–644. https://doi.org/10.1007/S00253-011-3256-9/TABLES/3

Ngara, T. R., & Zhang, H. (2018). Recent Advances in Function-based Metagenomic Screening. In *Genomics, Proteomics and Bioinformatics* (Vol. 16, Issue 6, pp. 405–415). Elsevier.

https://doi.org/10.1016/j.gpb.2018.01.002

Nguyen, C. C., Hugie, C. N., Kile, M. L., & Navab-Daneshmand, T. (2019). Association between heavy metals and antibiotic-resistant human pathogens in environmental reservoirs: A review. *Frontiers of Environmental Science & Engineering 2019 13:3*, *13*(3), 1–17. https://doi.org/10.1007/S11783-019-1129-0

Nicolaou, K. C., & Rigol, S. (2018). A brief history of antibiotics and select advances in their synthesis. *The Journal of Antibiotics*, *71*(2), 153–184. https://doi.org/10.1038/ja.2017.62

Nikaido, H. (2009). Multidrug Resistance in Bacteria. *Annual Review of Biochemistry*, *78*, 119. https://doi.org/10.1146/ANNUREV.BIOCHEM.78.082907.145923

Nishimuro, H., Ohnishi, H., Sato, M., Ohnishi-Kameyama, M., Matsunaga, I., Naito, S., Ippoushi, K., Oike, H., Nagata, T., Akasaka, H., Saitoh, S., Shimamoto, K., & Kobori, M. (2015). Estimated daily intake and seasonal food sources of quercetin in Japan. *Nutrients*, *7*(4), 2345–2358. https://doi.org/10.3390/nu7042345

Niu, S., Wei, J., Zou, C., Chavda, K. D., Lv, J., Zhang, H., Du, H., Tang, Y. W., Pitout, J. D. D., Bonomo, R. A., Kreiswirth, B. N., & Chen, L. (2020). In vitro selection of aztreonam/avibactam resistance in dual-carbapenemase-producing Klebsiella pneumoniae. *Journal of Antimicrobial Chemotherapy*, *75*(3), 559–565. https://doi.org/10.1093/JAC/DKZ468

Nm, J., Joseph, A., Maliakel, B., & Im, K. (2018). Dietary addition of a standardized extract of turmeric ({TurmaFEEDTM}) improves growth performance and carcass quality of broilers. *Journal of Animal Science and Technology*, *60*, 8. https://doi.org/10.1186/s40781-018-0167-7

Nordstrom, L., Liu, C. M., & Price, L. B. (2013). Foodborne urinary tract infections: a new paradigm for antimicrobial-resistant foodborne illness. *Frontiers in Microbiology*, *4*, 29. https://doi.org/10.3389/fmicb.2013.00029

Norton, M. D., Spilkia, A. J., & Godoy, V. G. (2013). Antibiotic Resistance Acquired through a DNA Damage-Inducible Response in Acinetobacter baumannii. *Journal of Bacteriology*, *195*(6), 1335. https://doi.org/10.1128/JB.02176-12

Noureen, N., Cheema, M. T., Anwar, S., Hasnain, S., & Sajid, I. (2020). PCR-based Screening Approach: A Rapid Method to Detect the Biosynthetic Potential of Antimicrobials in Actinobacterial Strains. *Polish Journal of Microbiology*, *69*(2), 139. https://doi.org/10.33073/PJM-2020-016

O'Neill, J. (2014). *Antimicrobial Resistance: Tackling a crisis for the health and wealth of nations*.

Oakley, B. B., & Kogut, M. H. (2016). Spatial and Temporal Changes in the Broiler Chicken Cecal and Fecal Microbiomes and Correlations of Bacterial Taxa with Cytokine Gene Expression. *Frontiers in Veterinary Science*, *3*(FEB). https://doi.org/10.3389/FVETS.2016.00011

Oh, S., Gadde, U. D., Bravo, D., Lillehoj, E. P., & Lillehoj, H. S. (2018). Growth-Promoting and Antioxidant Effects of Magnolia Bark Extract in Chickens Uninfected or Co-Infected with Clostridium perfringens and Eimeria maxima as an Experimental Model of Necrotic Enteritis. *Current Developments in Nutrition*, *2*(4), nzy009. https://doi.org/10.1093/cdn/nzy009

Ohene-Agyei, T., Mowla, R., Rahman, T., & Venter, H. (2014). Phytochemicals increase the antibacterial activity of antibiotics by acting on a drug efflux pump. *MicrobiologyOpen*, *3*(6), 885–896. https://doi.org/10.1002/MBO3.212

Ohore, O. E., Addo, F. G., Zhang, S., Han, N., & Anim-Larbi, K. (2019). Distribution and relationship between antimicrobial resistance genes and heavy metals in surface sediments of Taihu Lake, China. *Journal of Environmental Sciences (China)*, *77*, 323–335. https://doi.org/10.1016/j.jes.2018.09.004

Oladeinde, A., Abdo, Z., Zwirzitz, B., Woyda, R., Lakin, S. M., Press, M. O., Cox, N. A., Thomas, J. C., Looft, T., Rothrock, M. J., Zock, G., Lawrence, J. P., Cudnik, D., Ritz, C., Aggrey, S. E., Liachko, I., Grove, J. R., & Wiersma, C. (2021). Litter commensal bacteria can limit the horizontal gene transfer of antimicrobial resistance to Salmonella in chickens. *BioRxiv*, 2021.04.02.438293. https://doi.org/10.1101/2021.04.02.438293

Oliver, A., Cantón, R., Campo, P., Baquero, F., & Blázquez, J. (2000). High frequency of hypermutable Pseudomonas aeruginosa in cystic fibrosis lung infection. *Science*, *288*(5469), 1251–1253. https://doi.org/10.1126/SCIENCE.288.5469.1251/ASSET/CFA36892-C436-4822-9340-2275A31C780A/ASSETS/GRAPHIC/SE1708507002.JPEG

Oluwatuyi, M., Kaatz, G. W., & Gibbons, S. (2004). Antibacterial and resistance modifying activity of Rosmarinus officinalis. *Phytochemistry*, *65*(24), 3249–3254. https://doi.org/10.1016/j.phytochem.2004.10.009

Oost, M. J., Velkers, F. C., Kraneveld, A. D., & Venema, K. (2021). Development of the in vitro Cecal Chicken ALIMEntary tRact mOdel-2 to Study Microbiota Composition and Function. *Frontiers in Microbiology*, *12*. https://doi.org/10.3389/FMICB.2021.726447/FULL

Ortiz, L. M. G., Lombardi, P., Tillhon, M., & Scovassi, A. I. (2014). Berberine, an epiphany against cancer. *Molecules (Basel, Switzerland)*, *19*(8), 12349–12367. https://doi.org/10.3390/molecules190812349

Osmon, S., Ward, S., Fraser, V. J., & Kollef, M. H. (2004). Hospital mortality for patients with bacteremia due to Staphylococcus aureus or Pseudomonas aeruginosa. *Chest*, *125*(2), 607–616. https://doi.org/10.1378/chest.125.2.607

Ouji, M., Augereau, J.-M., Paloque, L., & Benoit-Vical, F. (2018). Plasmodium falciparum resistance to artemisinin-based combination therapies: A sword of Damocles in the path toward malaria elimination. *Parasite*, *25*, 24. https://doi.org/10.1051/parasite/2018021

Ouyang, J., Sun, F., Feng, W., Sun, Y., Qiu, X., Xiong, L., Liu, Y., & Chen, Y. (2016). Quercetin is an effective inhibitor of quorum sensing, biofilm formation and virulence factors in Pseudomonas aeruginosa. *Journal of Applied Microbiology*, *120*(4), 966–974. https://doi.org/10.1111/jam.13073

Ozma, M. A., Khodadadi, E., Pakdel, F., Kamounah, F. S., Yousefi, M., Yousefi, B., Asgharzadeh, M., Ganbarov, K., & Kafil, H. S. (2021). Baicalin, a natural antimicrobial and anti-biofilm agent. *Journal of Herbal Medicine*, *27*, 100432. https://doi.org/10.1016/J.HERMED.2021.100432

Pal, A., & Tripathi, A. (2019). Quercetin potentiates meropenem activity among pathogenic carbapenem resistant Pseudomonas aeruginosa and Acinetobacter baumannii. *Journal of Applied Microbiology*. https://doi.org/10.1111/jam.14388

Pal, G., & Srivastava, S. (2014). Cloning and heterologous expression of {plnE}, -F, -J and -K genes derived from soil metagenome and purification of active plantaricin peptides. *Applied Microbiology and Biotechnology*, *98*(3), 1441–1447. https://doi.org/10.1007/s00253-013-5097-1

Paltansing, S., Kraakman, M., Van Boxtel, R., Kors, I., Wessels, E., Goessens, W., Tommassen, J., & Bernards, A. (2015). Increased Expression Levels of Chromosomal AmpC β-Lactamase in Clinical Escherichia coli Isolates and Their Effect on Susceptibility to Extended-Spectrum Cephalosporins. *Https://Home.Liebertpub.Com/Mdr*, *21*(1), 7–16. https://doi.org/10.1089/MDR.2014.0108

Pang, Z., Raudonis, R., Glick, B. R., Lin, T.-J., & Cheng, Z. (2019). Antibiotic resistance in Pseudomonas aeruginosa: mechanisms and alternative therapeutic strategies. *Biotechnology Advances*, *37*(1), 177–192. https://doi.org/10.1016/j.biotechadv.2018.11.013

Pankey, G. A., & Sabath, L. D. (2004). Clinical relevance of bacteriostatic versus bactericidal mechanisms of action in the treatment of Gram-positive bacterial infections. *Clinical Infectious Diseases*, *38*(6), 864–870. https://doi.org/10.1086/381972

Pao, S. S., Paulsen, I. T., & Saier, M. H. (1998). Major facilitator superfamily. *Microbiology and Molecular Biology Reviews*, *62*(1), 1–34. https://doi.org/10.1128/{MMBR}.62.1.1-34.1998

Park, I., Oh, S., Lillehoj, E. P., & Lillehoj, H. S. (2020). Dietary supplementation with magnolia bark extract alters chicken intestinal metabolite levels. *Frontiers in Veterinary Science*, *7*, 157. https://doi.org/10.3389/fvets.2020.00157

Park, I., Zimmerman, N. P., Smith, A. H., Rehberger, T. G., Lillehoj, E. P., & Lillehoj, H. S. (2020). Dietary Supplementation With Bacillus subtilis Direct-Fed Microbials Alters Chicken Intestinal Metabolite Levels. *Frontiers in Veterinary Science*, *7*, 123. https://doi.org/10.3389/fvets.2020.00123

Patel, R. V, Mistry, B. M., Shinde, S. K., Syed, R., Singh, V., & Shin, H.-S. (2018). Therapeutic potential of quercetin as a cardiovascular agent. *European Journal of Medicinal Chemistry*, *155*, 889–904. https://doi.org/10.1016/j.ejmech.2018.06.053

Pathak, M., Devi, A., Sarma, H. K., & Lal, B. (2014). Application of bioflocculating property of Pseudomonas aeruginosa strain IASST201 in treatment of oil-field formation water. *Journal of Basic Microbiology*, *54*(7), 658–669. https://doi.org/10.1002/JOBM.201301011

Paulo, P. L., Azevedo, C., Begosso, L., Galbiati, A. F., & Boncz, M. A. (2013). Natural systems treating greywater and blackwater on-site: Integrating treatment, reuse and landscaping. *Ecological Engineering*, *50*, 95–100. https://doi.org/10.1016/J.ECOLENG.2012.03.022

Paulson, J. N., Stine, O. C., Bravo, H. C., & Pop, M. (2013). Differential abundance analysis for microbial marker-gene surveys. *Nature Methods*, *10*(12), 1200–1202. https://doi.org/10.1038/nmeth.2658

Pawlowski, A. C., Wang, W., Koteva, K., Barton, H. A., McArthur, A. G., & Wright, G. D. (2016). A diverse intrinsic antibiotic resistome from a cave bacterium. *Nature Communications*, *7*, 13803. https://doi.org/10.1038/ncomms13803

Pearcy, N., Hu, Y., Baker, M., Maciel-Guerra, A., Xue, N., Wang, W., Kaler, J., Peng, Z., Li, F., &

Dottorini, T. (2021). Genome-Scale Metabolic Models and Machine Learning Reveal Genetic Determinants of Antibiotic Resistance in Escherichia coli and Unravel the Underlying Metabolic Adaptation Mechanisms. *MSystems*, *6*(4). https://doi.org/10.1128/MSYSTEMS.00913-20

Pechmann, S., Chartron, J. W., & Frydman, J. (2014). Local slowdown of translation by nonoptimal codons promotes nascent-chain recognition by SRP in vivo. *Nature Structural & Molecular Biology*, *21*(12), 1100–1105. https://doi.org/10.1038/NSMB.2919

Pechmann, S., & Frydman, J. (2013). Evolutionary conservation of codon optimality reveals hidden signatures of cotranslational folding. *Nature Structural & Molecular Biology*, *20*(2), 237–243. https://doi.org/10.1038/NSMB.2466

Peleg, A. Y., Seifert, H., & Paterson, D. L. (2008). Acinetobacter baumannii: Emergence of a Successful Pathogen. *Clinical Microbiology Reviews*, *21*(3), 538. https://doi.org/10.1128/CMR.00058-07

Peng, Q., Zeng, X. F., Zhu, J. L., Wang, S., Liu, X. T., Hou, C. L., Thacker, P. A., & Qiao, S. Y. (2016). Effects of dietary Lactobacillus plantarum B1 on growth performance, intestinal microbiota, and short chain fatty acid profiles in broiler chickens. *Poultry Science*, *95*(4), 893–900. https://doi.org/10.3382/PS/PEV435

Pérez-Reytor, D., Pavón, A., Lopez-Joven, C., Ramírez-Araya, S., Peña-Varas, C., Plaza, N., Alegría-Arcos, M., Corsini, G., Jaña, V., Pavez, L., del Pozo, T., Bastías, R., Blondel, C. J., Ramírez, D., & García, K. (2020). Analysis of the Zonula occludens Toxin Found in the Genome of the Chilean Non-toxigenic Vibrio parahaemolyticus Strain PMC53.7. *Frontiers in Cellular and Infection Microbiology*, *10*, 482. https://doi.org/10.3389/FCIMB.2020.00482/BIBTEX

Perron, G. G., Zasloff, M., & Bell, G. (2006). Experimental evolution of resistance to an antimicrobial peptide. *Proceedings. Biological Sciences / the Royal Society*, *273*(1583), 251–256. https://doi.org/10.1098/rspb.2005.3301

Perron, K., Caille, O., Rossier, C., Van Delden, C., Dumas, J. L., & Köhler, T. (2004). CzcR-CzcS, a Two-component System Involved in Heavy Metal and Carbapenem Resistance in Pseudomonas aeruginosa. *Journal of Biological Chemistry*, *279*(10), 8761–8768. https://doi.org/10.1074/JBC.M312080200

Pessoa, L. Z. da S., Duarte, J. L., Ferreira, R. M. dos A., Oliveira, A. E. M. de F. M., Cruz, R. A. S., Faustino, S. M. M., Carvalho, J. C. T., Fernandes, C. P., Souto, R. N. P., & Araújo, R. S. (2018). Nanosuspension of quercetin: preparation, characterization and effects against Aedes aegypti larvae. *Revista Brasileira de Farmacognosia*, *28*(5), 618–625. https://doi.org/10.1016/J.BJP.2018.07.003

Peterfreund, G. L., Vandivier, L. E., Sinha, R., Marozsan, A. J., Olson, W. C., Zhu, J., & Bushman, F. D. (2012). Succession in the Gut Microbiome following Antibiotic and Antibody Therapies for Clostridium difficile. *PLOS ONE*, *7*(10), e46966. https://doi.org/10.1371/JOURNAL.PONE.0046966

Peters, K., Pazos, M., Edoo, Z., Hugonnet, J. E., Martorana, A. M., Polissi, A., VanNieuwenhze, M. S., Arthur, M., & Vollmer, W. (2018). Copper inhibits peptidoglycan LD-transpeptidases suppressing β-lactam resistance due to bypass of penicillin-binding proteins. *Proceedings of the National Academy of Sciences of the United States of America*, *115*(42), 10786–10791. https://doi.org/10.1073/PNAS.1809285115/SUPPL_FILE/PNAS.1809285115.SAPP.PDF

Petričević, V., Lukić, M., Škrbić, Z., Rakonjac, S., Dosković, V., Petričević, M., & Stanojković, A. (2018). The effect of using rosemary (Rosmarinus officinalis) in broiler nutrition on production parameters, slaughter characteristics, and gut microbiological population. *Turkish Journal of Veterinary and Animal Sciences*, *42*(6), 658–664. https://doi.org/10.3906/VET-1803-53

Petry, F., & Loos, M. (2005). Common silent mutations in all types of hereditary complement C1q deficiencies. *Immunogenetics*, *57*(8), 566–571. https://doi.org/10.1007/S00251-005-0023-Z

Piotrowska, M., Kowalska, S., & Popowska, M. (2019). Diversity of β-lactam resistance genes in Gram-negative rods isolated from a municipal wastewater treatment plant. *Annals of Microbiology*, *69*(6), 591–601. https://doi.org/10.1007/S13213-019-01450-1/TABLES/3

Plackett, B. (2020). Why big pharma has abandoned antibiotics. *Nature*, *586*(7830), S50–S52. https://doi.org/10.1038/d41586-020-02884-3

Plaper, A., Golob, M., Hafner, I., Oblak, M., Solmajer, T., & Jerala, R. (2003). Characterization of quercetin binding site on {DNA} gyrase. *Biochemical and Biophysical Research Communications*, *306*(2), 530–536. https://doi.org/10.1016/S0006-{291X}(03)01006-4

Plata, G., Baxter, N. T., Susanti, D., Volland-Munson, A., Gangaiah, D., Nagireddy, A., Mane, S. P., Balakuntla, J., Hawkins, T. B., & Kumar Mahajan, A. (2022). Growth promotion and antibiotic induced metabolic shifts in the chicken gut microbiome. *Communications Biology 2022 5:1*, *5*(1), 1–14. https://doi.org/10.1038/s42003-022-03239-6

Proença, J. T., Barral, D. C., & Gordo, I. (2017). Commensal-to-pathogen transition: One-single transposon insertion results in two pathoadaptive traits in Escherichia coli -macrophage interaction. *Scientific Reports*, *7*(1), 4504. https://doi.org/10.1038/s41598-017-04081-1

Putnins, M., & Androulakis, I. P. (2021). Self-selection of evolutionary strategies: adaptive versus non-adaptive forces. *Heliyon*, *7*(5), e06997. https://doi.org/10.1016/J.HELIYON.2021.E06997

Qiu, X., Kroeker, A., He, S., Kozak, R., Audet, J., Mbikay, M., & Chrétien, M. (2016). Prophylactic Efficacy of Quercetin 3-β-O-d-Glucoside against Ebola Virus Infection. *Antimicrobial Agents and Chemotherapy*, *60*(9), 5182–5188. https://doi.org/10.1128/{AAC}.00307-16

Qu, S., Dai, C., Shen, Z., Tang, Q., Wang, H., Zhai, B., Zhao, L., & Hao, Z. (2019). Mechanism of Synergy Between Tetracycline and Quercetin Against Antibiotic Resistant Escherichia coli. *Frontiers in Microbiology*, *10*, 2536. https://doi.org/10.3389/fmicb.2019.02536

Rabausch, U., Juergensen, J., Ilmberger, N., Böhnke, S., Fischer, S., Schubach, B., Schulte, M., & Streit, W. R. (2013). Functional screening of metagenome and genome libraries for detection of novel flavonoid-modifying enzymes. *Applied and Environmental Microbiology*, *79*(15), 4551–4563. https://doi.org/10.1128/{AEM}.01077-13

Rabbani, G. H., Butler, T., Knight, J., Sanyal, S. C., & Alam, K. (1987). Randomized controlled trial of berberine sulfate therapy for diarrhea due to enterotoxigenic Escherichia coli and Vibrio cholerae. *The Journal of Infectious Diseases*, *155*(5), 979–984. https://doi.org/10.1093/infdis/155.5.979

Rahman, A. (2017). *Chapter 1 (Introduction), Thesis*. University College London.

Rahman, M. A., Kaiser, F., Jamshidi, S., Freitas Monteiro, M., Rahman, K. M., Mullany, P., & Roberts, A. P. (2020). Integron gene cassettes harboring novel variants of D-alanine-D-alanine ligase confer high-level resistance to D-cycloserine. *Scientific Reports*, *10*(1), 20709. https://doi.org/10.1038/s41598-020-77377-4

Ranjitkar, S., Lawley, B., Tannock, G., & Engberg, R. M. (2016). Bacterial Succession in the Broiler Gastrointestinal Tract. *Applied and Environmental Microbiology*, *82*(8), 2399–2410. https://doi.org/10.1128/AEM.02549-15

Rasamiravaka, T., Labtani, Q., Duez, P., & El Jaziri, M. (2015). The formation of biofilms by pseudomonas aeruginosa: A review of the natural and synthetic compounds interfering with control mechanisms. *BioMed Research International*, *2015*. https://doi.org/10.1155/2015/759348

Ratner, H. K., Sampson, T. R., & Weiss, D. S. (2016). Overview of {CRISPR}-Cas9 Biology. *Cold Spring Harbor Protocols*, *2016*(12). https://doi.org/10.1101/pdb.top088849

Reygaert, W. C. (2018). An overview of the antimicrobial resistance mechanisms of bacteria. *AIMS Microbiology*, *4*(3), 482. https://doi.org/10.3934/MICROBIOL.2018.3.482

Reynolds, L. J. (2017). *The identification and characterisation of novel antimicrobial resistance genes from human and animal metagenomes*. UCL Eastman Dental Institute.

Reynolds, L. J., Roberts, A. P., & Anjum, M. F. (2016). Efflux in the oral metagenome: The discovery of a novel tetracycline and tigecycline ABC transporter. *Frontiers in Microbiology*, *7*(DEC), 1923. https://doi.org/10.3389/FMICB.2016.01923/BIBTEX

Rezaeiamiri, E., Bahramsoltani, R., & Rahimi, R. (2020). Plant-derived natural agents as dietary supplements for the regulation of glycosylated hemoglobin: A review of clinical trials. *Clinical Nutrition*, *39*(2), 331–342. https://doi.org/10.1016/j.clnu.2019.02.006

Richards, P., Fothergill, J., Bernardeau, M., & Wigley, P. (2019). Development of the caecal microbiota in three broiler breeds. *Frontiers in Veterinary Science*, *6*(JUN), 201. https://doi.org/10.3389/FVETS.2019.00201/FULL

Riesenfeld, C. S., Goodman, R. M., & Handelsman, J. (2004). Uncultured soil bacteria are a reservoir of new antibiotic resistance genes. *Environmental Microbiology*, *6*(9), 981–989. https://doi.org/10.1111/j.1462-2920.2004.00664.x

Roberts, A. P. (2020). Swab and Send: a citizen science, antibiotic discovery project. *Future Science OA*, *6*(6). https://doi.org/10.2144/FSOA-2020-0053

Roberts, M. (2005). Update on acquired tetracycline resistance genes. In *FEMS Microbiology Letters* (Vol. 245, Issue 2, pp. 195–203). Oxford Academic. https://doi.org/10.1016/j.femsle.2005.02.034

Round, J. L., & Mazmanian, S. K. (2009). The gut microbiota shapes intestinal immune responses during health and disease. *Nature Reviews Immunology 2009 9:5*, *9*(5), 313–323. https://doi.org/10.1038/nri2515

Rubio, L. A., Peinado, M. J., Ruiz, R., Suárez-Pereira, E., Ortiz Mellet, C., & García Fernández, J. M. (2015). Correlations between changes in intestinal microbiota composition and performance parameters in broiler chickens. *Journal of Animal Physiology and Animal Nutrition*, *99*(3), 418–423. https://doi.org/10.1111/JPN.12256

Rychlik, I. (2020). Composition and Function of Chicken Gut Microbiota. *Animals : An Open Access Journal from MDPI*, *10*(1). https://doi.org/10.3390/ANI10010103

Sadikot, R. T., Blackwell, T. S., Christman, J. W., & Prince, A. S. (2005). Pathogen-host interactions in Pseudomonas aeruginosa pneumonia. *American Journal of Respiratory and Critical Care Medicine*, *171*(11), 1209–1223. https://doi.org/10.1164/rccm.200408-{1044SO}

Sahu, J., Koley, K. M., & Sahu, B. D. (2017). Attribution of antibacterial and antioxidant activity of Cassia tora extract toward its growth promoting effect in broiler birds. *Veterinary World*, *10*(2), 221–226. https://doi.org/10.14202/vetworld.2017.221-226

Saier, M. H., & Paulsen, I. T. (2001). Phylogeny of multidrug transporters. *Seminars in Cell \& Developmental Biology*, *12*(3), 205–213. https://doi.org/10.1006/scdb.2000.0246

Salehi, B., Venditti, A., Sharifi-Rad, M., Kręgiel, D., Sharifi-Rad, J., Durazzo, A., Lucarini, M., Santini, A., Souto, E. B., Novellino, E., Antolak, H., Azzini, E., Setzer, W. N., & Martins, N. (2019). The therapeutic potential of apigenin. *International Journal of Molecular Sciences*, *20*(6). https://doi.org/10.3390/ijms20061305

Sallam, I. E., Abdelwareth, A., Attia, H., Aziz, R. K., Homsi, M. N., von Bergen, M., & Farag, M. A. (2021). Effect of gut microbiota biotransformation on dietary tannins and human health implications. In *Microorganisms* (Vol. 9, Issue 5, p. 965). Multidisciplinary Digital Publishing Institute. https://doi.org/10.3390/microorganisms9050965

Sampson, L., Rimm, E., Hollman, P. C. H., de Vries, J. H. M., & Katan, M. B. (2002). Flavonol and flavone intakes in {US} health professionals. *Journal of the American Dietetic Association*, *102*(10), 1414–1420. https://doi.org/10.1016/s0002-8223(02)90314-7

Santos-Lopez, A., Marshall, C. W., Scribner, M. R., Snyder, D. J., & Cooper, V. S. (2019). Evolutionary pathways to antibiotic resistance are dependent upon environmental structure and bacterial lifestyle. *ELife*, *8*. https://doi.org/10.7554/elife.47612

Sarabhai, S., Sharma, P., & Capalash, N. (2013). Ellagic Acid Derivatives from Terminalia chebula Retz. Downregulate the Expression of Quorum Sensing Genes to Attenuate Pseudomonas aeruginosa PAO1 Virulence. *PLOS ONE*, *8*(1), e53441. https://doi.org/10.1371/JOURNAL.PONE.0053441

Sauvage, E., & Terrak, M. (2016). Glycosyltransferases and Transpeptidases/Penicillin-Binding Proteins: Valuable Targets for New Antibacterials. *Antibiotics 2016, Vol. 5, Page 12*, *5*(1), 12. https://doi.org/10.3390/ANTIBIOTICS5010012

Schliep, K. P. (2011). phangorn: phylogenetic analysis in R. *Bioinformatics*, *27*(4), 592–593. https://doi.org/10.1093/BIOINFORMATICS/BTQ706

Thomas Schön, Jim Werngren, Diana Machado, Emanuele Borroni, Maria Wijkander, Gerard Lina, Johan Mouton, Erika Matuschek, Gunnar Kahlmeter, Christian Giske, Miguel Santin, Daniela Maria Cirillo, Miguel Viveiros, Emmanuelle Cambau, Antimicrobial susceptibility testing of Mycobacterium tuberculosis complex isolates – the EUCAST broth microdilution reference method for MIC determination, Clinical Microbiology and Infection, Volume 26, Issue 11, 2020, Pages 1488-1492, ISSN 1198-743X, https://doi.org/10.1016/j.cmi.2020.07.036. (https://www.sciencedirect.com/science/article/pii/S1198743X20304444)).

Seemann, T. (2022). *GitHub - tseemann/abricate: Mass screening of contigs for antimicrobial and virulence genes*. https://github.com/tseemann/abricate

Seiler, C., & Berendonk, T. U. (2012). Heavy metal driven co-selection of antibiotic resistance in soil and water bodies impacted by agriculture and aquaculture. *Frontiers in*

Microbiology, *3*, 399. https://doi.org/10.3389/fmicb.2012.00399

Selma, M. V., Tomás-Barberán, F. A., Beltrán, D., García-Villalba, R., & Espín, J. C. (2014). Gordonibacter urolithinfaciens sp. nov., a urolithin-producing bacterium isolated from the human gut. *International Journal of Systematic and Evolutionary Microbiology*, *64*(PART 7), 2346–2352. https://doi.org/10.1099/IJS.0.055095-0/CITE/REFWORKS

Shahi, S. K., Freedman, S. N., Murra, A. C., Zarei, K., Sompallae, R., Gibson-Corley, K. N., Karandikar, N. J., Murray, J. A., & Mangalam, A. K. (2019). Prevotella histicola, a human gut commensal, is as potent as COPAXONE® in an animal model of multiple sclerosis. *Frontiers in Immunology*, *10*(MAR), 462. https://doi.org/10.3389/FIMMU.2019.00462/BIBTEX

Shang, Y., Kumar, S., Oakley, B., & Kim, W. K. (2018). Chicken gut microbiota: Importance and detection technology. In *Frontiers in Veterinary Science* (Vol. 5, Issue OCT, p. 254). Frontiers Media S.A. https://doi.org/10.3389/fvets.2018.00254

Shapira, R., & Mimran, E. (2007). Isolation and characterization of Escherichia coli mutants exhibiting altered response to thymol. *Microbial Drug Resistance*, *13*(3), 157–165. https://doi.org/10.1089/mdr.2007.731

Sharma, U., Pal, D., & Prasad, R. (2014). Alkaline Phosphatase: An Overview. *Indian Journal of Clinical Biochemistry*, *29*(3), 269. https://doi.org/10.1007/S12291-013-0408-Y

Shaw, L., Ribeiro, A. L. R., Levine, A. P., Pontikos, N., Balloux, F., Segal, A. W., Roberts, A. P., & Smith, A. M. (2017). The human salivary microbiome is shaped by shared environment rather than genetics: Evidence from a large family of closely related individuals. *MBio*, *8*(5). https://doi.org/10.1128/MBIO.01237-17/SUPPL_FILE/MBO004173481SF7.TIF

Sherrard, L. J., Graham, K. A., McGrath, S. J., McIlreavey, L., Hatch, J., Muhlebach, M. S., Wolfgang, M. C., Gilpin, D. F., Elborn, J. S., Schneiders, T., & Tunney, M. M. (2013). Antibiotic resistance in Prevotella species isolated from patients with cystic fibrosis. *Journal of Antimicrobial Chemotherapy*, *68*(10), 2369. https://doi.org/10.1093/JAC/DKT191

Sherrard, L. J., Schaible, B., Graham, K. A., McGrath, S. J., McIlreavey, L., Hatch, J., Wolfgang, M. C., Muhlebach, M. S., Gilpin, D. F., Schneiders, T., Stuart Elborn, J., & Tunney, M. M. (2014). Mechanisms of reduced susceptibility and genotypic prediction of antibiotic resistance in Prevotella isolated from cystic fibrosis (CF) and non-CF patients. *Journal of Antimicrobial Chemotherapy*, *69*(10), 2690–2698. https://doi.org/10.1093/JAC/DKU192

Shi, S., & Ehrt, S. (2006). Dihydrolipoamide Acyltransferase Is Critical for Mycobacterium tuberculosis Pathogenesis. *Infection and Immunity*, *74*(1), 56. https://doi.org/10.1128/IAI.74.1.56-63.2006

Shin, W., Wu, A., Massidda, M. W., Foster, C., Thomas, N., Lee, D. W., Koh, H., Ju, Y., Kim, J., & Kim, H. J. (2019). A robust longitudinal co-culture of obligate anaerobic gut microbiome with human intestinal epithelium in an anoxic-oxic interface-on-a-chip. *Frontiers in Bioengineering and Biotechnology*, *7*(FEB). https://doi.org/10.3389/FBIOE.2019.00013/FULL

Shoemaker, N. B., Vlamakis, H., Hayes, K., & Salyers, A. A. (2001). Evidence for extensive resistance gene transfer among Bacteroides spp. and among Bacteroides and other genera in the human colon. *Applied and Environmental Microbiology*, *67*(2), 561–568.

https://doi.org/10.1128/AEM.67.2.561-568.2001

Siegerstetter, S. C., Schmitz-Esser, S., Magowan, E., Wetzels, S. U., Zebeli, Q., Lawlor, P. G., O'Connell, N. E., & Metzler-Zebeli, B. U. (2017). Intestinal microbiota profiles associated with low and high residual feed intake in chickens across two geographical locations. *PloS One*, *12*(11). https://doi.org/10.1371/JOURNAL.PONE.0187766

Sievers, F., Wilm, A., Dineen, D., Gibson, T. J., Karplus, K., Li, W., Lopez, R., McWilliam, H., Remmert, M., Söding, J., Thompson, J. D., & Higgins, D. G. (2011). Fast, scalable generation of high-quality protein multiple sequence alignments using Clustal Omega. *Molecular Systems Biology*, *7*(1), 539. https://doi.org/10.1038/MSB.2011.75

Silver, S., & Misra, T. K. (1988). Plasmid-mediated heavy metal resistances. *Annual Review of Microbiology*, *42*, 717–743. https://doi.org/10.1146/ANNUREV.MI.42.100188.003441

Singer, A., Kirchhelle, C., & Roberts, A. (2019a). Reinventing the antimicrobial pipeline in response to the global crisis of antimicrobial-resistant infections. *F1000Research*, *8*, 238. https://doi.org/10.12688/f1000research.18302.1

Singer, A., Kirchhelle, C., & Roberts, A. (2019b). (Inter)nationalising the antibiotic research and development pipeline. *The Lancet Infectious Diseases*. https://doi.org/10.1016/S1473-3099(19)30552-3

Singer, A., Shaw, H., Rhodes, V., & Hart, A. (2016). Review of antimicrobial resistance in the environment and its relevance to environmental regulators. *Frontiers in Microbiology*, *7*, 1728. https://doi.org/10.3389/fmicb.2016.01728

Sinha, R., Abnet, C. C., White, O., Knight, R., & Huttenhower, C. (2015). The microbiome quality control project: baseline study design and future directions. *Genome Biology 2015 16:1*, *16*(1), 1–6. https://doi.org/10.1186/S13059-015-0841-8

Siriwong, S., Teethaisong, Y., Thumanu, K., Dunkhunthod, B., & Eumkeb, G. (2016). The synergy and mode of action of quercetin plus amoxicillin against amoxicillin-resistant Staphylococcus epidermidis. *BMC Pharmacology and Toxicology*, *17*(1), 1–14. https://doi.org/10.1186/S40360-016-0083-8/FIGURES/11

Sivaraman, J., Li, Y., Banks, J., Cane, D. E., Matte, A., & Cygler, M. (2003). Crystal structure of Escherichia coli PdxA, an enzyme involved in the pyridoxal phosphate biosynthesis pathway. *The Journal of Biological Chemistry*, *278*(44), 43682–43690. https://doi.org/10.1074/JBC.M306344200

Smillie, C., Garcillán-Barcia, M. P., Francia, M. V., Rocha, E. P. C., & de la Cruz, F. (2010). Mobility of Plasmids. *Microbiology and Molecular Biology Reviews*, *74*(3), 434–452. https://doi.org/10.1128/MMBR.00020-10/SUPPL_FILE/SUPPLEMENTARY_TABLES2.DOC

Smith, A. J., Kavuru, P., Wojtas, L., Zaworotko, M. J., & Shytle, R. D. (2011). Cocrystals of quercetin with improved solubility and oral bioavailability. *Molecular Pharmaceutics*, *8*(5), 1867–1876. https://doi.org/10.1021/MP200209J

Smith, E. E., Buckley, D. G., Wu, Z., Saenphimmachak, C., Hoffman, L. R., D'Argenio, D. A., Miller, S. I., Ramsey, B. W., Speert, D. P., Moskowitz, S. M., Burns, J. L., Kaul, R., & Olson, M. V. (2006). Genetic adaptation by Pseudomonas aeruginosa to the airways of cystic fibrosis patients. *Proceedings of the National Academy of Sciences of the United States of America*, *103*(22), 8487–8492. https://doi.org/10.1073/PNAS.0602138103/SUPPL_FILE/02138TABLE6.XLS

Smith, S. R. (2009). A critical review of the bioavailability and impacts of heavy metals in municipal solid waste composts compared to sewage sludge. *Environment International*, *35*(1), 142–156. https://doi.org/10.1016/j.envint.2008.06.009

Sneath, P. H. A. (1994). Handbook of new bacterial systematics. *Trends in Ecology & Evolution*, *9*(5), 197. https://doi.org/10.1016/0169-5347(94)90093-0

Social Science Statistics. (2022). *T-Test Calculator for 2 Independent Means*. https://www.socscistatistics.com/tests/studentttest/default2.aspx

SoftBerry. (2020). *SoftBerry - BPROM HELP*. http://www.softberry.com/berry.phtml?topic=bprom&group=help&subgroup=gfindb

Somerset, S. M., & Johannot, L. (2008). Dietary flavonoid sources in Australian adults. *Nutrition and Cancer*, *60*(4), 442–449. https://doi.org/10.1080/01635580802143836

Sood, A., Ray, P., & Angrup, A. (2021). Phenotypic and genotypic antimicrobial resistance in clinical anaerobic isolates from India. *JAC-Antimicrobial Resistance*, *3*(2). https://doi.org/10.1093/JACAMR/DLAB044

Soong, G., Parker, D., Magargee, M., & Prince, A. S. (2008). The type III toxins of Pseudomonas aeruginosa disrupt epithelial barrier function. *Journal of Bacteriology*, *190*(8), 2814–2821. https://doi.org/10.1128/JB.01567-07

Spangenberg, C., Heuer, T., Bürger, C., & Tümmler, B. (1996). Genetic diversity of flagellins of Pseudomonas aeruginosa. *FEBS Letters*, *396*(2–3), 213–217. https://doi.org/10.1016/0014-5793(96)01099-X

Spanogiannopoulos, P., Waglechner, N., Koteva, K., & Wright, G. D. (2014). A rifamycin inactivating phosphotransferase family shared by environmental and pathogenic bacteria. *Proceedings of the National Academy of Sciences of the United States of America*, *111*(19), 7102–7107. https://doi.org/10.1073/PNAS.1402358111/-/DCSUPPLEMENTAL

Stanley, D., Geier, M. S., Chen, H., Hughes, R. J., & Moore, R. J. (2015). Comparison of fecal and cecal microbiotas reveals qualitative similarities but quantitative differences. *BMC Microbiology*, *15*(1), 1–11. https://doi.org/10.1186/S12866-015-0388-6/FIGURES/7

Stanley, D., Hughes, R. J., Geier, M. S., & Moore, R. J. (2016). Bacteria within the Gastrointestinal Tract Microbiota Correlated with Improved Growth and Feed Conversion: Challenges Presented for the Identification of Performance Enhancing Probiotic Bacteria. *Frontiers in Microbiology*, *7*(FEB). https://doi.org/10.3389/FMICB.2016.00187

Stanley, D., Keyburn, A. L., Denman, S. E., & Moore, R. J. (2012). Changes in the caecal microflora of chickens following Clostridium perfringens challenge to induce necrotic enteritis. *Veterinary Microbiology*, *159*(1–2), 155–162. https://doi.org/10.1016/J.VETMIC.2012.03.032

Stromberg, Z. R., Johnson, J. R., Fairbrother, J. M., Kilbourne, J., Van Goor, A., Curtiss, R., & Mellata, M. (2017). Evaluation of Escherichia coli isolates from healthy chickens to determine their potential risk to poultry and human health. *PloS One*, *12*(7). https://doi.org/10.1371/JOURNAL.PONE.0180599

Su, T., Liu, S., Wang, K., Chi, K., Zhu, D., Wei, T., Huang, Y., Guo, L., Hu, W., Xu, S., Lin, Z., & Gu, L. (2015). The REC domain mediated dimerization is critical for FleQ from Pseudomonas aeruginosa to function as a c-di-GMP receptor and flagella gene

regulator. *Journal of Structural Biology*, *192*(1), 1–13. https://doi.org/10.1016/J.JSB.2015.09.002

Su, X.-Z., & Miller, L. H. (2015). The discovery of artemisinin and the Nobel Prize in Physiology or Medicine. *Science China. Life Sciences*, *58*(11), 1175–1179. https://doi.org/10.1007/s11427-015-4948-7

Sun, C., Wang, H., Wang, D., Chen, Y., Zhao, Y., & Xia, W. (2015). Using an {FFQ} to assess intakes of dietary flavonols and flavones among female adolescents in the Suihua area of northern China. *Public Health Nutrition*, *18*(4), 632–639. https://doi.org/10.1017/S1368980014000780

Sun, Q., Wang, H., Shu, L., Dong, N., Yang, F., Zhou, H., Chen, S., & Zhang, R. (2019). Leclercia adecarboxylata From Human Gut Flora Carries mcr-4.3 and blaIMP-4-Bearing Plasmids. *Frontiers in Microbiology*, *10*, 2805. https://doi.org/10.3389/FMICB.2019.02805/BIBTEX

Swab & Send | LSTM. (n.d.). Retrieved March 17, 2022, from https://www.lstmed.ac.uk/public-engagement/swab-send

Sychantha, D., Brott, A. S., Jones, C. S., & Clarke, A. J. (2018). Mechanistic pathways for peptidoglycan O-acetylation and De-O-acetylation. *Frontiers in Microbiology*, *9*(OCT), 2332. https://doi.org/10.3389/FMICB.2018.02332/BIBTEX

Takala-Harrison, S., Jacob, C. G., Arze, C., Cummings, M. P., Silva, J. C., Dondorp, A. M., Fukuda, M. M., Hien, T. T., Mayxay, M., Noedl, H., Nosten, F., Kyaw, M. P., Nhien, N. T. T., Imwong, M., Bethell, D., Se, Y., Lon, C., Tyner, S. D., Saunders, D. L., … Plowe, C. V. (2015). Independent emergence of artemisinin resistance mutations among Plasmodium falciparum in Southeast Asia. *The Journal of Infectious Diseases*, *211*(5), 670–679. https://doi.org/10.1093/infdis/jiu491

Takase, H., Yamamoto, K., Ito, K., & Yumioka, E. (1993). [Pharmacological studies on antidiarrheal effects of berberine and geranii herba]. *Nippon Yakurigaku Zasshi. Folia Pharmacologica Japonica*, *102*(2), 101–112. https://doi.org/10.1254/fpj.102.101

Talundzic, E., Okoth, S. A., Congpuong, K., Plucinski, M. M., Morton, L., Goldman, I. F., Kachur, P. S., Wongsrichanalai, C., Satimai, W., Barnwell, J. W., & Udhayakumar, V. (2015). Selection and spread of artemisinin-resistant alleles in Thailand prior to the global artemisinin resistance containment campaign. *{PLoS} Pathogens*, *11*(4), e1004789. https://doi.org/10.1371/journal.ppat.1004789

Tamtaji, O. R., Hadinezhad, T., Fallah, M., Shahmirzadi, A. R., Taghizadeh, M., Behnam, M., & Asemi, Z. (2020). The Therapeutic Potential of Quercetin in Parkinson's Disease: Insights into its Molecular and Cellular Regulation. *Current Drug Targets*, *21*(5), 509–518. https://doi.org/10.2174/1389450120666191112155654

Tamura, K., Sakazaki, R., Kosako, Y., & Yoshizaki, E. (1986). Leclercia adecarboxylata Gen. Nov., Comb. Nov., formerly known asEscherichia adecarboxylata. *Current Microbiology 1986 13:4*, *13*(4), 179–184. https://doi.org/10.1007/BF01568943

Tan, J., Wang, J., Yang, C., Zhu, C., Guo, G., Tang, J., & Shen, H. (2019). Antimicrobial characteristics of Berberine against prosthetic joint infection-related Staphylococcus aureus of different multi-locus sequence types. *{BMC} Complementary and Alternative Medicine*, *19*(1), 218. https://doi.org/10.1186/s12906-019-2558-9

Tarantino, L. M., & Eisener-Dorman, A. F. (2012). Forward Genetic Approaches to

Understanding Complex Behaviors. *Current Topics in Behavioral Neurosciences*, *12*, 25. https://doi.org/10.1007/7854_2011_189

Taylor, R. G., Walker, D. C., & McInnes, R. R. (1993). E. coli host strains significantly affect the quality of small scale plasmid {DNA} preparations used for sequencing. *Nucleic Acids Research*, *21*(7), 1677–1678. https://doi.org/10.1093/nar/21.7.1677

Tchounwou, P. B., Yedjou, C. G., Patlolla, A. K., & Sutton, D. J. (2012). Heavy Metals Toxicity and the Environment. *Exs*, *101*, 133–164. https://doi.org/10.1007/978-3-7643-8340-4_6

Team, R. C. (2020). *R: A language and environment for statistical computing.* R Foundation for Statistical Computing.

Tegos, G., Stermitz, F. R., Lomovskaya, O., & Lewis, K. (2002). Multidrug pump inhibitors uncover remarkable activity of plant antimicrobials. *Antimicrobial Agents and Chemotherapy*, *46*(10), 3133–3141. https://doi.org/10.1128/AAC.46.10.3133-3141.2002

Teuscher, F., Lowther, J., Skinner-Adams, T. S., Spielmann, T., Dixon, M. W. A., Stack, C. M., Donnelly, S., Mucha, A., Kafarski, P., Vassiliou, S., Gardiner, D. L., Dalton, J. P., & Trenholme, K. R. (2007). The M18 aspartyl aminopeptidase of the human malaria parasite Plasmodium falciparum. *Journal of Biological Chemistry*, *282*(42), 30817–30826. https://doi.org/10.1074/JBC.M704938200/ATTACHMENT/334F270C-21A0-45B5-BE2A-2552B510534E/MMC1.PDF

Thermo Scientific Template Generation System II Kit Technical Manual (p. 20). (2021). Thermo Scientific. https://www.thermofisher.com/document-connect/document-connect.html?url=https%3A%2F%2Fassets.thermofisher.com%2FTFS-Assets%2FLSG%2Fmanuals%2FMAN0013385_Template_Generation_System_II_UG.pdf

This new index ranks companies' efforts in the fight against antimicrobial resistance. Science. (n.d.). Retrieved February 27, 2023, from https://www.science.org/content/article/new-index-ranks-companies-efforts-fight-against-antimicrobial-resistance

Thompson, C. L., Vier, R., Mikaelyan, A., Wienemann, T., & Brune, A. (2012). "Candidatus Arthromitus" revised: segmented filamentous bacteria in arthropod guts are members of Lachnospiraceae. *Environmental Microbiology*, *14*(6), 1454–1465. https://doi.org/10.1111/J.1462-2920.2012.02731.X

Tian, Y., Tan, Y., Liu, N., Yan, Z., Liao, Y., Chen, J., De Saeger, S., Yang, H., Zhang, Q., & Wu, A. (2016). Detoxification of Deoxynivalenol via Glycosylation Represents Novel Insights on Antagonistic Activities of Trichoderma when Confronted with Fusarium graminearum. *Toxins*, *8*(11), 335. https://doi.org/10.3390/TOXINS8110335

Tobie, W. (1946). The so-called Pseudomonas vendrelli. *Journal of Bacteriology*, *52*(6), 685. https://doi.org/10.1128/jb.52.6.685-686.1946

Toney, A., Xian, Y., Shao, J., Schmaltz, R., Chaidez, V., Chung, S., & Ramer-Tait, A. (2020). Introducing Gordonibacter urolithinfaciens into Gut Ecosystems to Study Its Role in Mediating the Metabolic Benefits of Dietary Polyphenols. *Current Developments in Nutrition*, *4*(Supplement_2), 1594–1594. https://doi.org/10.1093/CDN/NZAA062_051

Toth, M., Antunes, N. T., Stewart, N. K., Frase, H., Bhattacharya, M., Smith, C. A., & Vakulenko,

S. B. (2016). Class D β-lactamases do exist in Gram-positive bacteria. *Nature Chemical Biology*, *12*(1), 9. https://doi.org/10.1038/NCHEMBIO.1950

Traglia, G. M., Place, K., Dotto, C., Fernandez, J. S., Montaña, S., Bahiense, C. dos S., Soler-Bistue, A., Iriarte, A., Perez, F., Tolmasky, M. E., Bonomo, R. A., Melano, R. G., & Ramírez, M. S. (2019). Interspecies DNA acquisition by a naturally competent Acinetobacter baumannii strain. *International Journal of Antimicrobial Agents*, *53*(4), 483–490. https://doi.org/10.1016/J.IJANTIMICAG.2018.12.013

Triboulet, S., Dubée, V., Lecoq, L., Bougault, C., Mainardi, J. L., Rice, L. B., Ethève-Quelquejeu, M., Gutmann, L., Marie, A., Dubost, L., Hugonnet, J. E., Simorre, J. P., & Arthur, M. (2013). Kinetic Features of L,D-Transpeptidase Inactivation Critical for β-Lactam Antibacterial Activity. *PLOS ONE*, *8*(7), e67831. https://doi.org/10.1371/JOURNAL.PONE.0067831

Truglio, J. J., Croteau, D. L., van Houten, B., & Kisker, C. (2006). Prokaryotic nucleotide excision repair: the UvrABC system. *Chem. Rev.*, *106*(2), 233–252. https://doi.org/10.1021/cr040471u

Trunk, T., Khalil, H. S., & Leo, J. C. (2018). Bacterial autoaggregation. *AIMS Microbiology*, *4*(1), 140. https://doi.org/10.3934/MICROBIOL.2018.1.140

Tsay, T.-B., Jiang, Y.-Z., Hsu, C.-M., & Chen, L.-W. (2016). Pseudomonas aeruginosa colonization enhances ventilator-associated pneumonia-induced lung injury. *Respiratory Research*, *17*(1), 101. https://doi.org/10.1186/s12931-016-0417-5

Tyner, S., Briatte, F., & Hofmann, H. (2017). Network visualization with ggplot2. *R Journal*, *9*(1), 27–59. https://doi.org/10.32614/rj-2017-023

United States Department of Agriculture. (2022). *Livestock and Poultry: World Markets and Trade*. https://usda.library.cornell.edu/concern/publications/73666448x?locale=en

Vafadar, A., Shabaninejad, Z., Movahedpour, A., Fallahi, F., Taghavipour, M., Ghasemi, Y., Akbari, M., Shafiee, A., Hajighadimi, S., Moradizarmehri, S., Razi, E., Savardashtaki, A., & Mirzaei, H. (2020). Quercetin and cancer: new insights into its therapeutic effects on ovarian cancer cells. *Cell \& Bioscience*, *10*, 32. https://doi.org/10.1186/s13578-020-00397-0

Valenzuela-Grijalva, N. V., Pinelli-Saavedra, A., Muhlia-Almazan, A., Domínguez-Díaz, D., & González-Ríos, H. (2017). Dietary inclusion effects of phytochemicals as growth promoters in animal production. *Journal of Animal Science and Technology*, *59*(1), 8. https://doi.org/10.1186/s40781-017-0133-9

Valls-Fonayet, J., Vendramin, V., Pizzinato, D., Sparrow, C., Pagni, D., Cascella, F., Carapelli, C., Vincenzi, S., & Ricasoli, B. (2022). Prevention of quercetin precipitation in red wines: a promising enzymatic solution. *OENO One*, *56*(1), 41–51. https://doi.org/10.20870/OENO-ONE.2022.56.1.4699

Van Hoek, A. H. A. M., Mevius, D., Guerra, B., Mullany, P., Roberts, A. P., & Aarts, H. J. M. (2011). Acquired Antibiotic Resistance Genes: An Overview. *Frontiers in Microbiology*, *2*(SEP). https://doi.org/10.3389/FMICB.2011.00203

Van Immerseel, F., De Buck, J., Pasmans, F., Huyghebaert, G., Haesebrouck, F., & Ducatelle, R. (2004). Clostridium perfringens in poultry: an emerging threat for animal and public health. *Avian Pathology : Journal of the W.V.P.A*, *33*(6), 537–549. https://doi.org/10.1080/03079450400013162

van Kuijk, S. J. A., Han, Y., Garcia-Ruiz, A. I., & Rodiles, A. (2021). Hydroxychloride trace minerals have a positive effect on growth performance, carcass quality and impact ileal and cecal microbiota in broiler chickens. *Journal of Animal Science and Biotechnology 2021 12:1*, *12*(1), 1–13. https://doi.org/10.1186/S40104-021-00553-7

Vandeputte, O. M., Kiendrebeogo, M., Rasamiravaka, T., Stévigny, C., Duez, P., Rajaonson, S., Diallo, B., Mol, A., Baucher, M., & Jaziri, M. El. (2011). The flavanone naringenin reduces the production of quorum sensing-controlled virulence factors in Pseudomonas aeruginosa PAO1. *Microbiology*, *157*(7), 2120–2132. https://doi.org/10.1099/MIC.0.049338-0

Varmuzova, K., Kubasova, T., Davidova-Gerzova, L., Sisak, F., Havlickova, H., Sebkova, A., Faldynova, M., & Rychlik, I. (2016). Composition of Gut Microbiota Influences Resistance of Newly Hatched Chickens to Salmonella Enteritidis Infection. *Frontiers in Microbiology*, *7*(JUN). https://doi.org/10.3389/FMICB.2016.00957

Veloo, A. C. M., Baas, W. H., Haan, F. J., Coco, J., & Rossen, J. W. (2019). Prevalence of antimicrobial resistance genes in Bacteroides spp. and Prevotella spp. Dutch clinical isolates. *Clinical Microbiology and Infection*, *25*(9), 1156.e9-1156.e13. https://doi.org/10.1016/J.CMI.2019.02.017

Ventola, C. L. (2015). The antibiotic resistance crisis: part 1: causes and threats. *P \& T : A Peer-Reviewed Journal for Formulary Management*, *40*(4), 277–283. https://www.ncbi.nlm.nih.gov/pubmed/25859123

Vernon, G. (2019). Syphilis and Salvarsan. *The British Journal of General Practice*, *69*(682), 246. https://doi.org/10.3399/BJGP19X702533

Vesth, T., Ozen, A., Andersen, S. C., Sommer Kaas, R., Lukjancenko, O., Bohlin, J., Nookaew, I., Wassenaar, T. M., & Ussery, D. W. (2013). Veillonella, Firmicutes: Microbes disguised as Gram negatives. *Standards in Genomic Sciences*, *9*(2), 431. https://doi.org/10.4056/SIGS.2981345

Videnska, P., Sedlar, K., Lukac, M., Faldynova, M., Gerzova, L., Cejkova, D., Sisak, F., & Rychlik, I. (2014). Succession and replacement of bacterial populations in the caecum of egg laying hens over their whole life. *PLoS ONE*, *9*(12). https://doi.org/10.1371/JOURNAL.PONE.0115142

Vipin, C., Mujeeburahiman, M., Ashwini, P., Arun, A. B., & Rekha, P.-D. (2019). Anti-biofilm and cytoprotective activities of quercetin against Pseudomonas aeruginosa isolates. *Letters in Applied Microbiology*, *68*(5), 464–471. https://doi.org/10.1111/lam.13129

Vipin, C., Saptami, K., Fida, F., Mujeeburahiman, M., Rao, S. S., Athmika, Arun, A. B., & Rekha, P. D. (2020). Potential synergistic activity of quercetin with antibiotics against multidrug-resistant clinical strains of Pseudomonas aeruginosa. *PLoS ONE*, *15*(11). https://doi.org/10.1371/JOURNAL.PONE.0241304

Vogel, R. F., Bocker, G., Stolz, P., Ehrmann, M., Fanta, D., Ludwig, W., Pot, B., Kersters, K., Schleifer, K. H., & Hammes, W. P. (1994). Identification of lactobacilli from sourdough and description of Lactobacillus pontis sp. nov. *Int J Syst Bacteriol*, *44*(2), 223–229. https://doi.org/10.1099/00207713-44-2-223

Walsh, C., & Wright, G. (2005). Introduction: antibiotic resistance. *Chemical Reviews*, *105*(2), 391–394. https://doi.org/10.1021/cr030100y

Wang, D., Yu, L., Xiang, H., Fan, J., He, L., Guo, N., Feng, H., & Deng, X. (2008). Global

transcriptional profiles of Staphylococcus aureus treated with berberine chloride. *FEMS Microbiology Letters*, *279*(2), 217–225. https://doi.org/10.1111/J.1574-6968.2007.01031.X

Wang, M., Firrman, J., Liu, L., & Yam, K. (2019). A Review on Flavonoid Apigenin: Dietary Intake, {ADME}, Antimicrobial Effects, and Interactions with Human Gut Microbiota. *{BioMed} Research International*, *2019*, 7010467. https://doi.org/10.1155/2019/7010467

Wang, M., Guo, Q., Xu, X., Wang, X., Ye, X., Wu, S., Hooper, D., & Wang, M. (2009). New plasmid-mediated quinolone resistance gene, qnrC, found in a clinical isolate of Proteus mirabilis. *Antimicrobial Agents and Chemotherapy*, *53*(5), 1892–1897. https://doi.org/10.1128/AAC.01400-08

Wang, S., Yao, J., Zhou, B., Yang, J., Chaudry, M. T., Wang, M., Xiao, F., Li, Y., & Yin, W. (2018). Bacteriostatic effect of quercetin as an antibiotic alternative in vivo and its antibacterial mechanism in vitro. *Journal of Food Protection*, *81*(1), 68–78. https://doi.org/10.4315/0362-{028X}.{JFP}-17-214

Wang, W., Archbold, T., Kimber, M. S., Li, J., Lam, J. S., & Fan, M. Z. (2012). The porcine gut microbial metagenomic library for mining novel cellulases established from growing pigs fed cellulose-supplemented high-fat diets. *Journal of Animal Science*, *90*(suppl_4), 400–402. https://doi.org/10.2527/JAS.53942

Wang, X., Qiu, S., Yao, X., Tang, T., Dai, K., & Zhu, Z. (2009). Berberine inhibits Staphylococcus epidermidis adhesion and biofilm formation on the surface of titanium alloy. *Journal of Orthopaedic Research : Official Publication of the Orthopaedic Research Society*, *27*(11), 1487–1492. https://doi.org/10.1002/JOR.20917

Wang, Y., Shou, J. W., Li, X. Y., Zhao, Z. X., Fu, J., He, C. Y., Feng, R., Ma, C., Wen, B. Y., Guo, F., Yang, X. Y., Han, Y. X., Wang, L. L., Tong, Q., You, X. F., Lin, Y., Kong, W. J., Si, S. Y., & Jiang, J. D. (2017). Berberine-induced bioactive metabolites of the gut microbiota improve energy metabolism. *Metabolism: Clinical and Experimental*, *70*, 72–84. https://doi.org/10.1016/J.METABOL.2017.02.003

Wang, Y., Xu, C., Zhang, R., Chen, Y., Shen, Y., Hu, F., Liu, D., Lu, J., Guo, Y., Xia, X., Jiang, J., Wang, X., Fu, Y., Yang, L., Wang, J., Li, J., Cai, C., Yin, D., Che, J., … Shen, J. (2020). Changes in colistin resistance and mcr-1 abundance in Escherichia coli of animal and human origins following the ban of colistin-positive additives in China: an epidemiological comparative study. *The Lancet Infectious Diseases*, *20*(10), 1161–1171. https://doi.org/10.1016/S1473-3099(20)30149-3

Wani, M. C., Taylor, H. L., Wall, M. E., Coggon, P., & Mcphail, A. T. (1971). Plant antitumor agents. VI. The isolation and structure of taxol, a novel antileukemic and antitumor agent from Taxus brevifolia. *Journal of the American Chemical Society*, *93*(9), 2325–2327. https://doi.org/10.1021/JA00738A045

Warinner, C., Rodrigues, J. F. M., Vyas, R., Trachsel, C., Shved, N., Grossmann, J., Radini, A., Hancock, Y., Tito, R. Y., Fiddyment, S., Speller, C., Hendy, J., Charlton, S., Luder, H. U., Salazar-García, D. C., Eppler, E., Seiler, R., Hansen, L. H., Castruita, J. A. S., … Cappellini, E. (2014). Pathogens and host immunity in the ancient human oral cavity. *Nature Genetics*, *46*(4), 336–344. https://doi.org/10.1038/ng.2906

Waterhouse, A. M., Procter, J. B., Martin, D. M. A., Clamp, M., & Barton, G. J. (2009). Jalview Version 2—a multiple sequence alignment editor and analysis workbench. *Bioinformatics*, *25*(9), 1189–1191. https://doi.org/10.1093/BIOINFORMATICS/BTP033

Welsh, C. (2022, April 15). *The Russia-Ukraine War and Global Food Security: A Seven-Week Assessment, and the Way Forward for Policymakers*. Center for Strategic and International Studies. https://www.csis.org/analysis/russia-ukraine-war-and-global-food-security-seven-week-assessment-and-way-forward

Wexler, H. M. (2007). Bacteroides: the Good, the Bad, and the Nitty-Gritty. *Clinical Microbiology Reviews*, *20*(4), 593. https://doi.org/10.1128/CMR.00008-07

White, T., Bruns, T., Lee, S., & Taylor, J. (1990). Amplification and direct sequencing of fungal ribosomal RNA genes for phylogenetic. In M. Innis, D. Gelfand, J. Sninsky, & T. White (Eds.), *PCR protocols: a guide to methods and applications* (18th ed., Vol. 18, pp. 315–322). Academic Press. https://doi.org/10.1016/0168-9525(90)90186-a

Wick, R. R., Judd, L. M., Gorrie, C. L., & Holt, K. E. (2017). Unicycler: Resolving bacterial genome assemblies from short and long sequencing reads. *PLoS Computational Biology*, *13*(6). https://doi.org/10.1371/JOURNAL.PCBI.1005595

Wickham, H. (2009). ggplot2. *Ggplot2*. https://doi.org/10.1007/978-0-387-98141-3

Wiersema, M. L., Koester, L. R., Schmitz-Esser, S., & Koltes, D. A. (2021). Comparison of intestinal permeability, morphology, and ileal microbial communities of commercial hens housed in conventional cages and cage-free housing systems. *Poultry Science*, *100*(2), 1178–1191. https://doi.org/10.1016/J.PSJ.2020.10.052

Wilson, R., Sykes, D. A., Watson, D., Rutman, A., Taylor, G. W., & Cole, P. J. (1988). Measurement of Pseudomonas aeruginosa phenazine pigments in sputum and assessment of their contribution to sputum sol toxicity for respiratory epithelium. *Infection and Immunity*, *56*(9), 2515–2517. https://doi.org/10.1128/IAI.56.9.2515-2517.1988

Wimberly, B. T., Brodersen, D. E., Clemons, W. M., Morgan-Warren, R. J., Carter, A. P., Vonrheln, C., Hartsch, T., & Ramakrishnan, V. (2000). Structure of the 30S ribosomal subunit. *Nature*, *407*(6802), 327–339. https://doi.org/10.1038/35030006

Wintola, O. A., & Afolayan, A. J. (2015). The antibacterial, phytochemicals and antioxidants evaluation of the root extracts of Hydnora africanaThunb. used as antidysenteric in Eastern Cape Province, South Africa. *BMC Complementary and Alternative Medicine*, *15*(1). https://doi.org/10.1186/S12906-015-0835-9

Wiser, M. J., Ribeck, N., & Lenski, R. E. (2013). Long-term dynamics of adaptation in asexual populations. *Science (New York, N.Y.)*, *342*(6164), 1364–1367. https://doi.org/10.1126/SCIENCE.1243357

Wojtyczka, R. D., Dziedzic, A., Kępa, M., Kubina, R., Kabała-Dzik, A., Mularz, T., & Idzik, D. (2014). Berberine Enhances the Antibacterial Activity of Selected Antibiotics against Coagulase-Negative Staphylococcus Strains in Vitro. *Molecules*, *19*(5), 6583. https://doi.org/10.3390/MOLECULES19056583

Wong, G., He, S., Siragam, V., Bi, Y., Mbikay, M., Chretien, M., & Qiu, X. (2017). Antiviral activity of quercetin-3-β-O-D-glucoside against Zika virus infection. *Virologica Sinica*, *32*(6), 545–547. https://doi.org/10.1007/s12250-017-4057-9

Wong, J. L. C., David, S., Sanchez-Garrido, J., Woo, J. Z., Low, W. W., Morecchiato, F., Giani, T., Rossolini, G. M., Brett, S. J., Clements, A., Aanensen, D. M., Rouskin, S., & Frankel, G. (2022). Recurrent emergence of carbapenem resistance in Klebsiella pneumoniae mediated by an inhibitory ompK36 mRNA secondary structure. *BioRxiv*, *119*(38),

e2203593119. https://doi.org/10.1073/PNAS.2203593119

Wong, K., Shaw, T. I., Oladeinde, A., Glenn, T. C., Oakley, B., & Molina, M. (2016). Rapid microbiome changes in freshly deposited cow feces under field conditions. *Frontiers in Microbiology*, *7*(APR), 500. https://doi.org/10.3389/FMICB.2016.00500/BIBTEX

Woodrow, C. J., Haynes, R. K., & Krishna, S. (2005). Artemisinins. *Postgraduate Medical Journal*, *81*(952), 71–78. https://doi.org/10.1136/pgmj.2004.028399

Wright, E. S. (2016). Using DECIPHER v2.0 to analyze big biological sequence data in R. *R Journal*, *8*(1), 352–359. https://doi.org/10.32614/RJ-2016-025

Xiao, S.-S., Mi, J.-D., Mei, L., Liang, J., Feng, K.-X., Wu, Y.-B., Liao, X.-D., Wang, Y., & Microbial, Y. (2021). *Microbial Diversity and Community Variation in the Intestines of Layer Chickens*. *11*, 840. https://doi.org/10.3390/ani11030840

Xiao, Y., Nie, L., Chen, H., He, M., Liang, Q., Nie, H., Chen, W., & Huang, Q. (2021). The two-component system TarR–TarS is regulated by c-di-GMP/FleQ and FliA and modulates antibiotic susceptibility in Pseudomonas putida. *Environmental Microbiology*, *23*(9), 5239–5257. https://doi.org/10.1111/1462-2920.15555

Xiao, Y., Xiang, Y., Zhou, W., Chen, J., Li, K., & Yang, H. (2017). Microbial community mapping in intestinal tract of broiler chicken. *Poultry Science*, *96*(5), 1387–1393. https://doi.org/10.3382/PS/PEW372

Xie, Q., Johnson, B. R., Wenckus, C. S., Fayad, M. I., & Wu, C. D. (2012). Efficacy of berberine, an antimicrobial plant alkaloid, as an endodontic irrigant against a mixed-culture biofilm in an in vitro tooth model. *Journal of Endodontics*, *38*(8), 1114–1117. https://doi.org/10.1016/j.joen.2012.04.023

Xie, Y., Yao, L., Yu, X., Ruan, Y., Li, Z., & Guo, J. (2020). Action mechanisms and research methods of tRNA-derived small RNAs. *Signal Transduction and Targeted Therapy 2020 5:1*, *5*(1), 1–9. https://doi.org/10.1038/s41392-020-00217-4

Xu, J. H., Liu, X. Z., Pan, W., & Zou, D. J. (2017). Berberine protects against diet-induced obesity through regulating metabolic endotoxemia and gut hormone levels. *Molecular Medicine Reports*, *15*(5), 2765–2787. https://doi.org/10.3892/MMR.2017.6321/HTML

Xu, J., Zhou, F., Ji, B.-P., Pei, R.-S., & Xu, N. (2008). The antibacterial mechanism of carvacrol and thymol against Escherichia coli. *Letters in Applied Microbiology*, *47*(3), 174–179. https://doi.org/10.1111/j.1472-{765X}.2008.02407.x

Xu, R., Yang, Z. H., Zheng, Y., Wang, Q. P., Bai, Y., Liu, J. B., Zhang, Y. R., Xiong, W. P., Lu, Y., & Fan, C. Z. (2019). Metagenomic analysis reveals the effects of long-term antibiotic pressure on sludge anaerobic digestion and antimicrobial resistance risk. *Bioresource Technology*, *282*, 179–188. https://doi.org/10.1016/J.BIORTECH.2019.02.120

Xu, Z., Shah, H. N., Misra, R., Chen, J., Zhang, W., Liu, Y., Cutler, R. R., & Mkrtchyan, H. V. (2018). The prevalence, antibiotic resistance and mecA characterization of coagulase negative staphylococci recovered from non-healthcare settings in London, UK. *Antimicrobial Resistance and Infection Control*, *7*(1). https://doi.org/10.1186/S13756-018-0367-4

Yadav, S., & Jha, R. (2019). Strategies to modulate the intestinal microbiota and their effects on nutrient utilization, performance, and health of poultry. *Journal of Animal Science and Biotechnology*, *10*(1). https://doi.org/10.1186/S40104-018-0310-9

Yang, J., Li, Y., Wen, Z., Liu, W., Meng, L., & Huang, H. (2021). Oscillospira - a candidate for the next-generation probiotics. *Gut Microbes*, *13*(1). https://doi.org/10.1080/19490976.2021.1987783

Yang, Q., Liu, J., Wang, X., Robinson, K., Whitmore, M. A., Stewart, S. N., Zhao, J., & Zhang, G. (2021). Identification of an Intestinal Microbiota Signature Associated With the Severity of Necrotic Enteritis. *Frontiers in Microbiology*, *12*, 2377. https://doi.org/10.3389/FMICB.2021.703693/BIBTEX

Yao, Y., Chen, H., Yan, L., Wang, W., & Wang, D. (2020). Berberine alleviates type 2 diabetic symptoms by altering gut microbiota and reducing aromatic amino acids. *Biomedicine & Pharmacotherapy*, *131*, 110669. https://doi.org/10.1016/J.BIOPHA.2020.110669

Yousi, F., Kainan, C., Junnan, Z., Chuanxing, X., Lina, F., Bangzhou, Z., Jianlin, R., & Baishan, F. (2019). Evaluation of the effects of four media on human intestinal microbiota culture in vitro. *{AMB} Express*, *9*(1), 69. https://doi.org/10.1186/s13568-019-0790-9

Yu, C. H., Dang, Y., Zhou, Z., Wu, C., Zhao, F., Sachs, M. S., & Liu, Y. (2015). Codon usage influences the local rate of translation elongation to regulate co-translational protein folding. *Molecular Cell*, *59*(5), 744. https://doi.org/10.1016/J.MOLCEL.2015.07.018

Yu, H.-H., Kim, K.-J., Cha, J.-D., Kim, H.-K., Lee, Y.-E., Choi, N.-Y., & You, Y.-O. (2005). Antimicrobial activity of berberine alone and in combination with ampicillin or oxacillin against methicillin-resistant Staphylococcus aureus. *Journal of Medicinal Food*, *8*(4), 454–461. https://doi.org/10.1089/jmf.2005.8.454

Yu, Z., Gunn, L., Wall, P., & Fanning, S. (2017). Antimicrobial resistance and its association with tolerance to heavy metals in agriculture production. *Food Microbiology*, *64*, 23–32. https://doi.org/10.1016/j.fm.2016.12.009

Zaman, S. Bin, Hussain, M. A., Nye, R., Mehta, V., Mamun, K. T., & Hossain, N. (2017). A review on antibiotic resistance: alarm bells are ringing. *Cureus*, *9*(6), e1403. https://doi.org/10.7759/cureus.1403

Zamora-Ros, R., Andres-Lacueva, C., Lamuela-Raventós, R. M., Berenguer, T., Jakszyn, P., Barricarte, A., Ardanaz, E., Amiano, P., Dorronsoro, M., Larrañaga, N., Martínez, C., Sánchez, M. J., Navarro, C., Chirlaque, M. D., Tormo, M. J., Quirós, J. R., & González, C. A. (2010). Estimation of dietary sources and flavonoid intake in a Spanish adult population ({EPIC}-Spain). *Journal of the American Dietetic Association*, *110*(3), 390–398. https://doi.org/10.1016/j.jada.2009.11.024

Zandi, T. A., & Townsend, C. A. (2021). Competing off-loading mechanisms of meropenem from an L,D-transpeptidase reduce antibiotic effectiveness. *Proceedings of the National Academy of Sciences of the United States of America*, *118*(27). https://doi.org/10.1073/PNAS.2008610118/SUPPL_FILE/PNAS.2008610118.SAPP.PDF

Zankari, E., Hasman, H., Cosentino, S., Vestergaard, M., Rasmussen, S., Lund, O., Aarestrup, F. M., & Larsen, M. V. (2012). Identification of acquired antimicrobial resistance genes. *The Journal of Antimicrobial Chemotherapy*, *67*(11), 2640–2644. https://doi.org/10.1093/JAC/DKS261

Zeng, Y., Nikitkova, A., Abdelsalam, H., Li, J., & Xiao, J. (2019). Activity of quercetin and kaemferol against Streptococcus mutans biofilm. *Archives of Oral Biology*, *98*, 9–16. https://doi.org/10.1016/j.archoralbio.2018.11.005

Zenner, C., Hitch, T. C. A., Riedel, T., Wortmann, E., Tiede, S., Buhl, E. M., Abt, B., Neuhaus,

K., Velge, P., Overmann, J., Kaspers, B., & Clavel, T. (2021). Early-Life Immune System Maturation in Chickens Using a Synthetic Community of Cultured Gut Bacteria. *MSystems*, *6*(3). https://doi.org/10.1128/MSYSTEMS.01300-20/SUPPL_FILE/MSYSTEMS.01300-20-ST001.XLSX

Zhang, J., Liu, J., Wang, Y., Yu, D., Sui, Q., Wang, R., Chen, M., Tong, J., & Wei, Y. (2017). Profiles and drivers of antibiotic resistance genes distribution in one-stage and two-stage sludge anaerobic digestion based on microwave-{H2O2} pretreatment. *Bioresource Technology*, *241*, 573–581. https://doi.org/10.1016/j.biortech.2017.05.157

Zhang, R., Chen, L., Niu, Z., Song, S., & Zhao, Y. (2019). Water stress affects the frequency of Firmicutes, Clostridiales and Lysobacter in rhizosphere soils of greenhouse grape. *Agricultural Water Management*, *226*, 105776. https://doi.org/10.1016/J.AGWAT.2019.105776

Zhang, X.-W., Chen, J.-Y., Ouyang, D., & Lu, J.-H. (2020). Quercetin in animal models of alzheimer's disease: A systematic review of preclinical studies. *International Journal of Molecular Sciences*, *21*(2). https://doi.org/10.3390/ijms21020493

Zhang, X., Sun, X., Wu, J., Wu, Y., Wang, Y., Hu, X., & Wang, X. (2020a). Berberine Damages the Cell Surface of Methicillin-Resistant Staphylococcus aureus. *Frontiers in Microbiology*, *11*, 621. https://doi.org/10.3389/fmicb.2020.00621

Zhang, X., Sun, X., Wu, J., Wu, Y., Wang, Y., Hu, X., & Wang, X. (2020b). Berberine Damages the Cell Surface of Methicillin-Resistant Staphylococcus aureus. *Frontiers in Microbiology*, *11*. https://doi.org/10.3389/FMICB.2020.00621

Zhang, Y., Gu, A. Z., Cen, T., Li, X., He, M., Li, D., & Chen, J. (2018). Sub-inhibitory concentrations of heavy metals facilitate the horizontal transfer of plasmid-mediated antibiotic resistance genes in water environment. *Environmental Pollution*, *237*, 74–82. https://doi.org/10.1016/j.envpol.2018.01.032

Zhang, Y., Gu, Y., Ren, H., Wang, S., Zhong, H., Zhao, X., Ma, J., Gu, X., Xue, Y., Huang, S., Yang, J., Chen, L., Chen, G., Qu, S., Liang, J., Qin, L., Huang, Q., Peng, Y., Li, Q., … Wang, W. (2020). Gut microbiome-related effects of berberine and probiotics on type 2 diabetes (the PREMOTE study). *Nature Communications*, *11*(1). https://doi.org/10.1038/S41467-020-18414-8

Zhao, H., Li, Y., Lv, P., Huang, J., Tai, R., Jin, X., Wang, J., & Wang, X. (2022). Salmonella Phages Affect the Intestinal Barrier in Chicks by Altering the Composition of Early Intestinal Flora: Association With Time of Phage Use. *Frontiers in Microbiology*, *0*, 2489. https://doi.org/10.3389/FMICB.2022.947640

Zhao, W. H., Hu, Z. Q., Hara, Y., & Shimamura, T. (2002). Inhibition of penicillinase by epigallocatechin gallate resulting in restoration of antibacterial activity of penicillin against penicillinase-producing Staphylococcus aureus. *Antimicrobial Agents and Chemotherapy*, *46*(7), 2266–2268. https://doi.org/10.1128/AAC.46.7.2266-2268.2002

Zhao, Y., Wu, J., Li, J. V., Zhou, N. Y., Tang, H., & Wang, Y. (2013). Gut microbiota composition modifies fecal metabolic profiles in mice. *Journal of Proteome Research*, *12*(6), 2987–2999. https://doi.org/10.1021/PR400263N

Zhou, L., Zheng, H., Tang, Y., Yu, W., & Gong, Q. (2012). Eugenol inhibits quorum sensing at sub-inhibitory concentrations. *Biotechnology Letters 2012 35:4*, *35*(4), 631–637. https://doi.org/10.1007/S10529-012-1126-X

Zhu, P., Lu, J., Zhi, X., Zhou, Y., Wang, X., Wang, C., Gao, Y., Zhang, X., Yu, J., Sun, Y., & Zhou, P. (2021). tRNA-derived fragment tRFLys-CTT-010 promotes triple-negative breast cancer progression by regulating glucose metabolism via G6PC. *Carcinogenesis*, *42*(9), 1196–1207. https://doi.org/10.1093/CARCIN/BGAB058

Zou, K., Li, Z., Zhang, Y., Zhang, H.-Y., Li, B., Zhu, W.-L., Shi, J.-Y., Jia, Q., & Li, Y.-M. (2017). Advances in the study of berberine and its derivatives: a focus on anti-inflammatory and anti-tumor effects in the digestive system. *Acta Pharmacologica Sinica*, *38*(2), 157–167. https://doi.org/10.1038/aps.2016.125

Zymo Research. (2022). *ZymoBIOMICS^{TM} DNA Miniprep Kit DNA for microbiome or metagenome analyses*. https://files.zymoresearch.com/protocols/_d4300t_d4300_d4304_zymobiomics_dna_miniprep_kit.pdf

Appendix I: Plasmid Insert Snapgene Files

Access Link: https://lstmed-

my.sharepoint.com/:f:/g/personal/william_hutton_lstmed_ac_uk/Eg76QO7H4yRJjLRcJxdve

PABNumsnCDQV2tAvCCMyJvCFg?e=c3Ox0s

Password: WillHThesis2022

Appendix II: *Pseudomonas Aeruginosa*: Statistical Analysis

List of Abbreviations

M – Mean

SD – Standard deviation

Methods Restated

Two tailed t-tests for independent means were conducted using https://www.socscistatistics.com/tests/studentttest/default2.aspx (Social Science Statistics, 2022). Two tailed t-tests were selected as it was unknown if resistance level, or production would increase or decrease as a consequence of evolution in sub-inhibitory concentrations of phytochemicals. Significance value was set at $p > 0.05$.

Imipenem Resistance Changes

(1) NCTC 7244 vs. NCTC 7244 control 1

NCTC 7244 – NCTC 7244 C1 (12,21,-) – (21,21,21)

Imipenem resistance of NCTC 7244 (M = 16.5, SD = 40.5) was not significantly different to NCTC 7244 C1 (M = 21, SD = 0.00)

The *t*-value is -1.34164. The *p*-value is .272228. The result is *not* significant at *p* < .05.

(2) NCTC 7244 vs. NCTC 7244 control 2

NCTC 7244 – NCTC 7244 C1 (12, 21, -) – (21, 23, 21)

Imipenem resistance of NCTC 7244 (M = 16.5, SD = 40.5) was not significantly different to NCTC 7244 C2 (M = 21.67, SD = 2.67)

The *t*-value is -1.49206. The *p*-value is .232497. The result is *not* significant at *p* < .05.

(3) NCTC 7244 vs. NCTC 7244 control 3

NCTC 7244 – NCTC 7244 C3 (12, 21, -) – (21, 22, 26)

Imipenem resistance of NCTC 7244 (M = 16.5, SD = 40.5) was not significantly different to NCTC 7244 C3 (M = 23, SD = 14)

The *t*-value is -1.67058. The *p*-value is .193398. The result is *not* significant at *p* < .05.

(4) NCTC 9433 vs. NCTC 9433 control 1

NCTC 9433 – NCTC 9433 C1 (18, 21, 18) – (20, 19, 14)

Imipenem resistance of NCTC 9433 (M = 19.00, SD = 6.0) was not significantly different to NCTC 9433 C1 (M = 17.67, SD = 20.67)

The *t*-value is 0.63246. The *p*-value is .561438. The result is *not* significant at *p* < .05.

(5) NCTC 9433 vs. NCTC 9433 control 2

NCTC 9433 – NCTC 9433 C2 (18, 21, 18) – (18, 19, 18)

Imipenem resistance of NCTC 9433 (M = 19.00, SD = 6.0) was not significantly different to NCTC 9433 C2 (M = 18.33, SD = 0.67)

The *t*-value is 0.63246. The *p*-value is .561438. The result is *not* significant at *p* < .05.

(6) NCTC 9344 vs. NCTC 9433 control 3

NCTC 9433 – NCTC 9433 C3 (18, 21, 18) – (18, 18, 14)

Imipenem resistance of NCTC 9433 (M = 19.00, SD = 6.0) was not significantly different to NCTC 9433 C3 (M = 16.67, SD = 10.67)

The *t*-value is 1.4. The *p*-value is .234101. The result is *not* significant at $p < .05$.

(7) NCTC 9433 vs. NCTC 9433 quercetin 1

NCTC 9433 – NCTC 9433 Q1 (18, 21, 18) – (18, 18, 18)

Imipenem resistance of NCTC 9433 (M = 19.00, SD = 6.0) was not significantly different to NCTC 9433 Q1 (M = 18, SD = 0)

The *t*-value is 1. The *p*-value is .373901. The result is *not* significant at $p < .05$.

(8) NCTC 9433 vs. NCTC 9433 quercetin 2

NCTC 9433 – NCTC 9433 Q2 (18, 21, 18) – (18, 18, 18)

Imipenem resistance of NCTC 9433 (M = 19.00, SD = 6.0) was not significantly different to NCTC 9433 Q2 (M = 18, SD = 0)

The *t*-value is 1. The *p*-value is .373901. The result is *not* significant at $p < .05$.

(9) NCTC 9433 vs. NCTC 9433 quercetin 3

NCTC 9433 – NCTC 9433 Q3 (18, 21, 18) – (-, 18, 18)

Imipenem resistance of NCTC 9433 (M = 19.00, SD = 6.0) was not significantly different to NCTC 9433 Q3 (M = 18, SD = 0)

The *t*-value is 0.7746. The *p*-value is .495025. The result is *not* significant at $p < .05$.

(10) NCTC 7244 vs. NCTC 7244 quercetin 1

NCTC 7244 – NCTC 7244 Q1 (12,21,-) – (18,18,21)

Imipenem resistance of NCTC 7244 (M = 16.5, SD = 40.5) was not significantly different to NCTC 7244 Q1 (M = 19, SD = 6.00)

The *t*-value is -0.69561. The *p*-value is .536717. The result is *not* significant at $p < .05$.

(11) NCTC 7244 vs. NCTC 7244 quercetin 2

NCTC 7244 – NCTC 7244 Q2 (12,21,-) – (21,20,21)

Imipenem resistance of NCTC 7244 (M = 16.5, SD = 40.5) was not significantly different to NCTC 7244 Q2 (M = 20.67, SD = 0.67)

The *t*-value is -1.23216. The *p*-value is .305655. The result is *not* significant at $p < .05$.

(12) NCTC 7244 vs. NCTC 7244 quercetin 3

NCTC 7244 – NCTC 7244 Q3 (12,21,-) – (21,20,21)

Imipenem resistance of NCTC 7244 (M = 16.5, SD = 40.5) was not significantly different to NCTC 7244 Q3 (M = 20.67, SD = 0.67)

The *t*-value is -1.23216. The *p*-value is .305655. The result is *not* significant at $p < .05$.

(13) NCTC 7244 vs. NCTC 7244 berberine 1

NCTC 7244 – NCTC 7244 B1 (12,21,-) – (20,20,20)

Imipenem resistance of NCTC 7244 (M = 16.5, SD = 40.5) was not significantly different to NCTC 7244 Q1 (M = 20.00, SD = 0)

The t-value is -1.0435. The p-value is .373404. The result is *not* significant at $p < .05$.

(14) NCTC 7244 vs. NCTC 7244 berberine 2

NCTC 7244 – NCTC 7244 B2 (12,21,-) – (24,-,24)

Imipenem resistance of NCTC 7244 (M = 16.5, SD = 40.5) was not significantly different to NCTC 7244 B2 (M = 24, SD = 0)

The t-value is -1.66667. The p-value is .237507. The result is *not* significant at $p < .05$.

(15) NCTC 7244 vs. NCTC 7244 berberine 3

NCTC 7244 – NCTC 7244 B3 (12, 21, -) – (20,21,21)

Imipenem resistance of NCTC 7244 (M = 16.5, SD = 40.5) was not significantly different to NCTC 7244 B3 (M = 20.67, SD = 0.67)

The t-value is -1.23216. The p-value is .305655. The result is *not* significant at $p < .05$.

(16) NCTC 9433 vs. NCTC 9433 berberine 1

NCTC 9433 – NCTC 9433 B1 (18, 21, 18) – (18, 18, 16)

Imipenem resistance of NCTC 9433 (M = 19.00, SD = 6.0) was not significantly different to NCTC 9433 B1 (M = 17.33, SD = 2.67)

The t-value is 1.38675. The p-value is .237796. The result is *not* significant at $p < .05$.

(17) NCTC 9433 vs. NCTC 9433 berberine 2

NCTC 9433 – NCTC 9433 B2 (18, 21, 18) – (14, 18, 16)

Imipenem resistance of NCTC 9433 (M = 19.00, SD = 6.0) was not significantly different to NCTC 9433 B2 (M = 16, SD = 8)

The t-value is 1.96396. The p-value is .121004. The result is *not* significant at $p < .05$.

(18) NCTC 9433 vs. NCTC 9433 berberine 3

NCTC 9433 – NCTC 9433 B3 (18, 21, 18) – (20, 18, 16)

Imipenem resistance of NCTC 9433 (M = 19.00, SD = 6.0) was not significantly different to NCTC 9433 B3 (M = 18, SD = 8)

The t-value is 0.65465. The p-value is .548424. The result is *not* significant at $p < .05$.

Pyocyanin production differences

(1) NCTC 7244 vs. NCTC 7244 berberine 1

NCTC 7244 – NCTC 7244 B1 (0.01, 0.046, 7e-003, 7e-003, -6e-003, -8e-003, -0.026, 0.028, -0.041) – (0.009, 0.002, 0.017, 0.16, 0.194, 0.024, 0.005, -0.004, -0.007)

Pyocyanin production of NCTC 7244 (M = 0.00, SD = 0.01) was not significantly different to NCTC 7244 B1 (M = 0.04, SD = 0.05)

The *t*-value is -1.58319. The *p*-value is .132942. The result is *not* significant at *p* < .05.

(2) NCTC 7244 vs. NCTC 7244 berberine 2

NCTC 7244 – NCTC 7244 B2 (0.01, 0.046, 7e-003, 7e-003, -6e-003, -8e-003, -0.026, 0.028, -0.041) – (0.002, -0.006, 0.008, -0.005, -0.006, 0.021, -0.016, -0.017, -0.014)

Pyocyanin production of NCTC 7244 (M = 0.00, SD = 0.01) was not significantly different to NCTC 7244 B2 (M = 0.00, SD = 0.00)

The *t*-value is 0.62116. The *p*-value is .543242. The result is *not* significant at *p* < .05.

(3) NCTC 7244 vs. NCTC 7244 berberine 3

NCTC 7244 – NCTC 7244 B3 (0.01, 0.046, 7e-003, 7e-003, -6e-003, -8e-003, -0.026, 0.028, -0.041) – (0.008, 0.003, 0.01, -0.014, -0.014, 0.009, -0.013, -0.016   )

Pyocyanin production of NCTC 7244 (M = 0.00, SD = 0.01) was not significantly different to NCTC 7244 B3 (M = 0.02, SD = 0.03)

The *t*-value is -0.63378. The *p*-value is .53518. The result is *not* significant at *p* < .05.

(4) NCTC 7244 vs. NCTC 7244 control 1

NCTC 7244 – NCTC 7244 C1 (0.01, 0.046, 7e-003, 7e-003, -6e-003, -8e-003, -0.026, 0.028, -0.041) – (0.003, 0.007, 0.007, 0.037, 0.033, 0.046, 0.001, 0.002, 0.011)

Pyocyanin production of NCTC 7244 (M = 0.00, SD = 0.01) was not significantly different to NCTC 7244 C1 (M = 0.02, SD = 0.00)

The *t*-value is -1.37645. The *p*-value is .187641. The result is *not* significant at *p* < .05.

(5) NCTC 7244 vs. NCTC 7244 control 2

NCTC 7244 – NCTC 7244 C2 (0.01, 0.046, 7e-003, 7e-003, -6e-003, -8e-003, -0.026, 0.028, -0.041) – (0.06, 0.049, 0.034, 0.021, 0.017, 0.023, 3e-003, 2e-003, -1e-003)

Pyocyanin production of NCTC 7244 (M = 0.00, SD = 0.01) was not significantly different to NCTC 7244 C2 (M = 0.02, SD = 0.00)

The *t*-value is -1.88299. The *p*-value is .078014. The result is *not* significant at *p* < .05.

(6) NCTC 7244 vs. NCTC 7244 control 3

NCTC 7244 – NCTC 7244 C3 (0.01, 0.046, 7e-003, 7e-003, -6e-003, -8e-003, -0.026, 0.028, -0.041) – (0.025, 0.038, 0.048, 0.019, 0.029, 0.016, -0.012, -0.01, 0.022)

Pyocyanin production of NCTC 7244 (M = 0.00, SD = 0.01) was not significantly different to NCTC 7244 C2 (M = 0.02, SD = 0.00)

The *t*-value is -1.59898. The *p*-value is .129383. The result is *not* significant at *p* < .05.

(7) NCTC 7244 vs. NCTC 7244 quercetin 1

NCTC 7244 – NCTC 7244 Q1 (0.01, 0.046, 7e-003, 7e-003, -6e-003, -8e-003, -0.026, 0.028, -0.041) – (0.007, 5.83e-004, 0.01, 0.007, 5.83e-004, 0.01, -0.02, -0.02, -0.014)

Pyocyanin production of NCTC 7244 (M = 0.00, SD = 0.01) was not significantly different to NCTC 7244 Q1 (M = 0.00, SD = 0.00)

The *t*-value is 0.41036. The *p*-value is .686986. The result is *not* significant at *p* < .05.

(8) NCTC 7244 vs. NCTC 7244 quercetin 2

NCTC 7244 – NCTC 7244 Q2 (0.01, 0.046, 7e-003, 7e-003, -6e-003, -8e-003, -0.026, 0.028, -0.041) – (-0.002, 0.002, -0.002, -0.004, -0.012, -0.004, 1.14e-004, -0.022, -0.015)

Pyocyanin production of NCTC 7244 (M = 0.00, SD = 0.01) was not significantly different to NCTC 7244 Q2 (M = -0.01, SD = 0.00)

The *t*-value is 0.921. The *p*-value is .370728. The result is *not* significant at *p* < .05.

(9) NCTC 7244 vs. NCTC 7244 quercetin 3

NCTC 7244 – NCTC 7244 Q3 (0.01, 0.046, 7e-003, 7e-003, -6e-003, -8e-003, -0.026, 0.028, -0.041) – (0.009, 0.016, 0.011, 0.014, 0.016, 0.017, -0.016, -0.019, -0.011)

Pyocyanin production of NCTC 7244 (M = 0.00, SD = 0.01) was not significantly different to NCTC 7244 Q2 (M = -0.01, SD = 0.00)

The *t*-value is -0.22058. The *p*-value is .828211. The result is *not* significant at *p* < .05.

(10) NCTC 9433 vs. NCTC 9433 quercetin 1

NCTC 9433 – NCTC 9433 Q1 (-0.013, -0.019, -0.013, 0.003, -0.015, -0.02, -0.004, -0.026, -0.026) – (0.000567, -0.008, -0.007, -0.01, -0.005, 0.005, -0.014, -0.02, -0.01)

Pyocyanin production of NCTC 9433 (M = -0.01, SD = 0.00) was not significantly different to NCTC 9433 Q1 (M = -0.01, SD = 0.00)

The *t*-value is -1.77624. The *p*-value is .094711. The result is *not* significant at *p* < .05.

(11) NCTC 9433 vs. NCTC 9433 quercetin 2

NCTC 9433 – NCTC 9433 Q2 (-0.013, -0.019, -0.013, 0.003, -0.015, -0.02, -0.004, -0.026, -0.026) – (-0.013, -0.011, -0.008, -0.015, -0.018, -0.016, -0.013, -0.024, -0.016)

Pyocyanin production of NCTC 9433 (M = -0.01, SD = 0.00) was not significantly different to NCTC 9433 Q2 (M = -0.01, SD = 0.00)

The *t*-value is 0.03142. The *p*-value is .975324. The result is *not* significant at $p < .05$.

(12) NCTC 9433 vs. NCTC 9433 quercetin 3

NCTC 9433 − NCTC 9433 Q3 (-0.013, -0.019, -0.013, 0.003, -0.015, -0.02, -0.004, -0.026, -0.026) − (0.00073, 0.002, 0.8, -0.014, -0.023, -0.023, -0.016, -0.024, -0.02)

Pyocyanin production of NCTC 9433 (M = -0.01, SD = 0.00) was not significantly different to NCTC 9433 Q3 (M = 0.08, SD = 0.59)

The *t*-value is -1.00004. The *p*-value is .332177. The result is *not* significant at $p < .05$.

(13) NCTC 9433 vs. NCTC 9433 berberine 1

NCTC 9433 − NCTC 9433 B1 (-0.013, -0.019, -0.013, 0.003, -0.015, -0.02, -0.004, -0.026, -0.026) − (0.013, 0.004, 0.018, 0.005, -0.013, -0.022, -0.01, -0.019, -0.012)

Pyocyanin production of NCTC 9433 (M = -0.01, SD = 0.00) was not significantly different to NCTC 9433 B1 (M = 0.00, SD = 0.00)

The *t*-value is -1.87319. The *p*-value is .079428. The result is *not* significant at $p < .05$.

(14) NCTC 9433 vs. NCTC 9433 berberine 2

NCTC 9433 − NCTC 9433 B2 (-0.013, -0.019, -0.013, 0.003, -0.015, -0.02, -0.004, -0.026, -0.026) − (0.009, 2.67e-004, 0.012, 0.01, -3.8e-004, -0.006, 0.002, -0.002, -0.005)

Pyocyanin production of NCTC 9433 (M = -0.01, SD = 0.00) was significantly different to NCTC 9433 B2 (M = 0.00, SD = 0.00)

The *t*-value is -4.37435. The *p*-value is .000472. The result is significant at $p < .05$.

(15) NCTC 9433 vs. NCTC 9433 berberine 3

NCTC 9433 − NCTC 9433 B3 (-0.013, -0.019, -0.013, 0.003, -0.015, -0.02, -0.004, -0.026, -0.026) − (-0.004, -0.007, -0.003, 0.033, 0.008, 8.5e-004, 0.002, -0.017, -0.024)

Pyocyanin production of NCTC 9433 (M = -0.01, SD = 0.00) was significantly different to NCTC 9433 B3 (M = 0.00, SD = 0.00)

The *t*-value is -2.30082. The *p*-value is .035189. The result is significant at $p < .05$.

(16) NCTC 9433 vs. NCTC 9433 control 1

NCTC 9433 − NCTC 9433 C1 (-0.013, -0.019, -0.013, 0.003, -0.015, -0.02, -0.004, -0.026, -0.026) − (0.014, 0.007, 0.018, -0.009, -0.012, -0.02, -0.018, -0.026, -0.029)

Pyocyanin production of NCTC 9433 (M = -0.01, SD = 0.00) was not significantly different to NCTC 9433 C1 (M = -0.01, SD = 0.00)

The *t*-value is -0.975. The *p*-value is .344074. The result is *not* significant at $p < .05$.

(17) NCTC 9433 vs. NCTC 9433 control 2

NCTC 9433 – NCTC 9433 C2 (-0.013, -0.019, -0.013, 0.003, -0.015, -0.02, -0.004, -0.026, -0.026) – (0.002, -9.5e-004, 0.003, -0.01, -0.016, -0.016, -0.013, -0.024, -0.028)

Pyocyanin production of NCTC 9433 (M = -0.01, SD = 0.00) was not significantly different to NCTC 9433 C2 (M = -0.01, SD = 0.00)

The *t*-value is -0.68456. The *p*-value is .503418. The result is *not* significant at *p* < .05.

(18) NCTC 9433 vs. NCTC 9433 control 3

NCTC 9433 – NCTC 9433 C3 (-0.013, -0.019, -0.013, 0.003, -0.015, -0.02, -0.004, -0.026, -0.026) – (0.023, 0.017, 0.022, -0.002, -0.003, -0.012, 0.001, -0.02, -0.019)

Pyocyanin production of NCTC 9433 (M = -0.01, SD = 0.00) was significantly different to NCTC 9433 C3 (M = 0.00, SD = 0.00)

The *t*-value is -2.42974. The *p*-value is .027255. The result is significant at *p* < .05.

Biofilm Production Assay Statistics / 2-tailed T-tests

(1) NCTC 9433 vs. NCTC 9433 control 1

NCTC 9433 – NCTC 9433 C1 (0.025, 0.05, 0.045, 0.039, 0.106, 0.119, 0.062, 0.036, 0.037, 0.042, 0.042, 0.049) – (0.034, 0.038, 0.02, 0.043, 0.068, 0.043, 0.028, 0.066, 0.016, 0.037, 0.026, 0.028)

Biofilm production of NCTC 9433 (M = 0.05, SD = 0.01) and NCTC 9433 C1 (M = 0.04, SD = 0.01) was not significantly different

The t-value is 1.79344. The p-value is .086662. The result is *not* significant at $p < .05$.

(2) NCTC 9433 vs. NCTC 9433 control 2

NCTC 9433 – NCTC 9433 C2 (0.025, 0.05, 0.045, 0.039, 0.106, 0.119, 0.062, 0.036, 0.037, 0.042, 0.042, 0.049) – (0.035, 0.033, 0.04, 0.043, 0.036, 0.059, 0.034, 0.092, 0.028, 0.024, 0.042, 0.03)

Biofilm production of NCTC 9433 (M = 0.05, SD = 0.01) and NCTC 9433 C2 (M = 0.04, SD = 0.00) was not significantly different

The t-value is 1.32205. The p-value is .199733. The result is *not* significant at $p < .05$.

(3) NCTC 9433 vs. NCTC 9433 control 3

NCTC 9433 – NCTC 9433 C3 (0.025, 0.05, 0.045, 0.039, 0.106, 0.119, 0.062, 0.036, 0.037, 0.042, 0.042, 0.049) – (0.044, 0.061, 0.046, 0.057, 0.058, 0.061, 0.098, 0.05, 0.018, 0.04, 0.038, 0.026)

Biofilm production of NCTC 9433 (M = 0.05, SD = 0.01) and NCTC 9433 C3 (M = 0.05, SD = 0.00) was not significantly different

The t-value is 0.45096. The p-value is .656429. The result is *not* significant at $p < .05$.

(4) NCTC 9433 vs. NCTC 9433 berberine 1

NCTC 9433 – NCTC 9433 B1 (0.025, 0.05, 0.045, 0.039, 0.106, 0.119, 0.062, 0.036, 0.037, 0.042, 0.042, 0.049) – (0.046, 0.04, 0.036, 0.06, 0.023, 0.021, 0.017, 0.019, 0.082, 0.02, 0.032, 0.046)

Biofilm production of NCTC 9433 (M = 0.05, SD = 0.01) and NCTC 9433 B1 (M = 0.04, SD = 0.00) was not significantly different

The t-value is 1.74365. The p-value is .09518. The result is *not* significant at $p < .05$.

(5) NCTC 9433 vs. NCTC 9433 berberine 2

NCTC 9433 – NCTC 9433 B2 (0.025, 0.05, 0.045, 0.039, 0.106, 0.119, 0.062, 0.036, 0.037, 0.042, 0.042, 0.049) – (0.003, 0.031, 0.008, 0.005, 0.04, 0.034, 0.022, 0.079, 0.07, 0.036, 0.044, 0.02)

Biofilm production of NCTC 9433 (M = 0.05, SD = 0.01) and NCTC 9433 B3 (M = 0.03, SD = 0.01) was not significantly different

The *t*-value is 2.00938. The *p*-value is .056921. The result is *not* significant at *p* < .05.

(6) NCTC 9433 vs. NCTC 9433 berberine 3

NCTC 9433 – NCTC 9433 B3 (0.025, 0.05, 0.045, 0.039, 0.106, 0.119, 0.062, 0.036, 0.037, 0.042, 0.042, 0.049) – (0.051, 0.053, 0.063, 0.06, 0.055, 0.029, 0.044, 0.064, 0.227, 0.088, 0.166, 0.1)

Biofilm production of NCTC 9433 (M = 0.05, SD = 0.01) and NCTC 9433 B3 (M = 0.08, SD = 0.04) was not significantly different

The *t*-value is -1.5628. The *p*-value is .132372. The result is *not* significant at *p* < .05.

(7) NCTC 9433 vs. NCTC 9433 quercetin 1

NCTC 9433 – NCTC 9433 Q1 (0.025, 0.05, 0.045, 0.039, 0.106, 0.119, 0.062, 0.036, 0.037, 0.042, 0.042, 0.049) – (0.079, 0.052, 0.056, 0.077, 0.057, 0.03, 0.032, 0.067, 0.158, 0.102, 0.072, 0.046)

Biofilm production of NCTC 9433 (M = 0.05, SD = 0.01) and NCTC 9433 Q1 (M = 0.07, SD = 0.01) was not significantly different

The *t*-value is -1.12869. The *p*-value is .271185. The result is *not* significant at *p* < .05.

(8) NCTC 9433 vs. NCTC 9433 quercetin 2

NCTC 9433 – NCTC 9433 Q2 (0.025, 0.05, 0.045, 0.039, 0.106, 0.119, 0.062, 0.036, 0.037, 0.042, 0.042, 0.049) – (0.052, 0.042, 0.057, 0.051, 0.014, 0.021   , 0.019, 0.024, 0.012, 0.035, 0.027, 0.049)

Biofilm production of NCTC 9433 (M = 0.05, SD = 0.01) and NCTC 9433 Q2 (M = 0.03, SD = 0.00) was significantly different

The *t*-value is 2.18196. The *p*-value is .040077. The result is significant at *p* < .05.

(9) NCTC 9433 vs. NCTC 9433 quercetin 3

NCTC 9433 – NCTC 9433 Q3 (0.025, 0.05, 0.045, 0.039, 0.106, 0.119, 0.062, 0.036, 0.037, 0.042, 0.042, 0.049) – (0.058, 0.028, 0.047, 0.046, 0.065, 0.075, 0.029, 0.049, 0.018, 0.023, 0.018, 0.019)

Biofilm production of NCTC 9433 (M = 0.05, SD = 0.01) and NCTC 9433 Q3 (M = 0.04, SD = 0.00) was not significantly different

The *t*-value is 1.46496. The *p*-value is .157078. The result is *not* significant at *p* < .05.

(10) NCTC 7244 vs. NCTC 7244 control 1

NCTC 7244 – NCTC 7244 C1 (0.195, 0.121, 0.128, 0.142, 0.152, 0.169, 0.114, 0.14, 0.423, 0.349, 0.246, 0.205) – (0.166, 0.129, 0.103, 0.125, 0.138, 0.129, 0.167, 0.137, 0.793, 0.23, 0.246, 0.26)

Biofilm production of NCTC 7244(M = 0.2, SD = 0.10) and NCTC 7244 C1 (M = 0.22, SD = 0.39) was not significantly different

(11) NCTC 7244 vs. NCTC 7244 control 2

NCTC 7244 – NCTC 7244 C2 (0.195, 0.121, 0.128, 0.142, 0.152, 0.169, 0.114, 0.14, 0.423, 0.349, 0.246, 0.205) – (0.125, 0.129, 0.088, 0.105, 0.162, 0.159, 0.17, 0.155, 0.232, 0.293, 0.318, 0.251)

Biofilm production of NCTC 7244(M = 0.2, SD = 0.10) and NCTC 7244 C2 (M = 0.18, SD = 0.06) was not significantly different

(12) NCTC 7244 vs. NCTC 7244 control 3

NCTC 7244 – NCTC 7244 C3 (0.195, 0.121, 0.128, 0.142, 0.152, 0.169, 0.114, 0.14, 0.423, 0.349, 0.246, 0.205) – (0.135, 0.144, 0.09, 0.13 , 0.169, 0.146, 0.121, 0.166, 0.249, 0.242, 0.295, 0.295)

Biofilm production of NCTC 7244(M = 0.2, SD = 0.10) and NCTC 7244 C3 (M = 0.18, SD = 0.05) was not significantly different

(13) NCTC 7244 vs. NCTC 7244 berberine 1

NCTC 7244 – NCTC 7244 B1 (0.195, 0.121, 0.128, 0.142, 0.152, 0.169, 0.114, 0.14, 0.423, 0.349, 0.246, 0.205) – (0.125, 0.086, 0.057, 0.13, 0.139, 0.138, 0.117, 0.146, 0.223, 0.25, 0.319, 0.378)

Biofilm production of NCTC 7244(M = 0.2, SD = 0.10) and NCTC 7244 B1 (M = 0.18, SD = 0.10) was not significantly different

(14) NCTC 7244 vs. NCTC 7244 berberine 2

NCTC 7244 – NCTC 7244 B2 (0.195, 0.121, 0.128, 0.142, 0.152, 0.169, 0.114, 0.14, 0.423, 0.349, 0.246, 0.205) – (0.135, 0.178, 0.132, 0.17, 0.135, 0.147, 0.143, 0.122, 0.349, 0.358, 0.484, 0.345)

Biofilm production of NCTC 7244(M = 0.2, SD = 0.10) and NCTC 7244 B2 (M = 0.22, SD = 0.17) was not significantly different

(15) NCTC 7244 vs. NCTC 7244 berberine 3

NCTC 7244 – NCTC 7244 B3 (0.195, 0.121, 0.128, 0.142, 0.152, 0.169, 0.114, 0.14, 0.423, 0.349, 0.246, 0.205) – (0.136, 0.141, 0.092, 0.11, 0.136, 0.183, 0.148, 0.145, 0.238, 0.277, 0.271, 0.316)

Biofilm production of NCTC 7244(M = 0.2, SD = 0.10) and NCTC 7244 B3 (M = 0.18, SD = 0.06) was not significantly different

(16) NCTC 7244 vs. NCTC 7244 quercetin 1

NCTC 7244 – NCTC 7244 Q1 (0.195, 0.121, 0.128, 0.142, 0.152, 0.169, 0.114, 0.14, 0.423, 0.349, 0.246, 0.205) – (0.073, 0.079, 0.077, 0.061, 0.084, 0.05, 0.086, 0.064, 0.256, 0.27, 0.246, 0.297)

Biofilm production of NCTC 7244(M = 0.2, SD = 0.10) and NCTC 7244 Q1 (M = 0.14, SD = 0.10) was not significantly different

The *t*-value is 1.55708. The *p*-value is .133722. The result is *not* significant at *p* < .05.

(17) NCTC 7244 vs. NCTC 7244 quercetin 2

NCTC 7244 – NCTC 7244 Q2 (0.195, 0.121, 0.128, 0.142, 0.152, 0.169, 0.114, 0.14, 0.423, 0.349, 0.246, 0.205) – (0.044, 0.055, 0.039, 0.031, 0.086, 0.074, 0.06, 0.026, 0.202, 0.316, 0.307, 0.294)

Biofilm production of NCTC 7244(M = 0.2, SD = 0.10) and NCTC 7244 Q2 (M = 0.13, SD = 0.15) was not significantly different

The *t*-value is 1.61806. The *p*-value is .119898. The result is *not* significant at *p* < .05.

(18) NCTC 7244 vs. NCTC 7244 quercetin 3

NCTC 7244 – NCTC 7244 Q3 (0.195, 0.121, 0.128, 0.142, 0.152, 0.169, 0.114, 0.14, 0.423, 0.349, 0.246, 0.205) – (0.197, 0.152, 0.1, 0.103, 0.23, 0.158, 0.174, 0.191, 0.176, 0.257, 0.244, 0.333)

Biofilm production of NCTC 7244(M = 0.2, SD = 0.10) and NCTC 7244 Q3 (M = 0.19, SD = 0.05) was not significantly different

The *t*-value is 0.16994. The *p*-value is .866609. The result is *not* significant at *p* < .05.

Appendix III: A summary of research on the impact of essential oil supplementation in poultry species since 2017. Indicating plant of origin, known compounds the essential oil contained, the growth promotive, physiological, and antimicrobial effect noted in the study, and the reference

Plant	Sickle Senna (*Cassia tora*)
Extract Location	Methanol leaf extract
Growth Promotion Effect	Increased cumulative body weight. Decreased FCR. Increased heart, gizzard, and liver size.
Physiological Effect	Decreased lipid peri-oxidation. Increased gluthione and flutione peroxidation in the blood.
Antimicrobial Effect	Antibacterial effect against *E. coli, S. gallinarum, S. aureus, P. aeruginosa* and *S. pyogenes* via disc diffusion assay.
Citation	(Sahu et al., 2017)
Plant	Blueberry *(Vaccinium corymbosum)* and Blackberry *(Rubus fruticosus)*
Extraction Location	Pomaces of fruit phenolic extract
Growth Promotion Effect	Cobb-500 Broiler Chickens. Increased bodyweight of 5.8% compared to control, but a decrease of 3.7% compared to AGP supplement.
Physiological Effect	Animal to animal changes in genes associated with energy and carbohydrate metabolism.
Antimicrobial Effect	Higher firmicute to Bacteroidetes ratio. Supplementation with BPE did not lead to the same associated caecal resistome as AGP supplementation.
Citation	(Salaheen et al., 2017)
Plant	Black Cumin *(Nigella sativa)*
Extract Location	Seed Powder
Growth Promotion Effect	Bodyweight and daily feed intake increased in accordance with an increase in feed supplementation.

Physiological Effect	Nitrate excretion increased. Intestinal morphology was unaffected. Antibody titres to Newcastle disease were increased. Glucose and triglyceride levels were unaffected. Concentration of cholesterol was decreased.
Antimicrobial Effect	Total bacteria counts were unaffected, but the relative counts of *Salmonella spp.* were decreased.
Citation	(Kumar et al., 2017)
Plant	Magnolia Tree *(Magnolia officinalis)*
Extract Location	Bark Extract
Growth Promotion Effect	Increased feed intake, FCR and bodyweight gain compared to untreated controls.
Physiological Effect	Gut lesions decreased, serum alpha1-acid glycoprotein levels decreased, transcriptions for antioxidant enzymes increased in a necrotic enteritis challenge model.
Antimicrobial Effect	Increased growth performance in challenged with *C. perfringens* and *E. maxima.*
Citation	(Oh et al., 2018b)
Plant	Plume Poppy *(Macleaya cordata)*
Extract Location	Whole Plant Extract
Growth Promotion Effect	Seven different breeds of chicken. Improved BWG and FCR numerically and FI statistically
Physiological Effect	Amino acids, vitamin and bile acid biosynthesis pathways upregulated
Antimicrobial Effect	No accumulation of ARGs, an increase of lactobacillus spp. in the foregut. As opposed to chlortetracycline which did increase ARGs.
Citation	(Huang et al., 2018)
Plant	Fever Tea *(Lippia javanica)*
Extract Location	Leaves powder extract
Growth Promotion Effect	Potchefstroom koekoek chickens. No effect on FCR, BWG or FI in supplemented chickens.
Physiological Effect	Increased bilirubin, alanine aminotransferase and aspartate transaminase, sodium potassium and cholesterol levels in blood. Increased meat lightness and redness levels.
Antimicrobial Effect	N/A
Citation	(Matshogo et al., 2018)
Plant	Chestnut *(Castanea sativa)* and Quebracho *(Schinopsis lorentzii)*
Extract Location	Whole plant powder
Growth Promotion Effect	Bodyweight and FCR did not change significantly between bactericin, control and phytochemical treated group.
Physiological Effect	N/A

Antimicrobial Effect	Treatment with phytochemicals allowed for a more complex bacterial community than bactaricin treatment. Firmicutes were the most abundant group in all cases.
Citation	(Díaz Carrasco et al., 2018)
Plant	Black Cumin *(Nigella sativa)*
Extract Location	Seeds and humic acid
Growth Promotion Effect	Increase of BWG, FCR and FI increasing with increase in phytochemical treatment. Carcass weight and breast yield increased. Quail.
Physiological Effect	Increased antibody titres to Newcastle disease. Production of a protective film in the gastrointestinal tract. Reduction in blood serum cholesterol and low density lipoproteins.
Antimicrobial Effect	Gut microbial community concentration decreased. Specifically coliform spp, *E. coli* and *Clostridium perfringens*.
Citation	(Arif et al., 2018)
Plant Extract	Oregano *(Origanum vulgare L. spp. Hirtum) &* Tarragon *(Artemisia dracunculus L.)*
Extract Location	Whole Plant
Growth Promotion Effect	N/A
Physiological Effect	N/A
Antimicrobial Effect	Strongly inhibited the growth of the lesser mealworm *Alphitobius diaperinus* (Panzer); by around 90% at 1% concentration. Both compounds also inhibited the growth of *Candida albicans*.
Citation	(Szczepanik et al., 2018)
Plant	Red Ginger (*Zigiber offcinale var rubrum*); Tumeric (*Curcuma domestica*); Wild Ginger (*Curcuma xanthorrhiza*)
Extract Location	Whole plant. Both aqueous and ethanolic extracts.
Growth Promotion Effect	N/A
Physiological Effect	N/A
Antimicrobial Effect	All compounds Inhibitory to *Salmonella enteritidis* growth at 3.13% when grown on broiler epithelial cells and by disc diffusion assay
Citation	(Prakasita et al., 2019)
Plant	Blend of Thyme *(Thymus vulgaris)*, Peppermint *(Mentha piperita)* and Eucalyptus *(Eucalyptus globulus)*
Extract Location	Synthetic blend of all three whole plant extracts
Growth Promotion Effect	Increased weight gain, FCR and production index compared to control at essential oil blend 150ppm. Essential oil supplementation also increased carcass yield, thigh muscle.

Physiological Effect	Decrease hepatic enzyme concentration. Improved the VCR ratio. Improved antibody titres to Newcastle, bronchitis, and infective bursal disease.
Antimicrobial Effect	Increased ileal *Lactobacillus* spp. count and decreased ileal *E. coli* counts.
Citation	(Hesabi Nameghi et al., 2019)
Plant	Thyme *(Thymus vulgaris)*
Extract Location	Whole plant extract
Growth Promotion Effect	Increased FCR and improved VCR in quail.
Physiological Effect	Reduced level of oxidation in quail meat in storage.
Antimicrobial Effect	Inhibited *E. coli* measured by disc diffusion methodology.
Citation	(Dehghani et al., 2019)
Plant	False Fleabane *(Pulicaria gnophalodes)*
Extraction Location	Whole plant powder
Growth Promotion Effect	Ross-308 Broilers. Higher body weight and improved FCR.
Physiological Effect	Increased VCR. Increased superoxide dismutase, glutathione peroxidase and decrease malondialdehyde level in the serum, liver and thigh muscles. Decreased levels of fatty acid.
Antimicrobial Effect	Low *E. coli* counts and higher counts of *Lactobacillus* spp. at day 42. No disease challenge model.
Citation	(Shirani et al., 2019)
Plant Extract	Synthetic Blend
Extract Location	Synthetic blend which contained; fumaric, sorbic, malic and citric acids and thymol, vanillin, and eugenol.
Growth Promotion Effect	Improved bodyweight and FCR in the supplemented group. BWG and FCR was maintained in groups challenged with *Eimeria and Clostridium spp.*
Physiological Effect	Increased intestinal integrity lower blood FITC-D and greater expression of MUC2 CLDN1 and OCLN genes.
Antimicrobial Effect	N/A
Citation	(Stefanello et al., 2019)
Plant	Sumac Berries (*Rhus coriaria, L*) and Thyme (*Thymus vulgaris*)
Extract Location	Aqueous Extract
Growth Promotion Effect	Male Ross 308 Broiler Chickens. Feed Intake, Bodyweight and FCR unchanged with treatment. Abdominal Fat Decreased with Sumac supplementation.
Physiological Effect	Blood glucose levels decreased with supplementation. Sumac treatment reduced cholesterol, triglyceride high and low-density lipoprotein levels. Increased Antibody titres to Newcastle disease and Influenza.

Antimicrobial Effect	N/A
Citation	(A Al-Sagan et al., 2020)
Plant	Fennel *(Foeniculum vulgare.* Apinceae)
Extract Location	Fennel Seed Powder
Growth Promotion Effect	Ross-308 Broiler Chicks. In normal conditions no changes measured in bodyweight, FCR, feed intake, survival, or production. Improve nitrate intake. FSP supplementation had a negative effect on economic yields.
Physiological Effect	Under heat stress conditions supplementation with 3.2% fennel seed powder improved breast meat characteristics and lowered breast meat temperature.
Antimicrobial Effect	N/A
Citation	(A Al-Sagan et al., 2020)
Plant	Synthetic Combination of Curcumin, carvacrol, thymol and cinnamaldehyde
Extract Location	Synthetic blend of all compounds
Growth Promotion Effect	N/A
Physiological Effect	Increased proteins associated with circulating globulins. Lower levels of uric acid, cholesterol, and triglycerides. Fewer oocysts. Increased antioxidant levels, reduction of lipid peroxidation. Increased VCR.
Antimicrobial Effect	Bacterial counts lowered on day 21 but increased on day 44.
Citation	(Galli et al., 2020a)
Plant	Magnolia Tree *(Magnolia officinalis)*
Extract Location	Bark Extract
Growth Promotion Effect	2% Bodyweight Gain
Physiological Effect	Alters intestinal 278 metabolite levels
Antimicrobial Effect	N/A
Citation	(Park et al., 2020a)
Plant Extract	Egyptian Leek Extract *(Allium ampeloprasum var. kurrat)*
Extract Location	Leaf extract
Growth Promotion Effect	Increased BWG, FI and FCR compared to control.
Physiological Effect	Improved liver and kidney function and decreased serum glucose presence in the chicken
Antimicrobial Effect	N/A
Citation	(Al-Khalaifah et al., 2020)
Plant Extract	Garlic, Cinnamon, Peppermint, Green Tea, and black cumin

Extract Location	Powder of garlic and cinnamon, dried leaves of peppermint and green tea and seeds of black cumin.
Growth Promotion Effect	Increased BWG and FCI after 42 days in treatment compared to control.
Physiological Effect	Significantly decrease cholesterol levels recorded in the treatment groups.
Antimicrobial Effect	Encouraged growth of *Enterococcus* spp. And *Lactobacillus* spp., whilst discouraged growth of *E. coli and Campylobacter* spp.
Citation	(Rashid et al., 2020)
Plant	Date *Phoenix dactylfera*
Extract Location	Date pits
Growth Promotion Effect	No significant effects on growth performance, except for non-degraded date pit supplementation which led to a poorer FCR.
Physiological Effect	N/A
Antimicrobial Effect	Total bacterial count and reduced populations of *Salmonella, Campylobacter and Shigella* spp. and *E. coli* decreased with degraded date pit supplementation
Citation	(Alyileili et al., 2020)
Plant	Onion *(Allium cepa L.)*
Extract Location	Whole plant extract
Growth Promotion Effect	Increased in final bodyweight, BWG and overall feed consumption
Physiological Effect	Increased antioxidant enzyme activity and serum lysozyme activity.
Antimicrobial Effect	N/A
Citation	(Omar et al., 2020)
Plant	Curcumin and Yucca Extract
Extract Location	Whole plant
Growth Promotion Effect	N/A
Physiological Effect	Increased antioxidant level, and lowered protein oxidation and altered fatty acid composition levels depending on treatment to increase presence of omegas,
Antimicrobial Effect	Reduced total bacterial counts and oocyst levels
Citation	(Galli et al., 2020b)
Plant	*Dacryodes edulis*
Extract Location	Leaves, stem and bark combination
Growth Promotion Effect	Increased FI and BWG after eight weeks of consumption.
Physiological Effect	Did not alter any of the physiological conditions measured.
Antimicrobial Effect	Lowered total CFU counts of *E. coli and Salmonella* spp*.

Citation	(Tangomo et al., 2020)
Plant	*Lippia gracilis Schauer*
Extract Location	Whole plant extract
Growth Promotion Effect	Improved FCR rate in quail above antimicrobial supplemented control.
Physiological Effect	Lowered catalase and glutathione peroxidase expression levels.
Antimicrobial Effect	Restricted *E. coli* but not *Salmonella* spp*.* Growth
Citation	(Rocha et al., 2020)
Plant Extract	Oregano *(Lippia origanoides) essential oil*
Extract Location	Whole plant
Growth Promotion Effect	Improved FCR and improved egg production and quality in *ISA* brown laying hens
Physiological Effect	Improved intestinal quality
Antimicrobial Effect	N/A
Citation	(Ramirez et al., 2021)
Plant Extract	*Monarda didyma L.*
Extract Location	Whole plant essential oil
Growth Promotion Effect	Significantly increase bodyweight in broilers (2.64%) above control.
Physiological Effect	N/A
Antimicrobial Effect	Exhibited antimicrobial properties against *E. coli* ($87 \mu g/ml$), *S. aureus* ($47 \mu g/ml$) and *C. perfringens* ($35 \mu g/ml$).
Citation	(Côté et al., 2021)
Plant Extract	Turnip *(Brassica rapa)*
Extract Location	Whole plant extract
Growth Promotion Effect	Increased BWG, decreased gizzard weight at 150ppm compared to virginiamycin treatment.
Physiological Effect	Increased low density lipoproteins and reduced very low density lipoprotein concentration in the blood serum.
Antimicrobial Effect	Birds given 450 ppm turnip extract had lower counters of Gram-negative lactose and coliform bacteria, than those of the control or virginiamycin treatment.
Citation	(Eghbaldost-Jadid et al., 2021)
Plant Extract	Synthetic mixture including citric acids, ginger, liquorice, ashwagandha roots, black seeds and green tea.
Extract Location	Synthetic powder mix
Growth Promotion Effect	Increased FI and BWG above control.
Physiological Effect	Increased VCR and downregulated ghrelin gene expression levels.

Antimicrobial Effect	Decreased total coliform and *E. coli* counts compared to the control.
Citation	(Gilani et al., 2021)
Plant Extract	*Oregano* essential oil
Extract Location	Whole plant extract
Growth Promotion Effect	Increased average BWG and a lower FCR
Physiological Effect	Improved glutathione peroxidase, superoxide dismutase and glutathione reductase activity by day 21 and total antioxidant capacity on day 42.
Antimicrobial Effect	Increased *lactobacillus* and anaerobe carriage in the cecum, and restrained the concentration of *E. coli*.
Citation	(Zhang et al., 2021)
Plant Extract	Synthetic combination of Thymol, carvacrol and cinnamaldehyde
Extract Location	Synthetic
Growth Promotion Effect	No clear increase in growth promotive parameters when compared with the control group.
Physiological Effect	Increased digestibility of Crude protein, dried matter and ether extract. Further increased activity of mucosal disaccharidase, and increased levels of ileal sucrase. Improved VCR. Increased the expression level of genes associated with nutrient transportation and barrier function.
Antimicrobial Effect	N/A
Citation	(Su et al., 2021)
Plant Extract	Cinnamon Bark Powder
Extract Location	Bark
Growth Promotion Effect	Increased maximum chicken breast weight
Physiological Effect	Increased VCR, serum album concentration and goblet cell density.
Antimicrobial Effect	Controlled for levels of *E. coli* number in a dose dependant fashion.
Citation	(Qaid et al., 2021)
Plant	*Lavender (Lavandula angustifolia)*
Extract Location	Whole plants
Growth Promotion Effect	Improved final wait and FCR in ross broilers
Physiological Effect	Increased total serum antioxidant in blood.
Antimicrobial Effect	Improved the antibacterial effect of enrofloxacin in vitro against MDR *E. coli*.
Citation	(Adaszyńska-Skwirzyńska et al., 2021)
Plant	Commercial Mixtures AV/SSL12 and Superliv Gold

Extract Location	Commercial Mix
Growth Promotion Effect	N/A
Physiological Effect	Increased acetyl-CoA carboxylase alpha levels and downregulated SREBP-1 and adiponectin expression.
Antimicrobial Effect	N/A
Citation	(Flees et al., 2021)
Compound	Carvacrol and Thymol and Cinnamic aldehyde
Growth Promotion Effect	Improved BWG. Variable changes in VCR through the experiment.
Physiological Effect	Lowered lymphocyte and erythrocyte counts. Decreased levels of alanine and aspartate aminotransferase concentrations.
Antimicrobial Effect	Total bacterial count was reduced by 1% with phytochemical supplementation.
Citation	(Reis et al., 2018)
Compound	Fuctooligosacciride
Growth Promotion Effect	N/A
Physiological Effect	N/A
Antimicrobial Effect	No difference in the alpha, beta diversity and bacterial phyla presence in the ileal microbiota. However, there was a significant decrease in the relative concentrations of potentially pathogenic bacteria including heliobacteria and desulfvibrio
Citation	(Shang et al., 2018)
Compound	Thymol (alone or in combination with), Tocopherol and Ascorbyl Palmitate.
Growth Promotion Effect	Increased bodyweight noted for all supplementation apart from tocopherol + ascorbyl palmitate combination. No changes in FI and FCR noted.
Physiological Effect	No change in the severity or occurrence of skin injuries.
Antimicrobial Effect	N/A
Citation	(Luna et al., 2019)
Compound	Caffeic acid riboflavin and Carnosic acid
Growth Promotion Effect	All treatment groups increased BWG compared to control.
Physiological Effect	Inhibited the function of bile salt hydrolases. Carnosic acid specifically altered expression of genes associated with lipid and bile salt metabolism.
Antimicrobial Effect	N/A
Citation	(Geng et al., 2020)
Compound	β-carotene

Growth Promotion Effect	Improved FCR in the full production cycle and improved daily BWG in finishing broilers.
Physiological Effect	N/A
Antimicrobial Effect	N/A
Citation	(Riley et al., 2021)
Compound	Chestnut Tannins
Growth Promotion Effect	N/A
Physiological Effect	Significantly increased expression of IL-6 which marked a change in metabolism and IL-10 which indicated a change in regulation of proinflammatory cytokines,
Antimicrobial Effect	N/A
Citation	(Lee et al., 2021)
Compound	Maltol
Growth Promotion Effect	Improved BWG in broilers over 22 days.
Physiological Effect	In vitro, maltol increased tight junction proteins in chicken intestinal epithelial cells. Improved gut lesion scores, and fecal oocyst shedding, and decrease TNFSF15 and IL-1ß
Antimicrobial Effect	N/A
Citation	(Park et al., 2021)
Compound	Ferulic Acid
Growth Promotion Effect	Increased average daily BWG and carcass weight compared to control
Physiological Effect	N/A
Antimicrobial Effect	N/A
Citation	(Peña-Torres et al., 2021)

Appendix IV: Bioinformatics R code for work conducted in Chapter 6 and 7

---
title: "Bioconductor Workflow January - Will Hutton"
author:
- Name: Will Hutton
  Affilliation: Liverpool School of Tropical Medicine
  From:
https://github.com/spholmes/F1000_workflow/blob/master/MicrobiomeWorkflow/Microb
iomeWorkflowII.Rmd
Date: 20th January 2022
output:
  pdf_document: default
  html_document:
    df_print: paged

The first chunks load all the required packages that are required for the first steps of this analysis.

````
```{r Load-Packages, message=FALSE, warning=FALSE}
library("knitr")
library("BiocStyle")
.cran_packages <- c("ggplot2", "gridExtra")
.bioc_packages <- c("dada2", "phyloseq", "DECIPHER", "phangorn")
.inst <- .cran_packages %in% installed.packages()
if(any(!.inst)) {
   install.packages(.cran_packages[!.inst])
}
.inst <- .bioc_packages %in% installed.packages()
if(any(!.inst)) {
   source("http://bioconductor.org/biocLite.R")
   biocLite(.bioc_packages[!.inst], ask = F)
}
BiocManager::install("dada2")
BiocManager::install("phyloseq")
BiocManager::install("DECIPHER")
BiocManager::install("phangorn")
# Load packages into session, and print package version
sapply(c(.cran_packages, .bioc_packages), require, character.only = TRUE)
set.seed(100)
```
````

This chunk directs to the area that the files are stored.
````
```{r path}
````

```
miseq_path <- "./16s_microbiota-model"
list.files(miseq_path)
```


This chunk sorts the files into a specific order for analysis
```{r filenames}
# Sort ensures forward/reverse reads are in same order
fnFs <- sort(list.files(miseq_path, pattern="_R1_001.fastq"))
fnRs <- sort(list.files(miseq_path, pattern="_R2_001.fastq"))
# Extract sample names, assuming filenames have format: SAMPLENAME_XXX.fastq
sampleNames <- sapply(strsplit(fnFs, "_"), `[`, 1)
# Specify the full path to the fnFs and fnRs
fnFs <- file.path(miseq_path, fnFs)
fnRs <- file.path(miseq_path, fnRs)
fnFs[1:3]
fnRs[1:3]
```


(1) These two chunks plot the read quality of the files to determine the best way to trim them
to get all the data required.
```{r see-quality-F}
plotQualityProfile(fnFs[1:2])
```


```{r see-quality-R}
plotQualityProfile(fnRs[1:2])
```


```{r filt-names-1}
filt_path <- file.path(miseq_path, "filtered") # Place filtered files in filtered/ subdirectory
if(!file_test("-d", filt_path)) dir.create(filt_path)
filtFs <- file.path(filt_path, paste0(sampleNames, "_F_filt.fastq.gz"))
filtRs <- file.path(filt_path, paste0(sampleNames, "_R_filt.fastq.gz"))
```


This chunk trims the read in the optimal way to get the most reads.
```{r filter, message=FALSE, warning=FALSE}
out <- filterAndTrim(fnFs, filtFs, fnRs, filtRs, trimLeft=10, truncLen=c(265,200  ),
        maxN=0, maxEE=c(2,2), truncQ=2, rm.phix=TRUE,
        compress=TRUE, multithread=TRUE) # On Windows set multithread=FALSE
head(out)
```


This chunk dereplicates duplicate reads.
```{r dereplicate, message=FALSE}
derepFs <- derepFastq(filtFs, verbose=TRUE)
derepRs <- derepFastq(filtRs, verbose=TRUE)
# Name the derep-class objects by the sample names
names(derepFs) <- sampleNames
names(derepRs) <- sampleNames
```
```

(2) This chunk determines all the error rates in the sequencing process.
```r
```{r learnErrorRates}
errF <- learnErrors(filtFs, multithread=TRUE)
errR <- learnErrors(filtRs, multithread=TRUE)
```
```

```r
```{r plotrates, fig.show= "hold", fig.height = 8, fig.cap= "Estimated Error rates (both forward and reverse)"}
plotErrors(errF)
plotErrors(errF, nominalQ=TRUE) # sanity check
plotErrors(errR)
plotErrors(errR, nominalQ=TRUE) # sanity check
```
```

This chunk takes the error rate anduses it to correct all the sequences.
```r
```{r dadaStep}
dadaFs <- dada(derepFs, err=errF, multithread=TRUE)
dadaRs <- dada(derepRs, err=errR, multithread=TRUE)
```
```

```r
```{r see-dada}
dadaFs[[1]]
```
```

This step mergers the forward and reverse reads.
```r
```{r mergers}
mergers <- mergePairs(dadaFs, derepFs, dadaRs, derepRs, minOverlap = 4)
```
```

```r
```{r Mergers-table}
library(stringr)

file_len_derepFs <- length(derepFs)
Read_Number_derepFs <- vector()
uniqueseq_number_derepFs <- vector()
for(i in 1:file_len_derepFs) {
  temp <- derepFs[[i]]
  Read_Number_derepFs[i] <- length(temp$map)
  uniqueseq_number_derepFs[i] <- length(temp$uniques)
}

file_len_derepRs <- length(derepRs)
Read_Number_derepRs <- vector()
uniqueseq_number_derepRs <- vector()
for(i in 1:file_len_derepRs) {
  temp <- derepRs[[i]]
  Read_Number_derepRs[i] <- length(temp$map)
  uniqueseq_number_derepRs[i] <- length(temp$uniques)
}

file_len_denoiseFs <- length(dadaFs)
Read_Number_denoiseFs <- vector()
```

```
uniqueseq_number_denoiseFs <- vector()
for(i in 1:file_len_denoiseFs) {
  temp <- dadaFs[[i]]
  Read_Number_denoiseFs[i] <- length(temp$map)
  uniqueseq_number_denoiseFs[i] <- length(temp$denoise)
}

file_len_denoiseRs <- length(dadaRs)
Read_Number_denoiseRs <- vector()
uniqueseq_number_denoiseRs <- vector()
for(i in 1:file_len_denoiseRs) {
  temp <- dadaRs[[i]]
  Read_Number_denoiseRs[i] <- length(temp$map)
  uniqueseq_number_denoiseRs[i] <- length(temp$denoise)
}

file_len_mergers <- length(mergers)
merg_num <- vector()
for(i in 1:file_len_mergers) {
  temp <- mergers[[i]]
 merg_num[i] <- length(temp$sequence)
}

Muffin <-data.frame(input=out[,1], filtered=out[,2],
          RNderepF=Read_Number_derepFs,
          RNderepR=Read_Number_derepRs,
          RNdenoisF=Read_Number_denoiseFs,
          RNdenoisR=Read_Number_denoiseRs,
          mergers_num=merg_num)
row.names(Muffin) <- str_extract(row.names(Muffin), "^[^_]+")
View(Muffin)
```


```{r seqtab}
seqtabAll <- makeSequenceTable(mergers)
table(nchar(getSequences(seqtabAll)))
```

This step removes all chimeric data from the dataset, incorrectly combined forward and reversed reads.
```{r chimeras}
seqtabNoC <- removeBimeraDenovo(seqtabAll)
```

Uses a particular set of references to determine the taxonomy of the reads.
```{r tax}
fastaRef <- "./silva_nr99_v138_train_set.fa.gz"
taxTab <- assignTaxonomy(seqtabNoC, refFasta = fastaRef, multithread=TRUE)
unname(head(taxTab))
```
```

This step propagates the tips of the phylogentic tree with the read taxonomy as previously determined.
```{r msa, output=FALSE,message=FALSE}
seqs <- getSequences(seqtabNoC)
names(seqs) <- seqs # This propagates to the tip labels of the tree
alignment <- AlignSeqs(DNAStringSet(seqs), anchor=NA,verbose=FALSE)
```

This step makes the phylogentic tree.
```{r tree-for-total-phyloseq-object}
phangAlign <- phyDat(as(alignment, "matrix"), type="DNA")
dm <- dist.ml(phangAlign)
treeNJ <- NJ(dm) # Note, tip order != sequence order
fit = pml(treeNJ, data=phangAlign)
fitGTR <- update(fit, k=4, inv=0.2)
fitGTR <- optim.pml(fitGTR, model="GTR", optInv=TRUE, optGamma=TRUE,
      rearrangement = "stochastic", control = pml.control(trace = 0))
detach("package:phangorn", unload=TRUE)
```

This step propagates each sample the data comes from with the metadata surrounding it.
```{r samdat-propogates-samples-with-associated-data}
samdf <- read.csv("./16S_Datasheet.csv",header=TRUE)
rownames(seqtabAll) <- gsub("124", "125", rownames(seqtabAll)) # Fix discrepancy
all(rownames(seqtabAll) %in% samdf$SampleID) # TRUE
which(rownames(seqtabAll) %in% samdf$SampleID) # TRUE
rownames(samdf) <- samdf$SampleID
keep.cols <- c("collection_date", "N2_ContSparg",
"BOX", "Treatment", "Time", "SampleID", "Model", "Air", "Treatment2", "Experiment")
samdf <- samdf[rownames(seqtabAll), keep.cols]
```

This combines all the previous steps into a phylosec object.
```{r phyloseqObj-creates-total-phyloseq-object}
ps <- phyloseq(otu_table(seqtabNoC, taxa_are_rows=FALSE),
        sample_data(samdf),
        tax_table(taxTab),phy_tree(fitGTR$tree))
```

(3) This step shows all the phylum present across all the samples.
```{r taxfilter0}
# Show available ranks in the dataset
rank_names(ps)
# Create table, number of features for each phyla
table(tax_table(ps)[, "Phylum"], exclude = NULL)
```

This step removes all the NA categories from the phylosec object.
```{r removeNAphyla-from-total-phylosec-object}
ps2 <- subset_taxa(ps, !is.na(Phylum) & !Phylum %in% c("", "uncharacterized"))
table(tax_table(ps2)[, "Phylum"], exclude = NULL)
```

This step removes all batch culture data from the phylosec object.
```{r remove-batch-from-phylosec-object}
ps2Model <- subset_samples(ps2, Model == "Model")
table(tax_table(ps2Model)[, "Phylum"], exclude = NULL)
```


This step determines the prevalence of each taxonomic rank within the data set.
```{r prevfilter0-in-phyloseq-model-object}
# Compute prevalence of each feature, store as data.frame
prevdfModel = apply(X = otu_table(ps2Model),
        MARGIN = ifelse(taxa_are_rows(ps2Model), yes = 1, no = 2),
        FUN = function(x){sum(x > 0)})
# Add taxonomy and total read counts to this data.frame
prevdfModel = data.frame(Prevalence = prevdfModel,
          TotalAbundance = taxa_sums(ps2Model),
            tax_table(ps2Model))
```


```{r lowprev-in-model}
plyr::ddply(prevdfModel,                                              "Phylum",
function(df1){cbind(mean(df1$Prevalence),sum(df1$Prevalence))})
```


(4) this chunk plots the prevalence to show how the prevalence is split according to the phyla.
```{r plotprevalence-in-model, fig.width=9, fig.height=5, fig.cap="Taxa prevalence versus total counts."}
# Subset to the remaining phyla
prevdf1Model = subset(prevdfModel, Phylum %in% get_taxa_unique(ps2Model, "Phylum"))
ggplot(prevdf1Model, aes(TotalAbundance, Prevalence / nsamples(ps),color=Phylum)) +
  # Include a guess for parameter
  geom_hline(yintercept = 0.05, alpha = 0.5, linetype = 2) + geom_point(size = 2, alpha = 0.7)
+
  scale_x_log10() + xlab("Total Abundance") + ylab("Prevalence [Frac. Samples]") +
  facet_wrap(~Phylum) + theme(legend.position="none")
```


This defines how to filter the prevelence.
```{r prevalencefilter}
# Define prevalence threshold as 5% of total samples
prevalenceThresholdModel = 0.05 * nsamples(ps2Model)
prevalenceThresholdModel
# Execute prevalence filter, using `prune_taxa()` function
keepTaxaModel       =       rownames(prevdf1Model)[(prevdf1Model$Prevalence       >=
prevalenceThresholdModel)]
ps3Model = prune_taxa(keepTaxaModel, ps2Model)
table(tax_table(ps3Model)[, "Phylum"], exclude = NULL)

```

This chunk subsets the phylum via the prevelence of around 5%
```{r subset}
# Subset to the remaining phyla
prevdf1Model = subset(prevdfModel, Phylum %in% get_taxa_unique(ps3Model, "Phylum"))
ggplot(prevdf1Model, aes(TotalAbundance, Prevalence / nsamples(ps),color=Phylum)) +
  # Include a guess for parameter
  geom_hline(yintercept = 0.05, alpha = 0.5, linetype = 2) + geom_point(size = 2, alpha = 0.7)
+
  scale_x_log10() + xlab("Total Abundance") + ylab("Prevalence [Frac. Samples]") +
  facet_wrap(~Phylum) + theme(legend.position="none")
```


```{r taxglom}
# How many genera would be present after filtering?
length(get_taxa_unique(ps3Model, taxonomic.rank = "Phylum"))
table(tax_table(ps3Model)[, "Phylum"], exclude = NULL)
```


```{r tipglom}
h1 = 0.4
ps4Model = tip_glom(ps3Model, h = h1)
```


```{r plotglomprep}
multiPlotTitleTextSize = 15
p2treeModel = plot_tree(ps3Model, method = "treeonly",
            ladderize = "left",
            title = "Before Agglomeration") +
  theme(plot.title = element_text(size = multiPlotTitleTextSize))
p3treeModel = plot_tree(ps3Model, method = "treeonly",
            ladderize = "left", title = "By Genus") +
  theme(plot.title = element_text(size = multiPlotTitleTextSize))
p4treeModel = plot_tree(ps3Model, method = "treeonly",
            ladderize = "left", title = "By Height") +
  theme(plot.title = element_text(size = multiPlotTitleTextSize))
```


(5) This chunks all the previously made phylogenetic trees.
```{r plotglomtree, fig.width=14, fig.cap="Different types of agglomeration"}
# group plots together
grid.arrange(nrow = 1, p2treeModel, p3treeModel, p4treeModel)
```


(6-21) This subsets the phyla in the model by Firmacute.

```{r abundancetransformation2Modelrelativeabundance}
# Transform to relative abundance. Save as new object.
ps3Modelra = transform_sample_counts(ps3Model, function(x){x / sum(x)})
```

```{r abundancetransformationF}
plot_abundanceF = function(physeq,title = "",
                Facet = "Order", Color = "Phylum"){
```

```
# Arbitrary subset, based on Phylum, for plotting
p1f = subset_taxa(physeq, Phylum %in% c("Firmicutes"))
mphyseq = psmelt(p1f)
mphyseq <- subset(mphyseq, Abundance > 0)
ggplot(data = mphyseq, mapping = aes_string(x = "Treatment", y = "Abundance",
                color = Color, fill = Color)) +
  geom_violin(fill = NA) +
  geom_point(size = 1, alpha = 0.3,
        position = position_jitter(width = 0.3)) +
  facet_wrap(facets = Facet) + scale_y_log10()+
  theme(legend.position="none")
}
```

```{r abundancetransformation3F, fig.height=12, fig.width=10.5,fig.cap="Comparison of original abundances with transformed data"}
plotBeforeFModel = plot_abundanceF(ps3Model,"") + theme(axis.text.x = element_text(angle = 90, vjust = 0.5, hjust=1))
plotAfterFModel = plot_abundanceF(ps3Modelra,"") + theme(axis.text.x = element_text(angle = 90, vjust = 0.5, hjust=1))
# Combine each plot into one graphic.
grid.arrange(nrow = 2, plotBeforeFModel, plotAfterFModel)
```

```{r subsettaxa1F, fig.cap= "Violin plot of relative abundances of Ancholeplasmatales"}
psOrd3ModelAcholeplasmatales= subset_taxa(ps3Modelra, Order == "Acholeplasmatales")
plot_abundanceF(psOrd3ModelAcholeplasmatales, Facet = "Genus", Color = NULL)
```

```{r subsettaxa2F, fig.cap= "Violin plot of relative abundances of Acidaminococcales"}
psOrd3ModelAcidaminococcales = subset_taxa(ps3Modelra, Order == "Acidaminococcales")
plot_abundanceF(psOrd3ModelAcidaminococcales, Facet = "Genus", Color = NULL)
```

```{r subsettaxa3F, fig.cap= "Violin plot of relative abundances of Caldicoprobacterales"}
psOrd3ModelCaldicoprobacterales = subset_taxa(ps3Modelra, Order == "Caldicoprobacterales")
plot_abundanceF(psOrd3ModelCaldicoprobacterales, Facet = "Genus", Color = NULL)
```

```{r subsettaxa4F, fig.cap= "Violin plot of relative abundances of Christensenellales"}
psOrd3ModelChristensenellales = subset_taxa(ps3Modelra, Order == "Christensenellales")
plot_abundanceF(psOrd3ModelChristensenellales, Facet = "Genus", Color = NULL)
```

```{r subsettaxa5F, fig.cap= "Violin plot of relative abundances of Clostridia UCG-014"}
psOrd3ModelClostridiaUCG = subset_taxa(ps3Modelra, Order == "Clostridia UCG-014")
plot_abundanceF(psOrd3ModelClostridiaUCG, Facet = "Order", Color = NULL)
```

```{r subsettaxa6F, fig.cap= "Violin plot of relative abundances of Clostridia vandinBB60 Group"}
psOrd3ModelClostridiaBB = subset_taxa(ps3Modelra, Order == "Clostridia vandinBB60 group")
plot_abundanceF(psOrd3ModelClostridiaBB, Facet = "Order", Color = NULL)
```

```{r subsettaxa7F, fig.cap= "Violin plot of relative abundances of DTU014"}
psOrd3ModelDTU014= subset_taxa(ps3Modelra, Order == "DTU014")
plot_abundanceF(psOrd3ModelDTU014, Facet = "Order", Color = NULL)
```

```
```{r subsettaxa8F, fig.cap= "Violin plot of relative abundances of Clostridiales"}
psOrd3ModelClostridiales = subset_taxa(ps3Modelra, Order == "Clostridiales")
plot_abundanceF(psOrd3ModelClostridiales, Facet = "Genus", Color = NULL)
```

```{r subsettaxa8F.2, fig.cap= "Violin plot of relative abundances of Clostridiales"}
psOrd3ModelClostridiales = subset_taxa(ps3Modelra, Order == "Clostridiales")
plot_abundanceF(psOrd3ModelClostridiales, Facet = "Order", Color = NULL)
```

```{r subsettaxa9F, fig.cap= "Violin plot of relative abundances of Erysipelotrichales"}
psOrd5ModelErysipelotrichales = subset_taxa(ps3Modelra, Order == "Erysipelotrichales")
plot_abundanceF(psOrd5ModelErysipelotrichales , Facet = "Genus", Color = NULL)
```

```{r subsettaxa10F, fig.cap= "Violin plot of relative abundances of Eubacteriales"}
psOrd5ModelEubacteriales = subset_taxa(ps3Modelra, Order == "Eubacteriales")
plot_abundanceF(psOrd5ModelEubacteriales, Facet = "Genus", Color = NULL)
```

```{r subsettaxa11F, fig.cap= "Violin plot of relative abundances of Hungateiclostridiaceae"}
psOrd5ModelHungateiclostridiaceae=        subset_taxa(ps3Modelra,        Order        ==
"Hungateiclostridiaceae")
plot_abundanceF(psOrd5ModelHungateiclostridiaceae, Facet = "Order", Color = NULL)
```

```{r subsettaxa12F, fig.cap= "Violin plot of relative abundances of Lachnospirales"}
psOrd5ModelLachnospirales = subset_taxa(ps3Modelra, Order == "Lachnospirales")
plot_abundanceF(psOrd5ModelLachnospirales , Facet = "Genus", Color = NULL) +
theme(axis.text.x = element_text(angle = 90, vjust = 0.5, hjust=1))
```

```{r subsettaxa13F, fig.cap= "Violin plot of relative abundances of Lactobacillales"}
psOrd5ModelLactobacillales = subset_taxa(ps3Modelra, Order == "Lactobacillales")
plot_abundanceF(psOrd5ModelLactobacillales, Facet = "Genus", Color = NULL)
```

```{r subsettaxa14F, fig.cap= "Violin plot of relative abundances of Monoglobales"}
psOrd5ModelMonoglobales = subset_taxa(ps3Modelra, Order == "Monoglobales")
plot_abundanceF(psOrd5ModelMonoglobales , Facet = "Genus", Color = NULL)
```

```{r subsettaxa15F, fig.cap= "Violin plot of relative abundances of Oscillospirales"}
psOrd5ModelOscillospirales = subset_taxa(ps3Modelra, Order == "Oscillospirales")
plot_abundanceF(psOrd5ModelOscillospirales, Facet = "Genus", Color = NULL) +
theme(axis.text.x = element_text(angle = 90, vjust = 0.5, hjust=1))
```

```{r subsettaxa16F, fig.cap= "Violin plot of relative abundances of Peptostreptococcales-
Tissierellales"}
psOrd5ModelPT = subset_taxa(ps3Modelra, Order == "Peptostreptococcales-Tissierellales")
plot_abundanceF(psOrd5ModelPT, Facet = "Genus", Color = NULL) + theme(axis.text.x =
element_text(angle = 90, vjust = 0.5, hjust=1))
```
```

(22-25) This subsets the phyla in the model by Proteobacteria.
```
```{r abundancetransformationP}
plot_abundanceP = function(physeq,title = "",
                Facet = "Order", Color = "Phylum"){
 # Arbitrary subset, based on Phylum, for plotting
```

```
  p1P = subset_taxa(physeq, Phylum %in% c("Proteobacteria"))
  mphyseq = psmelt(p1P)
  mphyseq <- subset(mphyseq, Abundance > 0)
  ggplot(data = mphyseq, mapping = aes_string(x = "Treatment", y = "Abundance",
                  color = Color, fill = Color)) +
    geom_violin(fill = NA) +
    geom_point(size = 1, alpha = 0.3,
          position = position_jitter(width = 0.3)) +
    facet_wrap(facets = Facet) + scale_y_log10()+
    theme(legend.position="none")
}
```

```{r abundancetransformationPModel, fig.height=12, fig.width=10.5,fig.cap="Comparison of
original abundances with transformed data"}
plotBeforePModel = plot_abundanceP(ps3Model,"")
plotAfterPModel = plot_abundanceP(ps3Modelra,"")
# Combine each plot into one graphic.
grid.arrange(nrow = 2,  plotBeforePModel, plotAfterPModel)
```

```{r subsettaxa1PModel, fig.cap= "Violin plot of relative abundances of Burkholderiales"}
psOrd5ModelBurkholderiales = subset_taxa(ps3Modelra, Order == "Burkholderiales")
plot_abundanceP(psOrd5ModelBurkholderiales, Facet = "Genus", Color = NULL)
```

```{r subsettaxa2PModel, fig.cap= "Violin plot of relative abundances of Enterobacterales"}
psOrd5ModelEnterobacterales = subset_taxa(ps3Modelra, Order == "Enterobacterales")
plot_abundanceP(psOrd5ModelEnterobacterales, Facet = "Genus", Color = NULL)
```

```{r subsettaxa3PModel, fig.cap= "Violin plot of relative abundances of Rhodospirillales"}
psOrd5ModelRhodospirillales = subset_taxa(ps3Modelra, Order == "Rhodospirillales")
plot_abundanceP(psOrd5ModelRhodospirillales, Facet = "Order", Color = NULL)
```

(26-30) This subsets the phyla in the model by Acintobacteriota.
```{r abundancetransformationA}
plot_abundanceA = function(physeq,title = "",
              Facet = "Order", Color = "Phylum"){
  # Arbitrary subset, based on Phylum, for plotting
  p1A = subset_taxa(physeq, Phylum %in% c("Actinobacteriota"))
  mphyseq = psmelt(p1A)
  mphyseq <- subset(mphyseq, Abundance > 0)
  ggplot(data = mphyseq, mapping = aes_string(x = "Treatment", y = "Abundance",
                  color = Color, fill = Color)) +
    geom_violin(fill = NA) +
    geom_point(size = 1, alpha = 0.3,
          position = position_jitter(width = 0.3)) +
    facet_wrap(facets = Facet) + scale_y_log10()+
    theme(legend.position="none")
}
```

```{r abundancetransformationAModel, fig.height=12, fig.width=10.5,fig.cap="Comparison of
original abundances with transformed data"}
plotBeforeAModel = plot_abundanceA(ps3Model,"")
plotAfterAModel = plot_abundanceA(ps3Modelra,"")
```

```
# Combine each plot into one graphic.
grid.arrange(nrow = 2,  plotBeforeAModel, plotAfterAModel)
```

```{r subsettaxa1AModel, fig.cap= "Violin plot of relative abundances of Bifidobacteriales"}
psOrd5ModelBifidobacteriales = subset_taxa(ps3Modelra, Order == "Bifidobacteriales")
plot_abundanceA(psOrd5ModelBifidobacteriales, Facet = "Genus", Color = NULL)
```

```{r subsettaxa2AModel, fig.cap= "Violin plot of relative abundances of Coriobacteriales"}
psOrd5ModelCoriobacteriales = subset_taxa(ps3Modelra, Order == "Coriobacteriales")
plot_abundanceA(psOrd5ModelCoriobacteriales, Facet = "Genus", Color = NULL) +
theme(axis.text.x = element_text(angle = 90, vjust = 0.5, hjust=1))
```

```{r subsettaxa3AModel, fig.cap= "Violin plot of relative abundances of Corynebacteriales"}
psOrd5ModelCorynebacteriales = subset_taxa(ps3Modelra, Order == "Corynebacteriales")
plot_abundanceA(psOrd5ModelCorynebacteriales, Facet = "Genus", Color = NULL)
```

```{r subsettaxa4AModel, fig.cap= "Violin plot of relative abundances of Micrococcales"}
psOrd5ModelMicrococcales = subset_taxa(ps3Modelra, Order == "Micrococcales")
plot_abundanceA(psOrd5ModelMicrococcales , Facet = "Genus", Color = NULL)
```

(31) This subsets the phyla in the model by Bacteroidota.
```{r abundancetransformationB}
plot_abundanceB = function(physeq,title = "",
                Facet = "Order", Color = "Phylum"){
 # Arbitrary subset, based on Phylum, for plotting
 p1B = subset_taxa(physeq, Phylum %in% c("Bacteroidota"))
 mphyseq = psmelt(p1B)
 mphyseq <- subset(mphyseq, Abundance > 0)
 ggplot(data = mphyseq, mapping = aes_string(x = "Treatment", y = "Abundance",
                color = Color, fill = Color)) +
  geom_violin(fill = NA) +
  geom_point(size = 1, alpha = 0.3,
        position = position_jitter(width = 0.3)) +
  facet_wrap(facets = Facet) + scale_y_log10()+
  theme(legend.position="none")
}
```

```{r abundancetransformationBModel, fig.height=12, fig.width=10.5,fig.cap="Comparison of
original abundances with transformed data"}
plotBeforeBModel = plot_abundanceB(ps3Model,"")
plotAfterBModel = plot_abundanceB(ps3Modelra,"")
# Combine each plot into one graphic.
grid.arrange(nrow = 2,  plotBeforeBModel, plotAfterBModel)
```

```{r subsettaxa1BModel, fig.cap= "Violin plot of relative abundances of Bacteroidales"}
psOrd5ModelBacteroidales= subset_taxa(ps3Modelra, Order == "Bacteroidales")
plot_abundanceB(psOrd5ModelBacteroidales , Facet = "Genus", Color = NULL) +
theme(axis.text.x = element_text(angle = 90, vjust = 0.5, hjust=1))
```

(32) This subsets the phyla in the model by Cyanobacteria.
```{r abundancetransformationC}
plot_abundanceC = function(physeq,title = "",
```

```
              Facet = "Order", Color = "Phylum"){
  # Arbitrary subset, based on Phylum, for plotting
  P1C = subset_taxa(physeq, Phylum %in% c("Cyanobacteria"))
  mphyseq = psmelt(P1C)
  mphyseq <- subset(mphyseq, Abundance > 0)
  ggplot(data = mphyseq, mapping = aes_string(x = "Treatment", y = "Abundance",
                  color = Color, fill = Color)) +
    geom_violin(fill = NA) +
    geom_point(size = 1, alpha = 0.3,
          position = position_jitter(width = 0.3)) +
    facet_wrap(facets = Facet) + scale_y_log10()+
    theme(legend.position="none")
}
```

```{r abundancetransformationCModel, fig.height=12, fig.width=10.5,fig.cap="Comparison of original abundances with transformed data"}
plotBeforeCModel = plot_abundanceC(ps3Model,"")
plotAfterCModel = plot_abundanceC(ps3Modelra,"")
# Combine each plot into one graphic.
grid.arrange(nrow = 2,  plotBeforeCModel, plotAfterCModel)
```

```{r subsettaxa1CModel, fig.cap= "Violin plot of relative abundances of Gastranaerophilales"}
psOrd5CModelGastranaerophilales = subset_taxa(ps3Modelra, Order == "Gastranaerophilales")
plot_abundanceC(psOrd5CModelGastranaerophilales, Facet = "Genus", Color = NULL)
```


```{r init-analysis}
.cran_packages <- c( "shiny","miniUI", "caret", "pls", "e1071", "ggplot2", "randomForest", "dplyr", "ggrepel", "nlme", "devtools",
          "reshape2", "PMA", "structSSI", "ade4",
          "ggnetwork", "intergraph", "scales")
.github_packages <- c("jfukuyama/phyloseqGraphTest")
.bioc_packages <- c("genefilter", "impute")
# Install CRAN packages (if not already installed)
.inst <- .cran_packages %in% installed.packages()
if (any(!.inst)){
  install.packages(.cran_packages[!.inst],repos = "http://cran.rstudio.com/")
}
.inst <- .github_packages %in% installed.packages()
if (any(!.inst)){
  devtools::install_github(.github_packages[!.inst])
}
.inst <- .bioc_packages %in% installed.packages()
if(any(!.inst)){
  source("http://bioconductor.org/biocLite.R")
  biocLite(.bioc_packages[!.inst])
}
```

```{r Read Counts Model}
sample.sum.df.Model <- data.frame(sum = sample_sums(ps3Model))
```

sample.sum.df.Model

log10(sample.sum.df.Model)
```

````{r Histogram of Read Counts Model}
# Histogram of sample read counts
plotreadcount.Model = ggplot(sample.sum.df.Model, aes(x = sum)) +
  geom_histogram(color = "black", fill = "indianred", binwidth = 5000) +
  ggtitle("Distribution of sample sequencing depth") +
  xlab("Read counts") +
  theme(axis.title.y = element_blank())
```

````{r Histogram of Log Read Counts Model}
# Histogram of log sample read counts
Logplotreadcount.Model = ggplot(sample.sum.df.Model, aes(x = log10((sum)))) +
  geom_histogram(color = "black", fill = "indianred", binwidth = 0.025) +
  ggtitle("Log Distribution of sample sequencing depth") +
  xlab("Read counts") +
  theme(axis.title.y = element_blank())
```

(33)
``` {r grouped plots Model}
grid.arrange(nrow = 1, plotreadcount.Model, Logplotreadcount.Model)
```

(34)
````{r outlier-detect Model, fig.cap="Exploratory ordination analysis with log abundances using MDS-BRAY",fig.wide= TRUE}
sample_data(ps3Model)$Time=gsub(" ","",sample_data(ps3Model)$Time)
ps3Model.log <- transform_sample_counts(ps3Model, function(x) log(1 + x))
out.bray.log.ps3Model <- ordinate(ps3Model.log, method = "MDS", distance = "bray")
evals.bray.ps3model <- out.bray.log.ps3Model$values$Eigenvalues
plot_ordination(ps3Model.log,    out.bray.log.ps3Model,    color   =   "Time",    shape   =
"Treatment2")+
  scale_shape_manual(values=1:10)+
  labs(col = "Time", shape = "Treatment2") +
  coord_fixed(sqrt(evals.bray.ps3model[2] / evals.bray.ps3model[1]))
```

````{r outlier-detect2 Model, fig.cap="Exploratory ordination analysis with log abundances using MDS Wunifrac",fig.wide= TRUE}
sample_data(ps3Model)$Time=gsub(" ","",sample_data(ps3Model)$Time)
ps3Model.log <- transform_sample_counts(ps3Model, function(x) log(1 + x))
out.wuf.log.ps3Model <- ordinate(ps3Model.log, method = "MDS", distance = "wunifrac")
evals.wuf.ps3model <- out.wuf.log.ps3Model$values$Eigenvalues
plot_ordination(ps3Model.log,    out.wuf.log.ps3Model,    color   =   "Time",    shape   =
"Treatment2")+
  scale_shape_manual(values=1:10)+
  labs(col = "Time", shape = "Treatment2") +
  coord_fixed(sqrt(evals.wuf.ps3model[2] / evals.wuf.ps3model[1]))
```

````{r outlier-analyze, fig.width=9, fig.height=5, fig.cap="The outlier samples are dominated by a single ASV."}

```r
rel_abund.ps3Model <- t(apply(otu_table(ps3Model), 1, function(x) x / sum(x)))
qplot(rel_abund.ps3Model[, 12], geom = "histogram",binwidth=0.05) +
  xlab("Relative abundance")
```


```{r removelowreads Model}
which(!rowSums(otu_table(ps3Model)) > 1000)
ps5Model <- prune_samples(rowSums(otu_table(ps3Model)) > 1000, ps3Model)
ps5Model.log <- transform_sample_counts(ps5Model, function(x) log(1 + x))
```

(35)
```{r self exploration using ordination Model}
Ps5Model.ord.NMDSbray <- ordinate(ps5Model, "NMDS", "bray")
Ps5Model.ordNMDSbray.Plot   =   plot_ordination(ps5Model,   Ps5Model.ord.NMDSbray,
type="taxa", color="Phylum", shape = "Time", title="taxa")
print(Ps5Model.ordNMDSbray.Plot)
```

(36) Self Exploration 2
```{r self exploration using ordination 2 Model}
Ps5Model.ordNMDSbray.Plot + facet_wrap(~Phylum, 3)
```

(37)
```{r ordinations-bray-Model,fig.cap="A PCoA plot using Bray-Curtis between  samples."}
out.pcoa.log.ps5model.mdsbray <- ordinate(ps5Model.log,   method = "MDS", distance =
"bray")
evals.pcoa.ps5model.mdsbray <- out.pcoa.log.ps5model.mdsbray$values[,1]
plot_ordination(ps5Model.log,  out.pcoa.log.ps5model.mdsbray, color = "Time", shape =
"Treatment2")+
  scale_shape_manual(values=1:10)+
  labs(col = "Time", shape = "Treatment2")
  coord_fixed(sqrt(evals.pcoa.ps5model.mdsbray[2] / evals.pcoa.ps5model.mdsbray[1]))
```

(38)
```{r   ordinations-dpcoa-model,   fig.wide=TRUE,fig.cap="A   DPCoA   plot   incorporates
phylogenetic information, but is  dominated by the first axis."}
out.dpcoa.log.ps5model <- ordinate(ps5Model.log,method = "DPCoA")
evals.dpcoa.ps5model.log <- out.dpcoa.log.ps5model$eig
plot_ordination(ps5Model.log,  out.dpcoa.log.ps5model,  color  =  "Time",  shape  =
"Treatment2")+
  scale_shape_manual(values=1:10)+
  labs(col = "Time", shape = "Treatment2") +
  coord_fixed(sqrt(evals.dpcoa.ps5model.log[2] / evals.dpcoa.ps5model.log[1]))
```


(39) Samples  with  higher  scores  on  the  second  axis  have  altered  concentrations  of
BActeroidota, acintobacter and proteobacteria
```{r dpcoabiplot-Model,fig.wide=TRUE,fig.cap="Taxa responsible for Axis 1 and 2"}
plot_ordination(ps5Model.log, out.dpcoa.log.ps5model , type = "species", color = "Phylum")
+
  coord_fixed(sqrt(evals.dpcoa.ps5model.log[2] / evals.dpcoa.ps5model.log[1]))
```

(40)

````
```{r ordinations-wuf-model,fig.wide =TRUE, fig.cap="The sample positions produced by a
PCoA using weighted Unifrac."}
out.wuf.log.ps5Model <- ordinate(ps5Model.log, method = "PCoA", distance ="wunifrac")
evals.out.wuf.log.ps5Model<- out.wuf.log.ps5Model$values$Eigenvalues
plot_ordination(ps5Model.log,   out.wuf.log.ps5Model,   color  =  "Time",   shape  =
"Treatment2")+
 scale_shape_manual(values=1:10)+
 labs(col = "Time", shape = "Treatment2")  +
 coord_fixed(sqrt(evals.out.wuf.log.ps5Model[2] / evals.out.wuf.log.ps5Model[1])) +
 labs(col = "Time", shape = "Treatment")
```
```

(41)
````
```{r dwufplotplot-model,fig.wide=TRUE,fig.cap="Taxa responsible for Axis 1 and 2"}
plot_ordination(ps5Model.log, out.wuf.log.ps5Model, type = "species", color = "Phylum") +
 coord_fixed(sqrt(evals.out.wuf.log.ps5Model[2] / evals.out.wuf.log.ps5Model[1]))
```
```

````
```{r rankab model}
abund.Model <- otu_table(ps5Model.log)
abund_ranks.Model <- t(apply(abund.Model, 1, rank))
```
```

````
```{r rank# model}
abund_ranks.Model[]
```
```

Hi @chloelulu, this is a somewhat subtle transformation of the data. I think it's worth thinking
through each step carefully.

The first step is a rank-transformation on the abundance matrix. Specifically, abund_ranks[i,
j] gives the rank of species j in sample i. The most abundant species in the i^th row has rank
389, since there are 389 species. If there were no ties, the least abundant species would have
rank 1. However, there are usually many species with 0 counts in each sample -- these ties
explain why you don't see any rank equal to 1. For example, the smallest rank in the first
sample is 82.5, because there are 164 species with counts of 0 in that sample.

Working with the ranks is an improvement, but there is a problem -- the difference between
very abundant species (say, 389 vs. 383) looks the same as the difference between rare
species (e.g., 1 vs. 7, if we imagine we didn't have any ties). Really, we'd like our
dimensionality reduction to pay more attention to differences between abundant species.
To do this, we make the ranks for all the rare species look the same. This is why we do the
next two lines,

abund_ranks <- abund_ranks - 329
abund_ranks[abund_ranks < 1] <- 1

The first line shifts all the ranks down, and the second "squashes" all the ranks for all the less-
abundant species, so that they are all equal to 1. If we didn't do the subtraction, we could
still achieve the squashing effect, but there would be a big gap between the high ranks of
abundant species and those low abundance species that have been fixed to 1. The choice 329
ensures that about 85% of species will be squashed to 1 (because 329 / 389 = 84.6%), so
differences in abundance between rare species are ignored (they're all equal to 1), and the

ordination pays more attention to ranks of the abundant species. You can should change 329 to whatever gives you an appropriate percentage of squashed species. Let us know if you have any questions.

```{r rankthreshold}
abund_ranks.Model <- abund_ranks.Model - 912.9
abund_ranks.Model[abund_ranks.Model < 1] <- 1
```

(42)
```{r pca-rank-visualize-procedure-model, fig.cap="Rank threshold transformation"}
library(dplyr)
library(reshape2)
abund_df.Model <- melt(abund.Model, value.name = "abund") %>%
  left_join(melt(abund_ranks.Model, value.name = "rank"))
colnames(abund_df.Model) <- c("sample", "seq", "abund", "rank")
sample_ix <- sample(1:nrow(abund_df.Model), 8)
ggplot(abund_df.Model %>%
      filter(sample %in% abund_df.Model$sample[sample_ix])) +
  geom_point(aes(x = abund, y = rank, col = sample),
        position = position_jitter(width = 0.2), size = 1.5) +
  labs(x = "Abundance", y = "Thresholded rank") +
  scale_color_brewer(palette = "Set2")
```

```{r pca-rank-pca-setup-model-simple}
library(ade4)
ranks_pca.Model <- dudi.pca(abund_ranks.Model, scannf = F, nf = 3)
row_scores.Model <- data.frame(li = ranks_pca.Model$li,
            SampleID = rownames(abund_ranks.Model))
col_scores.Model <- data.frame(co = ranks_pca.Model$co,
            seq = colnames(abund_ranks.Model))
tax.Model <- tax_table(ps5Model.log) %>%
  data.frame(stringsAsFactors = FALSE)
tax.Model$seq <- rownames(tax.Model)
main_orders            <-            c("Clostridiales","Enterobacterales","Eubacteriales",
"Lactospirales","Lactobacillales","Monoglobales","Oscillospirales")
tax.Model$Order[!(tax.Model$Order %in% main_orders)] <- "Other"
tax.Model$Order <- factor(tax.Model$Order, levels = c(main_orders, "Other"))
tax.Model$otu_id <- seq_len(ncol(otu_table(ps5Model.log)))
row_scores.Model<- row_scores.Model %>%
  left_join(sample_data(ps5Model.log))
col_scores.Model <- col_scores.Model %>%
  left_join(tax.Model)
```

(44)
```{r pca-rank-pca-plot-model, fig.wide=TRUE,fig.height=8,fig.cap="The biplot resulting from the PCA after the truncated-ranking transformation."}
evals_prop.ranks_pca.Model <- 100 * (ranks_pca.Model$eig / sum(ranks_pca.Model$eig))
ggplot() +
  geom_point(data = row_scores.Model, aes(x = li.Axis1, y = li.Axis2), shape = 2) +
```

```
  geom_text_repel(data = row_scores.Model, aes(x = li.Axis1, y = li.Axis2), label =
row_scores.Model$SampleID) +
  geom_point(data = col_scores.Model, aes(x = 25 * co.Comp1, y = 25 * co.Comp2, col =
Order),
        size = .3, alpha = 0.6) +
  facet_grid(~ Treatment) +
  guides(col = guide_legend(override.aes = list(size = 3))) +
  labs(x = sprintf("Axis1 [%s%% variance]", round(evals_prop.ranks_pca.Model[1], 2)),
     y = sprintf("Axis2 [%s%% variance]", round(evals_prop.ranks_pca.Model[2], 2))) +
  coord_fixed(sqrt(ranks_pca.Model$eig[2] / ranks_pca.Model$eig[1])) +
  theme(panel.border = element_rect(color = "#787878", fill = alpha("white", 0)))
```

```{r pca-rank-pca-plot-model-2, fig.wide=TRUE,fig.height=8,fig.cap="The biplot resulting
from the PCA after the truncated-ranking transformation.2"}
ggplot() +
  geom_point(data = row_scores.Model, aes(x = li.Axis1, y = li.Axis2), shape = 2)+
  geom_text_repel(data = row_scores.Model, aes(x = li.Axis1, y = li.Axis2), label =
row_scores.Model$SampleID)+
  geom_point(data = col_scores.Model, aes(x = 25 * co.Comp1, y = 25 * co.Comp2, col =
Order),
        size = .3, alpha = 0.6) +
  facet_wrap(~ Time, ncol=5) +
  guides(col = guide_legend(override.aes = list(size = 3))) +
  labs(x = sprintf("Axis1 [%s%% variance]", round(evals_prop.ranks_pca.Model[1], 2)),
     y = sprintf("Axis2 [%s%% variance]", round(evals_prop.ranks_pca.Model[2], 2))) +
  coord_fixed(sqrt(ranks_pca.Model$eig[2] / ranks_pca.Model$eig[1])) +
  theme(panel.border = element_rect(color = "#787878", fill = alpha("white", 0)))
```

```{r ccpna-correspondence-analysis-model}
ps_ccpna.model.log <- ordinate(ps5Model.log, "CCA", formula = ps5Model.log ~ Time +
Treatment)
```

```{r ccpna-join-data-model, fig.cap="The mouse and bacteria scores generated by CCpnA.",
fig.wide=TRUE, fig.height=10}
library(ggrepel)
ps_scores.model.log <- vegan::scores(ps_ccpna.model.log)
sites <- data.frame(ps_scores.model.log$sites)
sites$SampleID <- rownames(sites)
sites <- sites %>%
  left_join(sample_data(ps5Model.log))
species <- data.frame(ps_scores.model.log$species)
species$otu_id <- seq_along(colnames(otu_table(ps5Model.log)))
species <- species %>%
  left_join(tax.Model)
evals_prop.ps_ccpna.model.log    <-    100    *    ps_ccpna.model.log$CCA$eig[1:2]    /
sum(ps_ccpna.model.log$CA$eig)
ggplot() +
  geom_point(data = sites, aes(x = CCA1, y = CCA2), shape = 17, alpha = 0.5) +
  geom_point(data = species, aes(x = CCA1, y = CCA2, col = Order), size = 0.5) +
  geom_text_repel(data = species %>% filter(CCA2 > 2.5),
          aes(x = CCA1, y = CCA2, label = otu_id),
```

```
                          size = 4, segment.size = 0.1,
                          max.overlaps = Inf) +
  facet_wrap(. ~ Treatment2, ncol=5) +
  guides(col = guide_legend(override.aes = list(size = 3))) +
  labs(x = sprintf("Axis1 [%s%% variance]", round(evals_prop.ps_ccpna.model.log [1], 2)),
      y = sprintf("Axis2 [%s%% variance]", round(evals_prop.ps_ccpna.model.log [2], 2))) +
  coord_fixed(sqrt(ps_ccpna.model.log$CCA$eig[2] / ps_ccpna.model.log$CCA$eig[1])*0.45
) +
  theme(panel.border = element_rect(color = "#787878", fill = alpha("white", 0)))
```

```{r ccpna-join-data-model-2, fig.cap="The mouse and bacteria scores generated by CCpnA.",
fig.wide=TRUE, fig.height=10}
ggplot() +
  geom_point(data = sites, aes(x = CCA1, y = CCA2), shape = 17, alpha = 0.5) +
  geom_point(data = species, aes(x = CCA1, y = CCA2, col = Order), size = 0.5) +
  geom_text_repel(data = species %>% filter(CCA2 > 2.5),
            aes(x = CCA1, y = CCA2, label = otu_id),
                      size = 4, segment.size = 0.1,
                      max.overlaps = Inf) +
  facet_wrap(. ~ Time, ncol=5) +
  guides(col = guide_legend(override.aes = list(size = 3))) +
  labs(x = sprintf("Axis1 [%s%% variance]", round(evals_prop.ps_ccpna.model.log [1], 2)),
      y = sprintf("Axis2 [%s%% variance]", round(evals_prop.ps_ccpna.model.log [2], 2))) +
  coord_fixed(sqrt(ps_ccpna.model.log$CCA$eig[2] / ps_ccpna.model.log$CCA$eig[1])*0.45
) +
  theme(panel.border = element_rect(color = "#787878", fill = alpha("white", 0)))
```


```{r xtrasetupknitr, echo=FALSE}
theme_set(theme_bw())
min_theme <- theme_update(panel.border = element_blank(),
                panel.grid = element_blank(),
                axis.ticks = element_blank(),
                legend.title = element_text(size = 8),
                legend.text = element_text(size = 6),
                axis.text = element_text(size = 6),
                axis.title = element_text(size = 8),
                strip.background = element_blank(),

                strip.text = element_text(size = 8),
                legend.key = element_blank())
```

```{r setup-ggnetwork}
library("phyloseqGraphTest")
library("igraph")
library("ggnetwork")
net.model <- make_network(ps5Model.log, max.dist=0.35)
sampledata <- as.data.frame(sample_data(ps5Model.log))
V(net.model)$Treatment2 <- sampledata[names(V(net.model)), "Treatment2"]
V(net.model)$Time <- sampledata[names(V(net.model)), "Time"]
```
```

````
```{r Plot_network, Fig.cap="A network created by thresholding the Jaccard dissimilarity matrix."}
plot_net(ps5Model.log, maxdist = 0.3, color = "Time", shape = "Treatment2", point_size = 5,
laymeth = "fruchterman.reingold") + scale_shape_manual(values=15:23)
```

```{r mst}
gt.model.mst <- graph_perm_test(ps5Model.log, "Treatment2", grouping = "SampleID",
            distance = "jaccard", type = "mst")
gt.model.mst$pval
gt.model.mstT <- graph_perm_test(ps5Model.log, "Time", grouping = "SampleID",
            distance = "jaccard", type = "mst")
gt.model.mstT$pval
```

```{r mst-plot, fig.width=8.5, fig.height=5, fig.cap="The graph and permutation histogram obtained from the minimal  spanning tree with Jaccard similarity."}
plotNet.gt.model.mst=plot_test_network(gt.model.mst)     +     theme(legend.text     =
element_text(size = 8),
    legend.title = element_text(size = 9))
plotPerm.gt.model.mst=plot_permutations(gt.model.mst)
grid.arrange(ncol = 2,  plotNet.gt.model.mst, plotPerm.gt.model.mst)

plotNet.gt.model.mstT=plot_test_network(gt.model.mstT)     +     theme(legend.text     =
element_text(size = 8),
    legend.title = element_text(size = 9))
plotPerm.gt.model.mstT=plot_permutations(gt.model.mstT)
grid.arrange(ncol = 2,  plotNet.gt.model.mstT, plotPerm.gt.model.mstT)
```

```{r knn-1}
gt.model.knn <- graph_perm_test(ps5Model.log, "Treatment2", grouping = "SampleID",
            distance = "jaccard", type = "knn", knn = 1)
gt.model.knn$pval
```

```{r knn-1-plot,fig.cap="k=1  nearest-neighbor  network  and  permutation  histogram", fig.wide=TRUE, fig.height=5}
plotNet.gt.model.knn=plot_test_network(gt.model.knn)     +     theme(legend.text     =
element_text(size = 8),
    legend.title = element_text(size = 9))
plotPerm.gt.model.knn=plot_permutations(gt.model.knn)
grid.arrange(ncol = 2,  plotNet.gt.model.knn, plotPerm.gt.model.knn)
```

```{r Bray}
gt.model.bray <- graph_perm_test(ps5Model.log, "Treatment2", grouping = "SampleID",
            distance = "bray", type = "knn", knn = 1)
plotNet.gt.model.bray=plot_test_network(gt.model.bray)     +     theme(legend.text     =
element_text(size = 8),
    legend.title = element_text(size = 9))
plotPerm.gt.model.bray=plot_permutations(gt.model.bray)
grid.arrange(ncol = 2,  plotNet.gt.model.bray, plotPerm.gt.model.bray)
gt.model.bray$pval
```

```{r Braydistance}
````

```
gt.model.breynedges    <-    graph_perm_test(ps5Model.log,    "Treatment2",    grouping    =
"SampleID",
                            distance = "bray", type = "threshold.nedges", nedges = 720,
                            keep.isolates = FALSE)
plotNet.gt.model.breynedges=          plot_test_network(gt.model.breynedges)          +
theme(legend.text = element_text(size = 8),
        legend.title = element_text(size = 9))
plotPerm.gt.model.breynedges=plot_permutations(gt.model.breynedges)
grid.arrange(ncol = 2, plotNet.gt.model.breynedges, plotPerm.gt.model.breynedges)
```

```{r Bray Distance 2}
gt.model.breynedges2    <-    graph_perm_test(ps5Model.log,    "Treatment2",    grouping    =
"SampleID",
                            distance = "bray", type = "threshold.nedges", nedges = 100,
                            keep.isolates = FALSE)
plotNet.gt.model.breynedges2=          plot_test_network(gt.model.breynedges2)          +
theme(legend.text = element_text(size = 8),
        legend.title = element_text(size = 9))
plotPerm.gt.model.breynedges2=plot_permutations(gt.model.breynedges2)
grid.arrange(ncol = 2, plotNet.gt.model.breynedges2, plotPerm.gt.model.breynedges2)
gt.model.breynedges2$pval
```

```{r lm-get-alpha-diversity}
library("nlme")
library("reshape2")
ps_alpha_div.model <- estimate_richness(ps5Model.log, split = TRUE, measure = "Shannon")
ps_alpha_div.model$SampleID <- rownames(ps_alpha_div.model) %>%
 as.factor()
ps_samp.model <- sample_data(ps5Model.log) %>%
 unclass() %>%
 data.frame() %>%
 left_join(ps_alpha_div.model, by = "SampleID") %>%
 melt(measure.vars = "Shannon",
    variable.name = "diversity_measure",
    value.name = "alpha_diversity")
# reorder's facet from lowest to highest diversity
diversity_means.model <- ps_samp.model %>%
 group_by(SampleID) %>%
 summarise(mean_div = mean(alpha_diversity)) %>%
 arrange(mean_div)
ps_samp$.modelSampleID <- factor(ps_samp.model$SampleID,
                diversity_means.model$SampleID)
```

```{r lm-Treatment2}
alpha_div.model <- lme(fixed = alpha_diversity ~ Treatment2, data = ps_samp.model,
            random = ~ 1 | SampleID)
```

```{r lm-prediction-intervals}
new_data.model <- expand.grid(SampleID = ps_samp.model$SampleID,
            Treatment2 = ps_samp.model$Treatment2)
new_data.model$pred <- predict(alpha_div.model, newdata.model = new_data)
X.model <- model.matrix(eval(eval(alpha_div.model$call$fixed)[-2]),
```

```
            new_data[-ncol(new_data.model)])
pred_var_fixed.model <- diag(X.model %*% alpha_div.model$varFix %*% t(X.model))
new_data.model$pred_var <- pred_var_fixed.model + alpha_div.model$sigma ^ 2
```

```{r lm-fitted-plot}
# fitted values, with error bars
ggplot(ps_samp.model %>% left_join(new_data.model)) +
  geom_errorbar(aes(x = Time, ymin = pred - 2 * sqrt(pred_var),
            ymax = pred + 2 * sqrt(pred_var)),
        col = "#858585", size = .1) +
  geom_point(aes(x = Time, y = alpha_diversity,
          col = Time), size = 0.8) +
  facet_wrap(~Treatment2) +
  scale_y_continuous(limits = c(0.7, 10), breaks = seq(0, 10, .5)) +
  scale_color_brewer(palette = "Set3") +
  labs(x = "Treatment", y = "Shannon Diversity", color = "Time") +
  guides(col = guide_legend(override.aes = list(size = 4))) +
  theme(panel.border = element_rect(color = "#787878", fill = alpha("white", 0)),
      axis.text.x = element_text(angle = -90, size = 6),
      axis.text.y = element_text(size = 6))
```


```{r install for HmT}
BiocManager::install("DESeq2")
BiocManager::install("rjson")
install.packages("/home/huttonw/lstm_data/Tars/structSSI_1.1.1.tar.gz",  repos  =  NULL,
type="source")
```


```{r deseq-transform}
library("reshape2")
library("DESeq2")
#New version of DESeq2 needs special levels
ps_dds.model <- phyloseq_to_deseq2(ps5Model, design = ~ Time + Treatment2)
# geometric mean, set to zero when all coordinates are zero
geo_mean_protected <- function(x) {
 if (all(x == 0)) {
   return (0)
 }
 exp(mean(log(x[x != 0])))
}
geoMeans.model <- apply(counts(ps_dds.model), 1, geo_mean_protected)
ps_dds.model <- estimateSizeFactors(ps_dds.model, geoMeans = geoMeans.model)
ps_dds.model <- estimateDispersions(ps_dds.model)
abund.ps_dds.model <- getVarianceStabilizedData(ps_dds.model)
```

```{r structssi-shorten-names}
short_names.model <- substr(rownames(abund.ps_dds.model), 1, 5)%>%
  make.names(unique = TRUE)
rownames(abund.ps_dds.model) <- short_names.model
```

```{r deseq-vis, fig.cap="DEseq transformation abundance"}
```

```
abund_sums.ps_dds.model <- rbind(data.frame(sum = colSums(abund.ps_dds.model),
                  sample = colnames(abund.ps_dds.model),
                  type = "DESeq2"),
            data.frame(sum = rowSums(otu_table(ps5Model.log)),
                  sample = rownames(otu_table(ps5Model.log)),
                  type = "log(1 + x)"))
ggplot(abund_sums.ps_dds.model) +
  geom_histogram(aes(x = sum), binwidth = 20) +
  facet_grid(type ~ .) +
  xlab("Total abundance within sample")
```

```{r structssi-unadjp }
library("structSSI")
el.model <- phy_tree(ps5Model.log)$edge
el0.model <- el.model
el0.model <- el0[nrow(el.model):1, ]
el_names.model <- c(short_names.model, seq_len(phy_tree(ps5Model.log)$Nnode))
el.model[, 1] <- el_names[el0.model[, 1]]
el.model[, 2] <- el_names.model[as.numeric(el0.model[, 2])]
unadj_p.model.time            <-            treePValues(el.model,            abund.ps_dds.model,
sample_data(ps5Model.log)$Time)
unadj_p.model.treatment       <-            treePValues(el.model,            abund.ps_dds.model,
sample_data(ps5Model.log)$Treatment2)
```

```{r structssi-test}
hfdr_res.model.time<- hFDR.adjust(unadj_p.model.time, el.model, .75)
hfdr_res.model.treatment<- hFDR.adjust(unadj_p.model.treatment, el.model, .75)
summary(hfdr_res.model.time)
```

```{r  structssi-test-plotres, eval=FALSE}
#interactive part: not run
plot(hfdr_res.model) # opens in a browser
```

```{r structssi-tax}
tax.ps_dds.model <- tax_table(ps5Model.log)[, c("Family", "Genus")] %>%
  data.frame()
tax.ps_dds.model$seq <- short_names.model
```

```{r structssi-test-res-time}
options(digits=3)
hfdr_res.model.time@p.vals$seq <- rownames(hfdr_res.model.time@p.vals)
tax.ps_dds.model %>%
  left_join(hfdr_res.model.time@p.vals) %>%
  arrange(adjp) %>% head(10)
```

```{r structssi-test-res-treatment}
options(digits=3)
hfdr_res.model.treatment@p.vals$seq <- rownames(hfdr_res.model.treatment@p.vals)
tax.ps_dds.model %>%
  left_join(hfdr_res.model.treatment@p.vals) %>%
  arrange(adjp) %>% head(10)
```
```

(45)
```r Overall-Abundance-Plot-model
plot_bar(ps5Model, fill = "Phylum") +
geom_bar(aes(color=Phylum, fill=Phylum), stat="identity", position="stack")
```


```r relative-abundance-plot-model
total = median(sample_sums(ps6Model))
standf = function(x, t=total) round(t * (x / sum(x)))
ps7Model = transform_sample_counts(ps5Model, standf)

plot_bar(ps7Model, fill = "Phylum") +
geom_bar(aes(color=Phylum, fill=Phylum), stat="identity", position="stack")
```
(47)
```r Abundance-plot-for-model
plot_bar(ps7Model, x="Phylum", fill = "Phylum", facet_grid = "Treatment2")
```
(48)
```r Abundance-plot-for-model~time
plot_bar(ps7Model, x="Time", fill = "Phylum", facet_grid = "Treatment2")+
geom_bar(aes(color=Phylum, fill=Phylum), stat="identity", position="stack")
```


```r Abundance-plot-for-model~time-Berberine2
ps7ModelB <- subset_samples(ps7Model, Experiment =="Berberine")
plot_bar(ps7ModelB, x="Time", fill = "Phylum", facet_grid = "Treatment2")+
geom_bar(aes(color=Phylum, fill=Phylum), stat="identity", position="stack")
```

```r Abundance-plot-for-model~time-Quercetin2
ps7ModelQ <- subset_samples(ps7Model, Experiment =="Quercetin")
plot_bar(ps7ModelQ, x="Time", fill = "Phylum", facet_grid = "Treatment2")+
geom_bar(aes(color=Phylum, fill=Phylum), stat="identity", position="stack")
```


```r Abundance-plot-for-model~time-Quercetin3
ps11 <- subset_samples(ps7ModelQ, Treatment =="Quercetin")
plot_bar(ps11, x="Time", fill = "Phylum", facet_grid = "Treatment2")+
geom_bar(aes(color=Phylum, fill=Phylum), stat="identity", position="stack")
```
```r removeModel
ps2Batch <- subset_samples(ps2, Model == "BatchC")
table(tax_table(ps2Batch)[, "Phylum"], exclude = NULL)
```
```r prevfilterBatch
# Compute prevalence of each feature, store as data.frame
prevdf.Batch = apply(X = otu_table(ps2Batch),
        MARGIN = ifelse(taxa_are_rows(ps2Batch), yes = 1, no = 2),
        FUN = function(x){sum(x > 0)})
# Add taxonomy and total read counts to this data.frame
prevdf.Batch = data.frame(Prevalence = prevdf.Batch,
            TotalAbundance = taxa_sums(ps2Batch),
```

```
                tax_table(ps2Batch))
```

````{r lowprevBatch}
plyr::ddply(prevdf.Batch,                                          "Phylum",
function(df1){cbind(mean(df1$Prevalence),sum(df1$Prevalence))})
````

(b-1)
````{r plotprevalenceBatch, fig.width=9, fig.height=5, fig.cap="Taxa prevalence versus total
counts."}
# Subset to the remaining phyla
prevdf1.Batch = subset(prevdf.Batch, Phylum %in% get_taxa_unique(ps2Batch, "Phylum"))
ggplot(prevdf1.Batch,              aes(TotalAbundance,           Prevalence           /
nsamples(ps2Batch),color=Phylum)) +
 # Include a guess for parameter
 geom_hline(yintercept = 0.05, alpha = 0.5, linetype = 2) +  geom_point(size = 2, alpha = 0.7)
+
 scale_x_log10() + xlab("Total Abundance") + ylab("Prevalence [Frac. Samples]") +
 facet_wrap(~Phylum) + theme(legend.position="none")
````

````{r prevalencefilterBatch}
# Define prevalence threshold as 5% of total samples
prevalenceThreshold.batch = 0.05 * nsamples(ps2Batch)
prevalenceThreshold.batch
# Execute prevalence filter, using `prune_taxa()` function
keepTaxa.batch        =       rownames(prevdf1.Batch)[(prevdf1.Batch$Prevalence        >=
prevalenceThreshold.batch)]
ps3Batch = prune_taxa(keepTaxa.batch, ps2Batch)
table(tax_table(ps3Batch)[, "Phylum"], exclude = NULL)

````

(b-2)
````{r subsetBatch}
# Subset to the remaining phyla
prevdf1.Batch = subset(prevdf.Batch, Phylum %in% get_taxa_unique(ps3Batch, "Phylum"))
ggplot(prevdf1.Batch,              aes(TotalAbundance,           Prevalence           /
nsamples(ps3Batch),color=Phylum)) +
 # Include a guess for parameter
 geom_hline(yintercept = 0.05, alpha = 0.5, linetype = 2) +  geom_point(size = 2, alpha = 0.7)
+
 scale_x_log10() + xlab("Total Abundance") + ylab("Prevalence [Frac. Samples]") +
 facet_wrap(~Phylum) + theme(legend.position="none")
````

````{r taxglomBatch}
# How many genera would be present after filtering?
length(get_taxa_unique(ps3Batch, taxonomic.rank = "Phylum"))
table(tax_table(ps3Batch)[, "Phylum"], exclude = NULL)
````

````{r tipglomBatch}
h1 = 0.4
ps4Batch = tip_glom(ps3Batch, h = h1)
````

````{r plotglomprepB}
```

```
multiPlotTitleTextSize = 15
p2treeB = plot_tree(ps3Batch, method = "treeonly",
              ladderize = "left",
              title = "Before Agglomeration") +
  theme(plot.title = element_text(size = multiPlotTitleTextSize))
p3treeB = plot_tree(ps3Batch, method = "treeonly",
              ladderize = "left", title = "By Genus") +
  theme(plot.title = element_text(size = multiPlotTitleTextSize))
p4treeB = plot_tree(ps3Batch, method = "treeonly",
              ladderize = "left", title = "By Height") +
  theme(plot.title = element_text(size = multiPlotTitleTextSize))
```

(B-3) This chunks all the previously made phylogenetic trees.
```{r plotglomtreeBatch, fig.width=14, fig.cap="Different types of agglomeration"}
# group plots together
grid.arrange(nrow = 1, p2treeB, p3treeB, p4treeB)
```

(b-4)
```{r abundancetransformationBatchF}
plot_abundanceF = function(physeq,title = "",
                  Facet = "Order", Color = "Phylum"){
  # Arbitrary subset, based on Phylum, for plotting
  p1f = subset_taxa(physeq, Phylum %in% c("Firmicutes"))
  mphyseq = psmelt(p1f)
  mphyseq <- subset(mphyseq, Abundance > 0)
  ggplot(data = mphyseq, mapping = aes_string(x = "Treatment", y = "Abundance",
                  color = Color, fill = Color)) +
    geom_violin(fill = NA) +
    geom_point(size = 1, alpha = 0.3,
          position = position_jitter(width = 0.3)) +
    facet_wrap(facets = Facet) + scale_y_log10()+
    theme(legend.position="none")
}
```

```{r abundancetransformation2Batch}
# Transform to relative abundance. Save as new object.
ps3Batchra = transform_sample_counts(ps3Batch, function(x){x / sum(x)})
```

```{r abundancetransformation3FBatch, fig.height=12, fig.width=10.5,fig.cap="Comparison
of original abundances with transformed data"}
plotBeforeFBatch = plot_abundanceF(ps3Batch,"")
plotAfterFBatch = plot_abundanceF(ps3Batchra,"")
# Combine each plot into one graphic.
grid.arrange(nrow = 2, plotBeforeFBatch, plotAfterFBatch)
```

```{r subsettaxa1FBatch, fig.cap= "Violin plot of relative abundances of Ancholeplasmatales"}
psOrd3BatchAcholeplasmatales= subset_taxa(ps3Batchra, Order == "Acholeplasmatales")
plot_abundanceF(psOrd3BatchAcholeplasmatales, Facet = "Genus", Color = NULL)
```

```{r subsettaxa2FBatch, fig.cap= "Violin plot of relative abundances of Acidaminococcales"}
psOrd3BatchAcidaminococcales = subset_taxa(ps3Batchra, Order == "Acidaminococcales")
plot_abundanceF(psOrd3BatchAcidaminococcales, Facet = "Genus", Color = NULL)
```
```

```
```{r subsettaxa3FBatch, fig.cap= "Violin plot of relative abundances of
Caldicoprobacterales"}
psOrd3BatchCaldicoprobacterales = subset_taxa(ps3Batchra, Order ==
"Caldicoprobacterales")
plot_abundanceF(psOrd3BatchCaldicoprobacterales, Facet = "Genus", Color = NULL)
```

```{r subsettaxa4FBatch, fig.cap= "Violin plot of relative abundances of Christensenellales"}
psOrd3BatchChristensenellales = subset_taxa(ps3Batchra, Order == "Christensenellales")
plot_abundanceF(psOrd3BatchChristensenellales, Facet = "Genus", Color = NULL)
```

```{r subsettaxa5FBatch, fig.cap= "Violin plot of relative abundances of Clostridia UCG-014"}
psOrd3BatchClostridiaUCG = subset_taxa(ps3Batchra, Order == "Clostridia UCG-014")
plot_abundanceF(psOrd3BatchClostridiaUCG, Facet = "Order", Color = NULL)
```

```{r subsettaxa6FBatch, fig.cap= "Violin plot of relative abundances of DTU014"}
psOrd3BatchDTU014= subset_taxa(ps3Batchra, Order == "DTU014")
plot_abundanceF(psOrd3BatchDTU014, Facet = "Order", Color = NULL)
```

```{r subsettaxa7FBatch, fig.cap= "Violin plot of relative abundances of Eubacteriales"}
psOrd5BatchEubacteriales = subset_taxa(ps3Batchra, Order == "Eubacteriales")
plot_abundanceF(psOrd5BatchEubacteriales, Facet = "Genus", Color = NULL)
```

```{r subsettaxa8FBatch, fig.cap= "Violin plot of relative abundances of
Hungateiclostridiaceae"}
psOrd5BatchHungateiclostridiaceae= subset_taxa(ps3Batchra, Order ==
"Hungateiclostridiaceae")
plot_abundanceF(psOrd5BatchHungateiclostridiaceae, Facet = "Order", Color = NULL)
```

```{r subsettaxa9FBatch, fig.cap= "Violin plot of relative abundances of Lachnospirales"}
psOrd5BatchLachnospirales = subset_taxa(ps3Batchra, Order == "Lachnospirales")
plot_abundanceF(psOrd5BatchLachnospirales , Facet = "Genus", Color = NULL) +
theme(axis.text.x = element_text(angle = 90, vjust = 0.5, hjust=1))
```

```{r subsettaxa10FBatch, fig.cap= "Violin plot of relative abundances of Lactobacillales"}
psOrd5BatchLactobacillales = subset_taxa(ps3Batchra, Order == "Lactobacillales")
plot_abundanceF(psOrd5BatchLactobacillales, Facet = "Genus", Color = NULL)
```

```{r subsettaxa11FBatch, fig.cap= "Violin plot of relative abundances of Monoglobales"}
psOrd5BatchMonoglobales = subset_taxa(ps3Batchra, Order == "Monoglobales")
plot_abundanceF(psOrd5BatchMonoglobales , Facet = "Genus", Color = NULL)
```

```{r subsettaxa12FBatch, fig.cap= "Violin plot of relative abundances of Oscillospirales"}
psOrd5BatchOscillospirales = subset_taxa(ps3Batchra, Order == "Oscillospirales")
plot_abundanceF(psOrd5BatchOscillospirales, Facet = "Genus", Color = NULL) +
theme(axis.text.x = element_text(angle = 90, vjust = 0.5, hjust=1))
```

```{r subsettaxa13FBatch, fig.cap= "Violin plot of relative abundances of
Peptostreptococcales-Tissierellales"}
psOrd5BatchPT = subset_taxa(ps3Batchra, Order == "Peptostreptococcales-Tissierellales")
plot_abundanceF(psOrd5BatchPT, Facet = "Genus", Color = NULL)
```
```

(b-18)
```{r abundancetransformationPBatch, fig.height=12, fig.width=10.5,fig.cap="Comparison of original abundances with transformed data"}
plotBeforePBatch = plot_abundanceP(ps3Batch,"")
plotAfterPbatch = plot_abundanceP(ps3Batchra,"")
# Combine each plot into one graphic.
grid.arrange(nrow = 2,  plotBeforePBatch, plotAfterPbatch)
```

```{r subsettaxa1PBatch, fig.cap= "Violin plot of relative abundances of Enterobacterales"}
psOrd5BatchEnterobacterales = subset_taxa(ps3Batchra, Order == "Enterobacterales")
plot_abundanceP(psOrd5BatchEnterobacterales, Facet = "Genus", Color = NULL)
```

```{r subsettaxa2Patch, fig.cap= "Violin plot of relative abundances of Rhodospirillales"}
psOrd5BatchRhodospirillales = subset_taxa(ps3Batchra, Order == "Rhodospirillales")
plot_abundanceP(psOrd5BatchRhodospirillales, Facet = "Genus", Color = NULL)
```

```{r abundancetransformationABatch, fig.height=12, fig.width=10.5,fig.cap="Comparison of original abundances with transformed data"}
plotBeforeABatch = plot_abundanceA(ps3Batch,"")
plotAfterABatch = plot_abundanceA(ps3Batchra,"")
# Combine each plot into one graphic.
grid.arrange(nrow = 2,  plotBeforeABatch, plotAfterABatch)
```

```{r subsettaxa1ABatch, fig.cap= "Violin plot of relative abundances of Bifidobacteriales"}
psOrd5BatchBifidobacteriales = subset_taxa(ps3Batchra, Order == "Bifidobacteriales")
plot_abundanceA(psOrd5BatchBifidobacteriales, Facet = "Genus", Color = NULL)
```

```{r subsettaxa2ABatch, fig.cap= "Violin plot of relative abundances of Coriobacteriales"}
psOrd5BatchCoriobacteriales = subset_taxa(ps3Batchra, Order == "Coriobacteriales")
plot_abundanceA(psOrd5BatchCoriobacteriales, Facet = "Genus", Color = NULL)
```

```{r subsettaxa3ABatch, fig.cap= "Violin plot of relative abundances of Corynebacteriales"}
psOrd5BatchCorynebacteriales = subset_taxa(ps3Batchra, Order == "Corynebacteriales")
plot_abundanceA(psOrd5BatchCorynebacteriales , Facet = "Genus", Color = NULL)
```

```{r subsettaxa4ABatch, fig.cap= "Violin plot of relative abundances of Micrococcales"}
psOrd5BatchMicrococcales = subset_taxa(ps3Batchra, Order == "Micrococcales")
plot_abundanceA(psOrd5BatchMicrococcales , Facet = "Genus", Color = NULL)
```

(b-26)
```{r abundancetransformationBBatch, fig.height=12, fig.width=10.5,fig.cap="Comparison of original abundances with transformed data"}
plotBeforeBBatch = plot_abundanceB(ps3Batch,"")
plotAfterBBatch = plot_abundanceB(ps3Batchra,"")
# Combine each plot into one graphic.
grid.arrange(nrow = 2,  plotBeforeBBatch, plotAfterBBatch)
```

```{r subsettaxa1BBatch, fig.cap= "Violin plot of relative abundances of Bacteroidales"}
psOrd5BatchBacteroidales= subset_taxa(ps3Batchra, Order == "Bacteroidales")
plot_abundanceB(psOrd5BatchBacteroidales , Facet = "Genus", Color = NULL)
```

```
```

(b-30)
```{r abundancetransformationCBatch, fig.height=12, fig.width=10.5,fig.cap="Comparison of original abundances with transformed data"}
plotBeforeCBatch = plot_abundanceC(ps3Batch,"")
plotAfterCBatch = plot_abundanceC(ps3Batchra,"")
# Combine each plot into one graphic.
grid.arrange(nrow = 2,  plotBeforeCBatch, plotAfterCBatch)
```


```{r subsettaxa1CBatch, fig.cap= "Violin plot of relative abundances of Cyanobacteria"}
psOrd5CBatch = subset_taxa(ps3Batchra, Order == "Gastranaerophilales")
plot_abundanceC(psOrd5CBatch, Facet = "Order", Color = NULL)
```
```{r Read Counts Batch}
sample.sum.df.batch <- data.frame(sum = sample_sums(ps3Batch))

sample.sum.df.batch

log10(sample.sum.df.batch)
```
```{r Histogram of Read Counts Batch}
# Histogram of sample read counts
plotreadcountBatch = ggplot(sample.sum.df.batch, aes(x = sum)) +
  geom_histogram(color = "black", fill = "indianred", binwidth = 5000) +
  ggtitle("Distribution of sample sequencing depth") +
  xlab("Read counts") +
  theme(axis.title.y = element_blank())
```
```{r Histogram of Log Read Counts Batch}
# Histogram of log sample read counts
LogplotreadcountBatch = ggplot(sample.sum.df.batch, aes(x = log10((sum)))) +
  geom_histogram(color = "black", fill = "indianred", binwidth = 0.025) +
  ggtitle("Log Distribution of sample sequencing depth") +
  xlab("Read counts") +
  theme(axis.title.y = element_blank())
```
(b-31)
``` {r grouped plots Batch}
grid.arrange(nrow = 1, plotreadcountBatch, LogplotreadcountBatch)
```
(b-32)
```{r   outlier-detect-Batch,   fig.cap="Exploratory   ordination   analysis   with   log abundances.",fig.wide= TRUE}
sample_data(ps3Batch)$Time=gsub(" ","",sample_data(ps3Batch)$Time)
ps3Batch.log <- transform_sample_counts(ps3Batch, function(x) log(1 + x))
out.wuf.log.ps3Batch <- ordinate(ps3Batch, method = "MDS", distance = "bray")
evals.out.wuf.log.ps3Batch <- out.wuf.log.ps3Batch$values$Eigenvalues
plot_ordination(ps3Batch.log,  out.wuf.log.ps3Batch, color = "Air", shape = "Treatment", label ="Time") +
  labs(col = "Air", shape = "Treatment") +
  coord_fixed(sqrt(evals.out.wuf.log.ps3Batch[2] / evals.out.wuf.log.ps3Batch[1]))
```

```
```

```{r removelowreads Batch}
which(!rowSums(otu_table(ps3Batch)) > 52000)
ps5Batch <- prune_samples(rowSums(otu_table(ps3Batch)) > 52000, ps3Batch)
ps5Batch.log <- transform_sample_counts(ps5Batch, function(x) log(1 + x))
```

```{r outlier-analyze-batch, fig.width=9, fig.height=5, fig.cap="The outlier samples are dominated by a single ASV."}
rel_abund <- t(apply(otu_table(ps3Batch), 1, function(x) x / sum(x)))
qplot(rel_abund[, 12], geom = "histogram",binwidth=0.05) +
  xlab("Relative abundance")
```

(b-33)
```{r outlier-detect-removed-Batch, fig.cap="Exploratory ordination analysis with log abundances.",fig.wide= TRUE}
out.wuf.log.ps5Batch <- ordinate(ps5Batch, method = "MDS", distance = "bray")
evals.out.wuf.log.ps5Batch  <- out.wuf.log.ps5Batch$values$Eigenvalues
plot_ordination(ps5Batch.log, out.wuf.log.ps5Batch, color = "Air", shape = "Treatment", label = "Time") +
  labs(col = "Air", shape = "Time") +
  coord_fixed(sqrt(evals.out.wuf.log.ps5Batch[2] / evals.out.wuf.log.ps5Batch[1]))
```

```{r ordinations-dpcoa-batch,  fig.wide=TRUE,fig.cap="A  DPCoA  plot  incorporates phylogenetic information, but is  dominated by the first axis."}
out.dpcoa.log.batch <- ordinate(ps5Batch.log, method = "DPCoA")
evals.out.dpcoa.log.batch <- out.dpcoa.log.batch$eig
plot_ordination(ps5Batch.log, out.dpcoa.log.batch, color = "Air", shape = "Treatment", label = "Time") +
  scale_shape_manual(values=1:10)+
  labs(col = "Air", shape = "Time")+
  coord_fixed(sqrt(evals.out.dpcoa.log.batch[2] / evals.out.dpcoa.log.batch[1]))
```

```{r dpcoabiplot-batch,fig.wide=TRUE,fig.cap="Taxa responsible for Axis 1 and 2 Batch"}
plot_ordination(ps5Batch.log, out.dpcoa.log.batch, type = "species", color = "Phylum") +
  coord_fixed(sqrt(evals.out.dpcoa.log.batch[2] / evals.out.dpcoa.log.batch[1]))
```

```{r ordinations-wuf-batch,fig.wide =TRUE, fig.cap="The sample positions produced by a PCoA using weighted Unifrac."}
out.wuf.log.ps5Batch.pcoa <- ordinate(ps5Batch.log, method = "PCoA", distance ="wunifrac")
evals.ut.wuf.log.ps5Batch.pcoa <- out.wuf.log.ps5Batch.pcoa $values$Eigenvalues
plot_ordination(ps5Batchlog, out.wuf.log.ps5Batch.pcoa, color = "Time", shape = "Treatment2")+
  scale_shape_manual(values=1:10)+
  labs(col = "Time", shape = "Treatment") +
  coord_fixed(sqrt(evals.ut.wuf.log.ps5Batch.pcoa[2] / evals.ut.wuf.log.ps5Batch.pcoa[1]))
```

```{r dwufplotplot-batch,fig.wide=TRUE,fig.cap="Taxa responsible for Axis 1 and 2 Batch"}
plot_ordination(ps5Batch.log, out.wuf.log.ps5Batch.pcoa, type = "species", color = "Phylum") +
  coord_fixed(sqrt(evals.ut.wuf.log.ps5Batch.pcoa[2] / evals.ut.wuf.log.ps5Batch.pcoa[1]))
```

```
```

```{r rankab batch}
abund.batch <- otu_table(ps5Batch.log)
abund_ranks.batch <- t(apply(abund.batch, 1, rank))
```

```{r rank# batch}
abund_ranks.batch[]
```

```{r rankthresholbatch}
abund_ranks.batch <- abund_ranks.batch - 1335.35
abund_ranks.batch[abund_ranks.batch < 1] <- 1
```

(42)
```{r pca-rank-visualize-procedure-batch, fig.cap="Rank threshold transformation"}
library(dplyr)
library(reshape2)
abund_df.batch <- melt(abund.batch, value.name = "abund") %>%
  left_join(melt(abund_ranks.batch, value.name = "rank"))
colnames(abund_df.batch) <- c("sample", "seq", "abund", "rank")
abund_df.batch <- melt(abund.batch, value.name = "abund") %>%
  left_join(melt(abund_ranks.batch, value.name = "rank"))
colnames(abund_df.batch) <- c("sample", "seq", "abund", "rank")
sample_ix <- sample(1:nrow(abund_df.batch), 8)
ggplot(abund_df.batch %>%
    filter(sample %in% abund_df.batch$sample[sample_ix])) +
  geom_point(aes(x = abund, y = rank, col = sample),
      position = position_jitter(width = 0.2), size = 1.5) +
  labs(x = "Abundance", y = "Thresholded rank") +
  scale_color_brewer(palette = "Set2")
```

```{r pca-rank-pca-setup-batchle}
library(ade4)
ranks_pca.batch <- dudi.pca(abund_ranks.batch, scannf = F, nf = 3)
row_scores.batch <- data.frame(li = ranks_pca.batch$li,
          SampleID = rownames(abund_ranks.batch))
col_scores.batch <- data.frame(co = ranks_pca.batch$co,
          seq = colnames(abund_ranks.batch))
tax.batch <- tax_table(ps5Batch.log) %>%
  data.frame(stringsAsFactors = FALSE)
tax.batch$seq <- rownames(tax.batch)
main_orders          <-          c("Clostridiales","Enterobacterales","Eubacteriales",
"Lactospirales","Lactobacillales","Monoglobales","Oscillospirales")
tax.batch$Order[!(tax.batch$Order %in% main_orders)] <- "Other"
tax.batch$Order <- factor(tax.batch$Order, levels = c(main_orders, "Other"))
tax.batch$otu_id <- seq_len(ncol(otu_table(ps5Batch)))
row_scores.batch <- row_scores.batch %>%
  left_join(sample_data(ps5Batch))
col_scores.batch <- col_scores.batch %>%
  left_join(tax.batch)
```

````
```{r pca-rank-pca-plot-batch-1, fig.wide=TRUE,fig.height=8,fig.cap="The biplot resulting
from the PCA after the truncated-ranking transformation."}
evals_prop.batch <- 100 * (ranks_pca.batch$eig / sum(ranks_pca.batch$eig))
ggplot() +
 geom_point(data = row_scores.batch, aes(x = li.Axis1, y = li.Axis2), shape = 2) +
 geom_text_repel(data = row_scores.batch %>% filter(li.Axis1 > 20), aes(x = li.Axis1, y =
li.Axis2, label = SampleID)) +
 geom_point(data = col_scores.batch, aes(x = 25 * co.Comp1, y = 25 * co.Comp2, col =
Order),
        size = .3, alpha = 0.6) +
 facet_grid(~ Treatment) +
 guides(col = guide_legend(override.aes = list(size = 3))) +
 labs(x = sprintf("Axis1 [%s%% variance]", round(evals_prop.batch[1], 2)),
    y = sprintf("Axis2 [%s%% variance]", round(evals_prop.batch[2], 2))) +
 coord_fixed(sqrt(ranks_pca.batch$eig[2] / ranks_pca.batch$eig[1])) +
 theme(panel.border = element_rect(color = "#787878", fill = alpha("white", 0)))
```

```{r pca-rank-pca-plot-batch-2, fig.wide=TRUE,fig.height=8,fig.cap="The biplot resulting
from the PCA after the truncated-ranking transformation.2"}
evals_prop.batch <- 100 * (ranks_pca.batch$eig / sum(ranks_pca.batch$eig))
ggplot() +
 geom_point(data = row_scores.batch, aes(x = li.Axis1, y = li.Axis2), shape = 2) +
 geom_point(data = col_scores.batch, aes(x = 25 * co.Comp1, y = 25 * co.Comp2, col =
Order),
        size = .3, alpha = 0.6) +
 geom_text_repel(data = row_scores.batch %>% filter(li.Axis1 > 20), aes(x = li.Axis1, y =
li.Axis2, label=SampleID),
                 size = 4, segment.size = 0.1, force = 3,
                 max.overlaps = Inf) +
 facet_wrap(~ Time, ncol=3) +
 guides(col = guide_legend(override.aes = list(size = 3))) +
 labs(x = sprintf("Axis1 [%s%% variance]", round(evals_prop.batch[1], 2)),
    y = sprintf("Axis2 [%s%% variance]", round(evals_prop.batch[2], 2))) +
 coord_fixed(sqrt(ranks_pca.batch$eig[2] / ranks_pca.batch$eig[1])) +
 theme(panel.border = element_rect(color = "#787878", fill = alpha("white", 0)))
```

```{r pca-rank-pca-plot-batch-3, fig.wide=TRUE,fig.height=8,fig.cap="The biplot resulting
from the PCA after the truncated-ranking transformation.2"}
evals_prop.batch <- 100 * (ranks_pca.batch$eig / sum(ranks_pca.batch$eig))
ggplot() +
 geom_point(data = row_scores.batch, aes(x = li.Axis1, y = li.Axis2), shape = 2) +
 geom_point(data = col_scores.batch, aes(x = 25 * co.Comp1, y = 25 * co.Comp2, col =
Order),
        size = .3, alpha = 0.6) +
 geom_text_repel(data = row_scores.batch %>% filter(li.Axis1 > 20), aes(x = li.Axis1, y =
li.Axis2, label=SampleID),
                 size = 4, segment.size = 0.1, force = 3,
                 max.overlaps = Inf) +
 facet_wrap(~ Air, ncol=3) +
 guides(col = guide_legend(override.aes = list(size = 3))) +
 labs(x = sprintf("Axis1 [%s%% variance]", round(evals_prop.batch[1], 2)),
    y = sprintf("Axis2 [%s%% variance]", round(evals_prop.batch[2], 2))) +
````

```
  coord_fixed(sqrt(ranks_pca.batch$eig[2] / ranks_pca.batch$eig[1])) +
  theme(panel.border = element_rect(color = "#787878", fill = alpha("white", 0)))
```

```{Packages to fix}
install.packages("devtools")
devtools::install_github("david-barnett/microViz")
```

```{r ccpna-correspondence-analysis-batch}
ps5Batch.logB <- ps5Batch.log
head(tax_table(ps5Batch.log))
ps5Batch.logNaomit <- phyloseq_rm_na_tax(ps5Batch.log)
ps_ccpna.batch <- ordinate(ps5Batch.logNaomit, "CCA", formula = ps5Batch.logNaomit ~
Time + Treatment)
```


```{r ccpna-join-data-batch-1, fig.cap="The mouse and bacteria scores generated by CCpnA.",
fig.wide=TRUE, fig.height=10}
library(ggrepel)
ps_scores.batch <- vegan::scores(ps_ccpna.batch)
sites.batch <- data.frame(ps_scores.batch$sites)
sites.batch$SampleID <- rownames(sites.batch)
sites.batch <- sites.batch %>%
  left_join(sample_data(ps5Batch))
species.batch <- data.frame(ps_scores.batch$species)
species.batch$otu_id <- seq_along(colnames(otu_table(ps5Batch.logNaomit)))
species.batch <- species.batch %>%
  left_join(tax.batch)
evals_prop.ps_ccpna.batch      <-     100     *     ps_ccpna.batch$CCA$eig[1:2]      /
sum(ps_ccpna.batch$CA$eig)
ggplot() +
  geom_point(data = sites.batch, aes(x = CCA1, y = CCA2), shape = 2, alpha = 0.5) +
  geom_point(data = species.batch, aes(x = CCA1, y = CCA2, col = Order), size = 0.5) +
  geom_text_repel(data = species.batch %>% filter(CCA2 < -2.5),
          aes(x = CCA1, y = CCA2, label = otu_id),
                  size = 4, segment.size = 0.1,
                  max.overlaps = Inf) +
  facet_grid(. ~ Treatment) +
  guides(col = guide_legend(override.aes = list(size = 3))) +
  labs(x = sprintf("Axis1 [%s%% variance]", round(evals_prop.ps_ccpna.batch[1], 2)),
     y = sprintf("Axis2 [%s%% variance]", round(evals_prop.ps_ccpna.batch[2], 2))) +
  coord_fixed(sqrt(ps_ccpna.batch$CCA$eig[2] / ps_ccpna.batch$CCA$eig[1])*0.45   ) +
  theme(panel.border = element_rect(color = "#787878", fill = alpha("white", 0)))
```

```{r Plot_network_batch}
plot_net(ps5Batch.log, maxdist = 0.3, color = "Air", shape = "Treatment", point_label = NULL,
point_size = 5, laymeth = "fruchterman.reingold") + scale_shape_manual(values=1:9)
```

```{r Plot_network_batch_2}
plot_net(ps5Batch.log, maxdist = 0.3, color = "Time", shape = "Treatment", point_label =
NULL, point_size = 5, laymeth = "fruchterman.reingold") + scale_shape_manual(values=1:9)
```

```{r mst_batch}
```

```
gt.mst.batch <- graph_perm_test(ps5Batch.log, "Treatment", grouping = "SampleID",
          distance = "jaccard", type = "mst")
gt.mst.batchA <- graph_perm_test(ps5Batch.log, "Air", grouping = "SampleID",
          distance = "jaccard", type = "mst")
gt.mst.batchT <- graph_perm_test(ps5Batch.log, "Time", grouping = "SampleID",
          distance = "jaccard", type = "mst")
gt.mst.batch$pval
gt.mst.batchA$pval
gt.mst.batchT$pval
```

```{r mst-plot-batch, fig.width=8.5, fig.height=5, fig.cap="The graph and permutation histogram obtained from the minimal  spanning tree with Jaccard similarity."}
plotNet.gt.batch.mst=plot_test_network(gt.mst.batch)      +      theme(legend.text     =
element_text(size = 8),
    legend.title = element_text(size = 9))
plotPerm.gt.batch.mst=plot_permutations(gt.mst.batch)
grid.arrange(ncol = 2,  plotNet.gt.batch.mst, plotPerm.gt.batch.mst)
gt.mst.batch
```

```{r mst_batch_air}
gt.mst.batch.air <- graph_perm_test(ps5Batch.log, "Air", grouping = "SampleID",
          distance = "jaccard", type = "mst")
gt.mst.batch.air$pval
plotNet.gt.batch.mstA=plot_test_network(gt.mst.batch.air)      +      theme(legend.text     =
element_text(size = 8),
    legend.title = element_text(size = 9))
plotPerm.gt.batch.mstA=plot_permutations(gt.mst.batch.air)
grid.arrange(ncol = 2,  plotNet.gt.batch.mstA, plotPerm.gt.batch.mstA)
```

```{r mst_batch_time}
gt.mst.batch.T <- graph_perm_test(ps5Batch.log, "Time", grouping = "SampleID",
          distance = "jaccard", type = "mst")
gt.mst.batch.air$pval
plotNet.gt.batch.mstT=plot_test_network(gt.mst.batch.T)      +      theme(legend.text     =
element_text(size = 8),
    legend.title = element_text(size = 9))
plotPerm.gt.batch.mstT=plot_permutations(gt.mst.batch.T)
grid.arrange(ncol = 2,  plotNet.gt.batch.mstT, plotPerm.gt.batch.mstT)
```

```{r knn-1-batch}
gt.batch.knn <- graph_perm_test(ps5Batch.log, "Treatment", grouping = "SampleID",
          distance = "jaccard", type = "knn", knn = 1)
gt.batch.knn$pval
```

```{r knn-1-plot-batch,fig.cap="k=1 nearest-neighbor network and permutation histogram",
fig.wide=TRUE, fig.height=5}
plotNet.gt.batch.knn=plot_test_network(gt.batch.knn)      +      theme(legend.text     =
element_text(size = 8),
    legend.title = element_text(size = 9))
plotPerm.gt.batch.knn=plot_permutations(gt.batch.knn)
grid.arrange(ncol = 2,  plotNet.gt.batch.knn, plotPerm.gt.batch.knn)
```
```

```{r BraydistanceBatch-1}
gt.Batch.breynedges    <-    graph_perm_test(ps5Batch.log,    "Treatment",    grouping    =
"SampleID",
                        distance = "bray", type = "threshold.nedges", nedges = 25,
                        keep.isolates = FALSE)
plotNet.gt.Batch.breynedges        =plot_test_network(gt.Batch.breynedges        )        +
theme(legend.text = element_text(size = 8),
        legend.title = element_text(size = 9))
plotPerm.gt.Batch.breynedges =plot_permutations(gt.Batch.breynedges )
grid.arrange(ncol = 2, plotNet.gt.Batch.breynedges , plotPerm.gt.Batch.breynedges)
gt.Batch.breynedges$pval


```

```{r BraydistanceBatch-2}
gt4Batch <- graph_perm_test(ps5Batch.log, "Treatment", grouping = "SampleID",
                        distance = "bray", type = "threshold.nedges", nedges = 200,
                        keep.isolates = FALSE)
plotNet5B=plot_test_network(gt4Batch) + theme(legend.text = element_text(size = 8),
        legend.title = element_text(size = 9))
plotPerm5B=plot_permutations(gt4Batch)
grid.arrange(ncol = 2, plotNet5B, plotPerm5B)
```
```{r lm-get-alpha-diversity-batch}
library("nlme")
library("reshape2")
ps_alpha_div.B <- estimate_richness(ps5Batch.log, split = TRUE, measure = "Shannon")
ps_alpha_div.B$SampleID <- rownames(ps_alpha_div.B) %>%
 as.factor()
ps_samp.B <- sample_data(ps5Batch.log) %>%
 unclass() %>%
 data.frame() %>%
 left_join(ps_alpha_div.B, by = "SampleID") %>%
 melt(measure.vars = "Shannon",
    variable.name = "diversity_measure",
    value.name = "alpha_diversity")
# reorder's facet from lowest to highest diversity
diversity_means.B <- ps_samp.B %>%
 group_by(SampleID) %>%
 summarise(mean_div = mean(alpha_diversity)) %>%
 arrange(mean_div)
ps_samp.B$SampleID <- factor(ps_samp.B$SampleID,
                diversity_means.B$SampleID)
```

```{r lm-Treatment-batch}
alpha_div_model.B <- lme(fixed = alpha_diversity ~ Treatment, data = ps_samp.B,
            random = ~ 1 | SampleID)
```

```{r lm-prediction-intervals-batch}
new_data.B <- expand.grid(SampleID = ps_samp.B$SampleID,
            Treatment = ps_samp.B$Treatment)
new_data.B$pred <- predict(alpha_div_model.B, newdata = new_data.B)
X.B <- model.matrix(eval(eval(alpha_div_model.B$call$fixed)[-2]),
```

```
            new_data.B[-ncol(new_data.B)])
pred_var_fixed.B <- diag(X.B %*% alpha_div_model.B$varFix %*% t(X.B))
new_data.B$pred_var <- pred_var_fixed.B + alpha_div_model.B$sigma ^ 2
```

```{r lm-fitted-plot-batch}
# fitted values, with error bars
ggplot(ps_samp.B %>% left_join(new_data.B)) +
  geom_errorbar(aes(x = Time, ymin = pred - 2 * sqrt(pred_var),
            ymax = pred + 2 * sqrt(pred_var)),
        col = "#858585", size = .1) +
  geom_point(aes(x = Time, y = alpha_diversity,
        col = Time), size = 0.8) +
  facet_wrap(~Treatment + Air) +
  scale_y_continuous(limits = c(6, 7), breaks = seq(0, 7, .1)) +
  scale_color_brewer(palette = "Set3") +
  labs(x = "Treatment", y = "Shannon Diversity", color = "Time") +
  guides(col = guide_legend(override.aes = list(size = 4))) +
  theme(panel.border = element_rect(color = "#787878", fill = alpha("white", 0)),
      axis.text.x = element_text(angle = -90, size = 6),
      axis.text.y = element_text(size = 6))
```

```{r deseq-transform-batch}
library("reshape2")
library("DESeq2")
#New version of DESeq2 needs special levels
ps_dds.batch <- phyloseq_to_deseq2(ps5Batch, design = ~ Treatment + Time + Air)
# geometric mean, set to zero when all coordinates are zero
geo_mean_protected <- function(x) {
  if (all(x == 0)) {
    return (0)
  }
  exp(mean(log(x[x != 0])))
}
geoMeans.batch <- apply(counts(ps_dds.batch), 1, geo_mean_protected)
ps_dds.batch <- estimateSizeFactors(ps_dds.batch, geoMeans = geoMeans.batch)
ps_dds.batch <- estimateDispersions(ps_dds.batch)
abund.pp_dds.batch <- getVarianceStabilizedData(ps_dds.batch)
```

```{r structssi-shorten-names-batch}
short_names.batch <- substr(rownames(abund.pp_dds.batch), 1, 5)%>%
  make.names(unique = TRUE)
rownames(abund.pp_dds.batch) <- short_names.batch
```

```{r deseq-vis-batch, fig.cap="DEseq transformation abundance"}
abund_sums.ps_dds.batch <- rbind(data.frame(sum = colSums(abund.pp_dds.batch),
              sample = colnames(abund.pp_dds.batch),
              type = "DESeq2"),
          data.frame(sum = rowSums(otu_table(ps5Batch.log)),
              sample = rownames(otu_table(ps5Batch.log)),
              type = "log(1 + x)"))
ggplot(abund_sums.ps_dds.batch) +
  geom_histogram(aes(x = sum), binwidth = 20) +
```

```
  facet_grid(type ~ .) +
  xlab("Total abundance within sample")
```

```{r structssi-unadjp.batch }
library("structSSI")
el.batch <- phy_tree(ps5Batch.log)$edge
el0.batch <- el.batch
el0.batch <- el0.batch[nrow(el.batch):1, ]
el_names.batch <- c(short_names.batch, seq_len(phy_tree(ps5Batch.log)$Nnode))
el.batch[, 1] <- el_names.batch[el0.batch[, 1]]
el.batch[, 2] <- el_names.batch[as.numeric(el0.batch[, 2])]
unadj_p.batch              <-              treePValues(el.batch,          abund.pp_dds.batch,
sample_data(ps5Batch.log)$Treatment)
unadj_p.batch.time         <-              treePValues(el.batch,          abund.pp_dds.batch,
sample_data(ps5Batch.log)$Time)
unadj_p.batch.Air          <-              treePValues(el.batch,          abund.pp_dds.batch,
sample_data(ps5Batch.log)$Air)
```

```{r structssi-test-1}
hfdr_res.batch <- hFDR.adjust(unadj_p.batch, el.batch, .75)
hfdr_res.batch.time <- hFDR.adjust(unadj_p.batch.time, el.batch, .75)
hfdr_res.batch.Air <- hFDR.adjust(unadj_p.batch.Air, el.batch, .75)
summary(hfdr_res.batch)
summary(hfdr_res.batch.time)
summary(hfdr_res.batch.Air)
```

```{r structssi-tax-1}
tax.ps_dds.batch <- tax_table(ps5Batch.log)[, c("Family", "Genus")] %>%
  data.frame()
tax.ps_dds.batch$seq <- short_names.batch
```

```{r structssi-test-res-batch-treatment}
options(digits=3)
hfdr_res.batch@p.vals$seq <- rownames(hfdr_res.batch@p.vals)
tax.ps_dds.batch %>%
  left_join(hfdr_res.batch@p.vals) %>%
  arrange(adjp) %>% head(10)
```

```{r structssi-test-res-batch-time}
options(digits=3)
hfdr_res.batch.time@p.vals$seq <- rownames(hfdr_res.batch.time@p.vals)
tax.ps_dds.batch %>%
  left_join(hfdr_res.batch.time@p.vals) %>%
  arrange(adjp) %>% head(10)
```

```{r structssi-test-res-batch-air}
options(digits=3)
hfdr_res.batch.Air@p.vals$seq <- rownames(hfdr_res.batch.Air@p.vals)
tax.ps_dds.batch %>%
  left_join(hfdr_res.batch.Air@p.vals) %>%
  arrange(adjp) %>% head(10)
```

(b-34)
```{r Abundance-plot-for-batch}
ps3BatchBerberine <- subset_samples(ps3Batch, Treatment == "Berberine")
ps3BatchBAT = plot_bar(ps3BatchBerberine, x="Phylum", fill = "Phylum", facet_grid = "Time~Air", title = "Berberine Air/Time")
plot(ps3BatchBAT)
```

```{r Abundance-plot-for-batch1.1}
ps3BatchBerberineT7 <- subset_samples(ps3BatchBerberine, Time == "T7")
ps3BatchBATT7 = plot_bar(ps3BatchBerberineT7, x="Phylum", fill = "Phylum", facet_grid = "Time~Air", title = "Berberine Air/Time")
plot(ps3BatchBATT7)
```
```{r Abundance-plot-for-batch1.2}
ps5BatchBerberineT14 <- subset_samples(ps5BatchBerberine, Time == "T14")
ps5BatchBATT14 = plot_bar(ps5BatchBerberineT14, x="Phylum", fill = "Phylum", facet_grid = "Time~Air", title = "Berberine Air/Time")
plot(ps5BatchBATT14)
```
```{r Abundance-plot-for-batch1.3}
ps5BatchBerberineT21 <- subset_samples(ps5BatchBerberine, Time == "T21")
ps5BatchBATT21 = plot_bar(ps5BatchBerberineT21, x="Phylum", fill = "Phylum", facet_grid = "Time~Air", title = "Berberine Air/Time")
plot(ps5BatchBATT21)
```

```{r Abundance-plot-for-batch2}
ps3BatchQuercetin <- subset_samples(ps3Batch, Treatment == "Quercetin")
PS3BatchQAT = plot_bar(ps3BatchQuercetin, x="Phylum", fill = "Phylum", facet_grid = "Time~Air", title = "Quercetin Air/Time")
plot(PS3BatchQAT)
```
```{r Abundance-plot-for-batch2.1}
ps3BatchQuercetinT7 <- subset_samples(ps3BatchQuercetin, Time == "T7")
PS3BatchQATT7 = plot_bar(ps3BatchQuercetinT7, x="Phylum", fill = "Phylum", facet_grid = "Time~Air", title = "Quercetin Air/Time")
plot(PS3BatchQATT7)
```
```{r Abundance-plot-for-batch2.2}
ps3BatchQuercetinT14 <- subset_samples(ps3BatchQuercetin, Time == "T14")
PS3BatchQATT14 = plot_bar(ps3BatchQuercetinT14, x="Phylum", fill = "Phylum", facet_grid = "Time~Air", title = "Quercetin Air/Time")
plot(PS3BatchQATT14)
```
```{r Abundance-plot-for-batch2.3}
ps3BatchQuercetinT21 <- subset_samples(ps3BatchQuercetin, Time == "T21")
PS3BatchQATT21 = plot_bar(ps3BatchQuercetinT21, x="Phylum", fill = "Order", facet_grid = "Time~Air", title = "Quercetin Air/Time")
plot(PS3BatchQATT21)
```

```{r Abundance-plot-for-batch3}
ps3BatchControl <- subset_samples(ps3Batch, Treatment == "Control")
ps3BatchCAT = plot_bar(ps3BatchControl, x="Phylum", fill = "Phylum", facet_grid =
"Time~Air", title = "Control Air/Time")
plot(ps3BatchCAT)
```

```{r Abundance-plot-for-batch3.1}
ps3BatchControlT7 <- subset_samples(ps3BatchControl, Time == "T7")
PS3BatchCATT7 = plot_bar(ps3BatchControlT7, x="Phylum", fill = "Phylum", facet_grid =
"Time~Air", title = "Control Air/Time")
plot(PS3BatchCATT7)
```

```{r Abundance-plot-for-batch3.2}
ps3BatchControlT14 <- subset_samples(ps3BatchControl, Time == "T14")
PS3BatchCATT14 = plot_bar(ps3BatchControlT14, x="Phylum", fill = "Phylum", facet_grid =
"Time~Air", title = "Control Air/Time")
plot(PS3BatchCATT14)
```

```{r Abundance-plot-for-batch3.3}
ps3BatchControlT21 <- subset_samples(ps3BatchControl, Time == "T21")
PS3BatchCATT21 = plot_bar(ps3BatchControlT14, x="Phylum", fill = "Phylum", facet_grid =
"Time~Air", title = "Control Air/Time")
plot(PS3BatchCATT21)
```

```{r relative-abundance-plot-batch1}
total = median(sample_sums(ps5Batch))
standf = function(x, t=total) round(t * (x / sum(x)))
ps6Batch = transform_sample_counts(ps5Batch, standf)

plot_bar(ps6Batch, fill = "Phylum") +
geom_bar(aes(color=Phylum, fill=Phylum), stat="identity", position="stack")
```


```{r relative-abundance-plot-batch2}
Plotps6BatchAbundance <- plot_bar(ps6Batch, fill = "Phylum") +
geom_bar(aes(color=Phylum, fill=Phylum), stat="identity", position="stack")
plot(Plotps6BatchAbundance)
```

```{r RAbundance-plot-for-batch1}
ps6BatchBerberine <- subset_samples(ps6Batch, Treatment == "Berberine")
ps6BatchBAT = plot_bar(ps6BatchBerberine, x="Phylum", fill = "Phylum", facet_grid =
"Time~Air", title = "Berberine Air/Time")
plot(ps6BatchBAT)
```

```{r RAbundance-plot-for-batch1.1}
ps6BatchBerberineT7 <- subset_samples(ps6BatchBerberine, Time == "T7")
ps6BatchBATT7 = plot_bar(ps6BatchBerberineT7, x="Phylum", fill = "Phylum", facet_grid =
"Time~Air", title = "Berberine Air/Time")
plot(ps6BatchBATT7)
```

```{r RAbundance-plot-for-batch1.2}
```

```
ps6BatchBerberineT14 <- subset_samples(ps6BatchBerberine, Time == "T14")
ps6BatchBATT14 = plot_bar(ps6BatchBerberineT14, x="Phylum", fill = "Phylum", facet_grid
= "Time~Air", title = "Berberine Air/Time")
plot(ps6BatchBATT14)
```

```{r RAbundance-plot-for-batch1.3}
ps6BatchBerberineT21 <- subset_samples(ps6BatchBerberine, Time == "T21")
ps6BatchBATT21 = plot_bar(ps6BatchBerberineT21, x="Phylum", fill = "Phylum", facet_grid
= "Time~Air", title = "Berberine Air/Time")
plot(ps6BatchBATT21)
```

```{r RAbundance-plot-for-batch2}
ps6BatchQuercetin <- subset_samples(ps6Batch, Treatment == "Quercetin")
ps6BatchQAT = plot_bar(ps6BatchQuercetin, x="Phylum", fill = "Phylum", facet_grid =
"Time~Air", title = "Quercetin Air/Time")
plot(ps6BatchQAT)
```

```{r RAbundance-plot-for-batch2.1}
ps6BatchQuercetinT7 <- subset_samples(ps6BatchQuercetin, Time == "T7")
ps6BatchQATT7 = plot_bar(ps6BatchQuercetinT7, x="Phylum", fill = "Phylum", facet_grid =
"Time~Air", title = "Quercetin Air/Time")
plot(ps6BatchQATT7)
```

```{r RAbundance-plot-for-batch2.2}
ps6BatchQuercetinT14 <- subset_samples(ps6BatchQuercetin, Time == "T14")
ps6BatchQATT14 = plot_bar(ps6BatchQuercetinT14, x="Phylum", fill = "Phylum", facet_grid
= "Time~Air", title = "Quercetin Air/Time")
plot(ps6BatchQATT14)
```


```{r RAbundance-plot-for-batch2.3}
ps6BatchQuercetinT21 <- subset_samples(ps6BatchQuercetin, Time == "T21")
ps6BatchQATT21 = plot_bar(ps6BatchQuercetinT21, x="Phylum", fill = "Phylum", facet_grid
= "Time~Air", title = "Quercetin Air/Time")
plot(ps6BatchQATT21)
```


```{r RAbundance-plot-for-batch3}
ps6BatchControl <- subset_samples(ps6Batch, Treatment == "Control")
ps6BatchCAT = plot_bar(ps6BatchControl, x="Phylum", fill = "Phylum", facet_grid =
"Time~Air", title = "ControlAir/Time")
plot(ps6BatchCAT)
```

```{r RAbundance-plot-for-batch3.1}
ps6BatchControlT7 <- subset_samples(ps6BatchControl, Time == "T7")
ps6BatchCATT7 = plot_bar(ps6BatchControlT7, x="Phylum", fill = "Phylum", facet_grid =
"Time~Air", title = "Quercetin Air/Time")
plot(ps6BatchCATT7)
```

```{r RAbundance-plot-for-batch3.2}
ps6BatchControlT14 <- subset_samples(ps6BatchControl, Time == "T14")
```

```
ps6BatchCATT14 = plot_bar(ps6BatchControlT14, x="Phylum", fill = "Phylum", facet_grid =
"Time~Air", title = "Quercetin Air/Time")
plot(ps6BatchCATT14)
```

```{r RAbundance-plot-for-batch3.3}
ps6BatchControlT21 <- subset_samples(ps6BatchControl, Time == "T21")
ps6BatchCATT21 = plot_bar(ps6BatchControlT21, x="Phylum", fill = "Phylum", facet_grid =
"Time~Air", title = "Quercetin Air/Time")
plot(ps6BatchCATT21)
```

(b-40)
```{r self exploration using ordination Batch}
GP.ord <- ordinate(ps5Batch, "NMDS", "bray")
p1Batch = plot_ordination(ps5Batch, GP.ord, type="taxa", color="Phylum", title="taxa")
print(p1Batch)
```

```{r self exploration using ordination 2 Batch}
p1Batch + facet_wrap(~Phylum, 3)
```

```{r Arrange all Batch Plots}
grid.arrange(nrow  =  3,  PS3BatchCATT7  +  theme(axis.title  =  element_blank()),
ps3BatchBATT7, PS3BatchQATT7)
```

```{r ordinations-bray-Batch, fig.cap="A PCoA plot using Bray-Curtis between  samples."}
out.pcoa.log <- ordinate(ps5Batch,  method = "MDS", distance = "bray")
evals <- out.pcoa.log$values[,1]
plot_ordination(ps5Batch, out.pcoa.log, col = "Treatment",
          shape = "Air", label = "Time") +
  labs(shape = "Air")+
  coord_fixed(sqrt(evals[2] / evals[1]))
```


```{r  ordinations-dpcoa-batch-2,   fig.wide=TRUE,fig.cap="A   DPCoA   plot   incorporates
phylogenetic information, but is  dominated by the first axis."}
out.dpcoa.log <- ordinate(ps5Batchlog,method = "DPCoA")
evals <- out.dpcoa.log$eig
plot_ordination(ps5Batchlog, out.dpcoa.log, color = "Time",
          shape = "Treatment") +
  labs(col = "Time", shape = "Treatment")+
  coord_fixed(sqrt(evals[2] / evals[1]))
```

```{r dpcoabiplot-Batch, fig.wide=TRUE,fig.cap="Taxa responsible for Axis 1 and 2"}
plot_ordination(ps5Batchlog, out.dpcoa.log, type = "species", color = "Phylum") +
  coord_fixed(sqrt(evals[2] / evals[1]))
```

```{r ordinations-wuf-Batch, fig.wide =TRUE, fig.cap="The sample positions produced by a
PCoA using weighted Unifrac."}
out.wuf.log <- ordinate(ps5Batchlog, method = "PCoA", distance ="wunifrac")
evals <- out.wuf.log$values$Eigenvalues
plot_ordination(ps5Batchlog, out.wuf.log, color = "Time",
          shape = "Treatment", label = "Air") +
  coord_fixed(sqrt(evals[2] / evals[1])) +
```

```
  labs(col = "Time", shape = "Treatment")
```


```{r dwufplotplot-batch-2,  fig.wide=TRUE,fig.cap="Taxa responsible for Axis 1 and 2"}
plot_ordination(ps5Batchlog, out.wuf.log, type = "species", color = "Phylum") +
  coord_fixed(sqrt(evals[2] / evals[1]))
```
```{r plots}
ps4_Treatment <- merge_samples(ps4, "Treatment")
plot_bar(ps4_Treatment, fill = "Phylum") +
geom_bar(aes(color=Phylum, fill=Phylum), stat="identity", position="stack")

plot_bar(ps4, x="Phylum", fill = "Phylum", facet_grid = Treatment~Model)

ps5 <- subset_samples(ps4, Model =="BatchC")
ps6 <- subset_samples(ps5, Treatment =="Beberine")
ps6 <- subset_samples(ps4, Model =="Model", Treatment =="Berberine")
ps5_anaero <- subset_samples(ps5, Air =="anaero")
ps5_microaero <- subset_samples(ps5, Air =="microaero")
ps5_anaero_otugraph <- plot_bar(ps5_anaero, fill = "Phylum", facet_grid = Air~Treatment)
ps5_microaero_otugraph  <-  plot_bar(ps5_microaero,  fill  =  "Phylum",  facet_grid  =
Air~Treatment)
ps5_aero_otugraph <- plot_bar(ps5_aerobic, fill = "Phylum", facet_grid = Air~Treatment)

grid.arrange(ps5_anaero_otugraph, ps5_microaero_otugraph, ps5_aero_otugraph, ncol=1)

plot_bar(ps4, fill = "Phylum")

total = median(sample_sums(ps3))
standf = function(x, t=total) round(t * (x / sum(x)))
ps4 = transform_sample_counts(ps3, standf)

plot_bar(ps4, fill = "Phylum") +
geom_bar(aes(color=Phylum, fill=Phylum), stat="identity", position="stack")

plot_bar(ps5, fill = "Phylum") +
geom_bar(aes(color=Phylum, fill=Phylum), stat="identity", position="stack")
plot_bar(ps6, fill = "Phylum") +
geom_bar(aes(color=Phylum, fill=Phylum), stat="identity", position="stack")
```
```

Appendix V: Statistical Analysis for *Escherichia-shigella* abundance chapter 9

List of Abbreviations

M – Mean

SD – Standard deviation

Methods Restated

Two tailed t-tests for independent means were conducted using https://www.socscistatistics.com/tests/studenttest/default2.aspx (Social Science Statistics, 2022). Two tailed t-tests were selected as it was unknown if resistance level, or production would increase or decrease as a consequence of evolution in sub-inhibitory concentrations of phytochemicals. Significance value was set at $p > 0.05$.

Escherichia-shigella **concentration changes**

(1) Berberine Ceca Day 14 (0.01665, 0.0298, 0.46383) vs. Control Ceca Day 14 (0.04606, 0.09776)

Berberine Ceca Day 14 (M = 0.17, SD = 0.13) was not statistically significantly different than Control Ceca Day 14 (M = 0.07, SD = 0.00).

The *t*-value is 0.515. The *p*-value is .642093. The result is *not* significant at *p* < .05.

(2) Berberine Ceca Day 21 (0.00466, 0.0062, 0.0111, 0.01915, 0.02109, 0.08032, 0.11586, 0.13926, 0.1429, 0.1608, 0.06601) vs Control Ceca Day 21 (0.00772, 0.008, 0.011464, 0.011464, 0.01916, 0.0221, 0.02564, 0.02966, 0.05898, 0.06269)

Berberine Ceca Day 21 (M = 0.07, SD = 0.04) was statistically significantly different from Control Ceca Day 21 (M = 0.03, SD = 0.00)

The *t*-value is 2.17248. The *p*-value is .042679. The result is significant at *p* < .05.

(3) Berberine Ileum Day 14 (0.88869, 0.42817, 0.06601) vs Control Ileum Day 14 (0.0786, 0.02667)

Berberine Ileum Day 14 (M = 0.46, SD = 0.34) was not statistically significantly different from Control Ileum Day 14 (M = 0.05, SD = 0.00)

The *t*-value is 1.32601. The *p*-value is .276757. The result is *not* significant at *p* < .05.

(4) Berberine Ileum Day 21 (0.09023, 0.276, 0.44204) vs. Control Ileum Day 21 (0.02685, 0.11251, 0.25434, 0.00309)

Berberine Ileum Day 21 (M = 0.27, SD = 0.06) was not statistically significantly different from Control Ileum Day 21 (M = 0.10, SD = 0.04).

The *t*-value is 1.57075. The *p*-value is .177039. The result is *not* significant at *p* < .05.

(5) Quercetin Ceca Day 14 (0.04606, 0.09776) vs Control Ceca Day 14 (0.05816, 0.09383, 0.13025)

Quercetin Ceca Day 14 (M = 0.09, SD = 0.00) was not statistically significantly different from the Control Ceca Day 14 (M = 0.07, SD = 0.00)

The *t*-value is 0.67057. The *p*-value is .550502. The result is *not* significant at *p* < .05.

(6) Quercetin Ceca Day 21 (0.00649, 0.01053, 0.01803, 0.01878, 0.02153, 0.02346, 0.02676, 0.03586, 0.04957, 0.15225) vs. Control Ceca Day 21 (0.00772, 0.008, 0.011464, 0.011464, 0.01916, 0.0221, 0.02564, 0.02966, 0.05898, 0.06269)

Quercetin Ceca Day 21 (M = 0.04, SD = 0.02) was not statistically significantly different from the Control Ceca Day 21 (M = 0.03, SD = 0.00)

The *t*-value is -0.71583. The *p*-value is .483279. The result is *not* significant at *p* < .05.

(7) Quercetin Ileum Day 14 (0.15739, 0.43489, 0.57191) vs Control Ileum Day 14 (0.0786, 0.02667)

Quercetin Ileum Day 14 (M = 0.39, SD = 0.09) was not statistically significantly different from the Control Ileum Day 14 (M = 0.05, SD = 0.00)

The *t*-value is -2.11497. The *p*-value is .124776. The result is *not* significant at $p < .05$.

(8) Quercetin Ileum Day 21 (0, 0.01636, 0.02421, 0.04062, 0.17608, 0.17857) vs. Control Ileum Day 21 (0.02685, 0.11251, 0.25434, 0.00309)

Quercetin Ileum Day 21 (M = 0.07, SD = 0.03) was not statistically significantly different from the Control Ileum Day 21 (M = 0.10, SS = 0.04)

The *t*-value is 0.43232. The *p*-value is .676923. The result is *not* significant at $p < .05$.

Appendix VI: List of papers published because of the work presented in this thesis

1. Tansirichaiya S, **Hutton W,** Roberts AP (2022) Functional and sequence-specific screening protocols for the detection of novel antimicrobial resistance genes in metagenomic DNA in Metagenomics - Methods and Protocols 3rd Edition. Methods Mol Biol. (submitted)

2. **William Hutton,** Amy McLeman , Natasha Niethamer , Daire Cantillon , Claudia McKeown , Edwin Panford-Quainoo , Ellie Allman , Richard Goodman , Aaron Dowling , Lee Haines , Adam P. Roberts. Antimicrobial Resistance and One Health. International Microbiology Literacy Frameworks. Ed; Kenneth Timmis. Society for Applied Microbiology, UK (Accepted).